PB86-212412

# Development and Testing of a Surrogate Species Chemical Reaction Mechanism. Volume 2

Volume 2

California Univ., Riverside

Prepared for

Environmental Protection Agency
Research Triangle Park, NC

Jun 86

U.S. Department of Commerce
National Technical Information Service
NTIS

PB86-212412
EPA/600/3-86/031b
June 1986

# DEVELOPMENT AND TESTING OF A SURROGATE SPECIES CHEMICAL REACTION MECHANISM

## VOLUME II

William P. L. Carter, Frederick W. Lurmann,

Roger Atkinson and Alan C. Lloyd

Statewide Air Pollution Research Center
University of California
Riverside, California 92521

and

Environmental Research and Technology
975 Business Center Circle
Newbury Park, CA 91320

EPA Contract No. 68-02-4104

Project Officer

Marcia C. Dodge

Atmospheric Chemistry and Physics Division
Atmospheric Sciences Research Laboratory
Research Triangle Park, NC 27711

ATMOSPHERIC SCIENCES RESEARCH LABORATORY
OFFICE OF RESEARCH AND DEVELOPMENT
U. S. ENVIRONMENTAL PROTECTION AGENCY
RESEARCH TRIANGLE PARK, NC 27711

REPRODUCED BY
NATIONAL TECHNICAL
INFORMATION SERVICE
U.S. DEPARTMENT OF COMMERCE
SPRINGFIELD, VA. 22161

## TECHNICAL REPORT DATA

*(Please read Instructions on the reverse before completing)*

| | | |
|---|---|---|
| 1. REPORT NO.<br>EPA/600/3-86/031b | 2. | 3. RECIPIENT'S ACCESSION NO.<br>PB86 212412/AS |
| 4. TITLE AND SUBTITLE<br>DEVELOPMENT AND TESTING OF A SURROGATE SPECIES CHEMICAL REACTION MECHANISM, VOLUME II | | 5. REPORT DATE<br>June 1986<br>6. PERFORMING ORGANIZATION CODE |
| 7. AUTHOR(S)<br>W. P. L. Carter, F. W. Lurmann, R. Atkinson, and A. C. Lloyd | | 8. PERFORMING ORGANIZATION REPORT NO. |
| 9. PERFORMING ORGANIZATION NAME AND ADDRESS<br>Statewide Air Pollution Research Center<br>University of California<br>Riverside, California 92521 | | 10. PROGRAM ELEMENT NO.<br>CDWA1A/01-4003 (FY-86)<br>11. CONTRACT/GRANT NO.<br>Contract 68-02-4104 |
| 12. SPONSORING AGENCY NAME AND ADDRESS<br>Atmospheric Sciences Research Laboratory-RTP, NC<br>Office of Research and Development<br>U. S. Environmental Protection Agency<br>Research Triangle Park, North Carolina 27711 | | 13. TYPE OF REPORT AND PERIOD COVERED<br>Interim (10/84 - 2/86)<br>14. SPONSORING AGENCY CODE<br>EPA/600/09 |
| 15. SUPPLEMENTARY NOTES<br>Volume I. (EPA/600/3-86/031a) | | |

16. ABSTRACT

A photochemical reaction mechanism has been updated and extensively evaluated. The testing and refinement of the surrogate species mechanism was performed in order to create an improved chemical mechanism for the atmospheric simulation models that are used to develop ozone control strategies. The updated mechanism was tested against 400 smog chamber experiments carried out in four different chambers. Tests were performed to assess the accuracy of the chamber characterization procedures, of reactions for single organic compounds, and of the overall mechanism for complex organic mixtures, including mixtures obtained from automobile exhaust. The results indicate that the mechanism's predictions are generally consistent with the experimental data. Volume 1 contains the introduction, the documentation of the chemical mechanism, and a discussion of the chamber and light intensity characterization. Volume II contains the results of the model simulations of the environmental chamber experiments and a summary and conclusion section that includes a discussion of work to be carried out in the future to adapt this mechanism for use in atmospheric modeling.

17. KEY WORDS AND DOCUMENT ANALYSIS

| a. DESCRIPTORS | b. IDENTIFIERS/OPEN ENDED TERMS | c. COSATI Field/Group |
|---|---|---|
| | | |

| | | |
|---|---|---|
| 18. DISTRIBUTION STATEMENT<br>RELEASE TO PUBLIC | 19. SECURITY CLASS (This Report)<br>UNCLASSIFIED | 21. NO. OF PAGES<br>346 |
| | 20. SECURITY CLASS (This page)<br>UNCLASSIFIED | 22. PRICE |

EPA Form 2220-1 (9-73)

# NOTICE

The information in this document has been funded by the United States Environmental Protection Agency under Contract Number 68-02-4104 to the University of California at Riverside. It has been subject to the Agency's peer and administrative review, and it has been approved for publication as an EPA document. Mention of trade names or commercial products does not constitute endorsement or recommendation for use.

# ABSTRACT

This interim report describes the work performed in the first year of a two-year program to develop and test a chemical mechanism using the "lumped molecule" approach for inclusion in models to assess control strategies for ozone. The specific tasks which were carried out during the period covered by this report are as follows:

- The detailed, "lumped-molecule," mechanism of Atkinson et al. (1982) was updated and expanded. A number of new species were added to the mechanism and substantial modifications were made to the aromatic photooxidation mechanism and to the approach used to represent the reactions of the higher ($\geq C_5$) alkanes. Several significant changes were also made to the mechanisms of the alkenes and the ketones, and a new approach was used for representing the reactions of peroxy radicals under conditions where radical-radical reactions become important. Explicit chemical mechanisms were developed for the following species: $C_2$ through $C_4$ alkanes; ethene, propene, 1-butene and trans-2-butene; benzene, toluene, o-xylene, m-xylene, and 1,3,5-trimethylbenzene; formaldehyde, acetaldehyde, propionaldehyde, acetone, methyl ethyl ketone, 3-pentanol, glyoxal, methylglyoxal, biacetyl, and benzaldehyde; and the representative organic nitrates 2-butyl nitrate and 4-heptyl nitrate. "Lumped reaction" schemes were also formulated for the higher alkanes n-pentane through n-nonane, 2-methylbutane, 2,3-dimethylbutane, and 2,2,4-trimethylpentane (isooctane), and for the reactions of cresols and the uncharacterized ring-opening products formed in the photooxidations of the aromatic hydrocarbons. These chemical mechanisms are fully documented in this report.

- The updated mechanism was tested against the results of experiments carried out in four different environmental chambers: The 150,000-liter dual outdoor chamber at the University of North Carolina (UNC), the 5800-liter evacuable chamber at the Statewide Air Pollution Research Center (SAPRC) at the University of California in Riverside, the 6400-liter SAPRC indoor Teflon chamber, and the 50,000-liter dual- or single-mode SAPRC outdoor Teflon chamber. Prior to conducting these computer simulations, it was necessary to review and evaluate methods to represent the major chamber effects and the intensities and spectral distributions of the light sources for each chamber. The results of this evaluation are also documented in this report.

- The data from a total of 415 environmental chamber irradiations were used for model testing. These included $NO_x$-air, CO-$NO_x$-air, and background air irradiations carried out for chamber characterization purposes, $NO_x$-air irradiations of single organic compounds, $NO_x$-air irradiations of simple and complex mixtures of organic compounds, including some carried out under multi-day conditions, irradiations of auto exhaust, and several organic-$NO_x$-air experiments carried out under dynamic conditions. This testing program has resulted in a detailed assessment of the strengths and weaknesses of this mechanism in simulating results of environmental chamber experiments; and its results, documented in this report, will serve as a basis against which the performance of future kinetic mechanisms can be compared.

Although there were a number of experiments which were not well simulated by the model, the model simulated reasonably well the majority of the experimental data used for model testing. Many of the discrepancies observed, particularly in the simulations of the UNC outdoor chamber experiments, were of a random nature and suggested that these were due primarily to run-to-run varying chamber-dependent parameters, rather than being due to systematic errors in the chemical mechanism. No run-to-run adjustment of uncharacterized parameters to optimize the quality of the fits of model calculations to the experimental results was carried out, since such a procedure could mask any systematic errors in the chemistry, and thus defeat the major purpose in carrying out this testing program. Indeed, certain systematic discrepancies were observed in the model simulations of some groups of experiments, indicating problem areas in either the chemical mechanism or the representation of the chamber effects. In general, however, the performance of the model in simulating the results of the 415 experiments modeled was consistent with our current state of knowledge of chamber effects and the $NO_x$-air photooxidation mechanisms of organic compounds.

This report is divided into two volumes. Volume I contains the introduction, the documentation of the chemical mechanism, and the discussion of the chamber and light intensity characterization. Volume II gives the results of the model simulations of the environmental chamber experiments, the references, and the summary and conclusions section of this report, which includes a discussion of the work to be carried out in adapting this mechanism for use in atmospheric modeling.

## TABLE OF CONTENTS

Page

Disclaimer ii

Abstract iii

Acknowledgments xi

VOLUME I

I. INTRODUCTION I-1

II. CHEMICAL MECHANISM II-1

- A. Inorganic Reactions II-4
- B. General Peroxy and Acyl Peroxy Radical Reactions II-27
  - 1. Peroxy + NO and Peroxy + $NO_2$ Reactions II-28
  - 2. Peroxy + $HO_2$ Reactions II-30
  - 3. Peroxy + Peroxy Radical Reactions II-33
  - 4. Tests of Effects of the Approximations Employed II-39
- C. Oxygenate and Alkyl Nitrate Reaction Mechanisms II-47
  - 1. Reactions of Formaldehyde II-47
  - 2. Reactions of Acetaldehyde II-55
  - 3. Reactions of Propionaldehyde II-61
  - 4. Reactions of Acetone II-67
  - 5. Reactions of Methyl Ethyl Ketone II-70
  - 6. Reactions of Glyoxal II-75
  - 7. Reactions of Methylglyoxal II-81
  - 8. Reactions of Biacetyl II-83
  - 9. Reactions of Glycolaldehyde II-86
  - 10. Reactions of 2-Butyl Nitrate II-90
  - 11. Reactions of 4-Heptyl Nitrate II-94
  - 12. Reactions of 3-Pentanol II-99
- D. Reactions of Alkenes II-103
  - 1. Reactions of Ethene II-103
  - 2. Reactions of Propene II-109
  - 3. Reactions of 1-Butene II-120
  - 4. Reactions of trans-2-Butene II-131
  - 5. Reactions of Isobutene II-138
  - 6. Reactions of the Thermalized Biradicals II-147
  - 7. General $\geq C_3$ Monoalkene Model II-150

TABLE OF CONTENTS
(continued)

Page

E. Reactions of the $C_2$-$C_4$ Alkanes II-157

  1. Reactions of Ethane II-157

  2. Reactions of Propane II-157

  3. Reactions of n-Butane II-160

  4. Reactions of Isobutane II-165

F. Reactions of the Higher Alkanes II-170

  1. Summary of Alkane Photooxidation Reactions II-170

    a. Initial Reaction with OH Radicals II-171

    b. Alkyl Nitrate Formation in the Reactions of Peroxy Radicals with NO II-172

    c. Alkoxy Radical Reactions II-176

    d. Reactions of $\alpha$-Hydroxy Radicals II-181

    e. Cycloalkanes II-182

  2. Representation of the Alkane Photooxidation Products II-182

    a. Compounds Represented Explicitly II-183

    b. "Lost Carbon" and "Lost Nitrogen" II-183

    c. Alkyl Nitrates II-183

    d. $\geq C_3$ Aldehydes II-184

    e. $\geq C_4$ Ketones II-184

    f. Other Products II-185

  3. Representation of Higher Alkane Reactions in the Model II-186

  4. Models for Specific Alkanes II-192

G. Reactions of Aromatic Hydrocarbons II-207

  1. Reactions of Benzene II-207

  2. Reactions of Toluene II-215

  3. Reactions of m-Xylene II-219

  4. Reactions of o-Xylene II-221

  5. Reactions of 1,3,5-Trimethylbenzene II-223

  6. Reactions of Benzaldehyde II-225

  7. Reactions of Phenols, Cresols, and Nitrophenols II-231

## TABLE OF CONTENTS
## (continued)

Page

8. Reactions of the Unknown Aromatic Ring-Opened Products II-241
    - a. OH Radical Reactions II-245
    - b. Photolysis Reactions II-252
    - c. Other Reactions II-258

III. CHAMBER AND LIGHT INTENSITY CHARACTERIZATION III-1
- A. Light Characterization III-5
    - 1. Indoor Chambers III-5
        - a. Light Intensity III-6
        - b. Spectral Distribution III-9
    - 2. Outdoor Chambers III-10
- B. Chamber Radical Sources III-29
    - 1. The SAPRC Evacuable Chamber III-30
        - a. Continuous Radical Source III-30
        - b. Initial Nitrous Acid III-35
    - 2. Teflon Film Chambers III-36
        - a. Continuous Radical Sources in the SAPRC Teflon Chambers III-36
        - b. OH Radical Flux in the UNC Chamber III-38
        - c. Formaldehyde Offgassing in the UNC Chamber III-39
        - d. Dark Formation of HONO from $NO_2$ III-46
        - e. Initial HONO in Teflon Chambers III-47
- C. $NO_x$ Offgassing III-48
    - 1. The SAPRC Evacuable Chamber III-56
    - 2. The SAPRC Indoor Teflon Chamber III-57
    - 3. The SAPRC Outdoor Teflon Chamber III-57
    - 4. The UNC Outdoor Chamber III-58
- D. Other Heterogeneous Processes III-60
    - 1. $N_2O_5$ Hydrolysis III-60
    - 2. Wall Loss of Ozone III-62
    - 3. Wall Loss of Nitric Acid III-63
    - 4. Wall Loss of $H_2O_2$ III-64
    - 5. Offgassed or Background Reactive Organics III-65

## TABLE OF CONTENTS
## (continued)

Page

E. Other Chamber- and Run-Dependent Parameters III-67
  1. Dilution III-67
  2. Temperature III-68
  3. Humidity III-69

VOLUME II

IV. MODEL SIMULATIONS OF ENVIRONMENTAL CHAMBER EXPERIMENTS IV-1
  A. Experiments Employed for Model Testing IV-3
    1. UNC Chamber Experiments IV-3
    2. SAPRC Evacuable Chamber Experiments IV-7
    3. SAPRC Indoor Teflon Chamber Experiments IV-9
    4. SAPRC Outdoor Teflon Chamber Experiments IV-10
  B. Criteria Employed to Assess Model Performance IV-14
    1. Maximum Ozone Yields IV-14
    2. Measurements of "Timing" of Ozone Formation and NO Oxidation IV-15
    3. Other Product Yields IV-18
    4. Reactant Consumption Rates IV-18
    5. Role of Analytical Uncertanties in Assessing Model Performance IV-19
      a. Ozone IV-19
      b. NO IV-21
      c. $NO_2$ IV-21
      d. Hydrocarbon Reactants IV-22
      e. PAN and PPN IV-23
      f. Formaldehyde IV-24
      g. Other Photooxidation Products IV-26
      h. Characterization Data IV-27
  C. Characterization Runs IV-28
    1. $NO_x$-Air, Tracer-$NO_x$-Air, and CO-$NO_x$-Air Runs IV-28
    2. Acetaldehyde-Air Irradiations IV-33
    3. Background Air Irradiations IV-35

## TABLE OF CONTENTS
(continued)

Page

D. Single-Component $NO_x$-Air Irradiations IV-38
  1. Formaldehyde-Air Runs IV-38
  2. Formaldehyde-$NO_x$-Air Runs IV-43
  3. Acetaldehyde-$NO_x$-Air Runs IV-53
  4. Propionaldehyde-$NO_x$-Air Runs IV-57
  5. Acetone-$NO_x$-Air and Methyl Ethyl Ketone-$NO_x$-Air Runs IV-57
  6. Ethene-$NO_x$-Air Runs IV-61
  7. Propene-$NO_x$-Air Runs IV-69
  8. 1-Butene-$NO_x$-Air Runs IV-87
  9. trans-2-Butene-$NO_x$-Air Runs IV-97
  10. Isobutene-$NO_x$-Air Run IV-100
  11. n-Butane-$NO_x$-Air Runs IV-101
  12. 2,3-Dimethylbutane-$NO_x$-Air Runs IV-120
  13. Isopentane and Isooctane-$NO_x$-Air Runs IV-127
  14. $\geq C_5$ n-Alkane-$NO_x$-Air Runs IV-130
  15. Benzene-$NO_x$-Air Runs IV-137
  16. Toluene-$NO_x$-Air Irradiations IV-144
  17. o- and m-Xylene-$NO_x$-Air Runs IV-154
  18. 1,3,5-Trimethylbenzene-$NO_x$-Air Runs IV-160

E. Multi-Component Irradiations and Dynamic Experiments IV-167
  1. Mixed Alkene Irradiations IV-167
  2. EC Mixed Alkane Runs IV-168
  3. UNC Mixed Aromatic Runs IV-184
  4. Mixed Alkane + Alkene Runs IV-184
  5. Other Two- or Three-Component Runs IV-195
  6. EC Seven-Hydrocarbon Mix Runs IV-206
  7. ITC "Mini-Surrogate," Incremental Reactivity Runs IV-206
  8. ITC "SAI Surrogate" Multi-Day Runs IV-225
  9. OTC "SAI Surrogate" Multi-Day Runs IV-236

TABLE OF CONTENTS
(concluded)

Page

10. Runs Employing Miscellaneous UNC Mixtures IV-249
    a. Lumping Technique Employed IV-249
    b. Results of Model Simulations IV-253
11. UNC Dynamic Experiments IV-263

F. UNC Auto Exhaust Experiments IV-274
    1. Hydrocarbon Speciation and Lumping IV-275
    2. Results of Model Calculations IV-280

V. SUMMARY, CONCLUSIONS, AND FUTURE EFFORTS V-1
  A. Updated Chemical Mechanisms and Remaining Uncertainties V-4
    1. Mechanism Updates and Species Represented V-4
    2. Major Uncertainties in the Mechanisms V-7
  B. Summary of Results of Testing Program V-14
    1. Chamber Effects and Light Source Characterization and Uncertainties V-15
    2. Results of Model Testing V-20
  C. Adaptation of the Mechanism for Atmospheric Modeling V-28

VI. REFERENCES VI-1

# ACKNOWLEDGMENTS

We wish to gratefully acknowledge the following people at SAPRC for their contributions to this program and their assistance in the preparation of this report: Ms. Joanne E. Lohnes and Ms. Virpi Lindfors for their major efforts in carrying out the data processing needed to carry out the model testing calculations, Ms. Minn P. Poe and Ms. Susan E. Heffron for computer programming assistance, Ms. Minn P. Poe for preparation of the plots used in this report, Ms. Christy J. LaClaire for carrying out the word processing tasks involved in preparation of this report, and the student assistants Monica L. Murata, Bret M. McMillan, Scott M. Harris, and John T. Wood. We are also extremely grateful to Dr. Harvey E. Jeffries and Dr. Kenneth G. Sexton of UNC for taking the time to explain in detail the operations of the UNC chamber and for many other helpful discussions. Finally, we wish to acknowledge the EPA Contract Officer, Dr. Marcia C. Dodge, for assistance in planning this program, and thank her for her detailed reviews and comments on drafts of this report, and for helpful discussions.

# SECTION IV

## MODEL SIMULATIONS OF ENVIRONMENTAL CHAMBER EXPERIMENTS

In this section, the testing of the chemical mechanism and chamber effects model is described. This consisted of model simulations of 420 environmental chamber experiments carried out in the dual 150,000-liter outdoor chamber at UNC, the SAPRC 5800-liter evacuable chamber (EC), the SAPRC 6400-liter indoor Teflon chamber (ITC) , and the SAPRC 50,000-liter single- or dual-mode outdoor Teflon chamber (OTC). The types of experiments employed included $NO_x$-air, CO-$NO_x$-air, and background air irradiations carried out for chamber characterization purposes, $NO_x$-air irradiations of single organic compounds, $NO_x$-air irradiations of simple and complex mixtures of organics, including some carried out under multi-day conditions, irradiations of auto exhaust, and several organic-$NO_x$-air experiments carried out under dynamic conditions. Although many of the simple and complex mixture runs were carried out in only one chamber, such as the auto exhaust and "dynamic" runs conducted only at UNC, data for many of the single component and "characterization" runs are available from two or more chambers. Thus it is possible in many cases to assess to what extent the nature of the fits of calculation to experiment depends on the chamber employed, and how well the chamber and experimental conditions are characterized. As far as we are aware, no single set of chemical mechanisms and chamber characterization approach has been tested against the results of such a large and varied set of environmental chamber experiments carried out in different chambers.

The sources of the environmental chamber data employed in this program, and the criteria employed in selecting or rejecting runs for use in model testing, are discussed in Section IV-A. The specific criteria employed to assess the quality of the fits of the model simulations to the experimental results, and the uncertainties associated with the experimental measurements against which the model predictions are compared, are summarized in Section IV-B. In Sections IV-C through IV-G, the results of the model simulations are summarized and discussed for the different types of runs. For the purpose of this discussion, the runs are categorized as follows: $NO_x$-air irradiations and other chamber characterization runs (Section IV-C); $NO_x$-air irradiations of single organic compounds (Section

IV-D); $NO_x$-air irradiations of simple mixtures of organic compounds where the chemistry of each organic is represented explicitly in the model (Section IV-E); $NO_x$-air irradiations of complex mixtures of organics, including but not limited to auto exhaust, where some "lumping" of organics was employed, and also propene-$NO_x$-air and propene-n-butane-toluene-$NO_x$-air runs carried out under "dynamic" conditions (Section IV-F); and the UNC auto exhaust irradiations (Section IV-G). These sections contain tables and figures summarizing the results of the calculations and the quality of the fits of the model simulations to the experimental results, followed by a discussion of these results for each group of experiments.

## IV. A. EXPERIMENTS EMPLOYED FOR MODEL TESTING

As indicated above, selected experiments carried out in the UNC outdoor chamber, and in the SAPRC evacuable chamber (EC), indoor teflon chamber (ITC), and outdoor teflon chamber (OTC) were employed in this study. The specific experiments employed, the criteria used for selecting or rejecting particular experiments for use in this program, the source(s) of the data used and the studies in which they were obtained are summarized below for each of the four chambers.

### 1. UNC Chamber Experiments

The 195 UNC chamber experiments employed for model testing were selected from a much larger set of experiments carried out by Jeffries and co-workers under EPA funding to generate data for testing photochemical models (Jeffries et al. 1982, 1985a,b.). A list of the UNC chamber experiments modeled, by run type, is shown in Table IV-1. All UNC chamber experiments are designated by the date the run was carried out, followed by the suffix "R" or "B" which indicates on which side of the chamber, designated "red" or "blue" by the UNC researchers, the experiments were conducted. Although irradiations in the "red" and the "blue" side are carried out at the same time, for the purpose of this program the irradiations on each side are treated as a separate experiment, since in general different reaction mixtures or experimental conditions were employed for each side of the chamber, and thus separate model simulations for each had to be carried out.

As indicated in Tables IV-1 and I-1, a variety of different types of experiments were modeled, with almost half of the experiments modeled in this program being carried out in the UNC chamber. The selection process for these runs was twofold, as indicated below:

(1) Of the chamber experiments carried out between 1978 and 1983 for which the data have been processed, Dr. Jeffries and co-workers, with the advice and assistance of Dr. Marcia Dodge, the EPA contract monitor for this program and for the experimental programs for which the UNC chamber experiments were carried out, selected a comprehensive and representative set of experiments to be used in this program. The data from the runs

Table IV-1. List of UNC Chamber Experiments Used for Model Testing, Given by Run Type

| Run Type | Experiments |
|---|---|
| Background air | JN0682R OC0684R OC0684B |
| $NO_x$-air | AU0282R AU2082R AU2282R AU2382R ST0582R<br>OC0882R JL2483R JN1782B JN2782B OC0882B<br>JL2483B JL2783B JN1782R AU0683B |
| CO-$NO_x$-air | JN2782R JL2783R AU0683R AU0282B AU2082B<br>AU2282B AU2382B ST0582B |
| Formaldehyde-air | JL1782R OC0784R OC1684R JL1782B OC0784B<br>OC1684B |
| Acetaldehyde-air | JL2683R AU0483R OC1584R JL2683B AU0483B<br>OC1584B |
| Formaldehyde-$NO_x$-air | OC0984R AU0179B AU0279B AU0479B AU0579B<br>JL2381B OC0984B |
| Acetaldehyde-$NO_x$-air | AU0179R JN1482R AU2482B |
| Propionaldehyde-$NO_x$-air | JN1482B AU2482R |
| Acetone-$NO_x$-air | JN0480R |
| Methyl ethyl ketone-$NO_x$-air | OC2079R JN0480B |
| Ethene-$NO_x$-air | AU0479R AU0579R OC0584R OC1184R OC1284R<br>OC0584B |
| Propene-$NO_x$-air | JA1078R OC2078R OC2178R JN1279R JN1379R<br>AU0279R JL1783R JL2183R JL3183R OC0484R<br>OC1278B OC2078B OC2578B JN1279B AU2780B<br>ST0482B ST1382B JL2983B ST2383B OC0484B<br>OC1184B OC1284B |
| 1-Butene-$NO_x$-air | ST2383R ST2583R ST2783R ST2583B |
| *trans*-2-Butene-$NO_x$-air | ST2783B |
| n-Butane-$NO_x$-air | JL2178R JL2278R OC0979R JL2178B JL2278B<br>ST1879B OC1879B |
| 2,3-Dimethylbutane-$NO_x$-air | OC1879R OC2079B |
| Isopentane-$NO_x$-air | AU1983R |
| Isooctane-$NO_x$-air | AU1983B |

(continued)

Table IV-1 (continued) - 2

| Run Type | Experiments | | | | |
|---|---|---|---|---|---|
| n-Pentane-$NO_x$-air | OC0979B | | | | |
| n-Octane-$NO_x$-air | ST1879R | | | | |
| Toluene-$NO_x$-air | JL3080R | AU2780R | OC2782R | AU0183R | AU2782B |
| o-Xylene-$NO_x$-air | AU2782R | JL3080B | OC2782B | AU0183B | |
| Ethene + acetaldehyde-$NO_x$-air | OC1278R | OC2578R | | | |
| Ethene + trans-2-butene-$NO_x$-air | AU0180RB | AU1480RB | | | |
| Toluene + o-xylene-$NO_x$-air | ST0682R | ST0682B | | | |
| Propene + n-butane-$NO_x$-air | JL1581R | JL1881R | ST2481R | | |
| Ethene + propene + n-butane + n-pentane-$NO_x$-air | AU2781R | OC0382R | NV1582R | OC0382B | |
| Toluene + propene-$NO_x$-air | JN1379B | | | | |
| Propene + n-butane + toluene-$NO_x$-air | JL1581B | ST2481B | JN0982B | JN2783B | JN1483R |
| | AU2683R | | | | |
| Propene + n-butane + m-xylene-$NO_x$-air | JL1881B | JN0982R | | | |
| Miscellaneous complex mixtures-$NO_x$-air | JL2281R | JL2181B | NV1582B | DE0782B | ST2081R |
| | DE0782R | AU2681R | ST0381R | ST1081R | ST2081B |
| | AU2681B | AU2781B | JL2081B | ST1682R | JL2081R |
| | OC1481R | JL2281B | ST1682B | ST2981B | ST2981R |
| | ST0381B | ST1081B | JL0882R | JL0882B | OC1481B |
| Dynamic propene-$NO_x$-air | ST0482R | JL1783B | ST1382R | JL2183B | JL2983R |
| Dynamic propene + n-butane + toluene-$NO_x$-air | JN1483B | AU1883R | JN2783R | AU2683B | |
| Auto exhaust: Volare | JN2582R | JN2982R | JN3082R | OC0682R | AU1183R |
| | JN2582B | JN2982B | JN3082B | ST2982B | JL0283B |
| | JL0883B | AU1183B | | | |
| Auto exhaust: Charger | JL0182R | AU0382R | ST1782R | ST2982R | JL0283R |
| | JL0883R | JL1583R | OC0483R | JL0182B | AU0382B |
| | ST1782B | OC0682B | JL1583B | | |
| Synthetic exhaust | OC0783R | OC0483B | OC0783B | | |

selected were then forwarded to SAPRC. Among the criteria employed in this selection process was the "quality" of the lighting conditions for the runs, since runs carried out under less than clear-sky conditions are considered to be more difficult to characterize for model testing purposes. However, a number of runs carried out under less than clear-sky conditions were selected, presumably due to a lack of comparable runs carried out under clear-sky conditions. As far as we are aware, this selection of UNC runs was carried out without any regard to the ability of previous models to simulate their results, or any other source of bias (other than light "quality") which would affect the validity and representativeness of this set of experiments for use in model testing.

(2) Of the the UNC chamber runs for which data were sent to SAPRC, a number of runs were rejected by SAPRC because either (a) important characterization or initial concentration data were either missing or clearly suspect, resulting in the run being judged to be insufficiently well characterized for model testing, or (b) modeling of the run was outside the scope of this program. The latter data set consisted of several runs involving isoprene and the isoprene photooxidation products and the runs carried out in the recent UNC methanol substitution study (Jeffries et al. 1986c). In addition, the dynamic runs employing complex mixtures were not modeled because of insufficient time in this phase of the program, and because modeling of the dynamic runs employing simpler mixtures was considered sufficient.

Only a few of the UNC chamber runs whose data were sent to SAPRC were judged not to be useful for modeling purposes. Most of these runs were judged to be unsuitable because they did not have sufficient UV radiometer data, or had obvious problems with these data. A few runs were rejected because there was insufficient information available concerning initial concentrations of reactive species. In some cases, experimental measurements of initial concentrations were missing but the UNC researchers provided estimates of these in the "documentation" section of the data sets, and these runs were then modeled. In addition, auto exhaust experiments with high levels of "unspeciated carbon" were also modeled; the composition of the unspeciated organics were estimated as discussed in Section IV-F.

### 2. SAPRC Evacuable Chamber Experiments

A list of the SAPRC EC chamber experiments modeled, given by run type, is shown in Table IV-2. The data from most of these experiments, and a discussion of the experimental procedures and results of associated control and characterization runs, have been published previously. For these EC runs, Table IV-2 indicates the appropriate reference. The results of a few experiments used have not been published previously, and the table also indicates these experiments. Information regarding the unpublished SAPRC experiments used in this program, and tabulations of the data, can be obtained from SAPRC upon request.

All SAPRC EC runs, including actinometry and characterization experiments, are numbered according to the order they were carried out, and in this report, SAPRC EC runs are designated by the prefix "EC-", followed by the run number. The earliest SAPRC EC experiment modeled in this program (run EC-106) was carried out in October 1975, with the latest (run EC-903) being carried out in August of 1983.

A large majority of the SAPRC EC runs used in this program were conducted by Pitts et al. (1979) during 1975 through 1978 as part of an EPA-funded study carried out for the purpose of providing data for model testing. All single- and multi-component hydrocarbon-$NO_x$-air irradiations for which data are reported by Pitts et al. (1979) (and summarized in Tables 5 through 8 of that report) were modeled in this study, with the exception of those carried out prior to run EC-106, which lacked spectral distribution data. The variety of single-component runs carried out in that program makes the set of EC chamber experiments employed in this study almost as comprehensive as the set of UNC chamber runs, though far more runs employing complex mixtures were carried out at UNC.

A number of EC runs carried out for other programs were also employed in this program. A large number of $NO_x$-air irradiations with radical tracers were carried out in the EC (and in other chambers) for the purpose of studying the chamber radical source (Carter et al. 1982, Pitts et al. 1983), and a selected sub-set of these runs were modeled in this program. All runs in this sub-set carried out under conditions representative of those reported by Pitts et al. (1979), i.e., 50% RH and T = ~303 K, with normal chamber conditioning. Irradiations carried out with a variety of

Table IV-2. List of SAPRC EC Chamber Experiments Used for Model Testing, Given by Run Type

| Run Type | Reference | EC Run Numbers | | | | | | | |
|---|---|---|---|---|---|---|---|---|---|
| $NO_x$-air | a | 436 | 440 | 442 | 457 | 464 | 597 | 599 | |
| Formaldehyde-air | b | 250 | 255 | | | | | | |
| Acetaldehyde-air | b | 253 | | | | | | | |
| Formaldehyde-$NO_x$-air | b | 251 | 252 | | | | | | |
| | c | 389 | 391 | 392 | | | | | |
| Acetaldehyde-$NO_x$-air | b | 164 | 254 | | | | | | |
| Ethene-$NO_x$-air | b | 142 | 143 | 156 | 285 | 286 | 287 | | |
| Propene-$NO_x$-air | b | 121 | 177 | 216 | 217 | 230 | 256 | 257 | 276 |
| | | 277 | 278 | 279 | 314 | 315 | 316 | 317 | |
| 1-Butene-$NO_x$-air | b | 122 | 123 | 124 | | | | | |
| *trans*-2-Butene-$NO_x$-air | b | 146 | 147 | 157 | | | | | |
| n-Butane-$NO_x$-air | c | 130 | 133 | 134 | 137 | | | | |
| | b | 162 | 163 | 168 | 178 | 304 | 305 | 306 | 307 |
| | | 308 | 309 | | | | | | |
| n-Pentane-$NO_x$-air | c | 135 | | | | | | | |
| n-Hexane-$NO_x$-air | c | 131 | | | | | | | |
| n-Nonane-$NO_x$-air | c | 155 | | | | | | | |
| 2,3-Dimethylbutane-$NO_x$-air | b | 165 | 169 | 171 | | | | | |
| Toluene-$NO_x$-air | b | 264 | 265 | 266 | 269 | 270 | 271 | 272 | 273 |
| | | 327 | 336 | 337 | 339 | 340 | | | |
| m-Xylene-$NO_x$-air | b | 343 | 344 | 345 | 346 | | | | |
| 1,3,5-Trimethylbenzene-$NO_x$-air | c | 900 | 901 | 903 | | | | | |
| o-Cresol-$NO_x$-air | b | 181 | | | | | | | |
| Ethene + propene-$NO_x$-air | b | 144 | 145 | 160 | | | | | |
| Propene + *trans*-2-butene-$NO_x$-air | b | 149 | | | | | | | |

(continued)

Table IV-2 (continued) - 2

| Run Type | Reference | EC Run Numbers | | | | | | | |
|---|---|---|---|---|---|---|---|---|---|
| Mixed alkene-$NO_x$-air | b | 150 | 151 | 152 | 153 | 161 | | | |
| n-Butane + 2,3-dimethylbutane-$NO_x$-air | b | 166 | 172 | | | | | | |
| Propene + n-butane-$NO_x$-air | b | 106 | 113 | 114 | 115 | 116 | | | |
| Toluene + acetaldehyde-$NO_x$-air | b | 335 | | | | | | | |
| Toluene + propene-$NO_x$-air | b | 329 | 330 | 334 | | | | | |
| Toluene + n-butane-$NO_x$-air | b | 328 | 331 | 338 | | | | | |
| Seven hydrocarbon mix-$NO_x$-air | b | 231<br>245 | 232<br>246 | 233<br>247 | 237 | 238 | 241 | 242 | 243 |

[a] Pitts et al. (1983).
[b] Pitts et al. (1979).
[c] Unpublished SAPRC data.

initial hydrocarbon and $NO_x$ levels were selected. In addition, several 1,3,5-trimethylbenzene-$NO_x$-air irradiations, carried out under United States Air Force (USAF) funding (Carter et al. 1984), and several alkane-$NO_x$-air and formaldehyde-$NO_x$-air runs carried out under NSF funding, whose results have not been previously published, were also modeled as part of this program. In general, the experimental conditions and procedures for these runs were similar to those employed in the runs reported by Pitts et al. (1979), and indeed many of the NSF-funded experiments were carried out at around the same time as the EPA-funded experiments of Pitts et al. (1979).

### 3. SAPRC Indoor Teflon Chamber Experiments

The 63 SAPRC ITC chamber experiments whose results were used in this program are summarized in Table IV-3, together with a reference to the published reports. These reports contain the detailed data for these experiments, and discuss the experimental procedures employed and the results of the associated characterization runs. As with the SAPRC EC runs, all SAPRC ITC runs are numbered consecutively, and they are designated by the prefix "ITC-", followed by the run number.

Of the single component and characterization runs, most of the benzene-$NO_x$-air and n-butane-$NO_x$-air irradiations, and all of the n-hexane and n-heptane-$NO_x$-air ITC runs used in this study were carried out as part of a California Air Resources Board (CARB)-funded program reported by Pitts et al. (1983). The other single-component aromatic-$NO_x$-air and alkane-$NO_x$-air ITC runs used in this study, and two each of the ITC propene-$NO_x$-air and tracer-$NO_x$-air runs, were carried out for the USAF and reported by Carter et al. (1984). The formaldehyde-$NO_x$-air and propene-$NO_x$-air and tracer-$NO_x$-air runs were carried out as control runs for an ARB-funded study which has just been concluded (Carter et al. 1986). The other propene-$NO_x$-air and tracer-$NO_x$-air irradiations used were carried out as part of an EPA-funded multi-day study (Carter et al. 1985).

Most of the ITC experiments used in this program were multi-component in nature. One such group of experiments were the 2-4 day, eight-component "urban surrogate"-$NO_x$-air runs carried out for the EPA for testing models for multi-day effects (Carter et al. 1985). In addition, results of selected experiments from a CARB-funded study of incremental reactivity, in which repeated irradiations of a four-component "mini-surrogate"-$NO_x$-air mixture were alternated with irradiations of the "mini-surrogate"-$NO_x$-air mixture with various organics added or with levels of various surrogate components reduced (Atkinson et al. 1983c), were also modeled in this program. The runs modeled included two representative "standard" "mini-surrogate" runs, "mini-surrogate" runs in which the levels of the surrogate components are varied, and "mini-surrogate" runs with added benzaldehyde.

### 4. SAPRC Outdoor Teflon Chamber Experiments

Finally, data from 44 irradiations carried out in the SAPRC OTC were also selected for use in this program. These experiments are listed in Table IV-4, together with the citations to the reports which discuss the data and associated characterization runs and discuss the experimental

Table IV-3. List of SAPRC ITC Chamber Experiments Used for Model Testing, Given by Run Type

| Run Type | Reference | ITC Run Numbers | | | | | | | |
|---|---|---|---|---|---|---|---|---|---|
| Tracer-$NO_x$-air | a | 625 | 634 | | | | | | |
| | b | 695 | 826 | 882 | | | | | |
| Acetaldehyde-air | a | 627 | 636 | | | | | | |
| Formaldehyde-$NO_x$-air | c | 864 | | | | | | | |
| Propene-$NO_x$-air | b | 693 | 810 | 860 | | | | | |
| Isobutene-$NO_x$-air | a | 694 | | | | | | | |
| n-Butane-$NO_x$-air | d | 507 | 533 | | | | | | |
| | b | 770 | | | | | | | |
| n-Hexane-$NO_x$-air | d | 559 | | | | | | | |
| n-Heptane-$NO_x$-air | d | 538 | 540 | | | | | | |
| n-Octane-$NO_x$-air | d | 552 | | | | | | | |
| | b | 761 | 762 | 763 | 797 | | | | |
| Benzene-$NO_x$-air | d | 560 | 561 | 562 | | | | | |
| | b | 698 | 710 | 831 | | | | | |
| Toluene-$NO_x$-air | b | 699 | 828 | | | | | | |
| m-Xylene-$NO_x$-air | b | 827 | 702 | | | | | | |
| 1,3,5-Trimethylbenzene-$NO_x$-air | b | 703 | 706 | 709 | 742 | 826 | | | |
| "Mini-surrogate"-$NO_x$-air | e | 479 | 584 | 579 | 472 | 474 | 581 | 585 | 478 |
| | | 482 | 488 | 492 | 494 | 498 | 500 | 502 | |
| "Mini-surrogate" + benzaldehyde-$NO_x$-air | e | 462 | 466 | 468 | | | | | |
| "SAI-surrogate"-$NO_x$-air (Multi-day runs) | a | 626 | 630 | 631 | 633 | 635 | 637 | | |

[a] Carter et al. (1985).
[b] Carter et al. (1984).
[c] Carter et al. (1986).
[d] Pitts et al. (1983).
[e] Atkinson et al. (1983c).

procedures employed. As with the runs from the other SAPRC chambers, the OTC runs are numbered consecutively, and in this report they are designated by the prefix "OTC-" followed by the run number. Most, though not all, of the OTC experiments modeled were carried out with the chamber in the divided mode, and, as with the UNC chamber experiments, irradiations of different mixtures on different chamber sides are treated as separate experiments. The runs carried out in side 1 (the eastern half of the chamber) are designated with the suffix "A", those carried out in side 2 are designated with the suffix "B", and those carried out with the chamber in the undivided mode have no suffix.

The largest set of OTC experiments employed were 25 of the 2-4 day "urban surrogate"-$NO_x$-air irradiations carried out for the EPA-funded study of multi-day effects (Carter et al. 1985). These experiments were exactly analogous, and employed the same reaction mixtures, as the multi-day ITC experiments referenced above. The experiments were carried out in 1982 and 1983, but because of problems with side equivalency and other anomalous chamber effects observed in the 1982 experiments, the data obtained during 1982 were not modeled in this study. However, all of the 1983 OTC multi-day surrogate experiments which were successfully concluded were modeled in this study.

Most of the other OTC runs modeled in this study were selected propene-$NO_x$-air, tracer-$NO_x$-air, or acetaldehyde-air irradiations carried out as part of the multi-day study of Carter et al. (1985) for characterization or control purposes. However, the formaldehyde-$NO_x$-air, n-butane-$NO_x$-air, and some of the propene-$NO_x$-air and acetaldehyde-air runs were carried out as part of the control and characterization runs for a recently completed ARB funded study of methanol substitution effects (Carter et al. 1986).

Table IV-4. List of SAPRC OTC Chamber Experiments Used for Model Testing, Given by Run Type

| Run Type | Reference | OTC Run Numbers |
|---|---|---|
| Tracer-NOx-air | a | 185 187 |
| CO-tracer-NOx-air | a | 188 201A 201B |
| Acetaldehyde-air | a | 200B 206A 206B |
|  | b | 234A 234B |
| Formaldehyde-NOx-air | b | 235A 235B |
| Propene-NOx-air | a | 186 191 |
|  | b | 210 233 236 |
| n-Butane-NOx-air | b | 211 |
| "SAI surrogate"-NOx-air (multi-day runs) | a | 189A 189B 190A 190B 192A 192B<br>194A 194B 195A 195B 196B 197A<br>197B 198A 198B 199A 199B 202A<br>202B 203A 203B 204A 204B 205A<br>205B |

[a] Carter et al. (1985).
[b] Carter et al. (1986).

## IV. B. CRITERIA EMPLOYED TO ASSESS MODEL PERFORMANCE

A number of criteria were employed to measure the quality of fits of the model simulations to the experimental data. The specific criteria employed, and the aspects of the mechanism to which the fits are sensitive and thus can be used to test are briefly discussed in this section. In addition, the uncertainties associated with the analytical techniques employed to obtain the experimental data used to test the model are briefly summarized, and the role of these uncertainites in assessing the performance of the model is discussed.

### 1. Maximum Ozone Yields

Since the chemical mechanism will be primarily used to predict ozone levels and effects of control measures on ozone, the fits to the observed maximum ozone yields are obviously a very important criterion. The predictions of ozone yields are affected by a number of factors, the relative importance of which will vary depending on the type of experiment, and especially on the overall reactivity of the mixture. For irradiations of less reactive mixtures, where the experiment ends (or the sun sets) before the maximum ozone formation potential is realized, the maximum observed or calculated ozone yields reflect primarily the rate of the overall photooxidation process, and not the true maximum ozone formation potential. On the other hand, in irradiations of more reactive mixtures, where all the initially present $NO_x$ is consumed and ozone formation stops before the end of the irradiation, the maximum ozone yields obtained are much less sensitive to the overall transformation rates. In these cases, the maximum $O_3$ yields are governed by other factors which include the amount of $NO_x$ present, the tendency of the organic to remove $NO_x$ from the system (since $NO_x$ is required for ozone formation to occur), the efficiency of the organics in converting NO to $NO_2$, and whether the organic itself reacts with ozone or forms products which react with ozone.

The observed and calculated maximum ozone yields are summarized for all experiments modeled in this program, except for the $NO_x$-air irradiations summarized in Section IV-C, where measurable ozone formation did not occur. In addition, the summaries contain the absolute and, where appropriate, relative errors in the calculated ozone maximum relative to the experimental results. Because ozone cannot be monitored reliably at low concentrations (see Section IV-B-5, below), relative errors in the ozone maximum are shown only if the observed ozone maximum is greater than 50 ppb.

Because of the different factors which affect ozone formation, the mechanistic implications of good or poor model performance in predicting maximum ozone yields depends on the type of experiment for which the model is being tested. For this reason it is important that maximum ozone yields not be the only criterion used to judge model performance, and that other criteria, which may have a more simple and direct relationship to specific aspects of the mechanism, and whose interpretation thus may be more straightforward, should also be employed. These other criteria are discussed below.

## 2. Measurements of "Timing" of Ozone Formation and NO Oxidation

Another important criterion which should be used in assessing model performance concerns the fits of the model to the "timing" observed in the experiments, i.e., to the overall rates of the transformations which result in NO oxidation and ozone formation. This aspect is particularly sensitive to predicted radical levels, and thus is useful for testing those portions of the model concerning radical sources and sinks.

However, the best way to measure this aspect of environmental chamber experiments and model simulations is not obvious, and a number of different approaches are possible. As indicated above, comparison of maximum ozone yields is clearly not satisfactory in this regard, since in irradiations of more reactive mixtures it is possible to have experiments with similar ozone yields, but where the rates at which ozone is formed, and the time its maximum concentration is reached, are significantly different. Timing measurements which have been employed previously include the times to maximum ozone, times to maximum $NO_2$, and times to NO and $NO_2$ crossover, but each of these measurements has problems and for each there are types of experiments for which they are not applicable. The time to maximum ozone is obviously not useful for experiments or model simulations where a "true" ozone maximum is not achieved. In addition for many experiments, the ozone concentration either exhibits a broad maxima, or it slowly increases following an initial rapid rise (in some cases forming a "second" ozone maximum). These factors make a precise measurement of time to ozone maximum difficult and sensitive to second-order effects. The time of maximum $NO_2$ is also not a satisfactory measurement of timing because of interferences by PAN and other organic nitrates in the $NO_2$ measurement technique employed in the chamber experiments (see Section IV-B-5, below). This results in the observed "$NO_2$" maximum being later than the true maximum, and in some cases results in the "$NO_2$" readings having no maximum, even though $NO_2$ was actually consumed. In addition, the time to maximum $NO_2$ is obviously not useful in experiments where the maximum $NO_2$ occurs at the start of the run, or for runs which are so unreactive that $NO_2$ does not achieve a true maximum. Finally, the times to NO to $NO_2$ crossover, though avoiding some of the problems of the other statistics, are not useful for runs where the initial $NO_2$ is higher than the initial NO (which is the case in a number of the UNC experiments), or which are so unreactive that NO and $NO_2$ do not cross during the irradiation. Moreover, the magnitudes of these times are extremely sensitive to the exact initial NO and $NO_2$ concentrations employed.

The statistic we use in this program to measure timing avoids some of the problems discussed above. The specific timing parameter employed is defined as the time required to change the quantity ($[O_3]-[NO]$) by an amount equal to one-half of the maximum change in that quantity observed in the experiment. Although this may appear to be an arbitrary and contrived statistic, it is useful for a number of reasons: (a) It can be used to measure model performance in simulations of essentially all types of organic-$NO_x$-air irradiations used for model testing, regardless of whether or not ozone is formed or of the initial NO and $NO_2$ concentrations employed. For example, for experiments where significant ozone formation occurs, the maximum of the quantity ($[O_3]-[NO]$) is just ($[O_3]_{max}-[NO]_{init}$), while for experiments with high initial NO where no ozone formation occurs, it is ($[NO]_{final}-[NO]_{init}$); and the time required to achieve half of these maximum values can in both cases be determined precisely. (b) Since it is defined in terms of half the maximum ozone, this does not lead to problems for runs where it is difficult to precisely define the time of the ozone maximum, e.g. due to broad ozone maxima, etc. (c) The rate of change of the quantity ($[O_3]$-[NO]) can be directly related to the main chemical processes responsible for both the consumption of NO and the formation of ozone, i.e., the conversion of NO to $NO_2$ by peroxy radicals. This can be shown by examining the differential equations for the following reactions, which are the most important in affecting NO consumption and ozone formation:

$$NO_2 + h\nu \xrightarrow{O_2} NO + O_3 \tag{1}$$

$$O_3 + NO \rightarrow NO_2 + O_2 \tag{2}$$

$$RO_2 \text{ (etc.)} + NO \rightarrow \text{products} \tag{3}$$

Other processes which involve ozone and NO obviously also occur, but during the times of the experiments which are characterized by NO consumption or $O_3$ formation, these three reactions have the highest overall rates. If only these major processes are considered, the differential equations are:

$$d[O_3]/dt = k_1\ [NO_2] - k_2\ [O_3]$$

$$d[NO]/dt = k_1\ [NO_2] - k_2\ [O_3] - k_3[RO_2][NO]$$

which can be rearranged to yield

$$d([O_3]-[NO])/dt = k_3[RO_2][NO] = R_3$$

where $R_3$ is the total rate of consumption of NO by reaction with peroxy radicals and other species. Thus the rate of change of the quantity ($[O_3]$-[NO]) has a direct relationship to the overall rate of NO oxidation which is ultimately responsible for ozone formation, and (to a first approximation) is not directly affected by the specific initial reactant concentrations employed or whether ozone or NO are in excess. Instead, this quantity directly reflects the overall levels of peroxy radicals and other intermediates which react with NO and cause ozone formation.

The observed and calculated times required for ($[O_3]$-[NO]) to achieve a level equal to half the maximum observed in the experiment are summarized for all experiments modeled in this program (except for the $NO_x$-air irradiations for which comparisons of the experimental and calculated changes in [NO] and $[NO_2]$ were employed). In the subsequent discussion, this statistic is referred to as the "NO oxidation time" for simplicity, but in all cases it is defined as described above. The absolute and relative errors of this timing parameter for the model relative to the experimental results will also be summarized.

### 3. Other Product Yields

Additional tests of specific aspects of model performance can be obtained by comparing the observed and predicted yields of organic photooxidation products. For example, PAN measurements were made for most of these experiments, and for experiments where measurable yields of PAN are observed, the experimental and calculated maximum PAN yields are summarized together with the absolute and relative errors of the model prediction. In addition, where appropriate, the fits of the model calculations to observed maximum yields of formaldehyde, acetaldehyde, and (for runs containing n-butane) methyl ethyl ketone are summarized.

### 4. Reactant Consumption Rates

A comparison of the observed and predicted rates of consumption of organic reactants is also a useful measure of the performance of the model. Reaction with OH radicals is an important consumption process for most of the organic reactants, and thus their consumption rates provide a more direct indication of OH radical levels than the rates of NO consumption and ozone formation, which are influenced by other factors in addition to radical levels. The observed and predicted half lives for selected rapidly reacting organics are hence also included in the summaries, where appropriate. (The half-lives in this context are defined as the times required for half of the initially present organic to be consumed.) The consumption rates for slower reacting compounds are not summarized, since these are highly sensitive to random variations in the experimental measurements and the exact dilution rates (which as indicated in Section III-E tend to be variable in the UNC chamber), and are thus not particularly suitable for model testing. However, the alkenes and the di- and trimethylbenzenes all react sufficiently rapidly that their consumption rates are useful for evaluating model performance.

## 5. Role of Analytical Uncertainties in Assessing Model Performance

All of the experimental data obtained from environmental chamber studies have associated analytical uncertainties and the potential for interferences and other experimental problems. All of these must be taken into account when using these data to test the performance of the chemical model. Although a detailed discussion of the analytical techniques and their associated problems and uncertainties is beyond the scope of this report, the estimated uncertainties of the various types of measurements used in assessing the model performance are summarized. In addition, known problems with certain types of measurements are discussed. For more detailed discussions of the analytical techniques, calibration techniques, and quality assurance procedures associated with the various chamber experiments, Jeffries et al. (1982, 1985a,b,d) should be consulted for the UNC experiments, and Pitts et al. (1979) and Carter et al. (1984, 1985, 1986) should be consulted for discussions of the analytical procedures employed in the SAPRC experiments. Brief discussions of the different types of data used in this report are given below.

### a. Ozone

The ozone data are highly important in assessing model performance, and were used in all runs (except for the $NO_x$-air irradiations) to calculate the NO oxidation "timing" parameter and in most runs to compare with predictions of the maximum ozone yields. Ozone is routinely monitored by chemiluminescence in the UNC chamber experiments, and by UV absorption for the SAPRC experiments. Generally, these ozone data are not subject to significant uncertainties, especially when monitoring ozone at levels above ~50 ppb and in the absence of NO. For most experiments, the ozone data are estimated to be accurate to within approximately 10%, with the precision in general being better than this.

The ozone data are expected to be less accurate at lower concentrations, where instrumental drift and noise become relatively more important. However, in most cases the most significant factor affecting ozone data at lower concentrations concerns the likelihood that the concurrent NO levels are relatively high, with this NO reacting with ozone in the sample line resulting in lower measured concentrations of ozone. In the chamber, ozone is in photostationary state with NO as determined by the rapid reactions

$$NO_2 + h\nu \xrightarrow{O_2} O_3 + NO$$

$$O_3 + NO \longrightarrow NO_2 + O_2$$

However, in the dark sample line, the photolysis reaction does not regenerate NO and ozone after they react with each other, and thus concentrations of both are reduced. Although it is possible to correct for this effect in the model if the exact residence time in the sampling tube is known, this was not done in the calculations carried out in this program. This is not an important factor in affecting observed ozone yields in runs where the initial NO was consumed and significant ozone formation occurred, nor does it affect the observed NO oxidation "timing" parameters since the reaction of NO with ozone does not cause a net change in ($[O_3]-[NO]$). However, for runs where significant NO remains in the chamber throughout the experiment, the ozone measurements should strictly speaking be considered to be upper limits to the true values.

An additional factor which may affect ozone measurements in certain types of experiments carried out at SAPRC is that some organics absorb at the 254 nm mercury line used to monitor ozone in the UV absorption ozone monitors, thus causing positive interferences. Such interferences were observed in the cresol-$NO_x$-air irradiations carried out at SAPRC (Atkinson et al. 1980), but except for the o-cresol-$NO_x$-air EC run, this is probably not a major factor affecting the data from the runs modeled in this program. Although cresols are formed as products in aromatic-$NO_x$-air runs and in complex mixture runs containing aromatics, their yields are generally low, and they are not expected to significantly affect the reported ozone data from those runs. This is not a problem with the ozone data from the UNC chamber, since a chemiluminescence ozone monitor is employed at that facility.

### b. NO

NO is monitored by chemiluminescence at both the SAPRC and UNC chamber facilities, and under favorable conditions the precision and accuracy of the NO data are comparable to those for ozone. The NO monitors tend to exhibit somewhat more drift than do the ozone monitors, and thus the systematic uncertainty may be slightly higher. However, the data are still generally considered to be good to within 10%. As with ozone, the data are less accurate at low concentrations, and the reaction between NO and ozone in the sample line, discussed above, is expected to affect the NO data when ozone is present in the chamber at higher or comparable concentrations. In addition, at least for the instruments employed at SAPRC, there appears to be some low-level interferences in the NO measurements, since readings of 10-20 ppb of NO are obtained under conditions where ozone is in large excess, and when measurable NO is obviously not present. However, the primary utility of the NO data in this program is in determining the initial conditions of the experiments and in calculating the NO oxidation "timing" parameter. Problems in monitoring NO at low levels are not significant in affecting either of these uses. In addition, errors in NO calibration would not significantly affect the values derived for the NO oxidation "timing" parameter, since this is determined primarily by how rapidly its concentration changes, on a relative basis.

### c. $NO_2$

$NO_2$ is monitored using the same chemiluminescence instrument used to monitor NO, with the $NO_2$ being quantitatively converted to NO by means of a catalyst analysis. Thus, under favorable conditions the accuracy of the $NO_2$ data approach that of NO. However, this technique for monitoring $NO_2$ suffers from significant interferences by other nitrogen-containing species, such as PAN, organic nitrates, and (under some conditions) nitric acid (Winer et al. 1974), which are also converted to NO by the catalyst employed. These interferences significantly limit the utility of the $NO_2$ data for model testing purposes, since PAN (or PAN analogues) and organic nitrates are formed in the photooxidations of a wide variety of organic compounds, and nitric acid is formed in essentially all $NO_x$-air irradiations. Although Winer et al. (1974) reported that the interfences by PAN and organic nitrates was quantitative, and thus (if reliable and complete data for those compounds are available) some corrections for these data may be possible, the interference by nitric acid is non-quantitative (primarily because nitric acid tends to be absorbed on the surfaces of the sample lines). Furthermore, quantitative conversion of the other compounds to NO has only been demonstrated for the specific type of catalyst employed by Winer et al. (1974). Thus, in general, accurate corrections to the $NO_2$ data are probably not reliable, and the $NO_2$ measurements can only be considered to be upper limits to the true values.

For this program, the $NO_2$ data were primarily used for determining the initial $NO_2$ concentrations to employ in the simulations. The initial $NO_2$ concentrations would not be affected by this interference for the runs modeled in this program, since these did not involve the initial presence of nitrogen-containing organics. The only case where $NO_2$ data were used to test the quality of the fits of the model to the data was for the $NO_x$-air irradiations, where interfering organics were absent. For those experiments, the potential for nitric acid interference exists, but, based on our experince at SAPRC, we assume that most of the nitric acid was lost on the walls of the sample lines, and did not interfere signficantly with the $NO_2$ data in $NO_x$-air irradiations.

### d. Hydrocarbon Reactants

The primary utility of the hydrocarbon data associated with these experiments was to determine the initial reactant concentrations for model simulations, though, as indicated above, the rates of consumption of some of the more rapidly reacting hydrocarbons was also used to assess model performance. The hydrocarbons are monitored primarily by gas chromatography (GC) at both the UNC and the SAPRC facilities. The accuracy and precision of GC analyses can vary from compound to compound, depending on its stability, affinity to surfaces, and other factors, but of most simple alkanes, alkenes and aromatic hydrocarbons used as the reactants in these experiments are relatively easy to analyze by gas chromatography, and under favorable conditions the data are probably accurate to within 10%. However, in runs employing very complex mixtures of organics, particularly the auto exhaust runs, GC interferences between different organics can be significant, resulting in no usable data for compounds known to be present. Data where such interferences are known or suspected were not used for model testing, so these interferences result primarily in problems with characterizing the initial conditions for the model testing calculations.

### e. PAN and PPN

PAN (peroxy acetyl nitrate) data were available for most of the experiments used for testing in this program, and provide a useful means to test the accuracy of the details of the mechanisms for many classes of compounds or mixtures. PAN is monitored by GC, using electron capture detection (ECD), at both the SAPRC and UNC chamber facilities. Although this technique is reasonably precise when PAN is monitored at levels above approximately 10 ppb, being similar to that in the GC analyses of the reactant hydrocarbons, the absolute accuracy of the PAN data is less than that for the hydrocarbons because of difficulties in calibrating for PAN, which is thermally unstable. In addition, the ECD detectors may exhibit a non-linear response at the higher PAN concentrations, and this introduces additional uncertainties. The overall accuracy of the PAN data at both the SAPRC and the UNC facilities is estimated to be approximately 20% (Pitts et al. 1979, Jeffries et al. 1982).

PPN (peroxy propionyl nitrate) data are available for a few of the experiments employed in this program. PPN is monitored on the same instrument as employed for PAN. As far as we are aware, no authentic samples of PPN were available for use for calibration purposes for any of these experiments, and the calibration factor had to be estimated.

Therefore, the PPN data are highly uncertain, and are useful for testing the model only in a qualitative sense.

### f. Formaldehyde

Formaldehyde data are also available for a majority of the experiments used for model testing, and such data are potentially useful for model testing since formaldehyde is formed in the photooxidations of almost all reactive hydrocarbons. In addition, several of the experiments modeled in this program involved initially present formaldehyde, so reliable formaldehyde data are required for model testing using these runs. At both the SAPRC and UNC laboratories, formaldehyde is routinely monitored using "wet chemical" techniques; at SAPRC it is monitored using the chromatropric acid technique (Pitts et al. 1979), and at UNC it is monitored using a CEA 555 automated colorimetric formaldehyde system which employs the reverse West and Gaeke technique (Jeffries et al. 1982). In addition, for several runs carried out during October of 1984, formaldehyde was also monitored by Unisearch, Inc., using a tuneable diode laser absorption spectrometer, and these data were included in the UNC chamber data sets employed in this program.

The reliability of the SAPRC formaldehyde data have been variable over the years, and there are a number of runs where anomalously low formaldehyde measurements (compared to yields observed in replicate runs, or amounts known to be injected into the chamber) were obtained. These anomalously low readings are attributed to problems with sample collection efficiency (Pitts et al. 1979). (Anomalously low formaldehyde readings are believed to be due to the analytical technique since there is no evidence for significant wall loss of formaldehyde in any of the SAPRC chambers.) More infrequently, anomalously high measurements (presumably due to contamination) are obtained, but usually these anomalous data points are isolated and thus can be readily identified as such. At best, the SAPRC formaldehyde data is precise to within ±20-30%, and is useful only for formaldehyde concentrations above approximately 50 ppb. If the system is being operated properly, the accuracy of the SAPRC formaldehyde data should be comparable to its precision; and tests in which known quantities of formaldehyde were injected into the SAPRC EC (whose volume is known accurately) using vacuum techniques have confirmed the accuracy of the SAPRC formaldehyde analysis technique when employed carefully. However, in view of the frequent examples of anomalously low formaldehyde readings in SAPRC chamber experiments, an overprediction by the model of formaldehyde yields in a particular experiment does not necessarily indicate a problem with the model, unless there is a consistent pattern of overprediction of formaldehyde in a large number of runs carried out during different periods of time.

The UNC formaldehyde data does not appear to have the same type of problems as the SAPRC data, but (based on the observed scatter of the data) the precision of the two techniques appears to be similar, at least under favorable conditions. Some positive interferences with acetaldehyde and other oxygenates are observed, but the UNC researchers do not consider this to be significant under the conditions of these experiments (Jeffries et al. 1982, 1985a). While experience at UNC has indicated that there can be problems with the formaldehyde data under low temperature, high humidity conditions, when it is believed to be absorbed to a significant extent on the walls of the chamber or the sample line, these problems are believed to be corrected by drying the air in the chamber prior to the experiments and by cooling the sample line. Tests carried out at UNC involving comparisons between calibrations using formaldehyde solutions directly, permeation tubes, and injections of known quantities of paraformaldehyde into the chamber yielded good agreement (Kamens et al. 1981). This tends to support the accuracy of the UNC formaldehyde data, at least under conditions when no interfering compounds are present. The calibrations of the UNC formaldehyde instrument generally does not vary by more than 20% during an experimental season (except during 1984, when there appeared to be a problems in this regard) [Sexton, private communication]. Thus, provided interferences are not a problem, the accuracy of the UNC formaldehyde data should be comparable to its precision.

The accuracy and precision of the Unisearch formaldehyde monitoring technique when it was employed at UNC during October of 1984 is not documented. This technique gave results which were consistent with the standard UNC measurements when monitoring formaldehyde directly injected into the chamber, though this may be due to these injections being used as calibrations for both instruments. However, it yielded consistently lower formaldehyde concentrations in the October, 1984, propene-$NO_x$-air and ethene-$NO_x$-air irradiations than did the standard UNC instrument. The UNC researchers suggest that this may be due to the fact that Unisearch did not heat their sampling manifold when experiments were being carried out at relatively low temperatures and high humidity, resulting in sample line losses. However, we are aware of no direct evidence that such sample line losses can account for the discrepancies between the two techniques.

The results of the model testing carried out in this program, discussed below in Sections IV-D and IV-E, indicate that there is also an inconsistency between the SAPRC formaldehyde data and the formaldehyde data obtained using the standard UNC instrument. In particular, the model predictions in most cases appear to be generally consistent with the SAPRC formaldehyde measurements (after taking the relatively large uncertainties associated with the SAPRC formaldehyde data into account), but in almost all cases the model consistently underpredicts the formaldehyde yields as measured by the UNC colorometric instrument. The model predictions were, however, consistent with the formaldehyde data obtained by the Unisearch instrument in the October, 1984, ethene-$NO_x$-air and propene-$NO_x$-air runs (see Sections IV-D-6 and IV-D-7). This tends to indicate that Unisearch and the SAPRC techniques are consistent with each other. Thus either (a) both the SAPRC and the Unisearch formaldehyde data are consistently low and the model significantly underpredicts formaldehyde yields from almost all compounds for which such data are available, or (b) there are interferences or other problems with the formaldehyde data with most of the UNC experiments used in this program. We believe that it is more likely that the latter is the case, but until these inconsistencies are resolved, the validity of the model predictions for formaldehyde will be uncertain.

### g. Other Photooxidation Products

Measured yields of other products such as acetaldehyde, acetone, methyl ethyl ketone, benzaldehyde, and o-cresol were also used for testing the model for certain compounds, and for establishing the initial conditions in several experiments. These compounds were monitored by gas chromatography, so the same types of considerations which affect the accuracy of the hydrocarbon data are also applicable to these data.

However, in general, these oxygenated products are more prone to adsorption problems than the hydrocarbons, resulting in greater difficulties in accurately calibrating these species. In addition, some of these compounds also have unsymmetrical GC peak shapes, which results in reduced precision in monitoring these species. A detailed discussion of the uncertainties associated with the analysis of each of these compounds is beyond the scope of this report, but in most cases, it is probably appropriate to consider these data to be uncertain by ±30%, unless specific information is available to indicate otherwise.

### h. Characterization Data

It is important to recognize that in most cases the uncertainties in characterizing the conditions of the experiments are more important factors in assessing whether the chemical mechanism being tested is consistent with the experimental data than are the uncertainties in the analytical techniques employed. For example, if the light intensity or the temperature in a given experiment is uncertain, or if there is a significant uncertainty in the initial concentrations of one of the reactants, or if the experiment being modeled is highly uncertain to some relatively variable chamber effect (such as the chamber radical source in the case of n-butane runs as discussed in Section IV-D-11), then the fact that the model does not fit the observed ozone yields within its estimated 10% measurement uncertainty does not necessarily indicate a problem with the chemical mechanism. The various types of data which need to be taken into account in characterizing the conditions of the experiments being used for model testing, and the uncertainties involved, are discussed in Section III.

## IV. C. CHARACTERIZATION RUNS

Several types of characterization runs were modeled in this program, and the results of the model simulations of these runs are summarized in this section. As discussed in Section III, while some of these runs were used to derive chamber-dependent parameters, others were modeled without optimization of parameters to determine how well the standard model treats chamber-dependent effects. Since these runs, by design, are particularly sensitive to the assumptions concerning various chamber-dependent parameters (many of which are known or expected to vary from run-to-run) a relatively large variablility in the quality of fits is expected. Indeed, this was observed. However, the primary purpose for modeling these runs was not to obtain the best possible fit to the results of each experiment, which requires varying the chamber-effects parameters such as the chamber radical sources, $NO_x$ offgassing rates, background organic levels, light intensity parameters, etc. (see Section III), but rather to determine whether the default set of chamber-dependent parameters used in this program without any run-to-run variation results in any systematic biases in the model predictions.

Five types of characterization runs were modeled in this program: (1) $NO_x$-air irradiations (UNC chamber only); (2) $NO_x$-air irradiations with low levels (10-20 ppb) of propene and propane, or propene and n-butane, added as radical tracers (all SAPRC chambers); (3) CO-$NO_x$-air irradiations (all chambers except the SAPRC EC); (4) acetaldehyde-air irradiations (all chambers), and (5) background air irradiations (UNC chamber only). The results of the model simulations of these different types of characterization runs are summarized and discussed below.

### 1. $NO_x$-Air, Tracer-$NO_x$ Air, and CO-$NO_x$-Air Runs

These runs are carried out primarily for the purpose of evaluating chamber radical sources and the presence of background or contaminant reactive organics. In the absence of added organics, the rate of conversion of NO to $NO_2$ is sensitive to background or contaminant reactive organics, since the radicals formed in the reactions of these organics will cause more NO to $NO_2$ conversion than would otherwise be the case. In addition, as discussed by Carter et al. (1982b), the rates of NO to $NO_2$ conversion in the CO-$NO_x$-air runs, and the propene decay rates in the tracer-$NO_x$-air runs, are influenced primarily by chamber radical sources. Thus these runs can be used to test these aspects of the chamber characterization model.

The results of the model simulations of these runs are summarized in Table IV-5 and Figure IV-1, and plots of model predictions against experimental results for UNC selected $NO_x$-air runs have already been given in Section III (See Figures III-11 and III-15). The observed and calculated changes in NO, $NO_2$ and (for the runs with added propene as a radical tracer) propene concentrations for all of these runs are summarized in Table IV-5, along with the absolute errors in the model predictions of these quantities. No significant ozone formation occurred in any of these runs, so ozone maxima, and the NO oxidation timing parameter calculated from the change in ($[O_3]$-[NO]), are not summarized for these runs. Distribution plots of the relative errors in the predictions of changes in NO, $NO_2$, and and the predictions of the changes in the propene concentrations are given in Figure IV-1.

It can be seen from the data in Table IV-5 and Figure IV-1 that, although not all runs are exactly fit by the model predictions, there does not appear to be any systematic discrepancies. In particular, the distributions shown in Figure IV-1 are uniformly centered around zero, with the number of runs where the quantity is overpredicted being approximately the same as the number where it is underpredicted. In view of the sensitivity of the results of these experiments to chamber-dependent radical sources and contamination effects, which are expected to vary from run-to-run, (but which were not adjusted from run-to-run in this program), some discrepancies are expected, and the results of these simulations are consistent with this.

As indicated in Section III, these calculations were carried out with no provision in the model for effects of contamination by reactive organics. These effects are manifested by the observed conversion of NO to $NO_2$ being greater than predicted in $NO_x$-air and tracer-$NO_x$-air runs, i.e., in positive discrepancies in final-initial [NO] and in negative descrepancies for initial-final $[NO_2]$. The majority of the $NO_x$-air and tracer-$NO_x$-air runs modeled in this program are runs in this category, but

Table IV-5. Initial NO, $NO_2$, and CO Concentrations and Observed and Predicted Changes in NO, $NO_2$, and (Where Applicable) Propene Concentrations for the $NO_x$-Air, Tracer-$NO_x$-Air, and CO-$NO_x$-Air Runs

| Experiment | Initial | | | Final - Init [NO] | | | Final - Init [$NO_2$] | | | Final - Init [Propene] | | |
|---|---|---|---|---|---|---|---|---|---|---|---|---|
| | NO (ppm) | $NO_2$ (ppm) | CO (ppm) | Expt (ppm) | Calc (ppm) | Calc -Expt (ppm) | Expt (ppm) | Calc (ppm) | Calc -Expt (ppm) | Expt (ppb) | Calc (ppb) | Calc -Expt (ppb) |
| 1: EC Tracer-$NO_x$-Air Runs | | | | | | | | | | | | |
| EC-436 | 1.426 | 0.364 | 1.0 | -0.098 | -0.049 | 0.049 | -0.071 | -0.060 | 0.011 | -4.1 | -4.0 | 0.2 |
| EC-440 | 0.674 | 0.084 | 1.0 | -0.063 | -0.048 | 0.015 | 0.024 | 0.013 | -0.011 | -5.3 | -5.3 | 0.0 |
| EC-442 | 0.144 | 0.435 | 1.0 | 0.069 | 0.093 | 0.024 | -0.172 | -0.160 | 0.012 | -6.1 | -4.8 | 1.3 |
| EC-457 | 0.403 | 0.092 | 0.0 | -0.066 | -0.043 | 0.023 | 0.008 | -0.008 | -0.016 | -6.8 | -8.1 | -1.2 |
| EC-464 | 0.100 | 0.093 | 1.0 | -0.019 | -0.003 | 0.015 | -0.002 | -0.011 | -0.009 | -6.3 | -7.2 | -0.9 |
| EC-597 | 0.480 | 0.083 | 5.0 | -0.061 | -0.032 | 0.029 | 0.041 | 0.005 | -0.036 | -6.7 | -6.6 | 0.1 |
| EC-599 | 0.024 | 3.380 | 1.0 | 2.276 | 1.890 | -0.386 | -2.685 | -2.546 | 0.139 | -7.5 | -7.9 | -0.4 |
| 2: ITC Tracer-$NO_x$-Air Runs | | | | | | | | | | | | |
| ITC-695 | 0.399 | 0.103 | 5.0 | -0.021 | -0.007 | 0.015 | 0.011 | -0.001 | -0.011 | -2.8 | -2.2 | 0.7 |
| ITC-826 | 0.720 | 0.732 | 1.0 | 0.017 | -0.015 | -0.032 | -0.005 | 0.005 | 0.010 | -1.8 | -1.5 | 0.3 |
| ITC-882 | 0.519 | 0.182 | 1.0 | -0.001 | -0.003 | -0.002 | -0.010 | -0.007 | 0.004 | -1.5 | -1.5 | 0.0 |
| 3: OTC Tracer-$NO_x$-Air Runs | | | | | | | | | | | | |
| OTC-185 | 0.195 | 0.085 | 1.0 | -0.002 | -0.005 | -0.002 | -0.003 | -0.002 | 0.001 | -0.5 | -2.5 | -2.0 |
| OTC-187 | 0.244 | 0.091 | 1.0 | -0.004 | -0.004 | 0.000 | 0.005 | -0.002 | -0.007 | -1.6 | -2.5 | -0.9 |
| 4: UNC $NO_x$-Air Runs | | | | | | | | | | | | |
| AU0282R | 0.095 | 0.295 | 0.563 | 0.036 | 0.048 | 0.012 | -0.136 | -0.101 | 0.034 | | | |
| AU2082R | 0.225 | 0.191 | 0.400 | -0.015 | -0.001 | 0.014 | -0.049 | -0.045 | 0.005 | | | |
| AU2282R | 0.176 | 0.283 | 0.400 | -0.006 | 0.031 | 0.036 | -0.157 | -0.101 | 0.056 | | | |
| AU2382R | 0.095 | 0.341 | 0.310 | 0.059 | 0.064 | 0.005 | -0.152 | -0.117 | 0.035 | | | |
| ST0582R | 0.110 | 0.385 | 0.500 | 0.070 | 0.076 | 0.006 | -0.181 | -0.143 | 0.037 | | | |
| OC0882R | 0.223 | 0.080 | 0.527 | -0.029 | -0.038 | -0.009 | 0.007 | 0.025 | 0.018 | | | |
| JL2483R | 0.224 | 0.067 | 1.0 | -0.052 | -0.027 | 0.025 | 0.015 | -0.005 | -0.021 | | | |
| JN1782B | 0.323 | 0.090 | 0.261 | 0.013 | -0.039 | -0.052 | -0.018 | 0.003 | 0.021 | | | |

(continued)

Table IV-5 (continued) - 2

| Experiment | Initial | | | Final - Init [NO] | | | Final - Init [$NO_2$] | | | Final - Init [Propene] | | |
|---|---|---|---|---|---|---|---|---|---|---|---|---|
| | NO (ppm) | $NO_2$ (ppm) | CO (ppm) | Expt (ppm) | Calc (ppm) | Calc -Expt (ppm) | Expt (ppm) | Calc (ppm) | Calc -Expt (ppm) | Expt (ppb) | Calc (ppb) | Calc -Expt (ppb) |
| JN2782B | 0.414 | 0.037 | 0.333 | -0.117 | -0.084 | 0.033 | 0.052 | 0.035 | -0.017 | | | |
| OC0882B | 0.222 | 0.078 | 0.507 | -0.019 | -0.038 | -0.019 | 0.011 | 0.025 | 0.014 | | | |
| JL2483B | 0.394 | 0.090 | 1.0 | -0.072 | -0.050 | 0.023 | 0.025 | 0.000 | -0.025 | | | |
| JL2783B | 0.376 | 0.055 | 0.300 | -0.091 | -0.054 | 0.037 | 0.043 | 0.010 | -0.033 | | | |
| JN1782R | 0.340 | 0.080 | 0.261 | -0.069 | -0.041 | 0.028 | 0.005 | 0.007 | 0.002 | | | |
| AU0683B | 0.145 | 0.229 | 0.407 | 0.000 | 0.015 | 0.015 | -0.096 | -0.058 | 0.038 | | | |
| **5: ITC CO-$NO_x$-Air Runs** | | | | | | | | | | | | |
| ITC-625 | 0.219 | 0.064 | 50.000 | -0.004 | -0.009 | -0.005 | 0.004 | 0.002 | -0.001 | -2.3 | -3.0 | -0.7 |
| ITC-634 | 0.462 | 0.136 | 52.000 | 0.001 | -0.006 | -0.007 | -0.009 | -0.002 | 0.006 | -2.4 | -1.7 | 0.7 |
| **6: OTC CO-$NO_x$-Air and CO-Tracer-$NO_x$-Air Runs** | | | | | | | | | | | | |
| OTC-188 | 0.250 | 0.098 | 72.5 | -0.008 | -0.005 | 0.003 | 0.002 | -0.005 | -0.006 | | | |
| OTC-201A | 0.287 | 0.087 | 68.0 | -0.024 | -0.007 | 0.017 | 0.011 | -0.002 | -0.013 | -2.8 | -3.7 | -0.9 |
| OTC-201B | 0.577 | 0.179 | 68.0 | -0.002 | -0.005 | -0.004 | -0.002 | -0.003 | 0.000 | | | |
| **7: UNC CO-$NO_x$-Air Runs** | | | | | | | | | | | | |
| JN2782R | 0.414 | 0.038 | 54.8 | -0.328 | -0.277 | 0.051 | 0.209 | 0.229 | 0.020 | | | |
| JL2783R | 0.400 | 0.055 | 50.0 | -0.268 | -0.233 | 0.035 | 0.215 | 0.184 | -0.031 | | | |
| AU0633R | 0.154 | 0.245 | 50.0 | -0.133 | -0.085 | 0.048 | 0.037 | 0.035 | -0.002 | | | |
| AU0282B | 0.095 | 0.295 | 47.0 | -0.043 | -0.037 | 0.006 | -0.006 | -0.022 | -0.016 | | | |
| AU2082B | 0.225 | 0.191 | 43.0 | -0.117 | -0.103 | 0.014 | 0.078 | 0.055 | -0.023 | | | |
| AU2282B | 0.176 | 0.283 | 40.4 | -0.089 | -0.076 | 0.013 | 0.010 | 0.002 | -0.008 | | | |
| AU2382B | 0.095 | 0.341 | 46.5 | -0.007 | -0.020 | -0.013 | -0.043 | -0.036 | 0.007 | | | |
| ST0582B | 0.110 | 0.385 | 50.0 | 0.022 | -0.009 | -0.031 | -0.084 | -0.061 | 0.023 | | | |

```
-----------------------------------------------------------------------
 Experimental-
Calculated Change/          NO                    NO2
  Initial NOx
-----------------------------------------------------------------------

          <  -0.22     :                       :
  -0.22 -  -0.18     :                       :
  -0.18 -  -0.14     :                       :
  -0.14 -  -0.10     :14                     :
  -0.10 -  -0.06     :47                     :1447
  -0.06 -  -0.02     :247                    :112344677
  -0.02 -   0.02    -:12334455667           -:11223445566777
   0.02 -   0.06     :111124444677           :114477
   0.06 -   0.10     :1444447                :4444
   0.10 -   0.14     :77                     :44
   0.14 -   0.18     :                       :
   0.18 -   0.22     :                       :
          >   0.22     :                       :
-----------------------------------------------------------------------
 Experimental-
Calculated Change          Propene
    (ppb)
-----------------------------------------------------------------------

          <  -2.20     :
  -2.20 -  -1.80     :3
  -1.80 -  -1.40     :
  -1.40 -  -1.00     :1
  -1.00 -  -0.60     :1356
  -0.60 -  -0.20     :1
  -0.20 -   0.20    -:1112
   0.20 -   0.60     :2
   0.60 -   1.00     :25
   1.00 -   1.40     :1
   1.40 -   1.80     :
   1.80 -   2.20     :
          >   2.20     :
-----------------------------------------------------------------------
```

Figure IV-1. Distribution plots of the errors in the predicted changes in NO and $NO_2$, divided by the initial $NO_x$ concentrations, and of the errors in the predicted changes in the propene concentrations for the $NO_x$-air, tracer-$NO_x$-air, and CO-$NO_x$-air runs modeled in this program. Run type symbols used:

| | |
|---|---|
| 1 = EC tracer-$NO_x$-air runs | 2 = ITC tracer-$NO_x$-air runs |
| 3 = OTC tracer-$NO_x$-air runs | 4 = UNC $NO_x$-air runs |
| 5 = ITC CO-$NO_x$-air runs | 6 = OTC CO-$NO_x$-air runs |
| 7 = UNC CO-$NO_x$-air runs | |

there are a number of runs where the discrepancy is in the opposite direction, and in most cases the discrepancies amount to less than 10% of the initial $NO_x$ levels. Thus these data do not indicate that the neglect of this effect in the model calculations introduces any significant bias in the model predictions.

## 2. Acetaldehyde-Air Irradiations

As discussed in Section III-C, acetaldehyde-air irradiations are useful characterization runs because the amount of ozone and PAN formed in these runs are extremely sensitive to $NO_x$ offgassing from the chamber walls. Runs of this type were carried out in all four chambers, and the default $NO_2$ offgassing rates used in the chamber effects models were adjusted, based on the results of these runs. Representative plots of observed and calculated data for these runs are given in Section III-C (see Figures III-13 and III-14), and the observed and calculated maximum ozone and PAN yields, the acetaldehyde half-lives, and the absolute and relative errors in the values are summarized for all of the acetaldehyde-air irradiations in Table IV-6.

As discussed in Section III-C, the $NO_x$ offgassing rates assumed for each chamber were adjusted to maximize the agreement of the model predictions of the PAN and ozone yields to the results of these experiments. For most of the indoor chamber runs, good fits to both these yields were obtained. For the outdoor chamber runs, particularly for the UNC chamber, the fits in general were not as good. For most of the OTC runs the model tended to underpredict ozone and overpredict PAN, while for most of the UNC runs the opposite results were obtained, and the discrepancies between model predictions and experimental results in general were larger. The results for the UNC runs OC1583R and OC1584R would be better fit if the model assumed lower $NO_x$ offgassing rates for the UNC chamber, since that would result in lower predicted yields for both PAN and ozone. For the other outdoor runs, adjusting the $NO_x$ offgassing rates to improve the fits to one of these two species would result in worse fits for the other. The default values used for the standard model simulations of the runs carried out in the outdoor chambers were chosen to be approximately half way between the values which fit the ozone data and those which gave best fits

Table IV-6. Summary of Observed and Calculated Maximum Ozone and PAN Yields and Acetaldehyde Half-Lives for All the Acetaldehyde-Air Runs Modeled in this Program

| Run | Maximum Ozone (ppm) | | | Maximum PAN (ppb) | | | Acetaldehyde Half-Life (min.) | | |
|---|---|---|---|---|---|---|---|---|---|
| | Expt | Calc | Calc -Expt | Expt | Calc | Calc -Expt | Expt | Calc | Calc -Expt /Expt |
| EC-253 | 0.134 | 0.129 | -0.005 | 40 | 44 | 4 | 329 | 264 | -0.20 |
| ITC-627 | 0.061 | 0.057 | -0.003 | 13 | 14 | 1 | 229 | 211 | -0.08 |
| ITC-636 | 0.047 | 0.057 | 0.011 | 11 | 14 | 3 | 304 | 207 | -0.32 |
| OTC-200A | 0.088 | 0.075 | -0.013 | 8 | 8 | 0 | 243 | 345 | 0.42 |
| OTC-200B | 0.076 | 0.069 | -0.006 | 6 | 8 | -2 | 300 | 285 | -0.05 |
| OTC-206A | 0.030 | 0.054 | 0.024 | 20 | 11 | -9 | 246 | 215 | -0.12 |
| OTC-206B | 0.023 | 0.081 | 0.058 | 13 | 9 | -4 | 330 | 329 | 0.00 |
| OTC-234A | 0.083 | 0.120 | 0.037 | 10 | 13 | -3 | 300 | 315 | 0.05 |
| OTC-234B | 0.084 | 0.127 | 0.043 | 17 | 12 | -5 | 331 | 315 | -0.05 |
| JL2683R | 0.422 | 0.410 | -0.012 | 26 | 54 | 28 | 590 | 630 | 0.07 |
| AU0483R | 0.548 | 0.455 | -0.092 | 40 | 54 | 14 | 581 | 630 | 0.08 |
| OC1583R | 0.140 | 0.218 | 0.078 | 23 | 64 | 41 | a | | |
| JL2683B | 0.324 | 0.281 | -0.043 | 27 | 60 | 32 | 518 | 595 | 0.15 |
| AU0483B | 0.431 | 0.373 | -0.059 | 40 | 67 | 27 | 476 | 531 | 0.11 |
| OC1584B | 0.193 | 0.264 | 0.071 | 35 | 64 | 29 | a | | |

[a] No data.

to the PAN yields, though in general the values employed tended to give somewhat better fits to ozone than to PAN, especially for the UNC chamber. (A more detailed discussion of offgassing in the chambers is given in Section III-C.)

The model simulations of the aldehyde consumption rates are not as sensitive to the assumed $NO_x$ offgassing rates, but are more sensitive to the photolysis rate constants used. The simulations of the indoor chamber experiments have a tendency to overpredict acetaldehyde consumption rates while the simulations of the UNC experiments tend to underpredict these rates. The simulations of the OTC experiments indicate no consistent discrepancy in this regard.

In addition to acetaldehyde-air, several acetaldehyde-$NO_x$-air irradiations were also carried out in the SAPRC EC and in the UNC outdoor chamber. These are not considered characterization runs because they are not unusually sensitive to $NO_x$ offgassing or other chamber effects. Thus the results of the model simulations of these runs are summarized below in Section IV-D, together with the results of the other single-component $NO_x$-air runs.

### 3. Background Air Irradiations

Three background air irradiations carried out in the UNC outdoor chamber on two separate days were also modeled in this program. Ozone formation was observed in all three irradiations, and the observed and calculated ozone yields are summarized in Table IV-7. It can be seen that the standard model ("Calc 1" in Table IV-7) significantly underpredicts ozone yields. However, as indicated in Section III-B-2-c, this can be attributed to the model not including any provision for background or contaminant organics, which is extremely important in affecting the results of these runs. The ozone yields calculated by assuming formaldehyde offgassing instead of the OH flux model for the chamber radical source (see discussion in Section III-B-2-c), gave much better fits to the results of these experiments, as indicated by the results of these calculations shown in Table IV-7 as "Calc 2".

However, as discussed in Section III-B-2-c, in the October 6, 1984 runs formaldehyde was monitored by Unisearch Associates, Inc. using a tunable diode laser absorption spectrometer. The results of those measurements indicated that the formaldehyde levels were significantly less than predicted if formaldehyde is offgassed at a rate sufficient to account for all of the chamber radical source in the UNC chamber. The observed and calculated formaldehyde data are also indicated in Table IV-7.

[It should be pointed out that the calculations designated "Calc 2" were carried out using a simple 1-step process for formaldehyde offgassing, with its rate being dependent on light intensity only, and alternative methods of representing formaldehyde offgassing in chambers in general would give differing results. As discussed in Section III-B-2-c,

Table IV-7. Observed and Calculated[a] Ozone and Formaldehyde Yields for the UNC Background Air Irradiations Modeled in this Program

| | Maximum Ozone (ppm) | | | | Maximum HCHO (ppm) | | |
|---|---|---|---|---|---|---|---|
| Run | Expt. | Calc 1 | Calc 2 | Calc 3 | Expt. | Calc 2 | Calc 1,3 |
| JN0682R | 0.203 | 0.084 | 0.178 | 0.219 | b | 0.050 | c |
| OC0684R | 0.097 | 0.052 | 0.100 | 0.102 | 0.012 | 0.059 | c |
| OC0684B | 0.119 | 0.020 | 0.110 | 0.113 | 0.011 | 0.059 | c |

[a] Calc 1 = standard model; Calc 2 = model using formaldehyde offgassing at a rate of 0.001 x $k_1$, the $NO_2$ photolysis rate, instead of OH flux for the radical source (see Section III-B-2-c); Calc 3 = standard model with an added reaction converting OH to $HO_2$ with a rate constant of 500 $min^{-1}$.

[b] No data.

[c] No formaldehyde predicted to be formed.

Jeffries (private communication) uses a more complex representation where the light-dependent rate of formaldehyde offgassing decreases with time as the amount of "wall formaldehyde" is consumed as it is offgassed. If this representation is assumed, the amount of "wall formaldehyde" required for the model simulations to fit the result of the UNC n-butane runs (if it is assumed that there is no other chamber radical sources) is in excess of 40 ppb, and simulations of the UNC pure air irradiations assuming this quantity of "wall formaldehyde" results in a predicted peak formaldehyde in excess of 25 ppb, which is also inconsistent with the Unisearch formaldehyde data obtained in the pure air irradiations. Lesser amounts of "wall formaldehyde" are not only inadequate to account for the chamber radical source, but also result in underpredictions of ozone yields in these pure air irradiations. Thus it appears unlikely that use of more complex representations of formaldehyde offgassing would significantly affect the conclusions which can be drawn based on the results of the calculations shown in Table IV-7, though this has not been comprehensively investigated.]

It is not necessary to assume that formaldehyde offgassing is the radical source in order for the model to fit the ozone yields observed in these experiments. The presence of low levels of biogenic organics in the rural air used to fill the chamber, or the emission of other organic contaminants from the chamber walls, could also account for the observed ozone formation. As shown in Table IV-7, (as "Calc 3") and in Figure III-11 in Section III-B-2-c, excellent fits to the data can be obtained by including in the model the "reaction"

$$OH \rightarrow HO_2, \qquad k = 500 \text{ min}^{-1}$$

to account for peroxy radical formation resulting from reactions of background or contaminant organics, with the rate constant being adjusted to fit the ozone yields observed in these runs. The peroxy radical input provided by this "reaction" corresponds to that provided by only ~7 ppb of propene (or by lower concentrations of more reactive biogenics such as isoprene and α-pinene), and does not indicate excessive contamination. Indeed, this contamination is insignificant in runs where sufficient reactive organic is present to cause ozone formation in the presence of $NO_x$, and is ignored in the model calculations discussed in the remainder of this section.

## IV. D. SINGLE-COMPONENT $NO_x$-AIR IRRADIATIONS

Perhaps the most useful type of environmental chamber experiment with respect to developing and testing detailed reaction mechanisms of individual organic compounds are $NO_x$-air irradiations of single organics, since they allow tests of the chemical mechanisms for individual compounds which are independent of uncertainties in the mechanisms for other compounds which are not present. Runs of this type modeled in this program include $NO_x$-air irradiations of 24 different compounds representative of organics emitted into the atmosphere and their oxidation products. These compounds include the three simplest aldehydes, the two simplest ketones, four alkenes, nine alkanes, five aromatic hydrocarbons, and ortho-cresol. For many of these compounds irradiations were carried out in more than one chamber, allowing a comprehensive test of the model for their reaction mechanisms.

A few of the runs included in this group of single component runs also had one of the organic's major oxidation products included in the reaction mixture. While strictly speaking these are two-component runs, they are included in this set of single component runs because the reactions of the major oxidation products must be included in the model, and hence the same model is being tested regardless of whether the product is initially present or not. The results of the model simulations of the $NO_x$-air irradiations of the various single organics are summarized below for each organic or set of organics.

### 1. Formaldehyde-Air Runs

Eight formaldehyde-air irradiations were modeled in this program, two carried out in the SAPRC EC and six carried out in the UNC outdoor chamber. The observed and calculated maximum ozone concentrations, times to reach half the experimental ozone maxima, and formaldehyde half-lives are summarized in Table IV-8. Distribution plots for the discrepancies in the model predictions of these quantities are summarized in Figure IV-2.

The model simulations of the two EC formaldehyde-air runs overpredicted the ozone yields by approximately 30% and underpredicted the formaldehyde half-lives by approximately 10%. These results are considered

Table IV-8. Initial Formaldehyde and Experimental and Calculated Maximum Ozone Concentrations, Times to Half the Experimental Ozone Maxima, and Formaldehyde Half-Lives for the Formaldehyde-Air Irradiations

| Experiment | Init. HCHO | Maximum Ozone Concentration | | | | Time to 1/2 Maximum Expt. $[O_3]$ | | | | Formaldehyde Half-Life | | | |
|---|---|---|---|---|---|---|---|---|---|---|---|---|---|
| | (ppm) | Expt (ppm) | Calc (ppm) | Calc -Expt (ppm) | Calc -Expt /Expt | Expt (min) | Calc (min) | Calc -Expt (min) | Calc -Expt /Expt | Expt (min) | Calc (min) | Calc -Expt (min) | Calc -Expt /Expt |
| 1: EC Runs | | | | | | | | | | | | | |
| EC-250 | 0.540 | 0.213 | 0.292 | 0.079 | 0.37 | 92 | 95 | 2 | 0.02 | 131 | 115 | -15 | -0.12 |
| EC-255 | 0.510 | 0.203 | 0.252 | 0.049 | 0.24 | 104 | 97 | -7 | -0.07 | 126 | 114 | -12 | -0.10 |
| Group Average | | 0.208 | 0.254 | 0.046 | 0.22 | 98 | 96 | -2 | -0.02 | 128 | 115 | 14 | -0.11 |
| S. Dev. | | 0.007 | 0.003 | 0.004 | 0.03 | 8 | 2 | 6 | 0.06 | 4 | 1 | 2 | 0.01 |
| Avg. Abs. Val | | | | 0.046 | 0.22 | | | 4 | 0.04 | | | | 0.11 |
| S. Dev. | | | | 0.004 | 0.03 | | | 3 | 0.03 | | | | 0.01 |
| 2: UNC Runs | | | | | | | | | | | | | |
| JL1782R | 0.520 | 0.239 | 0.293 | 0.054 | 0.23 | 354 | 212 | -142 | -0.40 | 219 | 125 | -94 | -0.43 |
| OC0784R | 0.442 | 0.087 | 0.236 | 0.149 | 1.72 | 292 | 182 | -110 | -0.38 | 450 | 197 | -253 | -0.56 |
| OC1684R | 0.420 | 0.153 | 0.239 | 0.086 | 0.56 | | | | | 283 | 196 | -87 | -0.31 |
| JL1782B | 0.576 | 0.264 | 0.269 | 0.005 | 0.02 | 354 | 320 | -34 | -0.10 | 240 | 185 | -55 | -0.23 |
| OC0784B | 1.032 | 0.138 | 0.339 | 0.200 | 1.45 | 308 | 289 | -19 | -0.06 | 450 | 218 | -232 | -0.52 |
| OC1684B | 0.250 | 0.133 | 0.176 | 0.042 | 0.32 | | | | | 318 | 209 | -109 | -0.34 |
| Group Average | | 0.169 | 0.259 | 0.089 | 0.72 | 326 | 250 | -76 | -0.23 | 327 | 188 | 138 | -0.40 |
| S. Dev. | | 0.068 | 0.056 | 0.073 | 0.70 | 32 | 64 | 59 | 0.18 | 102 | 33 | 83 | 0.13 |
| Avg. Abs. Val | | | | 0.089 | 0.72 | | | 76 | 0.23 | | | | 0.40 |
| S. Dev. | | | | 0.073 | 0.70 | | | 59 | 0.18 | | | | 0.13 |

```
------------------------------------------------------------------------
    Calc.-Expt.                               Calc.-Expt./Expt.
 Maximum Ozone (ppm)                      Time to 1/2 Expt. [O3]max
------------------------------------------------------------------------

       < -0.33     :                          < -0.55     :
 -0.33 - -0.27     :                    -0.55 - -0.45     :
 -0.27 - -0.21     :                    -0.45 - -0.35     :22
 -0.21 - -0.15     :                    -0.35 - -0.25     :
 -0.15 - -0.09     :                    -0.25 - -0.15     :
 -0.09 - -0.03     :                    -0.15 - -0.05     :122
 -0.03 -  0.03     :2                   -0.05 -  0.05     :12
  0.03 -  0.09     :11222                0.05 -  0.15     :2
  0.09 -  0.15     :2                    0.15 -  0.25     :
  0.15 -  0.21     :2                    0.25 -  0.35     :
  0.21 -  0.27     :                     0.35 -  0.45     :
  0.27 -  0.33     :                     0.45 -  0.55     :
       >  0.33     :                          >  0.55     :

------------------------------------------------------------------------
   Calc.-Expt./Expt.
 Formaldehyde Half-Lives
------------------------------------------------------------------------

       < -0.5     :22
  -0.5 - -0.4     :2
  -0.4 - -0.3     :22
  -0.3 - -0.2     :2
  -0.2 - -0.1     :1
  -0.1 -  0.0     :1
   0.0 -  0.1     :
   0.1 -  0.2     :
   0.2 -  0.3     :
   0.3 -  0.4     :
   0.4 -  0.5     :
       >  0.5     :

------------------------------------------------------------------------
```

Figure IV-2. Distribution plots of the errors in the predicted maximum ozone yields, the times required to achieve one-half the maximum experimental ozone yields, and the formaldehyde half-lives in the formaldehyde-air irradiations. Codes for chambers: 1 = EC, 2 = UNC.

to be reasonably satisfactory, in view of the facts that (1) the ozone yields in these runs, as in the acetaldehyde-air runs discussed above and in Section III-C, are very sensitive to the amount of $NO_x$ offgassing assumed in the chamber effects model, which in general would be expected to vary from run to run, and (2) the formaldehyde measurements carried out around the time of those experiments are known to be anomalously low due to a defect in the equipment employed. The initial concentrations used in the model simulations were obtained from the calculated amount injected into the chamber and not the experimental measurements; but if they are assumed to be valid in a relative sense, they indicate formaldehyde consumption rates which are reasonably consistent with model predictions. The observed and calculated ozone and formaldehyde data for one of these runs are shown in Figure IV-3; the results for the other experiments are similar.

In the model simulations of all but one the UNC formaldehyde-air irradiations, the ozone formation rates and yields and formaldehyde consumption rates were significantly overpredicted. The observed and calculated ozone and formaldehyde data for a representative run of this type is shown in Figure IV-4. The overprediction of the ozone yield in these runs may be due to our chamber effects model for the UNC chamber assuming too high a $NO_x$ offgassing rate. As indicated in Section III-C-4, the most appropriate way to represent this effect in the UNC chamber is presently uncertain, and the simulations of these runs suggest that it may need to be refined. However, it should be pointed out that the model consistently underpredicted the ozone yields in the acetaldehyde-air irradiations, and thus the overprediction of ozone in the formaldehyde-air runs may be due to some other problem. In particular, the overprediction of ozone in these experiments may be related to the fact that the model also consistently overpredicts the formaldehyde consumption rates observed in these experiments. The predicted formaldehyde consumption rates are expected to be affected primarily by the formaldehyde photolysis rates assumed in the model, and not by assumed $NO_x$ offgassing rates. This overprediction of formaldehyde consumption rate is also observed in the model simulations of the UNC formaldehyde-$NO_x$-air irradiations, and is discussed further in the following section.

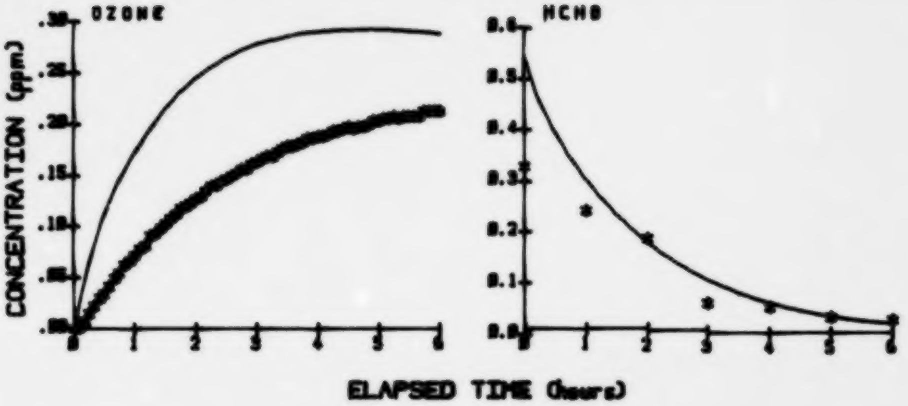

Figure IV-3. Experimental and calculated ozone and formaldehyde concentration-time profiles for the formaldehyde-air irradiation EC-250.
* = Experimental data.
---- = Model calculation.

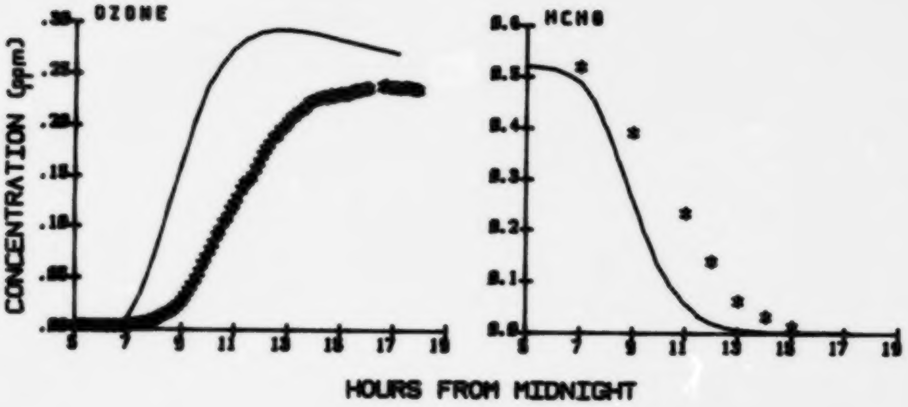

Figure IV-4. Experimental and calculated ozone and formaldehyde concentration-time profiles for the UNC formaldehyde-air irradiation JL1782R.
* = Experimental data.
---- = Model calculation.

### 2. Formaldehyde-$NO_x$-Air Runs

Several formaldehyde-$NO_x$-air irradiations carried out in the SAPRC EC and in the UNC chamber were modeled in this program, along with one such run carried out in the SAPRC ITC and one dual formaldehyde-$NO_x$-air run carried out in the SAPRC OTC. The observed and calculated maximum ozone yields, NO oxidation and ozone formation timing parameters, and formaldehyde half-lives are summarized in Table IV-9. Distribution plots of the discrepancies in these measures of reactivity are given in Figure IV-5.

The fits of the model simulations to the results of the runs carried out in the SAPRC EC and ITC were probably as good as can reasonably be expected considering the uncertainties in precisely monitoring formaldehyde with the technique employed at SAPRC. The ozone maximum yields were overpredicted by less than 15% in the two EC runs where sufficient ozone formation occurred, the NO oxidation time was reasonably well fit in the ITC run and two of the EC runs, but fit less well in the other three EC runs, and the formaldehyde consumption rate was fit (to within 10%) in two of the EC runs, was overpredicted in one and was underpredicted in two. These results do not indicate any consistent problems with the formaldehyde model or the method of calculating formaldehyde photolysis rates in these indoor chambers.

The results of the simulations of the dual-chamber formaldehyde-$NO_x$-air run carried out in the SAPRC outdoor chamber also do not indicate any consistent problems. In that run, the formaldehyde was injected after the second hour of a dual-chamber tracer-$NO_x$-air irradiation, and the observed and calculated concentration-time profiles are summarized in Figure IV-6. The predicted formaldehyde consumption rates and the rates of NO to $NO_2$ conversion on both sides of the chamber appear to be reasonably consistent with the experimental results, though it should be noted that since the exact amount of formaldehyde injected is unknown and had to be adjusted to fit the first formaldehyde measurement made 30 minutes after its injection, it does not provide a very good test of the model's prediction of formaldehyde consumption rates.

The results of the formaldehyde-$NO_x$-air irradiations carried out in the UNC chamber were much less satisfactory than the simulations of the runs carried out in the SAPRC chambers since they indicated a consistent

Table IV-9. Initial Concentrations and Experimental and Calculated Maximum Ozone Yields, Times to Half Maximum Experimental ($[O_3]-[NO]$), and Reactant Half-Lives for the Single-Component Aldehyde or Ketone-$NO_x$-Air Irradiations

| Experiment | Initial Concentrations | | | Maximum Ozone Concentration | | | | Time to 1/2 Maximum Expt. ($[O_3]-[NO]$) | | | | Reactant Half-Life | | |
|---|---|---|---|---|---|---|---|---|---|---|---|---|---|---|
| | $NO_x$ (ppm) | HC (ppmC) | $HC/NO_x$ | Expt (ppm) | Calc (ppm) | Calc -Expt (ppm) | Calc -Expt /Expt | Expt (min) | Calc (min) | Calc -Expt (min) | Calc -Expt /Expt | Expt (min) | Calc (min) | Calc -Expt /Expt |
| **1: EC Formaldehyde Runs** | | | | | | | | | | | | | | |
| EC-251 | 0.113 | 0.6 | 4.9 | 0.271 | 0.305 | 0.033 | 0.12 | 53 | 39 | -14 | -0.26 | 112 | 72 | -0.36 |
| EC-252 | 0.495 | 0.6 | 1.1 | 0.024 | 0.024 | 0.000 | | 81 | 68 | -13 | -0.16 | 99 | 133 | 0.34 |
| EC-389 | 4.930 | 9.1 | 1.9 | 0.002 | 0.032 | 0.029 | | 25 | 22 | -3 | -0.12 | 190 | 98 | -0.49 |
| EC-391 | 5.179 | 16.0 | 3.1 | 2.371 | 2.682 | 0.311 | 0.13 | 24 | 30 | 7 | 0.28 | 90 | 83 | -0.08 |
| EC-392 | 10.730 | 9.5 | 0.9 | 0.000 | 0.008 | 0.008 | | 47 | 29 | -19 | -0.39 | 129 | 117 | -0.10 |
| Group Average | 4.289 | 7.2 | 2.4 | 0.534 | 0.610 | 0.076 | 0.13 | 46 | 38 | -8 | -0.13 | 124 | 100 | -0.14 |
| S. Dev. | 4.316 | 6.6 | 1.6 | 1.033 | 1.165 | 0.132 | 0.01 | 24 | 18 | 10 | 0.25 | 40 | 25 | 0.32 |
| Avg. Abs. Value | | | | | | 0.076 | 0.13 | | | 10 | 0.24 | | | 0.27 |
| S. Dev. | | | | | | 0.132 | 0.01 | | | 6 | 0.11 | | | 0.18 |
| **2: ITC Formaldehyde Runs** | | | | | | | | | | | | | | |
| ITC-864 | 0.537 | 0.5 | 0.9 | 0.001 | 0.016 | 0.015 | | 185 | 167 | -18 | -0.10 | | | |
| **3: OTC Formaldehyde Runs** | | | | | | | | | | | | | | |
| OTC-235A | 0.558 | 0.0 | 0.0 | 0.273 | 0.196 | -0.077 | -0.28 | 170 | 179 | 9 | 0.05 | | | |
| OTC-235B | 0.580 | 0.0 | 0.0 | 0.308 | 0.262 | -0.046 | -0.15 | 173 | 168 | -5 | -0.03 | | | |
| Group Average | 0.569 | 0.0 | 0.0 | 0.291 | 0.229 | -0.061 | -0.22 | 172 | 173 | 1 | 0.01 | | | |
| S. Dev. | 0.016 | 0.0 | 0.0 | 0.025 | 0.046 | 0.022 | 0.09 | 2 | 8 | 10 | 0.06 | | | |
| Avg. Abs. Value | | | | | | 0.061 | 0.22 | | | 7 | 0.04 | | | |
| S. Dev. | | | | | | 0.022 | 0.09 | | | 3 | 0.02 | | | |

(continued)

Table IV-9 (continued) - 2

| Experiment | Initial Concentrations | | | Maximum Ozone Concentration | | | | Time to 1/2 Maximum Expt. ($[O_3]-[NO]$) | | | | Reactant Half-Life | | |
|---|---|---|---|---|---|---|---|---|---|---|---|---|---|---|
| | $NO_x$ (ppm) | HC (ppmC) | $HC/NO_x$ | Expt (ppm) | Calc (ppm) | Calc -Expt (ppm) | Calc -Expt /Expt | Expt (min) | Calc (min) | Calc -Expt (min) | Calc -Expt /Expt | Expt (min) | Calc (min) | Calc -Expt /Expt |
| **4: UNC Formaldehyde Runs** | | | | | | | | | | | | | | |
| OC0984R | 0.559 | 1.0 | 1.7 | 0.666 | 1.039 | 0.373 | 0.56 | 364 | 261 | -103 | -0.28 | 272 | 168 | -0.38 |
| AU0179B | 0.352 | 1.0 | 2.8 | 0.618 | 0.446 | -0.172 | -0.28 | 299 | 272 | -26 | -0.09 | 259 | 189 | -0.27 |
| AU0279B | 0.210 | 1.0 | 4.8 | 0.583 | 0.534 | -0.049 | -0.08 | 278 | 235 | -43 | -0.15 | 290 | 203 | -0.30 |
| AU0479B | 0.230 | 0.5 | 2.2 | 0.378 | 0.221 | -0.157 | -0.42 | 332 | 329 | -3 | -0.01 | 302 | 206 | -0.32 |
| AU0579B | 0.539 | 1.2 | 2.2 | 0.508 | 0.450 | -0.058 | -0.11 | 323 | 267 | -56 | -0.17 | 317 | 222 | -0.30 |
| JL2381B | 0.433 | 1.5 | 3.5 | 0.637 | 0.683 | 0.045 | 0.07 | 228 | 198 | -30 | -0.13 | 245 | 213 | -0.13 |
| OC0984B | 0.501 | 1.0 | 1.9 | 0.301 | 0.308 | 0.007 | 0.02 | 338 | 279 | -59 | -0.17 | 304 | 181 | -0.40 |
| Group Average | 0.403 | 1.0 | 2.7 | 0.527 | 0.526 | -0.002 | -0.03 | 309 | 263 | -46 | -0.14 | | 198 | -0.30 |
| S. Dev. | 0.143 | 0.3 | 1.1 | 0.139 | 0.271 | 0.183 | 0.31 | 45 | 40 | 32 | 0.08 | | 19 | 0.08 |
| Avg. Abs. Value | | | | | | 0.123 | 0.22 | | | 45 | 0.14 | | | 0.30 |
| S. Dev. | | | | | | 0.126 | 0.20 | | | 32 | 0.08 | | | 0.08 |
| **5: EC Acetaldehyde Runs** | | | | | | | | | | | | | | |
| EC-164 | 0.506 | 0.7 | 1.3 | 0.085 | 0.064 | -0.021 | -0.25 | 100 | 117 | 17 | 0.17 | | | |
| EC-254 | 0.110 | 1.0 | 8.7 | 0.264 | 0.248 | -0.015 | -0.06 | 129 | 131 | 2 | 0.01 | 258 | 337 | 0.30 |
| Group Average | 0.308 | 0.8 | 5.0 | 0.175 | 0.156 | -0.018 | -0.15 | 114 | 124 | 9 | 0.09 | | | |
| S. Dev. | 0.280 | 0.2 | 5.2 | 0.126 | 0.130 | 0.004 | 0.13 | 21 | 10 | 10 | 0.11 | | | |
| Avg. Abs. Value | | | | | | 0.018 | 0.15 | | | 9 | 0.09 | | | |
| S. Dev. | | | | | | 0.004 | 0.13 | | | 10 | 0.11 | | | |
| **6: UNC Acetaldehyde Runs** | | | | | | | | | | | | | | |
| AU0179R | 0.349 | 1.9 | 5.4 | 0.683 | 0.445 | -0.238 | -0.35 | 344 | 387 | 43 | 0.12 | 413 | 463 | 0.12 |
| JN1482R | 0.312 | 3.1 | 9.9 | 0.731 | 0.453 | -0.278 | -0.38 | 203 | 213 | 10 | 0.05 | 458 | 586 | 0.28 |
| AU2482B | 0.319 | 1.9 | 6.0 | 0.972 | 0.637 | -0.335 | -0.34 | 466 | 481 | 15 | 0.03 | 466 | 533 | 0.14 |

(continued)

Table IV-9 (continued) - 3

| Experiment | Initial Concentrations | | | Maximum Ozone Concentration | | | | Time to 1/2 Maximum Expt. ($[O_3]-[NO]$) | | | | Reactant Half-Life | | |
|---|---|---|---|---|---|---|---|---|---|---|---|---|---|---|
| | $NO_x$ (ppm) | HC (ppmC) | $HC/NO_x$ | Expt (ppm) | Calc (ppm) | Calc -Expt (ppm) | Calc -Expt /Expt | Expt (min) | Calc (min) | Calc -Expt (min) | Calc -Expt /Expt | Expt (min) | Calc (min) | Calc -Expt /Expt |
| Group Average | 0.327 | 2.3 | 7.1 | 0.795 | 0.512 | -0.283 | -0.36 | 337 | 360 | 23 | 0.07 | 446 | 528 | 0.18 |
| S. Dev. | 0.020 | 0.7 | 2.4 | 0.155 | 0.109 | 0.049 | 0.02 | 132 | 136 | 18 | 0.05 | 29 | 61 | 0.09 |
| Avg. Abs. Value | | | | | | 0.283 | 0.36 | | | 23 | 0.07 | | | 0.18 |
| S. Dev. | | | | | | 0.049 | 0.02 | | | 18 | 0.05 | | | 0.09 |
| 7: UNC Propionaldehyde Runs | | | | | | | | | | | | | | |
| JN1482B | 0.300 | 3.1 | 10.3 | 0.733 | 0.452 | -0.281 | -0.38 | 201 | 184 | -17 | -0.08 | 407 | 443 | 0.09 |
| AU2482R | 0.336 | 2.1 | 6.2 | 0.941 | 0.618 | -0.322 | -0.34 | 433 | 470 | 37 | 0.09 | 434 | 504 | 0.16 |
| Group Average | 0.318 | 2.6 | 8.2 | 0.837 | 0.535 | -0.302 | -0.36 | 317 | 327 | 10 | 0.00 | 420 | 473 | 0.12 |
| S. Dev. | 0.025 | 0.7 | 2.9 | 0.147 | 0.117 | 0.029 | 0.03 | 164 | 202 | 38 | 0.12 | 18 | 43 | 0.05 |
| Avg. Abs. Value | | | | | | 0.302 | 0.36 | | | 27 | 0.08 | | | 0.12 |
| S. Dev. | | | | | | 0.029 | 0.03 | | | 14 | 0.00 | | | 0.05 |
| 8: UNC Acetone Runs | | | | | | | | | | | | | | |
| JN0480R | 0.176 | 4.8 | 27.3 | 0.233 | 0.474 | 0.241 | 1.04 | 458 | 340 | -118 | -0.26 | 325 | 395 | 0.22 |
| 9: UNC MEK Runs | | | | | | | | | | | | | | |
| OC2079R | 0.224 | 13.8 | 61.6 | 0.563 | 0.463 | -0.100 | -0.18 | 456 | 397 | -59 | -0.13 | 175 | 196 | 0.12 |
| JN0480B | 0.178 | 3.8 | 21.3 | 0.652 | 0.566 | -0.086 | -0.13 | 431 | 448 | 17 | 0.04 | 480 | 515 | 0.07 |
| Group Average | 0.201 | 8.8 | 41.5 | 0.607 | 0.515 | -0.093 | -0.15 | 443 | 423 | -20 | -0.04 | 308 | 355 | 0.10 |
| S. Dev. | 0.033 | 7.1 | 28.5 | 0.063 | 0.073 | 0.010 | 0.03 | 17 | 36 | 53 | 0.12 | 216 | 226 | 0.03 |
| Avg. Abs. Value | | | | | | 0.093 | 0.15 | | | 38 | 0.08 | | | 0.10 |
| S. Dev. | | | | | | 0.010 | 0.03 | | | 29 | 0.06 | | | 0.03 |

```
--------------------------------------------------------------------------------
   Calc.-Expt.                                    Calc.-Expt./Expt.
 Maximum Ozone (ppm)                  Time to 1/2 Expt. ([O3]-[NO])max
--------------------------------------------------------------------------------

        < -0.33    :                             < -0.55    :
 -0.33 - -0.27    :                      -0.55 - -0.45    :
 -0.27 - -0.21    :                      -0.45 - -0.35    :1
 -0.21 - -0.15    :                      -0.35 - -0.25    :14
 -0.15 - -0.09    :4                     -0.25 - -0.15    :1444
 -0.09 - -0.03    :3344                  -0.15 - -0.05    :12444
 -0.03 -  0.03    :111244                -0.05 -  0.05    :3
  0.03 -  0.09    :14                     0.05 -  0.15    :3
  0.09 -  0.15    :                       0.15 -  0.25    :
  0.15 -  0.21    :                       0.25 -  0.35    :1
  0.21 -  0.27    :                       0.35 -  0.45    :
  0.27 -  0.33    :1                      0.45 -  0.55    :
        >  0.33    :4                            >  0.55    :

--------------------------------------------------------------------------------
   Calc.-Expt./Expt.
 Formaldehyde Half-Lives
--------------------------------------------------------------------------------

        < -0.5    :
   -0.5 - -0.4    :14
   -0.4 - -0.3    :144
   -0.3 - -0.2    :44
   -0.2 - -0.1    :4
   -0.1 -  0.0    :11
    0.0 -  0.1    :
    0.1 -  0.2    :
    0.2 -  0.3    :
    0.3 -  0.4    :1
    0.4 -  0.5    :
          > 0.5    :

--------------------------------------------------------------------------------
```

Figure IV-5. Distribution plots of the errors in the predicted maximum ozone yields, the times required to achieve one-half the maximum experimental change in ($[O_3]-[NO]$), and the formaldehyde half-lives in the formaldehyde-$NO_x$-air irradiations. Codes for chambers: 1 = EC, 2 = ITC, 3 = OTC, 4 = UNC.

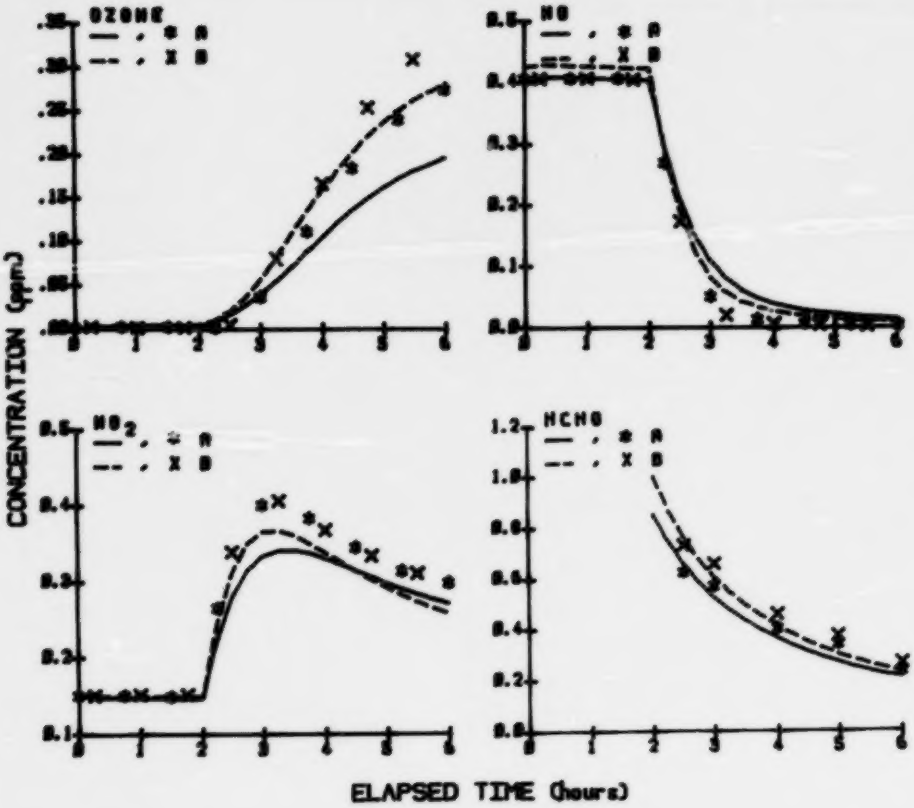

Figure IV-6. Experimental and calculated concentration-time profiles for selected species in the formaldehyde-$NO_x$-air irradiation OTC-235.
* = Experimental data, side 1.
x = Experimental data, side 2.
----- = Model calculation, side 1.
- - - = Model calculation, side 2.

pattern of discrepancy in underpredicting NO oxidation times and rates of formaldehyde consumption, particularly early in the experiment. The results shown for run AU0279B in Figure IV-7 are reasonably typical of all UNC formaldehyde runs modeled in this study. As indicated in the previous section, similar discrepancies in the formaldehyde consumption rates were observed in the model simulations of the formaldehyde-air runs carried out in the UNC chamber.

It should be pointed out that the source of this discrepancy in the model predictions of the formaldehyde consumption rates observed in the UNC chamber is unlikely to be related to the question of whether formaldehyde offgassing (discussed in Sections III-B-2-c and IV-C-3) is occurring in the UNC chamber. Calculations assuming formaldehyde offgassing result in no significant change in predicted formaldehyde consumption rates in the UNC formaldehyde experiments. This is because the maximum amount of formaldehyde offgassed which would be consistent with the magnitude of the chamber radical source for the UNC chamber is considerably less than the amount of formaldehyde initially present in these experiments.

The possiblilty that the descrepancies in the model simulations of the UNC experiments are due to problems with the UNC formaldehyde cannot be totally ruled out. In particular, as indicated above in Section IV-B-5-f and shown in the following sections, there may be interferences in the UNC formaldehyde analysis, since the formaldehyde yields, relative to model predictions, are consistently higher in the UNC chamber experiments than in the SAPRC experiments, or in the yields when measured in the UNC chamber by the Unisearch laser absorption technique in several October, 1984 runs. Indeed, the initial formaldehyde levels measured by Unisearch in the OC0984 formaldehyde-$NO_x$-air runs was 20% lower on each side than those measured by the standard technique employed at UNC. (Model simulations of that run using the initial formaldehyde levels measured by Unisearch give better fits to ozone on the "red" side, and worse fits on the "blue side". Unisearch formaldehyde data are only available for the initial period of the run, so fits to their measured decay rates could not be obtained.) On the other hand, the initial formaldehyde levels measured by the two techniques in the OC0784 formaldehyde-air run showed good agreement. It should be noted that, as indicated in Section IV-B-5, the Unisearch formaldehyde measurements are also subject to uncertainties, and

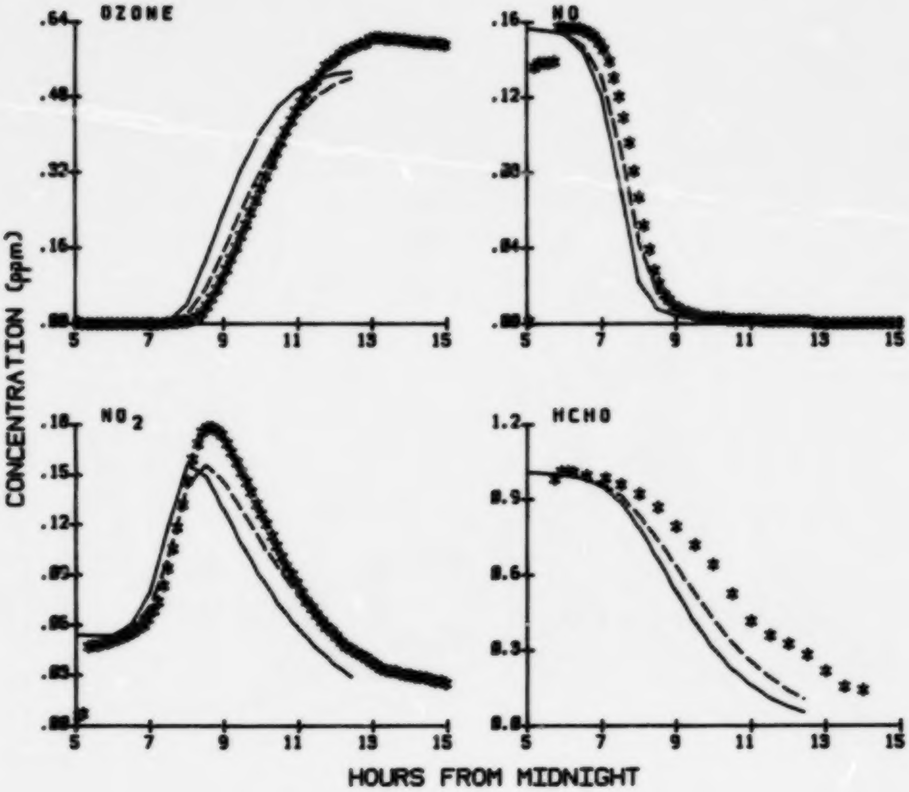

Figure IV-7. Experimental and calculated concentration-time profiles for selected species in the UNC formaldehyde-$NO_x$-air irradiation AU0279B.

* = Experimental data.
----- = Model calculation, standard model.
— — = Model calculation, formaldehyde photolysis reduced by a factor of 0.65

thus the discrepancies between the Unisearch data and the results of the standard UNC measurement technique are not conclusive. In addition, tests where known amounts of formaldehyde are introduced into the UNC chamber tend to indicate that the UNC formaldehyde measurements are probably valid when it is directly injected into the chamber when no other compounds are present.

A more likely cause for the fact that these simulations give consistent discrepancies in predictions of formaldehyde consumption rates in the UNC chamber is that there may be problems with the way the formaldehyde photolysis rates in that chamber are being calculated. If this is the case, it would be expected to be due to errors regarding the assumed light intensity and spectral distribution in the UNC chamber, since the absorption coefficients and quantum yields for formaldehyde photolysis (discussed in Section II-A) now appear to be reasonably well known, and, as discussed in Section III-A-2, there are significant uncertainties regarding the effects the chamber walls and the reflective floor have on intensity, spectral distribution, and zenith angle dependence of the light inside the UNC chamber. Thus the assumption incorporated in our standard model calculations that these factors have no significant effect (or tend to cancel each other out) may well be in error, especially at the lower wavelength regions (which affect formaldehyde photolysis) and at higher zenith angles.

Jeffries (private communication) suggests that the UNC chamber walls may be suppressing the UV intensity and thus use of a lower formaldehyde photolysis rate might be appropriate. In addition, Whitten et al. (1985) found the UNC formaldehyde runs are better fit by using formaldehyde photolysis rates which are approximately 65-70% those used in this model, though they only report fits to ozone and not formaldehyde consumption or NO oxidation rates. In order to determine if assuming lower formaldehyde consumption rates gave better fits to the data, test calculations were carried out in which the UNC formaldehyde-$NO_x$-air runs were simulated with formaldehyde photolyzing at 65% the rate assumed in the standard model. (Strictly speaking, if the UV intensity is suppressed such that formaldehyde photolysis is significantly slower, then photolyses of other species which are affected by the relative UV intensity, such as photolysis of $O_3$ to $O(^1D)$, should also be reduced, though this was not done in these test calculations. These reactions are expected to be much less important than formaldehyde photolysis in formaldehyde-$NO_x$-air systems.) The results of this calculation for run AU0279B, shown in Figure IV-7, is typical. Although a simple reduction of the formaldehyde photolysis rate by a constant amount results in some improvement in the fit to the "timing" for ozone formation, it can be seen that the model is still not correctly predicting the rate of formaldehyde consumption, particularly in the initial stages of the experiment. Thus the effects of the chamber walls and floor on spectral distribution of the light inside the UNC chamber, and thus on the formaldehyde photolysis rates, are probably more complicated than a simple reduction in photolysis rates applicable at all zenith angles, as assumed in these test calculations.

Model simulations of most of the other types of runs carried out at UNC, using the standard model without assuming any chamber effects on the light within the chamber, in general do not indicate the types of discrepancies observed in the simulations of the formaldehyde experiments. Indeed, in contrast to the simulations of these formaldehyde runs, the model tends to underpredict the consumption rates of the other aldehydes and ketones in the UNC acetaldehyde-$NO_x$-air, propionaldehyde-$NO_x$ -air, and ketone-$NO_x$-air runs, as shown in Table IV-9. Furthermore, the simulations of most of the other groups of UNC runs do not indicate any consistent pattern of discrepancies in the fits which could be attributed to the model using inappropriately high aldehyde photolysis rates (see following sections). Thus the model simulations of the UNC chamber runs as a group do not unambiguously indicate any ways in which our representation of light within the UNC chamber can be improved, so no modifications of this were made in the standard model simulations of the UNC chamber runs. However, some modifications are likely to be appropriate once the effects of the walls and the floor of the UNC chamber are better understood.

One possible reason that the type of discrepancy observed in the model simulations of the UNC formaldehyde runs was not observed in the simulations of most of the other runs is that most runs did not have significant levels of formaldehyde or other photoinitiators present initially. The calculated photolysis rates are expected to be particularly uncertain during the initial part of the UNC chamber experiments when the zenith angle is large, and a discrepancy in the early part of the irradiation would result in discrepancies throughout the experiment. In most other runs, the photoinitiators present are formed as products, so their photolyses do not become as important until later in the day, when the uncertainties in calculated photolysis rates are expected to be less. This is less of a problem in the model simulations of the OTC runs, since the OTC irradiations generally do not begin until 0900 local standard time, significantly later in the day than the beginning of the irradiations in the UNC chamber, which are initiated by sunrise.

### 3. Acetaldehyde-$NO_x$-Air Runs

Five acetaldehyde-$NO_x$-air irradiations were modeled in this program, two carried out in the SAPRC EC and three in the UNC chamber. The observed and calculated ozone yields, NO oxidation times, and acetaldehyde half-lives are summarized in Table IV-9, and the observed and calculated maximum PAN and formaldehyde yields are summarized in Table IV-10. Observed and calculated concentration-time data for representative runs carried out in the EC and the UNC chamber are given in Figures IV-8 and IV-9, respectively.

As for the formaldehyde runs discussed above, the model performed better in the simulations of the EC experiments than for the UNC runs, though in this case the differences were much less. The simulations of the UNC runs tended to underpredict the ozone maximum yields, and simulations of runs in both chambers tended to underpredict the NO oxidation and ozone formation rates and acetaldehyde consumption rates. However, the discrepencies in the NO oxidation/ozone formation times were relatively small and the discrepancies for the aldehyde consumption rates were not as great, and, in the opposite direction, as those observed in the simulations of the formaldehyde runs. The model also underpredicted the formaldehyde yields observed in the UNC experiments, though this may reflect problems with the formaldehyde data, since this is observed for essentially all groups of UNC chamber runs where formaldehyde formation is observed. No systematic discrepancies are observed in the model simulations of the PAN yields in these acetaldehyde-$NO_x$-air experiments.

Table IV-10. Experimental and Calculated Yields of Selected Organic Products Observed in the Acetaldehyde, Propionaldehyde, and Ketone-$NO_x$-Air Runs

| Experiment | Species | Expt (ppm) | Calc (ppm) | Calc -Expt (ppm) | Calc -Expt /Expt |
|---|---|---|---|---|---|
| 1: EC Acetaldehyde Runs | | | | | |
| EC-164 | PAN | 0.026 | 0.017 | -0.009 | -0.34 |
| | Formaldehyde | 0.050 | 0.081 | 0.031 | 0.62 |
| EC-254 | PAN | 0.071 | 0.088 | 0.017 | 0.24 |
| | Formaldehyde | 0.037 | 0.068 | 0.031 | 0.83 |
| 2: UNC Acetaldehyde Runs | | | | | |
| AU0179R | PAN | 0.210 | 0.188 | -0.022 | -0.10 |
| | Formaldehyde | 0.410 | 0.137 | -0.273 | -0.67 |
| JN1482R | PAN | 0.226 | 0.271 | 0.045 | 0.20 |
| | Formaldehyde | 0.150 | 0.097 | -0.053 | -0.36 |
| AU2482B | PAN | 0.174 | 0.200 | 0.026 | 0.15 |
| | Formaldehyde | 0.190 | 0.108 | -0.082 | -0.43 |
| 3: UNC Propionaldehyde Runs | | | | | |
| JN1482B | PPN | 0.034 | 0.220 | 0.185 | 5.42 |
| | PAN | 0.027 | 0.048 | 0.021 | 0.77 |
| AU2482R | PAN | 0.077 | 0.059 | -0.018 | -0.23 |
| | Formaldehyde | 0.110 | 0.014 | -0.096 | -0.87 |
| 4: UNC Acetone Run | | | | | |
| JN0480R | PAN | 0.006 | 0.066 | 0.060 | 10.00 |
| 5: UNC Methyl Ethyl Ketone Runs | | | | | |
| OC2079R | Acetaldehyde | 0.155 | 0.104 | -0.052 | -0.33 |
| JN0480B | PAN | 0.070 | 0.092 | 0.022 | 0.31 |
| | Acetaldehyde | 0.070 | 0.046 | -0.024 | -0.34 |

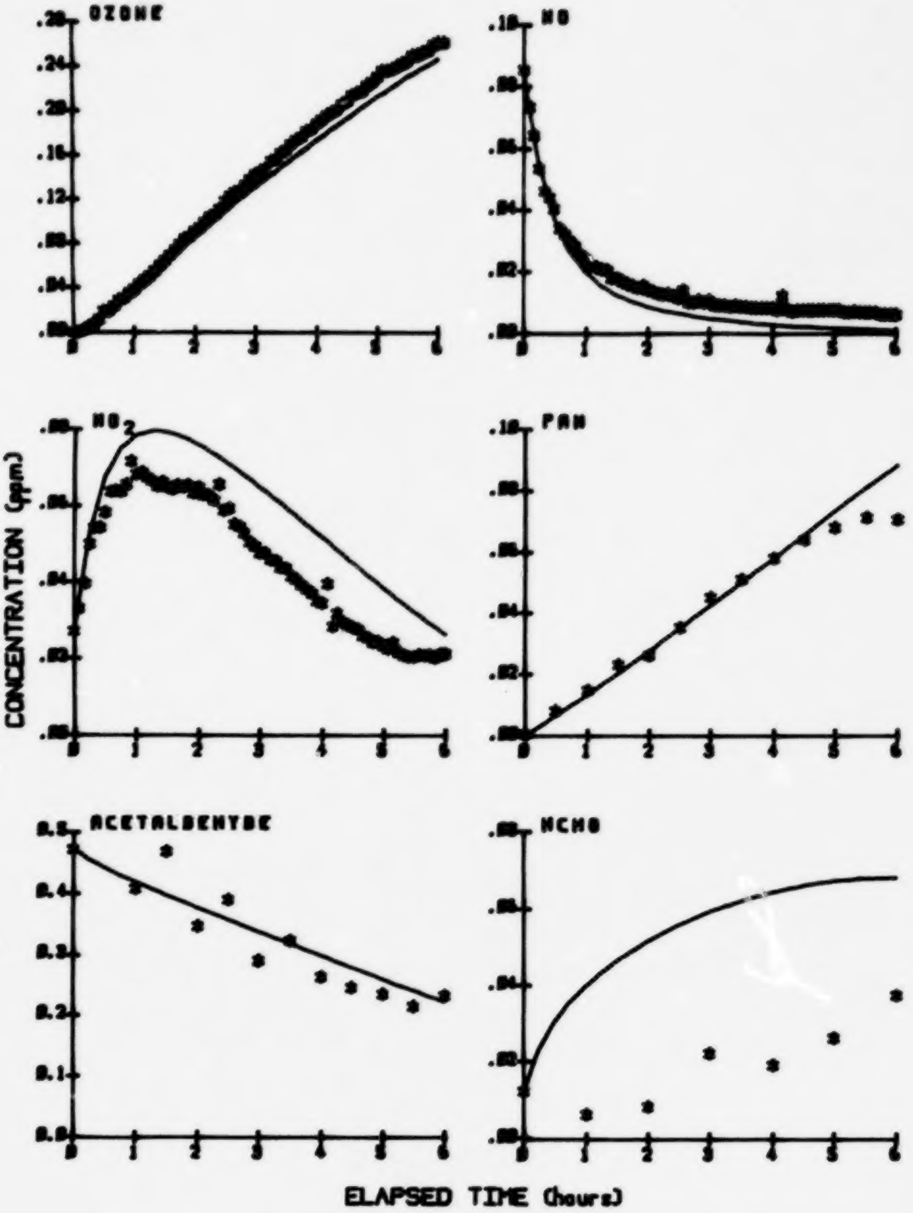

Figure IV-8. Experimental and calculated concentration-time profiles for selected species monitored in the acetaldehyde-NO$_x$-air run EC-254.

* = Experimental data.
―――― = Model calculation.

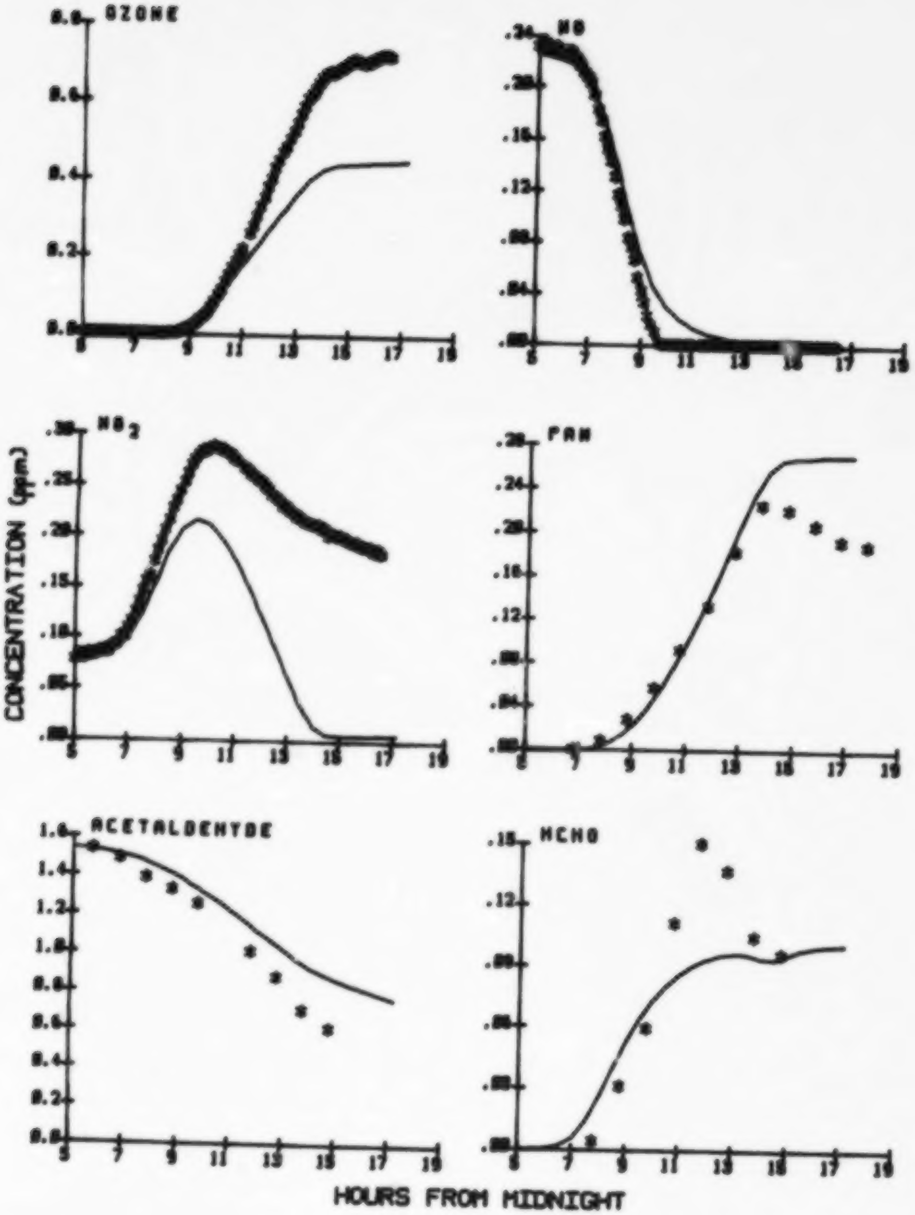

Figure IV-9. Experimental and calculated concentration-time profiles for selected species monitored in the UNC acetaldehyde-$NO_x$-air run JN1482R.
* = Experimental data.
----- = Model calculation.

### 4. Propionaldehyde-$NO_x$-Air Runs

Two propionaldehyde-$NO_x$-air irradiations were modeled in this program, both being carried out in the UNC chamber. The observed and calculated ozone yields and NO oxidation times are summarized in Table IV-9, and the observed and calculated propionaldehyde half-lives and maximum PAN, PPN, and formaldehyde yields are summarized in Table IV-10. The results of the model simulations of these two runs were similar, and Figure IV-10 shows the observed and calculated concentration-time data for one of those runs.

The model simulations of the UNC propionaldehyde runs were similar to those of the UNC acetaldehyde runs in that the ozone yields were overpredicted by approximately 35 percent in both runs. However, the model yielded good fits to the observed NO oxidation/ozone formation times, and had only a slight tendency to overpredict propionaldehyde consumption rates. (This slight overprediction of aldehyde consumption rates is consistent with the results of the simulations of the acetaldehyde runs, but contrasts with the results for formaldehyde, where consistent overprediction of the consumption rate is observed.) The fits to the PAN yields are variable, but do not indicate any systematic discrepancy in the model predictions. The model significantly overpredicts the PPN yield observed in the June 14, 1982 run, but, as indicated in Section IV-B-5, the accuracy of the experimental PPN data are highly uncertain.

### 5. Acetone-$NO_x$-Air and Methyl Ethyl Ketone-$NO_x$-Air Runs

One acetone-$NO_x$-air irradiation and two methyl ethyl ketone (MEK)-$NO_x$-air irradiations were carried out in the UNC chamber, with the acetone run and one of the MEK runs being carried out on the same day in different sides of the chamber. The observed and calculated ozone yields and NO oxidation times are summarized in Table IV-9, and the observed and calculated aldehyde half-lives and maximum PAN and acetaldehyde yields are summarized in Table IV-10. The observed and calculated concentration-time profiles for the acetone and the MEK irradiations carried out on June 4, 1980 are given in Figures IV-11 and IV-12, respectively.

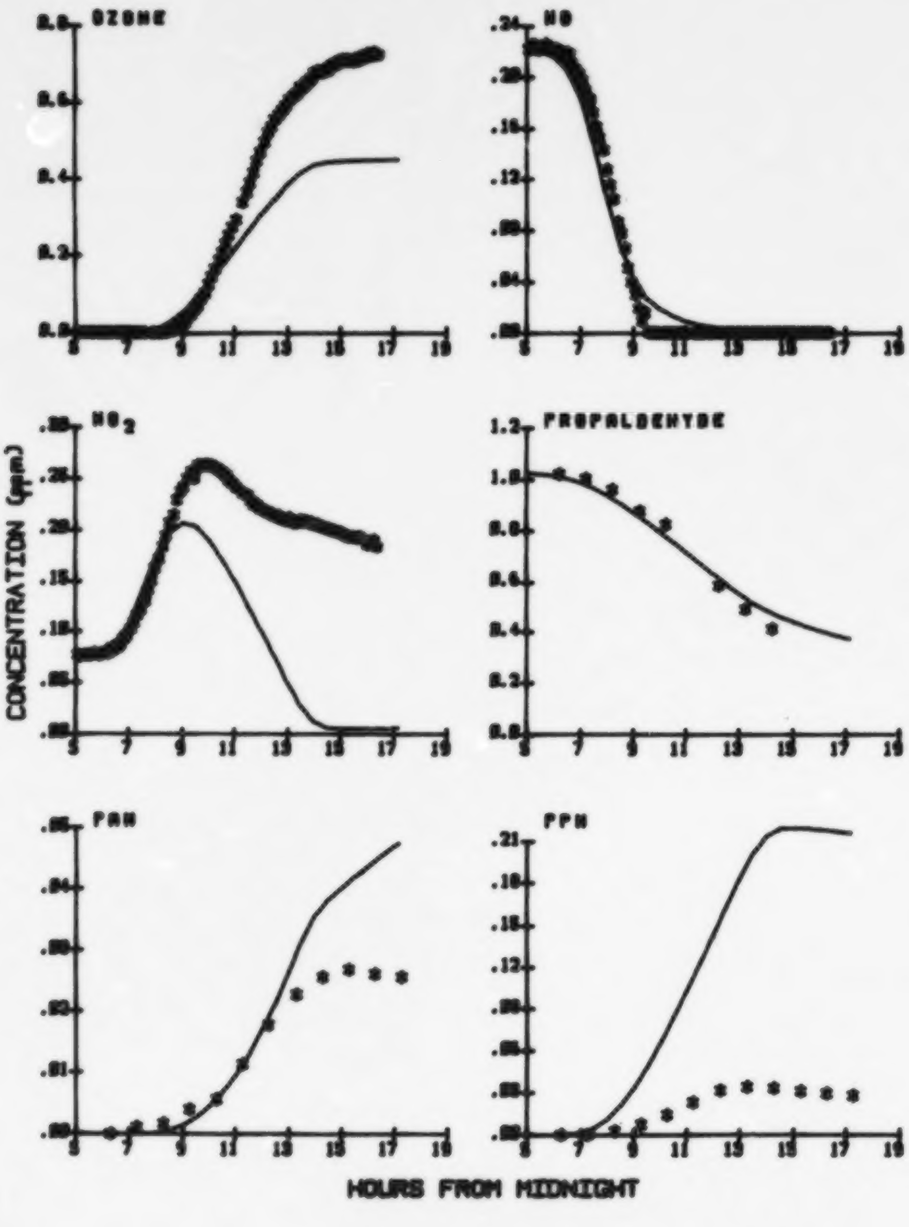

Figure IV-10. Experimental and calculated concentration-time profiles for selected species monitored in the UNC propionaldehyde-$NO_x$-air run JN1482B.
* = Experimental data.
----- = Model calculation.

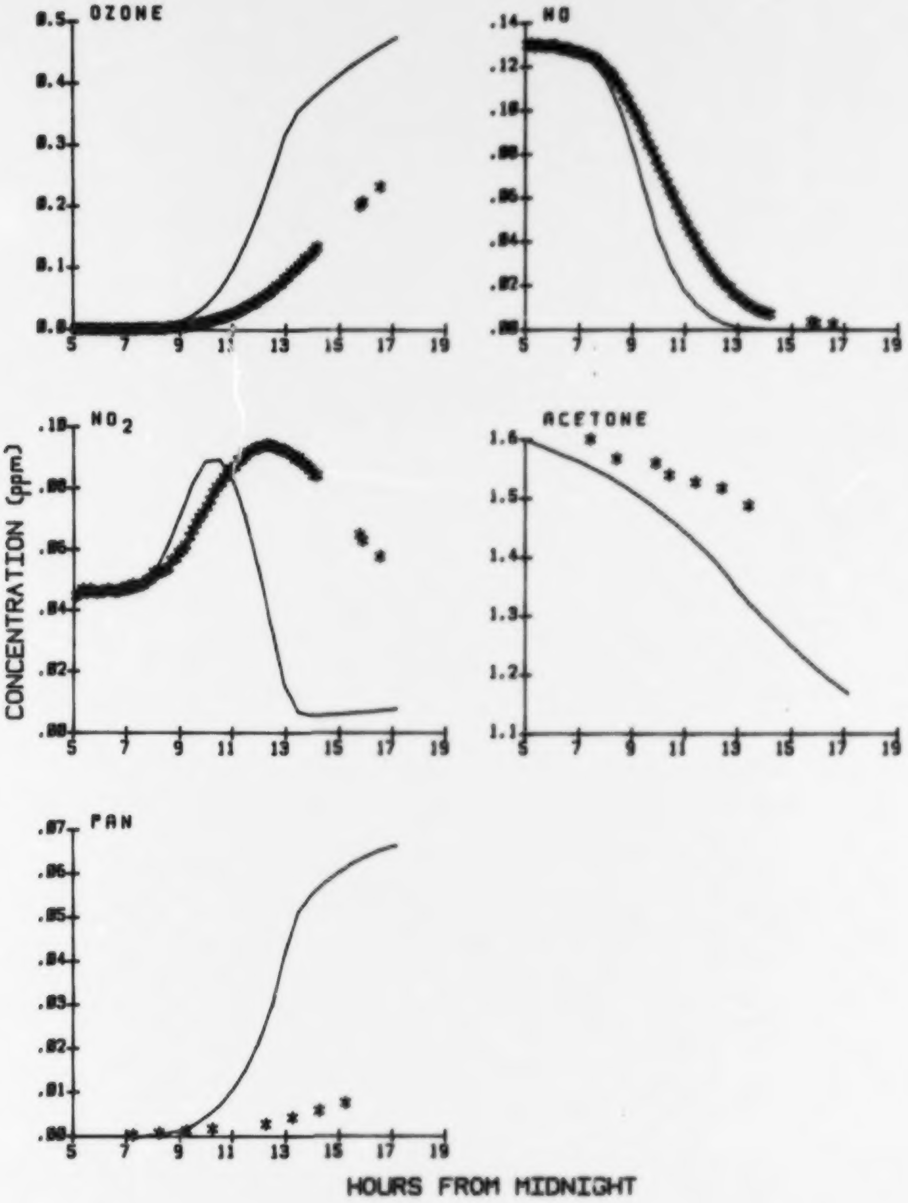

Figure IV-11. Experimental and calculated concentration-time profiles for selected species monitored in the UNC acetone-$NO_x$-air run JN0480B.
* = Experimental data.
----- = Model calculation.

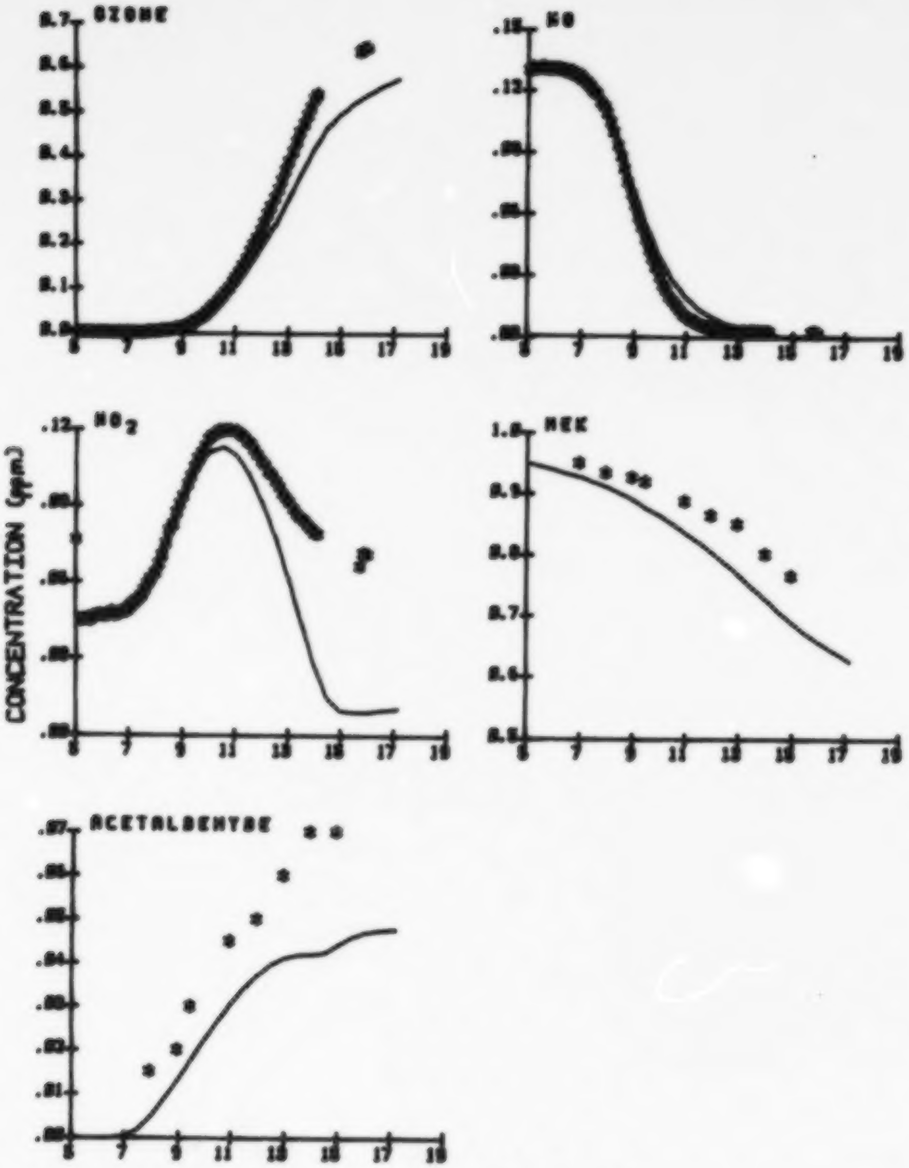

Figure IV-12. Experimental and calculated concentration-time profiles for selected species monitored in the UNC methyl ethyl ketone-$NO_x$-air run JN0480B.
* = Experimental data.
----- = Model calculation.

As shown in Figure IV-11, the model significantly overpredicted the reactivity observed in the acetone-$NO_x$-air irradiation. As discussed in Section II-C-4, the results of this run are much better simulated by assuming a zero quantum yield for acetone photolysis. However, because of the uncertainties in the light characterization for these experiments, adjusting the model to improve the fits to this run was not considered to be appropriate.

The fits of the model simulations to the results of the two UNC MEK runs were significantly better than the fits to the acetone runs, but, as was the case for the other UNC aldehyde and ketone runs (except for formaldehyde), the consumption rates of MEK tended to be underpredicted. The ozone maximum and acetaldehyde yields were slightly underpredicted in both runs, but the model gave a good fit to the PAN data for the June 4 run.

### 6. Ethene-$NO_x$-Air Runs

A total of 12 ethene-$NO_x$-air runs were modeled in this program, six carried out in the SAPRC EC and six in the UNC chamber. The observed and calculated ozone yields, NO oxidation times and ethene half-lives are summarized in Table IV-11, and the observed and calculated formaldehyde maximum yields are summarized in Tables IV-12. Three of the UNC ethene runs had Unisearch formaldehyde data as well as data from their standard technique (see Section IV-B-5-f), and a comparison of the model calculation results with the Unisearch formaldehyde is also shown in Table IV-12. Both the SAPRC and EC ethene runs consisted of two groups of runs carried out at different times, as indicated by the run numbers for the EC runs and the dates for the UNC runs. The results of the model simulations were consistent for runs within each of these four groups. Plots of experimental and calculated concentration-time data for runs representative of each of these groups are given in Figures IV-13 through IV-16.

As indicated in Tables IV-11 and IV-12 and Figures IV-13 and IV-14, the model tended to underpredict ozone yields and formation rates and ethene consumption rates in the earlier set of EC experiments, but tended to overpredict these aspects of reactivity in the simulations of the latter set of experiments. Interestingly, as indicated by the tables and Figures IV-15 and IV-16, the same is true of the UNC experiments -- the

Table IV-11. Initial Concentrations and Experimental and Calculated Ozone Maximum Yields, Times Required to Achieve Half the Maximum Experimental Change in ($[O_3]-[NO]$), and Ethene Half-Lives Observed in the Ethene-$NO_x$-Air Irradiations

| Experiment | Initial Concentrations | | | Maximum Ozone Concentration | | | | Time to 1/2 Maximum Expt. ($[O_3]-[NO]$) | | | | Reactant Half-Life | | | |
|---|---|---|---|---|---|---|---|---|---|---|---|---|---|---|---|
| | $NO_x$ (ppm) | HC (ppmC) | HC/$NO_x$ | Expt (ppm) | Calc (ppm) | Calc -Expt (ppm) | Calc -Expt /Expt | Expt (min) | #Calc (min) | Calc -Expt (min) | Calc -Expt /Expt | Expt (min) | Calc (min) | Calc -Expt (min) | Calc -Expt /Expt |
| **1: EC Runs** | | | | | | | | | | | | | | | |
| EC-142 | 0.480 | 1.9 | 4.1 | 0.782 | 0.577 | -0.205 | -0.26 | 171 | 210 | 39 | 0.23 | 222 | 282 | 60 | 0.27 |
| EC-143 | 0.500 | 4.1 | 8.1 | 1.087 | 0.858 | -0.229 | -0.21 | 86 | 129 | 43 | 0.49 | 155 | 222 | 68 | 0.44 |
| EC-156 | 0.500 | 4.0 | 8.0 | 1.105 | 0.816 | -0.289 | -0.26 | 83 | 130 | 47 | 0.56 | 153 | 222 | 69 | 0.45 |
| EC-285 | 1.006 | 3.9 | 3.9 | 0.840 | 1.082 | 0.242 | 0.29 | 161 | 128 | -33 | -0.20 | 265 | 240 | -25 | -0.09 |
| EC-286 | 0.945 | 7.5 | 8.0 | 1.081 | 1.283 | 0.202 | 0.19 | 76 | 61 | -15 | -0.20 | 174 | 159 | -16 | -0.09 |
| EC-287 | 0.528 | 8.0 | 15.2 | 0.965 | 1.107 | 0.142 | 0.15 | 49 | 39 | -11 | -0.22 | 171 | 152 | -19 | -0.11 |
| Group Average | 0.660 | 4.9 | 7.9 | 0.977 | 0.954 | -0.023 | -0.02 | 104 | 116 | 11 | 0.11 | 190 | 213 | 23 | 0.14 |
| S. Dev. | 0.246 | 2.4 | 4.1 | 0.139 | 0.252 | 0.243 | 0.25 | 50 | 61 | 35 | 0.37 | 45 | 50 | 47 | 0.27 |
| Avg. Abs. Value | | | | | | 0.218 | 0.23 | | | 30 | 0.32 | | | 43 | 0.24 |
| S. Dev. | | | | | | 0.049 | 0.05 | | | 15 | 0.17 | | | 25 | 0.17 |
| **2: UNC Runs** | | | | | | | | | | | | | | | |
| AU0479R | 0.227 | 0.9 | 3.9 | 0.729 | 0.547 | -0.082 | -0.25 | 368 | 459 | 84 | 0.26 | 359 | 430 | 71 | 0.20 |
| AU0579R | 0.638 | 4.1 | 6.4 | 1.294 | 1.114 | -0.180 | -0.14 | 372 | 376 | 4 | 0.01 | 351 | 379 | 28 | 0.08 |
| OC0584R | 0.365 | 3.1 | 8.5 | 0.856 | 1.013 | 0.157 | 0.18 | 379 | 321 | -59 | -0.15 | 405 | 330 | -75 | -0.19 |
| OC1184R | 0.348 | 2.9 | 8.2 | 0.858 | 1.104 | 0.246 | 0.29 | 373 | 320 | -54 | -0.14 | 315 | 251 | -64 | -0.20 |
| OC1284R | 0.721 | 2.7 | 3.7 | 0.495 | 0.621 | 0.126 | 0.25 | 441 | 395 | -46 | -0.10 | 539 | 478 | -62 | -0.11 |
| OC0584B | 0.370 | 1.8 | 4.9 | 0.675 | 0.791 | 0.115 | 0.17 | 443 | 390 | -53 | -0.12 | 506 | 421 | -86 | -0.17 |
| Group Average | 0.445 | 2.6 | 5.9 | 0.818 | 0.865 | 0.047 | 0.08 | 395 | 377 | -19 | -0.04 | 413 | 381 | -31 | -0.07 |
| S. Dev. | 0.191 | 1.1 | 2.1 | 0.269 | 0.248 | 0.183 | 0.22 | 37 | 52 | 61 | 0.16 | 91 | 81 | 64 | 0.17 |
| Avg. Abs. Value | | | | | | 0.168 | 0.21 | | | 51 | 0.13 | | | 64 | 0.16 |
| S. Dev. | | | | | | 0.047 | 0.06 | | | 29 | 0.08 | | | 20 | 0.05 |

**Table IV-12. Observed and Calculated Formaldehyde Yields in the Ethene-$NO_x$-Air Irradiations**

| Experiment | Expt (ppm) | Calc (ppm) | Calc -Expt (ppm) | Calc -Expt /Expt |
|---|---|---|---|---|
| **1: EC Runs** | | | | |
| EC-142 | 0.207 | 0.381 | 0.174 | 0.84 |
| EC-143 | 0.967 | 0.751 | -0.216 | -0.22 |
| EC-156 | 0.735 | 0.745 | 0.010 | 0.01 |
| EC-285 | 0.709 | 0.732 | 0.023 | 0.03 |
| EC-286 | 1.425 | 1.324 | -0.101 | -0.07 |
| EC-287 | 1.426 | 1.260 | -0.166 | -0.12 |
| Group average | | | -0.046 | 0.08 |
| Std. Dev. | | | 0.143 | 0.38 |
| Avg. Abs. Value | | | 0.115 | 0.22 |
| Std. Dev. | | | 0.085 | 0.31 |
| **2: UNC Runs** (Standard formaldehyde data) | | | | |
| AU0479R | 0.306 | 0.150 | -0.155 | -0.51 |
| AU0579R | 1.488 | 0.659 | -0.829 | -0.56 |
| OC0584R | 0.869 | 0.519 | -0.350 | -0.40 |
| OC1184R | 0.707 | 0.477 | -0.230 | -0.32 |
| OC1284R | 0.655 | 0.440 | -0.215 | -0.33 |
| OC0584B | 0.558 | 0.306 | -0.252 | -0.45 |
| Group average | | | -0.338 | -0.43 |
| Std. Dev. | | | 0.249 | 0.09 |
| Avg. Abs. Value | | | 0.338 | 0.43 |
| Std. Dev. | | | 0.249 | 0.09 |
| **2B: UNC Runs** (Unisearch formaldehyde data) | | | | |
| OC0584R | 0.550 | 0.519 | -0.031 | -0.06 |
| OC1184R | 0.465 | 0.477 | 0.012 | 0.03 |
| OC0584B | 0.342[a] | 0.306 | -0.036 | -0.11 |
| Group average | | | -0.018 | -0.05 |
| Std. Dev. | | | 0.026 | 0.07 |
| Avg. Abs. Value | | | 0.026 | 0.07 |
| Std. Dev. | | | 0.013 | 0.04 |

---

[a] Anomalously high dats points at end of run rejected.

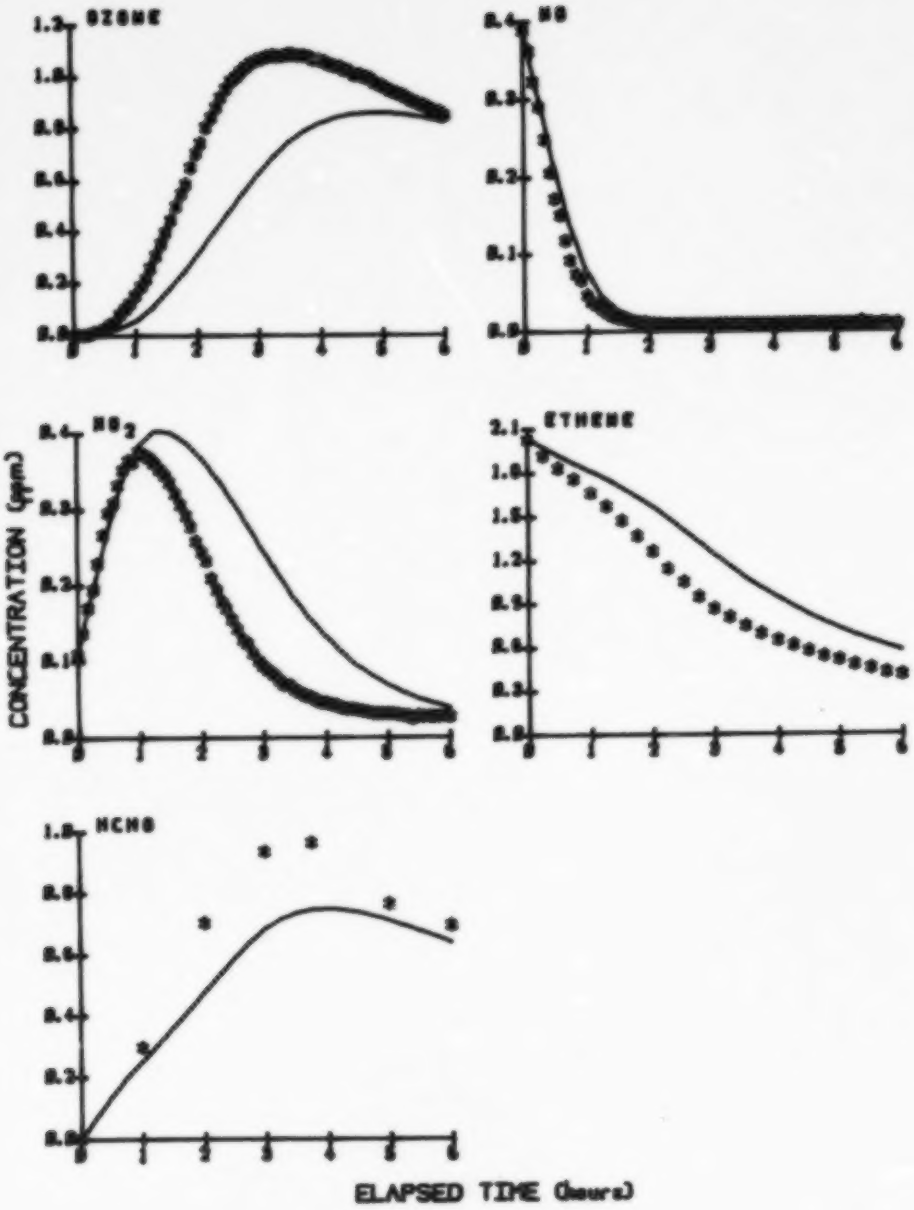

Figure IV-13. Experimental and calculated concentration-time profiles for selected species monitored in the ethene-$NO_x$-air run EC-143.

* = Experimental data.

---- = Model calculation.

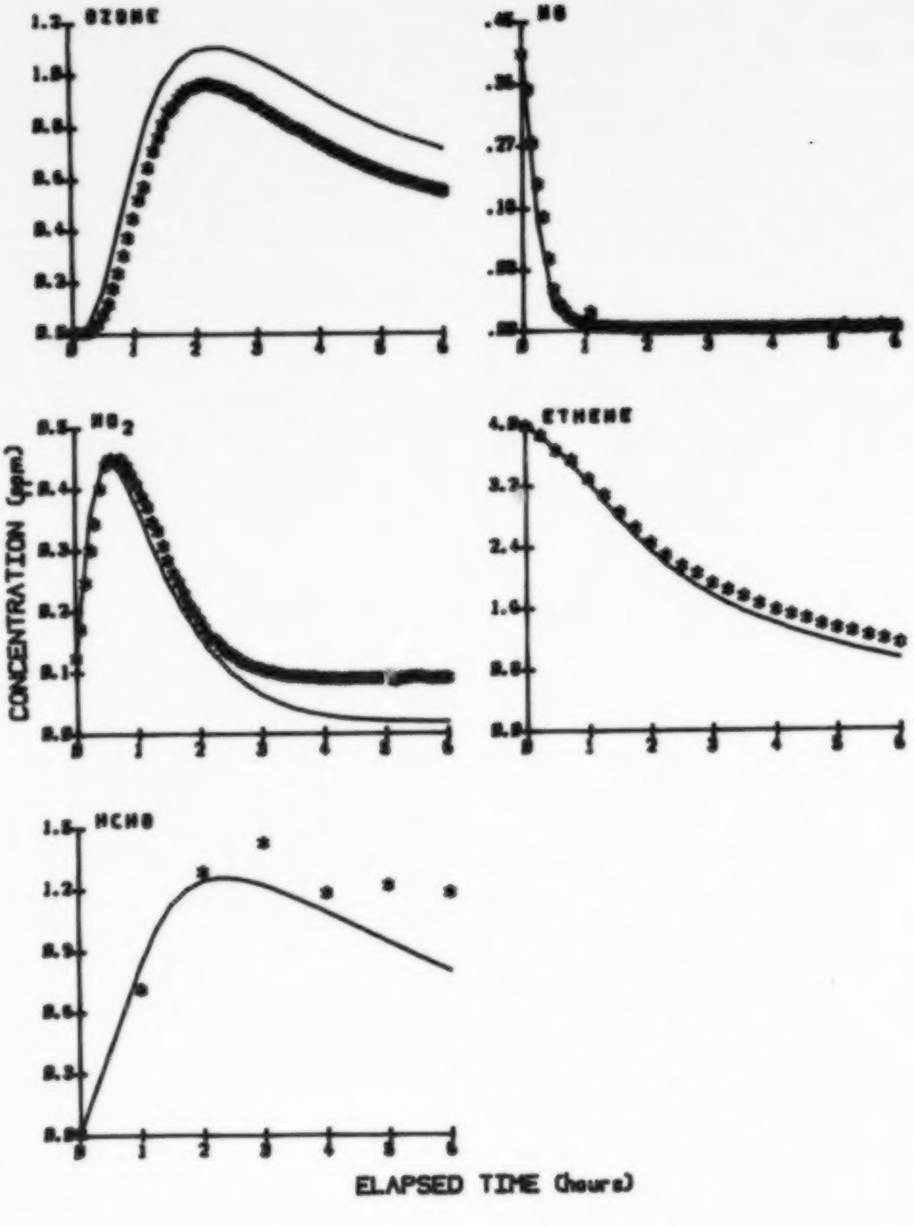

Figure IV-14. Experimental and calculated concentration-time profiles for selected species monitored in the ethene-$NO_x$-air run EC-287.

* = Experimental data.

----- = Model calculation.

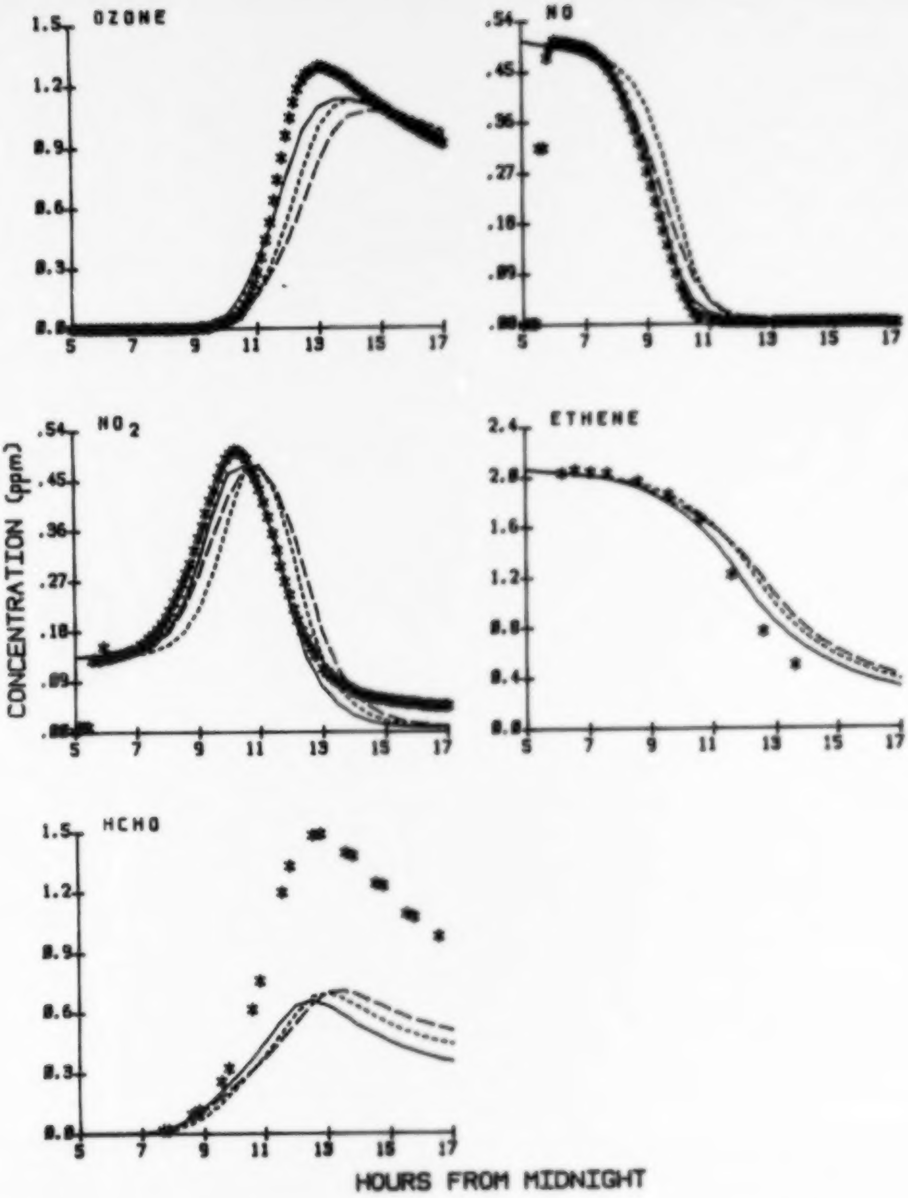

Figure IV-15. Experimental and calculated concentration-time profiles for selected species monitored in the UNC ethene-$NO_x$-air run AU0579R.

* = Experimental data.

—— = Model calculation, standard model.

-- -- = Model calculation, formaldehyde photolysis rate reduced by a factor of 0.65.

----- = Model calculation, formaldehyde offgassing from the wall at the rate of $k_1$ x 1 ppb.

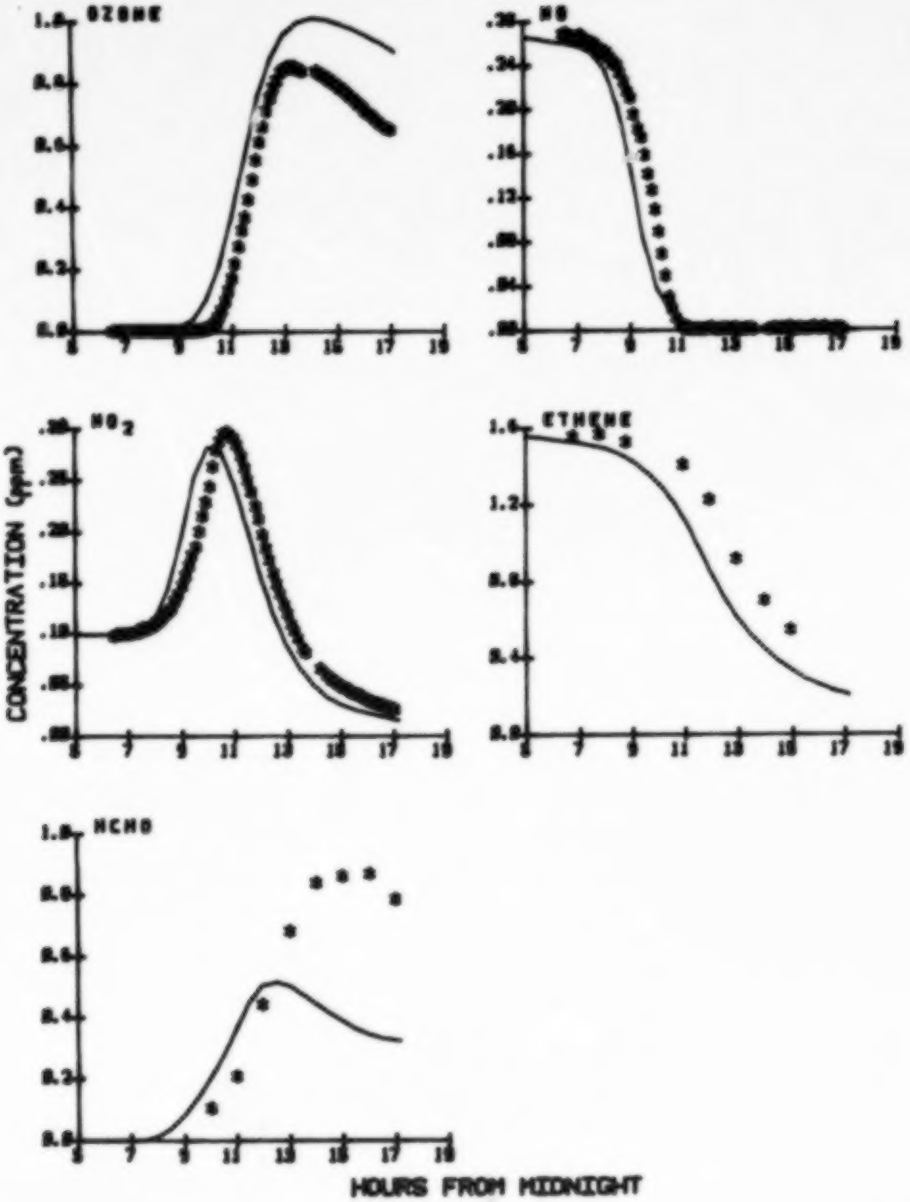

Figure IV-16. Experimental and calculated concentration-time profiles for selected species monitored in the UNC ethene-$NO_x$-air run OC0584R.

* = Experimental data.

——— = Model calculation.

reactivity tends to be underpredicted in the first group and overpredicted in the second. However, unlike many of the aldehyde runs discussed above, in general the model simulations of the ethene runs carried out in both chambers did not indicate any systematic discrepancies with regard to predictions of ozone formation, $NO_x$ oxidation, or reactant consumption rates.

The performance of the model in predicting formaldheyde yields is indicated in Table IV-12. Ethene forms formaldehyde in sufficiently large yields that the formaldehyde monitoring technique employed at UNC and SAPRC should yield usable data. It can be seen that for all but one of the SAPRC EC runs the model gave good fits to the formaldehyde yields, and in addition, the model gave very good fits to the formaldehyde data obtained by the Unisearch instrument in the three runs where such data are available. On the other hand, the formaldehyde measurements obtained by the standard UNC technique were consistently higher than the model predictions, for both the 1979 and the 1984 runs. Model simulations assuming the lower formaldehyde photolysis rates as assumed by Whitten et al. (1985) in their recent modeling of UNC data, or assuming formaldehyde offgassing from the UNC chamber walls at rates required to fit the chamber radical source (see Section III-B-2-c), shown in Figure IV-15, do not predict significantly higher maximum formaldehyde levels, and thus are also inconsistent with the UNC formaldehyde data. In view of the fact that the aspects of the ethene model which affect formaldehyde yields do not appear to be significantly uncertain (since they are based on the relatively straightforward laboratory results of Niki et al. (1981) -- see Section II-D-1], and the fact that the formaldehyde yields predicted by the ethene model appear to be consistent with the yields as measured both at SAPRC and in the UNC chamber using the Unisearch laser absorption technique, this strongly suggests that the UNC formaldehyde measurements may be consistently high, or suffer from interferences. The results of the modeling of the propene runs are consistent with this.

### 7. Propene-$NO_x$-Air Runs

By far the largest set of experiments which have been carried out in all four chambers and which have been modeled in this program are the propene-$NO_x$-air irradiations. This set includes 15 experiments carried out in the SAPRC EC, 22 carried out in the UNC chamber, 3 in the SAPRC OTC and 5 in the SAPRC ITC. In the case of the SAPRC EC and the UNC chamber, this large data set allows the propene experiments to be used for testing the consistency of the model in representing chamber effects over the entire time period during which most of the experiments modeled in this program were carried out, and assessing the variability of the experimental results relative to the model predictions.

The experimental and calculated ozone maximum yields and NO oxidation times for the propene-$NO_x$-air runs are summarized in Table IV-13. The propene decay rates and the maximum PAN, formaldehyde, and acetaldehyde yields are summarized in Table IV-14. Table IV-14 also shows the fits of the model calculation to the formaldehyde yields measured by Unisearch laser absorption technique for the three October, 1984, UNC runs for which such data are available. Distribution plots of the discrepancies in the model predictions of these data are given in Figure IV-17, and Figures IV-18 and IV-19, respectively, show plots of the discrepancies in the predictions of the ozone maxima and the NO oxidation and ozone formation timing parameter against the hydrocarbon/$NO_x$ ratio. Experimental and calculated concentration-time plots for EC propene runs carried out in 1977 and 1978, for UNC propene runs carried out in 1979 and 1984, and for recent, representative ITC and OTC propene runs are given in Figures IV-20 through IV-25, respectively.

In general, with a few exceptions the model simulations of the SAPRC propene runs were consistent and showed relatively little variability. The model has a tendency to overpredict the ozone, PAN, and aldehyde maxima and to underpredict the times required to achieve a given change in ($[O_3]-[NO]$) observed in the EC runs. Formaldehyde tended to be significantly overpredicted in a few EC runs, but this can be attributed to the periodic tendency of the SAPRC formaldehyde measurements to be anomalously low (see Section IV-B-5-f). If these runs are not counted, then the fits of the model to the formaldehyde yields observed in these runs are within

Table IV-13. Initial Concentrations and Experimental and Calculated Maximum Ozone Yields, Times Required to Achieve Half the Experimental Change in ($[O_3]-[NO]$), and Propene Half-Lives for the Propene-$NO_x$-Air Runs

| Experiment | Initial Concentrations | | | Maximum Ozone Concentration | | | | Time to 1/2 Maximum Expt. ($[O_3]-[NO]$) | | | | Reactant Half-Life | | | |
|---|---|---|---|---|---|---|---|---|---|---|---|---|---|---|---|
| | $NO_x$ (ppm) | HC (ppmC) | HC/$NO_x$ | Expt (ppm) | Calc (ppm) | Calc -Expt (ppm) | Calc -Expt /Expt | Expt (min) | Calc (min) | Calc -Expt (min) | Calc -Expt /Expt | Expt (min) | Calc (min) | Calc -Expt (min) | Calc -Expt /Expt |
| 1: EC Runs | | | | | | | | | | | | | | | |
| EC-121 | 0.511 | 1.4 | 2.8 | 0.506 | 0.506 | 0.000 | 0.00 | 61 | 107 | 46 | 0.76 | 56 | 111 | 55 | 0.97 |
| EC-177 | 0.463 | 1.5 | 3.2 | 0.540 | 0.500 | -0.040 | -0.07 | 115 | 110 | -5 | -0.04 | 95 | 116 | 21 | 0.22 |
| EC-216 | 0.515 | 1.6 | 3.1 | 0.564 | 0.596 | 0.032 | 0.06 | 116 | 83 | -33 | -0.29 | 105 | 89 | -16 | -0.16 |
| EC-217 | 0.479 | 0.6 | 1.3 | 0.149 | 0.279 | 0.130 | 0.87 | 235 | 126 | -109 | -0.46 | 116 | 122 | 6 | 0.05 |
| EC-230 | 0.518 | 1.8 | 3.4 | 0.186 | 0.322 | 0.137 | 0.74 | 91 | 51 | -40 | -0.44 | 15 | 15 | 0 | 0.00 |
| EC-256 | 0.564 | 0.3 | 0.6 | 0.002 | 0.010 | 0.007 | | 151 | 144 | -8 | -0.05 | 181 | 170 | -11 | -0.06 |
| EC-257 | 0.562 | 0.9 | 1.6 | 0.066 | 0.111 | 0.045 | 0.68 | 79 | 61 | -19 | -0.24 | 80 | 72 | -8 | -0.10 |
| EC-276 | 0.516 | 1.6 | 3.2 | 0.388 | 0.461 | 0.073 | 0.19 | 122 | 87 | -35 | -0.28 | 128 | 120 | -7 | -0.06 |
| EC-277 | 0.108 | 1.7 | 15.7 | 0.313 | 0.398 | 0.086 | 0.27 | 24 | 26 | 2 | 0.08 | 74 | 66 | -8 | -0.11 |
| EC-278 | 0.494 | 3.1 | 6.2 | 0.625 | 0.688 | 0.062 | 0.10 | 64 | 51 | -13 | -0.20 | 87 | 80 | -7 | -0.08 |
| EC-279 | 0.974 | 3.5 | 3.5 | 0.679 | 0.718 | 0.039 | 0.06 | 106 | 78 | -27 | -0.26 | 123 | 111 | -12 | -0.10 |
| EC-314 | 0.930 | 3.2 | 3.5 | 0.728 | 0.817 | 0.089 | 0.12 | 97 | 61 | -35 | -0.37 | 98 | 83 | -15 | -0.15 |
| EC-315 | 0.940 | 2.9 | 3.1 | 0.344 | 0.590 | 0.245 | 0.71 | 115 | 73 | -42 | -0.37 | 159 | 123 | -36 | -0.23 |
| EC-316 | 0.981 | 3.2 | 3.3 | 0.955 | 0.998 | 0.042 | 0.04 | 79 | 67 | -11 | -0.14 | 70 | 74 | 4 | 0.06 |
| EC-317 | 0.537 | 1.5 | 2.8 | 0.615 | 0.617 | 0.002 | 0.00 | 107 | 93 | -14 | -0.13 | 85 | 77 | -8 | -0.10 |
| Group Average | 0.606 | 1.9 | 3.8 | 0.444 | 0.507 | 0.063 | 0.27 | 104 | 81 | -23 | -0.16 | 98 | 95 | -3 | 0.01 |
| S. Dev. | 0.244 | 1.0 | 3.5 | 0.268 | 0.260 | 0.070 | 0.33 | 47 | 31 | 33 | 0.30 | 41 | 36 | 20 | 0.29 |
| Avg. Abs. Value | | | | | | 0.069 | 0.28 | | | 28 | 0.27 | | | 14 | 0.16 |
| S. Dev. | | | | | | 0.064 | 0.32 | | | 26 | 0.19 | | | 14 | 0.23 |

(continued)

Table IV-13 (continued) - 2

| Experiment | Initial Concentrations | | | Maximum Ozone Concentration | | | | Time to 1/2 Maximum Expt. ($[O_3]-[NO]$) | | | | Reactant Half-Life | | | |
|---|---|---|---|---|---|---|---|---|---|---|---|---|---|---|---|
| | $NO_x$ (ppm) | HC (ppmC) | $HC/NO_x$ | Expt (ppm) | Calc (ppm) | Calc -Expt (ppm) | Calc -Expt /Expt | Expt (min) | Calc (min) | Calc -Expt (min) | Calc -Expt /Expt | Expt (min) | Calc (min) | Calc -Expt (min) | Calc -Expt /Expt |
| **2: ITC Runs** | | | | | | | | | | | | | | | |
| ITC-693 | 0.491 | 3.3 | 6.7 | 0.779 | 0.707 | -0.072 | -0.09 | 114 | 100 | -14 | -0.13 | 126 | 125 | -1 | -0.01 |
| ITC-810 | 0.519 | 2.8 | 5.4 | 0.782 | 0.701 | -0.082 | -0.10 | 136 | 126 | -10 | -0.08 | 135 | 143 | 8 | 0.06 |
| ITC-860 | 0.521 | 3.0 | 5.7 | 0.585 | 0.730 | 0.145 | 0.25 | 137 | 94 | -43 | -0.31 | 142 | 133 | -8 | -0.06 |
| Group Average | 0.510 | 3.0 | 5.9 | 0.715 | 0.713 | -0.003 | 0.02 | 129 | 107 | -22 | -0.17 | 134 | 134 | 0 | 0.00 |
| S. Dev. | 0.017 | 0.3 | 0.7 | 0.113 | 0.015 | 0.128 | 0.20 | 13 | 17 | 18 | 0.12 | 8 | 9 | 8 | 0.06 |
| Avg. Abs. Value | | | | | | 0.100 | 0.15 | | | 22 | 0.17 | | | 6 | 0.04 |
| S. Dev. | | | | | | 0.040 | 0.09 | | | 18 | 0.12 | | | 4 | 0.03 |
| **3: OTC Runs** | | | | | | | | | | | | | | | |
| OTC-186 | 0.558 | 3.8 | 6.8 | 0.822 | 0.868 | 0.046 | 0.06 | 166 | 145 | -20 | -0.12 | 172 | 169 | -4 | -0.02 |
| OTC-191 | 0.540 | 3.6 | 6.7 | 0.903 | 1.098 | 0.195 | 0.22 | 65 | 63 | -3 | -0.04 | 74 | 79 | 5 | 0.07 |
| OTC-210 | 0.564 | 3.1 | 5.4 | 0.972 | 1.002 | 0.030 | 0.03 | 103 | 110 | 7 | 0.07 | | | | |
| OTC-233 | 0.457 | 3.0 | 6.6 | 0.633 | 0.934 | 0.301 | 0.48 | 133 | 90 | -43 | -0.33 | | | | |
| OTC-236 | 0.534 | 3.6 | 6.7 | 0.849 | 0.999 | 0.151 | 0.18 | 84 | 76 | -9 | -0.10 | | | | |
| Group Average | 0.531 | 3.4 | 6.4 | 0.836 | 0.980 | 0.145 | 0.19 | 110 | 97 | -14 | -0.10 | 123 | 124 | 1 | 0.02 |
| S. Dev. | 0.043 | 0.4 | 0.6 | 0.127 | 0.086 | 0.112 | 0.18 | 40 | 32 | 20 | 0.15 | 70 | 64 | 6 | 0.06 |
| Avg. Abs. Value | | | | | | 0.145 | 0.19 | | | 16 | 0.13 | | | 4 | 0.04 |
| S. Dev. | | | | | | 0.112 | 0.18 | | | 16 | 0.11 | | | 1 | 0.03 |

(continued)

Table IV-13 (continued) - 3

| Experiment | Initial Concentrations | | | Maximum Ozone Concentration | | | | Time to 1/2 Maximum Expt. ($[O_3]-[NO]$) | | | | Reactant Half-Life | | | |
|---|---|---|---|---|---|---|---|---|---|---|---|---|---|---|---|
| | $NO_x$ (ppm) | HC (ppmC) | $HC/NO_x$ | Expt (ppm) | Calc (ppm) | Calc -Expt (ppm) | Calc -Expt /Expt | Expt (min) | Calc (min) | Calc -Expt (min) | Calc -Expt /Expt | Expt (min) | Calc (min) | Calc -Expt (min) | Calc -Expt /Expt |
| **4: UNC Runs** | | | | | | | | | | | | | | | |
| JA1078R | 0.488 | 3.2 | 6.7 | 0.363 | 0.450 | 0.087 | 0.24 | 439 | 346 | -94 | -0.21 | 320 | 265 | -55 | -0.17 |
| OC2078R | 0.468 | 1.4 | 2.9 | 0.340 | 0.310 | -0.030 | -0.09 | 429 | 357 | -72 | -0.17 | 182 | 138 | -44 | -0.24 |
| OC2178R | 0.495 | 3.5 | 7.1 | 0.670 | 0.801 | 0.131 | 0.20 | 371 | 270 | -101 | -0.27 | 314 | 249 | -64 | -0.20 |
| JN1279R | 0.503 | 0.8 | 1.6 | 0.382 | 0.241 | -0.141 | -0.37 | 450 | 480 | 30 | 0.07 | 402 | 390 | -12 | -0.03 |
| JN1379R | 0.453 | 2.7 | 6.0 | 0.974 | 0.772 | -0.201 | -0.21 | 320 | 301 | -19 | -0.06 | 279 | 251 | -28 | -0.10 |
| AU0279R | 0.213 | 1.4 | 6.8 | 0.673 | 0.545 | -0.128 | -0.19 | 280 | 311 | 31 | 0.11 | 187 | 211 | 24 | 0.13 |
| JL1783R | 0.268 | 1.1 | 4.1 | 0.848 | 0.608 | -0.240 | -0.28 | 347 | 421 | 74 | 0.21 | 257 | 295 | 38 | 0.15 |
| JL2183R | 0.216 | 1.1 | 5.1 | 0.806 | 0.657 | -0.150 | -0.19 | 366 | 391 | 25 | 0.07 | 290 | 276 | -14 | -0.05 |
| JL3183R | 0.220 | 1.1 | 4.9 | 0.719 | 0.603 | -0.116 | -0.16 | 287 | 330 | 43 | 0.15 | 218 | 243 | 25 | 0.11 |
| OC0484R | 0.361 | 2.1 | 5.8 | 0.645 | 0.723 | 0.078 | 0.12 | 336 | 288 | -49 | -0.14 | 320 | 235 | -85 | -0.27 |
| OC1278B | 0.492 | 1.3 | 2.7 | 0.461 | 0.392 | -0.069 | -0.15 | 430 | 352 | -78 | -0.18 | 393 | 328 | -65 | -0.17 |
| OC2078B | 0.468 | 3.6 | 7.7 | 0.727 | 0.854 | 0.126 | 0.17 | 343 | 262 | -81 | -0.24 | 57 | 47 | -10 | -0.18 |
| OC2578B | 0.462 | 1.2 | 2.6 | 0.230 | 0.254 | 0.023 | 0.10 | 423 | 343 | -80 | -0.19 | 443 | 355 | -88 | -0.20 |
| JN1279B | 0.492 | 1.3 | 2.7 | 0.673 | 0.411 | -0.262 | -0.39 | 451 | 523 | 72 | 0.16 | 339 | 347 | 7 | 0.02 |
| AU2780B | 0.487 | 1.9 | 3.9 | 1.044 | 0.995 | -0.049 | -0.05 | 342 | 319 | -23 | -0.07 | 277 | 284 | 6 | 0.02 |
| ST0482B | 0.231 | 1.1 | 4.9 | 0.658 | 0.573 | -0.085 | -0.13 | 326 | 248 | -78 | -0.24 | 354 | 303 | -51 | -0.15 |
| ST1382B | 0.321 | 1.1 | 3.4 | 0.731 | 0.590 | -0.142 | -0.19 | 297 | 276 | -21 | -0.07 | 269 | 267 | -2 | -0.01 |
| JL2983B | 0.214 | 1.1 | 5.1 | 0.697 | 0.627 | -0.070 | -0.10 | 403 | 322 | -80 | -0.20 | 303 | 275 | -28 | -0.09 |
| ST2383B | 0.370 | 1.6 | 4.4 | 0.405 | 0.606 | 0.201 | 0.50 | 440 | 289 | -151 | -0.34 | 424 | 295 | -129 | -0.30 |
| OC0484B | 0.349 | 1.0 | 2.9 | 0.446 | 0.443 | -0.002 | -0.01 | 399 | 362 | -38 | -0.09 | 316 | 245 | -71 | -0.22 |
| OC1184B | 0.352 | 2.3 | 6.4 | 0.674 | 0.728 | 0.054 | 0.08 | 321 | 277 | -44 | -0.14 | 273 | 225 | -48 | -0.18 |
| OC1284B | 0.684 | 2.0 | 2.9 | 0.432 | 0.410 | -0.023 | -0.05 | 402 | 350 | -52 | -0.13 | 326 | 259 | -67 | -0.21 |
| Group Average | 0.391 | 1.7 | 4.6 | 0.618 | 0.572 | -0.046 | -0.05 | 373 | 337 | -36 | -0.09 | 297 | 263 | -35 | -0.11 |
| S. Dev. | 0.128 | 0.8 | 1.7 | 0.211 | 0.196 | 0.124 | 0.21 | 56 | 69 | 60 | 0.15 | 87 | 72 | 42 | 0.13 |
| Avg. Abs. Value | | | | | | 0.109 | 0.18 | | | 61 | 0.16 | | | 44 | 0.15 |
| S. Dev. | | | | | | 0.071 | 0.12 | | | 33 | 0.08 | | | 32 | 0.08 |

Table IV-14. Experimental and Calculated Maximum PAN, Acetaldehyde, and Formaldehyde Yields for the Propene-$NO_x$-Air Runs

| Experiment | Species | Expt (ppm) | Calc (ppm) | Calc -Expt (ppm) | Calc -Expt /Expt |
|---|---|---|---|---|---|
| 1: EC Runs | | | | | |
| EC-121 | PAN | 0.167 | 0.157 | -0.009 | -0.06 |
| | Acetaldehyde | 0.162 | 0.210 | 0.048 | 0.30 |
| | Formaldehyde | 0.278 | 0.224 | -0.054 | -0.19 |
| EC-177 | PAN | 0.165 | 0.185 | 0.020 | 0.12 |
| | Acetaldehyde | 0.186 | 0.215 | 0.029 | 0.16 |
| | Formaldehyde | 0.091 | 0.229 | 0.138 | 1.53 |
| EC-216 | PAN | 0.154 | 0.201 | 0.047 | 0.30 |
| | Acetaldehyde | 0.202 | 0.223 | 0.021 | 0.10 |
| | Formaldehyde | 0.181 | 0.260 | 0.079 | 0.44 |
| EC-217 | PAN | 0.019 | 0.038 | 0.019 | 1.05 |
| | Formaldehyde | 0.040 | 0.075 | 0.035 | 0.86 |
| EC-230 | PAN | 0.110 | 0.025 | -0.085 | -0.78 |
| | Formaldehyde | 0.266 | 0.295 | 0.029 | 0.11 |
| EC-256 | Acetaldehyde | 0.040 | 0.044 | 0.004 | 0.11 |
| EC-257 | Acetaldehyde | 0.037 | 0.049 | 0.012 | 0.32 |
| EC-276 | PAN | 0.100 | 0.136 | 0.036 | 0.36 |
| | Acetaldehyde | 0.192 | 0.237 | 0.045 | 0.24 |
| | Formaldehyde | 0.192 | 0.252 | 0.060 | 0.31 |
| EC-277 | PAN | 0.077 | 0.107 | 0.029 | 0.38 |
| | Acetaldehyde | 0.192 | 0.260 | 0.068 | 0.35 |
| | Formaldehyde | 0.213 | 0.242 | 0.029 | 0.14 |
| EC-278 | PAN | 0.260 | 0.263 | 0.003 | 0.01 |
| | Acetaldehyde | 0.378 | 0.464 | 0.086 | 0.23 |
| | Formaldehyde | 0.438 | 0.477 | 0.039 | 0.09 |
| EC-279 | PAN | 0.340 | 0.326 | -0.014 | -0.04 |
| | Acetaldehyde | 0.470 | 0.510 | 0.040 | 0.08 |
| | Formaldehyde | 0.522 | 0.531 | 0.009 | 0.02 |
| EC-314 | PAN | 0.226 | 0.379 | 0.153 | 0.68 |
| | Acetaldehyde | 0.441 | 0.476 | 0.035 | 0.08 |
| | Formaldehyde | 0.523 | 0.503 | -0.020 | -0.04 |

(continued)

Table IV-14 (continued) - 2

| Experiment | Species | Expt (ppm) | Calc (ppm) | Calc -Expt (ppm) | Calc -Expt /Expt |
|---|---|---|---|---|---|
| EC-315 | PAN | 0.116 | 0.294 | 0.178 | 1.53 |
| | Acetaldehyde | 0.382 | 0.421 | 0.038 | 0.10 |
| | Formaldehyde | 0.383 | 0.398 | 0.015 | 0.04 |
| EC-316 | PAN | 0.270 | 0.325 | 0.054 | 0.20 |
| | Acetaldehyde | 0.489 | 0.481 | -0.008 | -0.02 |
| | Formaldehyde | 0.586 | 0.533 | -0.053 | -0.09 |
| EC-317 | PAN | 0.130 | 0.194 | 0.064 | 0.49 |
| | Acetaldehyde | 0.205 | 0.217 | 0.013 | 0.06 |
| | Formaldehyde | 0.268 | 0.225 | -0.043 | -0.16 |
| Group Average | PAN | 0.164 | 0.202 | 0.038 | 0.33 |
| Std. Dev. | | 0.089 | 0.111 | 0.068 | 0.56 |
| Avg. Abs Value | | | | 0.055 | 0.46 |
| Std. Dev. | | | | 0.055 | 0.45 |
| Group Average | Acetaldehyde | 0.260 | 0.293 | 0.033 | 0.16 |
| Std. Dev. | | 0.155 | 0.161 | 0.026 | 0.11 |
| Avg. Abs Value | | | | 0.034 | 0.16 |
| Std. Dev. | | | | 0.024 | 0.11 |
| Group Average | Formaldehyde | 0.306 | 0.326 | 0.020 | 0.23 |
| Std. Dev. | | 0.172 | 0.146 | 0.055 | 0.48 |
| Avg. Abs Value | | | | 0.046 | 0.31 |
| Std. Dev. | | | | 0.034 | 0.43 |
| 2: ITC Runs | | | | | |
| ITC-693 | PAN | 0.311 | 0.254 | -0.057 | -0.18 |
| | Acetaldehyde | 0.320 | 0.534 | 0.214 | 0.67 |
| | Formaldehyde | 0.416 | 0.494 | 0.078 | 0.19 |
| ITC-810 | PAN | 0.140 | 0.231 | 0.091 | 0.65 |
| | Acetaldehyde | 0.174 | 0.447 | 0.273 | 1.57 |
| | Formaldehyde | 0.447 | 0.408 | -0.040 | -0.09 |
| ITC-860 | Acetaldehyde | 0.189 | 0.480 | 0.292 | 1.55 |
| | Formaldehyde | 0.617 | 0.440 | -0.177 | -0.29 |

(continued)

Table IV-14 (continued) - 3

| Experiment | Species | Expt (ppm) | Calc (ppm) | Calc -Expt (ppm) | Calc -Expt /Expt |
|---|---|---|---|---|---|
| Group Average | PAN | 0.225 | 0.242 | 0.017 | 0.23 |
| Std. Dev. | | 0.121 | 0.016 | 0.104 | 0.59 |
| Avg. Abs Value | | | | 0.074 | 0.42 |
| Std. Dev. | | | | 0.024 | 0.33 |
| Group Average | Acetaldehyde | 0.228 | 0.487 | 0.260 | 1.26 |
| Std. Dev. | | 0.081 | 0.044 | 0.041 | 0.51 |
| Avg. Abs Value | | | | 0.260 | 1.26 |
| Std. Dev. | | | | 0.041 | 0.51 |
| Group Average | Formaldehyde | 0.493 | 0.447 | -0.046 | -0.06 |
| Std. Dev. | | 0.109 | 0.044 | 0.128 | 0.24 |
| Avg. Abs Value | | | | 0.098 | 0.19 |
| Std. Dev. | | | | 0.071 | 0.10 |
| 3: OTC Runs | | | | | |
| OTC-186 | PAN | 0.260 | 0.300 | 0.040 | 0.15 |
| | Acetaldehyde | 0.508 | 0.596 | 0.088 | 0.17 |
| | Formaldehyde | 0.462 | 0.566 | 0.104 | 0.23 |
| OTC-191 | PAN | 0.190 | 0.270 | 0.080 | 0.42 |
| | Acetaldehyde | 0.433 | 0.569 | 0.136 | 0.31 |
| | Formaldehyde | 0.811 | 0.541 | -0.270 | -0.33 |
| OTC-210 | a | | | | |
| OTC-233 | a | | | | |
| OTC-236 | a | | | | |
| Group Average | PAN | 0.225 | 0.285 | 0.060 | 0.29 |
| Std. Dev. | | 0.049 | 0.021 | 0.028 | 0.19 |
| Avg. Abs Value | | | | 0.060 | 0.29 |
| Std. Dev. | | | | 0.028 | 0.19 |
| Group Average | Acetaldehyde | 0.470 | 0.582 | 0.112 | 0.24 |
| Std. Dev. | | 0.053 | 0.019 | 0.034 | 0.10 |
| Avg. Abs Value | | | | 0.112 | 0.24 |
| Std. Dev. | | | | 0.034 | 0.10 |
| Group Average | Formaldehyde | 0.636 | 0.554 | -0.083 | -0.05 |
| Std. Dev. | | 0.247 | 0.018 | 0.264 | 0.39 |
| Avg. Abs Value | | | | 0.187 | 0.28 |
| Std. Dev. | | | | 0.117 | 0.08 |

(continued)

Table IV-14 (continued) - 4

| Experiment | Species | Expt (ppm) | Calc (ppm) | Calc -Expt (ppm) | Calc -Expt /Expt |
|---|---|---|---|---|---|
| **4: UNC Runs** | | | | | |
| JA1078R | | | | | |
| OC2078R | PAN | 0.082 | 0.078 | -0.004 | -0.05 |
| | Formaldehyde | 0.440 | 0.158 | -0.282 | -0.64 |
| | Acetaldehyde | 0.190 | 0.187 | -0.003 | -0.01 |
| OC2178R | PAN | 0.162 | 0.275 | 0.113 | 0.70 |
| | Formaldehyde | 0.840 | 0.471 | -0.369 | -0.44 |
| | Acetaldehyde | 0.455 | 0.510 | 0.055 | 0.12 |
| JN1279R | PAN | 0.032 | 0.036 | 0.004 | 0.11 |
| | Acetaldehyde | 0.122 | 0.106 | -0.016 | -0.13 |
| JN1379R | PAN | 0.223 | 0.271 | 0.048 | 0.22 |
| | Formaldehyde | 0.410 | 0.374 | -0.036 | -0.09 |
| | Acetaldehyde | 0.419 | 0.397 | -0.022 | -0.05 |
| AU0279R | Formaldehyde | 0.440 | 0.212 | -0.228 | -0.52 |
| | Acetaldehyde | 0.201 | 0.209 | 0.007 | 0.04 |
| JL1783R | PAN | 0.086 | 0.103 | 0.017 | 0.19 |
| | Formaldehyde | 0.174 | 0.160 | -0.014 | -0.08 |
| | Acetaldehyde | 0.134 | 0.153 | 0.020 | 0.15 |
| JL2183R | PAN | 0.093 | 0.095 | 0.002 | 0.02 |
| | Formaldehyde | 0.214 | 0.164 | -0.050 | -0.23 |
| | Acetaldehyde | 0.124 | 0.156 | 0.032 | 0.26 |
| JL3183R | PAN | 0.088 | 0.113 | 0.025 | 0.28 |
| | Formaldehyde | 0.211 | 0.152 | -0.059 | -0.28 |
| | Acetaldehyde | 0.134 | 0.149 | 0.015 | 0.11 |
| OC0484R | PAN | 0.167 | 0.211 | 0.044 | 0.26 |
| | Formaldehyde | 0.424 | 0.285 | -0.139 | -0.33 |
| | (Unisearch Formaldehyde[b] | 0.268 | 0.285 | 0.017 | 0.06) |
| | Acetaldehyde | 0.293 | 0.300 | 0.007 | 0.02 |
| OC1278B | PAN | 0.069 | 0.095 | 0.026 | 0.38 |
| | Acetaldehyde | 0.214 | 0.185 | -0.029 | -0.14 |
| OC2078B | PAN | 0.241 | 0.287 | 0.046 | 0.19 |
| | Formaldehyde | 0.800 | 0.489 | -0.311 | -0.39 |
| | Acetaldehyde | 0.460 | 0.525 | 0.065 | 0.14 |

(continued)

Table IV-14 (continued) - 5

| Experiment | Species | Expt (ppm) | Calc (ppm) | Calc -Expt (ppm) | Calc -Expt /Expt |
|---|---|---|---|---|---|
| OC2578B | PAN | 0.050 | 0.063 | 0.013 | 0.27 |
| | Acetaldehyde | 0.166 | 0.170 | 0.004 | 0.03 |
| JN1279B | PAN | 0.134 | 0.131 | -0.003 | -0.02 |
| | Formaldehyde | 0.208 | 0.094 | -0.114 | -0.55 |
| AU2780B | PAN | 0.130 | 0.153 | 0.024 | 0.18 |
| ST0482B | PAN | 0.122 | 0.132 | 0.011 | 0.09 |
| ST1382B | PAN | 0.117 | 0.107 | -0.010 | -0.09 |
| JL2983B | PAN | 0.092 | 0.122 | 0.030 | 0.32 |
| | Formaldehyde | 0.185 | 0.154 | -0.030 | -0.16 |
| | Acetaldehyde | 0.129 | 0.155 | 0.026 | 0.20 |
| ST2383B | PAN | 0.099 | 0.206 | 0.107 | 1.07 |
| | Acetaldehyde | 0.215 | 0.231 | 0.016 | 0.08 |
| OC0484B | PAN | 0.086 | 0.088 | 0.002 | 0.02 |
| | Formaldehyde | 0.223 | 0.132 | -0.092 | -0.41 |
| | (Unisearch Formaldehyde | 0.128 | 0.132 | 0.004 | 0.03) |
| | Acetaldehyde | 0.145 | 0.142 | -0.003 | -0.02 |
| OC1184B | PAN | 0.180 | 0.226 | 0.047 | 0.26 |
| | Formaldehyde | 0.484 | 0.308 | -0.176 | -0.36 |
| | (Unisearch Formaldehyde | 0.322 | 0.308 | -0.014 | -0.04) |
| | Acetaldehyde | 0.287 | 0.326 | 0.038 | 0.13 |
| OC1284B | PAN | 0.144 | 0.124 | -0.020 | -0.14 |
| | Formaldehyde | 0.427 | 0.240 | -0.187 | -0.44 |
| | Acetaldehyde | 0.236 | 0.273 | 0.037 | 0.16 |
| Group Average | PAN | 0.120 | 0.146 | 0.026 | 0.21 |
| Std. Dev. | | 0.054 | 0.074 | 0.035 | 0.28 |
| Avg. Abs Value | | | | 0.030 | 0.24 |
| Std. Dev. | | | | 0.032 | 0.25 |
| Group Average | Formaldehyde | 0.391 | 0.242 | -0.149 | -0.35 |
| Std. Dev. | | 0.215 | 0.126 | 0.114 | 0.17 |
| Avg. Abs Value | | | | 0.149 | 0.35 |
| Std. Dev. | | | | 0.114 | 0.17 |
| Group Average | Acetaldehyde | 0.231 | 0.245 | 0.015 | 0.06 |
| Std. Dev. | | 0.115 | 0.127 | 0.026 | 0.11 |
| Avg. Abs Value | | | | 0.023 | 0.10 |
| Std. Dev. | | | | 0.018 | 0.07 |

[a] No data.

[b] Anomalously high data points at end of run rejected.

```
------------------------------------------------------------------------------
       Calc.-Expt.                          Calc.-Expt./Expt.
   Maximum Ozone (ppm)          Time to 1/2 Expt. Δ([O3]-[NO])max
------------------------------------------------------------------------------
       < -0.33     :                        < -0.55     :
 -0.33 - -0.27     :                  -0.55 - -0.45     :1
 -0.27 - -0.21     :44                -0.45 - -0.35     :111
 -0.21 - -0.15     :4                 -0.35 - -0.25     :1112344
 -0.15 - -0.09     :44444             -0.25 - -0.15     :114444444
 -0.09 - -0.03     :12244444          -0.15 - -0.05     :11122334444444
 -0.03 -  0.03     :1113444           -0.05 -  0.05     :13
  0.03 -  0.09     :111111113444       0.05 -  0.15     :134444
  0.09 -  0.15     :11244              0.15 -  0.25     :44
  0.15 -  0.21     :334                0.25 -  0.35     :
  0.21 -  0.27     :1                  0.35 -  0.45     :
  0.27 -  0.33     :3                  0.45 -  0.55     :
       >  0.33     :                        >  0.55     :1
------------------------------------------------------------------------------
      Calc.-Expt./Expt.                     Calc.-Expt./Expt.
     Propene Half-Lives                        PAN Yields
------------------------------------------------------------------------------
      < -0.5     :                          < -0.5     :1
 -0.5 - -0.4     :                     -0.5 - -0.4     :
 -0.4 - -0.3     :4                    -0.4 - -0.3     :
 -0.3 - -0.2     :144444               -0.3 - -0.2     :
 -0.2 - -0.1     :111444444            -0.2 - -0.1     :24
 -0.1 -  0.0     :11111122344444       -0.1 -  0.0     :11444
  0.0 -  0.1     :1112344               0.0 -  0.1     :1444
  0.1 -  0.2     :444                   0.1 -  0.2     :134444
  0.2 -  0.3     :1                     0.2 -  0.3     :144444
  0.3 -  0.4     :                      0.3 -  0.4     :11144
  0.4 -  0.5     :                      0.4 -  0.5     :13
      >  0.5     :1                         >  0.5     :111244
------------------------------------------------------------------------------
      Calc.-Expt./Expt.                     Calc.-Expt./Expt.
     Acetaldehyde Yields                   Formaldehyde Yields
------------------------------------------------------------------------------
      < -0.5     :                          < -0.5     :444
 -0.5 - -0.4     :                     -0.5 - -0.4     :444
 -0.4 - -0.3     :                     -0.4 - -0.3     :3444
 -0.3 - -0.2     :                     -0.3 - -0.2     :244
 -0.2 - -0.1     :44                   -0.2 - -0.1     :114
 -0.1 -  0.0     :1444                 -0.1 -  0.0     :11244UUU
  0.0 -  0.1     :1114444               0.0 -  0.1     :111
  0.1 -  0.2     :111134444444          0.1 -  0.2     :112
  0.2 -  0.3     :1114                  0.2 -  0.3     :3
  0.3 -  0.4     :113                   0.3 -  0.4     :1
  0.4 -  0.5     :                      0.4 -  0.5     :1
      >  0.5     :222                       >  0.5     :11
------------------------------------------------------------------------------
```

Figure IV-17. Distribution plots of the errors in the predicted maximum ozone yields, the times required to achieve one-half the maximum experimental change in ($[O_3]$-[NO]), the propene half-lives, and organic product yields observed in the propene-$NO_x$-air irradiations. Codes for chambers: 1 = EC, 2 = ITC, 3 = OTC, 4 = UNC, U = Fits to Unisearch formaldehyde data.

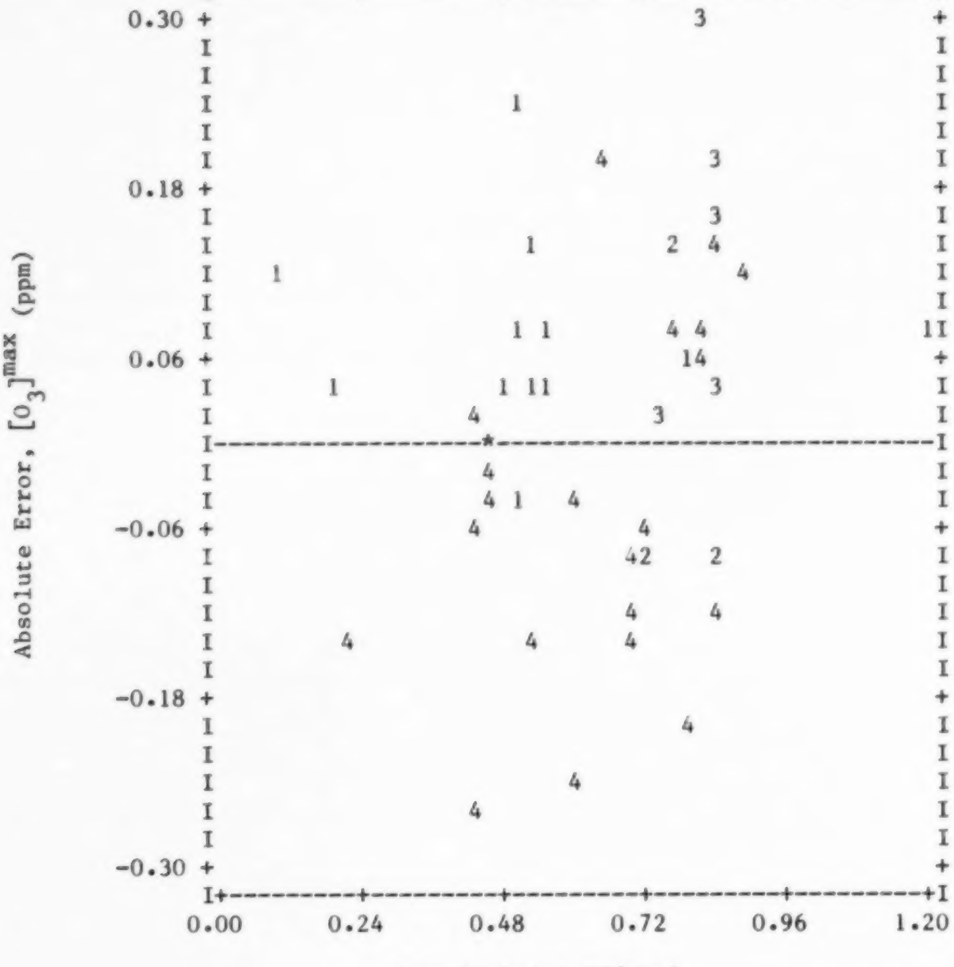

Figure IV-18. Plot of the discrepancies between the experimental and predicted ozone maximum yields against the log of the hydrocarbon/$NO_x$ ratio for the propene-$NO_x$-air runs. Codes for chambers: 1 = EC, 2 = ITC, 3 = OTC, 4 = UNC, * = overlap of 2 or more runs.

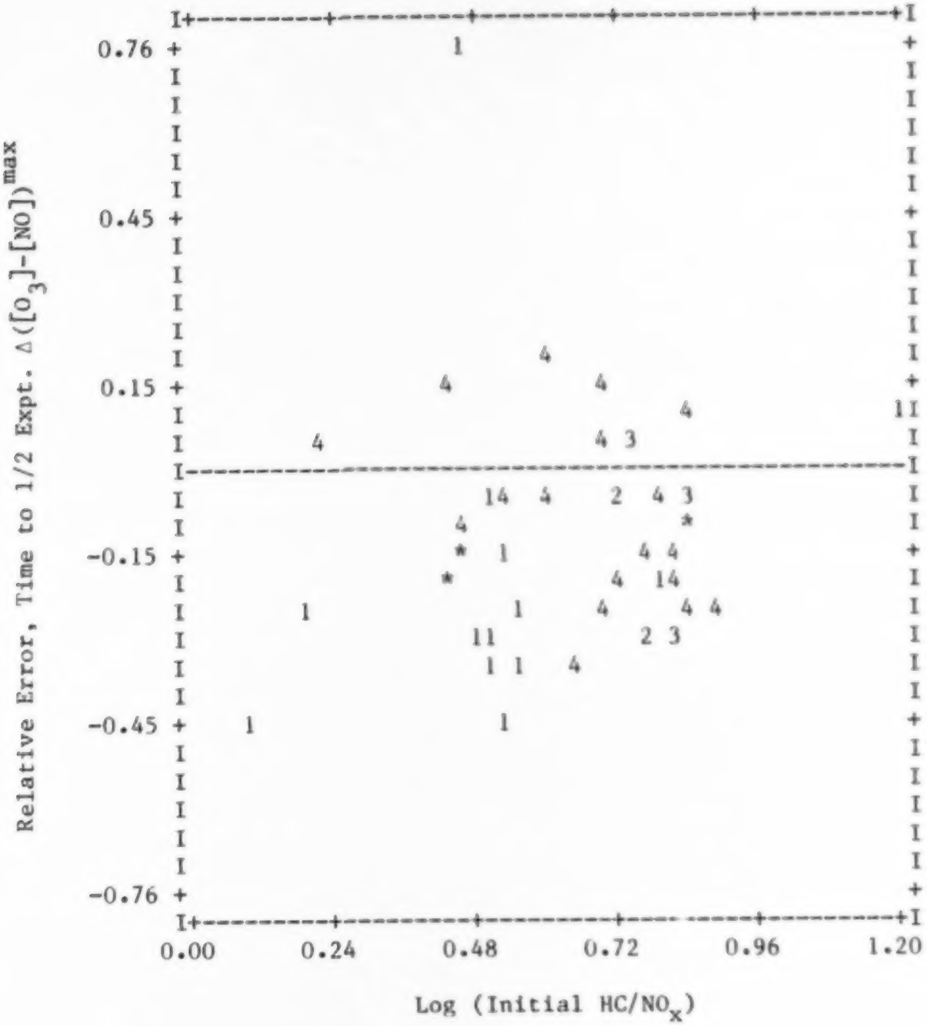

Figure IV-19 Plot of the discrepancies between the experimental and predicted times to achieve half the maximum experimental change in ($[O_3]$-[NO]) against the log of the hydrocarbon/$NO_x$ ratio for the propene-$NO_x$-air runs. Code for chambers: 1 = EC, 2 = ITC, 3 = OTC, 4 = UNC, * = overlap of 2 or more runs.

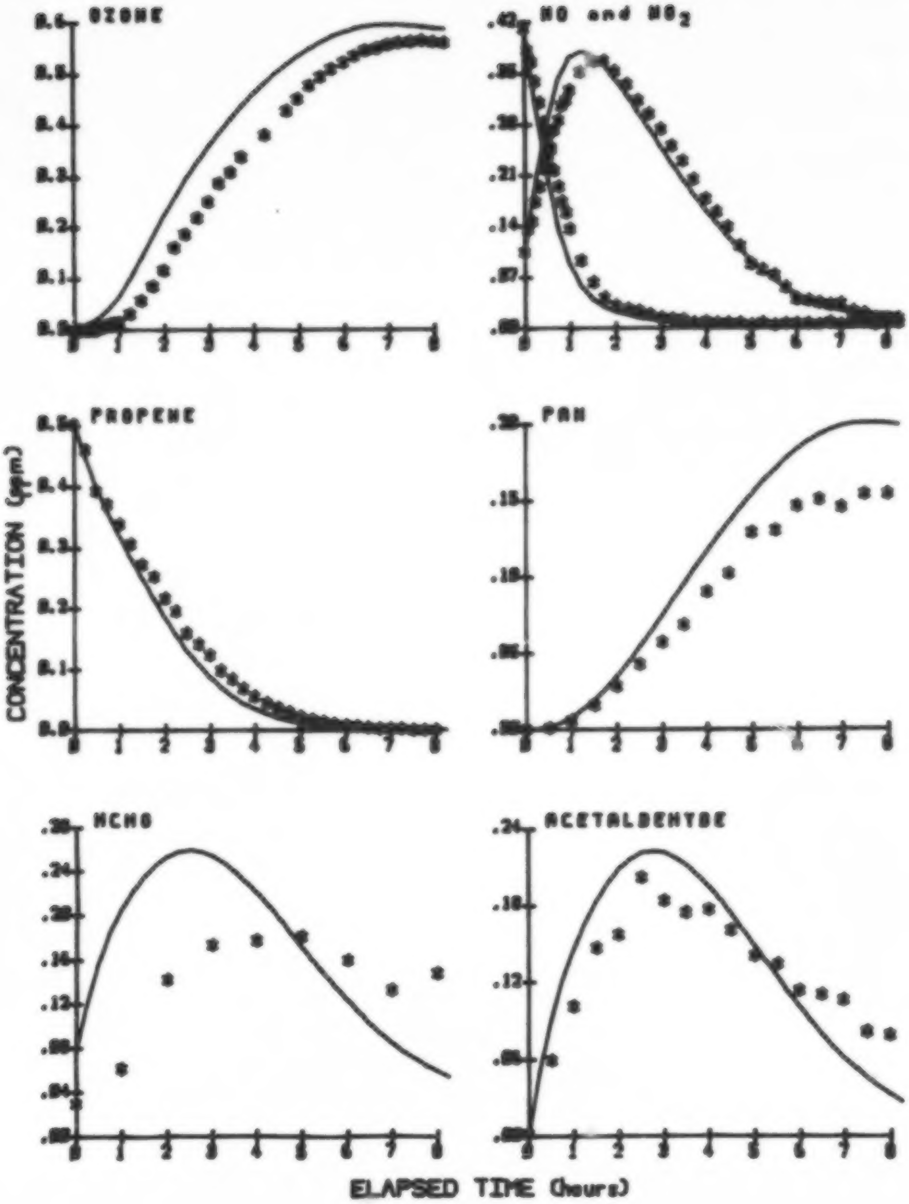

Figure IV-20. Experimental and calculated concentration-time profiles for selected species monitored in the propene-NO$_x$-air run EC-216.

* = Experimental data.

----- = Model calculation.

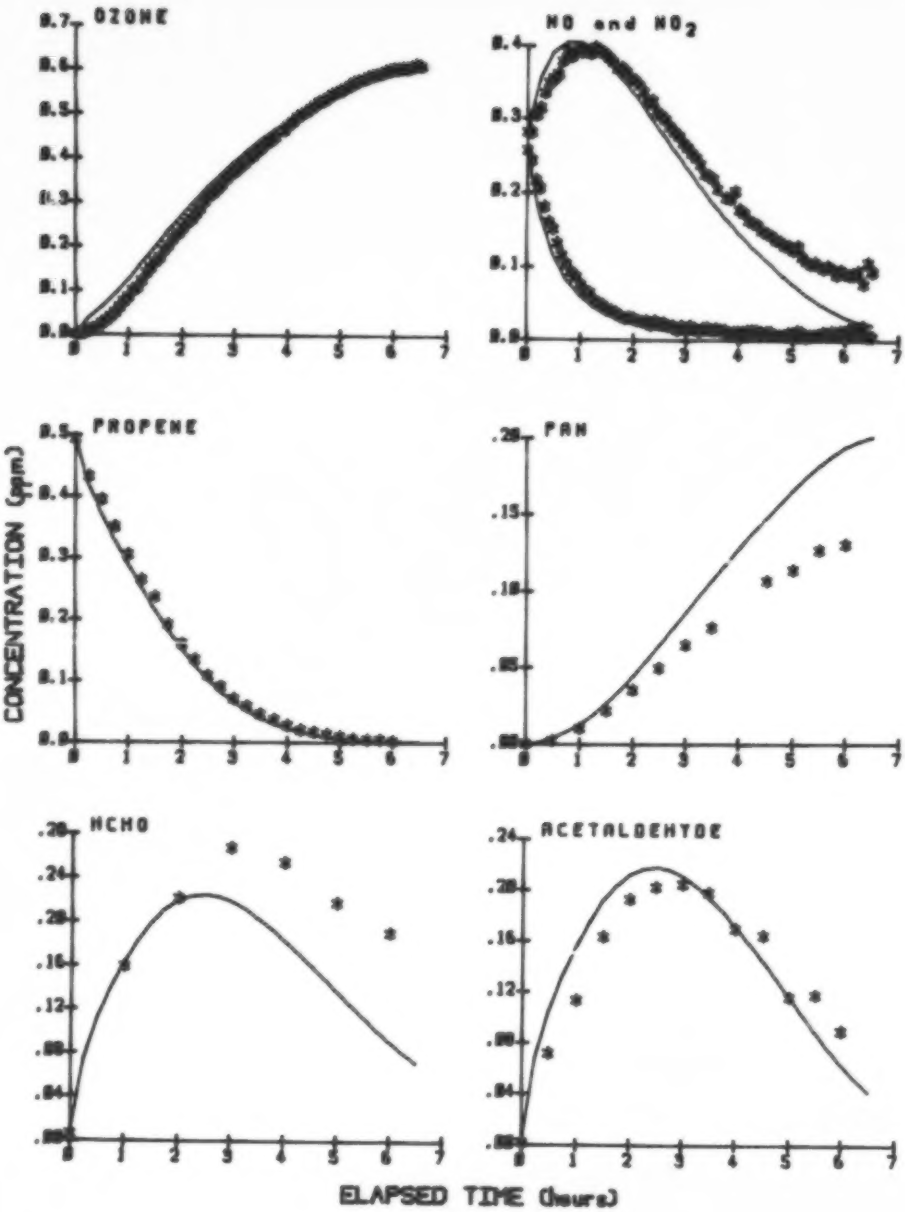

Figure IV-21. Experimental and calculated concentration-time profiles for selected species monitored in the propene-NO$_x$-air run EC-317.

* = Experimental data.

----- = Model calculation.

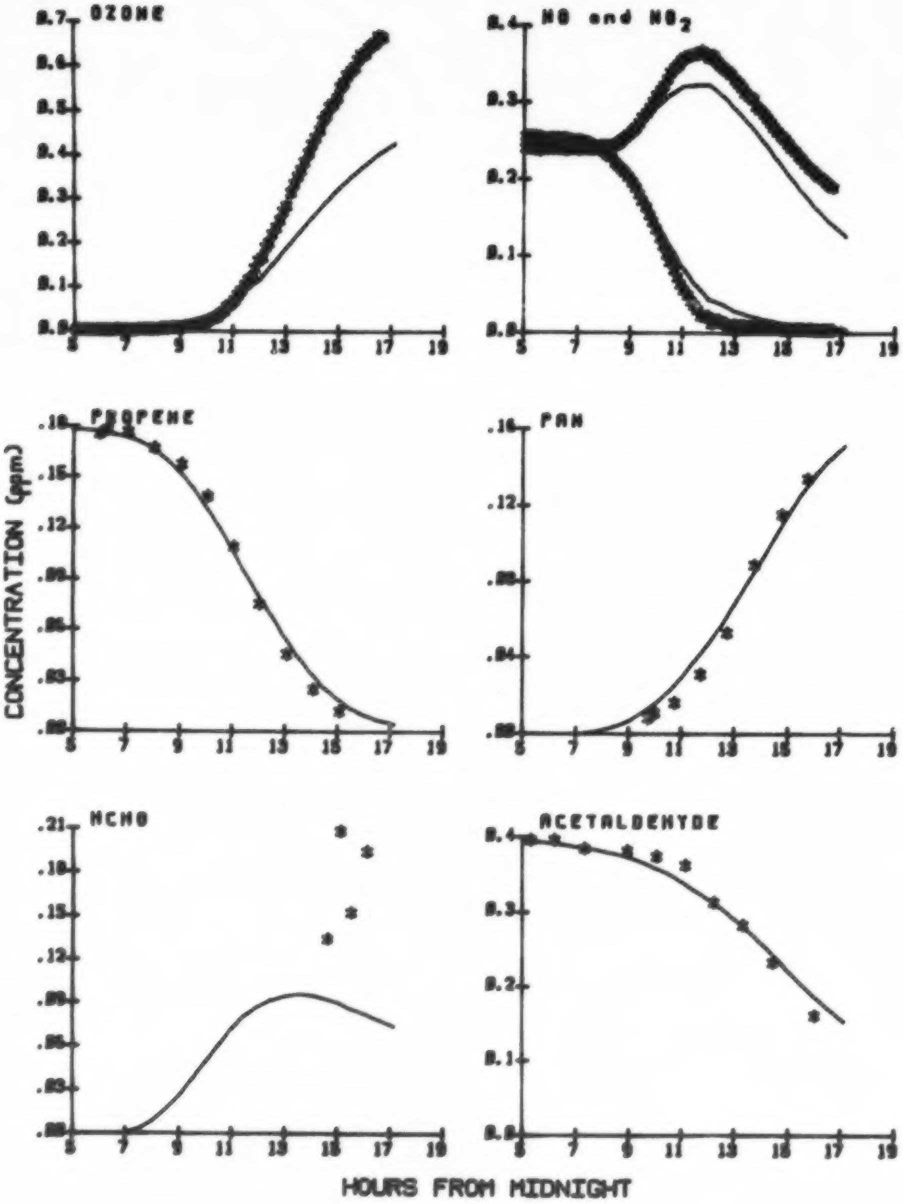

Figure IV-22. Experimental and calculated concentration-time profiles for selected species monitored in the UNC propene-$NO_x$-air run JN1279B.

* = Experimental data.

----- = Model calculation.

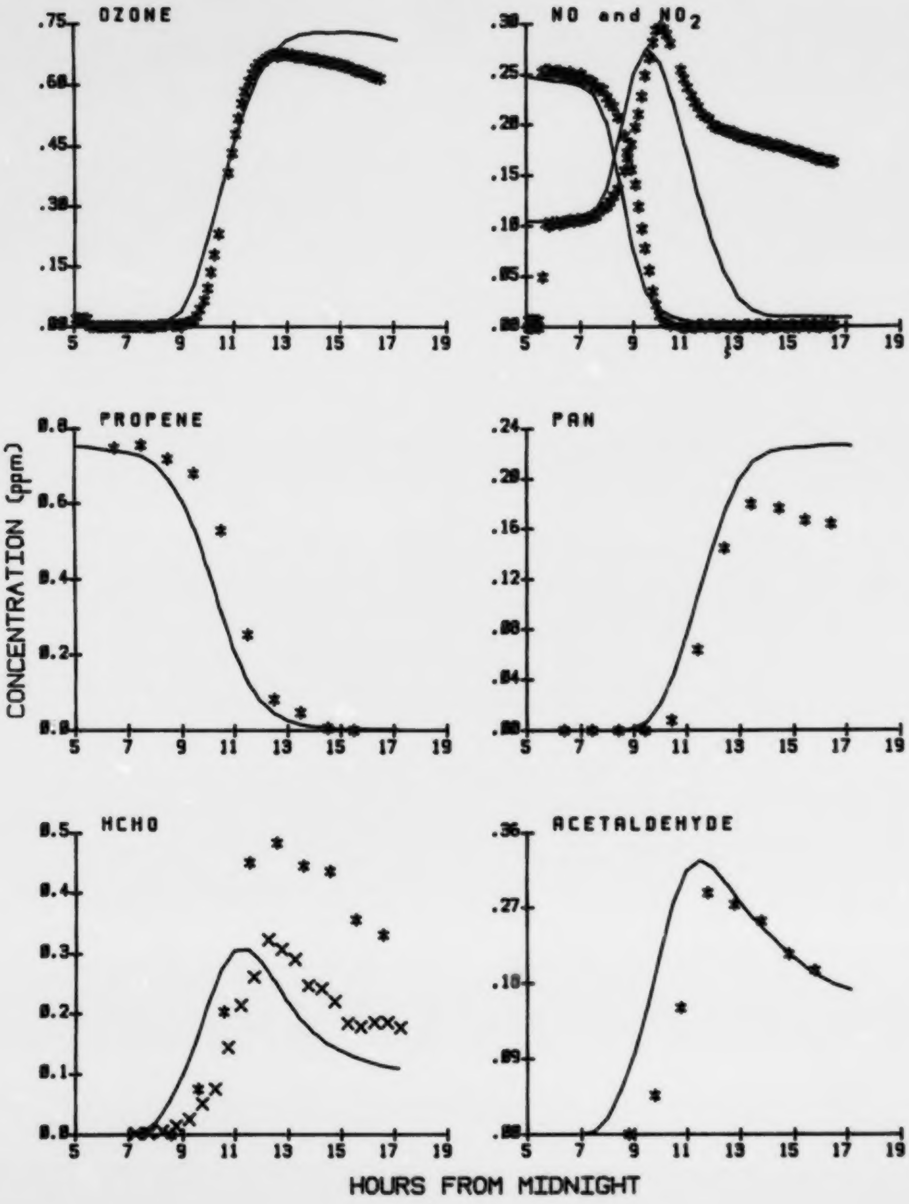

Figure IV-23. Experimental and calculated concentration-time profiles for selected species monitored in the UNC propene-$NO_x$-air run OC1184B.
* = Experimental data.
----- = Model calculation.
(x = Unisearch data).

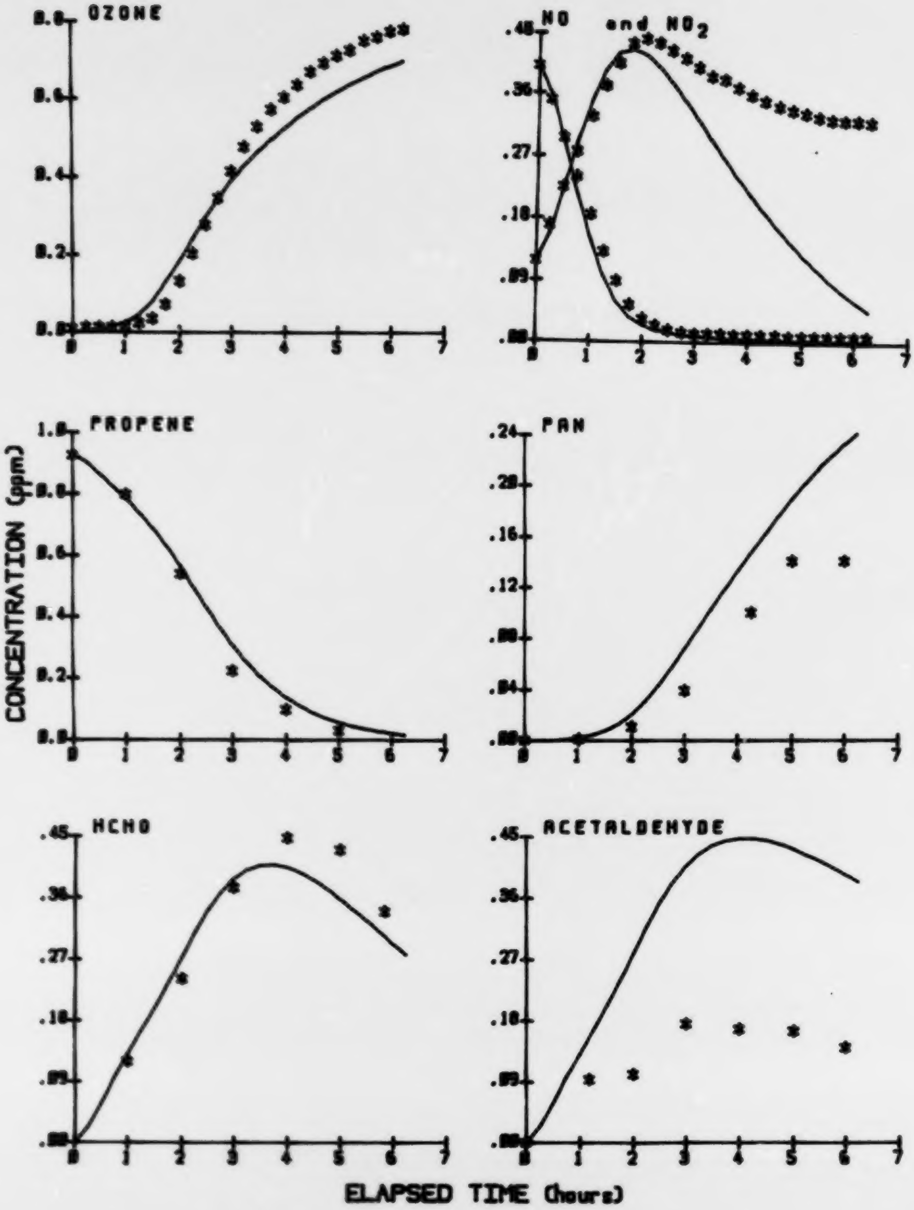

Figure IV-24. Experimental and calculated concentration-time profiles for selected species monitored in the propene-$NO_x$-air run ITC-810.

* = Experimental data.

---- = Model calculation.

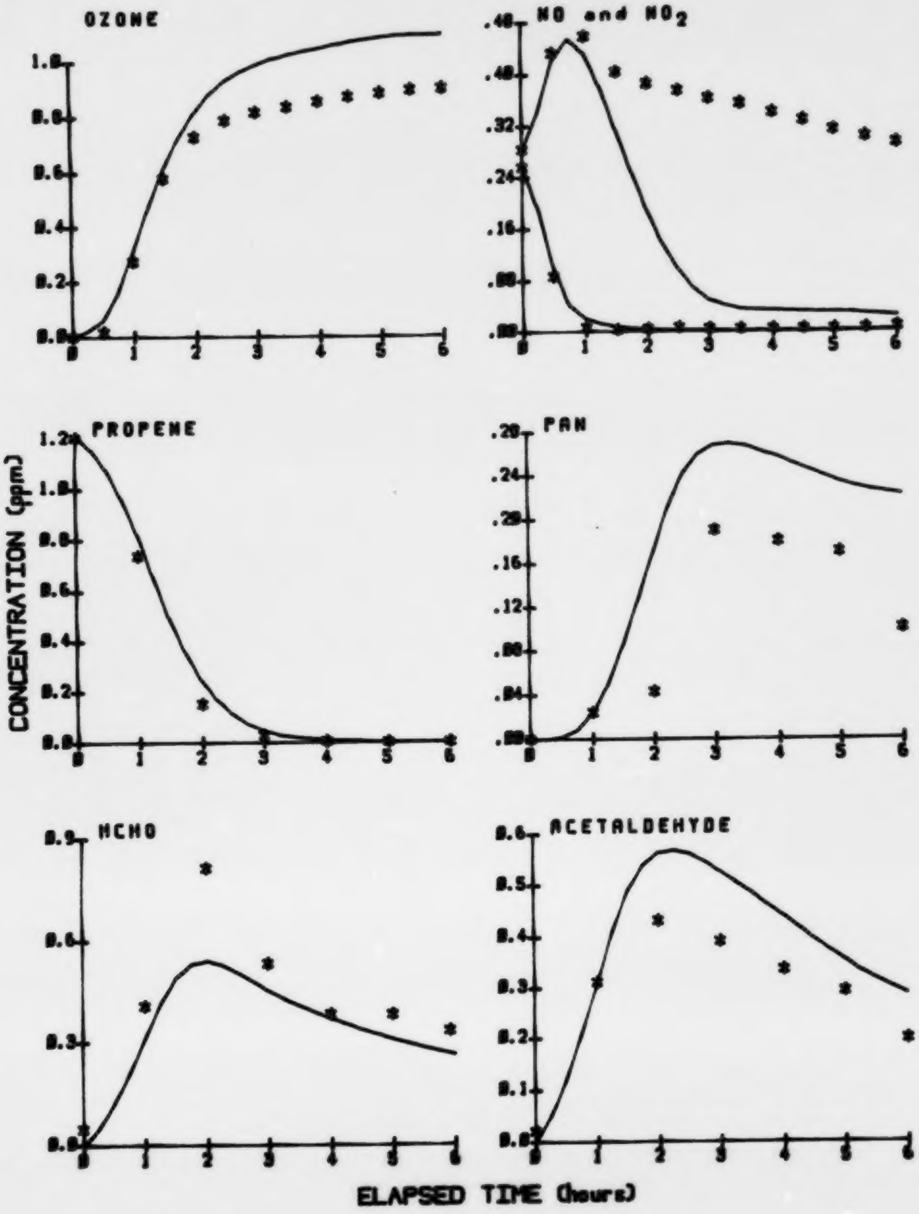

Figure IV-25. Experimental and calculated concentration-time profiles for selected species monitored in the propene-$NO_x$-air run OTC-191.
* = Experimental data.
----- = Model calculation.

the analytical uncertainty. The fits for the SAPRC ITC and OTC propene runs are of a similar quality as those for the EC runs, despite the differences in the chamber employed and the greater uncertainties involved in modeling the OTC runs relative to the indoor chamber runs. As shown in Figures IV-18 and IV-19, there appears to be no systematic dependence of the discrepancies in the model predictions of the reactivity observed in these experiments on the the hydrocarbon/$NO_x$ ratio.

The fits of the model simulations to the results of the propene runs carried out at UNC are much more variable, though, as shown in Figures IV-18 and IV-19, these discrepancies do not appear to have any systematic dependence on the propene/$NO_x$ ratio, and similar plots against initial propene or initial $NO_x$ also do not indicate any systematic discrepancies. Indeed, despite the relatively large variability in the quality of the fits, on the average the model gives good fits to the maximum ozone yields, the NO oxidation "timing" parameter, and the acetaldehyde yields, and the average discrepancy for the fits to the PAN yields is probably within the calibration uncertainty for that compound. As with the ethene runs, the model underpredicted the formaldehyde yields as when measured by the standard UNC formaldehyde technique, but gave very good fits to the Unisearch formaldehyde data for the three runs which had such data (Table IV-14).

The variability of the model fits to the UNC propene runs does not appear to be due to the fact that the runs were carried out over a period of several years, since, as shown in Figure IV-26, the variability of the fits for the 1982-1984 runs is almost as great as that for the 1978-1979 runs. Thus the exact reason for this greater variability in simulating the UNC chamber experiments is not known, but it is consistent with the greater uncertainties associated with modeling outdoor chamber experiments, particularly with regard to light characterization.

### 8. 1-Butene-$NO_x$-Air Runs

Three 1-butene-$NO_x$-air runs carried out in the SAPRC EC and four carried out in the UNC chamber were modeled in this program. For each of these chambers, the runs were carried out around the same time period, as indicated by the run numbers for the EC runs and the dates for the UNC

| Calculated-Observed $[O_3]$ Maximum (ppb) | 1978-1979 | 1982-1984 |
|---|---|---|
| < -0.33 | : | : |
| -0.33 - -0.27 | : | : |
| -0.27 - -0.21 | :9 | :3 |
| -0.21 - -0.15 | :9 | : |
| -0.15 - -0.09 | :99 | :233 |
| -0.09 - -0.03 | :88 | :23 |
| -0.03 - 0.03 | -:8 | -:44 |
| 0.03 - 0.09 | :8 | :44 |
| 0.09 - 0.15 | :88 | : |
| 0.15 - 0.21 | : | : |
| 0.21 - 0.27 | : | : |
| 0.27 - 0.33 | : | : |
| > 0.33 | : | : |

Figure IV-26. Summary of distributions of discrepancies in the maximum ozone yields observed in the model simulations of the propene-$NO_x$-air runs carried out in the UNC outdoor chamber. Symbols for UNC runs coded by year: 8 = 1978, 9 = 1979, 2 = 1982, 3 = 1983, 4 = 1984.

runs. The experimental and calculated ozone yields, NO oxidation and ozone formation timing parameters, and 1-butene half-lives are summarized in Table IV-15, and the PAN, PPN, and aldehyde product yields are summarized on Table IV-16. Experimental and calculated concentration-time plots for representative 1-butene runs carried out in the EC and in the UNC chamber are given in Figures IV-27 and IV-28, respectively.

In general, the fits of the model predictions to the results of the 1-butene runs carried out in either chamber were not as satisfactory as those for ethene and propene discussed above. For two of the three runs carried out in the SAPRC EC the model significantly underpredicts the observed reactivity. On the other hand, for the UNC runs the model significantly overpredicts reactivity. However, as noted above, the runs carried out in each chamber were carried out around the same time, and additional runs carried out at different times may give slightly different results. (Note, for example, the results of the model simulations of the

Table IV-15. Summary of Initial Concentrations and Experimental and Calculated Maximum Ozone Yields, Times Required to Achieve Half the Maximum Experimental Change in ($[O_3]-[NO]$), and Reactant Alkene Half-Lives for the Butene-$NO_x$-Air Irradiations

| Experiment | Initial Concentrations | | | Maximum Ozone Concentration | | | | Time to 1/2 Maximum Expt. ($[O_3]-[NO]$) | | | | Butene Half-Life | | | |
|---|---|---|---|---|---|---|---|---|---|---|---|---|---|---|---|
| | $NO_x$ (ppm) | HC (ppmC) | HC/$NO_x$ | Expt (ppm) | Calc (ppm) | Calc -Expt (ppm) | Calc -Expt /Expt) | Expt (min) | Calc (min) | Calc -Expt (min) | Calc -Exp /Exp | Expt (min) | Calc (min) | Calc -Expt (min) | Calc -Expt /Expt |
| **1: EC 1-Butene-$NO_x$-Air Runs** | | | | | | | | | | | | | | | |
| EC-122 | 0.501 | 0.9 | 1.7 | 0.220 | 0.122 | -0.098 | -0.45 | 132 | 177 | 45 | 0.34 | 97 | 143 | 46 | 0.48 |
| EC-123 | 0.507 | 1.6 | 3.2 | 0.506 | 0.329 | -0.177 | -0.35 | 108 | 166 | 58 | 0.54 | 84 | 142 | 58 | 0.70 |
| EC-124 | 0.993 | 1.7 | 1.7 | 0.247 | 0.200 | -0.047 | -0.19 | 210 | 192 | -17 | -0.08 | 122 | 166 | 44 | 0.36 |
| Group Average | 0.667 | 1.4 | 2.2 | 0.324 | 0.217 | -0.107 | -0.33 | 150 | 178 | 28 | 0.27 | 101 | 150 | 50 | 0.51 |
| S. Dev. | 0.282 | 0.5 | 0.8 | 0.158 | 0.104 | 0.066 | 0.13 | 53 | 13 | 40 | 0.32 | 19 | 13 | 8 | 0.17 |
| Avg. Abs. Value | | | | | | 0.107 | 0.33 | | | 39 | 0.32 | | | 50 | 0.51 |
| S. Dev. | | | | | | 0.066 | 0.13 | | | 21 | 0.23 | | | 8 | 0.17 |
| **2: UNC 1-Butene-$NO_x$-Air Runs** | | | | | | | | | | | | | | | |
| ST2383R | 0.399 | 1.4 | 3.6 | 0.206 | 0.440 | 0.234 | 1.13 | 430 | 300 | -130 | -0.30 | 463 | 330 | -134 | -0.29 |
| ST2583R | 0.463 | 1.6 | 3.5 | 0.266 | 0.446 | 0.180 | 0.67 | 429 | 321 | -108 | -0.25 | 409 | 317 | -92 | -0.22 |
| ST2783R | 0.453 | 1.6 | 3.5 | 0.285 | 0.438 | 0.153 | 0.54 | 425 | 331 | -94 | -0.22 | 415 | 321 | -94 | -0.23 |
| ST2583B | 0.425 | 2.9 | 6.7 | 0.594 | 0.710 | 0.117 | 0.20 | 410 | 287 | -124 | -0.30 | 403 | 318 | -85 | -0.21 |
| Group Average | 0.435 | 1.9 | 4.3 | 0.338 | 0.509 | 0.171 | 0.63 | 423 | 310 | -114 | -0.27 | 422 | 321 | -101 | -0.24 |
| S. Dev. | 0.029 | 0.7 | 1.6 | 0.174 | 0.134 | 0.049 | 0.39 | 9 | 20 | 16 | 0.04 | 28 | 6 | 22 | 0.03 |
| Avg. Abs. Value | | | | | | 0.171 | 0.63 | | | 114 | 0.27 | | | 101 | 0.24 |
| S. Dev. | | | | | | 0.049 | 0.39 | | | 16 | 0.04 | | | 22 | 0.03 |
| **3: EC trans-2-Butene-$NO_x$-Air Runs** | | | | | | | | | | | | | | | |
| EC-146 | 0.509 | 0.9 | 1.8 | 0.239 | 0.151 | -0.089 | -0.37 | 50 | 76 | 26 | 0.51 | 23 | 40 | 18 | 0.77 |
| EC-147 | 0.982 | 1.7 | 1.7 | 0.154 | 0.117 | -0.037 | -0.24 | 45 | 59 | 14 | 0.31 | 27 | 44 | 17 | 0.61 |
| EC-157 | 0.526 | 0.9 | 1.7 | 0.205 | 0.129 | -0.076 | -0.37 | 48 | 79 | 31 | 0.63 | 25 | 41 | 16 | 0.65 |

(continued)

Table IV-15 (continued) - 2

| Experiment | Initial Concentrations | | | Maximum Ozone Concentration | | | | Time to 1/2 Maximum Expt. ($[O_3]-[NO]$) | | | | Butene Half-Life | | | |
|---|---|---|---|---|---|---|---|---|---|---|---|---|---|---|---|
| | $NO_x$ (ppm) | HC (ppmC) | $HC/NO_x$ | Expt (ppm) | Calc (ppm) | Calc -Expt (ppm) | Calc -Expt /Expt) | Expt (min) | Calc (min) | Calc -Expt (min) | Calc -Exp /Exp | Expt (min) | Calc (min) | Calc -Expt (min) | Calc -Expt /Expt |
| Group Average | 0.672 | 1.2 | 1.7 | 0.200 | 0.132 | -0.067 | -0.33 | 48 | 71 | 23 | 0.48 | 25 | 42 | 17 | 0.68 |
| S. Dev. | 0.268 | 0.5 | 0.1 | 0.043 | 0.017 | 0.027 | 0.08 | 3 | 11 | 9 | 0.16 | 2 | 2 | 1 | 0.08 |
| Avg. Abs. Value | | | | | | 0.067 | 0.33 | | | 23 | 0.48 | | | 17 | 0.68 |
| S. Dev. | | | | | | 0.027 | 0.08 | | | 9 | 0.16 | | | 1 | 0.08 |
| 4: UNC trans-2-Butene-$NO_x$-Air Run | | | | | | | | | | | | | | | |
| ST2783B | 0.436 | 1.6 | 3.7 | 0.523 | 0.454 | -0.069 | -0.13 | 288 | 266 | -22 | -0.08 | 204 | 188 | -17 | -0.08 |
| 5: ITC Isobutene-$NO_x$-Air Run | | | | | | | | | | | | | | | |
| ITC-694 | 0.508 | 4.6 | 9.0 | 0.900 | 0.971 | 0.071 | 0.08 | 73 | 49 | -24 | -0.33 | 76 | 57 | -19 | -0.25 |

Table IV-16. Experimental and Calculated Product Yields for the Butene-$NO_x$-Air Runs

| Experiment | Species | Expt (ppm) | Calc (ppm) | Calc -Expt (ppm) | Calc -Expt /Expt |
|---|---|---|---|---|---|
| 1: EC 1-Butene-$NO_x$-Air Runs | | | | | |
| EC-122 | PAN | 0.021 | 0.005 | -0.016 | -0.77 |
| | PPN | 0.031 | 0.016 | -0.015 | -0.49 |
| | Formaldehyde | 0.111 | 0.086 | -0.025 | -0.22 |
| | Propionaldehyde | 0.073 | 0.088 | 0.015 | 0.20 |
| | Acetaldehyde | 0.041 | 0.042 | 0.001 | 0.02 |
| EC-123 | PAN | 0.065 | 0.023 | -0.042 | -0.64 |
| | PPN | 0.085 | 0.094 | 0.009 | 0.10 |
| | Formaldehyde | 0.181 | 0.163 | -0.018 | -0.10 |
| | Propionaldehyde | 0.131 | 0.170 | 0.039 | 0.29 |
| | Acetaldehyde | 0.059 | 0.057 | -0.002 | -0.03 |
| EC-124 | PAN | 0.038 | 0.023 | -0.015 | -0.40 |
| | PPN | 0.036 | 0.052 | 0.015 | 0.41 |
| | Formaldehyde | 0.161 | 0.156 | -0.005 | -0.03 |
| | Propionaldehyde | 0.119 | 0.167 | 0.048 | 0.41 |
| | Acetaldehyde | 0.073 | 0.084 | 0.010 | 0.14 |
| Group Average | PAN | 0.041 | 0.017 | -0.024 | -0.60 |
| Std. Dev. | | 0.022 | 0.011 | 0.015 | 0.19 |
| Avg. Abs Value | | | | 0.024 | 0.60 |
| Std. Dev. | | | | 0.015 | 0.19 |
| Group Average | PPN | 0.051 | 0.054 | 0.003 | 0.01 |
| Std. Dev. | | 0.030 | 0.039 | 0.016 | 0.46 |
| Avg. Abs Value | | | | 0.013 | 0.33 |
| Std. Dev. | | | | 0.004 | 0.21 |
| Group Average | Formaldehyde | 0.151 | 0.135 | -0.016 | -0.12 |
| Std. Dev. | | 0.036 | 0.043 | 0.010 | 0.10 |
| Avg. Abs Value | | | | 0.016 | 0.12 |
| Std. Dev. | | | | 0.010 | 0.10 |
| Group Average | Propionaldehyde | 0.108 | 0.142 | 0.034 | 0.30 |
| Std. Dev. | | 0.030 | 0.047 | 0.017 | 0.10 |
| Avg. Abs Value | | | | 0.034 | 0.30 |
| Std. Dev. | | | | 0.017 | 0.10 |

(continued)

Table IV-16 (continued) - 2

| Experiment | Species | Expt (ppm) | Calc (ppm) | Calc -Expt (ppm) | Calc -Expt /Expt |
|---|---|---|---|---|---|
| Group Average | Acetaldehyde | 0.058 | 0.061 | 0.003 | 0.04 |
| Std. Dev. | | 0.016 | 0.021 | 0.007 | 0.09 |
| Avg. Abs Value | | | | 0.004 | 0.07 |
| Std. Dev. | | | | 0.005 | 0.07 |

## 2: UNC 1-Butene-$NO_x$-Air Runs

| Experiment | Species | Expt (ppm) | Calc (ppm) | Calc -Expt (ppm) | Calc -Expt /Expt |
|---|---|---|---|---|---|
| ST2383R | PAN | 0.029 | 0.030 | 0.000 | 0.01 |
| | Propionaldehyde | 0.173 | 0.146 | -0.027 | -0.16 |
| ST2583R | PAN | 0.031 | 0.030 | -0.001 | -0.02 |
| ST2783R | PAN | 0.032 | 0.028 | -0.004 | -0.13 |
| | Formaldehyde | 0.154 | 0.131 | -0.023 | -0.15 |
| ST2583B | PAN | 0.052 | 0.047 | -0.005 | -0.09 |
| Group Average | PAN | 0.036 | 0.034 | -0.002 | -0.06 |
| Std. Dev. | | 0.011 | 0.009 | 0.003 | 0.06 |
| Avg. Abs Value | | | | 0.002 | 0.06 |
| Std. Dev. | | | | 0.002 | 0.06 |
| Group Average | Propionaldehyde | 0.173 | 0.146 | -0.027 | -0.16 |
| Avg. Abs Value | | | | 0.027 | 0.16 |
| Group Average | Formaldehyde | 0.154 | 0.131 | -0.023 | -0.15 |
| Avg. Abs Value | | | | 0.023 | 0.15 |

## 3: EC trans-2-Butene-$NO_x$-Air Runs

| Experiment | Species | Expt (ppm) | Calc (ppm) | Calc -Expt (ppm) | Calc -Expt /Expt |
|---|---|---|---|---|---|
| EC-146 | PAN | 0.063 | 0.045 | -0.019 | -0.30 |
| | Acetaldehyde | 0.204 | 0.267 | 0.063 | 0.31 |
| | Formaldehyde | 0.030 | 0.077 | 0.047 | 1.56 |
| EC-147 | PAN | 0.060 | 0.055 | -0.006 | -0.09 |
| | Acetaldehyde | 0.389 | 0.466 | 0.077 | 0.20 |
| | Formaldehyde | 0.095 | 0.140 | 0.046 | 0.48 |
| EC-157 | PAN | 0.052 | 0.037 | -0.015 | -0.29 |
| | Acetaldehyde | 0.220 | 0.248 | 0.028 | 0.13 |
| | Formaldehyde | 0.028 | 0.078 | 0.050 | 1.78 |

(continued)

Table IV-16 (continued) - 3

| Experiment | Species | Expt (ppm) | Calc (ppm) | Calc -Expt (ppm) | Calc -Expt /Expt |
|---|---|---|---|---|---|
| Group Average | PAN | 0.058 | 0.045 | -0.013 | -0.23 |
| Std. Dev. | | 0.006 | 0.009 | 0.007 | 0.11 |
| Avg. Abs Value | | | | 0.013 | 0.23 |
| Std. Dev. | | | | 0.007 | 0.11 |
| 3: EC trans-2-Butene-$NO_x$-Air Runs | | | | | |
| Group Average | Acetaldehyde | 0.271 | 0.327 | 0.056 | 0.21 |
| Std. Dev. | | 0.103 | 0.121 | 0.025 | 0.09 |
| Avg. Abs Value | | | | 0.056 | 0.21 |
| Std. Dev. | | | | 0.025 | 0.09 |
| Group Average | Formaldehyde | 0.051 | 0.099 | 0.048 | 1.27 |
| Std. Dev. | | 0.038 | 0.036 | 0.002 | 0.69 |
| Avg. Abs Value | | | | 0.048 | 1.27 |
| Std. Dev. | | | | 0.002 | 0.69 |
| 4: UNC trans-2-Butene-$NO_x$-Air Run | | | | | |
| ST2783B | PAN | 0.145 | 0.162 | 0.017 | 0.11 |
| 5: ITC Isobutene-$NO_x$-Air Run | | | | | |
| ITC-694 | PAN | 0.137 | 0.042 | -0.095 | -0.69 |
| | Acetone | 0.595 | 0.993 | 0.398 | 0.67 |
| | Formaldehyde | 0.644 | 0.688 | 0.044 | 0.07 |

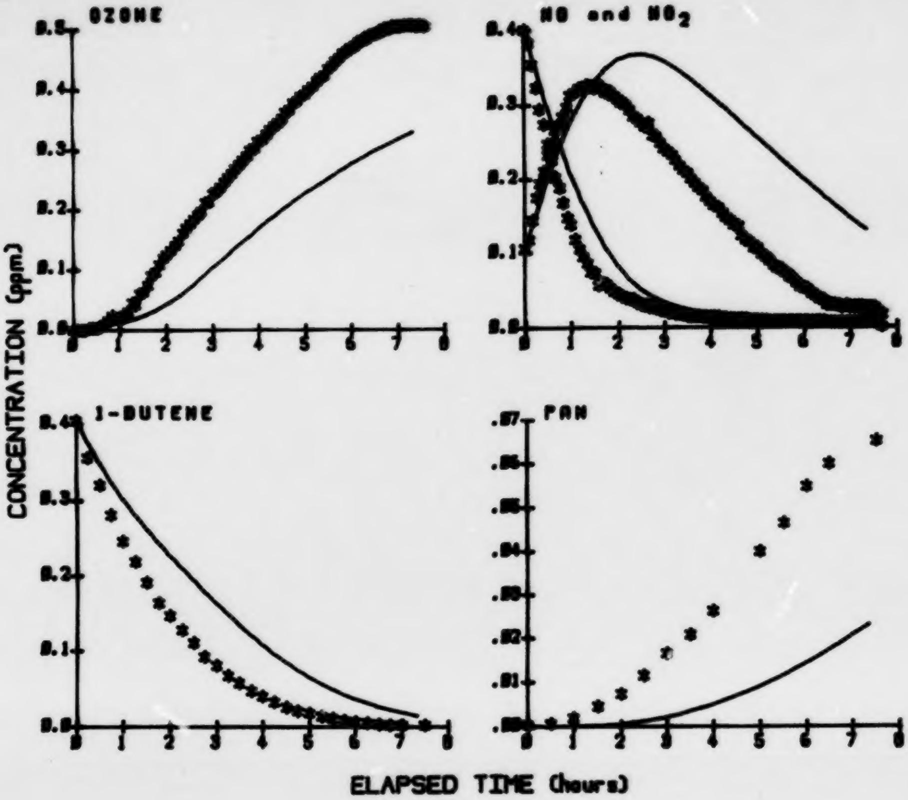

Figure IV-27. Experimental and calculated concentration-time plots for representative species observed in the 1-butene-$NO_x$-air run EC-123.
* = Experimental data.
----- = Model calculation.

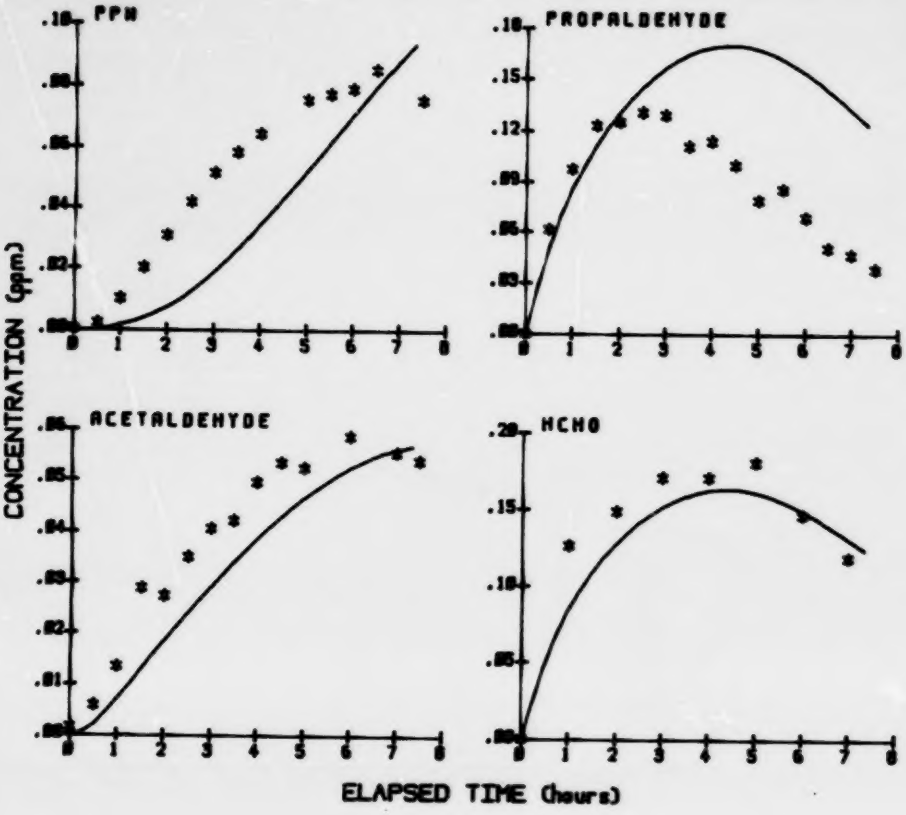

Figure IV-27 (continued)

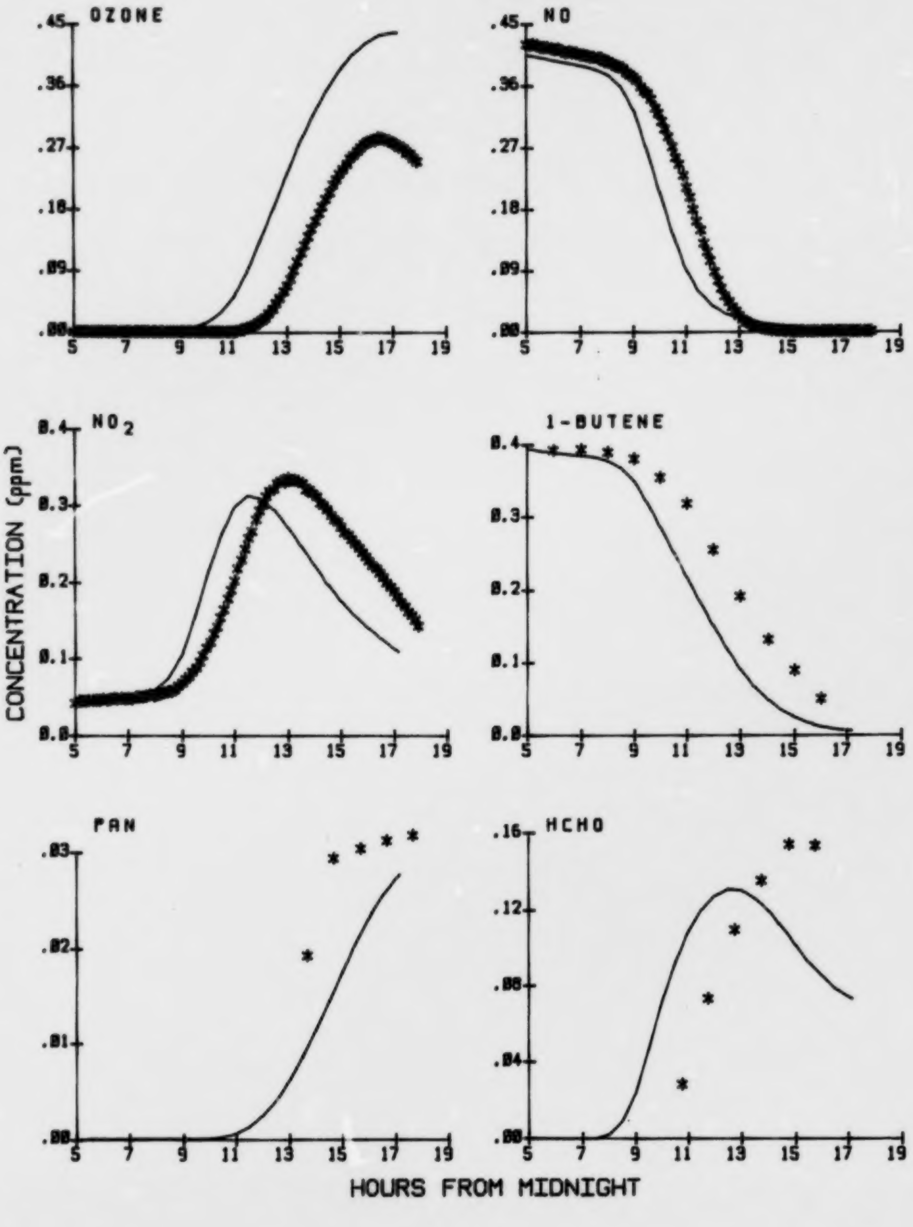

Figure IV-28. Experimental and calculated concentration-time plots for representative species observed in the UNC 1-butene-$NO_x$-air run ST2783R.
* = Experimental data.
----- = Model calculation.

different sets of ethene experiments discussed above.) In particular, it should be pointed out that the propene model also significantly overpredicted the reactivity observed in a propene run carried out at the same time as the September 23 UNC 1-butene run (see data for propene run ST2383B in Tables IV-13 and IV-14 and Figure II-11; Section II-D-3.) This suggests that the model may not be correctly representing the UNC chamber or light intensity parameters during the period that these runs were carried out, and that better fits may be obtained if the correct chamber-dependent parameters were known and employed.

If the differences in the predictions of overall reactivity are taken into account, the model predictions of the PAN and aldehyde yields are not necessarily inconsistent with the experimental data. The model would probably overpredict the PPN yields observed in the SAPRC EC experiments if the radical input fluxes were increased to better fit the overall reactivity. However, it should be noted that the PPN data are highly uncertain, since the calibration factors were estimated without the availability of authentic samples of PPN.

Better fits of the model predictions to the results of the SAPRC EC runs could be attained if the radical yields from the ozone + 1-butene reaction, which are highly uncertain (see Section II-D-3), were adjusted upwards. However, this would make the fits to the UNC chamber experiments even worse, and the possibility that additional experiments may indicate that the reactivity in runs EC-122 through EC-124 may be anomalously high cannot be ruled out. For that reason, no adjustment of the model was made to improve these fits.

### 9. trans-2-Butene-$NO_x$-Air Runs

Four *trans*-2-butene-$NO_x$ runs were modeled in this program, three carried out in the SAPRC EC at around the same time, and one carried out in the UNC chamber. The observed and calculated ozone yields, NO oxidation and ozone formation timing parameters, and butene half-lives for these runs are summarized in Table IV-15. The PAN, formaldehyde, and acetaldehyde maxima are summarized in Table IV-16. Plots of experimental and calculated concentration-time data for representative EC and UNC *trans*-2-butene runs are shown in Figures IV-29 and IV-30, respectively.

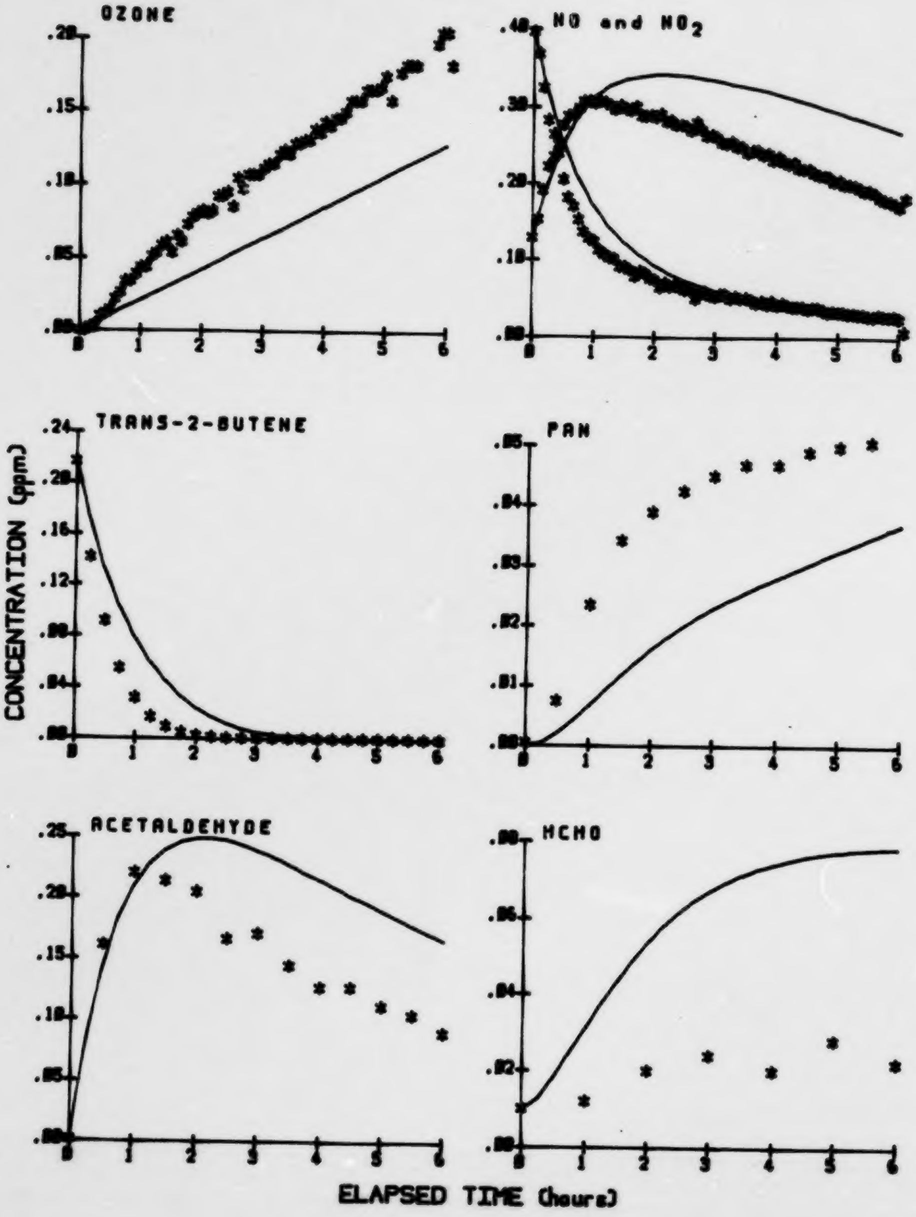

Figure IV-29. Experimental and calculated concentration-time plots for representative species observed in the trans-2-butene-$NO_x$-air run EC-157.
* = Experimental data.
----- = Model calculation.

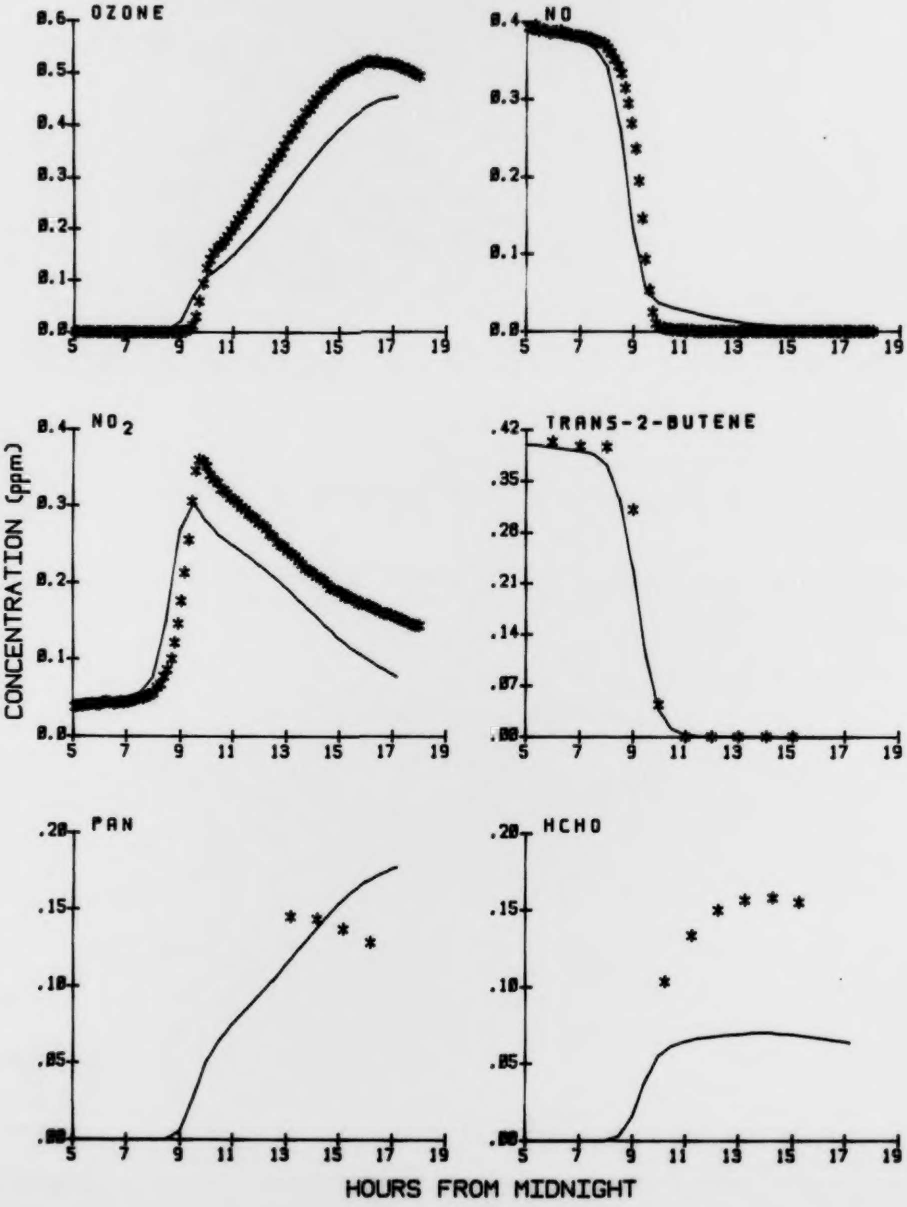

Figure IV-30. Experimental and calculated concentration-time plots for representative species observed in the UNC trans-2-butene-$NO_x$-air run ST2783B.
* = Experimental data.
----- = Model calculation.

The model consistently underpredicted the reactivity observed in the trans-2-butene runs carried out in the EC, but overpredicted the initial NO to $NO_2$ conversion rates and the butene consumption rates observed in the UNC runs. As discussed in Section IV-D-4, the fits of the model predictions to the results of the EC runs could be improved if several highly uncertain parameters in the trans-2-butene mechanism were adjusted, though this would probably make the fits to the UNC run worse. In view of this apparent inconsistency in the fits to the EC and the UNC data, and the fact that such adjustment would make the trans-2-butene model inconsistent with that used for propene (for which there are much more data), no such adjustments were carried out. The limited PAN data in the UNC experiment and the acetaldehyde yields in the EC runs are reasonably well fit by the model, and the underprediction of PAN in the EC runs is consistent with the general underprediction of reactivity for those runs.

The fits of the model predictions to the formaldehyde data are poor, with the yields observed in the SAPRC experiments being consistently lower than predicted, and that observed in the UNC experiment being higher than predicted. This is probably due to experimental problems in both cases, since, as noted above, the UNC formaldehyde measurements tend to be high, and the SAPRC formaldehyde values have tended to be anomalously low from time to time, and this may have been the case when these experiments were carried out.

### 10. Isobutene-$NO_x$-Air Run

One isobutene-$NO_x$-air run, carried out in the SAPRC ITC, was modeled in this program. The experimental and calculated ozone yields and NO oxidation and ozone formation timing parameters for this run are summarized in Table IV-15, and the isobutene half-lives and PAN and acetone yields are summarized in Table IV-16. Plots of the experimental and calculated concentration-time data for this run are given in Section II-D-5, in conjunction with the discussion of the isobutene + ozone reaction mechanism, which is by far the most uncertain aspect of its reaction mechanism for this alkene.

The problems with simulating the results of this run have been discussed in Section II-D-5. Briefly, it was found that if the radical input from the ozone + isobutene reaction was adjusted so that the model simulates the overall reactivity observed in that run, then the PAN yield is significantly underpredicted, while if the maximum radical input, which gives predicted PAN values almost as high as experimentally observed, is assumed in the model, then the model very significantly overpredicts reactivity. It appears that the experimental PAN data are valid, since the PAN measurements are consistent with the readings of the $NO_x$ monitor [which is known to have a 100% PAN interference (Winer et al. 1974)] at the end of the run when the $NO_2$ is expected to be consumed. The isobutene model employed in the standard calculations was based on a compromise between these two discrepancies, and the tendency of the model to overpredict overall reactivity and to very significantly underpredict the PAN yields reflects this.

### 11. n-Butane-$NO_x$-Air Runs

A total of 25 n-butane-$NO_x$-air irradiations were modeled in this program, including 14 carried out in the SAPRC EC, seven in the UNC chamber, three in the ITC and one in the OTC. The experimental and calculated ozone yields and NO oxidation and ozone formation times are summarized in Table IV-17 and the maximum yields of PAN, acetaldehyde and MEK are summarized on Table IV-18. Distribution plots of the discrepancies in the predictions of maximum ozone yields and the NO oxidation and ozone formation times for these standard model simulations are given in Figure IV-31.

It can be seen from Table IV-17 and Figure 31 that for all four chambers there is considerable variability in the fits of the standard model simulations to the reactivity observed in the n-butane experiments. This is attributed to the fact that, as discussed in Section III-B, results of model simulations of these runs are extremely sensitive to the chamber radical source, and relatively small variations in the magnitude of this radical source parameter, which tends to vary from run-to-run (Carter et al. 1982b, Pitts et al. 1983), can have a relatively large effect on the predicted "timing" for these runs. In particular, the

Table IV-17. Initial Concentrations and Experimental and Calculated Ozone Yields and Times Required to Achieve Half the Experimental Change in ($[O_3]-[NO]$) in the n-Butane-$NO_x$-Air Runs. Standard Model Calculations

| Experiment | Initial Concentrations | | | Maximum Ozone Concentration | | | | Time to 1/2 Maximum Expt. ($[O_3]-[NO]$) | | | |
|---|---|---|---|---|---|---|---|---|---|---|---|
| | $NO_x$ (ppm) | HC (ppmC) | $HC/NO_x$ | Expt (ppm) | Calc (ppm) | Calc -Expt (ppm) | Calc -Expt /Expt) | Expt (min) | Calc (min) | Calc -Expt (min) | Calc -Exp /Exp |
| **1: EC Runs** | | | | | | | | | | | |
| EC-130 | 0.098 | 17.4 | 178.0 | 0.459 | 0.496 | 0.037 | 0.08 | 57 | 85 | 27 | 0.48 |
| EC-133 | 0.502 | 8.6 | 17.1 | 0.249 | 0.080 | -0.169 | -0.68 | 128 | 232 | 104 | 0.82 |
| EC-134 | 0.507 | 8.3 | 16.3 | 0.034 | 0.061 | 0.027 | | 159 | 96 | -64 | -0.40 |
| EC-137 | 0.502 | 8.7 | 17.2 | 0.042 | 0.074 | 0.032 | | 147 | 94 | -53 | -0.36 |
| EC-162 | 0.505 | 8.2 | 16.3 | 0.112 | 0.086 | -0.026 | -0.24 | 125 | 140 | 15 | 0.12 |
| EC-163 | 0.490 | 8.7 | 17.8 | 0.430 | 0.235 | -0.195 | -0.45 | 114 | 174 | 60 | 0.53 |
| EC-168 | 0.493 | 8.1 | 16.4 | 0.655 | 0.465 | -0.190 | -0.29 | 239 | 302 | 63 | 0.26 |
| EC-178 | 0.098 | 7.8 | 80.0 | 0.384 | 0.438 | 0.054 | 0.14 | 144 | 126 | -18 | -0.12 |
| EC-304 | 0.466 | 17.1 | 36.7 | 0.354 | 0.652 | 0.298 | 0.84 | 166 | 120 | -46 | -0.28 |
| EC-305 | 0.098 | 17.2 | 175.5 | 0.398 | 0.592 | 0.194 | 0.49 | 98 | 61 | -37 | -0.37 |
| EC-306 | 0.187 | 25.8 | 137.8 | 0.535 | 0.746 | 0.211 | 0.39 | 140 | 77 | -63 | -0.45 |
| EC-307 | 0.102 | 25.8 | 253.0 | 0.420 | 0.647 | 0.227 | 0.54 | 94 | 39 | -56 | -0.59 |
| EC-308 | 0.483 | 16.2 | 33.5 | 0.046 | 0.217 | 0.171 | | 124 | 49 | -76 | -0.61 |
| EC-309 | 0.475 | 17.2 | 36.3 | 0.545 | 0.779 | 0.234 | 0.43 | 184 | 113 | -71 | -0.39 |
| Group Average | 0.358 | 13.9 | 73.7 | 0.333 | 0.398 | 0.065 | 0.11 | 137 | 122 | -15 | -0.10 |
| S. Dev. | 0.188 | 6.5 | 79.1 | 0.204 | 0.266 | 0.166 | 0.48 | 44 | 73 | 59 | 0.46 |
| Avg. Abs. Value | | | | | | 0.147 | 0.42 | | | 53 | 0.41 |
| S. Dev. | | | | | | 0.092 | 0.23 | | | 24 | 0.19 |
| **2: ITC Runs** | | | | | | | | | | | |
| ITC-507 | 0.092 | 15.0 | 162.8 | 0.149 | 0.583 | 0.434 | 2.92 | 157 | 41 | -116 | -0.74 |
| ITC-533 | 0.119 | 11.8 | 99.3 | 0.165 | 0.396 | 0.230 | 1.40 | 200 | 85 | -115 | -0.58 |
| ITC-770 | 0.539 | 37.8 | 70.1 | 0.042 | 0.051 | 0.009 | | 101 | 94 | -6 | -0.06 |

(continued)

Table IV-17 (continued) - 2

| Experiment | Initial Concentrations | | | Maximum Ozone Concentration | | | | Time to 1/2 Maximum Expt. ($[O_3]-[NO]$) | | | |
|---|---|---|---|---|---|---|---|---|---|---|---|
| | $NO_x$ (ppm) | HC (ppmC) | $HC/NO_x$ | Expt (ppm) | Calc (ppm) | Calc -Expt (ppm) | Calc -Expt /Expt) | Expt (min) | Calc (min) | Calc -Expt (min) | Calc -Exp /Exp |
| Group Average | 0.250 | 21.5 | 110.8 | 0.119 | 0.343 | 0.225 | 2.16 | 153 | 73 | -79 | -0.46 |
| S. Dev. | 0.250 | 14.2 | 47.4 | 0.067 | 0.270 | 0.213 | 1.08 | 50 | 29 | 63 | 0.35 |
| Avg. Abs. Value | | | | | | 0.225 | 2.16 | | | 79 | 0.46 |
| S. Dev. | | | | | | 0.213 | 1.08 | | | 63 | 0.35 |
| 3: OTC Runs | | | | | | | | | | | |
| OTC-211 | 0.553 | 42.7 | 77.3 | 0.008 | 0.242 | 0.234 | | 201 | 65 | -136 | -0.67 |
| 4: UNC Runs | | | | | | | | | | | |
| JL2178R | 0.238 | 7.6 | 31.9 | 0.763 | 0.461 | -0.301 | -0.40 | 496 | 582 | 86 | 0.17 |
| JL2278R | 0.547 | 8.8 | 16.1 | 0.149 | 0.053 | -0.096 | -0.64 | 411 | 508 | 97 | 0.24 |
| OC0979R | 0.206 | 14.6 | 70.9 | 0.191 | 0.366 | 0.174 | 0.91 | 452 | 326 | -126 | -0.28 |
| JL2178B | 0.238 | 16.0 | 67.2 | 0.986 | 0.831 | -0.155 | -0.16 | 448 | 501 | 53 | 0.12 |
| JL2278B | 0.547 | 17.6 | 32.2 | 0.735 | 0.236 | -0.499 | -0.68 | 470 | 634 | 164 | 0.35 |
| ST1879B | 0.205 | 5.3 | 25.9 | 0.184 | 0.266 | 0.083 | 0.45 | 480 | 382 | -98 | -0.20 |
| OC1879B | 0.200 | 14.2 | 71.0 | 0.208 | 0.427 | 0.219 | 1.05 | 443 | 314 | -129 | -0.29 |
| Group Average | 0.312 | 12.0 | 45.0 | 0.459 | 0.377 | -0.082 | 0.08 | 457 | 464 | 6 | 0.01 |
| S. Dev. | 0.162 | 4.7 | 23.7 | 0.354 | 0.243 | 0.262 | 0.73 | 28 | 125 | 121 | 0.27 |
| Avg. Abs. Value | | | | | | 0.218 | 0.61 | | | 108 | 0.24 |
| S. Dev. | | | | | | 0.144 | 0.31 | | | 36 | 0.08 |
| Grand Average | 0.340 | 15.5 | 70.3 | 0.330 | 0.379 | 0.049 | 0.31 | 231 | 210 | -22 | -0.13 |
| S. Dev. | 0.185 | 9.2 | 64.2 | 0.263 | 0.246 | 0.215 | 0.86 | 149 | 183 | 84 | 0.42 |
| Avg. Abs. Value | | | | | | 0.180 | 0.66 | | | 75 | 0.38 |
| S. Dev. | | | | | | 0.123 | 0.62 | | | 41 | 0.21 |

Table IV-18. Experimental and Calculated Product Yields Observed in the n-Butane-$NO_x$-Air Irradiations. Standard Model Used

| Experiment | Species | Expt (ppm) | Calc (ppm) | Calc -Expt (ppm) | Calc -Expt /Expt |
|---|---|---|---|---|---|
| 1: EC Runs | | | | | |
| EC-130 | PAN | 0.044 | 0.055 | 0.011 | 0.25 |
| | Methyl Ethyl Ketone | 0.165 | 0.185 | 0.020 | 0.12 |
| | Acetaldehyde | 0.130 | 0.196 | 0.066 | 0.51 |
| EC-133 | PAN | 0.031 | 0.007 | -0.024 | -0.78 |
| | Methyl Ethyl Ketone | 0.122 | 0.073 | -0.049 | -0.40 |
| | Acetaldehyde | 0.096 | 0.087 | -0.009 | -0.10 |
| EC-134 | Methyl Ethyl Ketone | 0.064 | 0.068 | 0.004 | 0.06 |
| | Acetaldehyde | 0.049 | 0.082 | 0.033 | 0.67 |
| EC-137 | Methyl Ethyl Ketone | 0.072 | 0.070 | -0.002 | -0.03 |
| | Acetaldehyde | 0.062 | 0.084 | 0.022 | 0.35 |
| EC-162 | PAN | 0.015 | 0.007 | -0.008 | -0.55 |
| | Methyl Ethyl Ketone | 0.068 | 0.073 | 0.005 | 0.08 |
| | Acetaldehyde | 0.098 | 0.086 | -0.011 | -0.11 |
| EC-163 | PAN | 0.106 | 0.047 | -0.059 | -0.56 |
| | Methyl Ethyl Ketone | 0.077 | 0.056 | -0.021 | -0.27 |
| EC-168 | PAN | 0.092 | 0.060 | -0.033 | -0.36 |
| | Methyl Ethyl Ketone | 0.193 | 0.134 | -0.059 | -0.31 |
| | Acetaldehyde | 0.114 | 0.117 | 0.003 | 0.02 |
| EC-178 | PAN | 0.045 | 0.057 | 0.011 | 0.25 |
| | Methyl Ethyl Ketone | 0.091 | 0.125 | 0.034 | 0.38 |
| | Acetaldehyde | 0.092 | 0.116 | 0.024 | 0.26 |
| EC-304 | PAN | 0.027 | 0.048 | 0.021 | 0.75 |
| | Methyl Ethyl Ketone | 0.092 | 0.171 | 0.079 | 0.85 |
| | Acetaldehyde | 0.149 | 0.190 | 0.041 | 0.28 |
| EC-305 | PAN | 0.031 | 0.056 | 0.025 | 0.80 |
| | Methyl Ethyl Ketone | 0.085 | 0.175 | 0.090 | 1.06 |
| | Acetaldehyde | 0.131 | 0.191 | 0.059 | 0.45 |
| EC-306 | PAN | 0.035 | 0.071 | 0.036 | 1.01 |
| | Methyl Ethyl Ketone | 0.098 | 0.230 | 0.132 | 1.34 |
| | Acetaldehyde | 0.166 | 0.248 | 0.082 | 0.49 |

(continued)

Table IV-18 (continued) - 2

| Experiment | Species | Expt (ppm) | Calc (ppm) | Calc -Expt (ppm) | Calc -Expt /Expt |
|---|---|---|---|---|---|
| EC-307 | PAN | 0.026 | 0.057 | 0.030 | 1.15 |
| | Methyl Ethyl Ketone | 0.139 | 0.212 | 0.073 | 0.52 |
| | Acetaldehyde | 0.161 | 0.243 | 0.083 | 0.51 |
| EC-308 | Methyl Ethyl Ketone | 0.076 | 0.153 | 0.077 | 1.01 |
| | Acetaldehyde | 0.037 | 0.082 | 0.045 | 1.22 |
| EC-309 | PAN | 0.034 | 0.071 | 0.037 | 1.07 |
| | Methyl Ethyl Ketone | 0.115 | 0.154 | 0.040 | 0.35 |
| | Acetaldehyde | 0.226 | 0.269 | 0.043 | 0.19 |
| Group Average | PAN | 0.044 | 0.049 | 0.004 | 0.28 |
| Std. Dev. | | 0.028 | 0.022 | 0.031 | 0.73 |
| Avg. Abs Value | | | | 0.027 | 0.68 |
| Std. Dev. | | | | 0.015 | 0.32 |
| Group Average | Methyl Ethyl Ketone | 0.104 | 0.134 | 0.030 | 0.34 |
| Std. Dev. | | 0.039 | 0.058 | 0.055 | 0.55 |
| Avg. Abs Value | | | | 0.049 | 0.49 |
| Std. Dev. | | | | 0.038 | 0.42 |
| Group Average | Acetaldehyde | 0.116 | 0.153 | 0.037 | 0.37 |
| Std. Dev. | | 0.053 | 0.072 | 0.031 | 0.35 |
| Avg. Abs Value | | | | 0.040 | 0.40 |
| Std. Dev. | | | | 0.027 | 0.31 |
| 2: ITC Runs | | | | | |
| ITC-507 | Methyl Ethyl Ketone | 0.075 | 0.123 | 0.048 | 0.63 |
| | Acetaldehyde | 0.029 | 0.146 | 0.117 | 4.02 |
| ITC-533 | Methyl Ethyl Ketone | 0.037 | 0.076 | 0.040 | 1.09 |
| | Acetaldehyde | 0.033 | 0.095 | 0.062 | 1.89 |
| ITC-770 | Methyl Ethyl Ketone | 0.047 | 0.066 | 0.020 | 0.42 |
| | Acetaldehyde | 0.056 | 0.094 | 0.039 | 0.69 |
| Group Average | Methyl Ethyl Ketone | 0.053 | 0.088 | 0.036 | 0.71 |
| Std. Dev. | | 0.020 | 0.030 | 0.014 | 0.34 |
| Avg. Abs Value | | | | 0.036 | 0.71 |
| Std. Dev. | | | | 0.014 | 0.34 |

(continued)

Table IV-18 (continued) - 3

| Experiment | Species | Expt (ppm) | Calc (ppm) | Calc -Expt (ppm) | Calc -Expt /Expt |
|---|---|---|---|---|---|
| Group Average | Acetaldehyde | 0.039 | 0.112 | 0.073 | 2.20 |
| Std. Dev. | | 0.014 | 0.029 | 0.040 | 1.68 |
| Avg. Abs Value | | | | 0.073 | 2.20 |
| Std. Dev. | | | | 0.040 | 1.68 |
| 3: OTC Run | | | | | |
| OTC-211 | PAN | 0.013 | 0.008 | -0.005 | -0.41 |
| | Acetaldehyde | 0.100 | 0.166 | 0.065 | 0.65 |
| 4: UNC Runs | | | | | |
| JL2178R | a | | | | |
| JL2278R | a | | | | |
| OC0979R | PAN | 1.100 | 0.014 | -1.086 | -0.99 |
| | Acetaldehyde | 0.095 | 0.093 | -0.002 | -0.02 |
| JL2178B | a | | | | |
| JL2278B | a | | | | |
| ST1879B | a | | | | |
| OC1879B | PAN | 4.590 | 0.020 | -4.570 | -1.00 |
| | Acetaldehyde | 0.095 | 0.099 | 0.004 | 0.04 |
| | Methyl Ethyl Ketone | 0.052 | 0.105 | 0.052 | 1.00 |
| Group Average | PAN | 2.845 | 0.017 | -2.828 | -0.99 |
| Std. Dev. | | 2.468 | 0.004 | 2.464 | 0.01 |
| Avg. Abs Value | | | | 2.828 | 0.99 |
| Std. Dev. | | | | 2.464 | 0.01 |
| Group Average | Acetaldehyde | 0.095 | 0.096 | 0.001 | 0.01 |
| Std. Dev. | | 0.000 | 0.004 | 0.004 | 0.04 |
| Avg. Abs Value | | | | 0.003 | 0.03 |
| Std. Dev. | | | | 0.001 | 0.01 |
| Group Average | Methyl Ethyl Ketone | 0.052 | 0.105 | 0.052 | 1.00 |
| Avg. Abs Value | | | | 0.052 | 1.00 |

[a] No data.

```
-------------------------------------------------------------
   Expt.-Calc.       Standard              Adjusted
   Ozone (ppm)        Model             Radical Input
-------------------------------------------------------------


        <  -0.33     :4                    :
 -0.33 -   -0.27     :4                    :
 -0.27 -   -0.21     :                     :
 -0.21 -   -0.15     :1114                 :
 -0.15 -   -0.09     :4                    :44
 -0.09 -   -0.03     :                     :114
 -0.03 -    0.03     :112                  :1111244
  0.03 -    0.09     :1114                 :1111234
  0.09 -    0.15     :                     :14
  0.15 -    0.21     :114                  :11
  0.21 -    0.27     :111234               :12
  0.27 -    0.33     :1                    :
        >   0.33     :2                    :

-------------------------------------------------------------
 Expt.-Calc.
  /Expt.           Standard              Adjusted
NO Oxidation       Model               Radical Input
   Times
-------------------------------------------------------------


        <  -0.55     :11223                :
 -0.55 -   -0.45     :                     :12
 -0.45 -   -0.35     :11111                :13
 -0.35 -   -0.25     :144                  :
 -0.25 -   -0.15     :4                    :12
 -0.15 -   -0.05     :12                   :1111111244
 -0.05 -    0.05     :                     :114444
  0.05 -    0.15     :14                   :114
  0.15 -    0.25     :44                   :
  0.25 -    0.35     :14                   :
  0.35 -    0.45     :                     :
  0.45 -    0.55     :11                   :
        >   0.55     :1                    :

-------------------------------------------------------------
```

Figure IV-31. Distribution plots of discrepancies in model predictions of ozone yields and times required to achieve half the maximum experimental change in ($[O_3]$-[NO]) for the standard model calculations and the calculations with run-to-run adjustment of the chamber radical source. Codes for chambers: 1 = EC, 2 = ITC, 3 = OTC, 4 = UNC.

discrepancies between the results of the standard model calculations and the experimental results appear to be random and do not depend on the reactant concentrations in the experiment, contrary to what one would expect if the discrepancies were due to errors in the homogeneous reaction mechanism. This is shown in Figures IV-32 and IV-33, where the discrepancies between the experimental and calculated NO oxidation and ozone formation "timing" parameter are plotted against the initial organic/$NO_x$ ratio and against the initial $NO_x$ concentration, respectively. A similar plot of the discrepancies against initial organic concentrations also does not indicate any apparent systematic dependences.

If run-to-run variability in the chamber radical source results in the standard model giving poor predictions of overall "timing" in the experiments, it is difficult to test other aspects of the model which are not directly related to timing, such as product yields. In order to provide a test for these aspects of the mechanism, model simulations of these runs were also carried out with the magnitude of the chamber radical source adjusted, by up to a factor of two, to improve the fits of the model calculations to the overall experimentally observed reactivity. (The criteria used to determine which adjustment factor for the radical source "fit" the data were subjective, and were based primarily on experimental and predicted ozone concentration-time profiles.) The experimental and calculated ozone yields, NO oxidation and ozone formation times, and radical source adjustment factors for the adjusted model calculations are summarized in Table IV-19, and the fits to the product yields for these calculations are summarized in Table IV-20. Distribution plots of the discrepancies in the predictions of maximum ozone yields and the NO oxidation and ozone formation times for the adjusted model simulations are given in Figure IV-31 together with the corresponding plots for the standard calculations, and distribution plots for the product yields in the adjusted model calculations are shown in Figure IV-34. Concentration-time plots of the experimental data and the results of both standard and adjusted model calculations for representative n-butane runs carried out in the SAPRC EC and in the UNC chamber are shown in Figures IV-35 and IV-36, respectively.

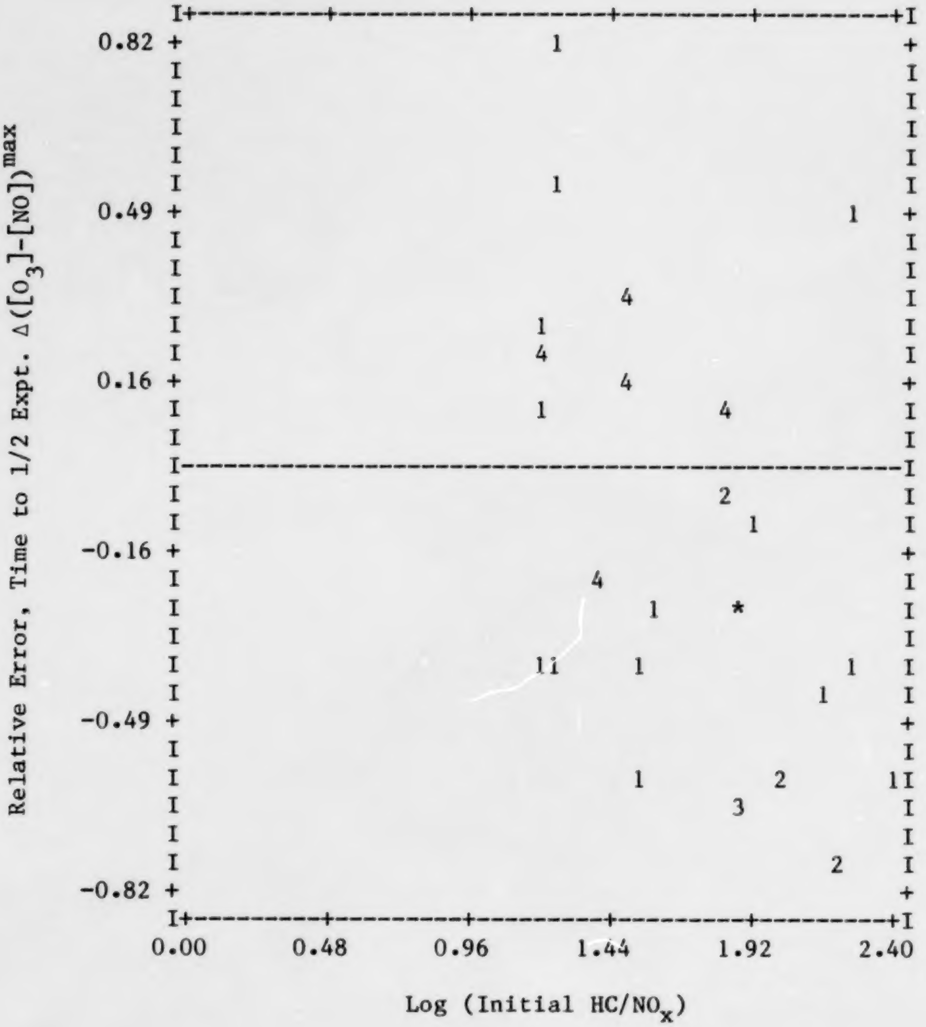

Figure IV-32. Plot of the discrepancy in the standard model prediction of the times required to achieve half the maximum experimental change in ($[O_3]-[NO]$) against the log of the initial hydrocarbon/$NO_x$ ratio. Codes for chambers: 1 = EC, 2 = ITC, 3 = OTC, 4 = UNC, * = overlap of 2 or more runs.

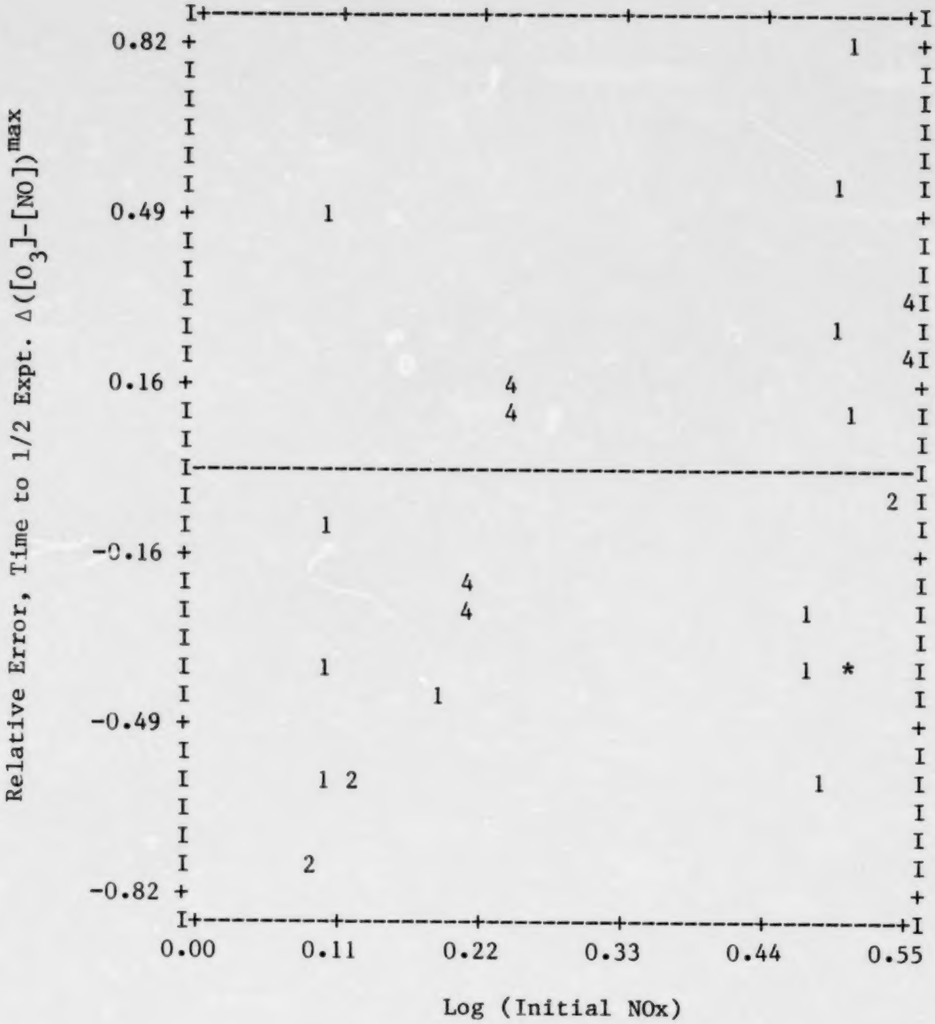

Figure IV-33. Plot of the discrepancy in the standard model prediction of the times required to achieve half the maximum experimental change in ($[O_3]$-[NO]) against the initial $NO_x$ concentrations. Codes for chambers: 1 = EC, 2 = ITC, 3 = OTC, 4 = UNC, * = overlap of 2 or more runs.

Table IV-19. Initial Concentrations and Experimental and Calculated Ozone Yields and Times Required to Achieve Half the Experimental Change in ([$O_3$]-[NO]) in the n-Butane-$NO_x$-Air Runs. Model Calculations Used Run-to-Run Adjusted Chamber Radical Input

| Experiment | Initial Concentrations | | | Maximum Ozone Concentration | | | | Time to 1/2 Maximum Expt. ([$O_3$]-[NO]) | | | | |
|---|---|---|---|---|---|---|---|---|---|---|---|---|
| | $NO_x$ (ppm) | HC (ppmC) | HC/$NO_x$ | Expt (ppm) | Calc (ppm) | Calc -Expt (ppm) | Calc -Expt /Expt) | Expt (min) | Calc (min) | Calc -Expt (min) | Calc -Exp /Exp | RS Adj. Fac.[a] |
| **1: EC Runs** | | | | | | | | | | | | |
| EC-130 | 0.098 | 17.4 | 178.0 | 0.459 | 0.493 | 0.034 | 0.07 | 57 | 59 | 2 | 0.03 | 1.8 |
| EC-133 | 0.502 | 8.6 | 17.1 | 0.249 | 0.261 | 0.012 | 0.05 | 128 | 137 | 10 | 0.08 | 2.0 |
| EC-134 | 0.507 | 8.3 | 16.3 | 0.034 | 0.022 | -0.012 | | 159 | 147 | -12 | -0.08 | 0.5 |
| EC-137 | 0.502 | 8.7 | 17.2 | 0.042 | 0.027 | -0.015 | | 147 | 147 | 0 | 0.00 | 0.5 |
| EC-162 | 0.505 | 8.2 | 16.2 | 0.112 | 0.152 | 0.040 | 0.35 | 125 | 110 | -15 | -0.12 | 1.4 |
| EC-163 | 0.490 | 8.7 | 17.8 | 0.430 | 0.382 | -0.048 | -0.11 | 114 | 123 | 9 | 0.08 | 2.0 |
| EC-168 | 0.493 | 7.8 | 15.9 | 0.655 | 0.578 | -0.076 | -0.12 | 239 | 212 | -27 | -0.11 | 1.8 |
| EC-178 | 0.098 | 7.8 | 80.0 | 0.384 | 0.438 | 0.054 | 0.14 | 144 | 126 | -18 | -0.12 | 1.0 |
| EC-304 | 0.466 | 17.1 | 36.7 | 0.354 | 0.481 | 0.127 | 0.36 | 166 | 153 | -12 | -0.07 | 0.7 |
| EC-305 | 0.098 | 17.2 | 175.5 | 0.398 | 0.598 | 0.200 | 0.50 | 98 | 85 | -13 | -0.14 | 0.6 |
| EC-306 | 0.187 | 25.8 | 137.8 | 0.535 | 0.742 | 0.207 | 0.39 | 140 | 115 | -25 | -0.18 | 0.5 |
| EC-307 | 0.102 | 25.8 | 252.5 | 0.420 | 0.654 | 0.234 | 0.56 | 94 | 50 | -44 | -0.47 | 0.5 |
| EC-308 | 0.483 | 16.2 | 33.5 | 0.046 | 0.092 | 0.046 | | 124 | 79 | -46 | -0.37 | 0.5 |
| EC-309 | 0.475 | 17.2 | 36.3 | 0.545 | 0.559 | 0.014 | 0.03 | 184 | 160 | -25 | -0.13 | 0.6 |
| Group Average | 0.358 | 13.9 | 73.6 | 0.333 | 0.391 | 0.058 | 0.20 | 137 | 122 | -15 | -0.11 | 1.0 |
| S. Dev. | 0.188 | 6.5 | 79.0 | 0.204 | 0.240 | 0.097 | 0.24 | 44 | 43 | 17 | 0.15 | 0.6 |
| Avg. Abs. Value | | | | | | 0.080 | 0.24 | | | 17 | 0.14 | |
| S. Dev. | | | | | | 0.079 | 0.19 | | | 14 | 0.13 | |
| **2: ITC Runs** | | | | | | | | | | | | |
| ITC-507 | 0.092 | 15.0 | 162.8 | 0.149 | 0.415 | 0.266 | 1.79 | 157 | 74 | -83 | -0.53 | 0.5 |
| ITC-533 | 0.119 | 11.8 | 99.3 | 0.165 | 0.227 | 0.061 | 0.37 | 200 | 153 | -47 | -0.23 | 0.5 |
| ITC-770 | 0.539 | 37.8 | 70.1 | 0.042 | 0.051 | 0.009 | | 101 | 94 | -6 | -0.06 | 1.0 |

(continued)

Table IV-19 (continued) - 2

| Experiment | Initial Concentrations | | | Maximum Ozone Concentration | | | | Time to 1/2 Maximum Expt. ($[O_3]-[NO]$) | | | | |
|---|---|---|---|---|---|---|---|---|---|---|---|---|
| | $NO_x$ (ppm) | HC (ppmC) | $HC/NO_x$ | Expt (ppm) | Calc (ppm) | Calc -Expt (ppm) | Calc -Expt /Expt) | Expt (min) | Calc (min) | Calc -Expt (min) | Calc -Exp /Exp | RS Adj. Fac.[a] |
| Group Average | 0.250 | 21.5 | 110.8 | 0.119 | 0.231 | 0.112 | 1.08 | 153 | 107 | -45 | -0.27 | 0.7 |
| S. Dev. | 0.250 | 14.2 | 47.4 | 0.067 | 0.182 | 0.136 | 1.00 | 50 | 41 | 39 | 0.24 | 0.3 |
| Avg. Abs. Value | | | | | | 0.112 | 1.08 | | | 45 | 0.27 | |
| S. Dev. | | | | | | 0.136 | 1.00 | | | 39 | 0.24 | |
| 3: OTC Runs | | | | | | | | | | | | |
| OTC-211 | 0.553 | 42.7 | 77.3 | 0.008 | 0.078 | 0.070 | | 201 | 111 | -90 | -0.45 | 0.5 |
| 4: UNC Runs | | | | | | | | | | | | |
| JL2178R | 0.238 | 7.6 | 31.9 | 0.763 | 0.650 | -0.113 | -0.15 | 496 | 505 | 9 | 0.02 | 1.5 |
| JL2278R | 0.547 | 8.8 | 16.1 | 0.149 | 0.200 | 0.051 | 0.34 | 411 | 401 | -10 | -0.02 | 1.8 |
| OC0979R | 0.206 | 14.6 | 70.9 | 0.191 | 0.178 | -0.013 | -0.07 | 452 | 410 | -42 | -0.09 | 0.5 |
| JL2178B | 0.238 | 16.0 | 67.2 | 0.986 | 0.912 | -0.074 | -0.08 | 448 | 449 | 1 | 0.00 | 1.5 |
| JL2278B | 0.547 | 17.6 | 32.2 | 0.735 | 0.624 | -0.111 | -0.15 | 470 | 481 | 11 | 0.02 | 2.0 |
| ST1879B | 0.205 | 5.3 | 25.9 | 0.184 | 0.203 | 0.019 | 0.11 | 480 | 414 | -67 | -0.14 | 0.8 |
| OC1879B | 0.200 | 14.2 | 71.0 | 0.208 | 0.306 | 0.098 | 0.47 | | | | | 0.7 |
| Group Average | 0.312 | 12.0 | 45.0 | 0.459 | 0.439 | -0.020 | 0.07 | 458 | 430 | -16 | -0.04 | 1.3 |
| S. Dev. | 0.162 | 4.7 | 23.7 | 0.354 | 0.289 | 0.082 | 0.25 | 30 | 53 | 31 | 0.07 | 0.6 |
| Avg. Abs. Value | | | | | | 0.068 | 0.19 | | | 23 | 0.05 | |
| S. Dev. | | | | | | 0.042 | 0.15 | | | 26 | 0.05 | |
| Grand Average | 0.340 | 15.4 | 70.2 | 0.330 | 0.373 | 0.043 | 0.24 | 222 | 206 | -23 | -0.13 | 1.0 |
| S. Dev. | 0.185 | 9.3 | 64.1 | 0.263 | 0.250 | 0.101 | 0.43 | 146 | 149 | 29 | 0.17 | 0.6 |
| Avg. Abs. Value | | | | | | 0.080 | 0.31 | | | 26 | 0.15 | |
| S. Dev. | | | | | | 0.074 | 0.39 | | | 25 | 0.15 | |

---

[a] Factor used to modify the radical input rate to improve fits of model calculation to experimental results.

Table IV-20. Experimental and Calculated Product Yields Observed in the n-Butane-$NO_x$-Air Irradiations. Model Calculation Used Run-to-Run Adjusted Chamber Radical Input

| Experiment | Species | Expt (ppm) | Calc (ppm) | Calc -Expt (ppm) | Calc -Expt /Expt |
|---|---|---|---|---|---|
| **1: EC Butane Runs** | | | | | |
| EC-130 | PAN | 0.044 | 0.057 | 0.013 | 0.29 |
| | Methyl Ethyl Ketone | 0.165 | 0.200 | 0.035 | 0.22 |
| | Acetaldehyde | 0.130 | 0.209 | 0.079 | 0.61 |
| EC-133 | PAN | 0.031 | 0.031 | 0.000 | 0.00 |
| | Methyl Ethyl Ketone | 0.122 | 0.113 | -0.009 | -0.08 |
| | Acetaldehyde | 0.096 | 0.117 | 0.021 | 0.22 |
| EC-134 | Methyl Ethyl Ketone | 0.064 | 0.046 | -0.018 | -0.27 |
| | Acetaldehyde | 0.049 | 0.059 | 0.010 | 0.21 |
| EC-137 | Methyl Ethyl Ketone | 0.072 | 0.048 | -0.024 | -0.33 |
| | Acetaldehyde | 0.062 | 0.062 | 0.000 | -0.01 |
| EC-162 | PAN | 0.015 | 0.014 | -0.001 | -0.06 |
| | Methyl Ethyl Ketone | 0.068 | 0.089 | 0.021 | 0.31 |
| | Acetaldehyde | 0.098 | 0.100 | 0.002 | 0.02 |
| EC-163 | PAN | 0.106 | 0.090 | -0.015 | -0.15 |
| | Methyl Ethyl Ketone | 0.077 | 0.080 | 0.002 | 0.03 |
| EC-168 | PAN | 0.092 | 0.101 | 0.008 | 0.09 |
| | Methyl Ethyl Ketone | 0.193 | 0.169 | -0.024 | -0.13 |
| | Acetaldehyde | 0.114 | 0.126 | 0.012 | 0.10 |
| EC-178 | PAN | 0.045 | 0.057 | 0.011 | 0.25 |
| | Methyl Ethyl Ketone | 0.091 | 0.125 | 0.034 | 0.38 |
| | Acetaldehyde | 0.092 | 0.116 | 0.024 | 0.26 |
| EC-304 | PAN | 0.027 | 0.027 | 0.000 | 0.00 |
| | Methyl Ethyl Ketone | 0.092 | 0.138 | 0.046 | 0.50 |
| | Acetaldehyde | 0.149 | 0.163 | 0.014 | 0.10 |
| EC-305 | PAN | 0.031 | 0.051 | 0.020 | 0.64 |
| | Methyl Ethyl Ketone | 0.085 | 0.162 | 0.078 | 0.92 |
| | Acetaldehyde | 0.131 | 0.180 | 0.049 | 0.37 |
| EC-306 | PAN | 0.035 | 0.057 | 0.022 | 0.62 |
| | Methyl Ethyl Ketone | 0.098 | 0.203 | 0.105 | 1.08 |
| | Acetaldehyde | 0.166 | 0.227 | 0.060 | 0.36 |

(continued)

Table IV-20 (continued) - 2

| Experiment | Species | Expt (ppm) | Calc (ppm) | Calc -Expt (ppm) | Calc -Expt /Expt |
|---|---|---|---|---|---|
| EC-307 | PAN | 0.026 | 0.055 | 0.029 | 1.10 |
| | Methyl Ethyl Ketone | 0.139 | 0.202 | 0.063 | 0.45 |
| | Acetaldehyde | 0.161 | 0.233 | 0.072 | 0.45 |
| EC-308 | Methyl Ethyl Ketone | 0.076 | 0.102 | 0.026 | 0.34 |
| | Acetaldehyde | 0.037 | 0.059 | 0.022 | 0.61 |
| EC-309 | PAN | 0.034 | 0.036 | 0.002 | 0.06 |
| | Methyl Ethyl Ketone | 0.115 | 0.121 | 0.006 | 0.06 |
| | Acetaldehyde | 0.226 | 0.230 | 0.004 | 0.02 |
| Group Average | PAN | 0.044 | 0.052 | 0.008 | 0.26 |
| Std. Dev. | | 0.028 | 0.026 | 0.013 | 0.38 |
| Avg. Abs Value | | | | 0.011 | 0.30 |
| Std. Dev. | | | | 0.010 | 0.35 |
| Group Average | Methyl Ethyl Ketone | 0.104 | 0.128 | 0.024 | 0.25 |
| Std. Dev. | | 0.039 | 0.053 | 0.039 | 0.41 |
| Avg. Abs Value | | | | 0.035 | 0.36 |
| Std. Dev. | | | | 0.029 | 0.31 |
| Group Average | Acetaldehyde | 0.116 | 0.145 | 0.028 | 0.26 |
| Std. Dev. | | 0.053 | 0.066 | 0.027 | 0.21 |
| Avg. Abs Value | | | | 0.028 | 0.26 |
| Std. Dev. | | | | 0.027 | 0.21 |
| 2: ITC Butane Runs | | | | | |
| ITC-507 | Methyl Ethyl Ketone | 0.075 | 0.088 | 0.013 | 0.17 |
| | Acetaldehyde | 0.029 | 0.112 | 0.083 | 2.85 |
| ITC-533 | Methyl Ethyl Ketone | 0.037 | 0.048 | 0.012 | 0.33 |
| | Acetaldehyde | 0.033 | 0.064 | 0.031 | 0.95 |
| ITC-770 | Methyl Ethyl Ketone | 0.047 | 0.066 | 0.020 | 0.42 |
| | Acetaldehyde | 0.056 | 0.094 | 0.039 | 0.69 |
| Group Average | Methyl Ethyl Ketone | 0.053 | 0.068 | 0.015 | 0.31 |
| Std. Dev. | | 0.020 | 0.020 | 0.004 | 0.13 |
| Avg. Abs Value | | | | 0.015 | 0.31 |
| Std. Dev. | | | | 0.004 | 0.13 |

(continued)

Table IV-20 (continued) - 3

| Experiment | Species | Expt (ppm) | Calc (ppm) | Calc -Expt (ppm) | Calc -Expt /Expt |
|---|---|---|---|---|---|
| Group Average | Acetaldehyde | 0.039 | 0.090 | 0.051 | 1.50 |
| Std. Dev. | | 0.014 | 0.024 | 0.028 | 1.18 |
| Avg. Abs Value | | | | 0.051 | 1.50 |
| Std. Dev. | | | | 0.028 | 1.18 |
| 3: OTC Butane Runs | | | | | |
| OTC-211 | PAN | 0.013 | 0.002 | -0.011 | -0.85 |
| | Acetaldehyde | 0.100 | 0.112 | 0.012 | 0.12 |
| 4: UNC Butane Runs | | | | | |
| JL2178R | a | | | | |
| JL2278R | a | | | | |
| OC0979R | PAN | 1.100 | 0.004 | -1.096 | -1.00 |
| | Acetaldehyde | 0.095 | 0.062 | -0.033 | -0.35 |
| JL2178B | a | | | | |
| JL2278B | a | | | | |
| ST1879B | a | | | | |
| OC1879B | PAN | 4.590 | 0.011 | -4.579 | -1.00 |
| | Acetaldehyde | 0.095 | 0.080 | -0.015 | -0.16 |
| | Methyl Ethyl Ketone | 0.052 | 0.081 | 0.028 | 0.54 |
| Group Average | PAN | 2.845 | 0.007 | -2.838 | -1.00 |
| Std. Dev. | | 2.468 | 0.005 | 2.463 | 0.00 |
| Avg. Abs Value | | | | 2.838 | 1.00 |
| Std. Dev. | | | | 2.463 | 0.00 |
| Group Average | Acetaldehyde | 0.095 | 0.071 | -0.024 | -0.25 |
| Std. Dev. | | 0.000 | 0.013 | 0.013 | 0.14 |
| Avg. Abs Value | | | | 0.024 | 0.25 |
| Std. Dev. | | | | 0.013 | 0.14 |
| Group Average | Methyl Ethyl Ketone | 0.052 | 0.081 | 0.028 | 0.54 |
| Std. Dev. | | | | | |
| Avg. Abs Value | | | | 0.028 | 0.54 |
| Std. Dev. | | | | | |

---

[a] No data.

| Calc.-Expt. /Expt. Yield | PAN | MEK | Acetaldehyde |
|---|---|---|---|
| < -0.5 | :344 | : | : |
| -0.5 - -0.4 | : | : | : |
| -0.4 - -0.3 | : | :1 | :4 |
| -0.3 - -0.2 | : | :1 | : |
| -0.2 - -0.1 | :1 | :1 | :4 |
| -0.1 - 0.0 | :11 | :1 | :1 |
| 0.0 - 0.1 | :111 | :11 | :111 |
| 0.1 - 0.2 | : | :2 | :13 |
| 0.2 - 0.3 | :11 | :1 | :111 |
| 0.3 - 0.4 | : | :1112 | :11 |
| 0.4 - 0.5 | : | :12 | :1 |
| > 0.5 | :111 | :1114 | :11222 |

Figure IV-34. Distribution plots for the discrepancies in the model predictions of the PAN, methyl ethyl ketone (MEK), and acetaldehyde yields observed in the n-butane-$NO_x$-air runs. Chamber radical source adusted from run-to-run in the model calculations. Code for chambers: 1 = EC, 2 = ITC, 3 = OTC, 4 = UNC.

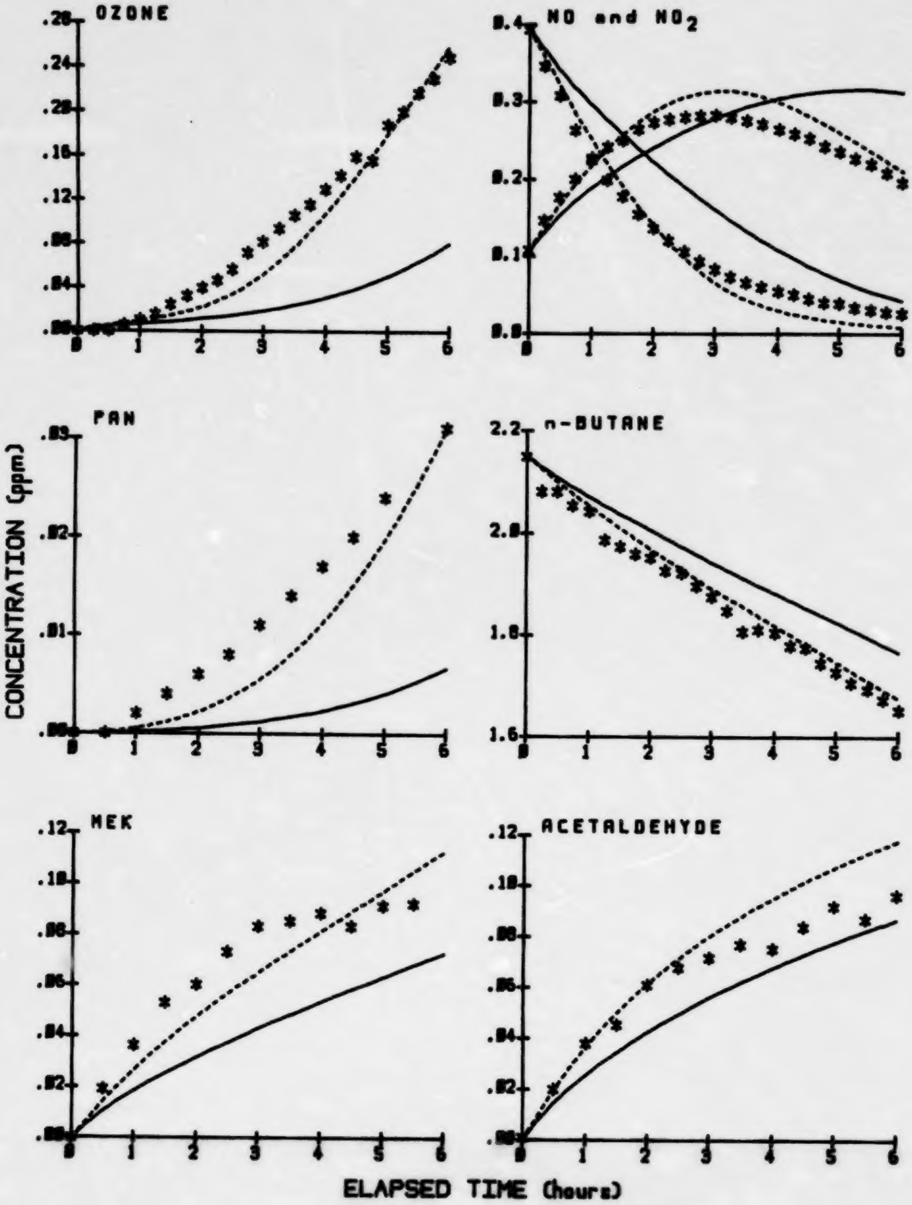

Figure IV-35. Experimental and calculated concentration-time plots for representative species observed in the n-butane-$NO_x$-air run EC-133.
* = Experimental data.
----- = Standard model calculation.
-- -- = Model calculation with adjusted chamber radical source.

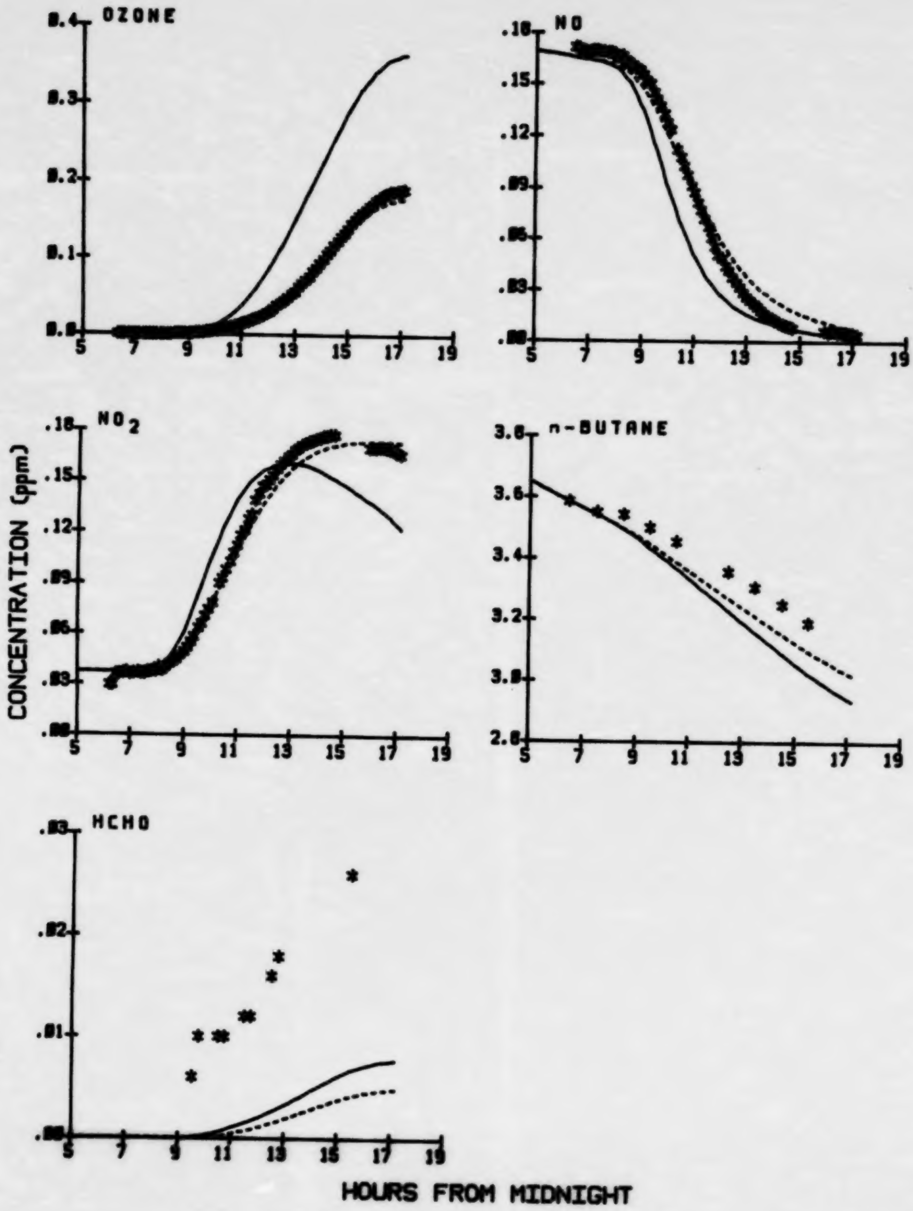

Figure IV-36. Experimental and calculated concentration-time plots for representative species observed in the UNC n-butane-$NO_x$-air run OC0979R.

* = Experimental data.

----- = Standard model calculation.

-- -- = Model calculation with adjusted chamber radical source.

As indicated above, the adjustment of the chamber radical source parameter was carried out in a subjective manner, and the distribution plots suggest that the reactivity parameters were not completely optimized. In a few cases, as discussed in Section III-B, adjustment of the radical source, within the factor of two, was not sufficient to yield acceptable fits to the experimentally observed reactivity; this was true of the apparently anomalous runs in the EC-300 series and also for two of the three ITC runs and the one OTC n-butane run modeled in this program. In most cases, the remaining variability of the discrepancies would be reduced by further refinement and optimization of the radical source adjustment factors, but this was not carried out. However, the distributions of the discrepancies obtained in the present set of adjusted model calculations indicate that if the adjustment is optimized to fit maximum ozone yields then the NO oxidation and ozone formation times will tend to be underpredicted, since in the present set the adjusted model calculations tend to underpredict ozone maximum yields and overpredict reactivity as measured by NO oxidation times. This indicates a probable systematic discrepancy between the model and the experimental data, but this evidence is too indirect to be conclusive.

Model predictions of product yields from n-butane runs are summarized only for SAPRC runs since oxygenate and PAN data are not available for the UNC runs, except for a few which have PAN measurements at levels too low for reliable model testing. There does not appear to be any systematic discrepancies in the predicted PAN yields in the SAPRC experiments where sufficient PAN was formed for reliable measurement. However, the adjusted model appears to consistently overpredict both the MEK and acetaldehyde yields observed in the EC runs, suggesting that the model is probably overpredicting the amount of n-butane consumed. (n-Butane reacts too slowly for the n-butane data itself to be useful for testing predictions of how much is consumed.) However, the model predictions of the acetaldehyde/MEK ratio appears to be consistent with the data; this is as expected, since as discussed in Section II-E-3, the relevant rate constant ratio was adjusted to fit the relative acetaldehyde/MEK yields observed in environmental chamber experiments.

## 12. 2,3-Dimethylbutane-$NO_x$-Air Runs

Five 2,3-dimethylbutane-$NO_x$-air runs were modeled in this program, three carried out in the SAPRC EC and two in the UNC chamber. The experimental and calculated ozone yields and NO oxidation and ozone formation times are summarized in Table IV-21. The maximum yields of PAN and acetone observed and calculated for these experiments are summarized in Table IV-22. In both of these tables, the corresponding data for the other $\geq C_6$ alkanes are also included. Experimental and calculated concentration-time plots for an EC 2,3-dimethylbutane run and for a representative UNC run are shown in Figures IV-37 and IV-38, respectively.

The overall reactivity observed in these experiments is overpredicted to varying extents in all the calculations. However, these discrepancies are not considered to be excessive in view of the fact that model simulations of these runs, like the n-butane runs, are highly sensitive to the magnitude of the chamber-dependent radical source assumed in the calculations. The tendency of the model to overpredict the PAN yields observed in the EC runs is consistent with the general overprediction of reactivity. For both the UNC and the EC chambers, the runs were carried out around the same time, so if the assumed radical source is high for one member of the group, it is reasonable to expect it to be high for the rest. The magnitude of the chamber radical source was not adjusted to improve the fits to the results of these experiments.

The calculated oxygenated product yields are reasonably consistent with the results of the 2,3-dimethylbutane experiments, if one takes into account the differences in overall reactivity between the calculations and the experiments. The model tends to slightly overpredict the acetone yields, but this discrepancy would be reduced if the magnitudes of the chamber radical source were adjusted to fit the overall reactivity. Only low yields of acetaldehyde and formaldehyde are observed in the SAPRC experiments, and these results are consistent with the model predictions.

Table IV-21. Initial Concentrations and Experimental and Calculated Ozone Yields and Times Required to Achieve Half the Experimental Change in ($[O_3]-[NO]$) for the $\geq C_6$ Alkane-$NO_x$-Air Runs

| Experiment | Initial Concentrations | | | Maximum Ozone Concentration | | | | Time to 1/2 Maximum Expt. ($[O_3]-[NO]$) | | | |
|---|---|---|---|---|---|---|---|---|---|---|---|
| | $NO_x$ (ppm) | HC (ppmC) | $HC/NO_x$ | Expt (ppm) | Calc (ppm) | Calc -Expt (ppm) | Calc -Expt /Expt) | Expt (min) | Calc (min) | Calc -Expt (min) | Calc -Expt /Expt |
| **1: EC 2,3-Dimethylbutane Runs** | | | | | | | | | | | |
| EC-165 | 0.097 | 11.3 | 116.3 | 0.488 | 0.650 | 0.162 | 0.33 | 161 | 103 | -58 | -0.36 |
| EC-169 | 0.191 | 4.4 | 23.2 | 0.493 | 0.529 | 0.036 | 0.07 | 307 | 240 | -67 | -0.22 |
| EC-171 | 0.098 | 3.5 | 35.7 | 0.403 | 0.477 | 0.074 | 0.18 | 184 | 172 | -12 | -0.06 |
| Group Average | 0.129 | 6.4 | 58.4 | 0.462 | 0.552 | 0.091 | 0.20 | 217 | 172 | -45 | -0.21 |
| S. Dev. | 0.054 | 4.2 | 50.5 | 0.051 | 0.089 | 0.065 | 0.13 | 78 | 69 | 29 | 0.15 |
| Avg. Abs. Value | | | | | | 0.091 | 0.20 | | | 44 | 0.21 |
| S. Dev. | | | | | | 0.065 | 0.13 | | | 29 | 0.15 |
| **2: UNC 2,3-Dimethylbutane Runs** | | | | | | | | | | | |
| OC1879R | 0.202 | 15.7 | 77.7 | 0.236 | 0.611 | 0.375 | 1.59 | 453 | 301 | -152 | -0.33 |
| OC2079B | 0.223 | 12.0 | 53.8 | 0.217 | 0.440 | 0.223 | 1.03 | 451 | 325 | -126 | -0.28 |
| Group Average | 0.213 | 13.9 | 65.8 | 0.226 | 0.525 | 0.299 | 1.31 | 452 | 313 | -139 | -0.31 |
| S. Dev. | 0.015 | 2.6 | 16.9 | 0.014 | 0.121 | 0.107 | 0.39 | 1 | 17 | 18 | 0.04 |
| Avg. Abs. Value | | | | | | 0.299 | 1.31 | | | 139 | 0.31 |
| S. Dev. | | | | | | 0.107 | 0.39 | | | 18 | 0.04 |
| **3: UNC Isopentane Run** | | | | | | | | | | | |
| AU1983R | 0.377 | 4.6 | 12.3 | 0.083 | 0.075 | -0.008 | -0.10 | 438 | 432 | -6 | -0.01 |

(continued)

Table IV-21 (continued) - 2

| Experiment | Initial Concentrations | | | Maximum Ozone Concentration | | | | Time to 1/2 Maximum Expt. ($[O_3]-[NO]$) | | | |
|---|---|---|---|---|---|---|---|---|---|---|---|
| | $NO_x$ (ppm) | HC (ppmC) | $HC/NO_x$ | Expt (ppm) | Calc (ppm) | Calc -Expt (ppm) | Calc -Expt /Expt) | Expt (min) | Calc (min) | Calc -Expt (min) | Calc -Expt /Expt |
| **4: UNC Isooctane Run** | | | | | | | | | | | |
| AU1983B | 0.374 | 4.0 | 10.7 | 0.055 | 0.038 | -0.017 | -0.31 | 450 | 467 | -17 | 0.04 |
| **5: EC n-Alkane Runs** | | | | | | | | | | | |
| n-Pentane | | | | | | | | | | | |
| EC-135 | 0.096 | 20.4 | 212.8 | 0.435 | 0.573 | 0.138 | 0.32 | 83 | 79 | -4 | -0.05 |
| n-Hexane | | | | | | | | | | | |
| EC-131 | 0.097 | 24.6 | 253.7 | 0.393 | 0.558 | 0.165 | 0.42 | 115 | 100 | -15 | -0.13 |
| n-Nonane | | | | | | | | | | | |
| EC-155 | 0.096 | 37.3 | 389.1 | 0.264 | 0.443 | 0.179 | 0.68 | 121 | 151 | 29 | 0.24 |
| Group Average | 0.096 | 27.5 | 285.2 | 0.364 | 0.525 | 0.161 | 0.47 | 106 | 110 | 3 | 0.02 |
| S. Dev. | 0.001 | 8.8 | 92.2 | 0.089 | 0.071 | 0.021 | 0.19 | 21 | 37 | 23 | 0.20 |
| Avg. Abs. Value | | | | | | 0.161 | 0.47 | | | 16 | 0.14 |
| S. Dev. | | | | | | 0.021 | 0.19 | | | 13 | 0.10 |
| **5: ITC n-Alkane Runs** | | | | | | | | | | | |
| n-Heptane | | | | | | | | | | | |
| ITC-559 | 0.113 | 279.4 | 2472.6 | 0.377 | 0.461 | 0.084 | 0.22 | 196 | 169 | -26 | -0.13 |
| ITC-538 | 0.118 | 60.3 | 511.1 | 0.150 | 0.254 | 0.104 | 0.69 | 161 | 130 | -31 | -0.19 |
| ITC-540 | 0.113 | 305.2 | 2700.9 | 0.360 | 0.319 | -0.042 | -0.12 | 118 | 224 | 106 | 0.90 |

(continued)

Table IV-21 (continued) - 3

| Experiment | Initial Concentrations | | | Maximum Ozone Concentration | | | | Time to 1/2 Maximum Expt. ([$O_3$]-[NO]) | | | |
|---|---|---|---|---|---|---|---|---|---|---|---|
| | $NO_x$ (ppm) | HC (ppmC) | HC/$NO_x$ | Expt (ppm) | Calc (ppm) | Calc -Expt (ppm) | Calc -Expt /Expt) | Expt (min) | Calc (min) | Calc -Expt (min) | Calc -Expt /Expt |
| n-Octane | | | | | | | | | | | |
| ITC-552 | 0.131 | 428.8 | 3273.3 | 0.315 | 0.201 | -0.115 | -0.36 | 165 | 256 | 91 | 0.55 |
| ITC-761 | 0.519 | 76.5 | 147.3 | 0.030 | 0.016 | -0.014 | | 141 | 203 | 62 | 0.44 |
| ITC-762 | 0.264 | 75.4 | 285.6 | 0.105 | 0.071 | -0.035 | -0.33 | 148 | 157 | 8 | 0.06 |
| ITC-763 | 0.259 | 7.6 | 29.5 | 0.041 | 0.034 | -0.007 | | 128 | 131 | 4 | 0.03 |
| ITC-797 | 0.540 | 7.3 | 13.5 | 0.004 | 0.008 | 0.003 | | 115 | 130 | 15 | 0.13 |
| Group Average | 0.257 | 155.1 | 1179.2 | 0.173 | 0.170 | -0.003 | 0.02 | 147 | 175 | 29 | 0.22 |
| S. Dev. | 0.179 | 159.5 | 1381.7 | 0.155 | 0.166 | 0.070 | 0.44 | 27 | 48 | 52 | 0.38 |
| Avg. Abs. Value | | | | | | 0.050 | 0.34 | | | 43 | 0.30 |
| S. Dev. | | | | | | 0.045 | 0.22 | | | 39 | 0.30 |
| 6: UNC n-Alkane Runs | | | | | | | | | | | |
| n-Pentane | | | | | | | | | | | |
| OC0979B | 0.205 | 14.1 | 68.5 | 0.184 | 0.346 | 0.162 | 0.88 | 446 | 338 | -108 | -0.24 |
| n-Octane | | | | | | | | | | | |
| ST1879R | 0.207 | 6.2 | 30.1 | 0.120 | 0.202 | 0.082 | 0.69 | 495 | 393 | -102 | -0.21 |
| Group Average | 0.206 | 10.1 | 49.3 | 0.152 | 0.274 | 0.122 | 0.79 | 470 | 365 | -105 | -0.22 |
| S. Dev. | 0.001 | 5.5 | 27.2 | 0.045 | 0.102 | 0.057 | 0.14 | 35 | 39 | 4 | 0.03 |
| Avg. Abs. Value | | | | | | 0.122 | 0.79 | | | 105 | 0.22 |
| S. Dev. | | | | | | 0.057 | 0.14 | | | 4 | 0.03 |

Table IV-22. Experimental and Calculated Product Yields Observed in the 2,3-Dimethylbutane, Isopentane, and Isooctane-$NO_x$-Air Irradiations

| Experiment | Species | Expt (ppm) | Calc (ppm) | Calc -Expt (ppm) | Calc -Expt /Expt |
|---|---|---|---|---|---|
| 1: EC 2,3-Dimethylbutane Runs | | | | | |
| EC-165 | PAN | 0.017 | 0.008 | -0.009 | -0.54 |
| | Acetone | 0.471 | 0.636 | 0.165 | 0.35 |
| EC-169. | PAN | 0.024 | 0.011 | -0.013 | -0.55 |
| | Acetone | 0.343 | 0.460 | 0.117 | 0.34 |
| EC-171 | PAN | 0.020 | 0.010 | -0.010 | -0.50 |
| | Acetone | 0.362 | 0.393 | 0.031 | 0.09 |
| | Acetaldehyde | 0.029 | 0.006 | -0.024 | -0.81 |
| Group Average | PAN | 0.020 | 0.010 | -0.011 | -0.53 |
| Std. Dev. | | 0.003 | 0.002 | 0.002 | 0.03 |
| Avg. Abs Value | | | | 0.011 | 0.53 |
| Std. Dev. | | | | 0.002 | 0.03 |
| Group Average | Acetone | 0.392 | 0.496 | 0.104 | 0.26 |
| Std. Dev. | | 0.069 | 0.126 | 0.068 | 0.15 |
| Avg. Abs Value | | | | 0.104 | 0.26 |
| Std. Dev. | | | | 0.068 | 0.15 |
| 2: UNC 2,3-Dimetylbutane Runs | | | | | |
| OC1879R | PAN | 1.260 | 0.003 | -1.257 | -1.00 |
| | Acetone | 0.253 | 0.407 | 0.153 | 0.61 |
| OC2079B | Acetone | 0.349 | 0.357 | 0.009 | 0.02 |
| Group Average | Acetone | 0.301 | 0.382 | 0.081 | 0.31 |
| Std. Dev. | | 0.067 | 0.035 | 0.102 | 0.41 |
| Avg. Abs Value | | | | 0.081 | 0.31 |
| Std. Dev. | | | | 0.102 | 0.41 |
| 3: UNC Isopentane Run | | | | | |
| AU1983B | Acetone | 0.233 | 0.014 | -0.220 | -0.94 |
| 4: UNC Isooctane Run | | | | | |
| AU1983R | Acetone | 0.340 | 0.052 | -0.288 | -0.85 |
| | Acetaldehyde | 0.064 | 0.045 | -0.019 | -0.30 |

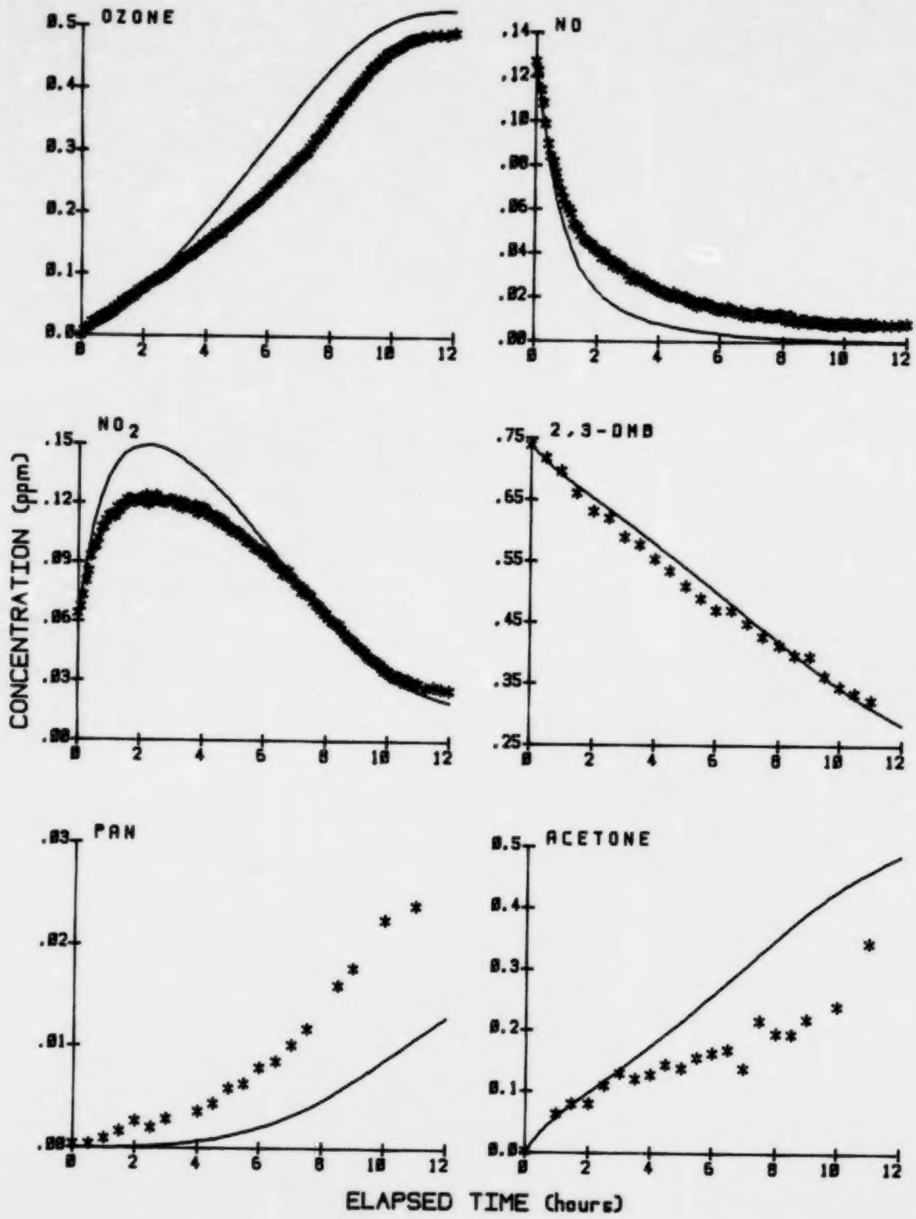

Figure IV-37. Experimental and calculated concentration-time plots for representative species observed in the 2,3-dimethylbutane-$NO_x$-air run EC-169.
* = Experimental data.
----- = Model calculation.

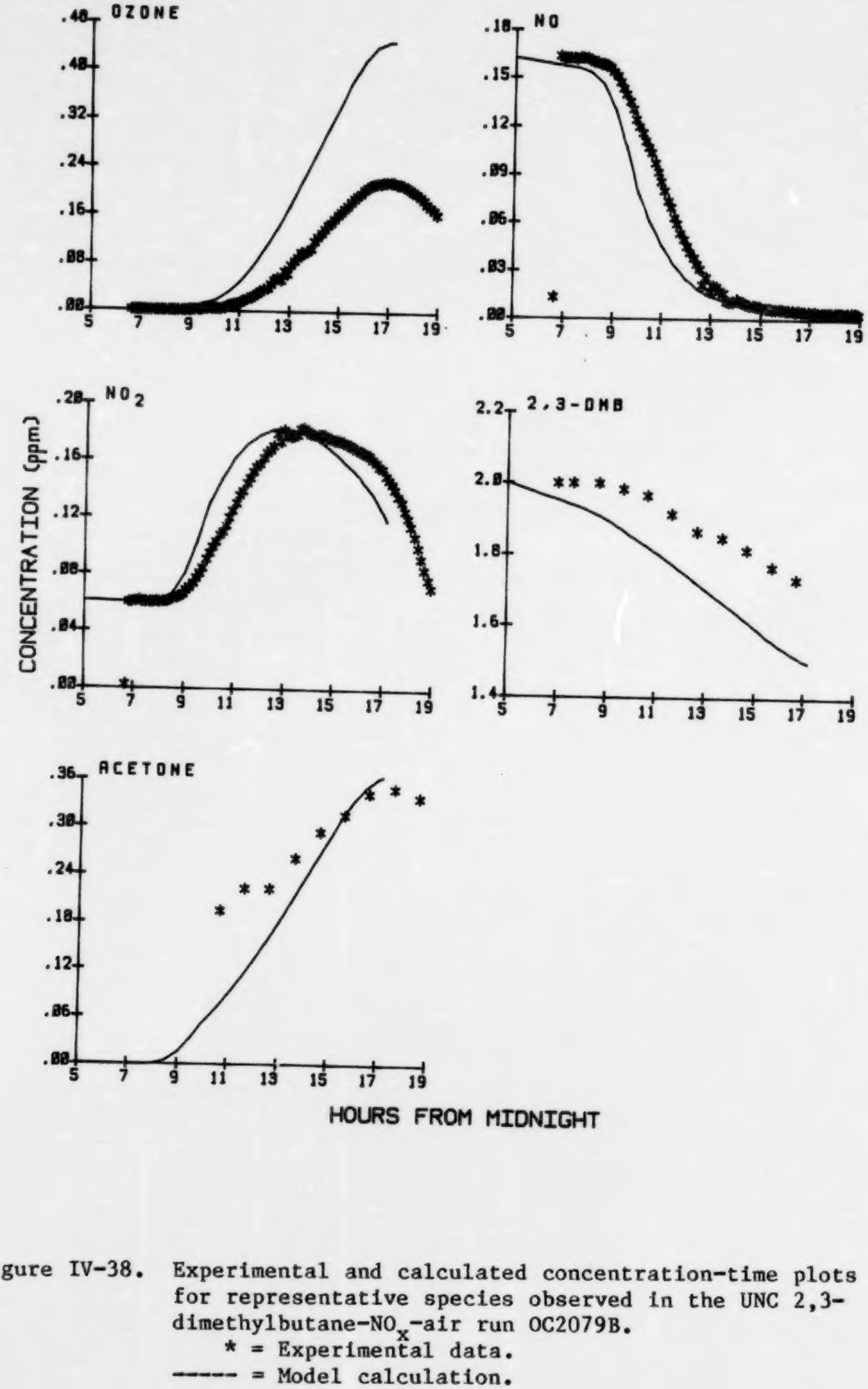

Figure IV-38. Experimental and calculated concentration-time plots for representative species observed in the UNC 2,3-dimethylbutane-$NO_x$-air run OC2079B.

* = Experimental data.

----- = Model calculation.

### 13. Isopentane and Isooctane-$NO_x$-Air Runs

One UNC chamber run modeled in this program consisted of an irradiation of an isopentane-$NO_x$-air mixture on the "red" side and an isooctane-$NO_x$-air mixture on the "blue" side. The experimental and calculated maximum ozone yields and NO oxidation and ozone formation times for these runs are summarized in Table IV-21, and the acetone and acetaldehyde yields are summarized in Table IV-22. Experimental and calculated concentration-time plots for these irradiations are given in Figures IV-39 and IV-40.

In both irradiations the model simulations gave good fits to the observed times to oxidize NO and form ozone, indicating that the default chamber radical source is appropriate for these runs. (Like other alkane-$NO_x$ irradiations, model simulations of these runs are expected to be highly sensitive to this.) On the other hand, the consumption of the alkane in the model calculation begins earlier than observed experimentally, though the model predictions of the total amount of alkane consumed during the run appears to fit the data. The major discrepancy concerns the predicted acetone yields, where the model is low by a factor of six in the isooctane simulation and by a factor of two in the isopentane simulation. This suggests that, if the experimental acetone measurements are accurate, the estimated rate constants for the decompositions of the alkoxy radicals formed in the photooxidations of these alkanes are too low, since according to the present mechanism these are the reactions which give rise to the formation of acetone in these systems. This would be especially so for the alkoxy radicals formed in the isooctane photooxidation, where the discrepancy in the acetone yields is a factor of six. For isopentane, the decomposition reactions which form acetone will also form acetaldehyde, and the model simulation underpredicts acetaldehyde by a factor of 1.4, which is comparable to the factor of two discrepancy for acetone. (Acetaldehyde is not expected to be formed in significant yields in the photooxidation of isooctane, and this is consistent with the experimental data.) These alkoxy radical decomposition reactions, and the alkane photooxidation mechanisms in general, are discussed in Section II-F. As discussed there, the decomposition rate constants for alkoxy radicals for which no experimental data are available (such as

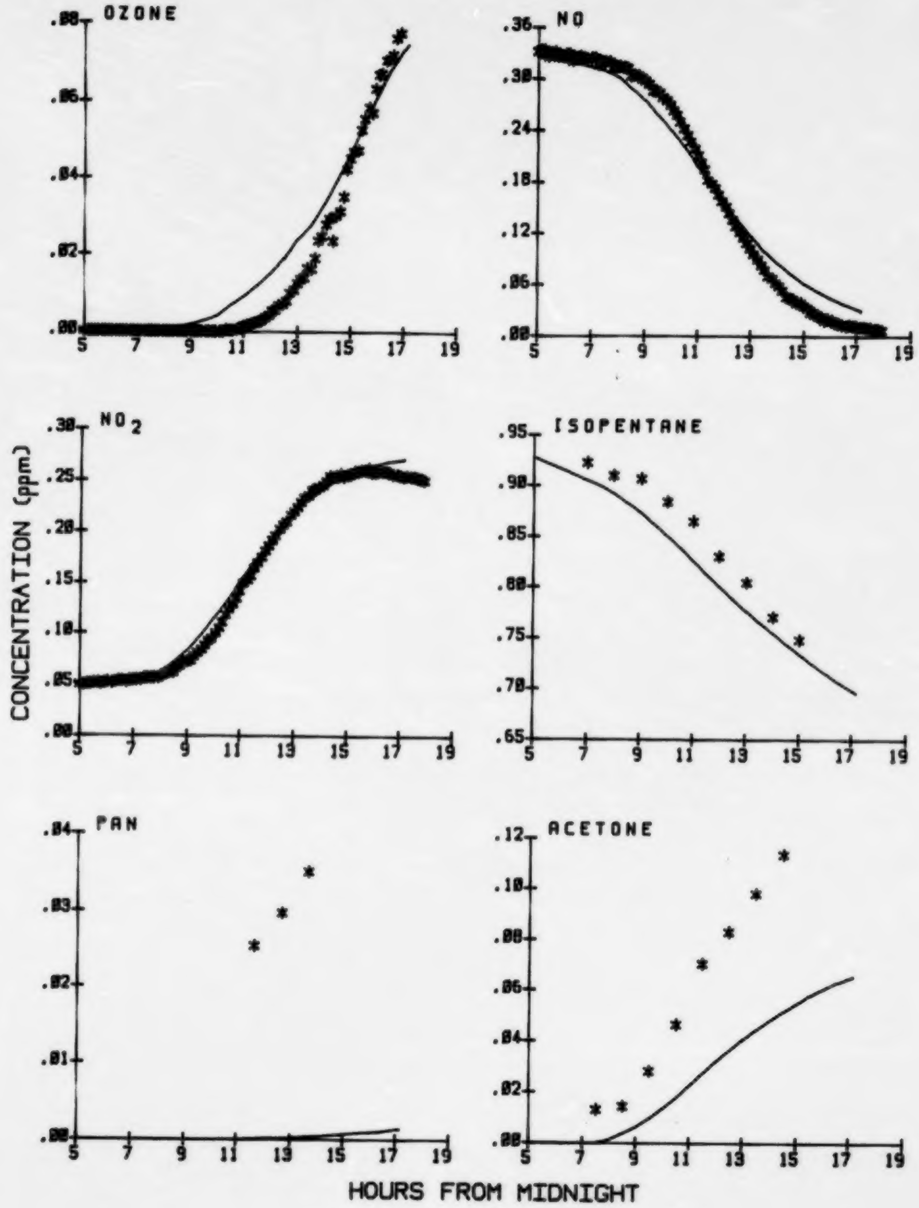

Figure IV-39. Experimental and calculated concentration-time plots for representative species observed in the UNC isopentane-$NO_x$-air run AU1983R.
* = Experimental data.
----- = Model calculation.

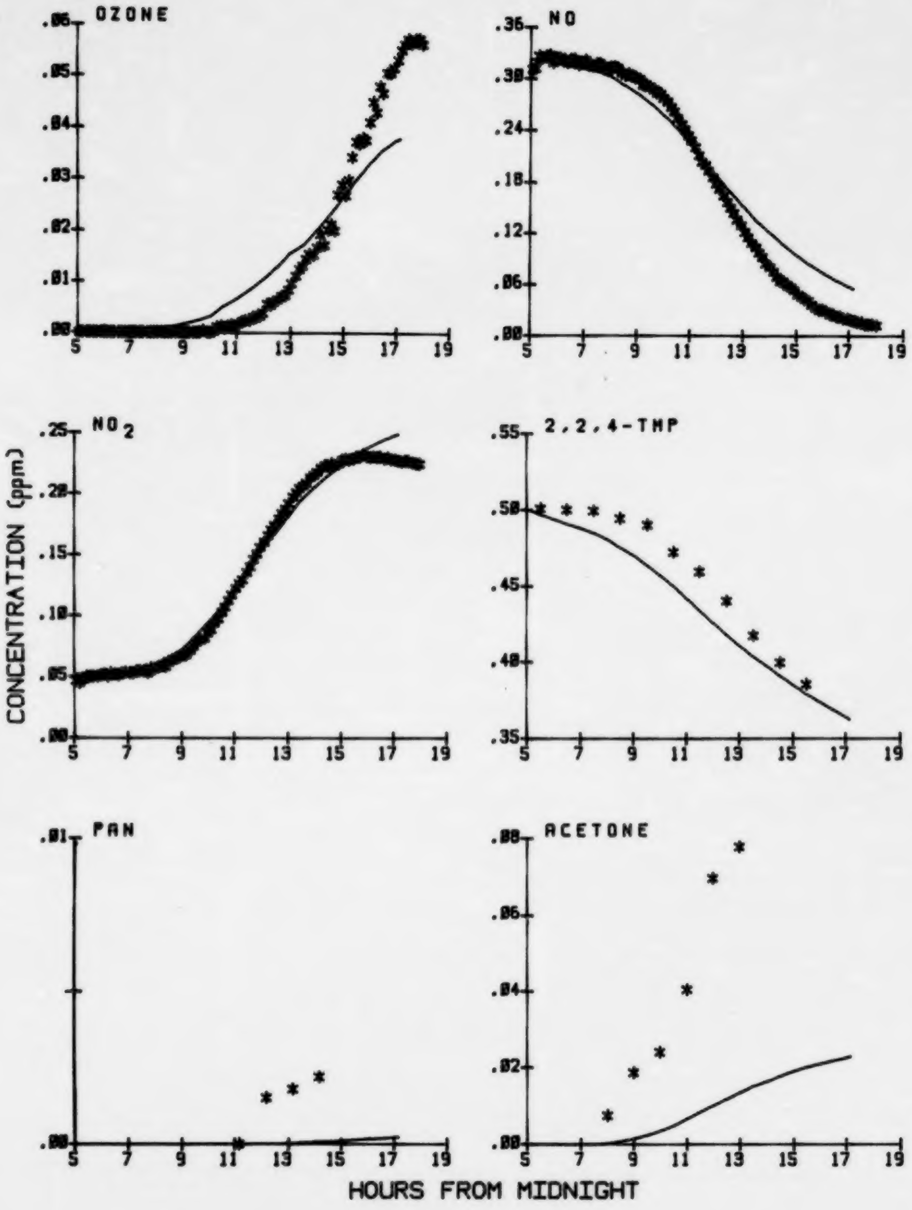

Figure IV-40. Experimental and calculated concentration-time plots for representative species observed in the UNC isooctane-$NO_x$-air run AU1983B.
* = Experimental data.
----- = Model calculation.

those formed from these alkanes) are uncertain by at least a factor of five, and thus the discrepancy observed in these runs is not suprising. No adjustment of the model was made to improve the predictions of the acetone yields in these experiments.

### 14. $\geq C_5$ n-Alkane-$NO_x$-Air Runs

$NO_x$-air irradiations of n-pentane through n-nonane were modeled in this program. These consist of one n-pentane run in the EC and one in the UNC chamber, one n-hexane run in the EC and one in the ITC, two n-heptane runs in the ITC, five n-octane runs in the ITC, and one n-nonane run in the EC. Four of the n-octane runs carried out in the ITC had low levels of propene added to serve as radical tracers. The experimental and calculated ozone maxima and NO oxidation and ozone formation times for these runs are summarized in Table IV-21. Distribution plots of the discrepancies in the model predictions of these values are given in Figure IV-41. Experimental and calculated concentration-time plots for n-pentane and the n-nonane runs carried out in the EC, for an ITC tracer-$NO_x$-air irradiation with n-octane added after two hours, and for the UNC n-octane run are given in Figures IV-42 through IV-45, respectively.

As expected for model simulations of alkane-$NO_x$-air runs, which are sensitive to the assumed chamber radical input rates, the fits of the model predictions to the timing parameter were variable, but there does not appear to be any consistent tendency for the model to overpredict or underpredict the timing parameters for these runs, when taken as a group. However, as discussed in Section II-F-1, in order to achieve these fits for the $\geq C_6$ n-alkane runs, it was necessary to assume, contrary to our initial estimate, that alkyl nitrates are not formed in significant yields from the reactions of the hydroxy-substituted peroxy radicals formed in the photooxidations of these compounds. If nitrate formation from these species is assumed, the model consistently and significantly underpredicts the reactivity observed in these experiments, more than can reasonably be attributed to variations in the chamber radical source. There are a sufficient number and variety of $\geq C_6$ n-alkane runs modeled in this program to justify modifying the mechanism in this highly uncertain area to reduce this discrepancy between the predictions of the model and the experimental results.

| Calc.-Expt./Calc.<br>Maximum Ozone | | Calc.-Expt./Calc.<br>Time to 1/2 Expt. $\Delta([O_3]-[NO])^{max}$ | |
|---|---|---|---|
| < -0.33 | : | < -0.55 | : |
| -0.33 - -0.27 | : | -0.55 - -0.45 | : |
| -0.27 - -0.21 | : | -0.45 - -0.35 | : |
| -0.21 - -0.15 | : | -0.35 - -0.25 | : |
| -0.15 - -0.09 | :2 | -0.25 - -0.15 | :233 |
| -0.09 - -0.03 | :22 | -0.15 - -0.05 | :12 |
| -0.03 - 0.03 | :222 | -0.05 - 0.05 | :12 |
| 0.03 - 0.09 | :23 | 0.05 - 0.15 | :22 |
| 0.09 - 0.15 | :12 | 0.15 - 0.25 | :1 |
| 0.15 - 0.21 | :113 | 0.25 - 0.35 | : |
| 0.21 - 0.27 | : | 0.35 - 0.45 | :2 |
| 0.27 - 0.33 | : | 0.45 - 0.55 | : |
| > 0.33 | : | > 0.55 | :22 |

Figure IV-41. Distribution plots of discrepancies in model predictions of ozone yields and times required to achieve half the maximum experimental change in ($[O_3]-[NO]$) for the $\geq C_5$ n-alkane runs. Codes for chambers: 1 = EC, 2 = ITC, 3 = UNC.

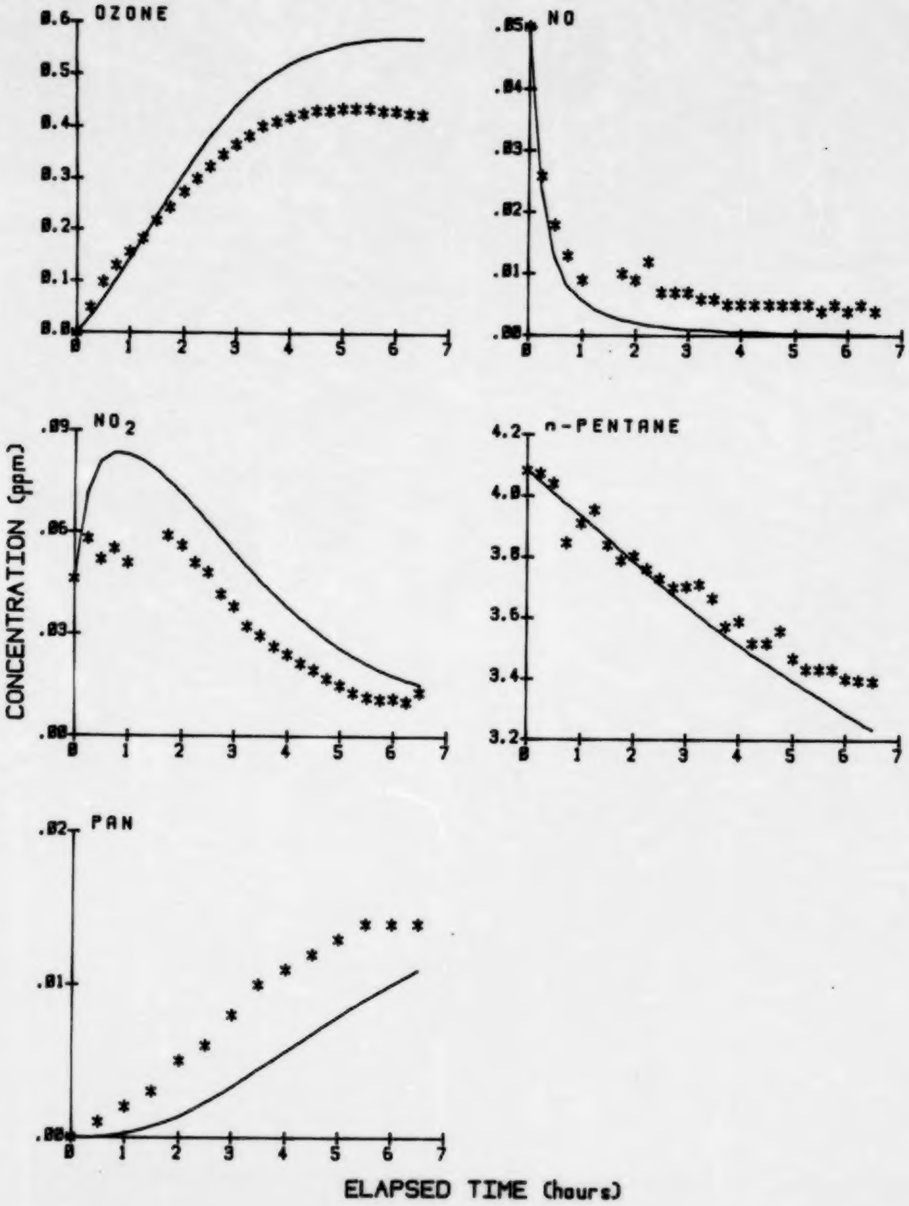

Figure IV-42. Experimental and calculated concentration-time plots for representative species observed in the n-pentane-NO$_x$-air run EC-135.
* = Experimental data.
----- = Model calculation.

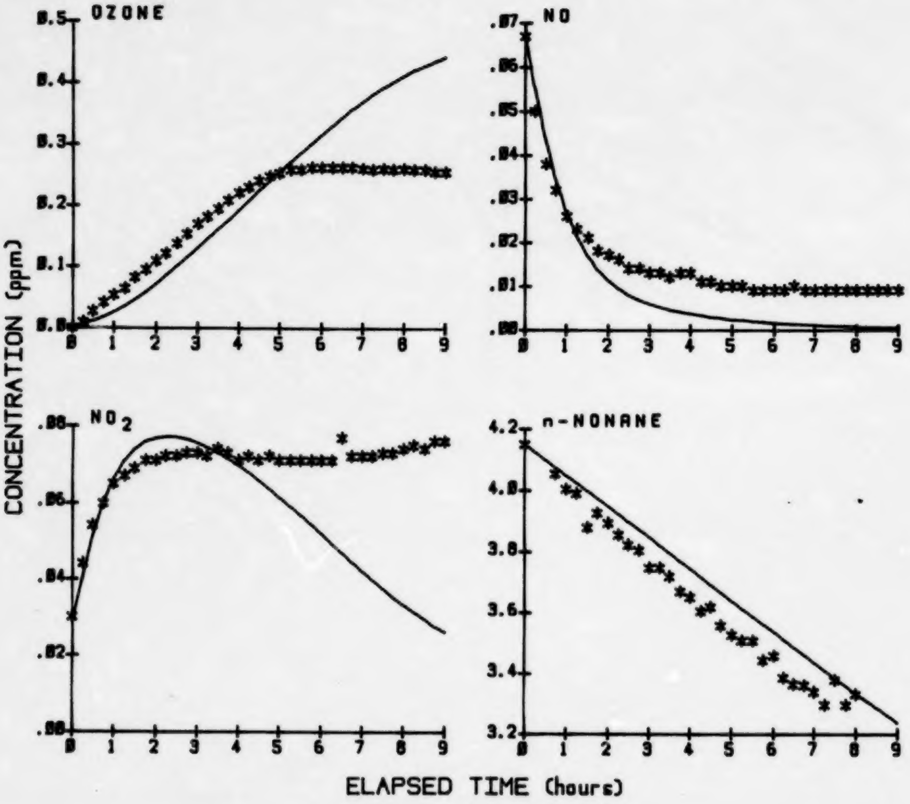

Figure IV-43. Experimental and calculated concentration-time plots for representative species observed in the n-nonane-NO$_x$-air run EC-155.
* = Experimental data.
----- = Model calculation.

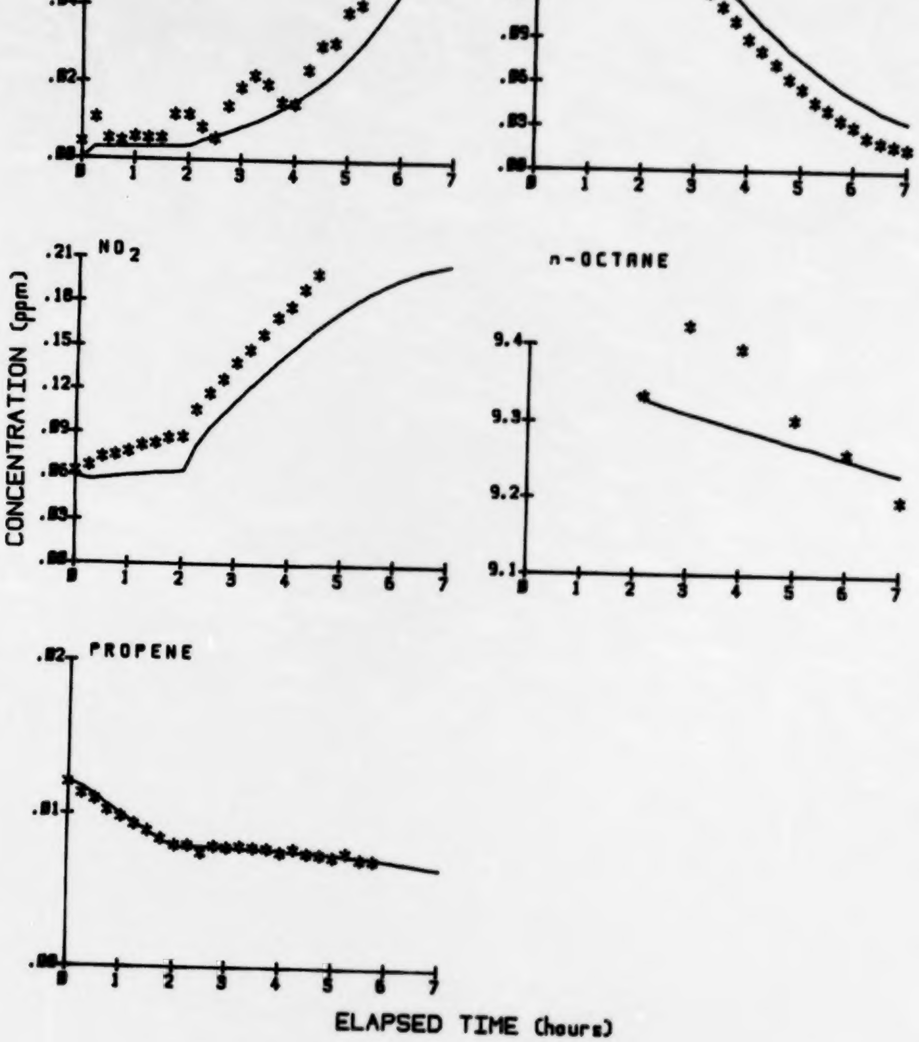

Figure IV-44. Experimental and calculated concentration-time plots for representative species observed in the n-octane-$NO_x$-air run ITC-762.
* = Experimental data.
----- = Model calculation.

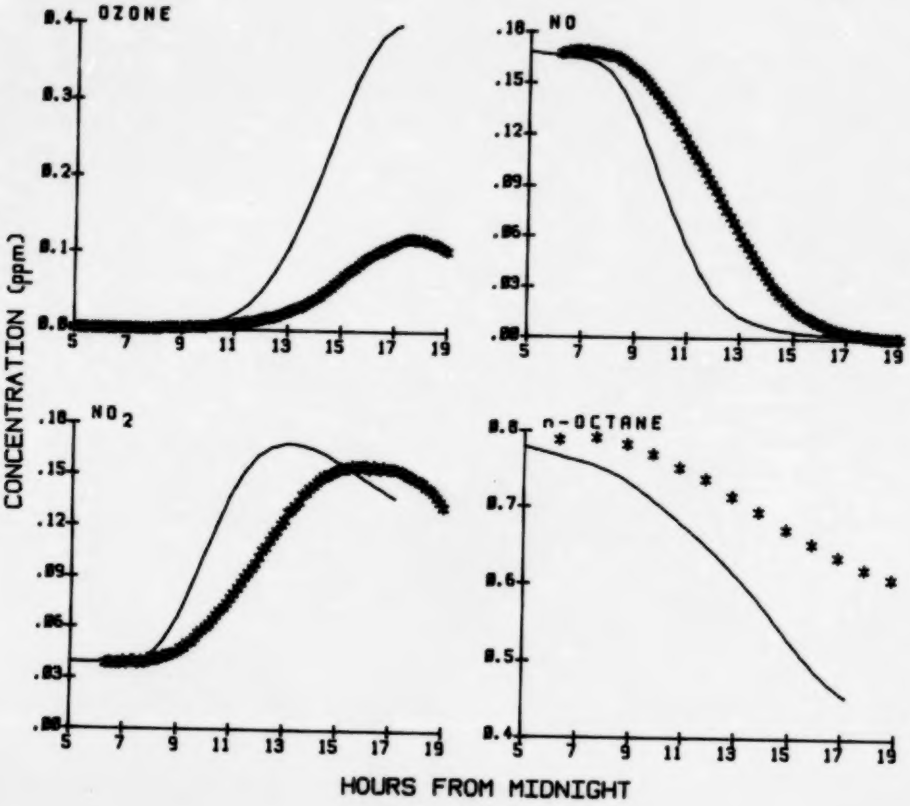

Figure IV-45. Experimental and calculated concentration-time plots for representative species observed in the UNC n-octane-$NO_x$-air run ST1879R.
* = Experimental data.
----- = Model calculation.

Of these n-alkane-$NO_x$-air runs, the only ones where a "true" ozone maxima were obtained were those carried out in the EC. This is attributed to the fact that the reactivity of alkane-$NO_x$ irradiations is greater in irradiations in the EC than in the other chambers because, as discussed in Section III-B, the EC has larger chamber radical fluxes than do the ITC, the OTC and the UNC chamber. For the runs carried out in the other chambers, the irradiation ended (or the sun set) while ozone formation was still occurring, and thus the fits to the maximum ozone yield reflect primarily the fits to the "timing" of the runs, which as indicated above is sensitive to the chamber radical source. In the model simulations of EC runs, where the "timing" was fit reasonably well (on the average), the maximum ozone yields were consistently overpredicted, with the extent of overprediction increasing with the size of the alkane. This could be attributed to the model underpredicting $NO_x$ sinks in the reaction mechanisms of the higher n-alkanes, since the availability of $NO_x$ is an important factor affecting the maximum amount of ozone which can be formed in these runs. Better predictions of "true" ozone maxima can be obtained if it is assumed that alkyl nitrates are formed in the reaction of NO with hydroxy-substituted alkoxy radicals, but as indicated above, this also results in significant underpredictions of reactivity as defined by "timing." This suggests that there may be other $NO_x$ sinks in the photooxidation mechanisms of the higher n-alkanes which are being overlooked by the present model.

The formation of the products 2- and 3-pentanone are expected in the n-pentane-$NO_x$-air irradiations, and indeed these products were observed in run EC-135. However, because the reactions of the various bi- and poly-functional products are lumped together and represented by the same species in the model used to represent the reactions of these higher ketones, this model makes no predictions of the yields of these specific products.

The photooxidations of the $\geq C_6$ n-alkanes are expected to give rise primarily to bi- and poly-functional products which could not be monitored by the analytical techniques employed during these chamber experiments. Thus the yields of measurable products in these experiments are expected to be low, and this is consistent with the experimental results.

### 15. Benzene-$NO_x$-Air Runs

Six benzene-$NO_x$-air runs carried out in the SAPRC ITC were modeled in this program. One of these experiments consisted of a tracer-$NO_x$-air run where benzene was added at the end of the second hour of the irradiation. The experimental and calculated maximum ozone yields and NO oxidation and ozone formation times for these runs are summarized in Table IV-23, and selected concentration-time plots for two representative benzene-$NO_x$-air runs and for the tracer-$NO_x$-air + benzene run are given in Figures IV-46 and IV-47, respectively. Distribution plots of the discrepancies in the predicted ozone maxima and the NO oxidation/ozone formation times for the benzene runs are given, together with the results for all the single component aromatic runs, in Figure IV-48. Plots of these discrepancies against the initial aromatic/$NO_x$ ratios are given in Figures IV-49 and IV-50.

The model simulations of the benzene-$NO_x$-air runs yielded fair fits to the overall reactivity observed in these runs, though it should be noted that, as discussed in Section II-G, this is a result of adjusting the photolysis rate of unknown ring-opened products. The performance of the model in other respects suggests some problems with the benzene mechanism. The maximum ozone yields tend to be consistently overpredicted, suggesting that the benzene mechanism may not be including enough $NO_x$ sinks, though this discrepancy is not large. In addition, as shown in Figure IV-46, the model does not accurately simulate the details of the NO and $NO_2$ concentration-time profiles. For the highest benzene/$NO_x$ run ITC-560, the model predicts an initial NO consumption rate which is far greater than observed experimentally, though the reactivity later in the run is well simulated.

The results of the simulation of the $NO_x$-air + benzene run, which was carried out at the lowest benzene/$NO_x$ ratio, also indicate a serious problem with the mechanism, since the rate of NO to $NO_2$ conversion, and the OH radical levels (as indicated by the rate of consumption of propene) after the benzene is added is significantly overpredicted. The propene data in that run indicate that the addition of benzene tends to initially inhibit radical levels, and this is not simulated by the model. Including a radical sink in the initial benzene photooxidation process in the model

Table IV-23. Initial Concentrations and Experimental and Calculated Ozone Yields and Times Required to Achieve Half the Experimental Change in ($[O_3]-[NO]$) for the Benzene-$NO_x$-Air Runs Carried Out in the SAPRC ITC

| Experiment | Initial Concentrations | | | Maximum Ozone Concentration | | | | Time to 1/2 Maximum Expt. ($[O_3]-[NO]$) | | | |
|---|---|---|---|---|---|---|---|---|---|---|---|
| | $NO_x$ (ppm) | HC (ppmC) | $HC/NO_x$ | Expt (ppm) | Calc (ppm) | Calc -Expt (ppm) | Calc -Expt /Expt) | Expt (min) | Calc (min) | Calc -Expt (min) | Calc -Exp /Exp |
| ITC-560 | 0.116 | 332 | 2865 | 0.323 | 0.398 | 0.075 | 0.23 | 28 | 19 | -9 | -0.33 |
| ITC-561 | 0.114 | 79.1 | 694.2 | 0.273 | 0.332 | 0.060 | 0.22 | 36 | 37 | 0 | 0.00 |
| ITC-562 | 0.559 | 83.8 | 149.8 | 0.412 | 0.458 | 0.046 | 0.11 | 146 | 124 | -22 | -0.15 |
| ITC-698 | 0.499 | 83.5 | 167.4 | 0.374 | 0.434 | 0.060 | 0.16 | 133 | 114 | -20 | -0.15 |
| ITC-710 | 0.553 | 83.6 | 151.1 | 0.367 | 0.444 | 0.077 | 0.21 | 145 | 123 | -22 | -0.15 |
| ITC-831 | 1.007 | 12.2 | 12.2 | 0.021 | 0.005 | -0.016 | | 205 | 177 | -28 | -0.14 |
| Group Average | 0.475 | 112.4 | 673.2 | 0.295 | 0.345 | 0.050 | 0.19 | 116 | 99 | -17 | -0.15 |
| S. Dev. | 0.333 | 111.3 | 1099.3 | 0.142 | 0.173 | 0.034 | 0.05 | 69 | 60 | 10 | 0.11 |
| Avg. Abs. Value | | | | | | 0.056 | 0.19 | | | 16 | 0.15 |
| S. Dev. | | | | | | 0.022 | 0.05 | | | 10 | 0.10 |

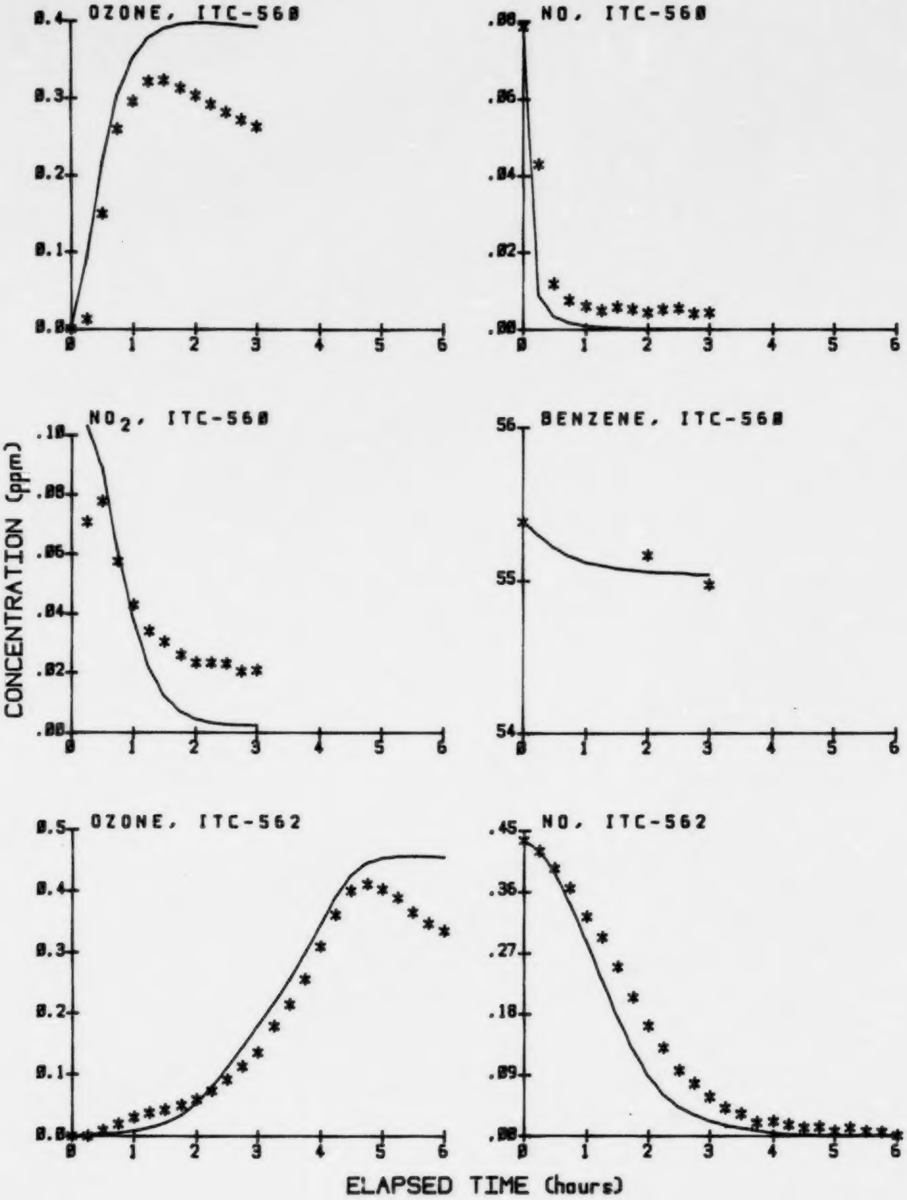

Figure IV-46. Experimental and calculated concentration-time plots for representative species observed in the benzene-$NO_x$-air runs ITC-560 and ITC-562.
* = Experimental data.
----- = Model calculation.

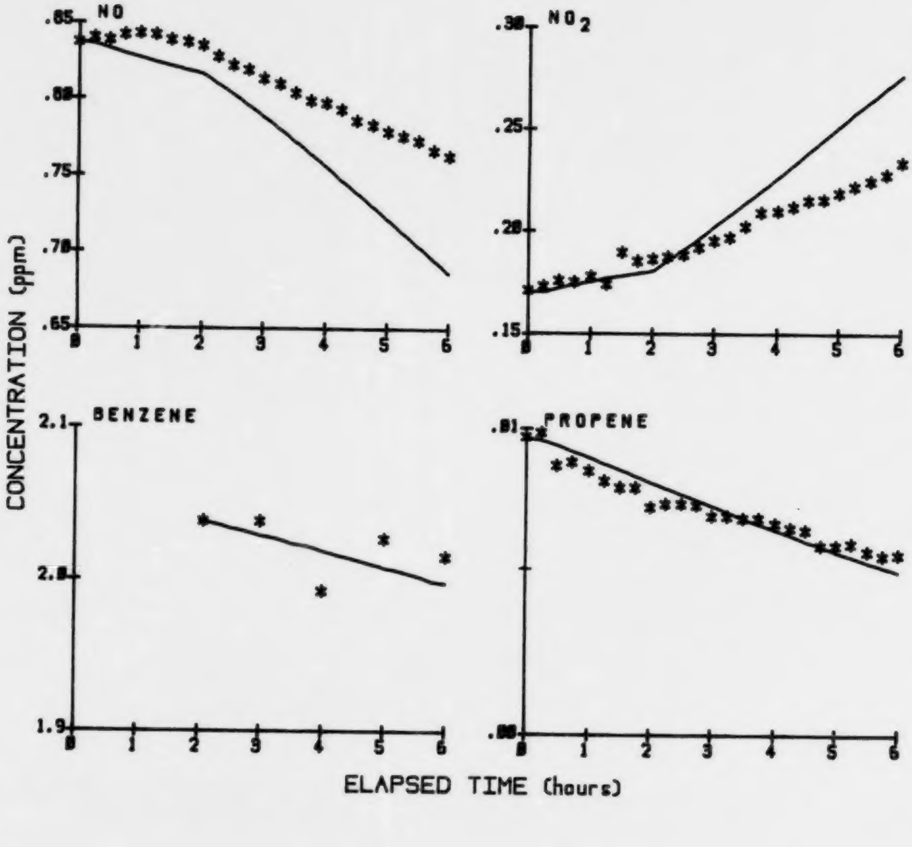

Figure IV-47. Experimental and calculated concentration-time plots for representative species observed in the benzene-$NO_x$-air run ITC-831.
* = Experimental data.
----- = Model calculation.

```
-------------------------------------------------------------
   Calc.-Expt.    Benzene     Toluene      Xylenes   1,3,5-TMB
  Ozone (ppm)
-------------------------------------------------------------

      <  -0.33  :       :            :         :2
-0.33 -  -0.27  :       :            :         :2
-0.27 -  -0.21  :       :            :3        :
-0.21 -  -0.15  :       :            :2        :22
-0.15 -  -0.09  :       :            :3        :
-0.09 -  -0.03  :       :            :1113     :
-0.03 -   0.03  :2      :1122        :23       :112
 0.03 -   0.09  :22222  :11111111133 :1        :1
 0.09 -   0.15  :       :13          :         :
 0.15 -   0.21  :       :3           :         :
 0.21 -   0.27  :       :            :         :
 0.27 -   0.33  :       :3           :         :
      >   0.33  :       :            :         :
-------------------------------------------------------------
 (Calc.-Expt)./Calc.
    Time to 1/2   Benzene     Toluene      Xylenes   1,3,5-TMB
Expt. Δ([O3]-[NO])max
-------------------------------------------------------------

      <  -0.55  :       :            :         :
-0.55 -  -0.45  :       :            :         :2
-0.45 -  -0.35  :       :12          :2        :
-0.35 -  -0.25  :2      :3           :         :2
-0.25 -  -0.15  :22     :1111111113  :133      :22
-0.15 -  -0.05  :22     :233         :23       :
-0.05 -   0.05  :2      :3           :11       :1112
 0.05 -   0.15  :       :1           :13       :
 0.15 -   0.25  :       :1           :         :
 0.25 -   0.35  :       :            :         :
 0.35 -   0.45  :       :            :         :
 0.45 -   0.55  :       :1           :         :
      >   0.55  :       :            :         :
-------------------------------------------------------------
```

Figure IV-48. Distribution plots for the discrepancies in the model predictions of the ozone yields and the times required to achieve half the experimental maximum ($[O_3]-[NO]$) for the benzene, toluene, xylene, and 1,3,5-trimethylbenzene (1,3,5-TMB) runs. Codes for chambers: 1 = EC, 2 = ITC, 3 = UNC.

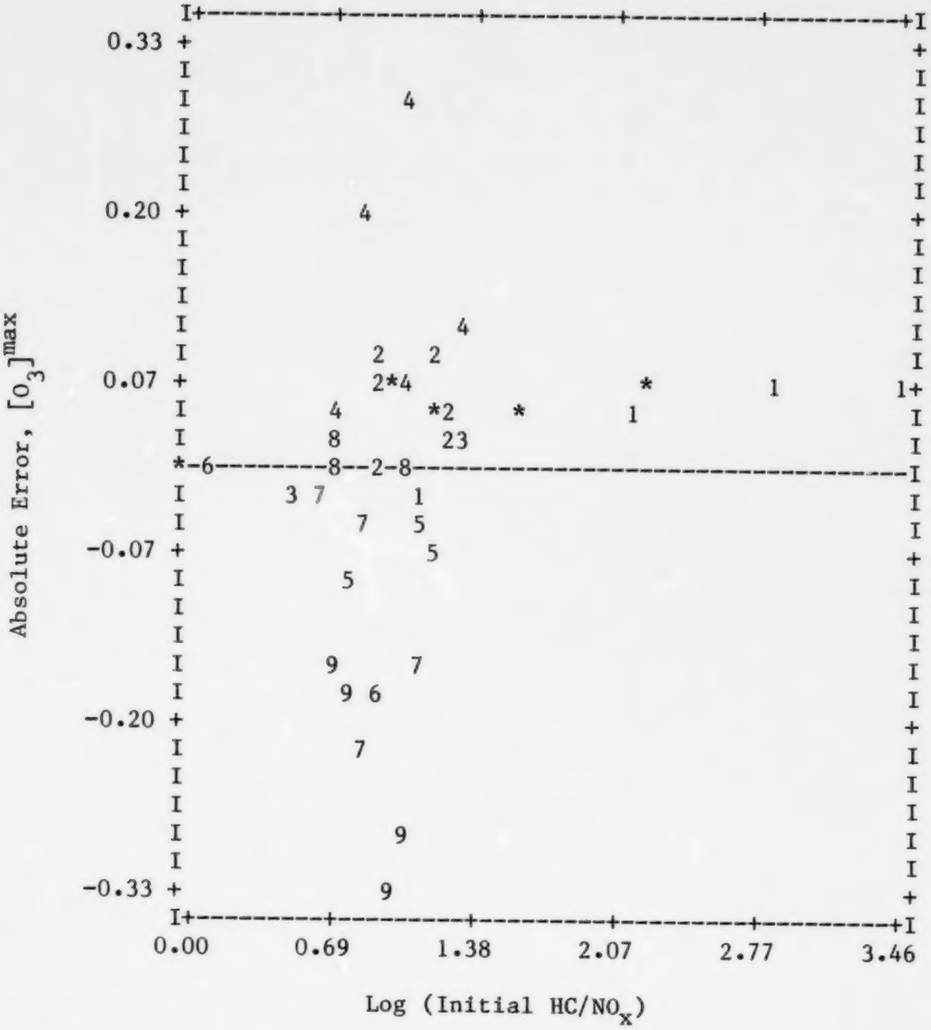

Figure IV-49. Plot of the discrepancies in the model predictions of the maximum ozone yields against the log of the initial hydrocarbon/$NO_x$ ratio for the aromatic hydrocarbon-$NO_x$-air runs. Codes for symbols:

Benzene runs: 1 = ITC
Toluene runs: 2 = EC, 3 = ITC, 4 = UNC
Xylene runs: 5 = EC, 6 = ITC, 7 = UNC
1,3,5-TMB runs: 8 = EC, 9 = ITC
* = overlap of 2 or more runs.

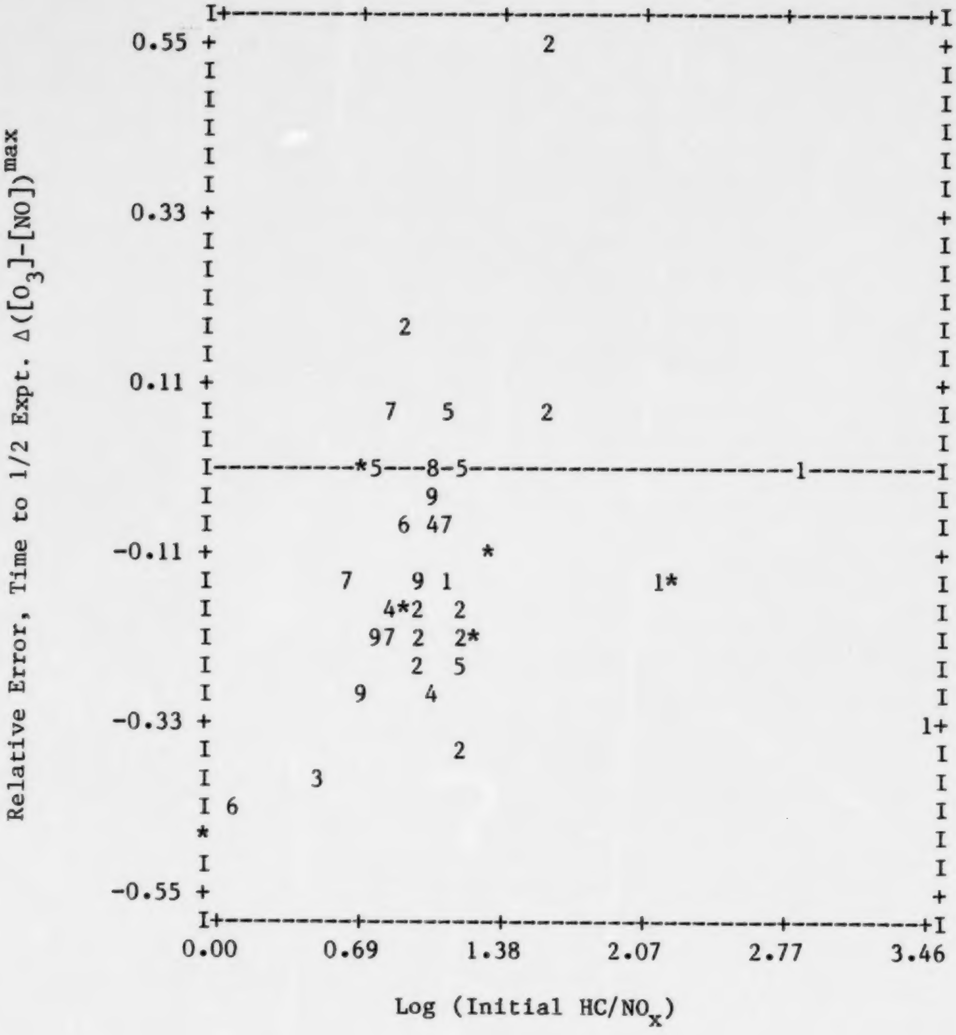

Figure IV-50. Plot of the discrepancies in the model predictions of the times required to achieve half the maximum change in ($[O_3]$-[NO]) against initial hydrocarbon/$NO_x$ ratio for the aromatic hydrocarbon-$NO_x$-air runs. Codes for symbols:

Benzene runs: 1 = ITC
Toluene runs: 2 = EC, 3 = ITC, 4 = UNC
Xylene runs: 5 = EC, 6 = ITC, 7 = UNC
1,3,5-TMB runs: 8 = EC, 9 = ITC
* = Overlap of 2 or more runs.

[such as, for example, nitrate formation in the reaction of NO with the OH-benzene-$O_2$ adduct (see Section II-G)] will yield a much better fit to the results of this experiment. However, inclusion of such a $NO_x$ sink results in either a significant underprediction of reactivity for the highest benzene-$NO_x$-air run ITC-560, or an overprediction of reactivity in the intermediate benzene-$NO_x$-air runs, depending on how the product photolysis rate is adjusted. Thus we are unable, using a single model, to simulate the reactivity observed in the full range of benzene-$NO_x$-air conditions for which we have data.

### 16. Toluene-$NO_x$-Air Irradiations

Twenty toluene-$NO_x$-air irradiations, 13 carried out in the SAPRC EC, five in the UNC chamber, and two in the SAPRC ITC, were modeled in this program. One of the ITC runs consisted of a tracer-$NO_x$-air run with toluene added after the end of the second hour, analogous to the benzene run discussed above. The experimental and calculated maximum ozone yields, NO oxidation and ozone formation times, and toluene half-lives for these runs are summarized in Table IV-24, and the yields of PAN and (where measured) benzaldehyde and o-cresol are given in Table IV-25. Distribution plots of the discrepancies in the predicted ozone maxima and the NO oxidation/ozone formation times for the toluene runs are given, together with the results for all the single-component aromatic runs in Figure IV-48, and plots of these discrepancies against the initial organic/$NO_x$ ratios are given in Figures IV-49 and IV-50. Concentration-time plots for a selected toluene-$NO_x$-air run carried out in the EC and the UNC chamber, and for the tracer-$NO_x$-air + benzene run carried out in the ITC are given in Figures IV-51 through IV-53, respectively.

As for benzene (and the other aromatics, discussed below), in general the model was able to simulate the overall reactivity observed in most of the toluene experiments, though as discussed in Section II-G it was necessary to adjust the photolysis rates of the unknown ring-opened products to achieve these fits. This adjustment was based entirely on the simulations of the EC and ITC runs, but despite this the model performed adequately in simulating three of the five UNC runs. The two UNC runs where the model significantly overpredicted reactivity were both in the

Table IV-24. Initial Concentrations and Experimental and Calculated Ozone Yields and Times Required to Achieve Half the Experimental Change in ($[O_3]-[NO]$) for the Toluene-$NO_x$-Air runs

| Experiment | Initial Concentrations | | | Maximum Ozone Concentration | | | | Time to 1/2 Maximum Expt. ($[O_3]-[NO]$) | | | |
|---|---|---|---|---|---|---|---|---|---|---|---|
| | $NO_x$ (ppm) | HC (ppmC) | $HC/NO_x$ | Expt (ppm) | Calc (ppm) | Calc -Expt (ppm) | Calc -Expt /Expt) | Expt (min) | Calc (min) | Calc -Expt (min) | Calc -Exp /Exp |
| 1: EC Runs | | | | | | | | | | | |
| EC-264 | 0.476 | 8.1 | 17.0 | 0.419 | 0.441 | 0.022 | 0.05 | 92 | 72 | -20 | -0.22 |
| EC-265 | 0.482 | 7.5 | 15.6 | 0.393 | 0.439 | 0.046 | 0.12 | 115 | 73 | -43 | -0.37 |
| EC-266 | 0.491 | 8.4 | 17.1 | 0.405 | 0.446 | 0.041 | 0.10 | 89 | 70 | -20 | -0.22 |
| EC-269 | 0.472 | 4.0 | 8.4 | 0.318 | 0.403 | 0.086 | 0.27 | 138 | 114 | -24 | -0.17 |
| EC-270 | 0.465 | 4.2 | 9.1 | 0.369 | 0.433 | 0.064 | 0.17 | 104 | 82 | -23 | -0.22 |
| EC-271 | 0.214 | 8.0 | 37.5 | 0.296 | 0.329 | 0.034 | 0.11 | 36 | 39 | 3 | 0.08 |
| EC-272 | 0.478 | 4.1 | 8.5 | 0.410 | 0.408 | -0.002 | -0.01 | 109 | 127 | 18 | 0.16 |
| EC-273 | 0.110 | 4.1 | 37.4 | 0.215 | 0.251 | 0.036 | 0.17 | 26 | 40 | 14 | 0.55 |
| EC-327 | 0.453 | 4.0 | 8.9 | 0.376 | 0.432 | 0.056 | 0.15 | 145 | 109 | -35 | -0.24 |
| EC-336 | 0.439 | 7.4 | 16.8 | 0.396 | 0.488 | 0.093 | 0.23 | 59 | 46 | -13 | -0.22 |
| EC-337 | 0.446 | 7.9 | 17.8 | 0.325 | 0.371 | 0.046 | 0.14 | 124 | 100 | -24 | -0.19 |
| EC-339 | 0.443 | 5.1 | 11.4 | 0.225 | 0.288 | 0.063 | 0.28 | 180 | 147 | -32 | -0.18 |
| EC-340 | 0.429 | 3.8 | 8.8 | 0.344 | 0.422 | 0.077 | 0.22 | 133 | 109 | -25 | -0.18 |
| Group Average | 0.415 | 5.9 | 16.5 | 0.345 | 0.396 | 0.051 | 0.16 | 104 | 87 | -17 | -0.11 |
| S. Dev. | 0.116 | 2.0 | 10.0 | 0.068 | 0.068 | 0.026 | 0.08 | 44 | 34 | 18 | 0.24 |
| Avg. Abs. Value | | | | | | 0.051 | 0.16 | | | 22 | 0.23 |
| S. Dev. | | | | | | 0.026 | 0.08 | | | 10 | 0.11 |
| 2: ITC Runs | | | | | | | | | | | |
| ITC-699 | 0.506 | 10.5 | 20.8 | 0.485 | 0.511 | 0.026 | 0.05 | 91 | 80 | -11 | -0.12 |
| ITC-828 | 0.999 | 3.0 | 3.0 | 0.021 | 0.009 | -0.012 | | 133 | 77 | -56 | -0.42 |
| Group Average | 0.752 | 6.7 | 11.9 | 0.253 | 0.260 | 0.007 | 0.05 | 112 | 79 | -33 | -0.27 |
| S. Dev. | 0.348 | 5.3 | 12.6 | 0.328 | 0.354 | 0.027 | 0.00 | 29 | 2 | 32 | 0.21 |
| Avg. Abs. Value | | | | | | 0.019 | 0.05 | | | 33 | 0.27 |
| S. Dev. | | | | | | 0.010 | 0.00 | | | 32 | 0.21 |

(continued)

Table IV-24 (continued) - 2

| Experiment | Initial Concentrations | | | Maximum Ozone Concentration | | | | Time to 1/2 Maximum Expt. ($[O_3]-[NO]$) | | | |
|---|---|---|---|---|---|---|---|---|---|---|---|
| | $NO_x$ (ppm) | HC (ppmC) | $HC/NO_x$ | Expt (ppm) | Calc (ppm) | Calc -Expt (ppm) | Calc -Expt /Expt) | Expt (min) | Calc (min) | Calc -Expt (min) | Calc -Exp /Exp |
| 3: UNC-Toluene Runs | | | | | | | | | | | |
| JL3080R | 0.180 | 3.7 | 20.8 | 0.273 | 0.386 | 0.112 | 0.41 | 287 | 256 | -31 | -0.11 |
| AU2780R | 0.482 | 2.2 | 4.6 | 0.736 | 0.785 | 0.049 | 0.07 | 439 | 442 | 3 | 0.01 |
| OC2782R | 0.391 | 4.5 | 11.6 | 0.122 | 0.401 | 0.278 | 2.27 | 444 | 321 | -123 | -0.28 |
| AU0183R | 0.395 | 4.6 | 11.6 | 0.458 | 0.533 | 0.075 | 0.16 | 329 | 302 | -28 | -0.08 |
| AU2782B | 0.430 | 3.0 | 7.0 | 0.116 | 0.325 | 0.209 | 1.81 | 444 | 369 | -75 | -0.17 |
| Group Average | 0.376 | 3.6 | 11.1 | 0.341 | 0.486 | 0.145 | 0.94 | 389 | 338 | -51 | -0.13 |
| S. Dev. | 0.115 | 1.0 | 6.2 | 0.261 | 0.183 | 0.096 | 1.02 | 75 | 71 | 49 | 0.11 |
| Avg. Abs. Value | | | | | | 0.145 | 0.94 | | | 52 | 0.13 |
| S. Dev. | | | | | | 0.096 | 1.02 | | | 47 | 0.10 |
| Grand Average | 0.439 | 5.4 | 14.7 | 0.335 | 0.405 | 0.070 | 0.36 | 176 | 149 | -27 | -0.13 |
| S. Dev. | 0.172 | 2.3 | 9.3 | 0.154 | 0.144 | 0.068 | 0.61 | 135 | 120 | 31 | 0.21 |
| Avg. Abs. Value | | | | | | 0.071 | 0.36 | | | 31 | 0.21 |
| S. Dev. | | | | | | 0.066 | 0.61 | | | 28 | 0.12 |

Table IV-25. Experimental and Calculated Yields of PAN and (When Measured) Benzaldehyde and o-Cresol for the Toluene-$NO_x$-Air Runs

| Experiment | Species | Expt (ppm) | Calc (ppm) | Calc -Expt (ppm) | Calc -Expt /Expt |
|---|---|---|---|---|---|
| 1: EC Runs | | | | | |
| | PAN | | | | |
| EC-264 | | 0.071 | 0.094 | 0.023 | 0.32 |
| EC-265 | | 0.072 | 0.091 | 0.019 | 0.27 |
| EC-266 | | 0.075 | 0.098 | 0.023 | 0.31 |
| EC-269 | | 0.050 | 0.063 | 0.013 | 0.26 |
| EC-270 | | 0.057 | 0.070 | 0.013 | 0.23 |
| EC-271 | | 0.053 | 0.068 | 0.015 | 0.28 |
| EC-272 | | 0.132 | 0.066 | -0.066 | -0.50 |
| EC-273 | | 0.032 | 0.044 | 0.012 | 0.38 |
| EC-327 | | 0.041 | 0.068 | 0.027 | 0.66 |
| EC-336 | | 0.059 | 0.088 | 0.029 | 0.48 |
| EC-337 | | 0.047 | 0.069 | 0.023 | 0.48 |
| EC-339 | | 0.024 | 0.037 | 0.013 | 0.55 |
| EC-340 | | 0.042 | 0.063 | 0.020 | 0.48 |
| Group Average | | 0.058 | 0.070 | 0.013 | 0.32 |
| Std. Dev. | | 0.027 | 0.018 | 0.024 | 0.28 |
| Avg. Abs Value | | | | 0.023 | 0.40 |
| Std. Dev. | | | | 0.014 | 0.14 |
| | Benzaldehyde | | | | |
| EC-266 | | 0.022 | 0.016 | -0.006 | -0.28 |
| EC-336 | | 0.016 | 0.014 | -0.002 | -0.14 |
| Group Average | | 0.019 | 0.015 | -0.004 | -0.21 |
| Std. Dev. | | 0.004 | 0.002 | 0.003 | 0.10 |
| Avg. Abs Value | | | | 0.004 | 0.21 |
| Std. Dev. | | | | 0.003 | 0.10 |
| | o-Cresol | | | | |
| EC-271 | | 0.013 | 0.010 | -0.003 | -0.26 |
| EC-337 | | 0.011 | 0.009 | -0.002 | -0.21 |
| EC-337 | | 0.012 | 0.007 | -0.005 | -0.44 |
| Group Average | | 0.012 | 0.008 | -0.004 | -0.30 |
| Std. Dev. | | 0.001 | 0.001 | 0.002 | 0.12 |
| Avg. Abs Value | | | | 0.004 | 0.30 |
| Std. Dev. | | | | 0.002 | 0.12 |

(continued)

Table IV-25 (continued) - 2

| Experiment | Species | Expt (ppm) | Calc (ppm) | Calc -Expt (ppm) | Calc -Expt /Expt |
|---|---|---|---|---|---|
| 2: ITC Runs | | | | | |
| | PAN | | | | |
| ITC-699 | | 0.145 | 0.116 | -0.029 | -0.20 |
| ITC-828 | a | | | | |
| Group Average | | 0.145 | 0.116 | -0.029 | -0.20 |
| Std. Dev. | | | | | |
| Avg. Abs Value | | | | 0.029 | 0.20 |
| Std. Dev. | | | | | |
| 3: UNC Runs | | | | | |
| | PAN | | | | |
| JL3080R | | 0.037 | 0.041 | 0.005 | 0.13 |
| AU2780R | | 0.020 | 0.026 | 0.005 | 0.27 |
| OC2782R | | 0.013 | 0.082 | 0.069 | 5.15 |
| AU0183R | | 0.043 | 0.060 | 0.017 | 0.39 |
| AU2782B | | 0.012 | 0.031 | 0.020 | 1.70 |
| Group Average | | 0.025 | 0.048 | 0.023 | 1.53 |
| Std. Dev. | | 0.014 | 0.023 | 0.026 | 2.12 |
| Avg. Abs Value | | | | 0.023 | 1.53 |
| Std. Dev. | | | | 0.026 | 2.12 |

[a] No data.

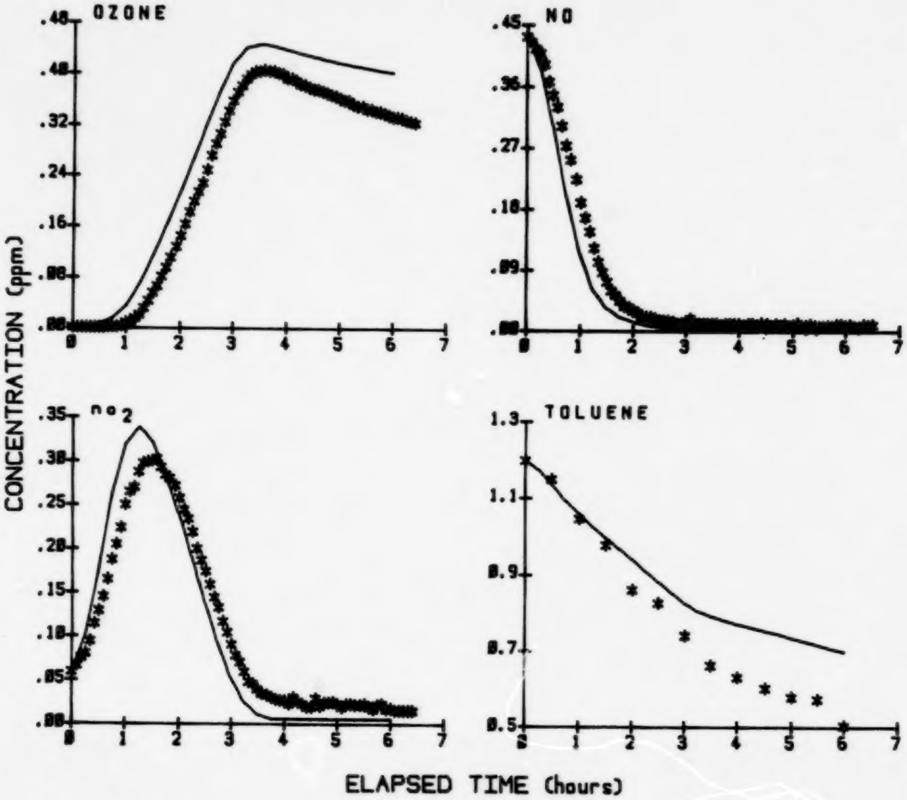

Figure IV-51. Experimental and calculated concentration-time plots for representative species observed in the toluene-$NO_x$-air run EC-266.
* = Experimental data.
——— = Model calculation.

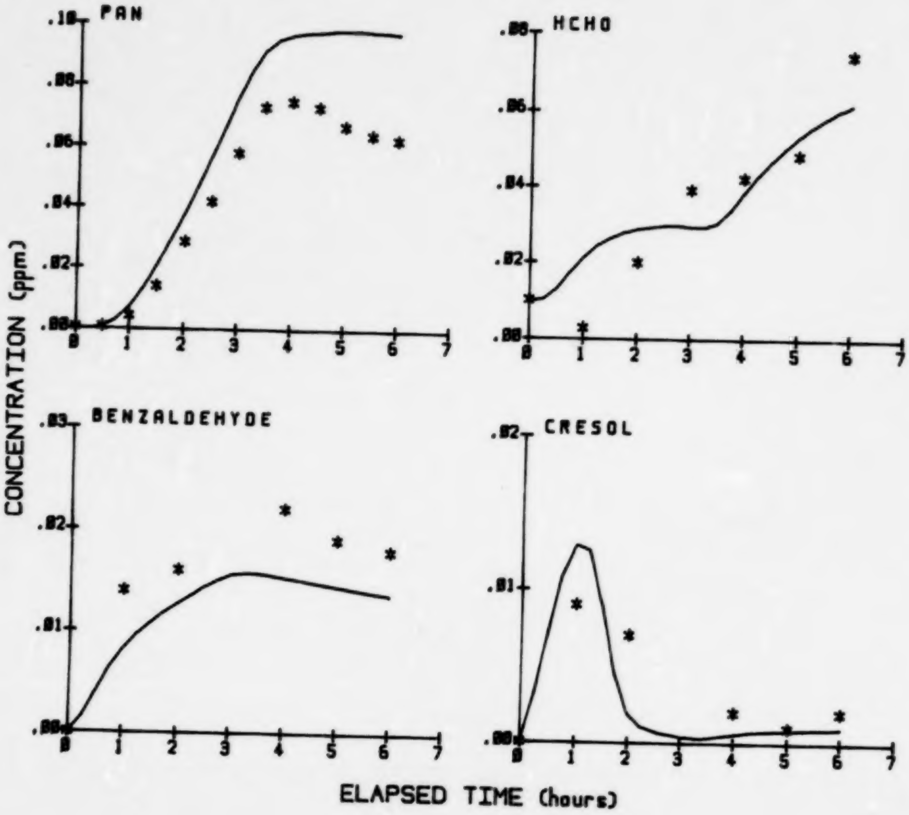

Figure IV-51 (continued)

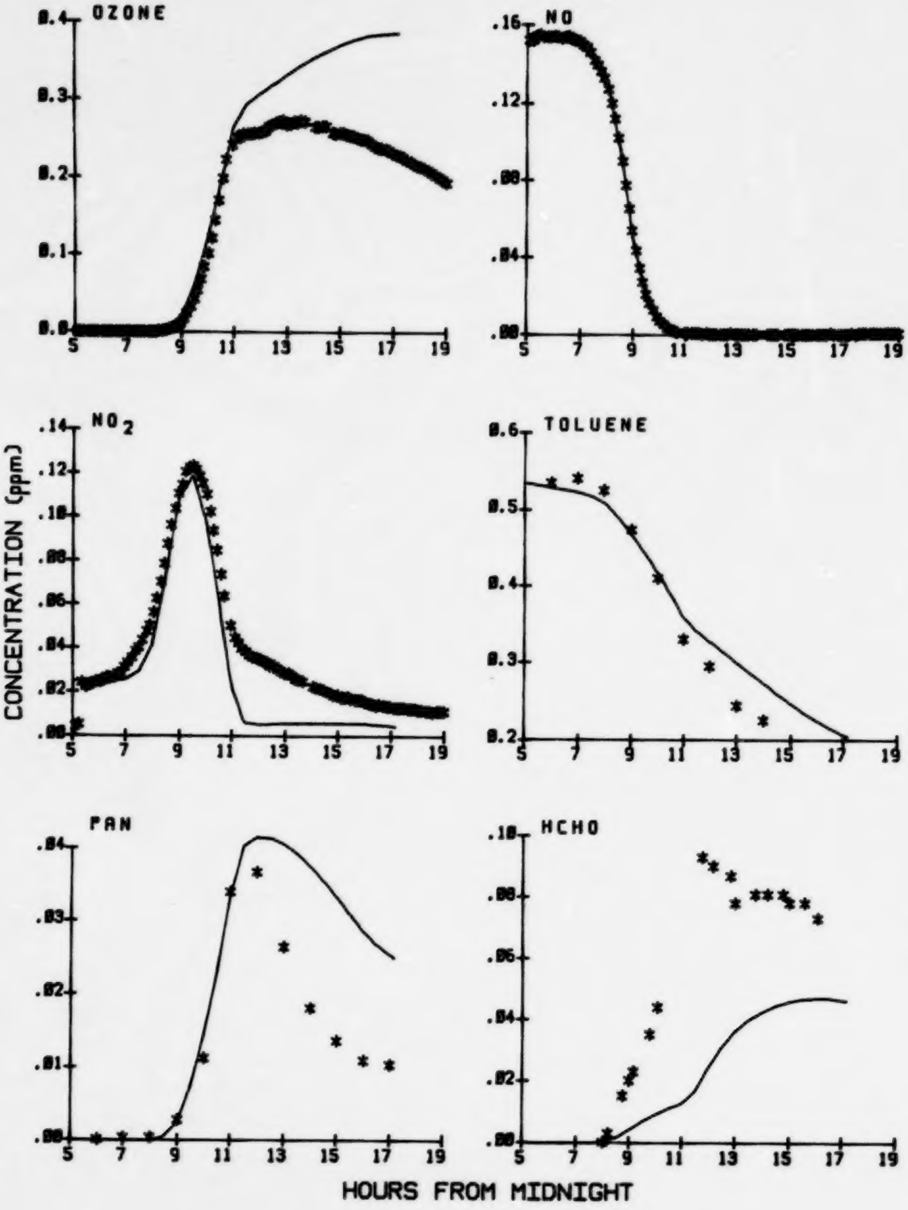

Figure IV-52. Experimental and calculated concentration-time plots for representative species observed in the UNC toluene-$NO_x$-air run JN3080R.
* = Experimental data.
----- = Model calculation.

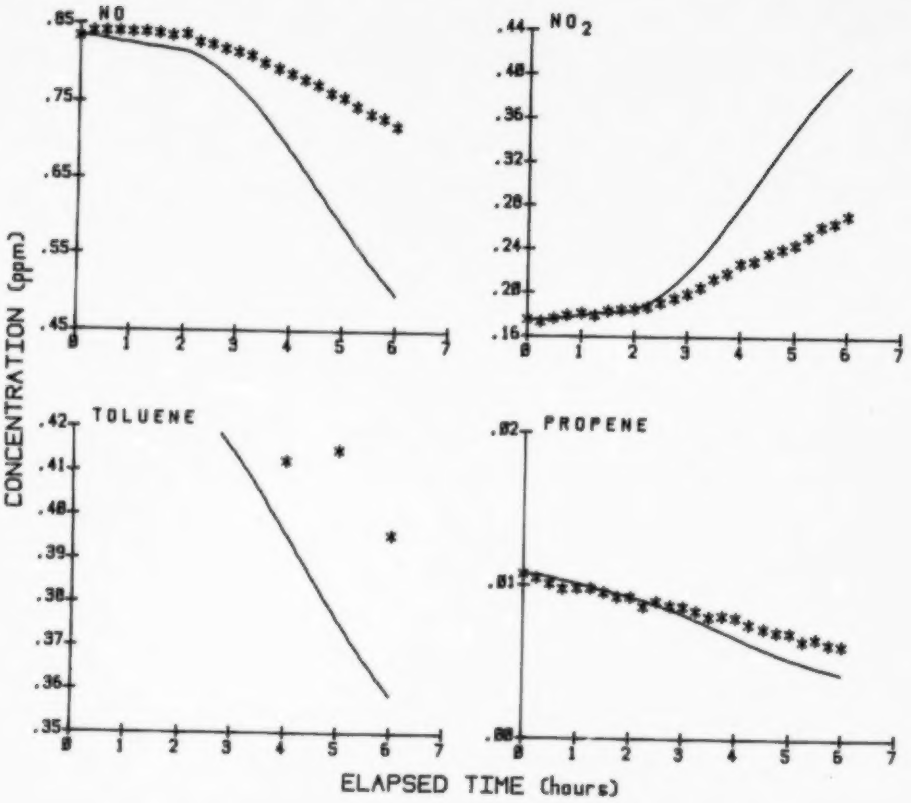

Figure IV-53. Experimental and calculated concentration-time plots for representative species observed in toluene-$NO_x$-air run ITC-828.

* = Experimental data.

----- = Model calculation.

middle of the range of toluene/$NO_x$ ratios employed in the UNC runs, so the poor fits for those runs are more likely indicative of the variability of the model in simulating results of UNC chamber experiments in general (as indicated in the model simulations of the propene runs discussed above in Section IV-D-7), rather than a problem with the chemical mechanism employed.

Several systematic discrepancies between the model predictions and the experimental data are noted, though in most cases the magnitude of these are not great. For all runs but two the model overpredicted the maximum ozone yield, and for all runs but two the PAN yields were overpredicted. On the other hand, the model tended to underpredict the toluene consumption rate, particularly at the end of the run (the toluene profiles shown in Figures 51 and 52 are typical).

Other than the two, possibly anomalous, UNC runs, the most serious discrepancy was obtained in the simulations of the ITC tracer-$NO_x$-air + toluene run where, as for the simulation of the analogous benzene run, the model significantly overpredicted the NO to $NO_x$ conversion rate and (to a lesser extent) the OH radical levels as measured by the propene consumption rate (see Figure IV-53). However, the model performed very well in the simulation of UNC run AU2780R, which was carried out at a similar toluene/$NO_x$ ratio (though it also contained 100 ppm of CO), and Figures IV-49 and IV-50 indicate no systematic dependences of the discrepancies of the model predictions of the ozone maxima and "timing" parameter on the organic/$NO_x$ ratio. However, the initial $NO_x$ concentration in the ITC run was almost a factor of two higher than employed in any of the other runs, indicating that there may be a problem with the mechanism under higher $NO_x$ conditions.

Benzaldehyde and o-cresol were monitored in several of the SAPRC EC runs, and the results of the model simulations were consistent with these data to within their experimental uncertainties (these are somewhat greater than uncertainties for most other species monitored in these chamber experiments, as discussed in Section IV-B-5). Some benzaldehyde data are available for one of the UNC experiments, which were over a factor of two higher than predicted by the model, but the quality of those data are unknown. The fits shown in Figure IV-51 are typical of those obtained in the EC experiments.

### 17. o- and m-Xylene-$NO_x$-Air Runs

Ten xylene-$NO_x$-air irradiations were modeled in this program, including four m-xylene experiments carried out in the SAPRC EC and two in the ITC, and four experiments employing o-xylene carried out in the UNC chamber. One of the ITC runs consisted of a tracer-$NO_x$-air run with m-xylene added after the end of the second hour, analogous to the benzene and toluene runs discussed above. The experimental and calculated maximum ozone yields, NO oxidation and ozone formation times, and xylene half-lives for these runs are summarized in Table IV-26, and the PAN yields are given in Table IV-27. Distribution plots of the discrepancies in the predicted ozone maxima and the NO oxidation/ozone formation times for the xylene runs are given, together with the results for all the single-component aromatic runs, in Figure IV-48, and plots of these discrepancies against initial organic/$NO_x$ ratios are given in Figures IV-49 and IV-50. Concentration-time plots for selected xylene runs carried out in the EC and the UNC chamber, and for the tracer-$NO_x$-air + o-xylene run carried out in the ITC are given in Figures IV-54 through IV-56, respectively.

As with the other aromatic hydrocarbons, for most runs the model was able to simulate the overall reactivity observed. This was achieved by adjusting the photolysis rate of the unknown ring-opened product(s) to fit the results of the EC and the ITC m-xylene runs. Use of the same parameter resulted in fits to the UNC o-xylene runs of similar quality as that observed in the simulations of the UNC toluene runs. In general, the model tends to underpredict ozone yields (in contrast to the toluene model, where the opposite result is seen) but has no consistent discrepancy with regard to the NO oxidation and ozone formation timing parameter. As for toluene, the model tends to overpredict PAN yields and underpredict the consumption rate of the aromatic. In addition, as shown in Figure IV-56, the model significantly overpredicted the NO to $NO_2$ conversion rate and the OH radical levels (i.e., propene consumption rate) in the high $NO_x$, low xylene/$NO_x$ ratio tracer-$NO_x$-air + m-xylene run, as was observed in the model simulations of the analogous toluene and benzene runs.

It should be noted that, although (as discussed in Section II-G) different reaction mechanisms are used for the two xylenes, we found that use of the m-xylene model in simulating the UNC o-xylene runs results in

Table IV-26. Initial Concentrations and Experimental and Calculated Ozone Yields, Times Required to Achieve Half the Experimental Change in ($[O_3]-[NO]$), and Xylene Half-Lives for the Xylene-$NO_x$-Air Runs

| Experiment | Initial Concentrations | | | Maximum Ozone Concentration | | | | Time to 1/2 Maximum Expt. ($[O_3]-[NO]$) | | | | Xylene Half-Life | | | |
|---|---|---|---|---|---|---|---|---|---|---|---|---|---|---|---|
| | $NO_x$ (ppm) | HC (ppmC) | HC/$NO_x$ | Expt (ppm) | Calc (ppm) | Calc -Expt (ppm) | Calc -Expt /Expt) | Expt (min) | Calc (min) | Calc -Expt (min) | Calc -Exp /Exp | Expt (min) | Calc (min) | Calc -Expt (min) | Calc -Expt /Expt |
| 1: EC m-Xylene Runs | | | | | | | | | | | | | | | |
| EC-343 | 0.280 | 3.9 | 14.1 | 0.283 | 0.338 | 0.055 | 0.19 | 29 | 22 | -7 | -0.24 | 192 | 225 | 33 | 0.17 |
| EC-344 | 0.674 | 3.9 | 5.8 | 0.589 | 0.503 | -0.086 | -0.15 | 51 | 51 | -1 | -0.01 | 70 | 84 | 15 | 0.21 |
| EC-345 | 0.279 | 3.8 | 13.8 | 0.396 | 0.347 | -0.049 | -0.12 | 27 | 28 | 2 | 0.06 | 57 | 110 | 53 | 0.94 |
| EC-346 | 0.263 | 3.9 | 14.8 | 0.384 | 0.320 | -0.063 | -0.17 | 40 | 40 | 0 | 0.00 | 52 | 117 | 64 | 1.22 |
| Group Average | 0.374 | 3.9 | 12.1 | 0.413 | 0.377 | -0.036 | -0.06 | 37 | 35 | -2 | -0.05 | 93 | 134 | 41 | 0.63 |
| S. Dev. | 0.200 | 0.0 | 4.2 | 0.128 | 0.085 | 0.062 | 0.17 | 11 | 13 | 4 | 0.13 | 67 | 62 | 22 | 0.52 |
| Avg. Abs. Value | | | | | | 0.063 | 0.16 | | | 1 | 0.08 | | | 41 | 0.63 |
| S. Dev. | | | | | | 0.016 | 0.03 | | | 3 | 0.11 | | | 22 | 0.52 |
| 2: ITC m-Xylene Runs | | | | | | | | | | | | | | | |
| ITC-702 | 0.519 | 4.0 | 7.8 | 0.627 | 0.454 | -0.173 | -0.28 | 66 | 62 | -4 | -0.06 | 87 | 121 | 34 | 0.39 |
| ITC-827 | 1.039 | 1.1 | 1.1 | 0.021 | 0.016 | -0.005 | | 140 | 79 | -61 | -0.44 | 193 | 179 | -14 | -0.07 |
| Group Average | 0.779 | 2.6 | 4.4 | 0.324 | 0.235 | -0.089 | -0.28 | 103 | 70 | -32 | -0.25 | 140 | 150 | 10 | 0.16 |
| S. Dev. | 0.368 | 2.0 | 4.7 | 0.429 | 0.310 | 0.119 | 0.00 | 52 | 12 | 40 | 0.26 | 75 | 41 | 34 | 0.33 |
| Avg. Abs. Value | | | | | | 0.089 | 0.28 | | | 32 | 0.25 | | | 24 | 0.23 |
| S. Dev. | | | | | | 0.119 | 0.00 | | | 40 | 0.26 | | | 14 | 0.23 |
| 3: UNC o-Xylene Runs | | | | | | | | | | | | | | | |
| AU2782R | 0.436 | 2.0 | 4.5 | 0.491 | 0.471 | -0.019 | -0.04 | 419 | 356 | -63 | -0.15 | 324 | 306 | -18 | -0.06 |
| JL3080B | 0.179 | 2.2 | 12.5 | 0.555 | 0.409 | -0.146 | -0.26 | 289 | 265 | -25 | -0.09 | 208 | 228 | 20 | 0.10 |
| OC2782B | 0.393 | 2.7 | 7.0 | 0.396 | 0.354 | -0.042 | -0.11 | 376 | 289 | -87 | -0.23 | 394 | 357 | -37 | -0.09 |
| AU0183B | 0.372 | 2.6 | 7.0 | 0.688 | 0.472 | -0.216 | -0.31 | 314 | 341 | 26 | 0.08 | 246 | 357 | 111 | 0.45 |
| Group Average | 0.345 | 2.4 | 7.8 | 0.532 | 0.427 | -0.106 | -0.18 | 349 | 312 | -36 | -0.10 | 293 | 312 | 19 | 0.10 |
| S. Dev. | 0.114 | 0.3 | 3.4 | 0.123 | 0.057 | 0.092 | 0.13 | 59 | 43 | 49 | 0.13 | 83 | 61 | 65 | 0.25 |
| Avg. Abs. Value | | | | | | 0.106 | 0.18 | | | 50 | 0.14 | | | 46 | 0.17 |
| S. Dev. | | | | | | 0.092 | 0.13 | | | 30 | 0.07 | | | 44 | 0.18 |

Table IV-27. Experimental and Calculated PAN Yields for the o- and m-Xylene-$NO_x$-Air Runs

| Experiment | Expt (ppm) | Calc (ppm) | Calc -Expt (ppm) | Calc -Expt /Expt |
|---|---|---|---|---|
| **1: EC m-Xylene-$NO_x$-Air Runs** | | | | |
| EC-343 | 0.081 | 0.149 | 0.069 | 0.85 |
| EC-344 | 0.175 | 0.251 | 0.076 | 0.43 |
| EC-345 | 0.107 | 0.149 | 0.042 | 0.39 |
| EC-346 | 0.102 | 0.142 | 0.041 | 0.40 |
| Group Average | 0.116 | 0.173 | 0.057 | 0.52 |
| Std. Dev. | 0.041 | 0.052 | 0.018 | 0.22 |
| Avg. Abs Value | | | 0.057 | 0.52 |
| Std. Dev. | | | 0.018 | 0.22 |
| **2: ITC m-Xylene-$NO_x$-Air Runs** | | | | |
| ITC-702 | 0.390 | 0.227 | -0.163 | -0.42 |
| ITC-827 | [a] | | | |
| **3: UNC o-Xylene-$NO_x$-Air Runs** | | | | |
| AU2782R | 0.093 | 0.113 | 0.020 | 0.22 |
| JL3080B | 0.091 | 0.084 | -0.007 | -0.08 |
| OC2782B | 0.112 | 0.160 | 0.049 | 0.44 |
| AU0183B | 0.102 | 0.106 | 0.004 | 0.04 |
| Group Average | 0.099 | 0.116 | 0.016 | 0.15 |
| Std. Dev. | 0.009 | 0.032 | 0.024 | 0.22 |
| Avg. Abs Value | | | 0.020 | 0.19 |
| Std. Dev. | | | 0.020 | 0.18 |

[a] No data.

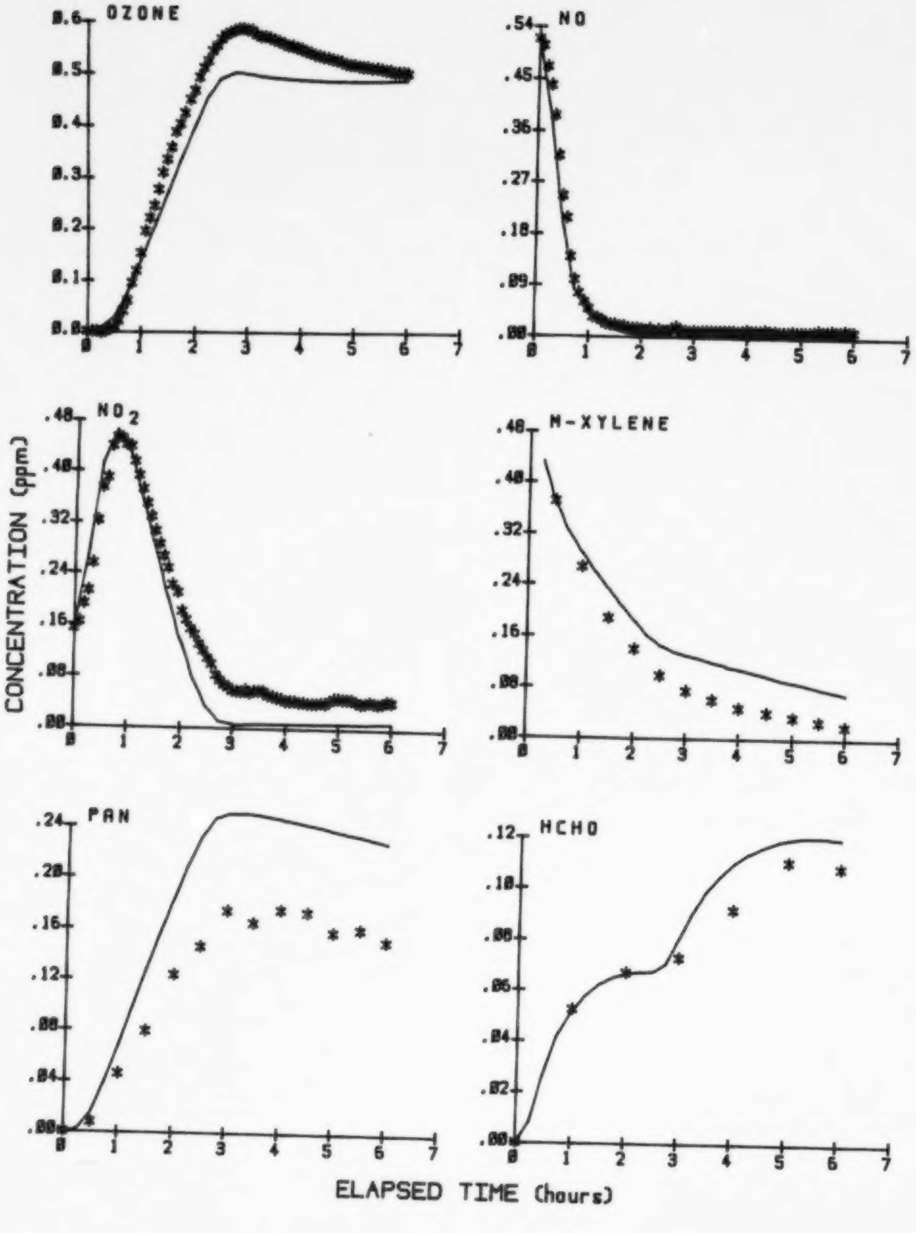

Figure IV-54. Experimental and calculated concentration-time plots for representative species observed in the m-xylene-$NO_x$-air run EC-344.
* = Experimental data.
----- = Model calculation.

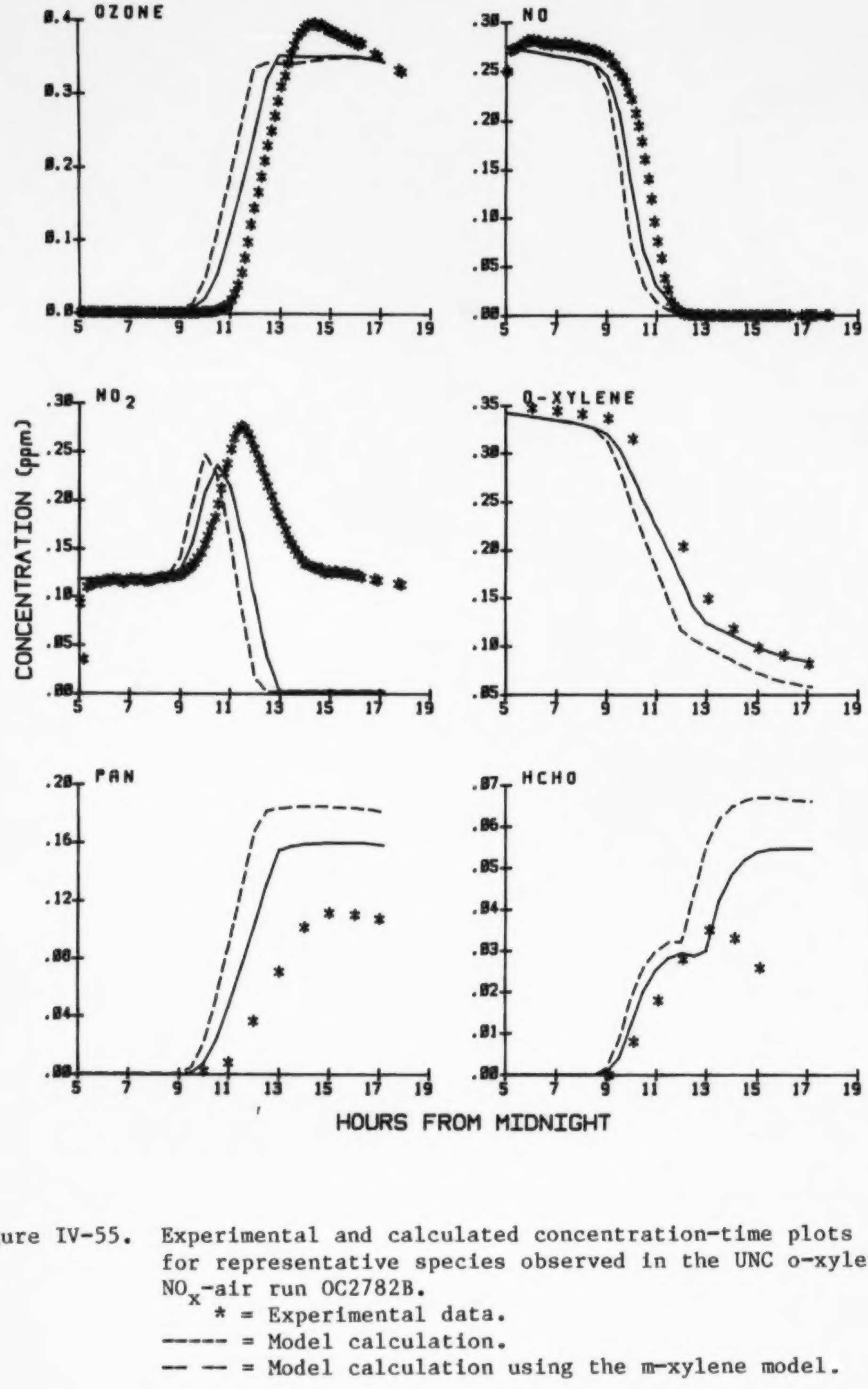

Figure IV-55. Experimental and calculated concentration-time plots for representative species observed in the UNC o-xylene-$NO_x$-air run OC2782B.

* = Experimental data.
----- = Model calculation.
— — = Model calculation using the m-xylene model.

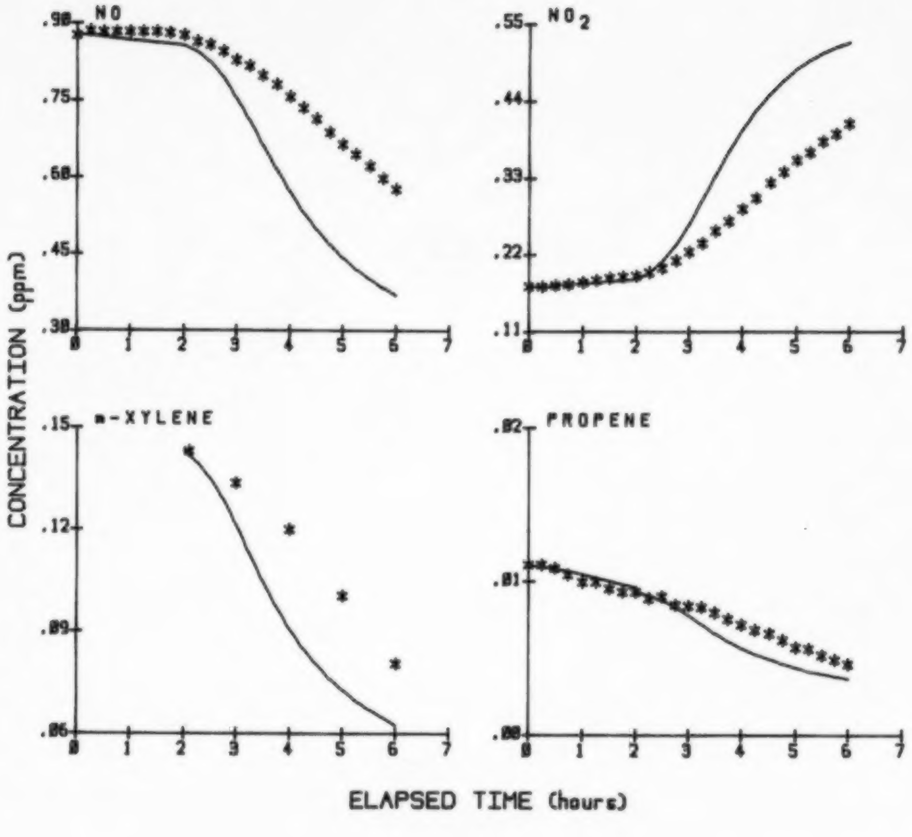

Figure IV-56. Experimental and calculated concentration-time plots for representative species observed in the m-xylene-$NO_x$-air run ITC-827.
* = Experimental data.
----- = Model calculation.

only a moderate change in the model predictions. This is shown in Figure IV-55, where the dashed lines are the model calculation using the m-xylene mechanism on this o-xylene experiment. This tends to justify lumping the xylenes together in "lumped molecule" models, as carried out for the simulations of the UNC complex mixture runs and the auto exhaust runs, discussed below in Sections IV-E-10 and IV-F, respectively.

### 18. 1,3,5-Trimethylbenzene-$NO_x$-Air Runs

Eight 1,3,5-trimethylbenzene (1,3,5-TMB) runs were modeled in this program, three carried out in the SAPRC EC and five in the SAPRC ITC. As with the other aromatics, one of the ITC runs consisted of a tracer-$NO_x$-air irradiation with 1,3,5-TMB added at the end of the second hour of the irradiation. The experimental and calculated maximum ozone yields, NO oxidation and ozone formation times, and 1,3,5-TMB half-lives for these runs are summarized in Table IV-28, and the PAN yields are given in Table IV-29. Distribution plots of the discrepancies in the predicted ozone maxima and the NO oxidation/ozone formation times for the xylene runs are given, together with the results for all the single-component aromatic runs, in Figure IV-48. Plots of these discrepancies against the initial organic/$NO_x$ ratios are given in Figures IV-49 and IV-50. Concentration-time plots for selected trimethylbenzene-$NO_x$-air runs carried out in the EC and the ITC, and for the tracer-$NO_x$ + 1,3,5-TMB run carried out in the ITC are given in Figures IV-57 through IV-59, respectively.

The fits of the model simulation to the overall reactivity observed in these runs were obtained by using the same product photolysis rate which was adjusted to fit the results of the SAPRC o-xylene runs. In general, the fits of the reactivity parameters to the results of the EC runs was excellent, but the model underpredicted, by an average of 30%, the maximum ozone yields observed in the ITC runs. Unfortunately, propene-$NO_x$ irradiations carried out in the EC around the same time as the 1,3,5-TMB runs gave anomalously low ozone yields (unpublished SAPRC data), and thus we believe the ITC experiments are more reliable for testing the model in this regard. Thus the good fits to the ozone yields in the EC experiments may be coincidental, and the discrepancy regarding ozone yields in the ITC may represent a problem with the chemical mechanism.

Table IV-28. Initial Concentrations and Experimental and Calculated Ozone Yields, Times Required to Achieve Half the Experimental Change in ($[O_3]-[NO]$), and 1,3,5-Trimethylbenzene Half-Lives for the 1,3,5-Trimethylbenzene-$NO_x$-Air Runs

| Experiment | Initial Concentrations | | | Maximum Ozone Concentration | | | | Time to 1/2 Maximum Expt. ($[O_3]-[NO]$) | | | | 1,3,5-TMB Half-Life | | | |
|---|---|---|---|---|---|---|---|---|---|---|---|---|---|---|---|
| | $NO_x$ (ppm) | HC (ppmC) | $HC/NO_x$ | Expt (ppm) | Calc (ppm) | Calc -Expt (ppm) | Calc -Expt /Expt) | Expt (min) | Calc (min) | Calc -Expt (min) | Calc -Exp /Exp | Expt (min) | Calc (min) | Calc -Expt (min) | Calc -Expt /Expt |
| 1: EC Runs | | | | | | | | | | | | | | | |
| EC-900 | 0.526 | 5.3 | 10.1 | 0.381 | 0.384 | 0.002 | 0.01 | 240 | 240 | 0 | 0.00 | 50 | 57 | 7 | 0.15 |
| EC-901 | 0.515 | 2.6 | 5.1 | 0.384 | 0.388 | 0.004 | 0.01 | 44 | 43 | -1 | -0.01 | 47 | 46 | -1 | -0.01 |
| EC-903 | 0.989 | 4.7 | 4.7 | 0.502 | 0.532 | 0.030 | 0.06 | 42 | 42 | 0 | -0.01 | 49 | 50 | 1 | 0.03 |
| Group Average | 0.677 | 4.2 | 6.7 | 0.422 | 0.435 | 0.012 | 0.03 | 109 | 108 | 0 | -0.01 | 48 | 51 | 3 | 0.05 |
| S. Dev. | 0.271 | 1.4 | 3.0 | 0.069 | 0.084 | 0.015 | 0.03 | 114 | 114 | 0 | 0.01 | 2 | 5 | 4 | 0.08 |
| Avg. Abs. Value | | | | | | 0.012 | 0.03 | | | 0 | 0.01 | | | 3 | 0.06 |
| S. Dev. | | | | | | 0.015 | 0.03 | | | 0 | 0.01 | | | 4 | 0.07 |
| 2: ITC Runs | | | | | | | | | | | | | | | |
| ITC-703 | 0.501 | 5.3 | 10.6 | 0.707 | 0.422 | -0.285 | -0.40 | 37 | 36 | -2 | -0.04 | 45 | 66 | 22 | 0.49 |
| ITC-706 | 0.493 | 2.7 | 5.4 | 0.641 | 0.469 | -0.172 | -0.27 | 71 | 56 | -15 | -0.21 | 45 | 44 | -1 | -0.02 |
| ITC-709 | 0.991 | 4.7 | 4.7 | 0.779 | 0.629 | -0.150 | -0.19 | 66 | 47 | -19 | -0.29 | 52 | 53 | 1 | 0.02 |
| ITC-742 | 0.481 | 4.6 | 9.7 | 0.773 | 0.441 | -0.332 | -0.43 | 34 | 29 | -5 | -0.16 | 42 | 60 | 18 | 0.42 |
| ITC-826 | 0.890 | 0.8 | 0.9 | 0.022 | 0.031 | 0.010 | | 105 | 56 | -49 | -0.47 | 106 | 58 | -48 | -0.45 |
| Group Average | 0.671 | 3.6 | 6.3 | 0.584 | 0.398 | -0.186 | -0.32 | 63 | 45 | -18 | -0.23 | 58 | 56 | -2 | 0.09 |
| S. Dev. | 0.248 | 1.9 | 3.9 | 0.320 | 0.221 | 0.133 | 0.11 | 29 | 12 | 19 | 0.16 | 27 | 8 | 28 | 0.38 |
| Avg. Abs. Value | | | | | | 0.190 | 0.32 | | | 17 | 0.23 | | | 18 | 0.28 |
| S. Dev. | | | | | | 0.126 | 0.11 | | | 19 | 0.16 | | | 19 | 0.24 |

Table IV-29. Experimental and Calculated PAN Yields for the 1,3,5-Trimethylbenzene-$NO_x$-Air Runs

| Experiment | Expt (ppm) | Calc (ppm) | Calc -Expt (ppm) | Calc -Expt /Expt |
|---|---|---|---|---|
| 1: EC Runs | | | | |
| EC-900 | 0.400 | 0.257 | -0.143 | -0.36 |
| EC-901 | 0.293 | 0.225 | -0.068 | -0.23 |
| EC-903 | 0.470 | 0.426 | -0.044 | -0.09 |
| Group Average | 0.388 | 0.302 | -0.085 | -0.23 |
| Std. Dev. | 0.089 | 0.108 | 0.052 | 0.13 |
| Avg. Abs Value | | | 0.085 | 0.23 |
| Std. Dev. | | | 0.052 | 0.13 |
| 2: ITC Runs | | | | |
| ITC-703 | 0.586 | 0.305 | -0.281 | -0.48 |
| ITC-706 | 0.440 | 0.258 | -0.182 | -0.41 |
| ITC-709 | 0.590 | 0.506 | -0.084 | -0.14 |
| ITC-742 | 0.470 | 0.293 | -0.177 | -0.38 |
| ITC-826 | [a] | | | |
| Group Average | 0.521 | 0.340 | -0.181 | -0.35 |
| Std. Dev. | 0.078 | 0.112 | 0.080 | 0.15 |
| Avg. Abs Value | | | 0.181 | 0.35 |
| Std. Dev. | | | 0.080 | 0.15 |

[a] No data.

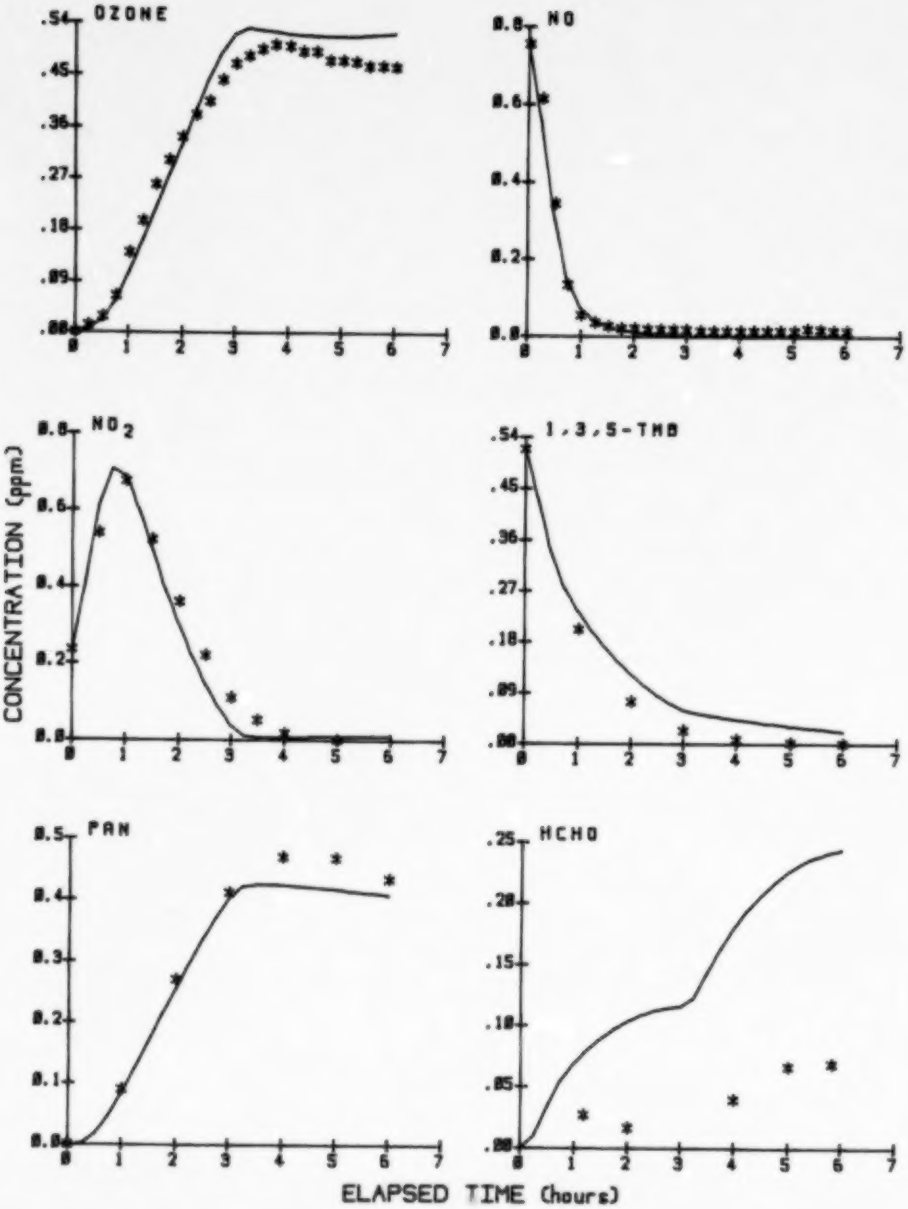

Figure IV-57. Experimental and calculated concentration-time plots for representative species observed in the 1,3,5-TMB-$NO_x$-air run EC-903.
* = Experimental data.
----- = Model calculation.

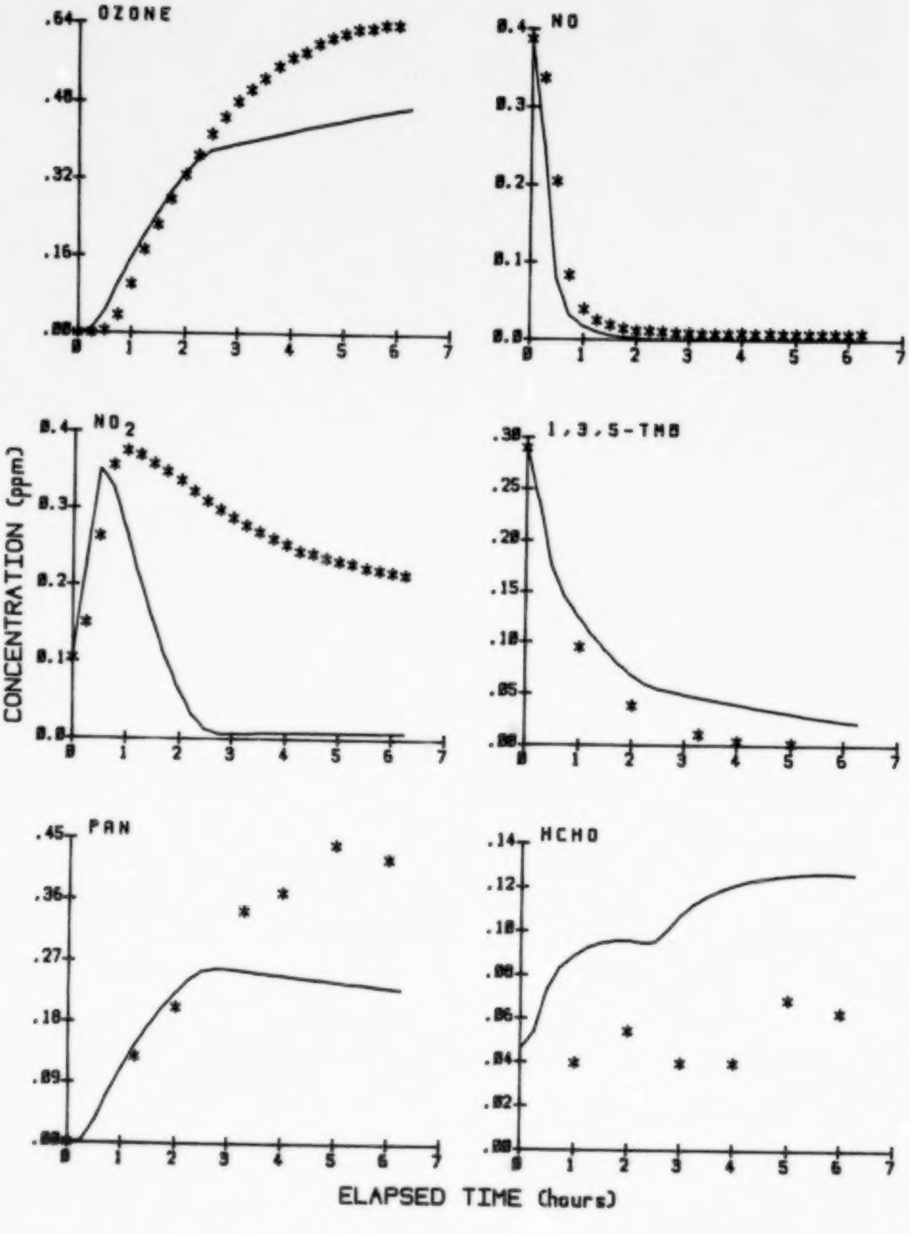

Figure IV-58. Experimental and calculated concentration-time plots for representative species observed in the 1,3,5-TMB-$NO_x$-air run ITC-706.
* = Experimental data.
----- = Model calculation.

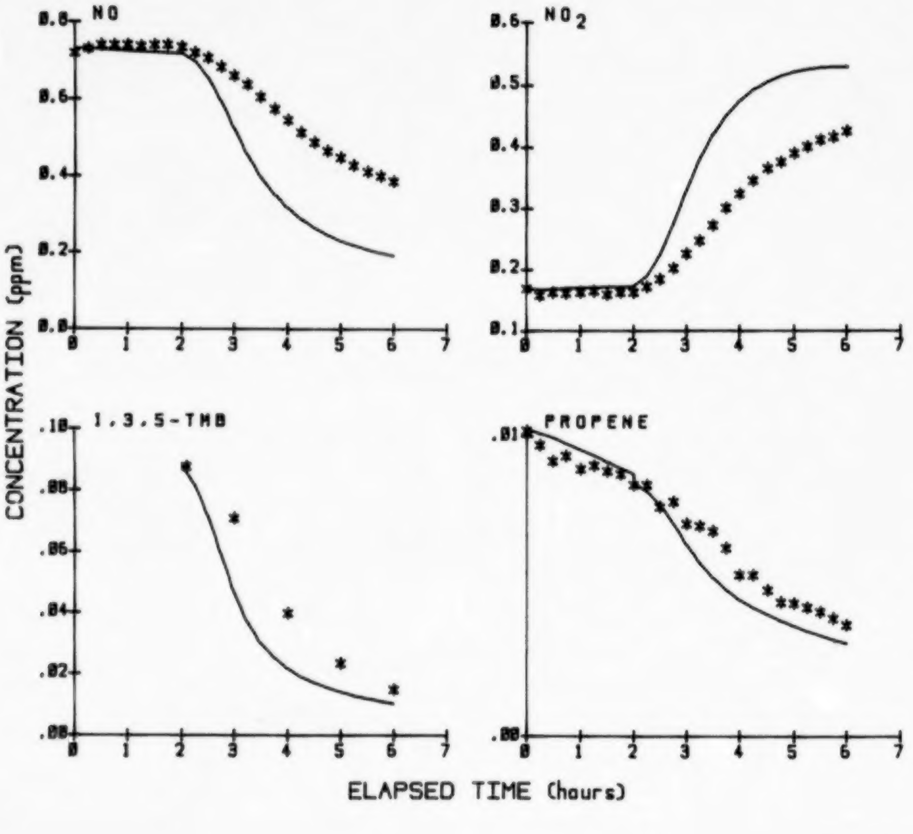

Figure IV-59. Experimental and calculated concentration-time plots for representative species observed in the 1,3,5-TMB-NO$_x$-air run ITC-826.
* = Experimental data.
----- = Model calculation.

As with the other aromatic hydrocarbons, the model tends to underpredict the 1,3,5-TMB consumption rate, though this discrepancy was not observed in all runs. Unlike the other aromatics, the 1,3,5-TMB model tends to underpredict PAN yields observed in both the EC and the ITC experiments. The model also underpredicts formaldehyde, but the yields are relatively low, and the reliability of the formaldehyde data at these levels is highly uncertain.

## IV. E. MULTI-COMPONENT IRRADIATIONS AND DYNAMIC EXPERIMENTS

While less useful for testing specific or detailed aspects of the chemical mechanism, $NO_x$-air irradiations of mixtures of organics, or irradiations carried out under dynamic conditions, are important for model testing because they are usually more representative of atmospheric conditions, and they allow the model to be tested under a wider range of conditions. For these reasons, a large number of experiments employing simple or complex mixtures of organics, and a more limited number of dynamic experiments, were modeled in this program. The mixtures of organics employed in the experiments whose simulations are discussed in this section, vary in complexity from dual- to multi-component mixtures of organics whose reactions are represented explicitly in the model to multi-component mixtures including species for which lumping was employed in the model simulations. (The auto exhaust irradiations and associated synthetic exhaust experiments are not included among these multi-component irradiations; they are discussed separately in Section IV-F). The "dynamic" experiments whose model simulations are discussed in this section consisted of propene-$NO_x$-air or propene-n-butane-toluene-$NO_x$-air irradiations carried out in the UNC chamber, where either some or all of the reactants were injected during the course of the irradiation, or the contents of the chamber were diluted at a significantly greater rate than usual, or both.

### 1. Mixed Alkene Irradiations

Thirteen mixed alkene runs carried out in the SAPRC EC or in the UNC chamber were modeled in this program. These included four ethene + propene runs and five multi-alkene runs carried out in the SAPRC EC and two ethene + acetaldehyde and two ethene + *trans*-2-butene runs carried out in the UNC chamber. (The ethene + acetaldehyde runs are classified with this group because acetaldehyde, which is a product from many other alkenes, is not formed from ethene, and thus a mixed alkene model was used to simulate them.) The experimental and calculated ozone maximum yields and NO oxidation and ozone formation times are summarized for these runs in Table IV-30, and the organic reactant half-lives and maximum product yields are summarized in Table IV-31. Selected distribution plots for the discrepancies obtained are given in Figure IV-60. Plots of the experimental and calculated concentration-time profiles for selected species are given for a representative EC ethene + propene run in Figure IV-61, for an EC mixed-alkene run in Figure IV-62, for an UNC ethene + acetaldehyde run in Figure IV-63, and for an UNC ethene + trans-2-butene run in Figure IV-64.

In general, the model tended to consistently underpredict reactivity in the mixed alkene runs carried out in the EC, with the discrepancies shown in Figures IV-61 and IV-62 being typical. For the UNC runs, the model gave good fits to the overall reactivity observed in the ethene + acetaldehyde runs (the run shown in Figure IV-63 being typical), but it significantly underpredicted the reactivity in the ethene + trans-2-butene runs, with the run shown in Figure IV-64 being the better of the two. However, in the case of the AU0180RB run, the trans-2-butene data appear to be anomalous, since it is observed to be "consumed" prior to sunrise, so that run may not be a reliable test for the model.

## 2. EC Mixed Alkane Runs

Two n-butane + 2,3-dimethylbutane runs carried out in the SAPRC EC were modeled in this program. The experimental and calculated ozone maximum yields and NO oxidation and ozone formation times are summarized for these runs in Table IV-32, and the organic reactant half-lives and product maximum yields are summarized in Table IV-33, together with the results for the UNC mixed aromatic runs discussed below. In both cases the model gave remarkably good fits to the data, especially considering the sensitivity of the model predictions to the chamber radical source, which tends to be variable (though somewhat less so for the SAPRC EC). Plots of the experimental and calculated concentration-time profiles for one of these runs are given in Figure IV-65; the corresponding profiles for the other are similar.

Table IV-30. Initial Concentrations and Experimental and Calculated Ozone Yields and Times Required to Achieve Half the Experimental Change in ($[O_3]-[NO]$) for the Mixed Alkene Runs

| Experiment | Initial Concentrations | | | Maximum Ozone Concentration | | | | Time to 1/2 Maximum Expt. ($[O_3]-[NO]$) | | | |
|---|---|---|---|---|---|---|---|---|---|---|---|
| | $NO_x$ (ppm) | HC (ppmC) | $HC/NO_x$ | Expt (ppm) | Calc (ppm) | Calc -Expt (ppm) | Calc -Expt /Expt) | Expt (min) | Calc (min) | Calc -Expt (min) | Calc -Exp /Exp |
| 1: EC Ethene + Propene Runs | | | | | | | | | | | |
| EC-144 | 0.509 | 4.7 | 9.3 | 1.065 | 0.837 | -0.228 | -0.21 | 69 | 97 | 28 | 0.41 |
| EC-145 | 0.991 | 3.4 | 3.4 | 0.777 | 0.516 | -0.261 | -0.34 | 148 | 157 | 9 | 0.06 |
| EC-160 | 0.993 | 3.2 | 3.3 | 0.874 | 0.461 | -0.414 | -0.47 | 138 | 186 | 48 | 0.35 |
| Group Average | 0.831 | 3.8 | 5.3 | 0.905 | 0.605 | -0.301 | -0.34 | 118 | 147 | 28 | 0.27 |
| S. Dev. | 0.279 | 0.8 | 3.4 | 0.147 | 0.203 | 0.099 | 0.13 | 43 | 45 | 20 | 0.19 |
| Avg. Abs. Value | | | | | | 0.301 | 0.34 | | | 27 | 0.27 |
| S. Dev. | | | | | | 0.099 | 0.13 | | | 20 | 0.19 |
| 2: EC Propene + trans-2-Butene Run | | | | | | | | | | | |
| EC-149 | 0.989 | 2.0 | 2.0 | 0.276 | 0.163 | -0.113 | -0.41 | 49 | 96 | 47 | 0.97 |
| 3: EC Four Alkene Runs | | | | | | | | | | | |
| EC-150 | 0.996 | 3.5 | 3.5 | 0.799 | 0.443 | -0.355 | -0.44 | 124 | 153 | 29 | 0.23 |
| EC-151 | 2.056 | 4.9 | 2.4 | 0.147 | 0.176 | 0.029 | 0.20 | 89 | 78 | -11 | -0.12 |
| EC-152 | 0.502 | 3.7 | 7.3 | 0.791 | 0.693 | -0.099 | -0.12 | 57 | 72 | 15 | 0.27 |
| EC-153 | 0.971 | 6.6 | 6.8 | 1.050 | 0.865 | -0.185 | -0.18 | 47 | 64 | 17 | 0.37 |
| EC-161 | 0.509 | 3.2 | 6.3 | 0.857 | 0.635 | -0.222 | -0.26 | 62 | 109 | 47 | 0.75 |
| Group Average | 1.007 | 4.4 | 5.3 | 0.729 | 0.562 | -0.166 | -0.16 | 76 | 95 | 20 | 0.30 |
| S. Dev. | 0.633 | 1.4 | 2.2 | 0.342 | 0.263 | 0.143 | 0.24 | 31 | 36 | 21 | 0.31 |
| Avg. Abs. Value | | | | | | 0.178 | 0.24 | | | 24 | 0.35 |
| S. Dev. | | | | | | 0.124 | 0.12 | | | 14 | 0.24 |

(continued)

Table IV-30 (continued) - 2

| Experiment | Initial Concentrations | | | Maximum Ozone Concentration | | | | Time to 1/2 Maximum Expt. ($[O_3]-[NO]$) | | | |
|---|---|---|---|---|---|---|---|---|---|---|---|
| | $NO_x$ (ppm) | HC (ppmC) | $HC/NO_x$ | Expt (ppm) | Calc (ppm) | Calc -Expt (ppm) | Calc -Expt /Expt) | Expt (min) | Calc (min) | Calc -Expt (min) | Calc -Exp /Exp |
| 4: UNC Ethene + Propene Runs | | | | | | | | | | | |
| OC1278R | 0.478 | 1.5 | 3.0 | 0.260 | 0.268 | 0.008 | 0.03 | 414 | 366 | -49 | -0.12 |
| OC2578R | 0.441 | 1.4 | 3.1 | 0.147 | 0.140 | -0.008 | -0.05 | 409 | 373 | -37 | -0.09 |
| Group Average | 0.460 | 1.4 | 3.1 | 0.204 | 0.204 | 0.000 | -0.01 | 412 | 369 | -43 | -0.10 |
| S. Dev. | 0.026 | 0.1 | 0.0 | 0.080 | 0.091 | 0.011 | 0.06 | 4 | 5 | 8 | 0.02 |
| Avg. Abs. Value | | | | | | 0.008 | 0.04 | | | 43 | 0.10 |
| S. Dev. | | | | | | 0.000 | 0.01 | | | 8 | 0.02 |
| 5: UNC Ethene + trans-2-Butene Runs | | | | | | | | | | | |
| AU0180RB | 0.555 | 0.7 | 1.3 | 0.256 | 0.052 | -0.204 | -0.80 | 383 | 630 | 248 | 0.65 |
| AU1480RB | 0.468 | 1.2 | 2.6 | 0.926 | 0.403 | -0.523 | -0.56 | 396 | 580 | 184 | 0.47 |
| Group Average | 0.512 | 1.0 | 1.9 | 0.591 | 0.228 | -0.363 | -0.68 | 389 | 605 | 216 | 0.56 |
| S. Dev. | 0.062 | 0.4 | 1.0 | 0.474 | 0.248 | 0.226 | 0.16 | 9 | 36 | 45 | 0.13 |
| Avg. Abs. Value | | | | | | 0.363 | 0.68 | | | 216 | 0.56 |
| S. Dev. | | | | | | 0.226 | 0.16 | | | 45 | 0.13 |
| Grand Average | 0.804 | 3.1 | 4.2 | 0.633 | 0.435 | -0.198 | -0.28 | 183 | 228 | 44 | 0.32 |
| S. Dev. | 0.449 | 1.7 | 2.4 | 0.355 | 0.268 | 0.166 | 0.27 | 154 | 196 | 83 | 0.34 |
| Avg. Abs. Value | | | | | | 0.204 | 0.31 | | | 59 | 0.37 |
| S. Dev. | | | | | | 0.158 | 0.22 | | | 72 | 0.28 |

Table IV-31. Experimental and Calculated Reactant Half-Lives and Product Yields for the Mixed Alkene Runs

| Experiment | Reactant Half-Life | | | | | Maximum Product Yields | | | | |
|---|---|---|---|---|---|---|---|---|---|---|
| | Species | Expt (min) | Calc (min) | Calc -Expt (min) | Calc -Expt /Expt | Species | Expt (ppm) | Calc (ppm) | Calc -Expt (ppm) | Calc -Expt /Expt |
| **1: EC Ethene + Propene Runs** | | | | | | | | | | |
| EC-144 | Ethene | 156 | 211 | 54 | 0.35 | PAN | 0.075 | 0.063 | -0.012 | -0.16 |
| | Propene | 63 | 94 | 31 | 0.50 | Formaldehyde | 0.846 | 0.815 | -0.031 | -0.04 |
| | | | | | | Acetaldehyde | 0.108 | 0.102 | -0.006 | -0.06 |
| EC-145 | Ethene | 267 | 326 | 59 | 0.22 | PAN | 0.112 | 0.085 | -0.027 | -0.24 |
| | Propene | 102 | 142 | 40 | 0.40 | Formaldehyde | 0.516 | 0.569 | 0.054 | 0.10 |
| | | | | | | Acetaldehyde | 0.174 | 0.185 | 0.011 | 0.07 |
| EC-160 | Ethene | 241 | 335 | 94 | 0.39 | PAN | 0.158 | 0.073 | -0.085 | -0.54 |
| | Propene | 86 | 145 | 60 | 0.70 | Formaldehyde | 0.500 | 0.542 | 0.042 | 0.08 |
| | | | | | | Acetaldehyde | 0.145 | 0.172 | 0.027 | 0.19 |
| Group Average | Ethene | 221 | 290 | 69 | 0.32 | PAN | 0.115 | 0.074 | -0.041 | -0.31 |
| Std. Dev. | | 58 | 69 | 21 | 0.09 | | 0.041 | 0.011 | 0.038 | 0.20 |
| Avg. Abs Value | | | | 69 | 0.32 | | | | 0.041 | 0.31 |
| Std. Dev. | | | | 21 | 0.09 | | | | 0.038 | 0.20 |
| Group Average | Propene | 84 | 127 | 44 | 0.53 | Formaldehyde | 0.620 | 0.642 | 0.022 | 0.05 |
| Std. Dev. | | 20 | 29 | 14 | 0.15 | | 0.196 | 0.150 | 0.046 | 0.08 |
| Avg. Abs Value | | | | 44 | 0.53 | | | | 0.042 | 0.08 |
| Std. Dev. | | | | 14 | 0.15 | | | | 0.011 | 0.03 |
| Group Average | | | | | | Acetaldehyde | 0.142 | 0.153 | 0.011 | 0.06 |
| Std. Dev. | | | | | | | 0.033 | 0.045 | 0.017 | 0.12 |
| Avg. Abs Value | | | | | | | | | 0.015 | 0.10 |
| Std. Dev. | | | | | | | | | 0.011 | 0.07 |

(continued)

Table IV-31 (continued) - 2

| Experiment | Reactant Half-Life |  |  |  |  | Maximum Product Yields |  |  |  |  |
|---|---|---|---|---|---|---|---|---|---|---|
|  | Species | Expt (min) | Calc (min) | Calc -Expt (min) | Calc -Expt /Expt | Species | Expt (ppm) | Calc (ppm) | Calc -Expt (ppm) | Calc -Expt /Expt |
| 2: EC Propene + trans-2-Butene Run |  |  |  |  |  |  |  |  |  |  |
| EC-149 | Propene | 75 | 154 | 80 | 1.07 | PAN | 0.112 | 0.065 | -0.047 | -0.42 |
|  | *trans*-2-Butene | 26 | 53 | 27 | 1.02 | Formaldehyde | 0.105 | 0.239 | 0.135 | 1.29 |
|  |  |  |  |  |  | Acetaldehyde | 0.339 | 0.370 | 0.031 | 0.09 |
| 3: EC Four Alkene Runs |  |  |  |  |  |  |  |  |  |  |
| EC-150 | Ethene | 265 | 341 | 76 | 0.29 | PAN | 0.145 | 0.077 | -0.068 | -0.47 |
|  | Propene | 102 | 142 | 40 | 0.39 | Formaldehyde | 0.433 | 0.516 | 0.083 | 0.19 |
|  | 1-Butene | 89 | 124 | 35 | 0.40 | Acetaldehyde | 0.139 | 0.195 | 0.056 | 0.40 |
|  | *trans*-2-Butene | 35 | 50 | 15 | 0.43 | Propionaldehyde | 0.036 | 0.041 | 0.005 | 0.14 |
| EC-151 | Ethene | 320 | 334 | 15 | 0.05 | PAN | 0.077 | 0.071 | -0.006 | -0.08 |
|  | Propene | 114 | 137 | 24 | 0.21 | Formaldehyde | 0.512 | 0.637 | 0.125 | 0.24 |
|  | 1-Butene | 99 | 118 | 19 | 0.19 | Acetaldehyde | 0.327 | 0.377 | 0.050 | 0.15 |
|  | *trans*-2-Butene | 34 | 42 | 7 | 0.21 | Propionaldehyde | 0.074 | 0.086 | 0.012 | 0.16 |
| EC-152 | Ethene | 180 | 231 | 51 | 0.28 | PAN | 0.115 | 0.102 | -0.013 | -0.11 |
|  | Propene | 64 | 88 | 25 | 0.39 | Formaldehyde | 0.262 | 0.521 | 0.259 | 0.99 |
|  | 1-Butene | 62 | 80 | 19 | 0.31 | Acetaldehyde | 0.124 | 0.171 | 0.047 | 0.38 |
|  | *trans*-2-Butene | 25 | 35 | 9 | 0.37 | Propionaldehyde | 0.074 | 0.100 | 0.026 | 0.35 |
| EC-153 | Ethene | 163 | 224 | 61 | 0.37 | PAN | 0.175 | 0.152 | -0.022 | -0.13 |
|  | Propene | 58 | 89 | 31 | 0.54 | Formaldehyde | 0.645 | 0.934 | 0.290 | 0.45 |
|  | 1-Butene | 45 | 82 | 37 | 0.82 | Acetaldehyde | 0.211 | 0.280 | 0.069 | 0.32 |
|  | *trans*-2-Butene | 25 | 37 | 12 | 0.48 | Propionaldehyde | 0.143 | 0.190 | 0.047 | 0.33 |
| EC-161 | Ethene | 175 | 255 | 80 | 0.46 | PAN | 0.125 | 0.088 | -0.037 | -0.29 |
|  | Propene | 58 | 100 | 42 | 0.71 | Formaldehyde | 0.423 | 0.470 | 0.047 | 0.11 |
|  | 1-Butene | 54 | 90 | 36 | 0.68 | Acetaldehyde | 0.133 | 0.148 | 0.015 | 0.11 |
|  | *trans*-2-Butene | 23 | 37 | 15 | 0.65 | Propionaldehyde | 0.078 | 0.084 | 0.006 | 0.08 |

(continued)

Table IV-31 (continued) - 3

| Experiment | Reactant Half-Life | | | | | Maximum Product Yields | | | | |
|---|---|---|---|---|---|---|---|---|---|---|
| | Species | Expt (min) | Calc (min) | Calc -Expt (min) | Calc -Expt /Expt | Species | Expt (ppm) | Calc (ppm) | Calc -Expt (ppm) | Calc -Expt /Expt |
| Group Average | Ethene | 220 | 277 | 57 | 0.29 | PAN | 0.127 | 0.098 | -0.029 | -0.22 |
| Std. Dev. | | 68 | 57 | 26 | 0.15 | | 0.036 | 0.033 | 0.025 | 0.16 |
| Avg. Abs Value | | | | 57 | 0.29 | | | | 0.029 | 0.22 |
| Std. Dev. | | | | 26 | 0.15 | | | | 0.025 | 0.16 |
| Group Average | Propene | 79 | 111 | 32 | 0.45 | Formaldehyde | 0.455 | 0.616 | 0.161 | 0.40 |
| Std. Dev. | | 27 | 26 | 8 | 0.19 | | 0.140 | 0.188 | 0.108 | 0.35 |
| Avg. Abs Value | | | | 32 | 0.45 | | | | 0.161 | 0.40 |
| Std. Dev. | | | | 8 | 0.19 | | | | 0.108 | 0.35 |
| Group Average | 1-Butene | 70 | 99 | 29 | 0.48 | Acetaldehyde | 0.187 | 0.234 | 0.047 | 0.27 |
| Std. Dev. | | 23 | 21 | 10 | 0.26 | | 0.086 | 0.094 | 0.020 | 0.13 |
| Avg. Abs Value | | | | 29 | 0.48 | | | | 0.047 | 0.27 |
| Std. Dev. | | | | 10 | 0.26 | | | | 0.020 | 0.13 |
| Group Average | *trans*-2-Butene | 28 | 40 | 12 | 0.43 | Propionaldehyde | 0.081 | 0.100 | 0.019 | 0.21 |
| Std. Dev. | | 6 | 6 | 3 | 0.16 | | 0.039 | 0.055 | 0.018 | 0.12 |
| Avg. Abs Value | | | | 12 | 0.43 | | | | 0.019 | 0.21 |
| Std. Dev. | | | | 3 | 0.16 | | | | 0.018 | 0.12 |
| 4: UNC Ethene + Acetaldehyde Runs | | | | | | | | | | |
| OC1278R | Ethene | 196 | 56C | 364 | 1.85 | PAN | 0.053 | 0.094 | 0.042 | 0.78 |
| | Acetaldehyde | 378 | 507 | 129 | 0.34 | | | | | |
| OC2578R | Ethene | 217 | 570 | 353 | 1.63 | PAN | 0.041 | 0.072 | 0.032 | 0.78 |
| | Acetaldehyde | 202 | 453 | 251 | 1.24 | | | | | |

(continued)

Table IV-31 (continued) - 4

| Experiment | Reactant Half-Life | | | | | Maximum Product Yields | | | | |
|---|---|---|---|---|---|---|---|---|---|---|
| | Species | Expt (min) | Calc (min) | Calc -Expt (min) | Calc -Expt /Expt | Species | Expt (ppm) | Calc (ppm) | Calc -Expt (ppm) | Calc -Expt /Expt |
| Group Average | Ethene | 207 | 565 | 359 | 1.74 | PAN | 0.047 | 0.083 | 0.037 | 0.78 |
| Std. Dev. | | 14 | 7 | 7 | 0.16 | | 0.009 | 0.016 | 0.007 | 0.01 |
| Avg. Abs Value | | | | 359 | 1.74 | | | | 0.037 | 0.78 |
| Std. Dev. | | | | 7 | 0.16 | | | | 0.007 | 0.01 |
| Group Average | Acetaldehyde | 290 | 480 | 190 | 0.79 | | | | | |
| Std. Dev. | | 124 | 38 | 86 | 0.64 | | | | | |
| Avg. Abs Value | | | | 190 | 0.79 | | | | | |
| Std. Dev. | | | | 86 | 0.64 | | | | | |
| 5: UNC Ethene + trans-2-Butene Runs | | | | | | | | | | |
| AU0180RB | Ethene | 526 | 570 | 44 | 0.08 | PAN | 0.013 | 0.001 | -0.011 | -0.89 |
| | | | | | | Formaldehyde | 0.230 | 0.064 | -0.166 | -0.72 |
| | | | | | | Acetaldehyde | 0.050 | 0.057 | 0.007 | 0.15 |
| AU1480RB | Ethene | 380 | 532 | 152 | 0.40 | PAN | 0.056 | 0.020 | -0.036 | -0.64 |
| | *trans*-2-Butene | 179 | 216 | 37 | 0.21 | Formaldehyde | 0.495 | 0.165 | -0.330 | -0.67 |
| Group Average | Ethene | 453 | 551 | 98 | 0.24 | PAN | 0.034 | 0.011 | -0.024 | -0.76 |
| Std. Dev. | | 103 | 27 | 76 | 0.22 | | 0.030 | 0.013 | 0.017 | 0.18 |
| Avg. Abs Value | | | | 98 | 0.24 | | | | 0.024 | 0.76 |
| Std. Dev. | | | | 76 | 0.22 | | | | 0.017 | 0.18 |
| Group Average | *trans*-2-Butene | 179 | 216 | 37 | 0.21 | Formaldehyde | 0.363 | 0.114 | -0.248 | -0.69 |
| Std. Dev. | | | | | | | 0.187 | 0.072 | 0.115 | 0.04 |
| Avg. Abs Value | | | | 37 | 0.21 | | | | 0.248 | 0.69 |
| Std. Dev. | | | | | | | | | 0.115 | 0.04 |
| Group Average | | | | | | Acetaldehyde | 0.050 | 0.057 | 0.007 | 0.15 |
| Std. Dev. | | | | | | | | | | |
| Avg. Abs Value | | | | | | | | | 0.007 | 0.15 |
| Std. Dev. | | | | | | | | | | |

```
----------------------------------------------------------------------------
        Calc.-Expt./Calc.                      Calc.-Expt./Calc.
          Maximum Ozone               Time to 1/2 Expt. Δ([O3]-[NO])max
----------------------------------------------------------------------------
         <  -0.33    :135                     <  -0.55    :
  -0.33 -   -0.27    :                  -0.55 -  -0.45    :
  -0.27 -   -0.21    :113               -0.45 -  -0.35    :
  -0.21 -   -0.15    :35                -0.35 -  -0.25    :
  -0.15 -   -0.09    :23                -0.25 -  -0.15    :
  -0.09 -   -0.03    :                  -0.15 -  -0.05    :344
  -0.03 -    0.03    :344               -0.05 -   0.05    :
   0.03 -    0.09    :                   0.05 -   0.15    :1
   0.09 -    0.15    :                   0.15 -   0.25    :3
   0.15 -    0.21    :                   0.25 -   0.35    :13
   0.21 -    0.27    :                   0.35 -   0.45    :13
   0.27 -    0.33    :                   0.45 -   0.55    :5
         >   0.33    :                        >   0.55    :235
----------------------------------------------------------------------------
(Calc.-Expt.)
  /Expt.       Ethene        Propene       trans-2-     1-Butene
 Half-Life                                  Butene
----------------------------------------------------------------------------
     < -0.5    :             :             :            :
-0.5 - -0.4    :             :             :            :
-0.4 - -0.3    :             :             :            :
-0.3 - -0.2    :             :             :            :
-0.2 - -0.1    :             :             :            :
-0.1 -  0.0    :             :             :            :
 0.0 -  0.1    :35           :             :            :
 0.1 -  0.2    :             :             :            :3
 0.2 -  0.3    :133          :3            :35          :
 0.3 -  0.4    :1135         :133          :3           :33
 0.4 -  0.5    :3            :1            :33          :
     >  0.5    :44           :1233         :23          :33
----------------------------------------------------------------------------
(Calc.-Expt.)
  /Expt.          PAN        Formaldehyde  Acetaldehyde  Propional-
Product Yield                                             dehyde
----------------------------------------------------------------------------
     < -0.5    :155          :55           :            :
-0.5 - -0.4    :23           :             :            :
-0.4 - -0.3    :             :             :            :
-0.3 - -0.2    :13           :             :            :
-0.2 - -0.1    :133          :             :            :
-0.1 -  0.0    :3            :1            :1           :
 0.0 -  0.1    :             :1            :12          :3
 0.1 -  0.2    :             :133          :1335        :33
 0.2 -  0.3    :             :3            :            :
 0.3 -  0.4    :             :             :33          :33
 0.4 -  0.5    :             :3            :3           :
     >  0.5    :44           :23           :            :
----------------------------------------------------------------------------
```

Figure IV-60. Distribution plots for discrepancies between calculated and experimental ozone maximum yields, times required to achieve half the maximum experimental change in ($[O_3]$-[NO]), and half lives or yields for selected reactants and products observed in the mixed olefin irradiations. Codes for symbols:

1 = EC Ethene + Propene Runs
2 = EC Propene + *trans*-2-Butene Run
3 = EC Four Alkene Runs
4 = UNC Ethene + Acetaldehyde Runs
5 = UNC Ethene + *trans*-2-Butene Runs

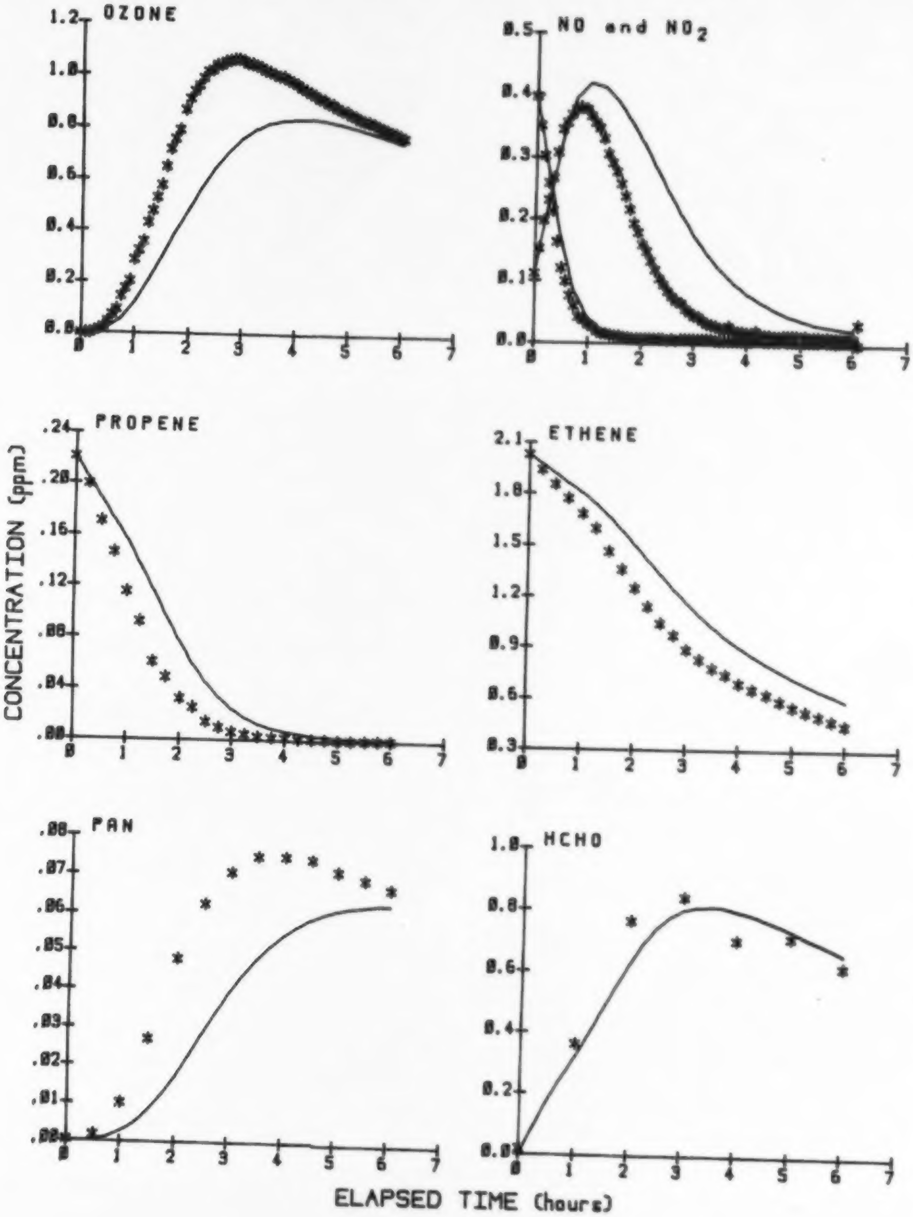

Figure IV-61. Experimental and calculated concentration-time profiles for selected species observed in the ethene + propene run EC-144.
* = Experimental data.
----- = Model calculation.

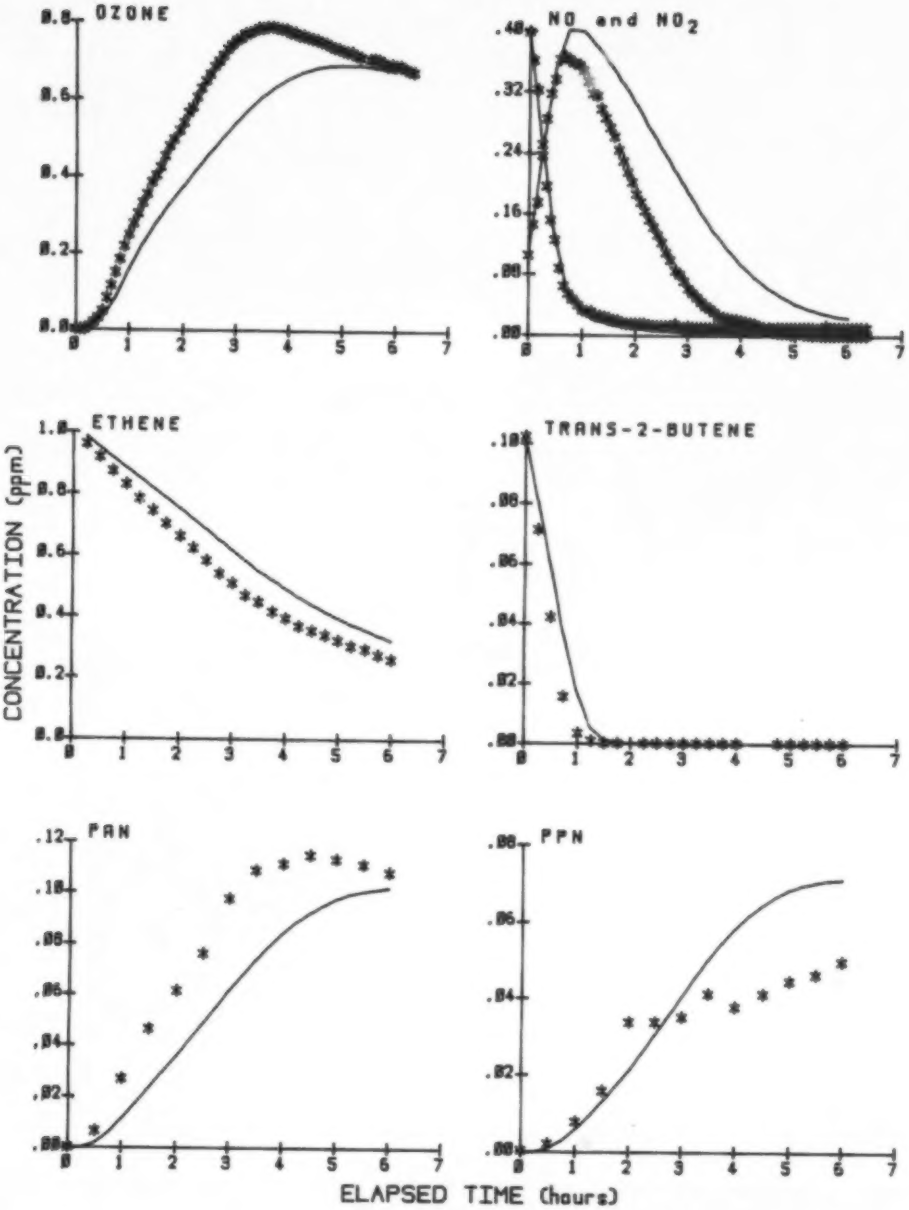

Figure IV-62. Experimental and calculated concentration-time profiles for selected species observed in the four alkene run EC-152.
* = Experimental data.
----- = Model calculation.

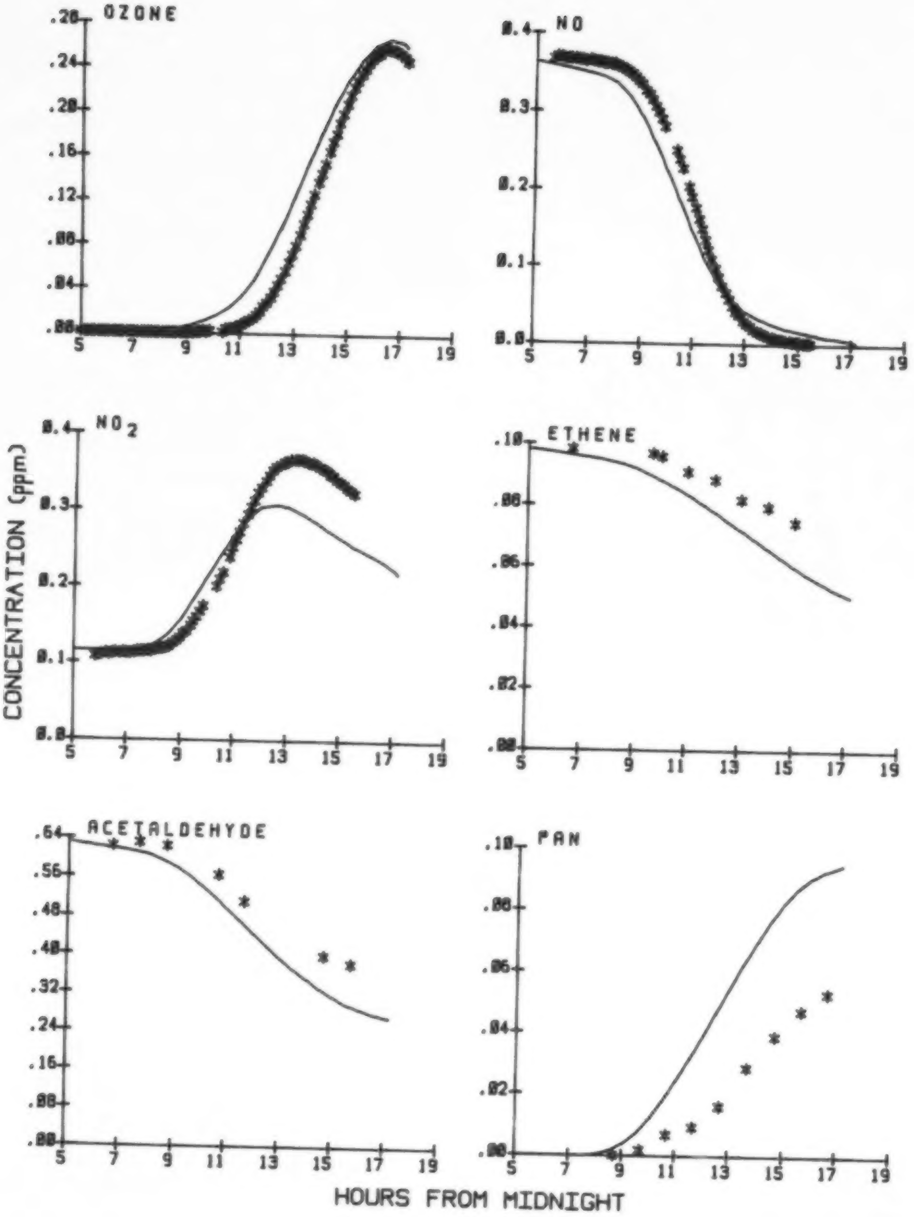

Figure IV-63. Experimental and calculated concentration-time profiles for selected species observed in the UNC ethene + acetaldehyde run OC1278R.
* = Experimental data.
---- = Model calculation.

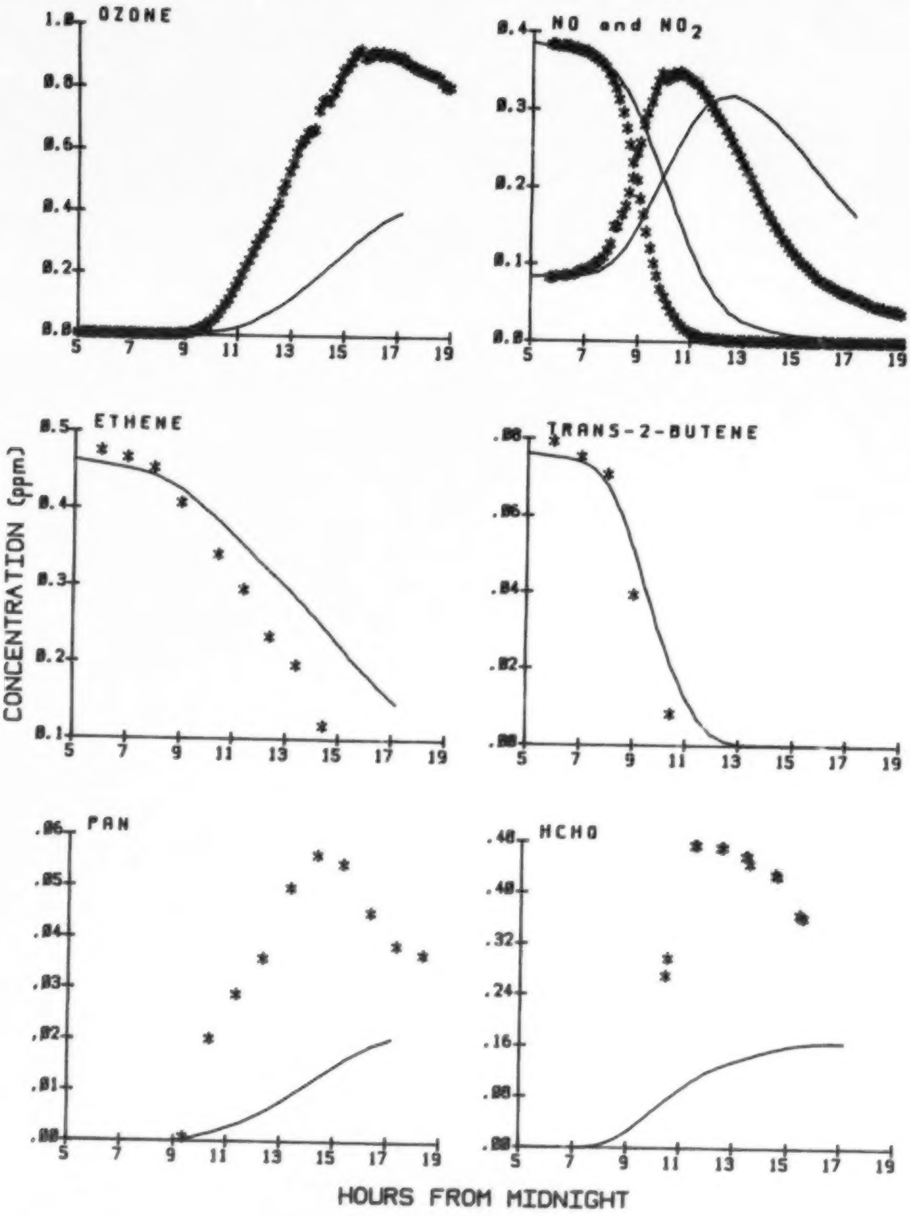

Figure IV-64. Experimental and calculated concentration-time profiles for selected species observed in the UNC ethene + trans-2-butene run AU1480RB.
* = Experimental data.
----- = Model calculation.

Table IV-32. Initial Concentrations and Experimental and Calculated Ozone Yields and Times Required to Achieve Half the Experimental Change in ($[O_3]-[NO]$) for the Mixed Alkane and the Mixed Aromatic Runs

| Experiment | Initial Concentrations | | | Maximum Ozone Concentration | | | | Time to 1/2 Maximum Expt. ($[O_3]-[NO]$) | | | |
|---|---|---|---|---|---|---|---|---|---|---|---|
| | $NO_x$ (ppm) | HC (ppmC) | $HC/NO_x$ | Expt (ppm) | Calc (ppm) | Calc -Expt (ppm) | Calc -Expt /Expt) | Expt (min) | Calc (min) | Calc -Expt (min) | Calc -Exp /Exp |
| 1: EC n-Butane + 2,3-Dimethylbutane Runs | | | | | | | | | | | |
| EC-166 | 0.100 | 9.2 | 91.9 | 0.462 | 0.475 | 0.013 | 0.03 | 128 | 143 | 15 | 0.11 |
| EC-172 | 0.096 | 2.8 | 29.1 | 0.369 | 0.405 | 0.037 | 0.10 | 220 | 209 | -11 | -0.05 |
| Group Average | 0.098 | 6.0 | 60.5 | 0.415 | 0.440 | 0.025 | 0.06 | 174 | 176 | 1 | 0.03 |
| S. Dev. | 0.003 | 4.5 | 44.4 | 0.066 | 0.049 | 0.017 | 0.05 | 65 | 47 | 18 | 0.12 |
| Avg. Abs. Value | | | | | | 0.025 | 0.06 | | | 12 | 0.08 |
| S. Dev. | | | | | | 0.017 | 0.05 | | | 2 | 0.04 |
| 2: UNC Toluene + o-Xylene Runs | | | | | | | | | | | |
| ST0682R | 0.456 | 2.8 | 6.2 | 0.378 | 0.475 | 0.097 | 0.26 | 440 | 381 | -59 | -0.13 |
| ST0682B | 0.447 | 2.8 | 6.4 | 0.478 | 0.475 | -0.003 | -0.01 | 416 | 365 | -52 | -0.12 |
| Group Average | 0.451 | 2.8 | 6.3 | 0.428 | 0.475 | 0.047 | 0.12 | 428 | 373 | -55 | -0.13 |
| S. Dev. | 0.006 | 0.0 | 0.1 | 0.070 | 0.000 | 0.070 | 0.18 | 16 | 12 | 5 | 0.01 |
| Avg. Abs. Value | | | | | | 0.050 | 0.13 | | | 55 | 0.13 |
| S. Dev. | | | | | | 0.066 | 0.18 | | | 5 | 0.01 |
| Grand Average | 0.275 | 4.4 | 33.4 | 0.422 | 0.457 | 0.036 | 0.09 | 301 | 274 | -27 | -0.05 |
| S. Dev. | 0.204 | 3.2 | 40.5 | 0.056 | 0.035 | 0.044 | 0.12 | 152 | 117 | 35 | 0.11 |
| Avg. Abs. Value | | | | | | 0.037 | 0.10 | | | 34 | 0.11 |
| S. Dev. | | | | | | 0.042 | 0.11 | | | 25 | 0.04 |

Table IV-33. Experimental and Calculated Maximum Product Yields for the Mixed Alkane Runs and Experimental and Calculated Maximum Product Yields and Aromatic Half-Lives for the Mixed Aromatic Runs

| Experiment | Maximum Product Yields | | | | |
|---|---|---|---|---|---|
| | Species | Expt (ppm) | Calc (ppm) | Calc -Expt (ppm) | Calc -Expt /Expt |
| **1: EC n-Butane + 2,3-Dimethylbutane Runs** | | | | | |
| EC-166 | Acetone | 0.128 | 0.117 | -0.011 | -0.08 |
| | PAN | 0.040 | 0.038 | -0.002 | -0.04 |
| | Acetaldehyde | 0.043 | 0.095 | 0.053 | 1.23 |
| EC-172 | Acetone | 0.150 | 0.174 | 0.024 | 0.16 |
| | PAN | 0.029 | 0.033 | 0.004 | 0.14 |
| | Acetaldehyde | 0.023 | 0.027 | 0.003 | 0.15 |
| Group Average | Acetone | 0.139 | 0.146 | 0.007 | 0.04 |
| Std. Dev. | | 0.016 | 0.040 | 0.024 | 0.17 |
| Avg. Abs Value | | | | 0.017 | 0.12 |
| Std. Dev. | | | | 0.009 | 0.05 |
| Group Average | PAN | 0.034 | 0.036 | 0.001 | 0.05 |
| Std. Dev. | | 0.008 | 0.004 | 0.004 | 0.13 |
| Avg. Abs Value | | | | 0.003 | 0.09 |
| Std. Dev. | | | | 0.002 | 0.07 |
| Group Average | Acetaldehyde | 0.033 | 0.061 | 0.028 | 0.69 |
| Std. Dev. | | 0.014 | 0.049 | 0.035 | 0.76 |
| Avg. Abs Value | | | | 0.028 | 0.69 |
| Std. Dev. | | | | 0.035 | 0.76 |
| **2: UNC Toluene + o-Xylene Runs** | | | | | |
| ST0682R | PAN | 0.043 | 0.070 | 0.028 | 0.65 |
| | Formaldehyde | 0.088 | 0.030 | -0.058 | -0.66 |
| ST0682B | PAN | 0.061 | 0.090 | 0.029 | 0.47 |
| | Formaldehyde | 0.100 | 0.038 | -0.062 | -0.62 |

(continued)

Table IV-33 (continued) - 2

| Experiment | Maximum Product Yields | | | | |
|---|---|---|---|---|---|
| | Species | Expt (ppm) | Calc (ppm) | Calc -Expt (ppm) | Calc -Expt /Expt |
| Group Average | PAN | 0.052 | 0.080 | 0.028 | 0.56 |
| Std. Dev. | | 0.013 | 0.014 | 0.001 | 0.12 |
| Avg. Abs Value | | | | 0.028 | 0.56 |
| Std. Dev. | | | | 0.001 | 0.12 |
| Group Average | Formaldehyde | 0.094 | 0.034 | -0.060 | -0.64 |
| Std. Dev. | | 0.008 | 0.005 | 0.003 | 0.02 |
| Avg. Abs Value | | | | 0.060 | 0.64 |
| Std. Dev. | | | | 0.003 | 0.02 |

| | Reactant Half-Lives | | | | |
|---|---|---|---|---|---|
| | Species | Expt (min) | Calc (min) | Calc -Expt (min) | Calc -Expt /Expt |
| ST0682R | o-Xylene | 402 | 388 | -14 | -0.03 |
| | Toluene | 375 | 525 | 150 | 0.40 |
| ST0682B | o-Xylene | 294 | 335 | 41 | 0.14 |
| | Toluene | 464 | 466 | 3 | 0.01 |
| Group Average | o-Xylene | 348 | 362 | 14 | 0.05 |
| Std. Dev. | | 76 | 37 | 39 | 0.12 |
| Avg. Abs Value | | | | 28 | 0.09 |
| Std. Dev. | | | | 20 | 0.08 |
| Group Average | Toluene | 419 | 496 | 76 | 0.20 |
| Std. Dev. | | 63 | 42 | 104 | 0.28 |
| Avg. Abs Value | | | | 76 | 0.20 |
| Std. Dev. | | | | 104 | 0.28 |

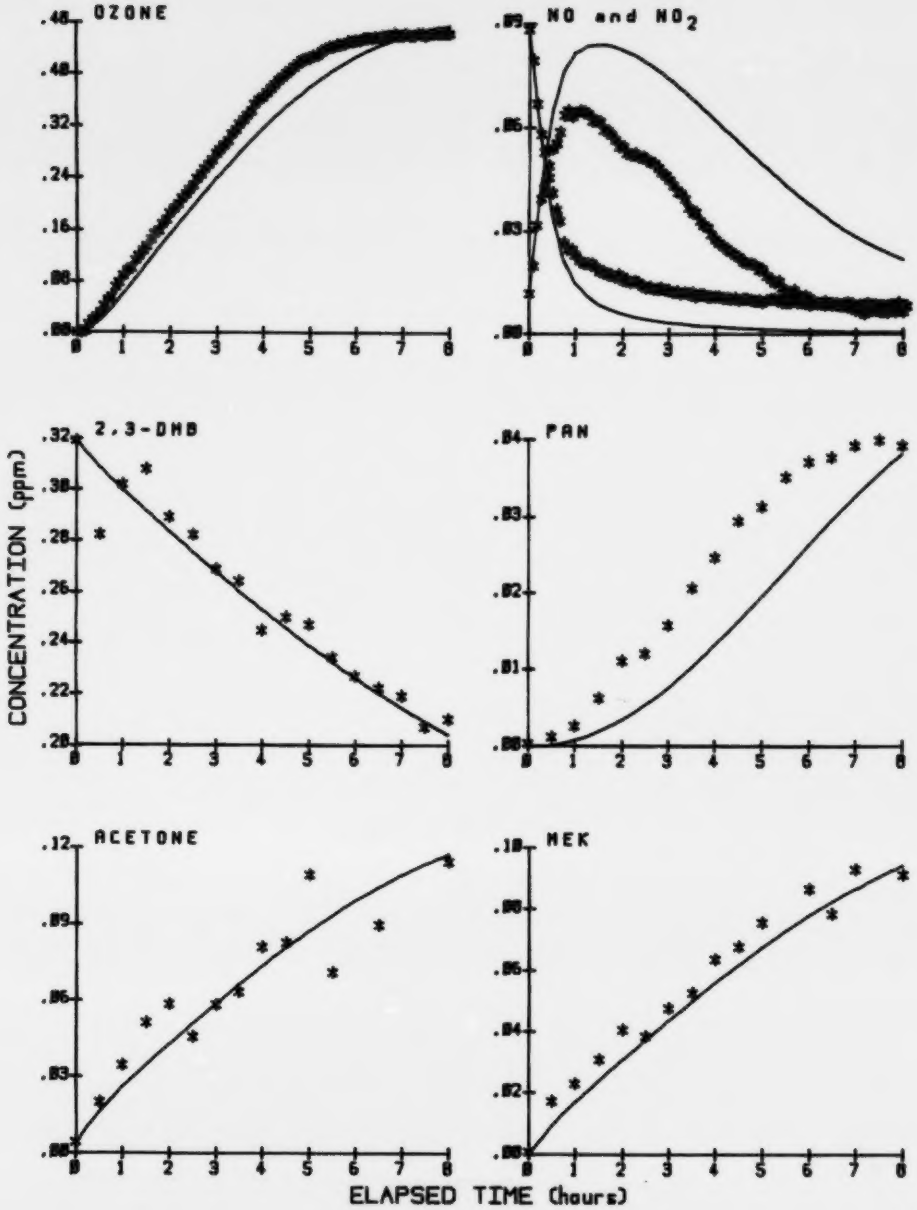

Figure IV-65. Experimental and calculated concentration-time plots for representative species observed in the mixed alkane run EC-166.

* = Experimental data.

----- = Model calculation.

### 3. UNC Mixed Aromatic Runs

Two toluene + o-xylene-$NO_x$-air irradiations, carried out on the same day in the two sides of the UNC chamber, were modeled in this program. The experimental and calculated ozone maximum yields and NO oxidation and ozone formation times for these runs are summarized in Table IV-32, and the organic reactant half-lives and product maximum yields are summarized in Table IV-33. The model tended to overpredict the NO oxidation and ozone formation rates for both runs, though not to a large extent. Concentration-time plots for the data from the "red" side are shown in Figure IV-66; the fits for the "blue" side were similar.

### 4. Mixed Alkane + Alkene Runs

The runs in this catagory which were modeled include five propene + n-butane runs carried out in the EC and three carried out in the UNC chamber, and four UNC runs employing an ethene, propene, n-butane and n-pentane mixture (called SIMMIX by the UNC researchers). The experimental and calculated ozone maximum yields and NO oxidation and ozone formation times for these runs are summarized in Table IV-34, and the organic reactant half-lives and maximum product yields are summarized in Table IV-35. Selected distribution plots for the discrepancies obtained are given in Figure IV-67. Concentration-time plots of selected data from representative EC and UNC propene + n-butane run are shown in Figures IV-68 and IV-69, respectively, and plots for a representative UNC "SIMMIX" run are shown in Figure IV-70.

The EC propene + n-butane run whose data are shown in Figure IV-68 is typical in that for all of these runs the model tended to slightly overpredict ozone maximum yields. However, in general, fair fits of the model to the experimental data were obtained. The fits obtained in the simulations of the UNC runs were more variable, but do not indicate any systematic discrepancies. Runs JL1581R and OC0382B shown in Figures IV-69 and IV-70, respectively, are fairly typical of this group.

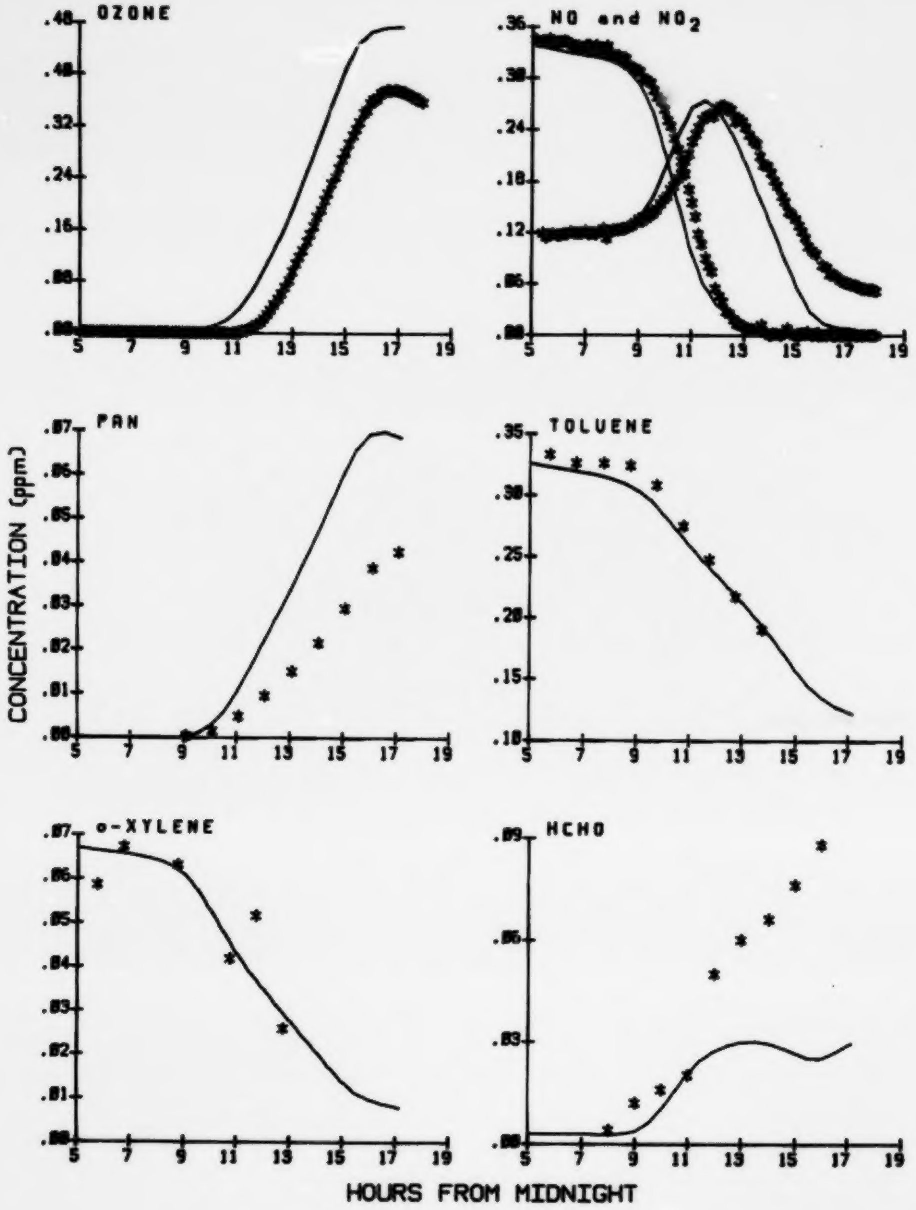

Figure IV-66. Experimental and calculated concentration-time plots for representative species observed in the UNC mixed aromatic run ST0682R.

* = Experimental data.
----- = Model calculation.

Table IV-34. Initial Concentrations and Experimental and Calculated Ozone Yields and Times Required to Achieve Half the Experimental Change in ($[O_3]$-[NO]) for the Alkane + Alkene Runs

| Experiment | Initial Concentrations | | | Maximum Ozone Concentration | | | | Time to 1/2 Maximum Expt. ($[O_3]$-[NO]) | | | |
|---|---|---|---|---|---|---|---|---|---|---|---|
| | $NO_x$ (ppm) | HC (ppmC) | $HC/NO_x$ | Expt (ppm) | Calc (ppm) | Calc -Expt (ppm) | Calc -Expt /Expt) | Expt (min) | Calc (min) | Calc -Expt (min) | Calc -Exp /Exp |
| **1: EC Propene + n-Butane Runs** | | | | | | | | | | | |
| EC-106 | 0.503 | 9.2 | 18.3 | 0.592 | 0.698 | 0.106 | 0.18 | 130 | 112 | -18 | -0.14 |
| EC-113 | 0.111 | 9.4 | 84.6 | 0.352 | 0.471 | 0.120 | 0.34 | 42 | 32 | -9 | -0.23 |
| EC-114 | 0.998 | 16.9 | 17.0 | 0.744 | 0.836 | 0.092 | 0.12 | 95 | 108 | 12 | 0.13 |
| EC-115 | 0.506 | 12.7 | 25.1 | 0.590 | 0.721 | 0.131 | 0.22 | 130 | 128 | -2 | -0.02 |
| EC-116 | 0.495 | 18.5 | 37.3 | 0.743 | 0.828 | 0.086 | 0.12 | 68 | 58 | -10 | -0.14 |
| Group Average | 0.523 | 13.3 | 36.5 | 0.604 | 0.711 | 0.107 | 0.20 | 93 | 88 | -5 | -0.08 |
| S. Dev. | 0.315 | 4.3 | 28.1 | 0.160 | 0.148 | 0.019 | 0.09 | 39 | 41 | 11 | 0.14 |
| Avg. Abs. Value | | | | | | 0.107 | 0.20 | | | 9 | 0.13 |
| S. Dev. | | | | | | 0.019 | 0.09 | | | 6 | 0.08 |
| **2: UNC Propene + n-Butane Runs** | | | | | | | | | | | |
| JL1581R | 0.272 | 2.2 | 8.2 | 0.485 | 0.428 | -0.057 | -0.12 | 336 | 372 | 36 | 0.11 |
| JL1881R | 0.262 | 2.1 | 8.1 | 0.658 | 0.391 | -0.267 | -0.41 | 341 | 367 | 26 | 0.08 |
| ST2481R | 0.235 | 1.5 | 6.5 | 0.211 | 0.293 | 0.082 | 0.39 | 455 | 343 | -112 | -0.25 |
| Group Average | 0.256 | 2.0 | 7.6 | 0.452 | 0.371 | -0.081 | -0.05 | 377 | 361 | -17 | -0.02 |
| S. Dev. | 0.019 | 0.4 | 1.0 | 0.226 | 0.070 | 0.176 | 0.40 | 67 | 16 | 83 | 0.20 |
| Avg. Abs. Value | | | | | | 0.135 | 0.30 | | | 58 | 0.14 |
| S. Dev. | | | | | | 0.115 | 0.16 | | | 47 | 0.09 |

(continued)

Table IV-34 (continued) - 2

| Experiment | Initial Concentrations | | | Maximum Ozone Concentration | | | | Time to 1/2 Maximum Expt. ([$O_3$]-[NO]) | | | |
|---|---|---|---|---|---|---|---|---|---|---|---|
| | $NO_x$ (ppm) | HC (ppmC) | HC/$NO_x$ | Expt (ppm) | Calc (ppm) | Calc -Expt (ppm) | Calc -Expt /Expt) | Expt (min) | Calc (min) | Calc -Expt (min) | Calc -Exp /Exp |
| 3: UNC Ethene + Propene + n-Butane + n-Pentane Runs | | | | | | | | | | | |
| AU2781R | 0.231 | 2.1 | 9.0 | 0.548 | 0.525 | -0.022 | -0.04 | 503 | 446 | -57 | -0.11 |
| OC0382R | 0.247 | 2.8 | 11.1 | 0.247 | 0.437 | 0.190 | 0.77 | 428 | 349 | -79 | -0.19 |
| NV1582R | 0.180 | 2.5 | 13.9 | 0.061 | 0.259 | 0.198 | 3.24 | 412 | 311 | -101 | -0.25 |
| OC0382B | 0.244 | 1.5 | 6.4 | 0.158 | 0.255 | 0.097 | 0.62 | 416 | 352 | -64 | -0.15 |
| Group Average | 0.226 | 2.2 | 10.1 | 0.253 | 0.369 | 0.116 | 1.15 | 440 | 364 | -75 | -0.17 |
| S. Dev. | 0.031 | 0.5 | 3.2 | 0.210 | 0.135 | 0.103 | 1.44 | 43 | 58 | 20 | 0.06 |
| Avg. Abs. Value | | | | | | 0.127 | 1.17 | | | 75 | 0.17 |
| S. Dev. | | | | | | 0.083 | 1.42 | | | 20 | 0.06 |

Table IV-35. Experimental and Calculated Product Yields and Alkene Consumption Rates for the Alkane + Alkene Runs

| Experiment | Reactant Half-Life | | | | | Maximum Product Yields | | | | |
|---|---|---|---|---|---|---|---|---|---|---|
| | Species | Expt (min) | Calc (min) | Calc -Expt (min) | Calc -Expt /Expt | Species | Expt (ppm) | Calc (ppm) | Calc -Expt (ppm) | Calc -Expt /Expt |
| 1: EC Propene + n-Butane Runs | | | | | | | | | | |
| EC-106 | Propene | 134 | 130 | -5 | -0.04 | PAN | 0.162 | 0.190 | 0.028 | 0.17 |
| | | | | | | Formaldehyde | 0.207 | 0.184 | -0.023 | -0.11 |
| | | | | | | Acetaldehyde | 0.199 | 0.266 | 0.067 | 0.34 |
| EC-113 | Propene | 82 | 75 | -7 | -0.09 | PAN | 0.060 | 0.090 | 0.029 | 0.49 |
| | | | | | | Acetaldehyde | 0.194 | 0.269 | 0.075 | 0.39 |
| EC-114 | Propene | 112 | 141 | 30 | 0.27 | PAN | 0.231 | 0.262 | 0.031 | 0.14 |
| | | | | | | Formaldehyde | 0.433 | 0.355 | -0.078 | -0.18 |
| | | | | | | Acetaldehyde | 0.427 | 0.492 | 0.065 | 0.15 |
| EC-115 | Propene | 130 | 147 | 17 | 0.13 | PAN | 0.134 | 0.166 | 0.033 | 0.24 |
| | | | | | | Formaldehyde | 0.201 | 0.147 | -0.054 | -0.27 |
| | | | | | | Acetaldehyde | 0.222 | 0.265 | 0.044 | 0.20 |
| EC-116 | Propene | 90 | 88 | -2 | -0.02 | PAN | 0.186 | 0.211 | 0.025 | 0.14 |
| | | | | | | Formaldehyde | 0.463 | 0.381 | -0.082 | -0.18 |
| | | | | | | Acetaldehyde | 0.440 | 0.538 | 0.098 | 0.22 |
| Group Average | Propene | 110 | 116 | 7 | 0.05 | PAN | 0.155 | 0.184 | 0.029 | 0.24 |
| Std. Dev. | | 23 | 33 | 16 | 0.15 | | 0.064 | 0.064 | 0.003 | 0.15 |
| Avg. Abs Value | | | | 12 | 0.11 | | | | 0.029 | 0.24 |
| Std. Dev. | | | | 11 | 0.10 | | | | 0.003 | 0.15 |
| Group Average | | | | | | Formaldehyde | 0.326 | 0.267 | -0.059 | -0.18 |
| Std. Dev. | | | | | | | 0.141 | 0.118 | 0.027 | 0.06 |
| Avg. Abs Value | | | | | | | | | 0.059 | 0.18 |
| Std. Dev. | | | | | | | | | 0.027 | 0.06 |

(continued)

Table IV-35 (continued) - 2

| Experiment | Reactant Half-Life | | | | | Maximum Product Yields | | | | |
|---|---|---|---|---|---|---|---|---|---|---|
| | Species | Expt (min) | Calc (min) | Calc -Expt (min) | Calc -Expt /Expt | Species | Expt (ppm) | Calc (ppm) | Calc -Expt (ppm) | Calc -Expt /Expt |
| Group Average | | | | | | Acetaldehyde | 0.296 | 0.366 | 0.070 | 0.26 |
| Std. Dev. | | | | | | | 0.126 | 0.137 | 0.020 | 0.10 |
| Avg. Abs Value | | | | | | | | | 0.070 | 0.26 |
| Std. Dev. | | | | | | | | | 0.020 | 0.10 |
| 2: UNC Propene + n-Butane Runs | | | | | | | | | | |
| JL1581R | Propene | 283 | 323 | 40 | 0.14 | PAN | 0.097 | 0.047 | -0.051 | -0.52 |
| JL1881R | Propene | 326 | 340 | 15 | 0.04 | PAN | 0.046 | 0.057 | 0.011 | 0.24 |
| ST2481R | Propene | 447 | 382 | -65 | -0.15 | | | | | |
| Group Average | Propene | 352 | 348 | -4 | 0.01 | PAN | 0.072 | 0.052 | -0.020 | -0.14 |
| Std. Dev. | | 85 | 30 | 55 | 0.15 | | 0.037 | 0.007 | 0.044 | 0.54 |
| Avg. Abs Value | | | | 40 | 0.11 | | | | 0.031 | 0.38 |
| Std. Dev. | | | | 25 | 0.06 | | | | 0.028 | 0.20 |
| 3: UNC Ethene, Propene, n-Butane and n-Pentane Runs | | | | | | | | | | |
| AU2781R | Ethene | 497 | 445 | -52 | -0.10 | Formaldehyde | 0.164 | 0.085 | -0.080 | -0.48 |
| | Propene | 285 | 280 | -5 | -0.02 | | | | | |
| OC0382R | Ethene | 444 | 466 | 22 | 0.05 | | | | | |
| | Propene | 346 | 328 | -17 | -0.05 | | | | | |
| NV1582R | Ethene | 476 | 670 | 195 | 0.41 | | | | | |
| | Propene | 547 | 408 | -139 | -0.25 | | | | | |
| | Formaldehyde | 180 | 205 | 25 | 0.14 | | | | | |

(continued)

Table IV-35 (continued) - 3

| Experiment | Reactant Half-Life | | | | | Maximum Product Yields | | | | |
|---|---|---|---|---|---|---|---|---|---|---|
| | Species | Expt (min) | Calc (min) | Calc -Expt (min) | Calc -Expt /Expt | Species | Expt (ppm) | Calc (ppm) | Calc -Expt (ppm) | Calc -Expt /Expt |
| OC0382B | Ethene | 420 | 466 | 46 | 0.11 | | | | | |
| | Propene | 296 | 286 | -10 | -0.03 | | | | | |
| Group Average | Ethene | 459 | 512 | 53 | 0.12 | Formaldehyde | 0.164 | 0.085 | -0.080 | -0.48 |
| Std. Dev. | | 34 | 106 | 103 | 0.22 | | | | | |
| Avg. Abs Value | | | | 79 | 0.17 | | | | 0.080 | 0.48 |
| Std. Dev. | | | | 78 | 0.16 | | | | | |
| Group Average | Propene | 368 | 326 | -43 | -0.09 | | | | | |
| Std. Dev. | | 122 | 59 | 65 | 0.11 | | | | | |
| Avg. Abs Value | | | | 43 | 0.09 | | | | | |
| Std. Dev. | | | | 65 | 0.11 | | | | | |
| Group Average | Formaldehyde | 180 | 205 | 25 | 0.14 | | | | | |
| Std. Dev. | | | | | | | | | | |
| Avg. Abs Value | | | | 25 | 0.14 | | | | | |
| Std. Dev. | | | | | | | | | | |

```
--------------------------------------------------------------------------------
        Calc.-Expt./Calc.                       Calc.-Expt./Calc.
         Maximum Ozone                  Time to 1/2 Expt. Δ([O3]-[NO])max
--------------------------------------------------------------------------------
          <  -0.33    :                            <  -0.55    :
   -0.33 -   -0.27    :                     -0.55 -   -0.45    :
   -0.27 -   -0.21    :2                    -0.45 -   -0.35    :
   -0.21 -   -0.15    :                     -0.35 -   -0.25    :
   -0.15 -   -0.09    :                     -0.25 -   -0.15    :12333
   -0.09 -   -0.03    :2                    -0.15 -   -0.05    :113
   -0.03 -    0.03    :3                    -0.05 -    0.05    :1
    0.03 -    0.09    :12                    0.05 -    0.15    :122
    0.09 -    0.15    :11113                 0.15 -    0.25    :
    0.15 -    0.21    :33                    0.25 -    0.35    :
    0.21 -    0.27    :                      0.35 -    0.45    :
    0.27 -    0.33    :                      0.45 -    0.55    :
          >   0.33    :                            >   0.55    :
--------------------------------------------------------------------------------
 (Calc.-Expt.)
   /Expt.         Ethene          Propene
  Half Life
--------------------------------------------------------------------------------
     < -0.5      :               :
 -0.5 - -0.4     :               :
 -0.4 - -0.3     :               :
 -0.3 - -0.2     :               :3
 -0.2 - -0.1     :3              :2
 -0.1 -  0.0     :               :111333
  0.0 -  0.1     :3              :2
  0.1 -  0.2     :3              :12
  0.2 -  0.3     :               :1
  0.3 -  0.4     :               :
  0.4 -  0.5     :3              :
     >  0.5      :               :
--------------------------------------------------------------------------------
 (Calc.-Expt.)
   /Expt.         PAN             Formaldehyde  Acetaldehyde
 Product Yield
--------------------------------------------------------------------------------
     < -0.5      :               :             :
 -0.5 - -0.4     :               :3            :
 -0.4 - -0.3     :               :             :
 -0.3 - -0.2     :               :1            :
 -0.2 - -0.1     :               :111          :
 -0.1 -  0.0     :               :             :
  0.0 -  0.1     :               :             :
  0.1 -  0.2     :111            :             :11
  0.2 -  0.3     :12             :             :1
  0.3 -  0.4     :               :             :11
  0.4 -  0.5     :1              :             :
     >  0.5      :               :             :
--------------------------------------------------------------------------------
```

Figure IV-67. Distribution plots for discrepancies between calculated and experimental ozone maximum yields, times required to achieve half the maximum experimental change in ($[O_3]$-[NO]), and half-lives or yields for selected reactants and products observed in the alkane + alkene irradiations. Codes for symbols:
1 = EC Propene + n-Butane Runs
2 = UNC Propene + n-Butane Runs
3 = UNC Ethene + Propene + n-Butane + n-Pentane Runs

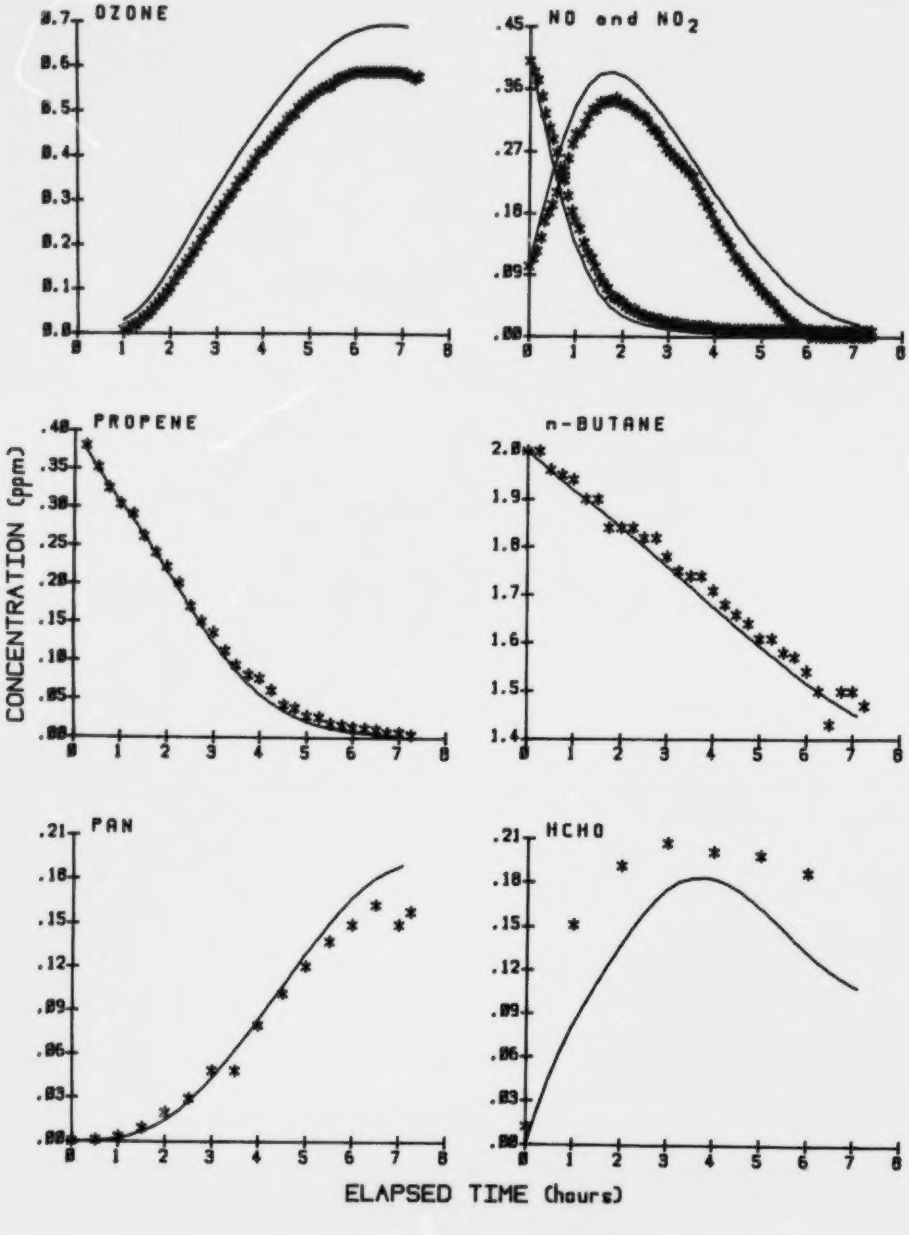

Figure IV-68. Experimental and calculated concentration-time plots for representative species observed in the propene + n-butane run EC-106.
* = Experimental data.
----- = Model calculation.

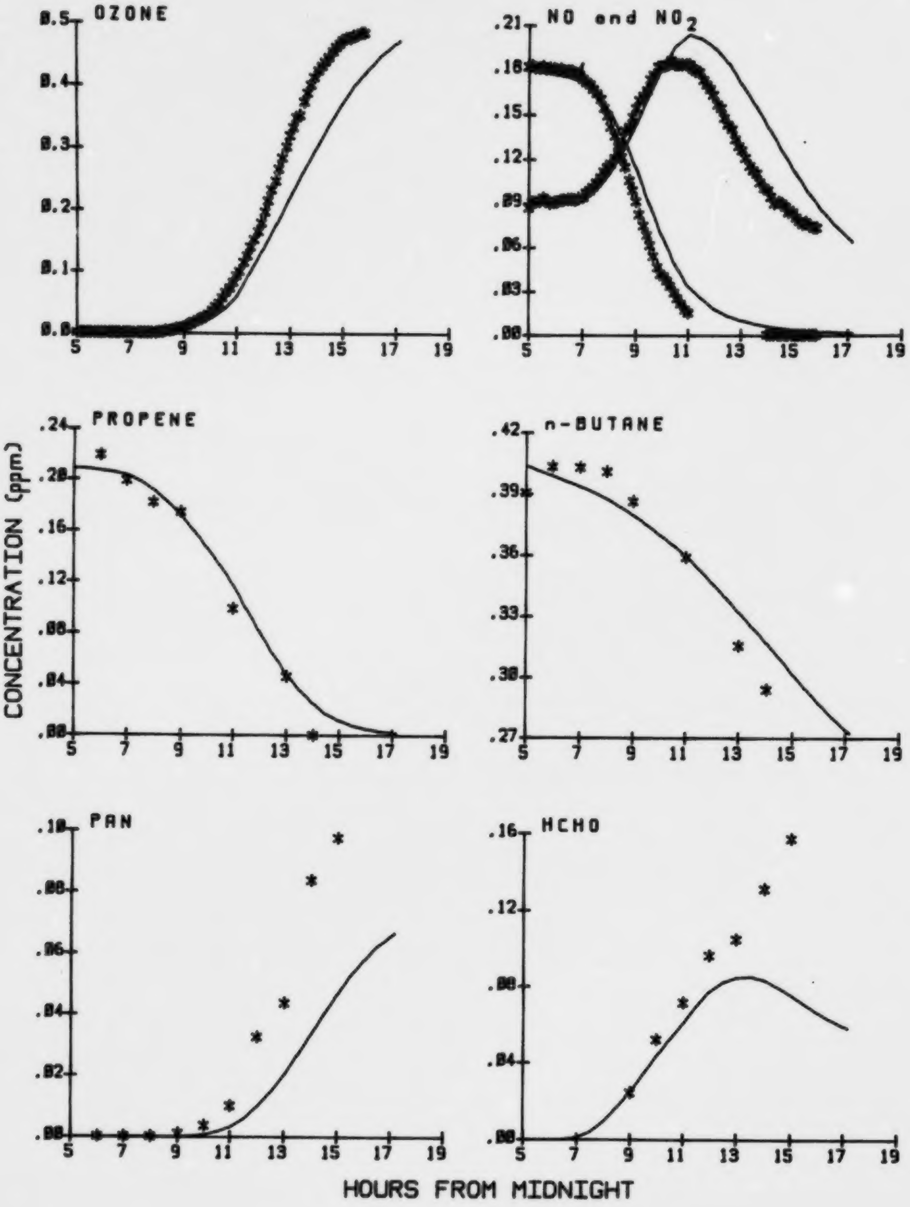

Figure IV-69. Experimental and calculated concentration-time plots for representative species observed in the UNC propene + n-butane run JL1581R.

* = Experimental data.
----- = Model calculation.

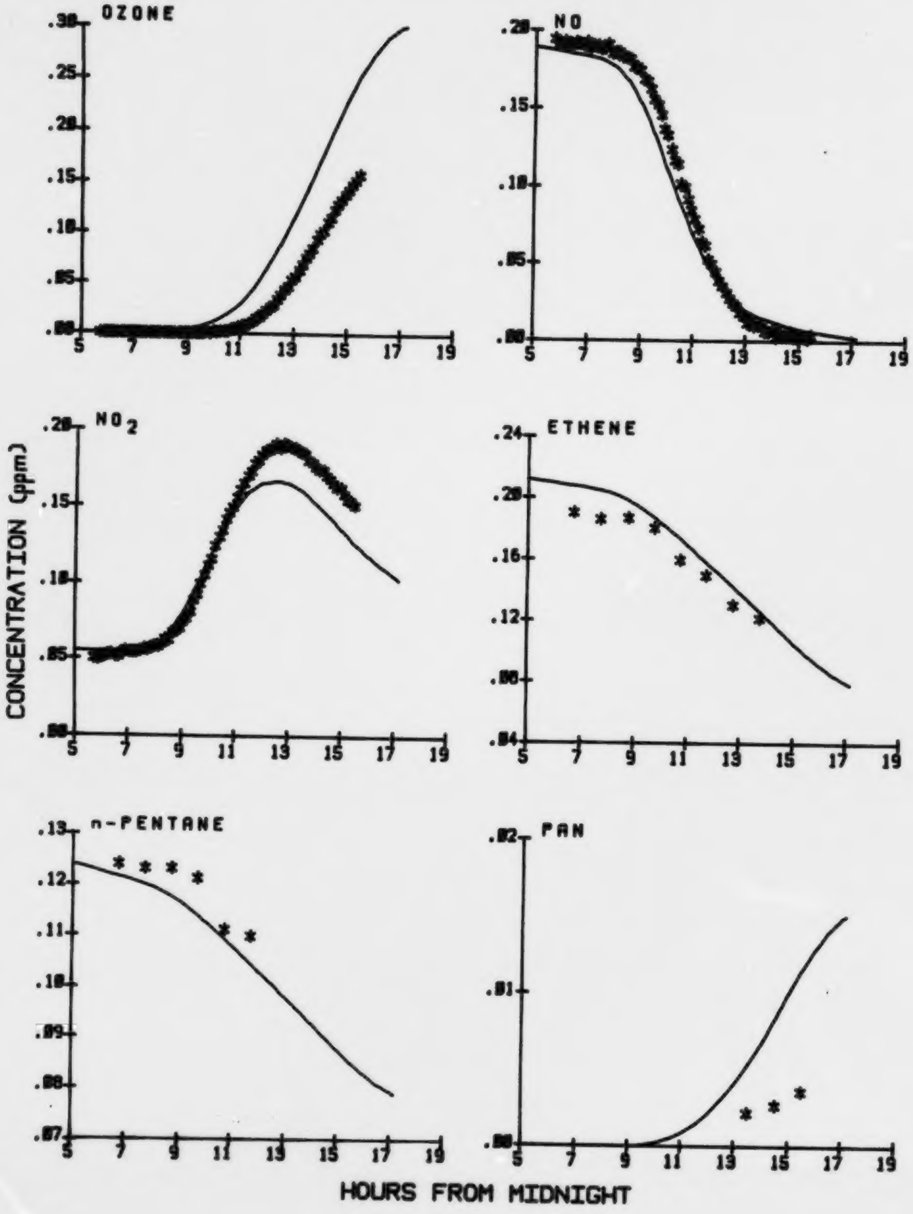

Figure IV-70. Experimental and calculated concentration-time plots for representative species observed in the UNC "SIMMIX" run OC0382B.

* = Experimental data.
----- = Model calculation.

## 5. Other Two- or Three-Component Runs

The two- or three-component runs modeled in this program which do not fall into the groups discussed above include one toluene + acetaldehyde run, three toluene + propene runs, and three toluene + n-butane runs carried out in the SAPRC EC, one toluene + propene and six toluene + propene + n-butane carried out in the UNC chamber, and two UNC m-xylene + propene + n-butane runs. The experimental and calculated ozone maximum yields and NO oxidation and ozone formation times for these runs are summarized in Table IV-36, and the organic reactant half-lives and product maximum yields are summarized in Table IV-37. Selected distribution plots of the discrepancies obtained are given in Figure IV-71, and concentration-time plots of selected data from runs representative of these groups are given in Figures IV-72 through IV-74.

In general, the quality of fits of the model simulations to the results of the toluene + acetaldehyde, propene, or n-butane runs carried out in the SAPRC EC were good, and the results shown for the toluene + n-butane run EC-328 (Figure IV-72) are typical. The main discrepancy observed was that for all runs the model overpredicted the maximum ozone yield. This overprediction of maximum ozone yields is consistent with a similar result observed in the model simulations of the single-component propene and toluene runs carried out in the EC.

The fits of the model predictions to the results of the UNC runs in this group were more variable, but the variability was less than observed in many other groups of UNC runs. Most, though not all, of these simulations tended to underpredict the ozone yields, in contrast to the simulations of the EC runs. Because of the variability of the fits it is not clear whether this can be considered to be a systematic discrepancy. Figure IV-73 shows the results for a representative propene + n-butane + toluene run, and the results for one of the two propene + n-butane + m-xylene runs are shown in Figure IV-74.

Table IV-36. Initial Concentrations and Experimental and Calculated Ozone Yields and Time Required to Achieve Half the Experimental Change in ($[O_3]-[NO]$) for the Miscellaneous 2- and 3-component Mixture Runs

| Experiment | Initial Concentrations | | | Maximum Ozone Concentration | | | | Time to 1/2 Maximum Expt. ($[O_3]-[NO]$) | | | |
|---|---|---|---|---|---|---|---|---|---|---|---|
| | $NO_x$ (ppm) | HC (ppmC) | $HC/NO_x$ | Expt (ppm) | Calc (ppm) | Calc -Expt (ppm) | Calc -Expt /Expt) | Expt (min) | Calc (min) | Calc -Expt (min) | Calc -Expt /Expt |
| **1: EC Toluene + Acetaldehyde Run** | | | | | | | | | | | |
| EC-335 | 0.444 | 7.6 | 17.2 | 0.398 | 0.469 | 0.071 | 0.18 | 79 | 73 | -6 | -0.08 |
| **2: EC Propene + Toluene Runs** | | | | | | | | | | | |
| EC-329 | 0.454 | 4.2 | 9.2 | 0.403 | 0.467 | 0.064 | 0.16 | 114 | 99 | -15 | -0.13 |
| EC-330 | 0.292 | 4.3 | 14.6 | 0.344 | 0.399 | 0.054 | 0.16 | 68 | 68 | 0 | 0.00 |
| EC-334 | 0.448 | 7.3 | 16.2 | 0.408 | 0.478 | 0.070 | 0.17 | 66 | 65 | -1 | -0.02 |
| Group Average | 0.398 | 5.2 | 13.3 | 0.385 | 0.448 | 0.063 | 0.16 | 83 | 77 | -6 | -0.05 |
| S. Dev. | 0.092 | 1.7 | 3.6 | 0.035 | 0.043 | 0.008 | 0.01 | 27 | 18 | 8 | 0.07 |
| Avg. Abs. Value | | | | | | 0.063 | 0.16 | | | 6 | 0.05 |
| S. Dev. | | | | | | 0.008 | 0.01 | | | 8 | 0.07 |
| **3: EC n-Butane + Toluene Runs** | | | | | | | | | | | |
| EC-328 | 0.449 | 12.1 | 27.0 | 0.523 | 0.639 | 0.116 | 0.22 | 123 | 108 | -15 | -0.12 |
| EC-331 | 0.466 | 22.1 | 47.4 | 0.525 | 0.609 | 0.084 | 0.16 | 49 | 45 | -4 | -0.08 |
| EC-338 | 0.446 | 14.8 | 33.2 | 0.484 | 0.619 | 0.136 | 0.28 | 79 | 74 | -4 | -0.05 |
| Group Average | 0.454 | 16.3 | 35.9 | 0.511 | 0.622 | 0.112 | 0.22 | 83 | 76 | -8 | -0.09 |
| S. Dev. | 0.011 | 5.2 | 10.5 | 0.023 | 0.015 | 0.026 | 0.06 | 37 | 32 | 6 | 0.03 |
| Avg. Abs. Value | | | | | | 0.112 | 0.22 | | | 8 | 0.09 |
| S. Dev. | | | | | | 0.026 | 0.06 | | | 6 | 0.03 |

(continued)

Table IV-36 (continued) - 2

| Experiment | Initial Concentrations | | | Maximum Ozone Concentration | | | | Time to 1/2 Maximum Expt. ($[O_3]-[NO]$) | | | |
|---|---|---|---|---|---|---|---|---|---|---|---|
| | $NO_x$ (ppm) | HC (ppmC) | $HC/NO_x$ | Expt (ppm) | Calc (ppm) | Calc -Expt (ppm) | Calc -Expt /Expt) | Expt (min) | Calc (min) | Calc -Expt (min) | Calc -Expt /Expt |
| **4: UNC Propene + Toluene Run** | | | | | | | | | | | |
| JN1379B | 0.443 | 5.8 | 13.1 | 0.756 | 0.749 | -0.007 | -0.01 | 299 | 257 | -42 | -0.14 |
| **5: UNC Propene + n-Butane + Toluene Runs** | | | | | | | | | | | |
| JL1581B | 0.283 | 2.2 | 7.8 | 0.474 | 0.397 | -0.076 | -0.16 | 331 | 381 | 50 | 0.15 |
| ST2479B | 0.233 | 1.8 | 7.8 | 0.246 | 0.342 | 0.096 | 0.39 | 437 | 346 | -91 | -0.21 |
| JN0982B | 0.284 | 3.1 | 10.9 | 0.666 | 0.480 | -0.186 | -0.28 | 389 | 441 | 52 | 0.13 |
| JN2783B | 0.256 | 2.8 | 11.1 | 0.511 | 0.535 | 0.025 | 0.05 | 450 | 426 | -24 | -0.05 |
| JN1483R | 0.222 | 2.6 | 11.7 | 0.585 | 0.518 | -0.067 | -0.12 | 425 | 405 | -20 | -0.05 |
| AU2683R | 0.317 | 2.5 | 7.9 | 0.646 | 0.487 | -0.159 | -0.25 | 453 | 478 | 25 | 0.06 |
| Group Average | 0.266 | 2.5 | 9.5 | 0.521 | 0.460 | -0.061 | -0.06 | 414 | 413 | 0 | 0.01 |
| S. Dev. | 0.036 | 0.4 | 1.9 | 0.154 | 0.075 | 0.107 | 0.25 | 47 | 46 | 55 | 0.14 |
| Avg. Abs. Value | | | | | | 0.102 | 0.21 | | | 44 | 0.11 |
| S. Dev. | | | | | | 0.060 | 0.12 | | | 27 | 0.07 |
| **6: UNC Propene + n-Butane + m-Xylene Runs** | | | | | | | | | | | |
| JL1881B | 0.267 | 2.3 | 8.5 | 0.693 | 0.509 | -0.183 | -0.26 | 277 | 279 | 2 | 0.01 |
| JN0982R | 0.290 | 3.1 | 10.7 | 0.714 | 0.519 | -0.195 | -0.27 | 330 | 373 | 43 | 0.13 |
| Group Average | 0.278 | 2.7 | 9.6 | 0.704 | 0.514 | -0.189 | -0.27 | 303 | 326 | 23 | 0.07 |
| S. Dev. | 0.016 | 0.6 | 1.6 | 0.015 | 0.007 | 0.008 | 0.01 | 37 | 66 | 29 | 0.09 |
| Avg. Abs. Value | | | | | | 0.189 | 0.27 | | | 23 | 0.07 |
| S. Dev. | | | | | | 0.008 | 0.01 | | | 29 | 0.09 |

Table IV-37. Experimental and Calculated Product Yields and Alkene and Aromatic Half-Lives for the Miscellaneous 2- and 3-Component Mixture Runs

| Experiment | Reactant Half-Life | | | | | Maximum Product Yields | | | | |
|---|---|---|---|---|---|---|---|---|---|---|
| | Species | Expt (min) | Calc (min) | Calc -Expt (min) | Calc -Expt /Expt | Species | Expt (ppm) | Calc (ppm) | Calc -Expt (ppm) | Calc -Expt /Expt |
| **1: EC Toluene + Acetaldehyde Run** | | | | | | | | | | |
| EC-335 | Toluene | 331 | 282 | -49 | -0.15 | PAN | 0.115 | 0.151 | 0.036 | 0.32 |
| | Acetaldehyde | 139 | 197 | 58 | 0.42 | Formaldehyde | 0.117 | 0.082 | -0.035 | -0.30 |
| **2: EC Propene + Toluene Runs** | | | | | | | | | | |
| EC-329 | Toluene | 294 | 360 | 65 | 0.22 | PAN | 0.067 | 0.093 | 0.026 | 0.38 |
| | Propene | 73 | 90 | 17 | 0.23 | Acetaldehyde | 0.042 | 0.044 | 0.002 | 0.05 |
| | | | | | | Formaldehyde | 0.088 | 0.071 | -0.016 | -0.19 |
| EC-330 | Toluene | 312 | 375 | 63 | 0.20 | PAN | 0.058 | 0.076 | 0.018 | 0.30 |
| | Propene | 59 | 78 | 19 | 0.32 | Acetaldehyde | 0.041 | 0.043 | 0.002 | 0.06 |
| | | | | | | Formaldehyde | 0.098 | 0.063 | -0.035 | -0.36 |
| EC-334 | Toluene | 355 | 365 | 9 | 0.03 | PAN | 0.071 | 0.104 | 0.032 | 0.46 |
| | Propene | 63 | 84 | 20 | 0.32 | Acetaldehyde | 0.046 | 0.043 | -0.002 | -0.05 |
| | | | | | | Formaldehyde | 0.113 | 0.080 | -0.033 | -0.29 |
| Group Average | Toluene | 321 | 366 | 46 | 0.15 | PAN | 0.065 | 0.091 | 0.025 | 0.38 |
| Std. Dev. | | 31 | 8 | 32 | 0.11 | | 0.007 | 0.014 | 0.007 | 0.08 |
| Avg. Abs Value | | | | 46 | 0.15 | | | | 0.025 | 0.38 |
| Std. Dev. | | | | 32 | 0.11 | | | | 0.007 | 0.08 |
| Group Average | Propene | 65 | 84 | 19 | 0.29 | Acetaldehyde | 0.043 | 0.043 | 0.001 | 0.02 |
| Std. Dev. | | 7 | 6 | 2 | 0.05 | | 0.003 | 0.001 | 0.003 | 0.06 |
| Avg. Abs Value | | | | 19 | 0.29 | | | | 0.002 | 0.05 |
| Std. Dev. | | | | 2 | 0.05 | | | | 0.000 | 0.00 |

(continued)

Table IV-37 (continued) - 2

| Experiment | Reactant Half-Life | | | | | Maximum Product Yields | | | | |
|---|---|---|---|---|---|---|---|---|---|---|
| | Species | Expt (min) | [illegible]lc ([illegible]in) | Calc -Expt (min) | Calc -Expt /Expt | Species | Expt (ppm) | Calc (ppm) | Calc -Expt (ppm) | Calc -Expt /Expt |
| Group Average | | | | | | Formaldehyde | 0.100 | 0.071 | -0.028 | -0.28 |
| Std. Dev. | | | | | | | 0.013 | 0.008 | 0.010 | 0.09 |
| Avg. Abs Value | | | | | | | | | 0.028 | 0.28 |
| Std. Dev. | | | | | | | | | 0.010 | 0.09 |
| **3: EC n-Butane + Toluene Runs** | | | | | | | | | | |
| EC-328 | Toluene | 307 | 375 | 68 | 0.22 | PAN | 0.074 | 0.109 | 0.035 | 0.47 |
| EC-331 | Toluene | 276 | 366 | 90 | 0.32 | PAN | 0.076 | 0.124 | 0.048 | 0.63 |
| EC-338 | Toluene | 291 | 368 | 77 | 0.26 | PAN | 0.076 | 0.117 | 0.041 | 0.54 |
| Group Average | Toluene | 292 | 370 | 78 | 0.27 | PAN | 0.075 | 0.116 | 0.041 | 0.55 |
| Std. Dev. | | 16 | 5 | 11 | 0.05 | | 0.001 | 0.008 | 0.007 | 0.08 |
| Avg. Abs Value | | | | 78 | 0.27 | | | | 0.041 | 0.55 |
| Std. Dev. | | | | 11 | 0.05 | | | | 0.007 | 0.08 |
| **4: UNC Propene + Toluene Run** | | | | | | | | | | |
| JN1379B | Toluene | 428 | 585 | 157 | 0.37 | PAN | 0.181 | 0.217 | 0.036 | 0.20 |
| | Propene | 306 | 264 | -43 | -0.14 | Acetaldehyde | 0.415 | 0.401 | -0.014 | -0.03 |

(continued)

Table IV-37 (continued) - 3

| Experiment | Reactant Half-Life | | | | | Maximum Product Yields | | | | |
|---|---|---|---|---|---|---|---|---|---|---|
| | Species | Expt (min) | Calc (min) | Calc -Expt (min) | Calc -Expt /Expt | Species | Expt (ppm) | Calc (ppm) | Calc -Expt (ppm) | Calc -Expt /Expt |
| **5: UNC Propene + n-Butane + Toluene Runs** | | | | | | | | | | |
| JL1581B | Toluene | 411 | 570 | 159 | 0.39 | PAN | 0.079 | 0.045 | -0.034 | -0.43 |
| | Propene | 294 | 351 | 57 | 0.19 | | | | | |
| ST2479B | Toluene | 403 | 630 | 227 | 0.56 | | | | | |
| | Propene | 387 | 336 | -52 | -0.13 | | | | | |
| JN0982B | Toluene | 360 | 390 | 30 | 0.08 | | | | | |
| | Propene | 217 | 196 | -21 | -0.10 | | | | | |
| JN2783B | Toluene | 635 | 635 | 1 | 0.00 | PAN | 0.065 | 0.072 | 0.006 | 0.10 |
| | Propene | 387 | 362 | -25 | -0.07 | | | | | |
| JN1483R | Toluene | 540 | 566 | 26 | 0.05 | PAN | 0.063 | 0.075 | 0.013 | 0.20 |
| | Propene | 351 | 313 | -38 | -0.11 | | | | | |
| AU2683R | Toluene | 540 | 572 | 32 | 0.06 | | | | | |
| | Propene | 241 | 301 | 60 | 0.25 | | | | | |
| Group Average | Toluene | 481 | 560 | 79 | 0.19 | PAN | 0.069 | 0.064 | -0.005 | -0.04 |
| Std. Dev. | | 106 | 89 | 92 | 0.23 | | 0.009 | 0.017 | 0.025 | 0.34 |
| Avg. Abs Value | | | | 79 | 0.19 | | | | 0.018 | 0.24 |
| Std. Dev. | | | | 92 | 0.23 | | | | 0.014 | 0.17 |
| Group Average | Propene | 313 | 310 | -3 | 0.01 | | | | | |
| Std. Dev. | | 74 | 60 | 49 | 0.17 | | | | | |
| Avg. Abs Value | | | | 42 | 0.14 | | | | | |
| Std. Dev. | | | | 16 | 0.07 | | | | | |

(continued)

Table IV-37 (continued) - 4

| Experiment | Reactant Half-Life |  |  |  |  | Maximum Product Yields |  |  |  |  |
|---|---|---|---|---|---|---|---|---|---|---|
|  | Species | Expt (min) | Calc (min) | Calc -Expt (min) | Calc -Expt /Expt | Species | Expt (ppm) | Calc (ppm) | Calc -Expt (ppm) | Calc -Expt /Expt |
| 6: UNC Propene + n-Butane + m-Xylene Runs |  |  |  |  |  |  |  |  |  |  |
| JL1881B | Propene | 289 | 302 | 13 | 0.05 | PAN | 0.061 | 0.111 | 0.050 | 0.83 |
|  | m-Xylene | 318 | 330 | 12 | 0.04 |  |  |  |  |  |
| JN0982R | Propene | 197 | 189 | -8 | -0.04 |  |  |  |  |  |
|  | m-Xylene | 208 | 227 | 19 | 0.09 |  |  |  |  |  |
| Group Average | Propene | 243 | 245 | 2 | 0.00 | PAN | 0.061 | 0.111 | 0.050 | 0.83 |
| Std. Dev. |  | 65 | 80 | 15 | 0.06 |  |  |  |  |  |
| Avg. Abs Value |  |  |  | 11 | 0.04 |  |  |  | 0.050 | 0.83 |
| Std. Dev. |  |  |  | 3 | 0.00 |  |  |  |  |  |
| Group Average | m-Xylene | 263 | 278 | 15 | 0.06 |  |  |  |  |  |
| Std. Dev. |  | 78 | 73 | 5 | 0.04 |  |  |  |  |  |
| Avg. Abs Value |  |  |  | 15 | 0.06 |  |  |  |  |  |
| Std. Dev. |  |  |  | 5 | 0.04 |  |  |  |  |  |

```
-------------------------------------------------------------------------------
        Calc.-Expt./Calc.                         Calc.-Expt./Calc.
         Maximum Ozone                  Time to 1/2 Expt. Δ([O3]-[NO])max
-------------------------------------------------------------------------------
          <  -0.33    :                            <  -0.55    :
     -0.33 - -0.27    :                      -0.55 - -0.45    :
     -0.27 - -0.21    :                      -0.45 - -0.35    :
     -0.21 - -0.15    :5566                  -0.35 - -0.25    :
     -0.15 - -0.09    :                      -0.25 - -0.15    :5
     -0.09 - -0.03    :55                    -0.15 - -0.05    :1233345
     -0.03 -  0.03    :45                    -0.05 -  0.05    :2256
      0.03 -  0.09    :12223                  0.05 -  0.15    :556
      0.09 -  0.15    :335                    0.15 -  0.25    :5
      0.15 -  0.21    :                       0.25 -  0.35    :
      0.21 -  0.27    :                       0.35 -  0.45    :
      0.27 -  0.33    :                       0.45 -  0.55    :
          >   0.33    :                            >  0.55    :
-------------------------------------------------------------------------------
 (Calc.-Expt.)
   /Expt.         Propene      Toluene      m-Xylene
  Half-Life
-------------------------------------------------------------------------------
       < -0.5     :            :            :
  -0.5 - -0.4     :            :            :
  -0.4 - -0.3     :            :            :
  -0.3 - -0.2     :            :            :
  -0.2 - -0.1     :455         :1           :
  -0.1 -  0.0     :556         :            :
   0.0 -  0.1     :6           :25555       :66
   0.1 -  0.2     :5           :            :
   0.2 -  0.3     :25          :2233        :
   0.3 -  0.4     :22          :345         :
   0.4 -  0.5     :            :            :
       >  0.5     :            :5           :
-------------------------------------------------------------------------------
 (Calc.-Expt.)
   /Expt.         PAN          Formaldehyde  Acetaldehyde
 Product Yield
-------------------------------------------------------------------------------
       < -0.5     :            :            :
  -0.5 - -0.4     :5           :            :
  -0.4 - -0.3     :            :12          :
  -0.3 - -0.2     :            :2           :
  -0.2 - -0.1     :            :2           :
  -0.1 -  0.0     :            :            :24
   0.0 -  0.1     :5           :            :22
   0.1 -  0.2     :4           :            :
   0.2 -  0.3     :5           :            :
   0.3 -  0.4     :122         :            :
   0.4 -  0.5     :23          :            :
       >  0.5     :336         :            :
-------------------------------------------------------------------------------
```

Figure IV-71. Distribution plots for discrepancies between calculated and experimental ozone maximum yields, times required to achieve half the maximum experimental change in ($[O_3]$-[NO]), and half-lives or yields for selected reactants and products observed in the mixed miscellaneous 2- or 3- component mixture runs. Codes for symbols:

1 = EC Toluene + Acetaldehyde Run
2 = EC Propene + Toluene Runs
3 = EC n-Butane + Toluene Runs
4 = UNC Propene + Toluene Run
5 = UNC Propene + n-Butane + Toluene Runs
6 = UNC Propene + n-Butane + m-Xylene Runs

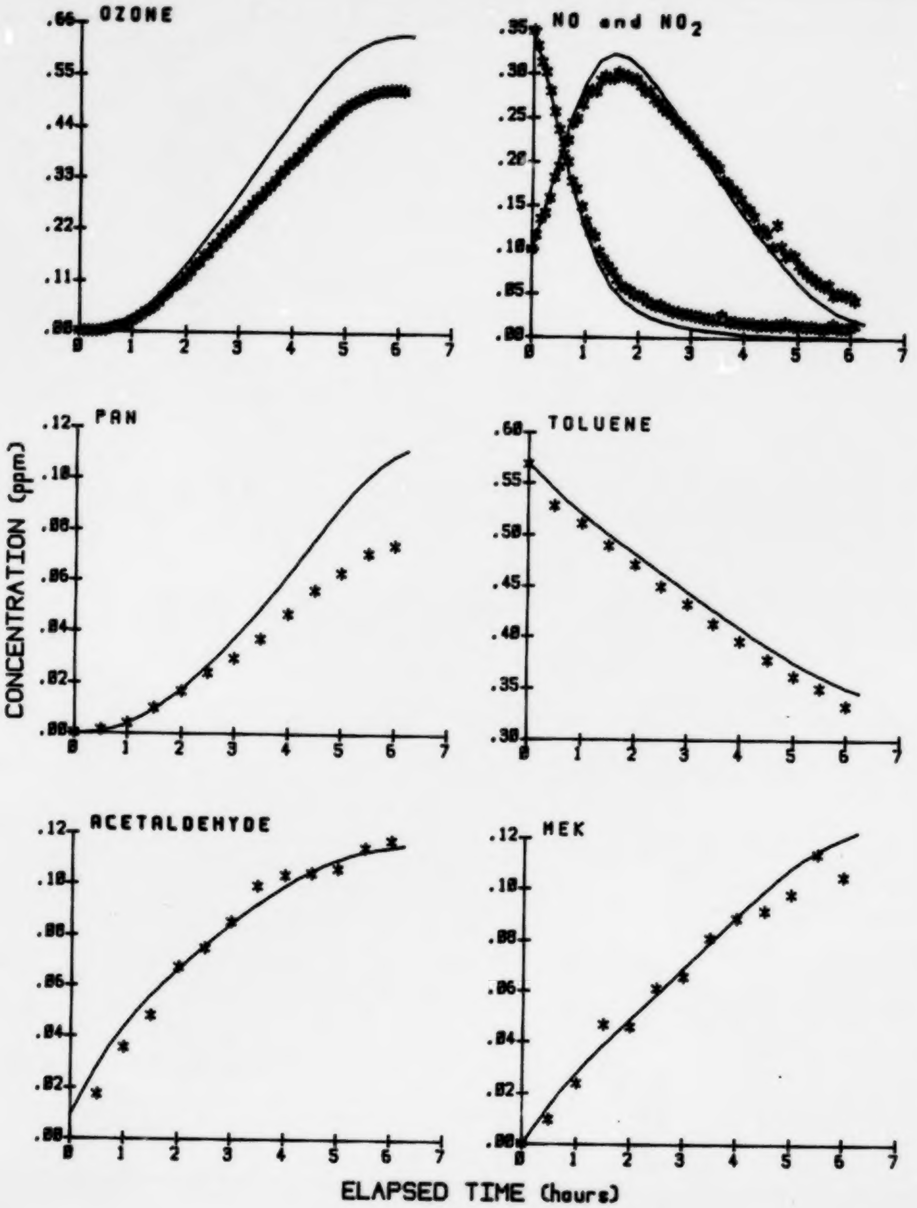

Figure IV-72. Experimental and calculated concentration-time plots for representative species observed in the toluene + n-butane run EC-328.

* = Experimental data.

----- = Model calculation.

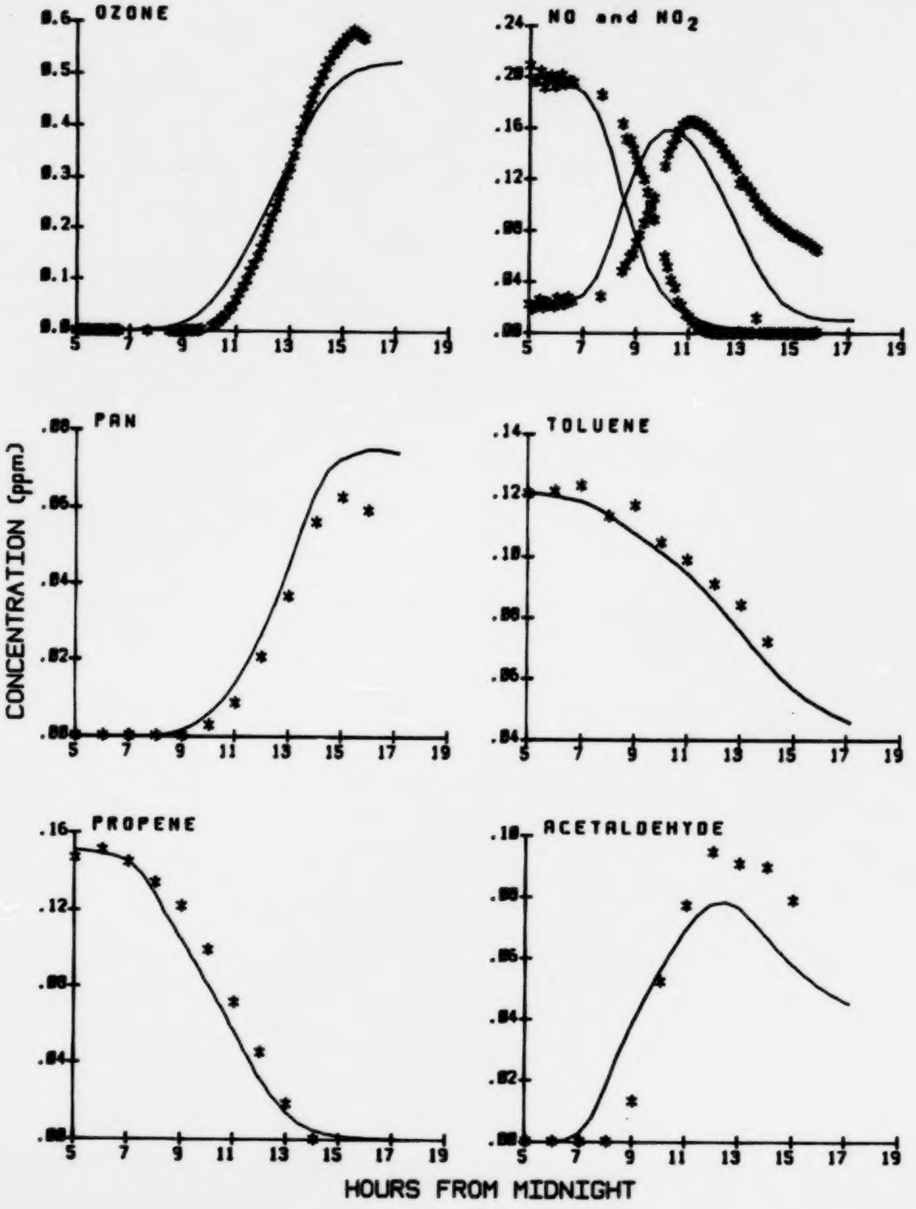

Figure IV-73. Experimental and calculated concentration-time plots for representative species observed in the UNC propene + n-butane + toluene run JN1483R.
* = Experimental data.
----- = Model calculation.

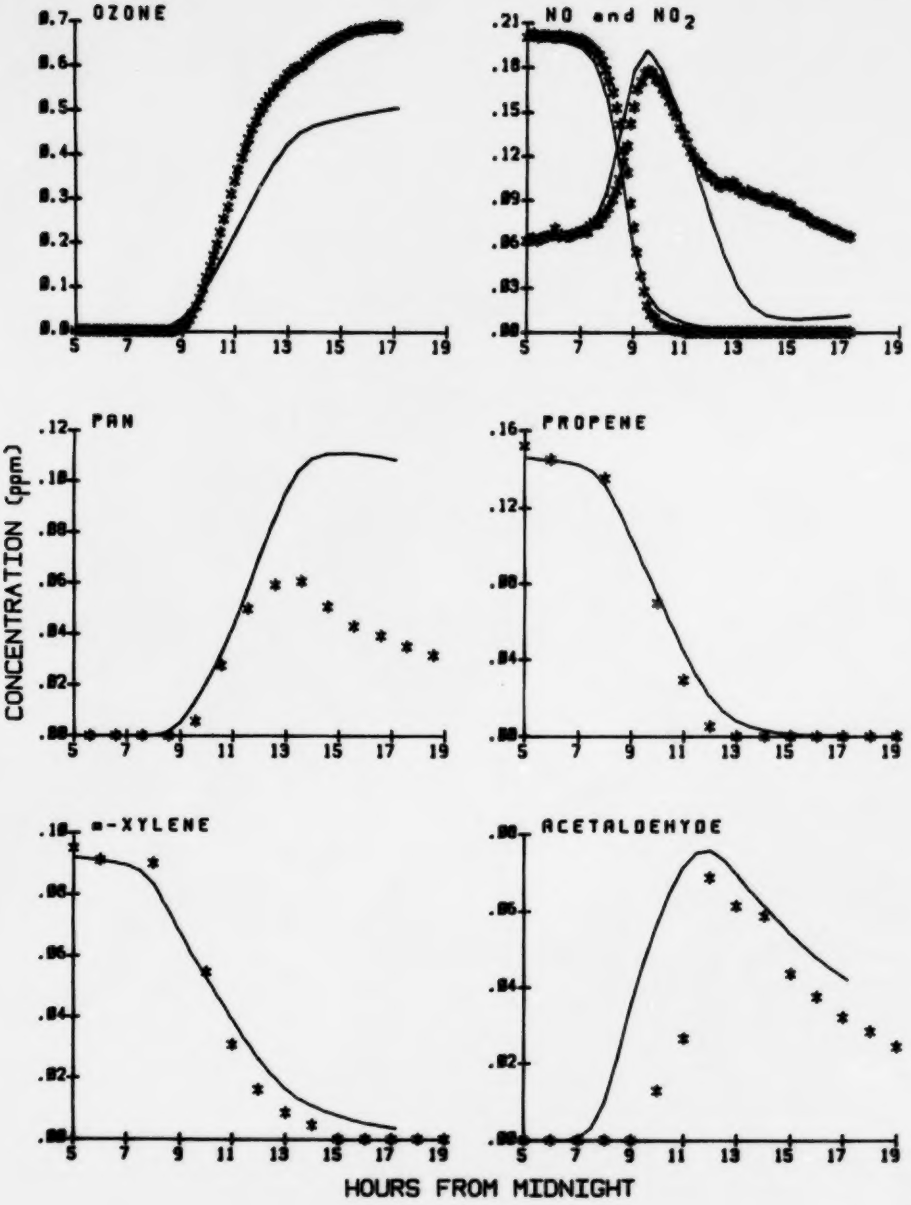

Figure IV-74. Experimental and calculated concentration-time plots for representative species observed in the UNC propene + n-butane + m-xylene run JN0982R.
* = Experimental data.
----- = Model calculation.

## 6. EC Seven-Hydrocarbon Mix Runs

Eleven runs carried out in the SAPRC EC employing a mixture of seven alkanes, alkenes and aromatic hydrocarbons were modeled in this program. The mixture consisted of ethene, propene, trans-2-butene, n-butane, 2,3-dimethylbutane, toluene, and m-xylene, all of whose reactions are represented explicitly in this model. The experimental and calculated ozone maximum yields and NO oxidation and ozone formation times for these runs are summarized in Table IV-38, and the organic reactant half-lives and product maximum yields are summarized in Table IV-39. Selected distribution plots of the discrepancies obtained are given in Figure IV-75, and Figures IV-76 and IV-77 give plots of the discrepancies in the ozone maxima and the NO oxidation/ozone formation timing parameter, respectively, against the initial hydrocarbon/$NO_x$ ratios for these runs.

As with the simulations of most of the other EC runs employing mixtures of organics, the fits of the model predictions to the results were reasonably good and showed relatively little variability. However, in general, the model tended to overpredict the maximum ozone yields and the rates of ozone formation, though the discrepancies were not large and (Figures IV-76 and IV-77) had no apparent systematic dependence on the initial hydrocarbon/$NO_x$ ratio. Concentration-time plots for the runs carried out at the lowest $NO_x$ concentration (the highest hydrocarbon/$NO_x$ ratio) are shown in Figure IV-78, and plots for the run carried out with the highest initial $NO_x$ are shown in Figure IV-79. The results for most runs carried out at intermediate $NO_x$ levels or hydrocarbon/$NO_x$ ratios are similar.

## 7. ITC "Mini-Surrogate," Incremental Reactivity Runs

A series of irradiations of a standard "mini-surrogate"-$NO_x$ mixture alternating with irradiations of the same mixture, except with selected organics added or removed, were carried out in the SAPRC ITC for the purpose of evaluating incremental reactivity effects (Atkinson et al. 1983c). The standard experiment consisted of irradiations of a 4 ppmC mixture of propene, trans-2-butene, n-butane, and m-xylene (the "mini-surrogate) with an initial $NO_x$ of 0.1 ppm. The standard experiments and runs with added or modified initial propene, n-butane, trans-2-butene, or

Table IV-38. Initial Concentrations and Experimental and Calculated Ozone Yields and Times Required to Achieve Half the Experimental Change in ($[O_3]-[NO]$) for the EC Seven-Hydrocarbon Mixture Runs

| Experiment | Initial Concentrations | | | Maximum Ozone Concentration | | | | Time to 1/2 Maximum Expt. ($[O_3]-[NO]$) | | | |
|---|---|---|---|---|---|---|---|---|---|---|---|
| | $NO_x$ (ppm) | HC (ppmC) | $HC/NO_x$ | Expt (ppm) | Calc (ppm) | Calc -Expt (ppm) | Calc -Expt /Expt) | Expt (min) | Calc (min) | Calc -Expt (min) | Calc -Expt /Expt |
| EC-231 | 0.492 | 13.2 | 26.8 | 0.623 | 0.766 | 0.143 | 0.23 | 75 | 57 | -18 | -0.24 |
| EC-232 | 0.493 | 9.3 | 18.9 | 0.340 | 0.530 | 0.191 | 0.56 | 128 | 110 | -18 | -0.14 |
| EC-233 | 0.103 | 9.5 | 92.3 | 0.327 | 0.438 | 0.111 | 0.34 | 52 | 39 | -13 | -0.25 |
| EC-237 | 0.483 | 10.5 | 21.7 | 0.652 | 0.702 | 0.049 | 0.08 | 70 | 73 | 3 | 0.04 |
| EC-238 | 0.952 | 10.1 | 10.6 | 0.691 | 0.796 | 0.104 | 0.15 | 138 | 113 | -24 | -0.18 |
| EC-241 | 0.489 | 5.0 | 10.1 | 0.408 | 0.504 | 0.096 | 0.24 | 135 | 109 | -26 | -0.19 |
| EC-242 | 0.502 | 12.8 | 25.6 | 0.682 | 0.672 | -0.009 | -0.01 | 30 | 28 | -2 | -0.06 |
| EC-243 | 0.501 | 9.7 | 19.4 | 0.716 | 0.725 | 0.009 | 0.01 | 38 | 39 | 1 | 0.03 |
| EC-245 | 1.002 | 12.9 | 12.8 | 0.894 | 0.868 | -0.026 | -0.03 | 61 | 54 | -7 | -0.12 |
| EC-246 | 0.508 | 8.6 | 16.9 | 0.574 | 0.626 | 0.052 | 0.09 | 179 | 176 | -3 | -0.02 |
| EC-247 | 0.505 | 6.2 | 12.2 | 0.657 | 0.641 | -0.016 | -0.02 | 68 | 71 | 3 | 0.04 |
| Group Average | 0.548 | 9.8 | 24.3 | 0.597 | 0.661 | 0.064 | 0.15 | 89 | 79 | -8 | -0.10 |
| S. Dev. | 0.243 | 2.6 | 23.3 | 0.173 | 0.131 | 0.071 | 0.18 | 48 | 44 | 11 | 0.11 |
| Avg. Abs. Value | | | | | | 0.073 | 0.16 | | | 10 | 0.12 |
| S. Dev. | | | | | | 0.060 | 0.17 | | | 9 | 0.09 |

Table IV-39. Experimental and Calculated Half-Lives or Yields for Selected Reactants and Products in the EC Seven-Hydrocarbon Mixture Runs

| Experiment | Reactant Half-Life | | | | | Maximum Product Yields | | | | |
|---|---|---|---|---|---|---|---|---|---|---|
| | Species | Expt (min) | Calc (min) | Calc -Expt (min) | Calc -Expt /Expt | Species | Expt (ppm) | Calc (ppm) | Calc -Expt (ppm) | Calc -Expt /Expt |
| EC-231 | Ethene | 220 | 239 | 19 | 0.09 | PAN | 0.095 | 0.136 | 0.040 | 0.43 |
| | Propene | 99 | 97 | -2 | -0.02 | Formaldehyde | 0.453 | 0.402 | -0.052 | -0.11 |
| | *trans*-2-Butene | 52 | 45 | -7 | -0.13 | | | | | |
| | Toluene | 326 | 262 | -64 | -0.20 | | | | | |
| | m-Xylene | 136 | 152 | 16 | 0.12 | | | | | |
| EC-232 | Ethene | 334 | 368 | 34 | 0.10 | PAN | 0.040 | 0.048 | 0.009 | 0.22 |
| | Propene | 163 | 172 | 10 | 0.06 | Formaldehyde | 0.157 | 0.125 | -0.033 | -0.21 |
| | *trans*-2-Butene | 74 | 75 | 1 | 0.02 | | | | | |
| | Toluene | 264 | 375 | 111 | 0.42 | | | | | |
| | m-Xylene | 204 | 221 | 17 | 0.08 | | | | | |
| EC-233 | Ethene | 356 | 310 | -46 | -0.13 | PAN | 0.037 | 0.047 | 0.010 | 0.28 |
| | Propene | 97 | 90 | -7 | -0.07 | Formaldehyde | 0.145 | 0.102 | -0.043 | -0.30 |
| | Toluene | 360 | 375 | 15 | 0.04 | | | | | |
| | m-Xylene | 198 | 183 | -16 | -0.08 | | | | | |
| EC-237 | Ethene | 259 | 254 | -5 | -0.02 | PAN | 0.100 | 0.127 | 0.027 | 0.27 |
| | Propene | 85 | 104 | 19 | 0.23 | Formaldehyde | 0.387 | 0.356 | -0.030 | -0.08 |
| | *trans*-2-Butene | 38 | 43 | 5 | 0.12 | | | | | |
| | Toluene | 292 | 370 | 78 | 0.27 | | | | | |
| | m-Xylene | 136 | 159 | 23 | 0.17 | | | | | |
| EC-238 | Ethene | 327 | 310 | -17 | -0.05 | PAN | 0.113 | 0.150 | 0.037 | 0.33 |
| | Propene | 142 | 140 | -2 | -0.01 | Formaldehyde | 0.404 | 0.431 | 0.027 | 0.07 |
| | *trans*-2-Butene | 52 | 51 | -1 | -0.01 | | | | | |
| | Toluene | 441 | 495 | 54 | 0.12 | | | | | |
| | m-Xylene | 187 | 186 | -1 | 0.00 | | | | | |

(continued)

Table IV-39 (continued) - 2

| Experiment | Reactant Half-Life | | | | | Maximum Product Yields | | | | |
|---|---|---|---|---|---|---|---|---|---|---|
| | Species | Expt (min) | Calc (min) | Calc -Expt (min) | Calc -Expt /Expt | Species | Expt (ppm) | Calc (ppm) | Calc -Expt (ppm) | Calc -Expt /Expt |
| EC-241 | Ethene | 341 | 318 | -23 | -0.07 | PAN | 0.047 | 0.059 | 0.012 | 0.26 |
| | Propene | 142 | 136 | -6 | -0.04 | Formaldehyde | 0.137 | 0.219 | 0.082 | 0.59 |
| | *trans*-2-Butene | 55 | 51 | -4 | -0.08 | | | | | |
| | Toluene | 360 | 365 | 5 | 0.01 | | | | | |
| | m-Xylene | 180 | 171 | -9 | -0.05 | | | | | |
| EC-242 | Ethene | 246 | 259 | 13 | 0.05 | PAN | 0.140 | 0.182 | 0.042 | 0.30 |
| | Propene | 57 | 62 | 6 | 0.10 | Formaldehyde | 0.673 | 0.644 | -0.028 | -0.04 |
| | *trans*-2-Butene | 23 | 24 | 1 | 0.05 | | | | | |
| | Toluene | 369 | 365 | -4 | -0.01 | | | | | |
| | m-Xylene | 118 | 203 | 85 | 0.72 | | | | | |
| EC-243 | Ethene | 150 | 165 | 15 | 0.10 | PAN | 0.100 | 0.131 | 0.031 | 0.31 |
| | Propene | 61 | 70 | 10 | 0.16 | | | | | |
| | *trans*-2-Butene | 28 | 30 | 1 | 0.04 | | | | | |
| | Toluene | 150 | 165 | 15 | 0.10 | | | | | |
| | m-Xylene | 108 | 129 | 22 | 0.20 | | | | | |
| EC-245 | Ethene | 205 | 217 | 12 | 0.06 | PAN | 0.194 | 0.274 | 0.080 | 0.41 |
| | Propene | 84 | 87 | 3 | 0.04 | Formaldehyde | 0.778 | 0.766 | -0.012 | -0.02 |
| | *trans*-2-Butene | 39 | 36 | -4 | -0.09 | | | | | |
| | Toluene | 366 | 375 | 9 | 0.03 | | | | | |
| | m-Xylene | 108 | 136 | 27 | 0.25 | | | | | |
| EC-246 | Ethene | 382 | 386 | 4 | 0.01 | PAN | 0.070 | 0.079 | 0.009 | 0.13 |
| | Propene | 167 | 170 | 3 | 0.02 | Formaldehyde | 0.121 | 0.124 | 0.003 | 0.03 |
| | *trans*-2-Butene | 57 | 59 | 2 | 0.04 | | | | | |
| | Toluene | 533 | 575 | 42 | 0.08 | | | | | |
| | m-Xylene | 218 | 227 | 9 | 0.04 | | | | | |

(continued)

Table IV-39 (continued) - 3

| Experiment | Reactant Half-Life | | | | | Maximum Product Yields | | | | |
|---|---|---|---|---|---|---|---|---|---|---|
| | Species | Expt (min) | Calc (min) | Calc -Expt (min) | Calc -Expt /Expt | Species | Expt (ppm) | Calc (ppm) | Calc -Expt (ppm) | Calc -Expt /Expt |
| EC-247 | Ethene | 215 | 238 | 23 | 0.11 | PAN | 0.106 | 0.143 | 0.037 | 0.34 |
| | Propene | 82 | 95 | 14 | 0.17 | Formaldehyde | 0.377 | 0.398 | 0.021 | 0.06 |
| | trans-2-Butene | 39 | 38 | -1 | -0.02 | | | | | |
| | Toluene | 307 | 305 | -2 | -0.01 | | | | | |
| | m-Xylene | 112 | 133 | 22 | 0.20 | | | | | |
| Group Average | Ethene | 276 | 278 | 3 | 0.02 | PAN | 0.095 | 0.125 | 0.030 | 0.30 |
| Std. Dev. | | 75 | 66 | 23 | 0.08 | | 0.047 | 0.067 | 0.021 | 0.08 |
| Avg. Abs Value | | | | 19 | 0.07 | | | | 0.030 | 0.30 |
| Std. Dev. | | | | 12 | 0.04 | | | | 0.021 | 0.08 |
| Group Average | Propene | 107 | 111 | 4 | 0.06 | Formaldehyde | 0.363 | 0.357 | -0.007 | 0.00 |
| Std. Dev. | | 39 | 38 | 8 | 0.10 | | 0.231 | 0.224 | 0.041 | 0.24 |
| Avg. Abs Value | | | | 7 | 0.08 | | | | 0.033 | 0.15 |
| Std. Dev. | | | | 5 | 0.07 | | | | 0.022 | 0.18 |
| Group Average | trans-2-Butene | 46 | 45 | -1 | -0.01 | | | | | |
| Std. Dev. | | 15 | 15 | 3 | 0.08 | | | | | |
| Avg. Abs Value | | | | 3 | 0.06 | | | | | |
| Std. Dev. | | | | 2 | 0.04 | | | | | |
| Group Average | Toluene | 343 | 366 | 24 | 0.08 | | | | | |
| Std. Dev. | | 98 | 107 | 46 | 0.16 | | | | | |
| Avg. Abs Value | | | | 36 | 0.12 | | | | | |
| Std. Dev. | | | | 36 | 0.13 | | | | | |
| Group Average | m-Xylene | 155 | 173 | 18 | 0.15 | | | | | |
| Std. Dev. | | 43 | 35 | 26 | 0.22 | | | | | |
| Avg. Abs Value | | | | 22 | 0.17 | | | | | |
| Std. Dev. | | | | 22 | 0.20 | | | | | |

```
------------------------------------------------------------------------------
         Calc.-Expt./Calc.                      Calc.-Expt./Calc.
           Maximum Ozone                 Time to 1/2 Expt. Δ([O3]-[NO])max
------------------------------------------------------------------------------
          < -0.33    :                             < -0.55    :
  -0.33 - -0.27      :                     -0.55 - -0.45      :
  -0.27 - -0.21      :                     -0.45 - -0.35      :
  -0.21 - -0.15      :                     -0.35 - -0.25      :
  -0.15 - -0.09      :                     -0.25 - -0.15      :1111
  -0.09 - -0.03      :                     -0.15 - -0.05      :111
  -0.03 -   0.03     :1111                 -0.05 -   0.05     :1111
   0.03 -   0.09     :11                    0.05 -   0.15     :
   0.09 -   0.15     :1111                  0.15 -   0.25     :
   0.15 -   0.21     :1                     0.25 -   0.35     :
   0.21 -   0.27     :                      0.35 -   0.45     :
   0.27 -   0.33     :                      0.45 -   0.55     :
          >  0.33    :                             >  0.55    :
------------------------------------------------------------------------------
(Calc.-Expt.)
  /Expt.        Ethene          Propene        trans-2-
Half-Life                                       Butene
------------------------------------------------------------------------------
     < -0.5     :               :               :
-0.5 - -0.4     :               :               :
-0.4 - -0.3     :               :               :
-0.3 - -0.2     :               :               :
-0.2 - -0.1     :1              :               :1
-0.1 -  0.0     :111            :1111           :1111
 0.0 -  0.1     :1111           :1111           :1111
 0.1 -  0.2     :111            :11             :1
 0.2 -  0.3     :               :1              :
 0.3 -  0.4     :               :               :
 0.4 -  0.5     :               :               :
     >  0.5     :               :               :
------------------------------------------------------------------------------
(Calc.-Expt.)
  /Expt.        Toluene         m-Xylene
Half-Life
------------------------------------------------------------------------------
     < -0.5     :               :
-0.5 - -0.4     :               :
-0.4 - -0.3     :               :
-0.3 - -0.2     :               :
-0.2 - -0.1     :1              :
-0.1 -  0.0     :11             :111
 0.0 -  0.1     :1111           :11
 0.1 -  0.2     :11             :111
 0.2 -  0.3     :1              :11
 0.3 -  0.4     :               :
 0.4 -  0.5     :1              :
     >  0.5     :               :1
------------------------------------------------------------------------------
(Calc.-Expt.)
  /Expt.        PAN             Formaldehyde
Product Yield
------------------------------------------------------------------------------
     < -0.5     :               :
-0.5 - -0.4     :               :
-0.4 - -0.3     :               :
-0.3 - -0.2     :               :11
-0.2 - -0.1     :               :1
-0.1 -  0.0     :               :111
 0.0 -  0.1     :               :111
 0.1 -  0.2     :1              :
 0.2 -  0.3     :11111          :
 0.3 -  0.4     :111            :
 0.4 -  0.5     :11             :
     >  0.5     :               :1
------------------------------------------------------------------------------
```

Figure IV-75. Distribution plots for discrepancies between calculated and experimental ozone maximum yields, times required to achieve half the maximum experimental change in ($[O_3]$-[NO]), and half-lives or yields for selected reactants and products observed in the EC seven-hydrocarbon mixture irradiations.

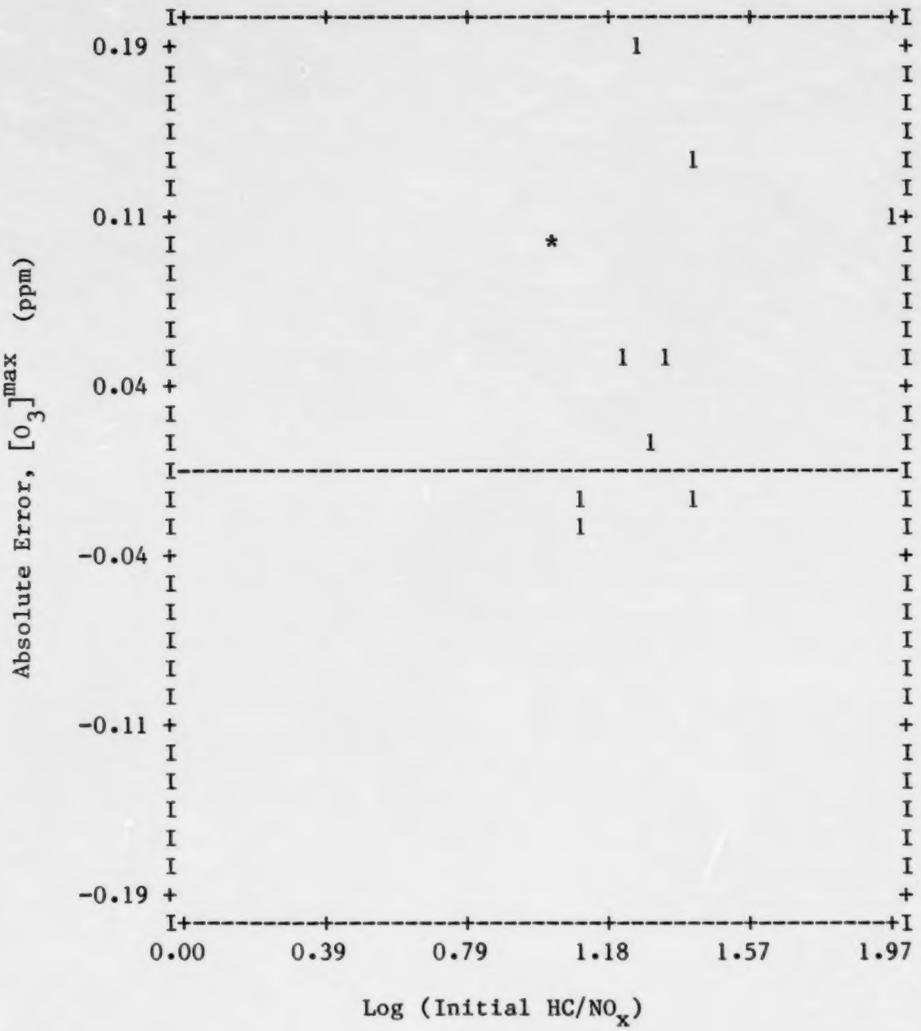

Figure IV-76. Plot of the discrepancies between calculated and experimental maximum ozone yields against the log of the hydrocarbon/$NO_x$ ratio for the EC seven-hydrocarbon mixture irradiations (* = two data points).

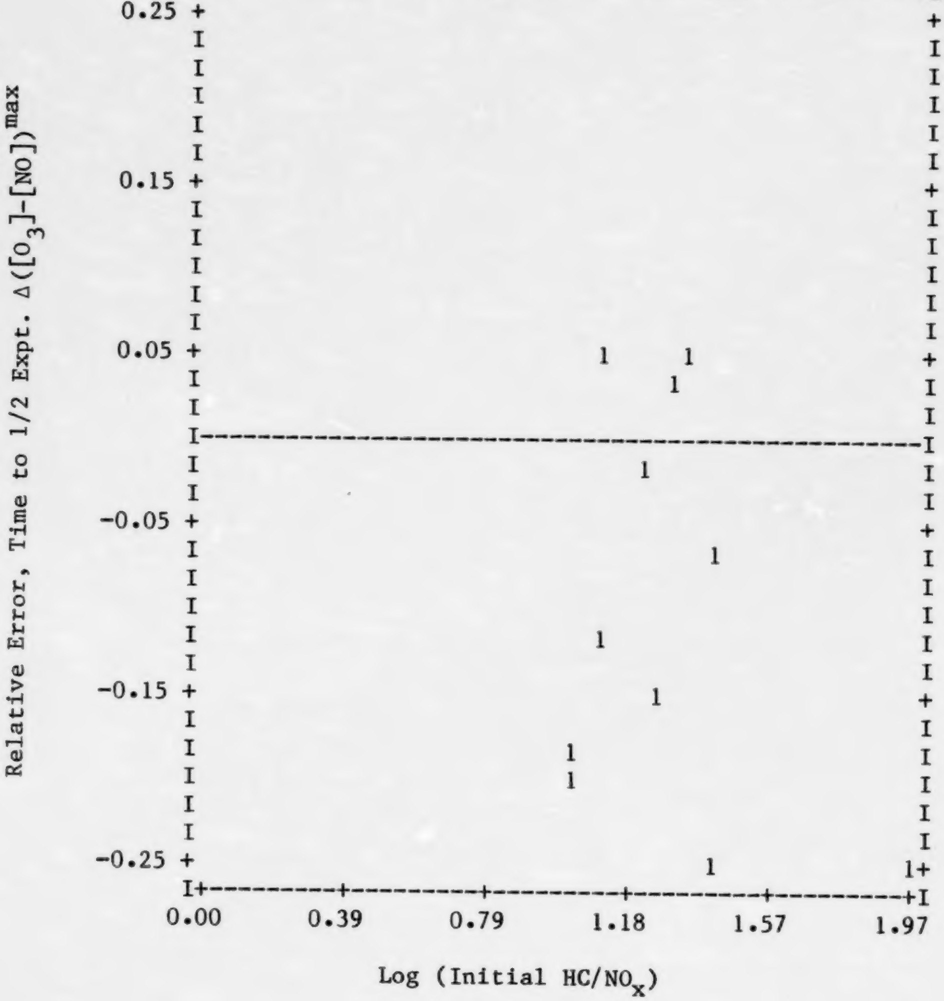

Figure IV-77. Plot of the discrepancies between calculated and experimental maximum times required to achieve half the maximum experimental change in $([O_3]-[NO])$ against the log of the hydrocarbon/$NO_x$ ratio for the EC seven-hydrocarbon mixture irradiations.

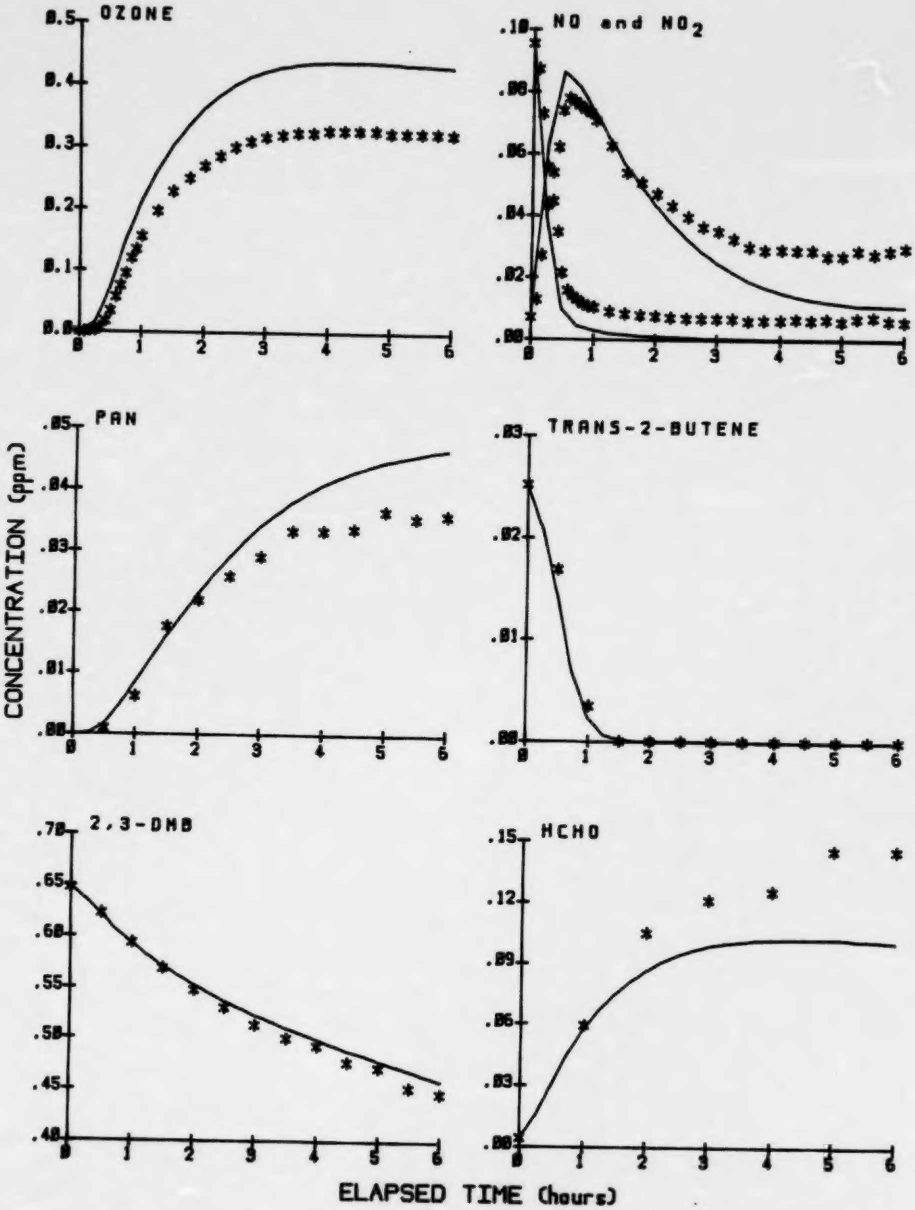

Figure IV-78. Experimental and calculated concentration-time plots for representative species observed in the seven-hydrocarbon mixture run EC-233.
* = Experimental data.
----- = Model calculation.

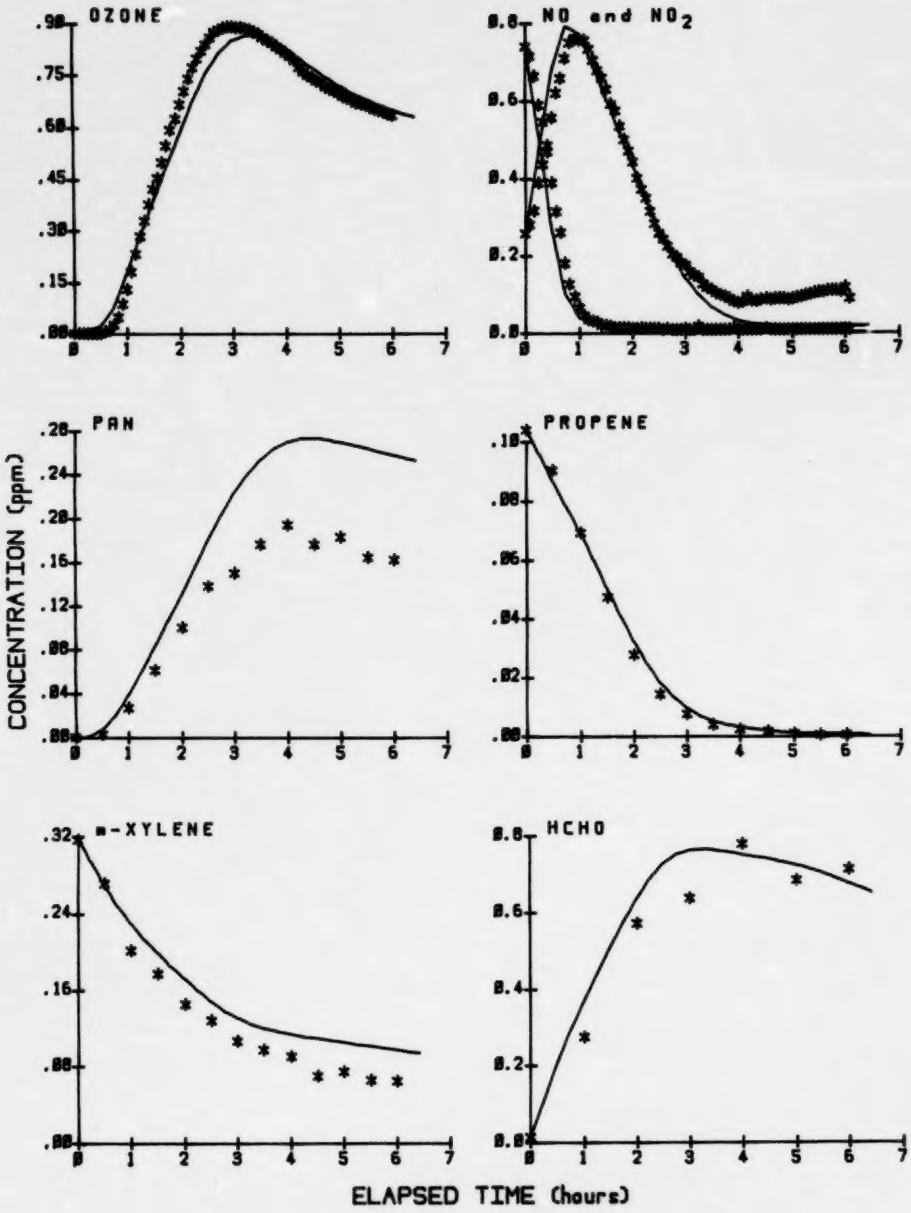

Figure IV-79. Experimental and calculated concentration-time plots for representative species observed in the seven-hydrocarbon mixture run EC-245.
* = Experimental data.
----- = Model calculation.

benzaldehyde were modeled in this program. The experimental and calculated maximum ozone yields and NO oxidation and ozone formation times for these runs are summarized in Table IV-40, selected reactant half-lives and product yields are summarized in Table IV-41, and selected distribution plots are given in Figure IV-80. Concentration-time plots for two representative standard experiments are given in Figure IV-81.

Except for one added benzaldehyde run, the quality of fits of the model simulations to the results of these experiments are similar to that shown in Figure IV-81 for the standard run, i.e., the model generally gave good predictions of the maximum ozone yields and reactant consumption rates, but consistently overpredicted the rates of NO conversion and ozone formation. This discrepancy in the NO oxidation and ozone formation times is not consistent with the results of modeling the ITC propene-$NO_x$ and m-xylene-$NO_x$ runs discussed above, where no consistent discrepancy of this nature was observed. However, it is consistent with the results of modeling other multi-component mixture runs, specifically the ITC "SAI surrogate" runs discussed in the following section.

The problem in predicting NO oxidation and ozone formation rates in these multi-component runs carried out in the SAPRC ITC is unlikely to be due to problems with the n-butane or the trans-2-butene models, since run ITC-482 was carried out without initial n-butane and run ITC-498 was carried out without initial trans-2-butene, and the results of modeling these runs were consistent with the other runs. It may be that too high a chamber radical source was used when modeling ITC experiments since, as indicated in Section IV-D-11, the model using the default radical source overpredicted the reactivity of all three n-butane runs which were modeled. (The modeling of the ITC propene and aromatic runs are not a good test of the magnitude of the radical source used, since in these cases mechanistic parameters affecting timing were adjusted to improve fits to the data.) Use of a lower chamber radical source (not shown) was found to improve the predictions of ozone formation times for most runs, but also resulted in a consistent underprediction of the organic reactant consumption rates. In addition, for some runs the model overpredicted the ozone formation rates even if a zero chamber radical source is used. This suggests that some other aspect of the model may be the source of this discrepancy in the model simulations of multi-component mixture runs carried out in the ITC.

Table IV-40. Initial Concentrations and Experimental and Calculated Ozone Yields and Times Required to Achieve Half the Experimental Change in ($[O_3]-[NO]$) for the ITC "Mini-Surrogate" Incremental Reactivity Runs

| Experiment | Initial Concentrations | | | Maximum Ozone Concentration | | | | Time to 1/2 Maximum Expt. ($[O_3]-[NO]$) | | | |
|---|---|---|---|---|---|---|---|---|---|---|---|
| | $NO_x$ (ppm) | HC (ppmC) | $HC/NO_x$ | Expt (ppm) | Calc (ppm) | Calc -Expt (ppm) | Calc -Expt /Expt) | Expt (min) | Calc (min) | Calc -Expt (min) | Calc -Expt /Expt |
| 1: "Mini-Surrogate" Runs: Standard and Varied Surrogate Components | | | | | | | | | | | |
| Standard Surrogate Runs | | | | | | | | | | | |
| ITC-479 | 0.092 | 4.0 | 43.4 | 0.332 | 0.326 | -0.006 | -0.02 | 68 | 39 | -29 | -0.43 |
| ITC-584 | 0.098 | 4.0 | 41.0 | 0.375 | 0.320 | -0.055 | -0.15 | 74 | 54 | -20 | -0.27 |
| Initial Propene Varied | | | | | | | | | | | |
| ITC-579 | 0.100 | 3.4 | 34.3 | 0.356 | 0.309 | -0.048 | -0.13 | 139 | 84 | -56 | -0.40 |
| ITC-472 | 0.103 | 3.6 | 35.1 | 0.258 | 0.336 | 0.078 | 0.30 | 98 | 47 | -51 | -0.52 |
| ITC-474 | 0.092 | 4.2 | 45.2 | 0.293 | 0.332 | 0.039 | 0.13 | 53 | 27 | -26 | -0.49 |
| ITC-581 | 0.091 | 4.3 | 46.8 | 0.352 | 0.309 | -0.043 | -0.12 | 55 | 37 | -18 | -0.33 |
| ITC-585 | 0.095 | 4.8 | 50.9 | 0.311 | 0.310 | -0.001 | 0.00 | 38 | 26 | -12 | -0.32 |
| ITC-478 | 0.095 | 5.0 | 52.6 | 0.322 | 0.326 | 0.004 | 0.01 | 41 | 22 | -19 | -0.46 |
| Initial n-Butane Varied | | | | | | | | | | | |
| ITC-482 | 0.096 | 1.2 | 12.3 | 0.279 | 0.295 | 0.016 | 0.06 | 70 | 37 | -33 | -0.48 |
| ITC-488 | 0.090 | 6.0 | 66.2 | 0.293 | 0.337 | 0.043 | 0.15 | 58 | 31 | -27 | -0.46 |
| ITC-492 | 0.092 | 8.1 | 87.8 | 0.326 | 0.361 | 0.035 | 0.11 | 59 | 33 | -25 | -0.43 |
| ITC-494 | 0.093 | 8.5 | 91.8 | 0.321 | 0.369 | 0.048 | 0.15 | 57 | 32 | -25 | -0.43 |
| Initial trans-2-Butene Varied | | | | | | | | | | | |
| ITC-498 | 0.098 | 3.9 | 40.2 | 0.320 | 0.338 | 0.017 | 0.05 | 88 | 48 | -41 | -0.46 |
| ITC-500 | 0.096 | 4.1 | 42.9 | 0.286 | 0.324 | 0.038 | 0.13 | 34 | 23 | -11 | -0.34 |
| ITC-502 | 0.093 | 4.6 | 49.4 | 0.271 | 0.308 | 0.037 | 0.14 | 24 | 13 | -11 | -0.46 |

(continued)

Table IV-40 (continued) - 2

| Experiment | Initial Concentrations | | | Maximum Ozone Concentration | | | | Time to 1/2 Maximum Expt. ($[O_3]-[NO]$) | | | |
|---|---|---|---|---|---|---|---|---|---|---|---|
| | $NO_x$ (ppm) | HC (ppmC) | $HC/NO_x$ | Expt (ppm) | Calc (ppm) | Calc -Expt (ppm) | Calc -Expt /Expt) | Expt (min) | Calc (min) | Calc -Expt (min) | Calc -Expt /Expt |
| Group Average | 0.095 | 4.6 | 49.3 | 0.313 | 0.327 | 0.013 | 0.05 | 64 | 37 | -27 | -0.42 |
| S. Dev. | 0.004 | 1.8 | 20.1 | 0.033 | 0.020 | 0.039 | 0.12 | 29 | 17 | 14 | 0.07 |
| Avg. Abs. Value | | | | | | 0.034 | 0.11 | | | 26 | 0.42 |
| S. Dev. | | | | | | 0.021 | 0.07 | | | 14 | 0.07 |
| 2: "Mini-Surrogate" with Benzaldehyde Added | | | | | | | | | | | |
| ITC-462 | 0.105 | 7.5 | 71.5 | 0.099 | 0.199 | 0.100 | 1.01 | 111 | 74 | -38 | -0.34 |
| ITC-466 | 0.104 | 6.5 | 62.5 | 0.131 | 0.221 | 0.090 | 0.69 | 127 | 70 | -57 | -0.45 |
| ITC-468 | 0.094 | 4.6 | 49.3 | 0.176 | 0.264 | 0.088 | 0.50 | 103 | 45 | -58 | -0.56 |
| Group Average | 0.101 | 6.2 | 61.1 | 0.135 | 0.228 | 0.093 | 0.73 | 114 | 63 | -51 | -0.45 |
| S. Dev. | 0.006 | 1.5 | 11.2 | 0.039 | 0.033 | 0.007 | 0.26 | 12 | 16 | 11 | 0.11 |
| Avg. Abs. Value | | | | | | 0.093 | 0.73 | | | 51 | 0.45 |
| S. Dev. | | | | | | 0.007 | 0.26 | | | 11 | 0.11 |
| Grand Average | 0.096 | 4.9 | 51.3 | 0.283 | 0.310 | 0.027 | 0.17 | 72 | 41 | -31 | -0.42 |
| S. Dev. | 0.005 | 1.8 | 19.2 | 0.076 | 0.043 | 0.046 | 0.30 | 33 | 19 | 16 | 0.08 |
| Avg. Abs. Value | | | | | | 0.044 | 0.21 | | | 31 | 0.42 |
| S. Dev. | | | | | | 0.030 | 0.26 | | | 16 | 0.08 |

Table IV-41. Experimental and Calculated Selected Reactant Half-Lives and Product Yields for the ITC "Mini-Surrogate" Incremental Reactivity Runs

| Experiment | Reactant Half-Life | | | | | Maximum Product Yields | | | | |
|---|---|---|---|---|---|---|---|---|---|---|
| | Species | Expt (min) | Calc (min) | Calc -Expt (min) | Calc -Expt /Expt | Species | Expt (ppm) | Calc (ppm) | Calc -Expt (ppm) | Calc -Expt /Expt |
| **1: "Mini-Surrogate": Standard and Varied Surrogate** | | | | | | | | | | |
| ITC-479 | Propene | 84 | 80 | -3 | -0.04 | PAN | 0.050 | 0.052 | 0.002 | 0.03 |
| | m-Xylene | 118 | 201 | 84 | 0.71 | Formaldehyde | 0.084 | 0.078 | -0.006 | -0.07 |
| ITC-584 | Propene | 98 | 90 | -7 | -0.08 | PAN | 0.080 | 0.054 | -0.026 | -0.33 |
| | m-Xylene | 145 | 207 | 62 | 0.43 | Formaldehyde | 0.046 | 0.079 | 0.033 | 0.72 |
| ITC-472 | m-Xylene | 117 | 116 | -1 | -0.01 | PAN | 0.044 | 0.050 | 0.006 | 0.14 |
| ITC-579 | m-Xylene | 141 | 133 | -8 | -0.06 | PAN | 0.058 | 0.048 | -0.010 | -0.17 |
| | | | | | | Formaldehyde | 0.025 | 0.028 | 0.003 | 0.11 |
| ITC-474 | Propene | 90 | 78 | -12 | -0.13 | PAN | 0.051 | 0.055 | 0.004 | 0.07 |
| | m-Xylene | 163 | 248 | 85 | 0.52 | Formaldehyde | 0.128 | 0.115 | -0.013 | -0.10 |
| ITC-581 | Propene | 94 | 86 | -8 | -0.08 | PAN | 0.090 | 0.053 | -0.037 | -0.41 |
| | m-Xylene | 163 | 302 | 139 | 0.85 | Formaldehyde | 0.102 | 0.119 | 0.016 | 0.16 |
| ITC-585 | Propene | 91 | 85 | -6 | -0.07 | PAN | 0.066 | 0.058 | -0.008 | -0.12 |
| | m-Xylene | 286 | 348 | 62 | 0.22 | Formaldehyde | 0.094 | 0.177 | 0.083 | 0.88 |
| ITC-478 | Propene | 80 | 78 | -2 | -0.03 | PAN | 0.056 | 0.059 | 0.003 | 0.05 |
| | m-Xylene | 194 | 356 | 162 | 0.84 | Formaldehyde | 0.197 | 0.184 | -0.012 | -0.06 |
| ITC-482 | Propene | 80 | 72 | -8 | -0.10 | PAN | 0.052 | 0.056 | 0.004 | 0.08 |
| | m-Xylene | 105 | 108 | 3 | 0.03 | | | | | |
| ITC-488 | Propene | 90 | 85 | -4 | -0.05 | PAN | 0.051 | 0.050 | -0.001 | -0.03 |
| | m-Xylene | 168 | 293 | 125 | 0.74 | Formaldehyde | 0.092 | 0.077 | -0.015 | -0.16 |

(continued)

Table IV-41 (continued) - 2

| Experiment | Reactant Half-Life |  |  |  |  | Maximum Product Yields |  |  |  |  |
|---|---|---|---|---|---|---|---|---|---|---|
|  | Species | Expt (min) | Calc (min) | Calc -Expt (min) | Calc -Expt /Expt | Species | Expt (ppm) | Calc (ppm) | Calc -Expt (ppm) | Calc -Expt /Expt |
| ITC-492 | Propene | 89 | 89 | 0 | 0.00 | PAN | 0.054 | 0.050 | -0.004 | -0.07 |
|  | m-Xylene | 189 | 358 | 169 | 0.89 | Formaldehyde | 0.084 | 0.078 | -0.006 | -0.07 |
| ITC-494 | Propene | 92 | 90 | -2 | -0.03 | PAN | 0.053 | 0.050 | -0.003 | -0.05 |
|  | m-Xylene | 202 | 356 | 155 | 0.77 | Formaldehyde | 0.092 | 0.078 | -0.014 | -0.15 |
| ITC-498 | Propene | 101 | 88 | -13 | -0.13 | PAN | 0.048 | 0.052 | 0.004 | 0.08 |
|  | m-Xylene | 144 | 162 | 18 | 0.13 | Formaldehyde | 0.094 | 0.077 | -0.017 | -0.18 |
| ITC-500 | Propene | 62 | 74 | 11 | 0.18 | PAN | 0.060 | 0.059 | -0.001 | -0.02 |
|  | m-Xylene | 129 | 260 | 131 | 1.01 | Formaldehyde | 0.098 | 0.083 | -0.015 | -0.15 |
| ITC-502 | Propene | 64 | 77 | 13 | 0.21 | PAN | 0.066 | 0.063 | -0.003 | -0.04 |
|  | *trans*-2-Butene | 30 | 17 | -14 | -0.45 |  |  |  |  |  |
|  | m-Xylene | 196 | 348 | 152 | 0.78 |  |  |  |  |  |
| Group Average | Propene | 86 | 83 | -3 | -0.03 | PAN | 0.059 | 0.054 | -0.005 | -0.05 |
| Std. Dev. |  | 12 | 6 | 8 | 0.10 |  | 0.012 | 0.004 | 0.012 | 0.15 |
| Avg. Abs Value |  |  |  | 7 | 0.09 |  |  |  | 0.008 | 0.11 |
| Std. Dev. |  |  |  | 4 | 0.06 |  |  |  | 0.010 | 0.11 |
| Group Average | m-Xylene | 164 | 253 | 89 | 0.52 | Formaldehyde | 0.095 | 0.098 | 0.003 | 0.08 |
| Std. Dev. |  | 46 | 93 | 64 | 0.37 |  | 0.042 | 0.045 | 0.029 | 0.36 |
| Avg. Abs Value |  |  |  | 90 | 0.53 |  |  |  | 0.019 | 0.23 |
| Std. Dev. |  |  |  | 62 | 0.36 |  |  |  | 0.021 | 0.27 |

(continued)

Table IV-41 (continued) - 3

| Experiment | Reactant Half-Life | | | | | Maximum Product Yields | | | | |
|---|---|---|---|---|---|---|---|---|---|---|
| | Species | Expt (min) | Calc (min) | Calc -Expt (min) | Calc -Expt /Expt | Species | Expt (ppm) | Calc (ppm) | Calc -Expt (ppm) | Calc -Expt /Expt |
| 2: "Mini-Surrogate" with Added Benzaldehyde | | | | | | | | | | |
| ITC-462 | Propene | 329 | 221 | -109 | -0.33 | | | | | |
| | trans-2-Butene | 90 | 83 | -7 | -0.08 | | | | | |
| | m-Xylene | 303 | 345 | 42 | 0.14 | | | | | |
| | Benzaldehyde | 324 | 184 | -140 | -0.43 | | | | | |
| ITC-466 | Propene | 281 | 187 | -94 | -0.33 | | | | | |
| | trans-2-Butene | 99 | 76 | -24 | -0.24 | | | | | |
| | m-Xylene | 240 | 124 | -116 | -0.48 | | | | | |
| | Benzaldehyde | 236 | 174 | -62 | -0.26 | | | | | |
| ITC-468 | Propene | 160 | 121 | -39 | -0.25 | PAN | 0.021 | 0.037 | 0.016 | 0.74 |
| | m-Xylene | 360 | 327 | -33 | -0.09 | | | | | |
| | Benzaldehyde | 294 | 152 | -142 | -0.48 | | | | | |
| Group Average | Propene | 257 | 176 | -80 | -0.30 | PAN | 0.021 | 0.037 | 0.016 | 0.74 |
| Std. Dev. | | 87 | 51 | 36 | 0.05 | | | | | |
| Avg. Abs Value | | | | 80 | 0.30 | | | | 0.016 | 0.74 |
| Std. Dev. | | | | 36 | 0.05 | | | | | |
| Group Average | trans-2-Butene | 95 | 79 | -15 | -0.16 | | | | | |
| Std. Dev. | | 7 | 5 | 12 | 0.11 | | | | | |
| Avg. Abs Value | | | | 15 | 0.16 | | | | | |
| Std. Dev. | | | | 12 | 0.11 | | | | | |

(continued)

Table IV-41 (continued) - 4

| Experiment | Reactant Half-Life | | | | | Maximum Product Yields | | | | |
|---|---|---|---|---|---|---|---|---|---|---|
| | Species | Expt (min) | Calc (min) | Calc -Expt (min) | Calc -Expt /Expt | Species | Expt (ppm) | Calc (ppm) | Calc -Expt (ppm) | Calc -Expt /Expt |
| Group Average | m-Xylene | 301 | 265 | -36 | -0.15 | | | | | |
| Std. Dev. | | 60 | 123 | 79 | 0.31 | | | | | |
| Avg. Abs Value | | | | 64 | 0.24 | | | | | |
| Std. Dev. | | | | 46 | 0.21 | | | | | |
| Group Average | Benzaldehyde | 285 | 170 | -115 | -0.39 | | | | | |
| Std. Dev. | | 45 | 16 | 45 | 0.11 | | | | | |
| Avg. Abs Value | | | | 115 | 0.39 | | | | | |
| Std. Dev. | | | | 45 | 0.11 | | | | | |

```
-----------------------------------------------------------------------------
        Calc.-Expt./Calc.                     Calc.-Expt./Calc.
          Maximum Ozone              Time to 1/2 Expt. Δ([O3]-[NO])max
-----------------------------------------------------------------------------
        <  -0.33    :                        <  -0.55    :2
  -0.33 -  -0.27    :                 -0.55 -  -0.45    :1111111
  -0.27 -  -0.21    :                 -0.45 -  -0.35    :11112
  -0.21 -  -0.15    :                 -0.35 -  -0.25    :11112
  -0.15 -  -0.09    :                 -0.25 -  -0.15    :
  -0.09 -  -0.03    :111              -0.15 -  -0.05    :
  -0.03 -   0.03    :11111            -0.05 -   0.05    :
   0.03 -   0.09    :11111112          0.05 -   0.15    :
   0.09 -   0.15    :22                0.15 -   0.25    :
   0.15 -   0.21    :                  0.25 -   0.35    :
   0.21 -   0.27    :                  0.35 -   0.45    :
   0.27 -   0.33    :                  0.45 -   0.55    :
        >   0.33    :                       >   0.55    :
-----------------------------------------------------------------------------
(Calc.-Expt.)
  /Expt.        Propene        m-Xylene        Benzaldehyde
 Half Life
-----------------------------------------------------------------------------
     < -0.5    :               :               :
-0.5 - -0.4    :               :2              :22
-0.4 - -0.3    :22             :               :
-0.3 - -0.2    :2              :               :2
-0.2 - -0.1    :11             :               :
-0.1 -  0.0    :111111111      :112            :
 0.0 -  0.1    :               :1              :
 0.1 -  0.2    :1              :12             :
 0.2 -  0.3    :1              :1              :
 0.3 -  0.4    :               :               :
 0.4 -  0.5    :               :1              :
     >  0.5    :               :111111111      :
-----------------------------------------------------------------------------
(Calc.-Expt.)
  /Expt.          PAN           Formaldehyde
Product Yield
-----------------------------------------------------------------------------
     < -0.5    :               :
-0.5 - -0.4    :1              :
-0.4 - -0.3    :1              :
-0.3 - -0.2    :               :
-0.2 - -0.1    :11             :11111
-0.1 -  0.0    :11111          :111
 0.0 -  0.1    :11111          :
 0.1 -  0.2    :1              :11
 0.2 -  0.3    :               :
 0.3 -  0.4    :               :
 0.4 -  0.5    :               :
     >  0.5    :2              :11
-----------------------------------------------------------------------------
```

Figure IV-80. Distribution plots for discrepancies between calculated and experimental ozone maximum yields, times required to achieve half the maximum experimental change in ($[O_3]-[NO]$), and half-lives or yields for selected reactants and products observed in the ITC "mini-surrogate" incremental reactivity irradiations. Codes for symbols:

1 = Standard runs and runs with initial concentrations of surrogate components varied.
2 = Runs with added benzaldehyde.

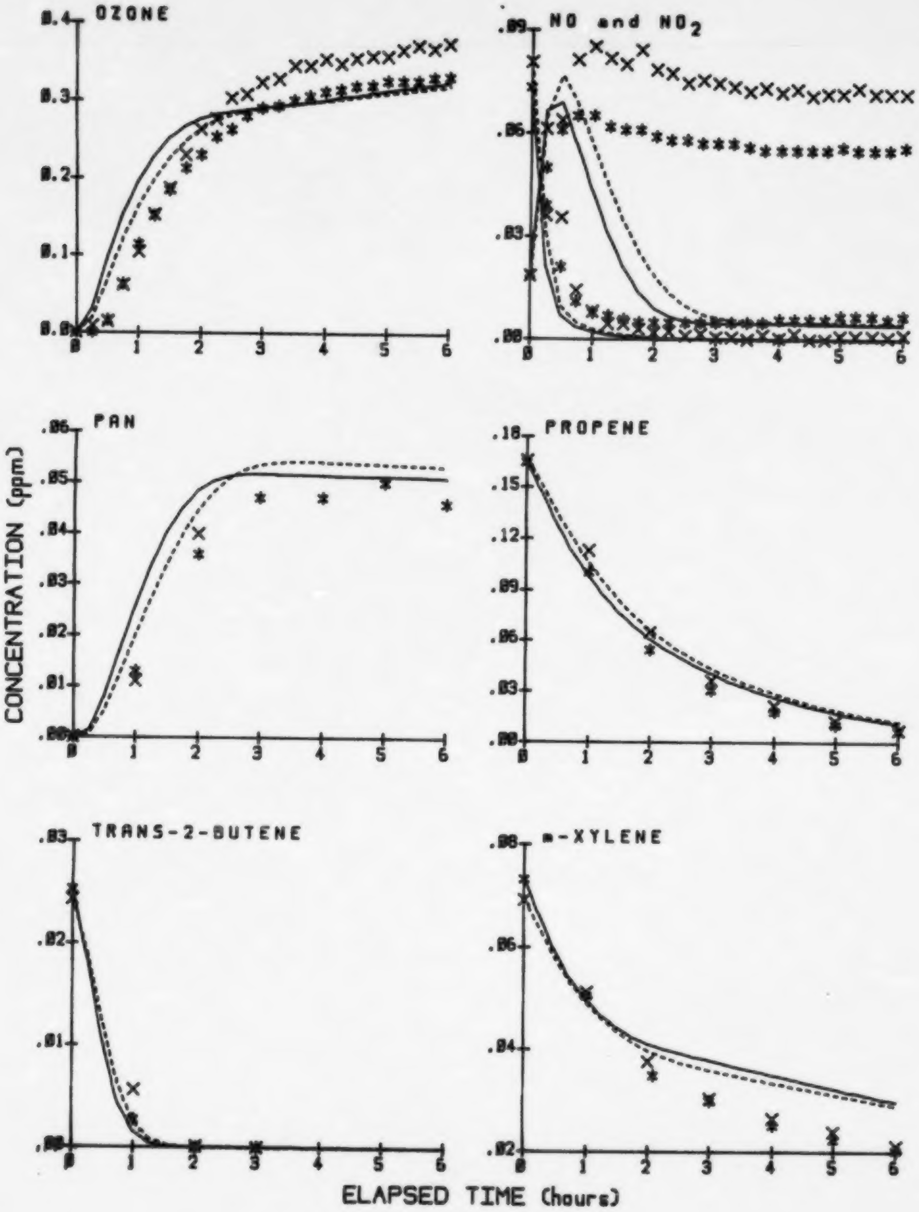

Figure IV-81. Experimental and calculated concentration-time plots for representative species observed in the standard "mini-surrogate" runs ITC-479 and ITC-584.
ITC-479:
* = Experimental data.
----- = Model calculation.

ITC-584:
x = Experimental data.
— — = Model calculation.

Despite the discrepancy in predictions of ozone formation rates, as indicated above, the model generally gave good fits of maximum ozone yields and other measures of reactivity. In addition, except for the added benzaldehyde runs, the model gave appropriate predictions of the effects of increasing or decreasing the initial concentrations of individual organics on the maximum ozone yields and (in a relative sense) on the ozone formation rates. The fits for the added benzaldehyde runs are less consistent and in general not as good, with the model tending to overpredict the ozone yields, though the model is qualitatively consistent with the experiments in that both indicate that benzaldehyde is a very effective inhibitor of reactivity. The relatively poor performance of the model predictions for the added benzaldehyde runs, where the model tends to overpredict the maximum ozone yields and reactant consumption rates, may be due to the model using too large a benzaldehyde photolysis rate (which was adjusted based on fits of the model simulations to results of EC runs, where the spectral distribution of the light source is significantly different), as indicated by the fact that the benzaldehyde consumption rates in these ITC runs are consistently underpredicted in the model calculations. However, although assuming lower benzaldehyde photolysis rates in these ITC runs improves the fits to the benzaldehyde data, the model still tends to overpredict ozone yields and other measures of reactivity. Concentration-time plots for selected species in an added benzaldehyde run are shown in Figure IV-82, where the fits using the standard model and a model assuming no benzaldehyde photolysis are compared.

### 8. ITC "SAI Surrogate" Multi-Day Runs

Six two- to four-day $NO_x$-air irradiations of the 8-component "SAI surrogate," carried out at varying initial hydrocarbon/$NO_x$ ratios in the SAPRC ITC as part of an EPA-funded program to study multi-day effects (Carter et al. 1985), were modeled in this program. (A similar set of experiments carried out in the OTC were also modeled; these are discussed separately in the following section since somewhat different results were obtained.) The eight-component surrogate, designated the "SAI surrogate" because it was designed by the modelers at SAI to represent urban emissions (Whitten, private communication), consists of a constant-composition mixture of ethene, propene, isobutene, n-butane, n-pentane, isooctane,

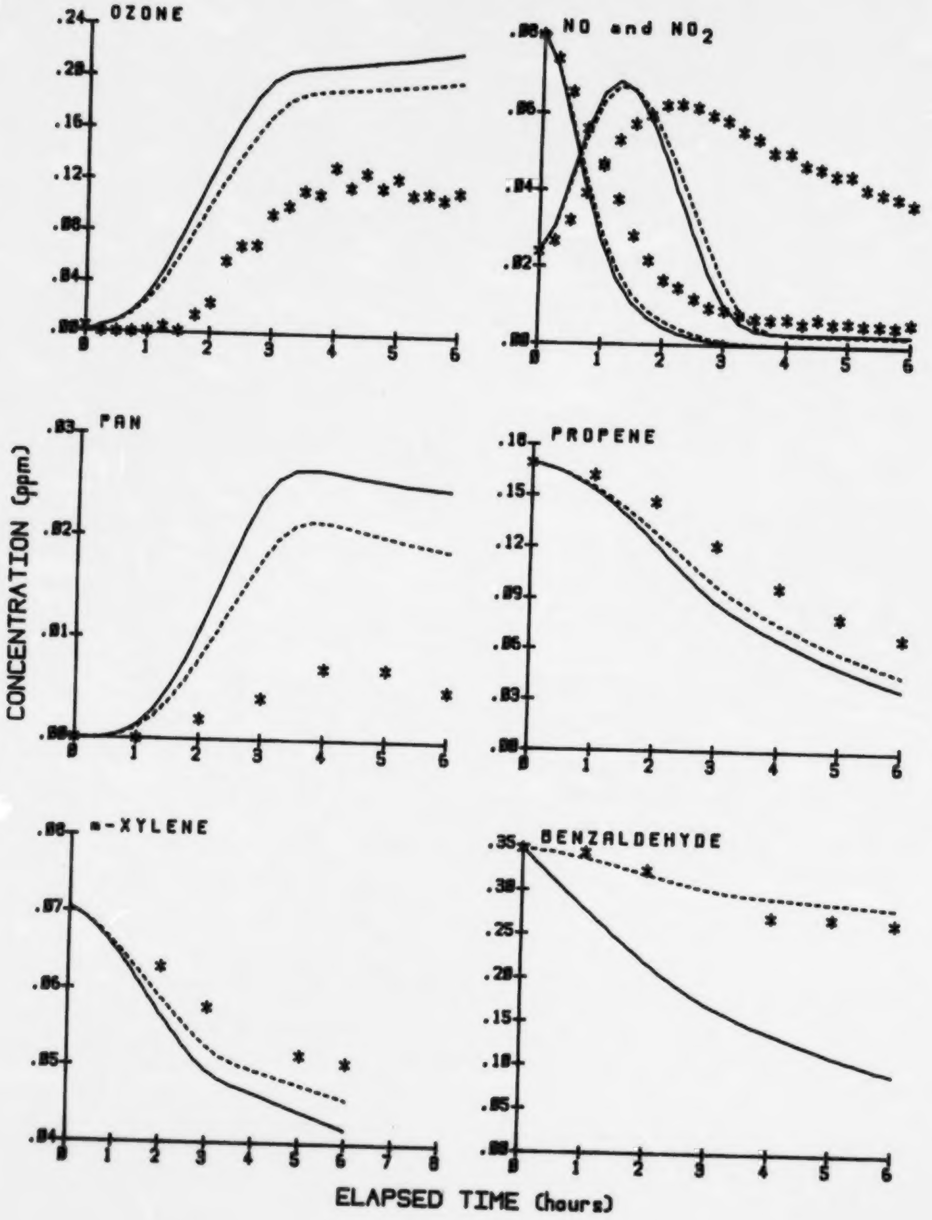

Figure IV-82. Experimental and calculated concentration-time plots for representative species observed in the "mini-surrogate" + benzaldehyde run ITC-466.

* = Experimental data.
————— = Model calculation (standard).
— — = Model calculation (no benzaldehyde photolysis assumed).

toluene, and m-xylene. In some experiments, NO was added on the second and subsequent days of the run to allow ozone formation to continue. The initial concentrations and special conditions and the experimental and calculated first-day ozone yields and NO oxdiation and ozone formation times are summarized in Table IV-42. The experimental and calculated maximum ozone yields for days 2 through 4 are summarized in Table IV-43, and selected reactant half-lives and first-day product yields are summarized in Table IV-44. Distribution plots of selected discrepancies are given in Figure IV-83 and concentration-time plots of selected data for three of these runs, carried out at differing initial hydrocarbon/$NO_x$ ratios, are given in Figures IV-84 through IV-86.

The results of the model simulations of these runs are consistent with the modeling of the ITC "mini-surrogate" runs discussed in the previous section in that in the simulations of the first day of these runs the model consistently overpredicted the rates of ozone formation and NO oxidation. However, as was the case for the "mini-surrogate" runs the model did not consistently overpredict the organic reactant consumption rates or, in runs which were sufficiently reactive to attain a "true" ozone maximum, the maximum ozone yields. For lower reactivity runs, the overprediction of ozone formation rates resulted in overpredicted first-day ozone yields, and this led to even greater discrepancies in the model predictions of ozone formation and other aspects of reactivity on subsequent days of the irradiation, as shown, for example, in Figures IV-84 and IV-85.

The discrepancies on the subsequent days were not as great for the higher reactivity runs, where the model more accurately simulated the conditions at the end of the day, and thus at the start of the subsequent days. For example, run ITC-637 was a high hydrocarbon/$NO_x$ run in which NO was injected at the beginning of each subsequent day of the irradiation to determine the ozone forming potential of the partially reacted (or "aged") organic mixture initially present on these days. As shown in Figure IV-86, the performance of the model in simulating the results of this run on days 2-4 was significantly better, both in terms of ozone formation and reactant consumption rates, than the simulations of most of the other runs in this group. This suggests that the poor performance of the model in simulating second and subsequent day data for the lower hydrocarbon/$NO_x$

Table IV-42. Initial Concentrations, Special Conditions, and Experimental and Calculated First Day Ozone Yields and Times Required to Achieve Half the Experimental Change in ([$O_3$]-[NO]) for the Multi-Day Surrogate-$NO_x$-Air Irradiations Carried Out in the SAPRC ITC

| Experiment | Special Conditions | | Initial Concentrations | | | Maximum Ozone Concentration | | | | Time to 1/2 Maximum Expt. ([$O_3$]-[NO]) | | | |
|---|---|---|---|---|---|---|---|---|---|---|---|---|---|
| | No. Run Days | Subsequent NO Injections (ppm [day])[a] | $NO_x$ (ppm) | HC (ppmC) | HC/$NO_x$ | Expt (ppm) | Calc (ppm) | Calc -Expt (ppm) | Calc -Expt /Expt) | Expt (min) | Calc (min) | Calc -Expt (min) | Calc -Expt /Expt |
| ITC-626 | 2 | 0.77 [2] | 0.301 | 4.0 | 13.4 | 0.618 | 0.594 | -0.024 | -0.04 | 193 | 134 | -59 | -0.31 |
| ITC-630 | 3 | 0.25 [2] | 0.306 | 1.9 | 6.3 | 0.284 | 0.425 | 0.142 | 0.50 | 294 | 163 | -130 | -0.44 |
| ITC-631 | 3 | | 0.323 | 1.0 | 3.2 | 0.042 | 0.108 | 0.066 | | 247 | 142 | -106 | -0.43 |
| ITC-633 | 2 | | 0.639 | 4.0 | 6.2 | 0.231 | 0.490 | 0.259 | 1.12 | 266 | 138 | -127 | -0.48 |
| ITC-635 | 2 | | 1.206 | 4.0 | 3.3 | 0.006 | 0.029 | 0.023 | | 224 | 130 | -94 | -0.42 |
| ITC-637 | 4 | 0.19 [2], 0.19 [3], 0.29 [4] | 0.310 | 4.0 | 12.7 | 0.617 | 0.593 | -0.024 | -0.04 | 184 | 136 | -48 | -0.26 |
| Group Average | | | 0.514 | 3.2 | 7.5 | 0.300 | 0.373 | 0.073 | 0.39 | 235 | 140 | -94 | -0.39 |
| S. Dev. | | | 0.364 | 1.3 | 4.5 | 0.268 | 0.246 | 0.110 | 0.55 | 42 | 12 | 34 | 0.09 |
| Avg. Abs. Value | | | | | | | | 0.090 | 0.43 | | | 93 | 0.39 |
| S. Dev. | | | | | | | | 0.095 | 0.51 | | | 34 | 0.09 |

[a] When indicated, NO injections were made at the end of the first hour of the irradiation on the day(s) given in brackets, except for run ITC-630, where the NO was injected at the end of the third hour.

Table IV-43. Experimental and Calculated Maximum Ozone Concentrations for Days 2-4 for the ITC Multi-Day Surrogate-$NO_x$-Air Irraditions

| Experiment | Day 2 Ozone Maximum | | | | Day 3 Ozone Maximum | | | | Day 4 Ozone Maximum | | | |
|---|---|---|---|---|---|---|---|---|---|---|---|---|
| | Expt (ppm) | Calc (ppm) | Calc -Expt (ppm) | Calc -Expt /Expt | Expt (ppm) | Calc (ppm) | Calc -Expt (ppm) | Calc -Expt /Expt | Expt (ppm) | Calc (ppm) | Calc -Expt (ppm) | Calc -Expt /Expt |
| ITC-626 | 0.505 | 0.437 | -0.068 | -0.13 | | | | | | | | |
| ITC-630 | 0.213 | 0.378 | 0.165 | 0.77 | 0.274 | 0.380 | 0.106 | 0.39 | | | | |
| ITC-631 | 0.165 | 0.336 | 0.171 | 1.04 | 0.242 | 0.353 | 0.111 | 0.46 | | | | |
| ITC-633 | 0.340 | 0.446 | 0.107 | 0.31 | 0.272 | 0.388 | 0.116 | 0.43 | | | | |
| ITC-635 | 0.008 | 0.058 | 0.050 | | | | | | | | | |
| ITC-637 | 0.577 | 0.624 | 0.047 | 0.08 | 0.537 | 0.612 | 0.075 | 0.14 | 0.384 | 0.523 | 0.139 | 0.36 |
| Group Average | 0.301 | 0.380 | 0.079 | 0.41 | 0.331 | 0.433 | 0.102 | 0.35 | 0.384 | 0.523 | 0.139 | 0.36 |
| S. Dev. | 0.215 | 0.186 | 0.090 | 0.48 | 0.138 | 0.120 | 0.018 | 0.15 | | | | |
| Avg. Abs. Value | | | 0.101 | 0.47 | | | 0.102 | 0.35 | | | 0.139 | 0.36 |
| S. Dev. | | | 0.056 | 0.42 | | | 0.018 | 0.15 | | | | |

Table IV-44. Experimental and Calculated Reactant Half-Lives and Product Yields for Selected Species Observed on the First Day of the Multi-Day Surrogate-$NO_x$-Air Irradiations Carried Out in the ITC

| Experiment | Reactant Half-Life | | | | | Maximum Product Yields | | | | |
|---|---|---|---|---|---|---|---|---|---|---|
| | Species | Expt (min) | Calc (min) | Calc -Expt (min) | Calc -Expt /Expt | Species | Expt (ppm) | Calc (ppm) | Calc -Expt (ppm) | Calc -Expt /Expt |
| ITC-626 | Ethene | 366 | 328 | -38 | -0.10 | PAN | 0.116 | 0.089 | -0.027 | -0.23 |
| | Propene | 165 | 135 | -29 | -0.18 | Formaldehyde | 0.045 | 0.135 | 0.090 | 2.00 |
| | Isobutene | 107 | 87 | -20 | -0.19 | | | | | |
| | Toluene | 596 | 705 | 109 | 0.18 | | | | | |
| | m-Xylene | 205 | 174 | -30 | -0.15 | | | | | |
| ITC-630 | Ethene | 619 | 500 | -119 | -0.19 | PAN | 0.027 | 0.037 | 0.010 | 0.38 |
| | Propene | 230 | 186 | -45 | -0.19 | Formaldehyde | 0.025 | 0.066 | 0.041 | 1.63 |
| | Isobutene | 118 | 102 | -17 | -0.14 | | | | | |
| | Toluene | 567 | 720 | 153 | 0.27 | | | | | |
| | m-Xylene | 302 | 236 | -66 | -0.22 | | | | | |
| ITC-631 | Ethene | 583 | 720 | 137 | 0.24 | Formaldehyde | 0.069 | 0.035 | -0.034 | -0.49 |
| | Propene | 267 | 231 | -36 | -0.13 | | | | | |
| | Isobutene | 120 | 120 | 0 | 0.00 | | | | | |
| | Toluene | 455 | 720 | 265 | 0.58 | | | | | |
| | m-Xylene | 415 | 273 | -142 | -0.34 | | | | | |
| ITC-633 | Ethene | 699 | 571 | -128 | -0.18 | PAN | 0.034 | 0.066 | 0.032 | 0.93 |
| | Propene | 272 | 228 | -44 | -0.16 | | | | | |
| | Isobutene | 145 | 131 | -14 | -0.10 | | | | | |
| | Toluene | 720 | 720 | 0 | 0.00 | | | | | |
| | m-Xylene | 376 | 316 | -60 | -0.16 | | | | | |
| ITC-635 | Ethene | 535 | 720 | 185 | 0.35 | Formaldehyde | 0.092 | 0.113 | 0.021 | 0.23 |
| | Propene | 353 | 327 | -27 | -0.08 | | | | | |
| | Isobutene | 165 | 173 | 9 | 0.05 | | | | | |
| | Toluene | 461 | 720 | 259 | 0.56 | | | | | |
| | m-Xylene | 510 | 426 | -83 | -0.16 | | | | | |

(continued)

Table IV-44 (continued) - 2

| Experiment | Reactant Half-Life | | | | | Maximum Product Yields | | | | |
|---|---|---|---|---|---|---|---|---|---|---|
| | Species | Expt (min) | Calc (min) | Calc -Expt (min) | Calc -Expt /Expt | Species | Expt (ppm) | Calc (ppm) | Calc -Expt (ppm) | Calc -Expt /Expt |
| ITC-637 | Ethene | 340 | 331 | -9 | -0.03 | PAN | 0.117 | 0.090 | -0.027 | -0.23 |
| | Propene | 151 | 137 | -14 | -0.09 | Formaldehyde | 0.127 | 0.137 | 0.010 | 0.08 |
| | Isobutene | 97 | 88 | -9 | -0.09 | | | | | |
| | Toluene | 680 | 720 | 40 | 0.06 | | | | | |
| | m-Xylene | 216 | 191 | -25 | -0.11 | | | | | |
| Group Average | Ethene | 524 | 529 | 5 | 0.01 | PAN | 0.073 | 0.071 | -0.003 | 0.21 |
| Std. Dev. | | 143 | 176 | 130 | 0.23 | | 0.050 | 0.025 | 0.029 | 0.56 |
| Avg. Abs Value | | | | 103 | 0.18 | | | | 0.024 | 0.44 |
| Std. Dev. | | | | 66 | 0.11 | | | | 0.009 | 0.33 |
| Group Average | Propene | 240 | 207 | -32 | -0.14 | Formaldehyde | 0.072 | 0.097 | 0.026 | 0.69 |
| Std. Dev. | | 75 | 72 | 11 | 0.05 | | 0.040 | 0.045 | 0.045 | 1.07 |
| Avg. Abs Value | | | | 32 | 0.14 | | | | 0.039 | 0.88 |
| Std. Dev. | | | | 11 | 0.05 | | | | 0.031 | 0.87 |
| Group Average | Isobutene | 125 | 117 | -8 | -0.08 | | | | | |
| Std. Dev. | | 25 | 33 | 11 | 0.09 | | | | | |
| Avg. Abs Value | | | | 11 | 0.10 | | | | | |
| Std. Dev. | | | | 7 | 0.06 | | | | | |
| Group Average | Toluene | 580 | 718 | 138 | 0.28 | | | | | |
| Std. Dev. | | 109 | 6 | 110 | 0.25 | | | | | |
| Avg. Abs Value | | | | 138 | 0.28 | | | | | |
| Std. Dev. | | | | 110 | 0.25 | | | | | |
| Group Average | m-Xylene | 337 | 269 | -68 | -0.19 | | | | | |
| Std. Dev. | | 119 | 93 | 43 | 0.08 | | | | | |
| Avg. Abs Value | | | | 68 | 0.19 | | | | | |
| Std. Dev. | | | | 43 | 0.08 | | | | | |

```
---------------------------------------------------------------------------
       Calc.-Expt./Calc.                     Calc.-Expt./Calc.
         Maximum Ozone               Time to 1/2 Expt. Δ([O3]-[NO])max
---------------------------------------------------------------------------
          <  -0.33    :                       <  -0.55    :
   -0.33 -  -0.27    :                -0.55 -  -0.45    :1
   -0.27 -  -0.21    :                -0.45 -  -0.35    :111
   -0.21 -  -0.15    :                -0.35 -  -0.25    :11
   -0.15 -  -0.09    :                -0.25 -  -0.15    :
   -0.09 -  -0.03    :                -0.15 -  -0.05    :
   -0.03 -   0.03    :111             -0.05 -   0.05    :
    0.03 -   0.09    :1                0.05 -   0.15    :
    0.09 -   0.15    :1                0.15 -   0.25    :
    0.15 -   0.21    :                 0.25 -   0.35    :
    0.21 -   0.27    :1                0.35 -   0.45    :
    0.27 -   0.33    :                 0.45 -   0.55    :
          >   0.33    :                       >   0.55    :
-------------------------------------------------------------------------
(Calc.-Expt.)
  /Expt.       Ethene        Propene        Isobutene      Toluene
 Half-Life
-------------------------------------------------------------------------
     < -0.5    :             :              :              :
-0.5 - -0.4    :             :              :              :
-0.4 - -0.3    :             :              :              :
-0.3 - -0.2    :             :              :              :
-0.2 - -0.1    :111          :1111          :11            :
-0.1 -  0.0    :1            :11            :11            :
 0.0 -  0.1    :             :              :11            :11
 0.1 -  0.2    :             :              :              :1
 0.2 -  0.3    :1            :              :              :1
 0.3 -  0.4    :1            :              :              :
 0.4 -  0.5    :             :              :              :
     >  0.5    :             :              :              :11
---------------------------------------------------------------------------
(Calc.-Expt.)                (Calc.-Expt.)
  /Expt.       m-Xylene        /Expt.         PAN           Formaldehyde
 Half-Life                   Product Yield
---------------------------------------------------------------------------
     < -0.5    :                  < -0.5    :              :
-0.5 - -0.4    :             -0.5 - -0.4    :              :1
-0.4 - -0.3    :1            -0.4 - -0.3    :              :
-0.3 - -0.2    :1            -0.3 - -0.2    :11            :
-0.2 - -0.1    :1111         -0.2 - -0.1    :              :
-0.1 -  0.0    :             -0.1 -  0.0    :              :
 0.0 -  0.1    :              0.0 -  0.1    :              :1
 0.1 -  0.2    :              0.1 -  0.2    :              :
 0.2 -  0.3    :              0.2 -  0.3    :              :1
 0.3 -  0.4    :              0.3 -  0.4    :1             :
 0.4 -  0.5    :              0.4 -  0.5    :              :
     >  0.5    :                  >  0.5    :1             :11
---------------------------------------------------------------------------
```

Figure IV-83. Distribution plots for discrepancies between calculated and experimental first day maximum ozone yields, times required to achieve half the maximum experimental change in ($[O_3]$-[NO]), and selected reactant half-lives and organic product yields in the model simulations of the first day of the multi-day surrogate-$NO_x$-air experiments carried out in the SAPRC ITC.

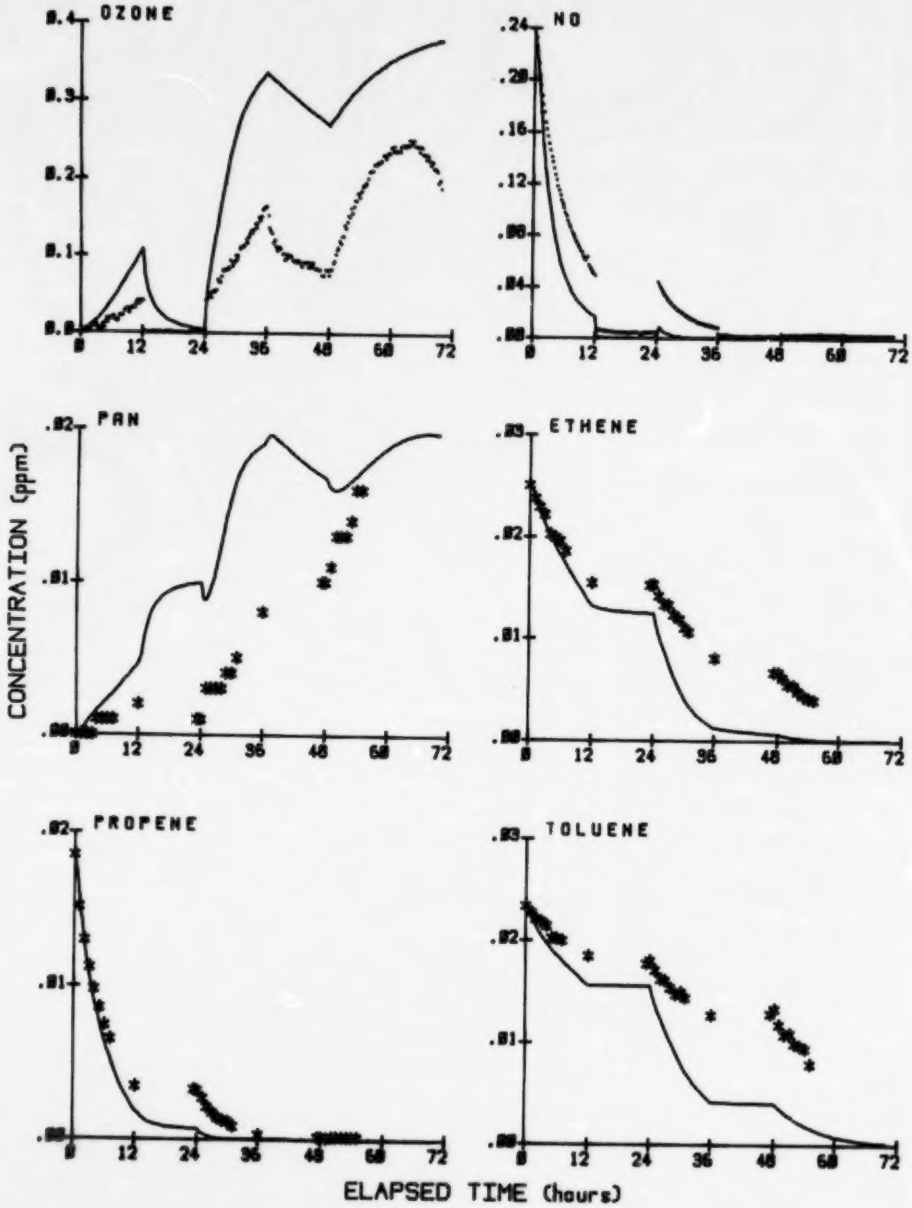

Figure IV-84. Experimental and calculated concentration-time plots for representative species observed in the multi-day surrogate run ITC-631.
... or * = Experimental data.
----- = Model calculation.

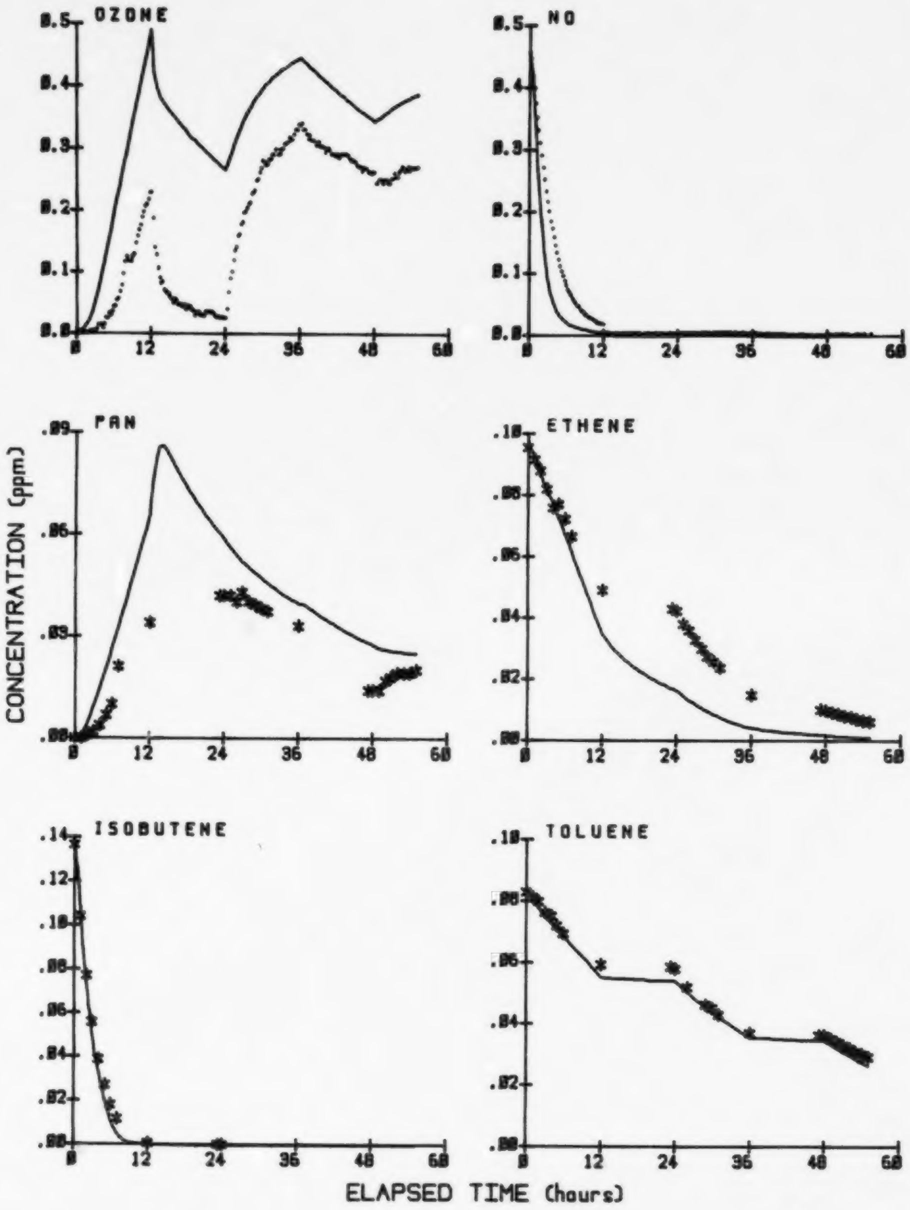

Figure IV-85. Experimental and calculated concentration-time plots for representative species observed in the multi-day surrogate run ITC-633.
.... or * = Experimental data.
----- = Model calculation.

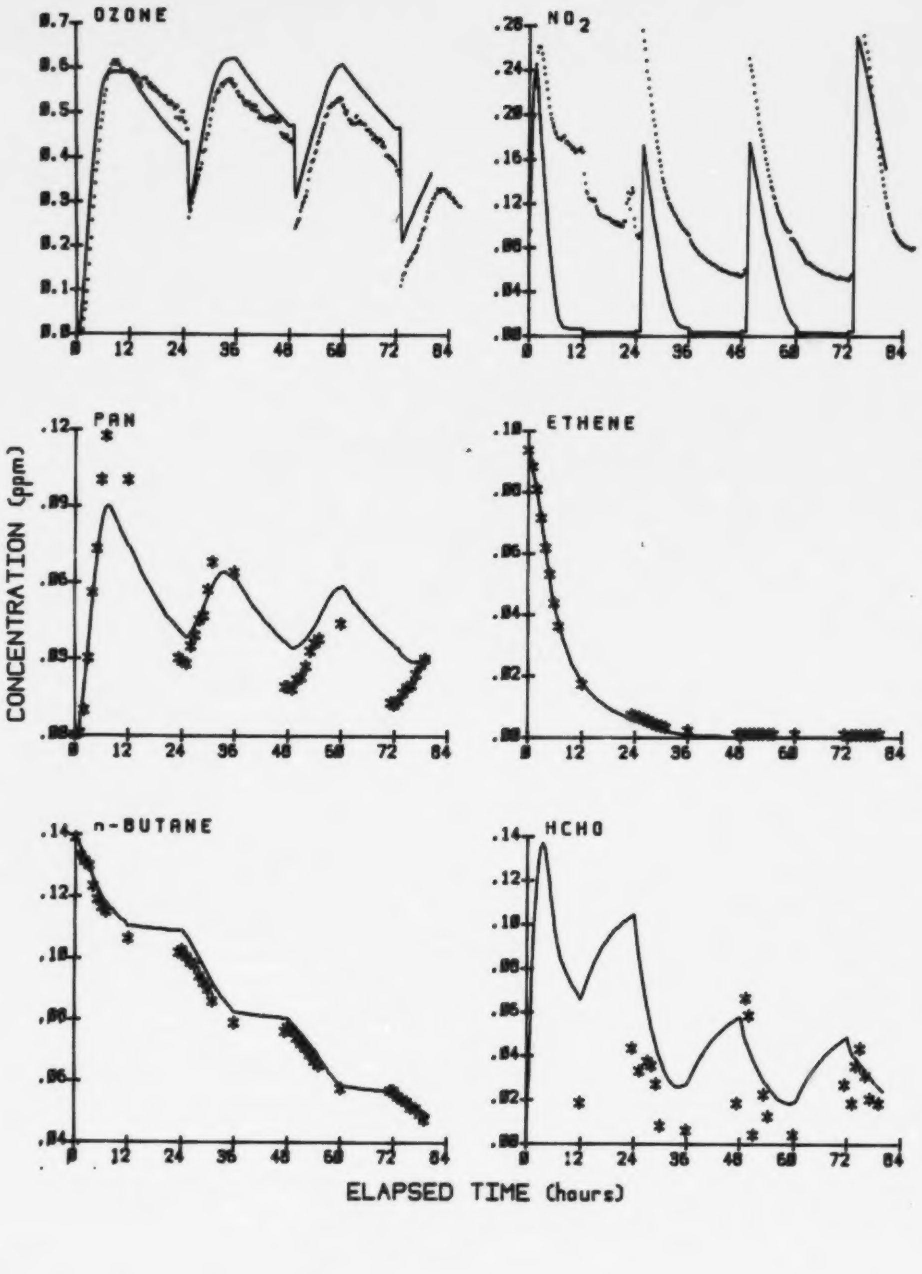

Figure IV-86. Experimental and calculated concentration-time plots for representative species observed in the multi-day surrogate run ITC-637.
.... or * = Experimental data.
----- = Model calculation.

runs is due to the model overpredicting the first day ozone formation rates and final ozone yields, and not necessarily due to a problem with the model in simulating multi-day effects as such. It is clear that accurately simulating the results of multi-day runs is more difficult than simulating one-day experiments since under some, though not all, conditions, relatively small discrepancies can be magnified on subsequent days.

### 9. OTC "SAI Surrogate" Multi-Day Runs

A total of 25 one- to four-day $NO_x$-air irradiations of the eight-component "SAI surrogate" mixture carried out in the SAPRC OTC were modeled in this program. These experiments employed the same surrogate mixture and were otherwise analogous to the ITC experiments discussed in the previous section, except that they were carried out in the outdoor chamber, and more such experiments were carried out. As with the ITC runs, in some runs NO was injected on subsequent days of some of the runs to allow ozone formation to continue. The initial reactant concentrations, special conditions and experimental and calculated first day maximum ozone yields and NO oxidation and ozone formation times are summarized in Table IV-45. The experimental and calculated second day through fourth day maximum ozone yields are summarized in Table IV-46, and selected hydrocarbon consumption rates and product yields are summarized in Table IV-47. Selected distribution plots of the discrepancies obtained are given in Figure IV-87 and selected concentration-time plots for two selected runs carried out at a low initial hydrocarbon/$NO_x$ ratio, two at a medium ratio, and one at a high ratio, are given in Figures IV-88 through IV-92, respectively.

In contrast to the results of the model simulations of the analogous "SAI surrogate" runs carried out in the ITC, the model simulations of these runs generally yielded good fits, on the average, to the rates of NO oxidation and ozone formation, but tended to overpredict the maximum ozone yields. Because of the better fits to the "timing" of these runs, the model gave much better fits to the results of several of the lower reactivity runs (e.g., run OTC-195A, shown in Figure IV-88, and run OTC-197B, where the fits are similar to that shown for OTC-195A), though the reactivity on subsequent days of OTC-205A, shown in Figure IV-89, was

Table IV-45. Initial Concentrations, Special Conditions, and Experimental and Calculated First Day Ozone Yields and Times Required to Achieve Half the Experimental Change in ([$O_3$]-[NO]) for the Multi-Day Surrogate-$NO_x$-Air Irradiations Carried Out in the SAPRC OTC

| Experiment | Special Conditions | | Initial Concentrations | | | Maximum Ozone Concentration | | | | Time to 1/2 Maximum Expt. ([$O_3$]-[NO]) | | | |
|---|---|---|---|---|---|---|---|---|---|---|---|---|---|
| | No. Run Days | Subsequent NO Injections (ppm [day])[a] | $NO_x$ (ppm) | HC (ppmC) | HC/$NO_x$ | Expt (ppm) | Calc (ppm) | Calc -Expt (ppm) | Calc -Expt /Expt) | Expt (min) | Calc (min) | Calc -Expt (min) | Calc -Expt /Expt |
| OTC-189A | 2 | | 0.453 | 3.3 | 7.4 | 0.576 | 0.815 | 0.239 | 0.41 | 130 | 114 | -16 | -0.12 |
| OTC-189B | 2 | | 0.452 | 3.4 | 7.5 | 0.712 | 0.889 | 0.176 | 0.25 | 147 | 123 | -24 | -0.17 |
| OTC-190A | 2 | | 0.415 | 3.1 | 7.5 | 0.702 | 0.880 | 0.177 | 0.25 | 126 | 135 | 9 | 0.07 |
| OTC-190B | 2 | | 0.417 | 3.0 | 7.3 | 0.669 | 0.837 | 0.168 | 0.25 | 134 | 136 | 2 | 0.02 |
| OTC-192A | 2 | | 0.465 | 3.5 | 7.5 | 0.735 | 0.904 | 0.169 | 0.23 | 128 | 126 | -3 | -0.02 |
| OTC-192B | 2 | 0.14 [2] | 0.527 | 3.4 | 6.4 | 0.754 | 0.823 | 0.070 | 0.09 | 141 | 148 | 7 | 0.05 |
| OTC-194A | 2 | | 0.379 | 6.1 | 16.2 | 0.737 | 1.020 | 0.283 | 0.38 | 67 | 54 | -13 | -0.20 |
| OTC-194B | 2 | | 0.380 | 3.1 | 8.2 | 0.603 | 0.753 | 0.149 | 0.25 | 82 | 57 | -25 | -0.31 |
| OTC-195A | 3 | | 0.413 | 1.5 | 3.7 | 0.164 | 0.157 | -0.007 | -0.04 | 122 | 132 | 10 | 0.08 |
| OTC-195B | 3 | | 0.413 | 3.5 | 8.4 | 0.681 | 0.835 | 0.155 | 0.23 | 112 | 101 | -11 | -0.10 |
| OTC-196B | 2 | | 0.411 | 3.0 | 7.3 | 0.597 | 0.849 | 0.251 | 0.42 | 122 | 110 | -12 | -0.10 |
| OTC-197A | 3 | | 0.380 | 3.0 | 8.0 | 0.621 | 0.610 | -0.011 | -0.02 | 117 | 137 | 19 | 0.16 |
| OTC-197B | 3 | | 0.771 | 3.1 | 4.0 | 0.152 | 0.161 | 0.010 | 0.06 | 134 | 124 | -10 | -0.07 |
| OTC-198A | 3 | | 0.693 | 4.1 | 5.9 | 0.704 | 0.657 | -0.047 | -0.07 | 97 | 117 | 19 | 0.20 |
| OTC-198B | 3 | | 0.375 | 3.0 | 8.0 | 0.674 | 0.671 | -0.003 | 0.00 | 108 | 132 | 25 | 0.23 |
| OTC-199A | 2 | | 0.369 | 3.0 | 8.0 | 0.591 | 0.696 | 0.105 | 0.18 | 121 | 116 | -5 | -0.04 |
| OTC-199B | 2 | 0.15 [2] | 0.365 | 2.9 | 8.1 | 0.606 | 0.682 | 0.076 | 0.13 | 130 | 127 | -3 | -0.03 |
| OTC-202A | 3 | | 0.780 | 5.8 | 7.5 | 0.714 | 0.590 | -0.124 | -0.17 | 89 | 106 | 16 | 0.18 |
| OTC-202B | 3 | 0.10 [3] | 0.396 | 3.3 | 8.3 | 0.522 | 0.484 | -0.038 | -0.07 | 112 | 108 | -4 | -0.04 |
| OTC-203A | 1 | | 0.389 | 3.0 | 7.6 | 0.231 | 0.325 | 0.094 | 0.41 | 133 | 107 | -26 | -0.19 |
| OTC-203B | 1 | | 0.187 | 2.9 | 15.7 | 0.394 | 0.503 | 0.109 | 0.28 | 127 | 81 | -46 | -0.36 |
| OTC-204A | 1 | 0.14 [3] | 0.335 | 2.9 | 8.8 | 0.302 | 0.422 | 0.120 | 0.40 | 125 | 98 | -26 | -0.21 |
| OTC-204B | 3 | 0.12 [3] | 0.171 | 3.0 | 17.6 | 0.381 | 0.528 | 0.147 | 0.39 | 98 | 72 | -25 | -0.26 |
| OTC-205A | 4 | | 0.651 | 3.1 | 4.7 | 0.039 | 0.108 | 0.069 | | 101 | 99 | -2 | -0.02 |
| OTC-205B | 4 | 0.11 [2], 0.11 [3], 0.07 [4] | 0.188 | 3.1 | 16.7 | 0.392 | 0.603 | 0.211 | 0.54 | 55 | 55 | 0 | 0.01 |
| Group Average | | | 0.431 | 3.3 | 8.6 | 0.530 | 0.632 | 0.102 | 0.20 | 114 | 108 | -6 | -0.05 |
| S. Dev. | | | 0.156 | 0.9 | 3.8 | 0.212 | 0.249 | 0.103 | 0.19 | 23 | 27 | 17 | 0.16 |
| Avg. Abs. Value | | | | | | | | 0.120 | 0.23 | | | 13 | 0.13 |
| S. Dev. | | | | | | | | 0.079 | 0.15 | | | 11 | 0.10 |

---

[a] When indicated, NO injections were made around the end of the first hour of the irradiation on the day(s) given in brackets.

Table IV-46. Experimental and Calculated Maximum Ozone Concentrations for Days 2-4 for the OTC Multi-Day Surrogate-$NO_x$-Air Irradiation

| Experiment | Day 2 Ozone Maximum | | | | Day 3 Ozone Maximum | | | | Day 4 Ozone Maximum | | | |
|---|---|---|---|---|---|---|---|---|---|---|---|---|
| | Expt (ppm) | Calc (ppm) | Calc -Expt (ppm) | Calc -Expt /Expt | Expt (ppm) | Calc (ppm) | Calc -Expt (ppm) | Calc -Expt /Expt | Expt (ppm) | Calc (ppm) | Calc -Expt (ppm) | Calc -Expt /Expt |
| OTC-189A | 0.352 | 0.644 | 0.292 | 0.83 | | | | | | | | |
| OTC-190A | 0.443 | 0.564 | 0.120 | 0.27 | | | | | | | | |
| OTC-192A | 0.394 | 0.700 | 0.306 | 0.78 | | | | | | | | |
| OTC-194A | 0.428 | 0.758 | 0.330 | 0.77 | | | | | | | | |
| OTC-195A | 0.398 | 0.484 | 0.086 | 0.22 | 0.196 | 0.423 | 0.227 | 1.16 | | | | |
| OTC-197A | 0.406 | 0.533 | 0.127 | 0.31 | | | | | | | | |
| OTC-198A | 0.525 | 0.624 | 0.100 | 0.19 | | | | | | | | |
| OTC-199A | 0.384 | 0.520 | 0.136 | 0.36 | | | | | | | | |
| OTC-202A | 0.371 | 0.415 | 0.045 | 0.12 | 0.278 | 0.380 | 0.102 | 0.37 | | | | |
| OTC-203A | a | | | | | | | | | | | |
| OTC-204A | 0.205 | 0.342 | 0.137 | 0.67 | 0.356 | 0.521 | 0.165 | 0.46 | | | | |
| OTC-205A | 0.456 | 0.743 | 0.287 | 0.63 | 0.338 | 0.597 | 0.259 | 0.77 | 0.131 | 0.442 | 0.311 | 2.39 |
| OTC-189B | 0.429 | 0.644 | 0.216 | 0.50 | | | | | | | | |
| OTC-190B | 0.403 | 0.570 | 0.167 | 0.41 | | | | | | | | |
| OTC-192B | 0.637 | 0.882 | 0.245 | 0.38 | | | | | | | | |
| OTC-194B | 0.468 | 0.624 | 0.155 | 0.33 | | | | | | | | |
| OTC-195B | 0.425 | 0.560 | 0.136 | 0.32 | 0.341 | 0.435 | 0.094 | 0.27 | | | | |
| OTC-196B | 0.366 | 0.502 | 0.135 | 0.37 | | | | | | | | |
| OTC-197B | b | | | | | | | | | | | |
| OTC-198B | 0.414 | 0.557 | 0.143 | 0.34 | | | | | | | | |
| OTC-199B | 0.587 | 0.732 | 0.145 | 0.25 | | | | | | | | |
| OTC-202B | 0.305 | 0.343 | 0.038 | 0.12 | | | | | | | | |
| OTC-204B | 0.265 | 0.381 | 0.116 | 0.44 | 0.375 | 0.556 | 0.181 | 0.48 | | | | |
| OTC-205B | 0.513 | 0.676 | 0.164 | 0.32 | 0.449 | 0.699 | 0.250 | 0.56 | 0.281 | 0.553 | 0.272 | 0.97 |
| Group Average | 0.417 | 0.582 | 0.165 | 0.41 | 0.333 | 0.516 | 0.183 | 0.58 | 0.206 | 0.498 | 0.292 | 1.68 |
| S. Dev. | 0.096 | 0.140 | 0.081 | 0.21 | 0.079 | 0.112 | 0.067 | 0.30 | 0.106 | 0.079 | 0.028 | 1.00 |
| Avg. Abs. Valu | | | 0.165 | 0.41 | | | 0.183 | 0.58 | | | 0.292 | 1.68 |
| S. Dev. | | | 0.081 | 0.21 | | | 0.067 | 0.30 | | | 0.028 | 1.00 |

---

[a] Run ended before start of day 2.
[b] Only day 1 of this experiment was modeled.

Table IV-47. Experimental and Calculated Reactant Half-Lives and Product Yields for Selected Species Observed on the First Day of the Multi-Day Surrogate-$NO_x$-Air Irradiations Carried Out in the OTC

| Experiment | Reactant Half-Life | | | | | Maximum Product Yields | | | | |
|---|---|---|---|---|---|---|---|---|---|---|
| | Species | Expt (min) | Calc (min) | Calc -Expt (min) | Calc -Expt /Expt | Species | Expt (ppm) | Calc (ppm) | Calc -Expt (ppm) | Calc -Expt /Expt |
| OTC-189A | Ethene | 252 | 254 | 2 | 0.01 | PAN | 0.021 | 0.083 | 0.062 | 2.97 |
| | Propene | 125 | 123 | -2 | -0.01 | Formaldehyde | 0.199 | 0.162 | -0.037 | -0.18 |
| | Toluene | 308 | 375 | 67 | 0.22 | | | | | |
| | m-Xylene | 156 | 152 | -5 | -0.03 | | | | | |
| OTC-190A | Ethene | 204 | 245 | 41 | 0.20 | PAN | 0.026 | 0.059 | 0.033 | 1.25 |
| | Propene | 105 | 124 | 19 | 0.18 | Formaldehyde | 0.276 | 0.153 | -0.123 | -0.44 |
| | Toluene | 344 | 390 | 46 | 0.13 | | | | | |
| | m-Xylene | 142 | 153 | 12 | 0.08 | | | | | |
| OTC-192A | Ethene | 208 | 240 | 32 | 0.15 | PAN | 0.056 | 0.079 | 0.023 | 0.40 |
| | Propene | 104 | 120 | 16 | 0.15 | Formaldehyde | 0.255 | 0.170 | -0.085 | -0.33 |
| | Toluene | 334 | 358 | 24 | 0.07 | | | | | |
| | m-Xylene | 142 | 151 | 9 | 0.06 | | | | | |
| OTC-194A | Ethene | 202 | 172 | -30 | -0.15 | PAN | 0.100 | 0.123 | 0.023 | 0.23 |
| | Propene | 80 | 75 | -5 | -0.07 | Formaldehyde | 0.251 | 0.311 | 0.060 | 0.24 |
| | Toluene | 340 | 390 | 50 | 0.15 | | | | | |
| | m-Xylene | 142 | 104 | -37 | -0.26 | | | | | |
| OTC-195A | Ethene | 270 | 300 | 30 | 0.11 | Formaldehyde | 0.069 | 0.071 | 0.002 | 0.03 |
| | Propene | 126 | 148 | 22 | 0.18 | | | | | |
| | Toluene | 270 | 300 | 30 | 0.11 | | | | | |
| | m-Xylene | 189 | 194 | 5 | 0.03 | | | | | |
| OTC-197A | Ethene | 208 | 255 | 47 | 0.23 | PAN | 0.062 | 0.064 | 0.002 | 0.03 |
| | Propene | 84 | 108 | 24 | 0.28 | Formaldehyde | 0.186 | 0.133 | -0.053 | -0.28 |
| | Toluene | 270 | 300 | 30 | 0.11 | | | | | |
| | m-Xylene | 117 | 147 | 30 | 0.26 | | | | | |

(continued)

Table IV-47 (continued) - 2

| Experiment | Reactant Half-Life | | | | | Maximum Product Yields | | | | |
|---|---|---|---|---|---|---|---|---|---|---|
| | Species | Expt (min) | Calc (min) | Calc -Expt (min) | Calc -Expt /Expt | Species | Expt (ppm) | Calc (ppm) | Calc -Expt (ppm) | Calc -Expt /Expt |
| OTC-198A | Ethene | 207 | 265 | 57 | 0.28 | PAN | 0.087 | 0.072 | -0.015 | -0.17 |
| | Propene | 78 | 108 | 30 | 0.39 | Formaldehyde | 0.426 | 0.274 | -0.152 | -0.36 |
| | Toluene | 270 | 300 | 30 | 0.11 | | | | | |
| | m-Xylene | 118 | 161 | 42 | 0.36 | | | | | |
| OTC-199A | Ethene | 236 | 267 | 32 | 0.13 | PAN | 0.057 | 0.060 | 0.003 | 0.06 |
| | Propene | 111 | 126 | 15 | 0.13 | Formaldehyde | 0.205 | 0.147 | -0.058 | -0.28 |
| | Toluene | 330 | 360 | 30 | 0.09 | | | | | |
| | m-Xylene | 131 | 158 | 26 | 0.20 | | | | | |
| OTC-202A | Ethene | 207 | 240 | 33 | 0.16 | PAN | 0.086 | 0.073 | -0.013 | -0.15 |
| | Propene | 99 | 108 | 9 | 0.09 | Formaldehyde | 0.219 | 0.259 | 0.040 | 0.18 |
| OTC-203A | Ethene | 327 | 330 | 3 | 0.01 | PAN | 0.016 | 0.036 | 0.020 | 1.27 |
| | Propene | 192 | 191 | -1 | -0.01 | Formaldehyde | 0.178 | 0.131 | -0.047 | -0.26 |
| | Toluene | 345 | 330 | -15 | -0.04 | | | | | |
| | m-Xylene | 258 | 253 | -5 | -0.02 | | | | | |
| OTC-204A | Ethene | 316 | 327 | 11 | 0.03 | PAN | 0.049 | 0.048 | -0.001 | -0.03 |
| | Propene | 131 | 143 | 12 | 0.09 | Formaldehyde | 0.251 | 0.138 | -0.113 | -0.45 |
| OTC-205A | Ethene | 283 | 299 | 17 | 0.06 | Formaldehyde | 0.184 | 0.138 | -0.046 | -0.25 |
| | Propene | 171 | 188 | 17 | 0.10 | | | | | |
| OTC-189B | Ethene | 220 | 212 | -8 | -0.04 | PAN | 0.025 | 0.072 | 0.047 | 1.88 |
| | Propene | 103 | 95 | -8 | -0.07 | Formaldehyde | 0.157 | 0.168 | 0.012 | 0.07 |
| | Toluene | 311 | 315 | 4 | 0.01 | | | | | |
| | m-Xylene | 130 | 125 | -5 | -0.04 | | | | | |
| OTC-190B | Ethene | 178 | 226 | 49 | 0.27 | PAN | 0.018 | 0.060 | 0.042 | 2.32 |
| | Propene | 85 | 104 | 19 | 0.22 | Formaldehyde | 0.228 | 0.149 | -0.079 | -0.35 |
| | Toluene | 315 | 330 | 15 | 0.05 | | | | | |
| | m-Xylene | 108 | 137 | 30 | 0.28 | | | | | |

(continued)

Table IV-47 (continued) - 3

| Experiment | Reactant Half-Life | | | | | Maximum Product Yields | | | | |
|---|---|---|---|---|---|---|---|---|---|---|
| | Species | Expt (min) | Calc (min) | Calc -Expt (min) | Calc -Expt /Expt | Species | Expt (ppm) | Calc (ppm) | Calc -Expt (ppm) | Calc -Expt /Expt |
| OTC-192B | Ethene | 205 | 244 | 39 | 0.19 | PAN | 0.058 | 0.070 | 0.012 | 0.21 |
| | Propene | 91 | 112 | 21 | 0.23 | Formaldehyde | 0.284 | 0.162 | -0.122 | -0.43 |
| | Toluene | 326 | 360 | 34 | 0.11 | | | | | |
| | m-Xylene | 120 | 152 | 32 | 0.26 | | | | | |
| OTC-194B | Ethene | 218 | 224 | 7 | 0.03 | PAN | 0.055 | 0.071 | 0.016 | 0.28 |
| | Propene | 102 | 96 | -6 | -0.06 | Formaldehyde | 0.190 | 0.142 | -0.049 | -0.26 |
| | Toluene | 330 | 300 | -30 | -0.09 | | | | | |
| | m-Xylene | 130 | 130 | 0 | 0.00 | | | | | |
| OTC-195B | Ethene | 198 | 214 | 16 | 0.08 | PAN | 0.055 | 0.065 | 0.010 | 0.18 |
| | Propene | 93 | 102 | 9 | 0.09 | Formaldehyde | 0.171 | 0.168 | -0.003 | -0.02 |
| | Toluene | 360 | 300 | -60 | -0.17 | | | | | |
| | m-Xylene | 111 | 129 | 19 | 0.17 | | | | | |
| OTC-196B | Ethene | 224 | 226 | 2 | 0.01 | Formaldehyde | 0.207 | 0.169 | -0.038 | -0.18 |
| | Propene | 107 | 120 | 13 | 0.12 | | | | | |
| | Toluene | 240 | 270 | 30 | 0.12 | | | | | |
| | m-Xylene | 103 | 110 | 7 | 0.07 | | | | | |
| OTC-197B | Ethene | 288 | 300 | 12 | 0.04 | Formaldehyde | 0.213 | 0.133 | -0.080 | -0.37 |
| | Propene | 109 | 186 | 77 | 0.71 | | | | | |
| | Toluene | 360 | 300 | -60 | -0.17 | | | | | |
| | m-Xylene | 205 | 230 | 26 | 0.13 | | | | | |
| OTC-198B | Ethene | 199 | 252 | 53 | 0.26 | PAN | 0.059 | 0.051 | -0.008 | -0.14 |
| | Propene | 95 | 115 | 21 | 0.22 | | | | | |
| | Toluene | 270 | 300 | 30 | 0.11 | | | | | |
| | m-Xylene | 120 | 159 | 39 | 0.32 | | | | | |
| OTC-199B | Ethene | 199 | 245 | 46 | 0.23 | PAN | 0.055 | 0.055 | 0.000 | 0.00 |
| | Propene | 94 | 105 | 11 | 0.11 | Formaldehyde | 0.215 | 0.146 | -0.069 | -0.32 |
| | Toluene | 270 | 300 | 30 | 0.11 | | | | | |
| | m-Xylene | 132 | 140 | 8 | 0.06 | | | | | |

(continued)

Table IV-47 (continued) - 4

| Experiment | Reactant Half-Life | | | | | Maximum Product Yields | | | | |
|---|---|---|---|---|---|---|---|---|---|---|
| | Species | Expt (min) | Calc (min) | Calc -Expt (min) | Calc -Expt /Expt | Species | Expt (ppm) | Calc (ppm) | Calc -Expt (ppm) | Calc -Expt /Expt |
| OTC-202B | Ethene | 269 | 287 | 18 | 0.07 | PAN | 0.046 | 0.047 | 0.001 | 0.02 |
| | | | | | | Formaldehyde | 0.123 | 0.138 | 0.015 | 0.12 |
| OTC-203B | Ethene | 305 | 291 | -14 | -0.05 | PAN | 0.026 | 0.067 | 0.041 | 1.58 |
| | Propene | 122 | 98 | -24 | -0.20 | Formaldehyde | 0.221 | 0.137 | -0.085 | -0.38 |
| | Toluene | 315 | 330 | 15 | 0.05 | | | | | |
| | m-Xylene | 162 | 144 | -18 | -0.11 | | | | | |
| OTC-204B | Ethene | 240 | 250 | 10 | 0.04 | PAN | 0.061 | 0.056 | -0.005 | -0.07 |
| | Propene | 95 | 82 | -14 | -0.15 | Formaldehyde | 0.203 | 0.137 | -0.066 | -0.32 |
| OTC-205B | Ethene | 192 | 196 | 4 | 0.02 | PAN | 0.046 | 0.055 | 0.009 | 0.19 |
| | Propene | 53 | 59 | 6 | 0.11 | Formaldehyde | 0.224 | 0.149 | -0.075 | -0.33 |
| Group Average | Ethene | 234 | 254 | 20 | 0.10 | PAN | 0.051 | 0.065 | 0.014 | 0.59 |
| Std. Dev. | | 43 | 39 | 22 | 0.11 | | 0.023 | 0.017 | 0.021 | 0.91 |
| Avg. Abs Value | | | | 24 | 0.11 | | | | 0.018 | 0.64 |
| Std. Dev. | | | | 18 | 0.09 | | | | 0.017 | 0.87 |
| Group Average | Propene | 107 | 118 | 12 | 0.12 | Formaldehyde | 0.214 | 0.162 | -0.052 | -0.22 |
| Std. Dev. | | 29 | 33 | 19 | 0.19 | | 0.065 | 0.051 | 0.053 | 0.21 |
| Avg. Abs Value | | | | 17 | 0.17 | | | | 0.063 | 0.27 |
| Std. Dev. | | | | 15 | 0.14 | | | | 0.039 | 0.12 |
| Group Average | Toluene | 311 | 327 | 16 | 0.06 | | | | | |
| Std. Dev. | | 36 | 35 | 34 | 0.10 | | | | | |
| Avg. Abs Value | | | | 33 | 0.11 | | | | | |
| Std. Dev. | | | | 17 | 0.05 | | | | | |
| Group Average | m-Xylene | 143 | 154 | 11 | 0.10 | | | | | |
| Std. Dev. | | 38 | 37 | 20 | 0.16 | | | | | |
| Avg. Abs Value | | | | 19 | 0.14 | | | | | |
| Std. Dev. | | | | 14 | 0.11 | | | | | |

```
-----------------------------------------------------------------------
       Calc.-Expt./Calc.                     Calc.-Expt./Calc.
         Maximum Ozone               Time to 1/2 Expt. Δ([O3]-[NO])max
-----------------------------------------------------------------------
         <  -0.33    :                          <  -0.55     :
    -0.33 -  -0.27    :                  -0.55 -  -0.45     :
    -0.27 -  -0.21    :                  -0.45 -  -0.35     :1
    -0.21 -  -0.15    :                  -0.35 -  -0.25     :11
    -0.15 -  -0.09    :1                 -0.25 -  -0.15     :1111
    -0.09 -  -0.03    :11                -0.15 -  -0.05     :1111
    -0.03 -   0.03    :1111              -0.05 -   0.05     :11111111
     0.03 -   0.09    :111                0.05 -   0.15     :11
     0.09 -   0.15    :111111             0.15 -   0.25     :1111
     0.15 -   0.21    :11111              0.25 -   0.35     :
     0.21 -   0.27    :111                0.35 -   0.45     :
     0.27 -   0.33    :1                  0.45 -   0.55     :
         >   0.33    :                          >   0.55     :
--------------------------------------------------------------------
(Calc.-Expt.)
  /Expt.       Ethene         Propene        Toluene       m-Xylene
 Half Life
--------------------------------------------------------------------
     < -0.5    :              :              :             :
-0.5 - -0.4    :              :              :             :
-0.4 - -0.3    :              :              :             :
-0.3 - -0.2    :              :              :             :1
-0.2 - -0.1    :1             :11            :11           :1
-0.1 -  0.0    :11            :11111         :11           :111
 0.0 -  0.1    :11111111111   :111           :11111        :111111
 0.1 -  0.2    :11111         :11111111      :111111111    :11
 0.2 -  0.3    :111111        :1111          :1            :1111
 0.3 -  0.4    :              :1             :             :11
 0.4 -  0.5    :              :              :             :
     >  0.5    :              :1             :             :
-----------------------------------------------------------------------
(Calc.-Expt.)
  /Expt.        PAN           Formaldehyde
Product Yield
-----------------------------------------------------------------------
     < -0.5    :              :
-0.5 - -0.4    :              :111
-0.4 - -0.3    :              :11111111
-0.3 - -0.2    :              :11111
-0.2 - -0.1    :111           :11
-0.1 -  0.0    :11            :1
 0.0 -  0.1    :1111          :11
 0.1 -  0.2    :11            :11
 0.2 -  0.3    :111           :1
 0.3 -  0.4    :              :
 0.4 -  0.5    :1             :
     >  0.5    :111111        :
-----------------------------------------------------------------------
```

Figure IV-87. Distribution plots for discrepancies between calculated and experimental first day maximum ozone yields, times required to achieve half the maximum experimental change in ($[O_3]-[NO]$), and selected reactant half-lives and organic product yields in the model simulations of the first day of the multi-day surrogate-$NO_x$-air irradiations carried out in the SAPRC OTC.

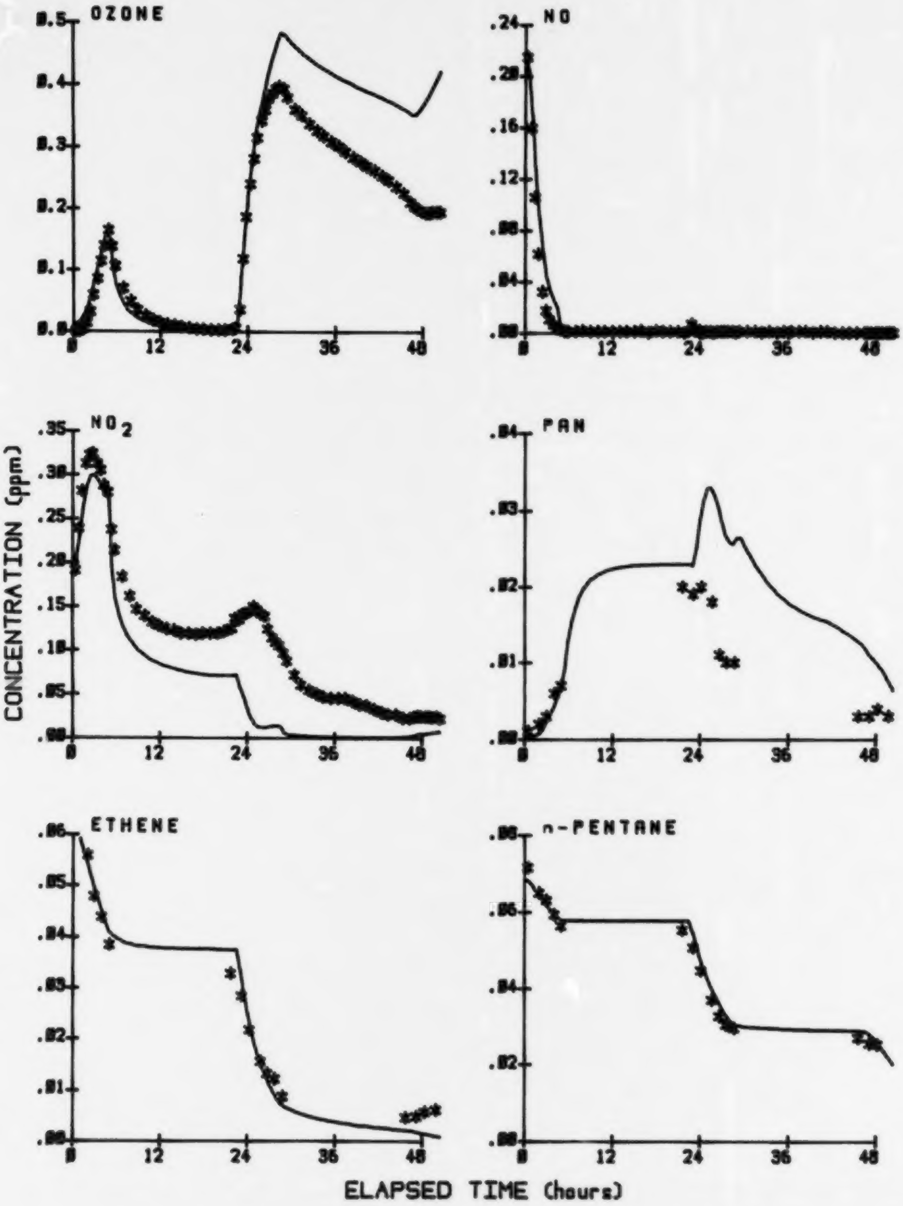

Figure IV-88. Experimental and calculated concentration-time plots for representative species observed in the multi-day surrogate run OTC-195A.
.... or * = Experimental data.
----- = Model calculation.

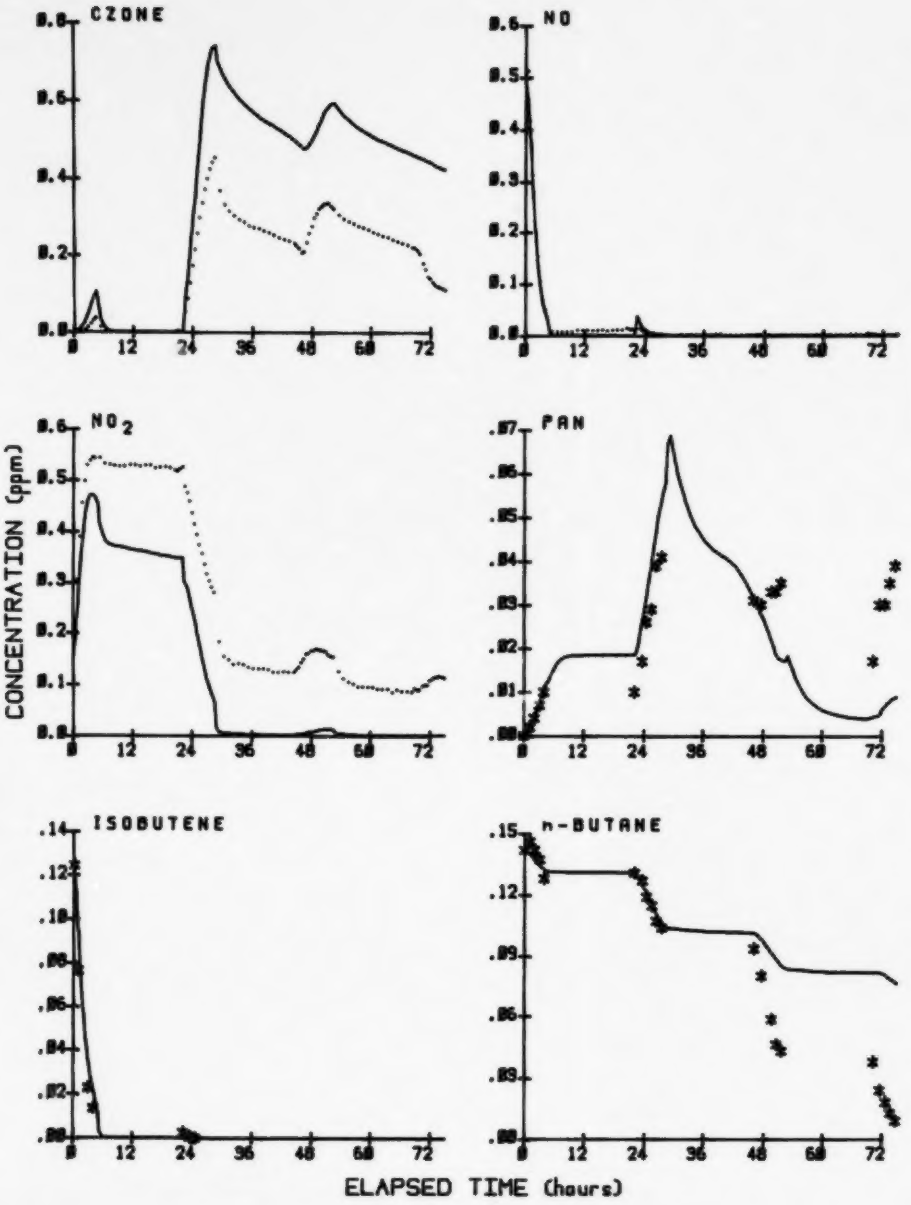

Figure IV-89. Experimental and calculated concentration-time plots for representative species observed in the multi-day surrogate run OTC-205A.
.... or * = Experimental data.
----- = Model calculation.

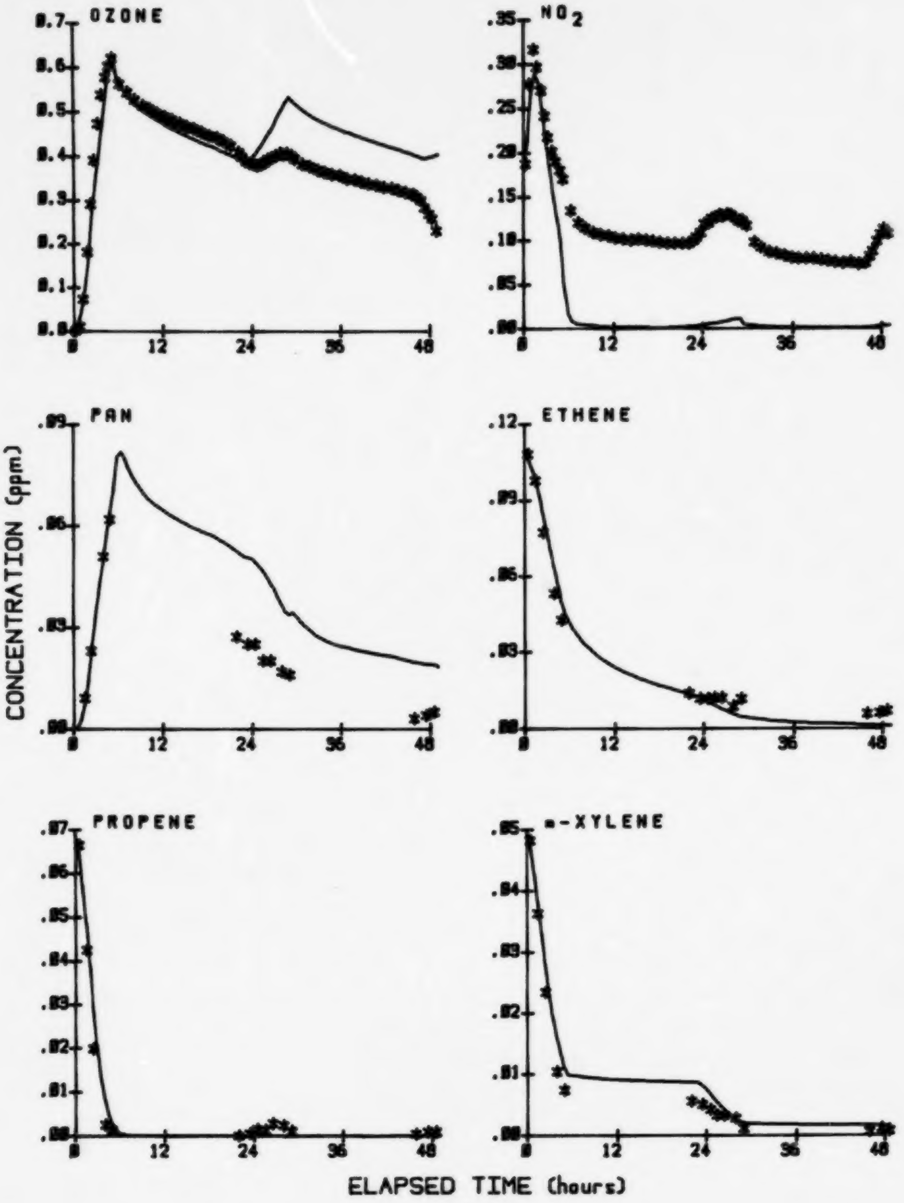

Figure IV-90. Experimental and calculated concentration-time plots for representative species observed in the multi-day surrogate run OTC-197A.
.... or * = Experimental data.
----- = Model calculation.

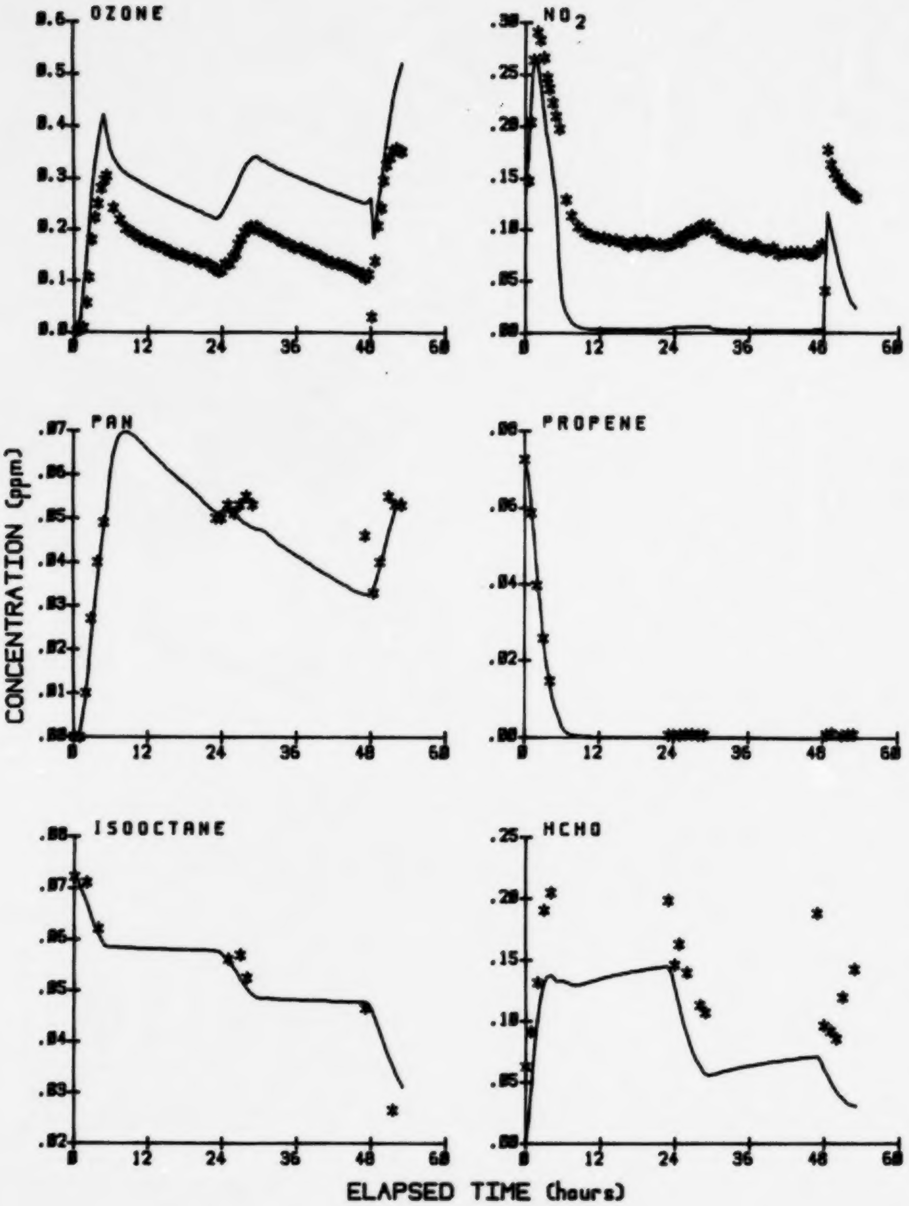

Figure IV-91. Experimental and calculated concentration-time plots for representative species observed in the multi-day surrogate run OTC-204A.
.... or * = Experimental data.
----- = Model calculation.

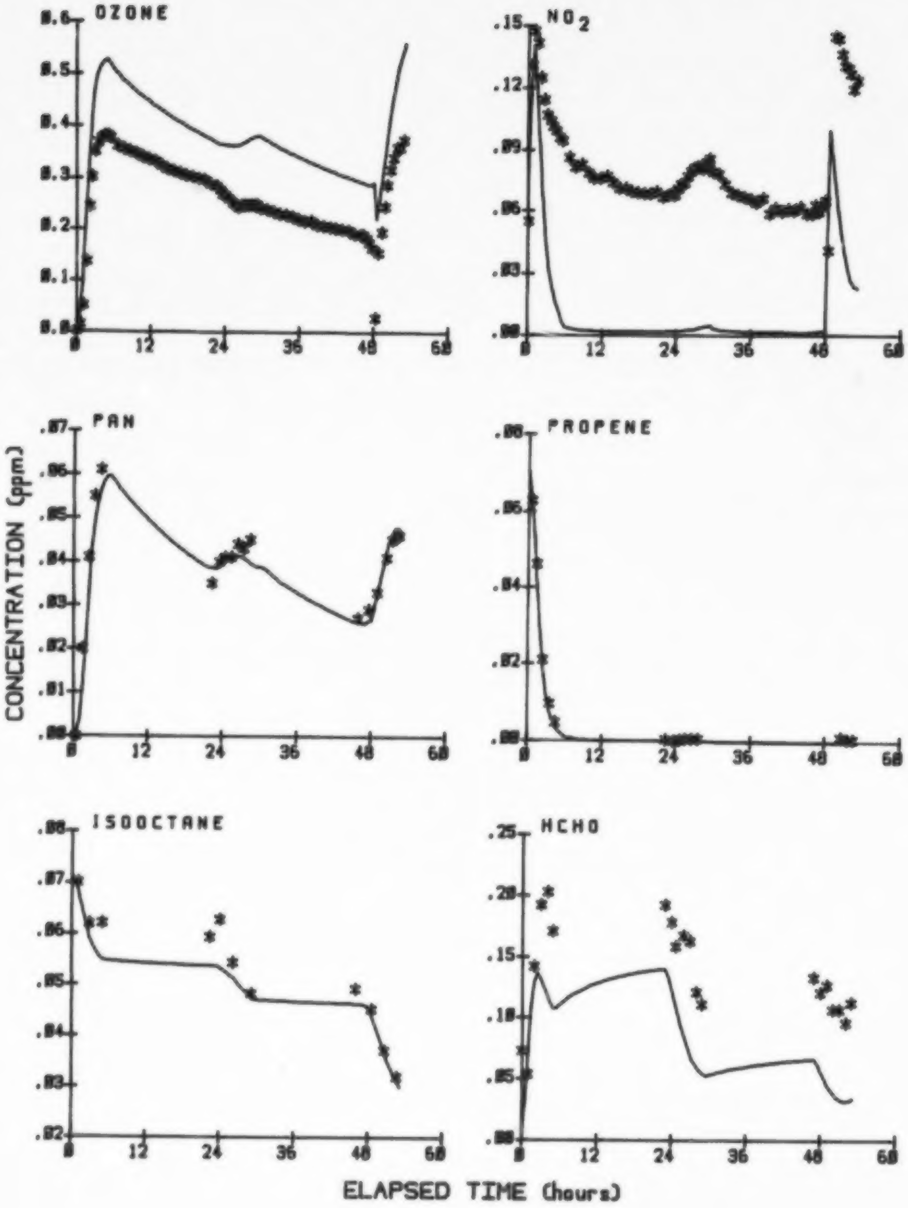

Figure IV-92. Experimental and calculated concentration-time plots for representative species observed in the multi-day surrogate run OTC-204B
.... or * = Experimental data.
----- = Model calculation.

overpredicted. In the intermediate and high hydrocarbon/$NO_x$ runs, the model tended to overpredict ozone, but usually by a consistent amount, as shown in Figures IV-91 and IV-92. As shown in Figures IV-91 and IV-92, the model also tends to overpredict the amount of ozone which is formed when NO was injected on subsequent days of the runs. In some cases, on subsequent days of runs where the initially present $NO_x$ was consumed and where NO was not injected, the model predicts that a small amount of ozone is formed while no increase in ozone is observed experimentally (e.g., the last day of run OTC-195A, shown in Figure IV-88), but in others (e.g., the second day of run OTC-204B) the model correctly predicts that no increase of ozone occurs.

However, despite the discrepancies noted above, in general the model was at least qualitatively consistent with the experimental data in terms of predicting multi-day effects, and in some cases quantitative agreement was also obtained. In view of the greater difficulty in exactly simulating results of multi-day experiments as compared to single day runs, and the greater uncertainties and variability associated with outdoor chamber experiments as compared with those carried out in indoor chambers, the performance of the model in simulating the results of these multi-day, outdoor chamber runs is probably as good as one might reasonably expect.

### 10. Runs Employing Miscellaneous UNC Mixtures

Twenty-five irradiations carried out at UNC, and which were modeled in this program, involved mixtures of organics including compounds which are not represented explicitly in this model. The mixtures and compounds employed in each of these runs are indicated in Table IV-48. The method used to represent the reactions of these mixtures in the model, and the results of the model simulations of these runs, are summarized below.

#### a. Lumping Technique Employed

For each of the 25 runs in this group, species lumping was accomplished by employing a pre-processing computer program which read the initial concentrations of the individual organics in each run. Using

Table IV-48. Summary of Initial Reactant Concentrations, Organic Mixtures Present and Experimental and Calculated Ozone Yields and Times Required to Achieve Half the Maximum Experimental Change in ($[O_3]-[NO]$) for the UNC Complex Mixture Runs

| Experiment | Mixtures[a] and Organics Present | Initial Concentrations | | | Maximum Ozone Concentration | | | | Time to 1/2 Maximum Expt. ($[O_3]-[NO]$) | | | |
|---|---|---|---|---|---|---|---|---|---|---|---|---|
| | | $NO_x$ (ppm) | HC (ppmC) | $HC/NO_x$ | Expt (ppm) | Calc (ppm) | Calc -Expt (ppm) | Calc -Expt /Expt) | Expt (min) | Calc (min) | Calc -Expt (min) | Calc -Expt /Expt |
| JL2281R | UNCMIX | 0.262 | 2.4 | 9.2 | 0.626 | 0.419 | -0.208 | -0.33 | 239 | 275 | 35 | 0.15 |
| JL2181B | UNCMIX | 0.244 | 1.3 | 5.5 | 0.237 | 0.216 | -0.021 | -0.09 | 379 | 349 | -30 | -0.08 |
| NV1582B | UNCMIX | 0.183 | 2.7 | 15.0 | 0.167 | 0.294 | 0.127 | 0.76 | 399 | 293 | -106 | -0.27 |
| DE0782B | UNCMIX | 0.186 | 3.5 | 18.8 | 0.093 | 0.322 | 0.230 | 2.48 | 423 | 258 | -165 | -0.39 |
| ST2081R | UNCMIX + COMARO | 0.231 | 2.3 | 9.9 | 0.403 | 0.467 | 0.063 | 0.16 | 436 | 332 | -104 | -0.24 |
| DE0782R | UNCMIX + COMARO | 0.185 | 3.4 | 18.2 | 0.076 | 0.368 | 0.292 | 3.82 | 415 | 246 | -169 | -0.41 |
| AU2681R | UNCMIX + SIMARO | 0.244 | 2.0 | 8.3 | 0.506 | 0.515 | 0.009 | 0.02 | 402 | 357 | -45 | -0.11 |
| ST0381R | UNCMIX + SIMARO | 0.240 | 1.8 | 7.4 | 0.541 | 0.431 | -0.110 | -0.20 | 369 | 396 | 27 | 0.07 |
| ST1081R | UNCMIX + SIMARO | 0.237 | 2.8 | 11.8 | 0.610 | 0.585 | -0.026 | -0.04 | 378 | 297 | -81 | -0.21 |
| ST2081B | UNCMIX + SIMARO | 0.229 | 2.1 | 9.1 | 0.414 | 0.439 | 0.025 | 0.06 | 404 | 342 | -61 | -0.15 |
| AU2681B | SIMMIX + SIMARO | 0.236 | 2.0 | 8.3 | 0.544 | 0.452 | -0.092 | -0.17 | 413 | 401 | -11 | -0.03 |
| AU2781B | SIMMIX + SIMARO | 0.229 | 2.0 | 8.8 | 0.625 | 0.489 | -0.135 | -0.22 | 434 | 416 | -18 | -0.04 |
| JL2081B | UNCMIX + Toluene | 0.422 | 1.8 | 4.2 | 0.165 | 0.077 | -0.087 | -0.53 | 406 | 475 | 69 | 0.17 |
| ST1682R | UNCMIX + Ethylbenzene | 0.422 | 3.2 | 7.6 | 0.410 | 0.445 | 0.035 | 0.09 | 399 | 403 | 4 | 0.01 |
| JL2081R | UNCMIX + m-Xylene | 0.411 | 1.8 | 4.3 | 0.635 | 0.354 | -0.281 | -0.44 | 323 | 367 | 44 | 0.14 |
| OC1481R | UNCMIX + m-Xylene | 0.281 | 3.3 | 11.8 | 0.462 | 0.510 | 0.048 | 0.10 | 310 | 284 | -26 | -0.08 |
| JL2281B | UNCMIX + m-Xylene | 0.258 | 2.7 | 10.3 | 0.722 | 0.503 | -0.219 | -0.30 | 320 | 334 | 13 | 0.04 |
| ST1682B | UNCMIX + m-Xylene | 0.426 | 3.1 | 7.3 | 0.840 | 0.725 | -0.115 | -0.14 | 365 | 369 | 3 | 0.01 |
| ST2981B | UNCMIX + m-Xylene | 0.241 | 2.5 | 10.2 | 0.485 | 0.452 | -0.033 | -0.07 | 391 | 346 | -45 | -0.11 |
| ST2981R | UNCMIX + Toluene | 0.238 | 2.5 | 10.4 | 0.294 | 0.461 | 0.167 | 0.57 | 450 | 325 | -125 | -0.28 |
| ST0381B | UNCMIX + SIMARO + Propene | 0.235 | 2.0 | 8.4 | 0.611 | 0.481 | -0.130 | -0.21 | 349 | 327 | -22 | -0.06 |
| ST1081B | UNCMIX + SIMARO + n-Butane | 0.246 | 1.0 | 4.1 | 0.626 | 0.500 | -0.126 | -0.20 | 424 | 424 | -1 | 0.00 |
| JL0882R | SIMARO + Propene + n-Butane | 0.290 | 2.1 | 7.2 | 0.598 | 0.633 | 0.035 | 0.06 | 352 | 302 | -49 | -0.14 |
| JL0882B | COMARO + Propene + n-Butane | 0.283 | 2.1 | 7.5 | 0.541 | 0.612 | 0.071 | 0.13 | 350 | 279 | -71 | -0.20 |
| OC1481B | UNCMIX + 1,2,4-Trimethylbenzene | 0.294 | 2.7 | 9.3 | 0.458 | 0.476 | 0.018 | 0.04 | 331 | 272 | -59 | -0.18 |

(continued)

Table IV-48 (continued) - 2

| Experiment | Mixtures[a] and Organics Present | Initial Concentrations | | | Maximum Ozone Concentration | | | | Time to 1/2 Maximum Expt. ($[O_3]-[NO]$) | | | |
|---|---|---|---|---|---|---|---|---|---|---|---|---|
| | | $NO_x$ (ppm) | HC (ppmC) | $HC/NO_x$ | Expt (ppm) | Calc (ppm) | Calc -Expt (ppm) | Calc -Expt /Expt) | Expt (min) | Calc (min) | Calc -Expt (min) | Calc -Expt /Expt |
| Group Average | | 0.270 | 2.4 | 9.3 | 0.468 | 0.449 | -0.019 | 0.21 | 378 | 339 | -40 | -0.10 |
| S. Dev. | | 0.073 | 0.6 | 3.7 | 0.199 | 0.133 | 0.137 | 0.95 | 49 | 58 | 61 | 0.15 |
| Avg. Abs. Value | | | | | | | 0.108 | 0.45 | | | 54 | 0.14 |
| S. Dev. | | | | | | | 0.084 | 0.86 | | | 47 | 0.11 |

[a] Compounds present in UNC mixtures (Jeffries et al. 1985a).

UNCMIX = n-pentane + isopentane + 2-methylpentane + 2,4-dimethylpentane + 2,2,4-trimethylpentane + ethene + propene + 1-butene + cis-2-butene + 2-methyl-1-butene + 2-methyl-2-butene.

COMARO = toluene + m-xylene + 1,2,4-trimethylbenzene + n-propylbenzene + s-butylbenzene.

SIMARO = toluene + m-xylene + 1,2,4-trimethylbenzene.

SIMMIX = n-butane + n-pentane + ethene + propene.

these data, and a data base giving the rate constants and (where applicable) other reactivity parameters for the individual reactants, this program determined the initial concentrations or reactivity parameters for lumped or representative species used in the model. The program thus produced output data which were used as input to the model simulation program. The lumping methods employed were somewhat different for alkanes, alkenes, and aromatics, and these are discussed separately below.

Alkanes. All of the $\geq C_5$ alkanes present in a given run were lumped together as a single species which reacted with the OH radical with a rate constant which is the weighed average of those for the alkanes in the run, and whose mechanistic and product yield parameters (p1 through pC, and p'1 through p'C, as defined in Section II-F-3) were also weighed averages of those for the individual alkanes. n-Butane was not lumped but was represented explicitly in the model. The alkane lumping technique employed is discussed in Section II-F-3, where the specific equations used to derive the parameters for the lumped species, which in general were different for each run which had different mixtures of $\geq C_5$ alkanes, are given. The OH radical rate constants for the individual alkanes which were used to determine the rate constant for the lumped $\geq C_5$ alkane are given in Table II-21, and the mechanistic and product yield parameters are given in Tables II-22 through II-31. The average kinetic parameters and rate constants were calculated for 270, 300, and 330 K, and the values used at a given temperature when carrying out a model simulation were determined by linear extrapolation (for the mechanistic and product yield parameters) or by fitting them to an Arrhenius expression (for the OH radical rate constants).

Alkenes. The reactions of the alkenes present in a given run were represented by a maximum of three species: ethene, whose reactions were represented explicitly; a lumped 1-alkene; and a lumped internal alkene. The lumping technique employed for the 1-alkenes and the internal alkenes is analogous to that employed for the alkanes and is described in Section II-D-7. Specifically, the OH radical, ozone, $O(^3P)$ atom, and $NO_3$ radical rate constants used for the lumped 1-alkene were weighed averages of the corresponding rate constants for the specific 1-alkenes in the run (which in general varied from run to run), and the alkene structural and product yield parameters, designated p1 through p6 in Section II-D-7, used for the lumped specie were weighed averages of the corresponding parameters for the individual alkenes that the particular specie represents. The rate constants and parameters for the lumped internal alkene were determined in exactly the same way. The rate constants for the specific alkenes present in these runs, which were used for determining the lumped rate constants employed, are given in Table II-17. The temperature dependencies for the rate constants for the lumped species were determined as indicated above for the alkanes.

Aromatics. The reactions of the aromatic hydrocarbons present in a given run were represented by a maximum of three species: a lumped monoalkyl benzene, a lumped dialkylbenzene, and a lumped trialkylbenzene. (Benzene was not present in any of these mixtures; if it were, its reactions would have been treated separately.) The lumped monoalkylbenzene was represented in the model as reacting with the same mechanism, and forming the same products, as toluene, except that its OH radical rate constant was a weighed average of those for the monoalkylbenzenes present in the runs, which in general varied from run to run. Likewise, the dialkylbenzenes were represented by the m-xylene mechanism, and the trialkylbenzenes were represented by the 1,3,5-trimethylbenzene (1,3,5-TMB) mechanism, but with the OH radical rate constant determined by weighed averages of the rate constants for the individual compounds those lumped species represent. The Arrhenius parameters used to determine the OH radical rate constants for the specific aromatics present in these runs, which were used to determine the rate constants for the lumped aromatic species, are given in Table IV-49. The temperature dependencies for the rate constants for the lumped species were determined as indicated above for the alkanes.

### b. Results of Model Simulations

The experimental and calculated ozone yields, NO oxidation and ozone formation times, and PAN yields are summarized for each of these 25 runs in Table IV-48, and experimental and calculated ethene half-lives and PAN and formaldehyde yields are summarized in Table IV-50. Figure IV-93 gives the distribution plots for the discrepancies in the predictions of these measures of reactivity. The discrepancies in the predictions of the maximum ozone yields and in the predictions of the NO oxidation/ozone formation times are plotted against initial hydrocarbon/$NO_x$ ratios in Figures IV-94 and IV-95, respectively. Selected concentration-time profiles for one of the runs which was relatively well simulated, for one of those where reactivity was overpredicted, and one where it was underpredicted are given in Figures IV-96 through IV-98, respectively.

Table IV-49. Arrhenius Parameters and 298 K Rate Constants for the Reaction of the OH Radical with Aromatic Hydrocarbons Represented in the Model Calculations Carried Out in this Program

| Aromatic | A (cm$^3$ mole$^{-1}$ sec$^{-1}$) | Ea (Cal mole$^{-1}$) | k (289 K) (cm$^3$ mole$^{-1}$ sec$^{-1}$) | Notes |
|---|---|---|---|---|
| Benzene | 7.57 x 10-12 | 1050 | 1.29 x 10-12 | a,b |
| Toluene | 2.10 x 10-12 | -640 | 6.19 x 10-12 | a,b |
| m-Xylene | 1.66 x 10-11 | -231 | 2.45 x 10-11 | a,b |
| o-Xylene | 1.47 x 10-11 | 0 | 1.47 x 10-11 | a,b |
| p-Xylene | 1.52 x 10-11 | 0 | 1.52 x 10-11 | b |
| Ethylbenzene | 7.5 x 10-12 | 0 | 7.5 x 10-12 | b,c |
| i-Propylbenzene | 6.6 x 10-12 | 0 | 6.6 x 10-12 | c,d |
| n-Propylbenzene | 5.7 x 10-12 | 0 | 5.7 x 10-12 | b,c |
| s-Butylbenzene | 6.6 x 10-12 | 0 | 6.6 x 10-12 | e |
| 1,2,3-TMB | 3.3 x 10-11 | 0 | 3.33 x 10-11 | c,f |
| 1,2,4-TMB | 4.0 x 10-11 | 0 | 4.0 x 10-11 | c,f |
| 1,3,5-TMB | 6.2 x 10-11 | 0 | 6.24 x 10-11 | c,f |

[a] Discussed in Section II-F of this report.

[b] Recommended by Atkinson (1986).

[c] No recommendation for temperature dependence. Temperature dependence ignored.

[d] See Atkinson (1986). No recommendation made.

[e] Assumed to be the same as i-propyl benzene.

[f] Room temperature value of Perry et al. (1977a) used. See Atkinson (1986).

Table IV-50. Experimental and Calculated Ethene Half-Lives and PAN and Formaldehyde Yields for the UNC Chamber Runs Employing Miscellaneous Complex Mixtures

| Experiment | Ethene Half-Life | | | | | Maximum Product Yields | | | | |
|---|---|---|---|---|---|---|---|---|---|---|
| | Species | Expt (min) | Calc (min) | Calc -Expt (min) | Calc -Expt /Expt | Species | Expt (ppm) | Calc (ppm) | Calc -Expt (ppm) | Calc -Expt /Expt |
| JL2281R | | | | | | PAN | 0.055 | 0.020 | -0.035 | -0.64 |
| | | | | | | Formaldehyde | 0.174 | 0.051 | -0.123 | -0.71 |
| JL2181B | Ethene | 509 | 550 | 41 | 0.08 | PAN | 0.013 | 0.013 | 0.001 | 0.07 |
| NV1582B | Ethene | 412 | 583 | 171 | 0.41 | | | | | |
| DE0782B | Ethene | 447 | 537 | 90 | 0.20 | Formaldehyde | 0.100 | 0.085 | -0.015 | -0.15 |
| ST2081R | Ethene | 531 | 483 | -48 | -0.09 | | | | | |
| DE0782R | Ethene | 453 | 467 | 14 | 0.03 | PAN | 0.010 | 0.081 | 0.071 | 6.80 |
| | | | | | | Formaldehyde | 0.064 | 0.070 | 0.006 | 0.09 |
| AU2681R | Ethene | 452 | 456 | 4 | 0.01 | PAN | 0.020 | 0.022 | 0.002 | 0.08 |
| | | | | | | Formaldehyde | 0.106 | 0.052 | -0.054 | -0.51 |
| ST0381R | a | | | | | | | | | |
| ST1081R | Ethene | 367 | 325 | -42 | -0.11 | | | | | |
| ST2081B | Ethene | 500 | 479 | -21 | -0.04 | | | | | |
| AU2681B | Ethene | 427 | 430 | 3 | 0.01 | PAN | 0.014 | 0.029 | 0.014 | 1.01 |
| | | | | | | Formaldehyde | 0.150 | 0.056 | -0.094 | -0.63 |
| AU2781B | Ethene | 435 | 421 | -14 | -0.03 | Formaldehyde | 0.208 | 0.068 | -0.140 | -0.67 |
| JL2081B | Ethene | 472 | 570 | 99 | 0.21 | Formaldehyde | 0.176 | 0.038 | -0.138 | -0.78 |
| ST1682R | Ethene | 485 | 562 | 77 | 0.16 | PAN | 0.015 | 0.032 | 0.017 | 1.17 |
| | | | | | | Formaldehyde | 0.140 | 0.085 | -0.054 | -0.39 |
| JL2081R | Ethene | 374 | 529 | 155 | 0.41 | PAN | 0.037 | 0.025 | -0.011 | -0.31 |
| | | | | | | Formaldehyde | 0.058 | 0.063 | 0.005 | 0.08 |

(continued)

Table IV-50 (continued) - 2

| Experiment | Ethene Half-Life | | | | | Maximum Product Yields | | | | |
|---|---|---|---|---|---|---|---|---|---|---|
| | Species | Expt (min) | Calc (min) | Calc -Expt (min) | Calc -Expt /Expt | Species | Expt (ppm) | Calc (ppm) | Calc -Expt (ppm) | Calc -Expt /Expt |
| OC1481R | Ethene | 482 | 455 | -27 | -0.06 | PAN | 0.137 | 0.098 | -0.038 | -0.28 |
| | | | | | | Formaldehyde | 0.204 | 0.064 | -0.140 | -0.69 |
| JL2281B | Ethene | 366 | 434 | 67 | 0.18 | PAN | 0.097 | 0.089 | -0.008 | -0.08 |
| | | | | | | Formaldehyde | 0.174 | 0.063 | -0.111 | -0.64 |
| ST1682B | Ethene | 379 | 413 | 34 | 0.09 | PAN | 0.047 | 0.109 | 0.061 | 1.30 |
| | | | | | | Formaldehyde | 0.190 | 0.110 | -0.080 | -0.42 |
| ST2981B | Ethene | 465 | 493 | 28 | 0.06 | | | | | |
| ST2981R | Ethene | 540 | 488 | -52 | -0.10 | | | | | |
| ST0381B | a | | | | | | | | | |
| ST1081B | Ethene | 510 | 462 | -48 | -0.09 | | | | | |
| JL0882R | | | | | | PAN | 0.085 | 0.090 | 0.005 | 0.06 |
| | | | | | | Formaldehyde | 0.141 | 0.069 | -0.071 | -0.51 |
| JL0882B | | | | | | PAN | 0.072 | 0.085 | 0.013 | 0.18 |
| | | | | | | Formaldehyde | 0.144 | 0.065 | -0.080 | -0.55 |
| OC1481B | Ethene | 498 | 460 | -38 | -0.08 | PAN | 0.117 | 0.135 | 0.018 | 0.16 |
| | | | | | | Formaldehyde | 0.166 | 0.074 | -0.092 | -0.55 |
| Group Average | Ethene | 455 | 480 | 25 | 0.06 | PAN | 0.055 | 0.064 | 0.008 | 0.73 |
| Std. Dev. | | 54 | 63 | 67 | 0.16 | | 0.043 | 0.041 | 0.031 | 1.92 |
| Avg. Abs Value | | | | 54 | 0.12 | | | | 0.023 | 0.93 |
| Std. Dev. | | | | 46 | 0.12 | | | | 0.022 | 1.82 |
| Group Average | | | | | | Formaldehyde | 0.146 | 0.068 | -0.079 | -0.47 |
| Std. Dev. | | | | | | | 0.046 | 0.017 | 0.049 | 0.27 |
| Avg. Abs Value | | | | | | | | | 0.080 | 0.49 |
| Std. Dev. | | | | | | | | | 0.047 | 0.22 |

[a] No data for ethene, PAN, or formaldehyde.

```
----------------------------------------------------------------------------
        Calc.-Expt./Calc.                      Calc.-Expt./Calc.
         Maximum Ozone                 Time to 1/2 Expt. Δ([O3]-[NO])max
----------------------------------------------------------------------------

       <  -0.33    :                          <  -0.55    :
  -0.33 - -0.27    :1                   -0.55 -  -0.45    :
  -0.27 - -0.21    :1                   -0.45 -  -0.35    :11
  -0.21 - -0.15    :1                   -0.35 -  -0.25    :11
  -0.15 - -0.09    :111111              -0.25 -  -0.15    :11111
  -0.09 - -0.03    :11                  -0.15 -  -0.05    :111111
  -0.03 -  0.03    :11111               -0.05 -   0.05    :111111
   0.03 -  0.09    :11111                0.05 -   0.15    :111
   0.09 -  0.15    :1                    0.15 -   0.25    :1
   0.15 -  0.21    :1                    0.25 -   0.35    :
   0.21 -  0.27    :1                    0.35 -   0.45    :
   0.27 -  0.33    :1                    0.45 -   0.55    :
       >   0.33    :                          >   0.55    :
----------------------------------------------------------------------------
(Calc.-Expt.)                 (Calc.-Expt.)
  /Expt.        Ethene           /Expt.        PAN            Formaldehyde
 Half Life                    Product Yield
----------------------------------------------------------------------------

     < -0.5    :                   < -0.5    :1              :1111111111
-0.5 - -0.4    :              -0.5 - -0.4    :               :1
-0.4 - -0.3    :              -0.4 - -0.3    :1              :1
-0.3 - -0.2    :              -0.3 - -0.2    :1              :
-0.2 - -0.1    :1             -0.2 - -0.1    :               :1
-0.1 -  0.0    :1111111       -0.1 -  0.0    :1              :
 0.0 -  0.1    :111111         0.0 -  0.1    :111            :11
 0.1 -  0.2    :11             0.1 -  0.2    :11             :
 0.2 -  0.3    :11             0.2 -  0.3    :               :
 0.3 -  0.4    :               0.3 -  0.4    :               :
 0.4 -  0.5    :11             0.4 -  0.5    :               :
     >  0.5    :                   >  0.5    :1111           :
----------------------------------------------------------------------------
```

Figure IV-93. Distribution plots for discrepancies between calculated and experimental first day maximum ozone yields, times required to achieve half the maximum experimental change in ([$O_3$]-[NO]), and ethene half-lives and PAN and formaldehyde product yields in the model simulations of UNC complex mixture runs.

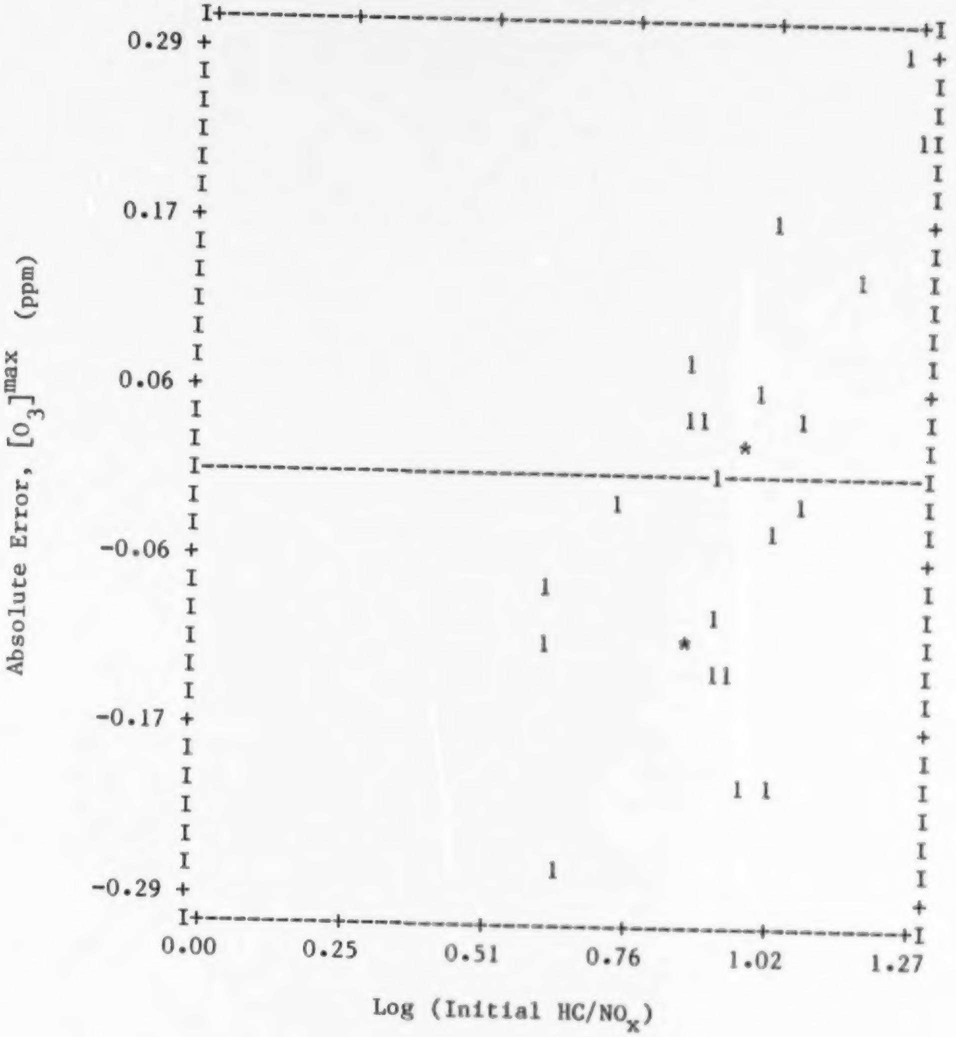

Figure IV-94. Plots of the discrepancies between the calculated and experimental maximum ozone yields against the log of the hydrocarbon/$NO_x$ ratio for the UNC complex mixture experiments.

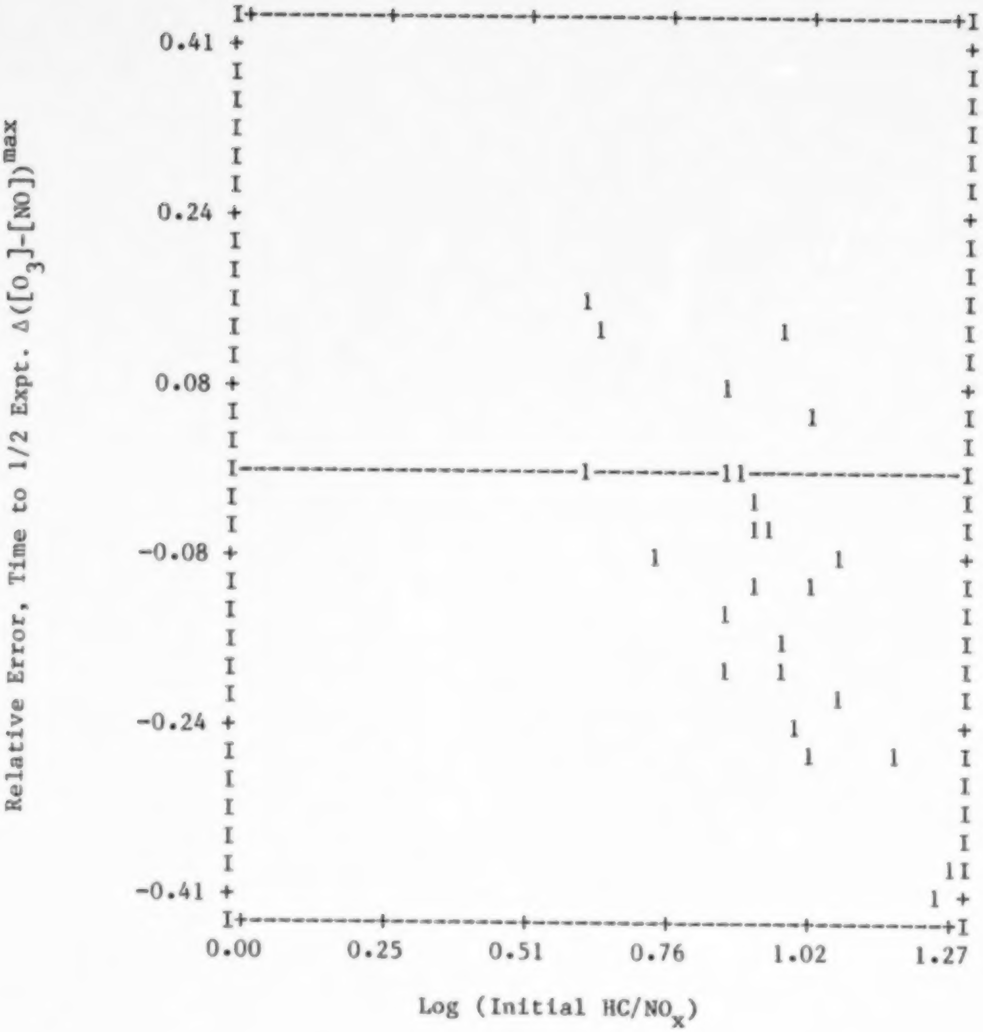

Figure IV-95. Plots of the relative discrepancies between the calculated and experimental times required to achieve half the experimental change in ($[O_3]$-[NO]) against the log of the hydrocarbon/$NO_x$ ratio for the UNC complex mixture experiments.

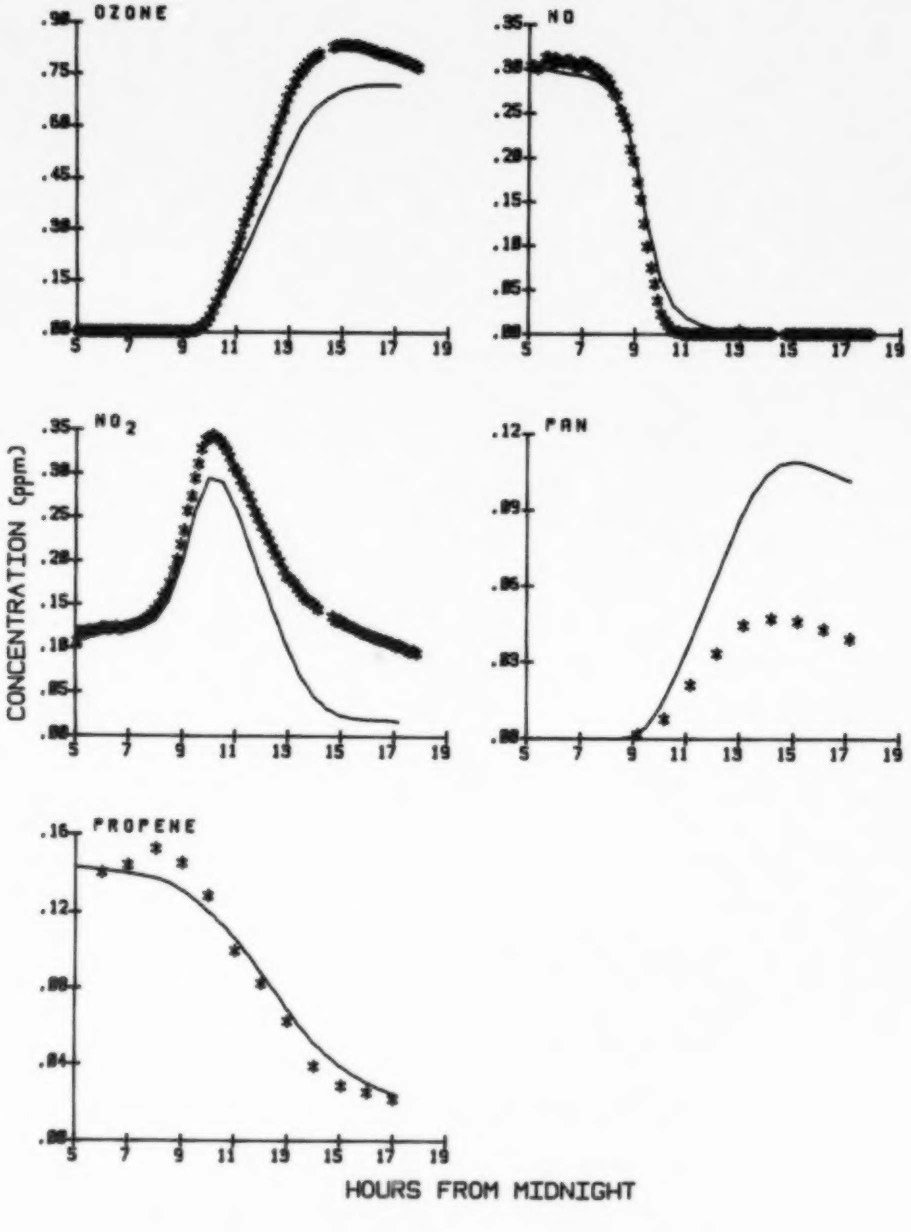

Figure IV-96. Experimental and calculated concentration-time plots for representative species observed in the "UNCMIX" + x-xylene run ST1682B.
* = Experimental data.
----- = Model calculation.

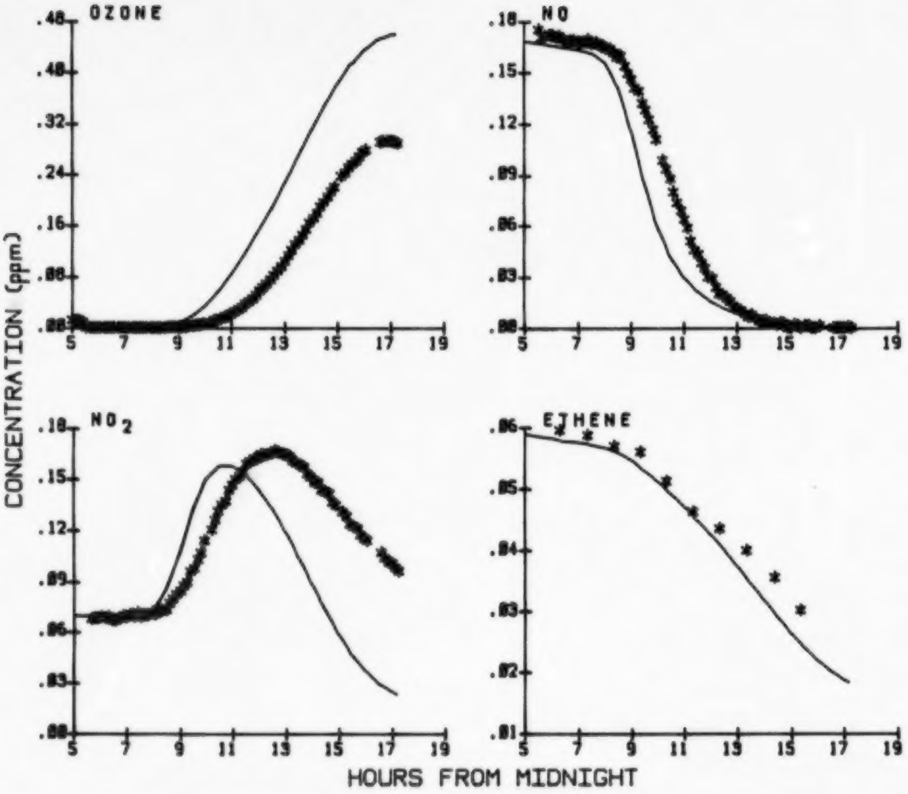

Figure IV-97. Experimental and calculated concentration-time plots for representative species observed in the "UNCMIX" + toluene + acetaldehyde run ST2981R.
* = Experimental data.
----- = Model calculation.

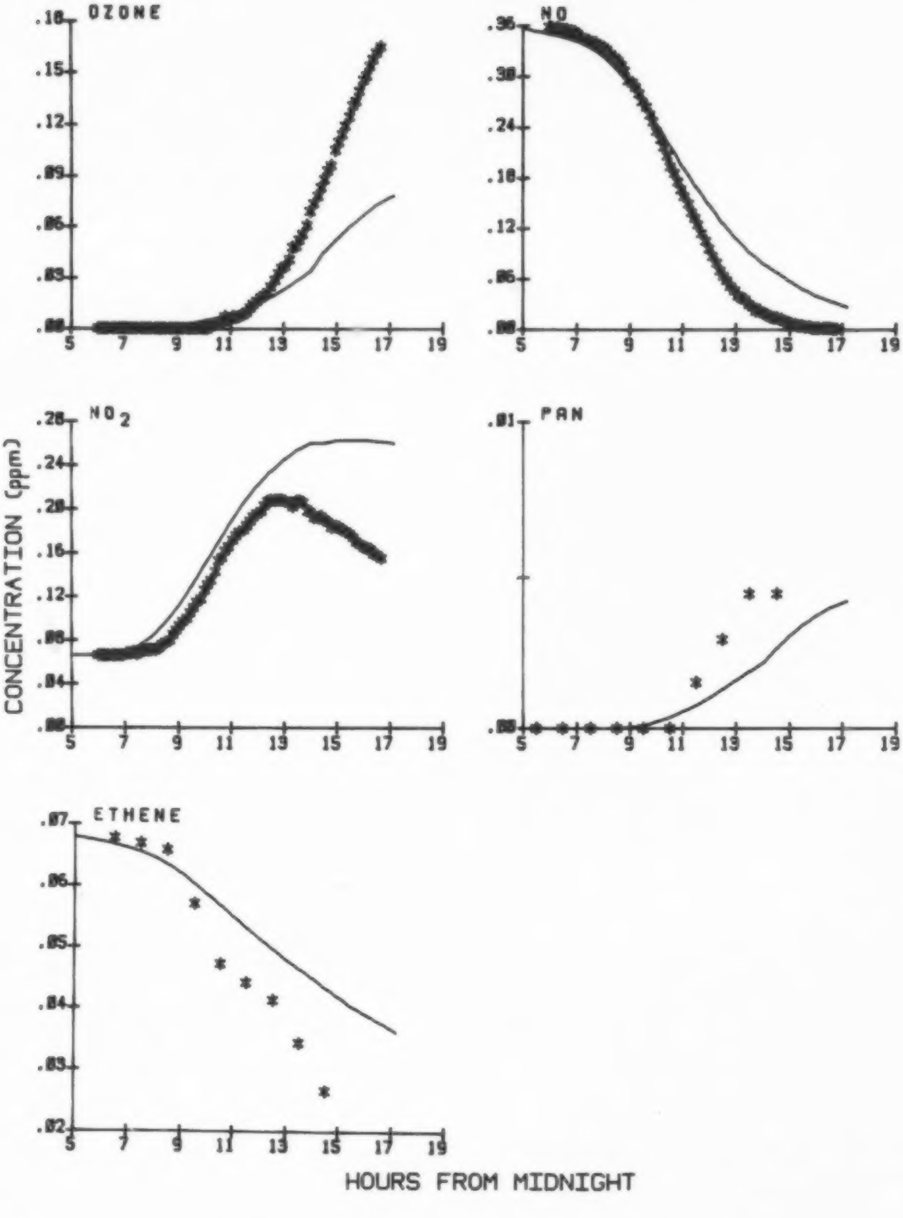

Figure IV-98. Experimental and calculated concentration-time plots for representative species observed in the "UNCMIX" + toluene run JL2081B.
* = Experimental data.
----- = Model calculation.

It can be seen that, as with the simulations of the propene runs carried out in the UNC chamber, the quality of the fits of the model simulations to the results of these runs was highly variable. As shown in Figure IV-93, there does not appear to be any systematic tendency to overpredict or underpredict the ozone yields, though the distribution of the discrepancies for the NO oxidation/ozone formation times suggests that the model tends to overpredict reactivity as defined in this manner. In addition, the plots in Figures IV-94 and IV-95 suggest that there may be a dependence of the discrepancies in the predicted measurements of reactivity on the initial organic/$NO_x$ ratio, with runs at the higher organic/$NO_x$ ratios having a greater chance of the reactivity being overpredicted, and vice-versa. However, this apparent dependence on organic/$NO_x$ ratio may be an artifact due to the specific set of experiments carried out and the time of year in which they were carried out. In particular, there may be a problem with the model in simulating runs under winter conditions, since the greatest discrepancies (with the reactivity in all cases being overpredicted) are obtained in modeling the three irradiations carried out in November and December (two carried out at the same time on different sides of the chamber), and these three runs have the three highest hydrocarbon/$NO_x$ ratios employed. If these three runs are removed from the plots on Figures IV-94 and IV-95, the appearance of a dependence on the hydrocarbon/$NO_x$ ratio is considerably reduced.

### 11. UNC Dynamic Experiments

Five propene-$NO_x$-air irradiations and four propene-n-butane-toluene-$NO_x$-air irradiations carried out in the UNC chamber employing non-standard, "dynamic" experimental conditions were modeled in this program. In these experiments, either some or all of the reactants were injected during the course of the irradiation, or the chamber contents were deliberately diluted with ambient air at rates much greater than usual, or both. In all cases, a corresponding standard, "static" irradiation of the same mixture was carried out at the same time on the other side of the chamber. The special techniques employed in carrying out these runs are discussed by Jeffries et al. (1985a), and that report should be consulted for details of how these experiments were carried out. These are summarized briefly below.

Dynamic Injection. In some experiments, one or more of the reactants were injected at an exponentially decaying rate using a continuously stirred tank reactor (CSTR) system with the outlet attached to the chamber injection mainfold. At the beginning of this experiment, this reactor contained the reactant(s) to be injected, and during the experiments the contents of the reactor were flushed into the chamber while being continuously diluted. This procedure results in an exponentially decaying input rate of the reactant(s). The resulting reactant injection rates assumed when modeling these experiments were thus calculated as a function of time (t) by the expression

$$\text{Reactant Injection Rate} = k_I\ C\ e^{-k_I(t-t_o)}$$

where $t_o$ is the start time of the injection, $k_I$ is a parameter reflecting how rapidly the contents of the CSTR are being introduced into the chamber, and C is the final concentration of the injected reactant in the chamber, if no chemical reaction or dilution of the chamber were occurring. In experiments where both $NO_x$ and the hydrocarbon(s) were dynamically injected, two separate CSTR's were used, but the value of $k_I$ associated with each were sufficiently similar that a single average $k_I$ value was used in modeling all dynamic injections in a given run. Although separate values of $k_I$ were used in modeling each dynamic injection experiment, their run-to-run variation was small, being in the range of 0.0046 to 0.0050 $min^{-1}$ for the runs discussed here. This corresponds to half the reactants being injected in 2.3 to 2.5 hours.

Dynamic Dilution In some experiments, the contents of the chamber were diluted at greater than the usual rate by introducing ambient air at a constant flowrate into the chamber after the beginning of the irradiation. The dilution rates recommended by the UNC researchers, and given as a function of time in the documentation included in the data sets for these runs, were used in the model simulations without adjustment. In some cases the air introduced into the chamber contained ozone, either because it was present in the ambient air, or because it was deliberately introduced using an ozone generator, in order to simulate entrainment of ozone from aloft. In the model simulations of these runs, this injection of ozone into this chamber was represented using the expression

$$\text{Ozone Injection Rate} = d\ [\text{diluent } O_3]$$

where d is the recommended dilution rate, and [diluent $O_3$] is the concentration of ozone in the air used to dilute the chamber. The concentration of ozone in the diluent air was monitored during the course of the experiments, and reported along with the data for the runs; the values used in the model calculations were averages over appropriate time intervals. The dilution rates employed in the dynamic dilution experiments ranged from 20% to 33% per hour.

For each of the dynamic runs modeled, Table IV-51 indicates the special conditions employed and the total amounts of reactants injected during the irradiation. The experimental and calculated maximum ozone yields and the NO oxidation/ozone formation times are also given in Table IV-51 and the experimental and calculated reactant half-lives or maxima for selected reactants and products are summarized in Table IV-52. Figures IV-99 through IV-100 give the experimental and calculated concentration-time plots for the representative dynamic runs JL1783B and JL2983R.

The performance of the model in simulating the data are typified by the fits shown in Figures IV-99 and IV-100. The model performance in simulating two of the four propene-n-butane-toluene (PBT) runs are similar, as shown in Figures IV-101 and IV-102. The model significantly underpredicted the reactivity observed in the other two PBT runs; this could be due to the general variability observed in modeling these runs (as seen in the results of modeling the other types of runs, discussed above), although the possibility cannot be ruled out that the conditions employed in those two runs are not being represented correctly in the model. However, the quality of the fits observed in modeling the other dynamic runs suggest that in these cases the model is representing the special conditions in an appropriate manner.

For most of these dynamic runs, the corresponding static run carried out at the same time on the other chamber was also modeled, and those

Table IV-51. Special Conditions, Initial or Injected Hydrocarbon and $NO_x$ Concentrations, and Experimental and Calculated Ozone Yields and Times Required to Achieve Half the Maximum Experimental Change in ($[O_3]-[NO]$) for Selected UNC "Dynamic" Experiments

| Experiment | Special Conditions | Initial or Injected Concentrations | | | Maximum Ozone Concentration | | | | Time to 1/2 Maximum Expt. ($[O_3]-[NO]$) | | | |
|---|---|---|---|---|---|---|---|---|---|---|---|---|
| | | $NO_x$ (ppm) | HC (ppmC) | $HC/NO_x$ | Expt (ppm) | Calc (ppm) | Calc -Expt (ppm) | Calc -Expt /Expt | Expt (min) | Calc (min) | Calc -Expt (min) | Calc -Expt /Expt |
| **1: Dynamic Propene Runs** | | | | | | | | | | | | |
| ST0482R | Dynamic injection: propene | 0.220 | 1.1 | 5.0 | 0.542 | 0.543 | 0.001 | 0.00 | 271 | 214 | -57 | -0.21 |
| JL1783B | Dynamic injection: propene | 0.265 | 1.1 | 4.1 | 0.728 | 0.580 | -0.148 | -0.20 | 351 | 384 | 34 | 0.10 |
| ST1382R | Dynamic injection: propene and $NO_x$ | 0.211 | 1.1 | 5.2 | 0.682 | 0.502 | -0.180 | -0.26 | 214 | 246 | 31 | 0.15 |
| JL2183B | Dynamic injection: propene and $NO_x$ | 0.217 | 1.1 | 5.1 | 0.740 | 0.648 | -0.093 | -0.13 | 321 | 354 | 33 | 0.10 |
| JL2983R | Dynamic dilution: maximum diluent ozone = 60 ppb | 0.216 | 1.1 | 5.1 | 0.234 | 0.191 | -0.043 | -0.18 | 200 | 178 | -21 | -0.11 |
| Group Average | | 0.226 | 1.1 | 4.9 | 0.585 | 0.493 | -0.092 | -0.15 | 271 | 275 | 3 | 0.01 |
| S. Dev. | | 0.022 | 0.0 | 0.4 | 0.212 | 0.177 | 0.074 | 0.10 | 66 | 90 | 41 | 0.16 |
| Avg. Abs. Value | | | | | | | 0.093 | 0.16 | | | 34 | 0.13 |
| S. Dev. | | | | | | | 0.073 | 0.10 | | | 13 | 0.05 |
| **2: Dynamic Propene-n-Butane-Toluene Runs** | | | | | | | | | | | | |
| JN1483B | Dynamic injection: HC´s and $NO_x$ | 0.221 | 2.6 | 11.8 | 0.573 | 0.503 | -0.070 | -0.12 | 400 | 422 | 22 | 0.05 |
| AU1883R | Dynamic dilution: maximum diluent ozone = 55 ppb | 0.276 | 2.6 | 9.4 | 0.346 | 0.186 | -0.160 | -0.46 | 262 | 503 | 241 | 0.92 |
| JN2783R | Dynamic dilution and dynamic injection of HC´s and $NO_x$ | 0.236 | 2.9 | 12.2 | 0.198 | 0.243 | 0.045 | 0.23 | 318 | 295 | -23 | -0.07 |
| AU2683B | Dynamic dilution and dynamic injection of HC´s and $NO_x$. Some $NO_2$ present initially | 0.319 | 2.5 | 8.0 | 0.256 | 0.200 | -0.056 | -0.22 | 165 | 271 | 106 | 0.64 |
| Group Average | | 0.263 | 2.7 | 10.3 | 0.343 | 0.283 | -0.060 | -0.14 | 286 | 373 | 87 | 0.39 |
| S. Dev. | | 0.044 | 0.2 | 2.0 | 0.165 | 0.149 | 0.084 | 0.29 | 99 | 109 | 116 | 0.47 |
| Avg. Abs. Value | | | | | | | 0.083 | 0.26 | | | 98 | 0.42 |
| S. Dev. | | | | | | | 0.053 | 0.15 | | | 103 | 0.43 |

Table IV-52. Experimental and Calculated Maximum Concentrations or Half-Lives for Selected Reactants and Products for the UNC "Dynamic" Experiments

| Experiment | Reactant Half-Life | | | | | Maximum Concentrations | | | | |
|---|---|---|---|---|---|---|---|---|---|---|
| | Species | Expt (min) | Calc (min) | Calc -Expt (min) | Calc -Expt /Expt | Species | Expt (ppm) | Calc (ppm) | Calc -Expt (ppm) | Calc -Expt /Expt |
| 1: Dynamic Propene Runns | | | | | | | | | | |
| ST0482R | NO | 237 | 187 | -50 | -0.21 | $NO_2$ | 0.178 | 0.162 | -0.017 | -0.09 |
| | | | | | | Propene | 0.190 | 0.179 | -0.011 | -0.06 |
| JL1783B | NO | 219 | 208 | -11 | -0.05 | $NO_2$ | 0.207 | 0.197 | -0.010 | -0.05 |
| | | | | | | Propene | 0.186 | 0.184 | -0.002 | -0.01 |
| ST1382R | | | | | | NO | 0.078 | 0.113 | 0.035 | 0.45 |
| | | | | | | $NO_2$ | 0.248 | 0.238 | -0.010 | -0.04 |
| | | | | | | Propene | 0.152 | 0.190 | 0.038 | 0.25 |
| JL2183B | | | | | | NO | 0.066 | 0.024 | -0.042 | -0.64 |
| | | | | | | $NO_2$ | 0.104 | 0.115 | 0.011 | 0.10 |
| | | | | | | Propene | 0.158 | 0.160 | 0.002 | 0.01 |
| JL2983R | NO | 156 | 136 | -20 | -0.13 | $NO_2$ | 0.115 | 0.113 | -0.002 | -0.02 |
| | Propene | 208 | 183 | -25 | -0.12 | | | | | |
| 2: Dynamic Propene-n-Butane-Toluene Runs | | | | | | | | | | |
| JN1483B | | | | | | NO | 0.046 | 0.060 | 0.013 | 0.29 |
| | | | | | | $NO_2$ | 0.116 | 0.126 | 0.010 | 0.09 |
| | | | | | | Propene | 0.073 | 0.071 | -0.002 | -0.03 |
| | | | | | | Toluene | 0.081 | 0.084 | 0.002 | 0.03 |

(continued)

Table IV-52 (continued) - 2

| Experiment | Reactant Half-Life | | | | | Maximum Concentrations | | | | |
|---|---|---|---|---|---|---|---|---|---|---|
| | Species | Expt (min) | Calc (min) | Calc -Expt (min) | Calc -Expt /Expt | Species | Expt (ppm) | Calc (ppm) | Calc -Expt (ppm) | Calc -Expt /Expt |
| AU1883R | $NO_2$ | 270 | 294 | 24 | 0.09 | NO | 0.024 | 0.039 | 0.015 | 0.62 |
| | Propene | 222 | 234 | 12 | 0.05 | | | | | |
| | Toluene | 286 | 310 | 24 | 0.08 | | | | | |
| JN2783R | | | | | | NO | 0.035 | 0.073 | 0.038 | 1.06 |
| | | | | | | $NO_2$ | 0.105 | 0.102 | -0.003 | -0.03 |
| | | | | | | Propene | 0.067 | 0.077 | 0.010 | 0.14 |
| | | | | | | Toluene | 0.060 | 0.073 | 0.012 | 0.21 |
| AU2683B | | | | | | NO | 0.036 | 0.076 | 0.040 | 1.13 |
| | | | | | | $NO_2$ | 0.146 | 0.116 | -0.030 | -0.21 |
| | | | | | | Propene | 0.050 | 0.073 | 0.023 | 0.46 |
| | | | | | | Toluene | 0.046 | 0.059 | 0.012 | 0.26 |

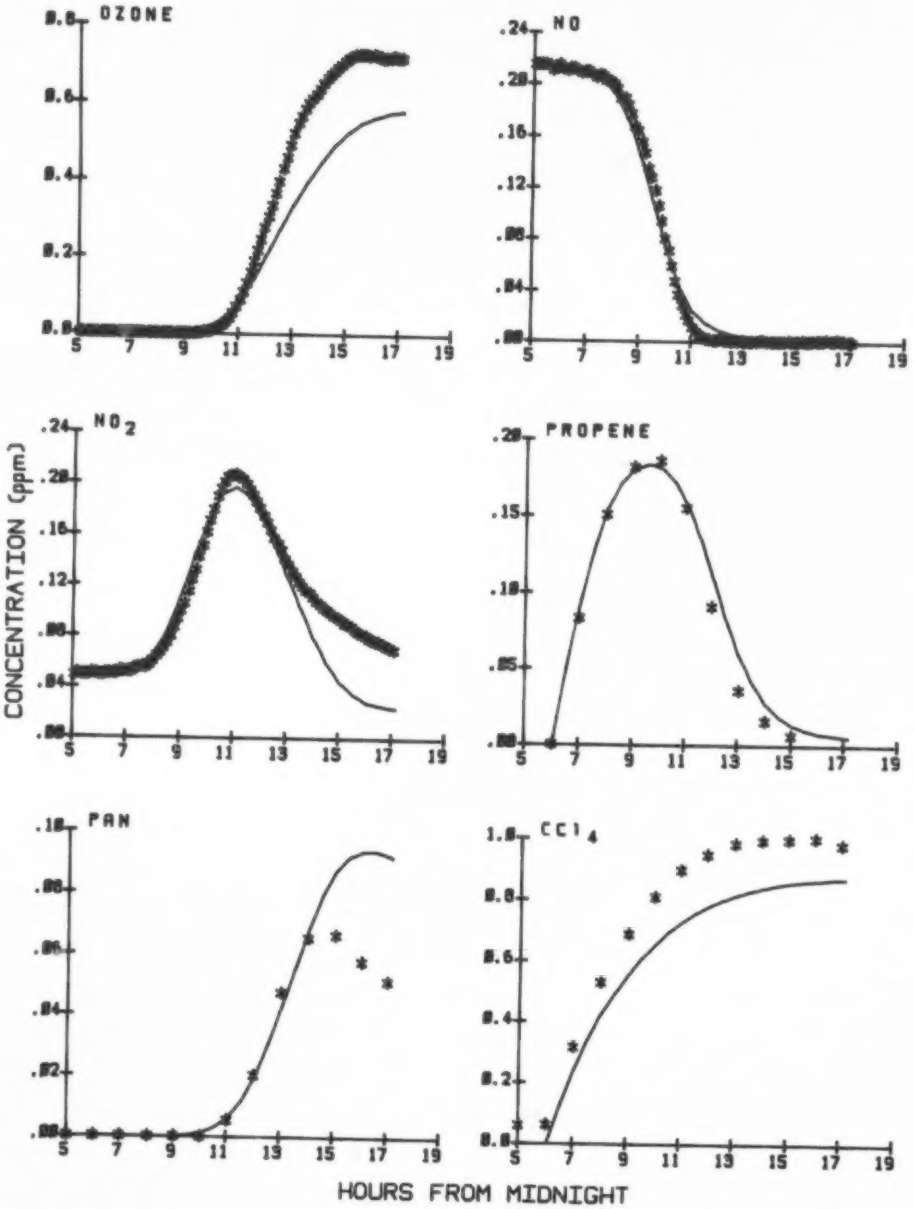

Figure IV-99. Experimental and calculated concentration-time plots for representative species observed in the UNC dynamic propene injection run JL1783B.
* = Experimental data.
----- = Model calculation.

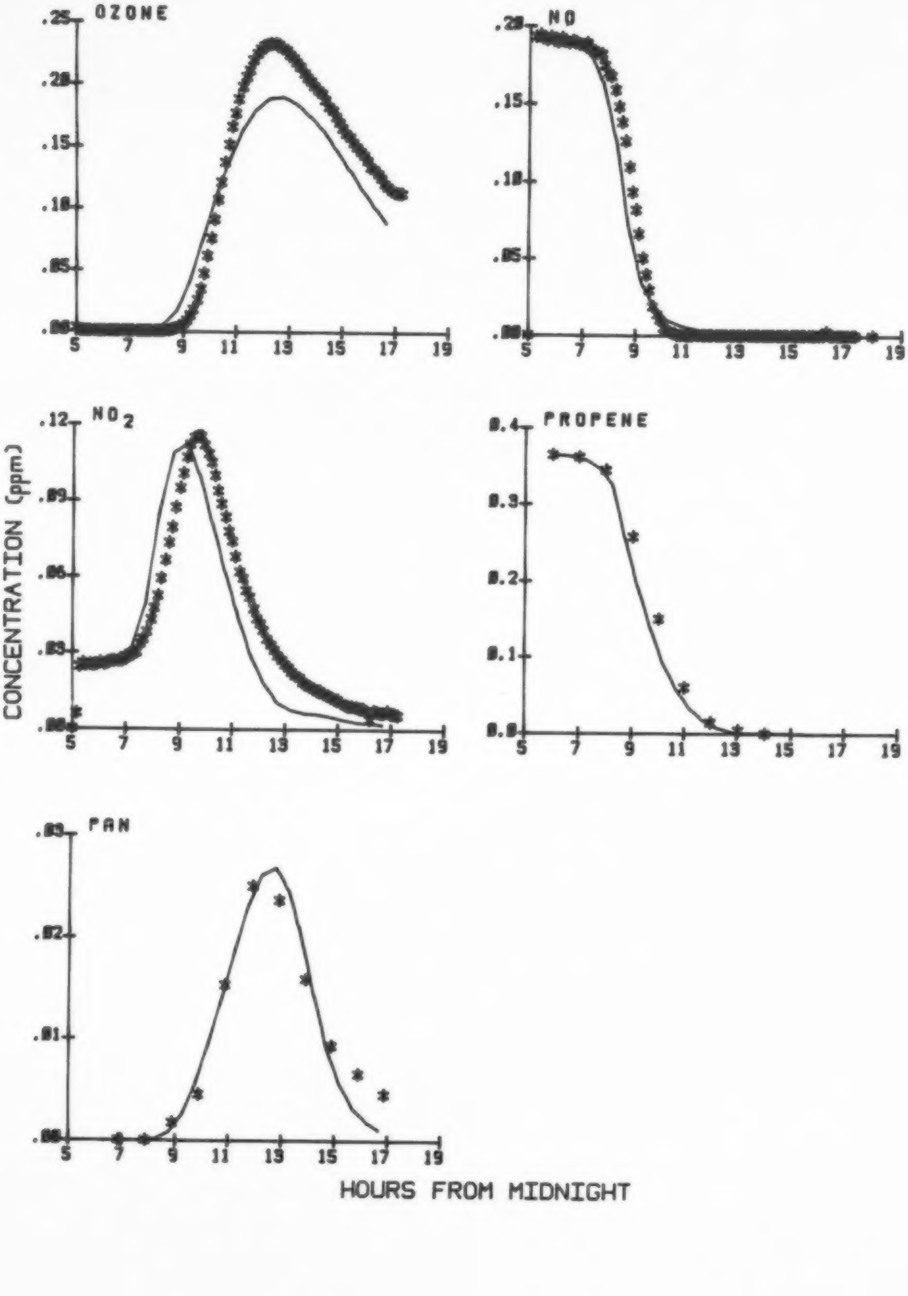

Figure IV-100. Experimental and calculated concentration-time plots for representative species observed in the UNC dynamic dilution propene run JL2983R.

* = Experimental data.

---- = Model calculation.

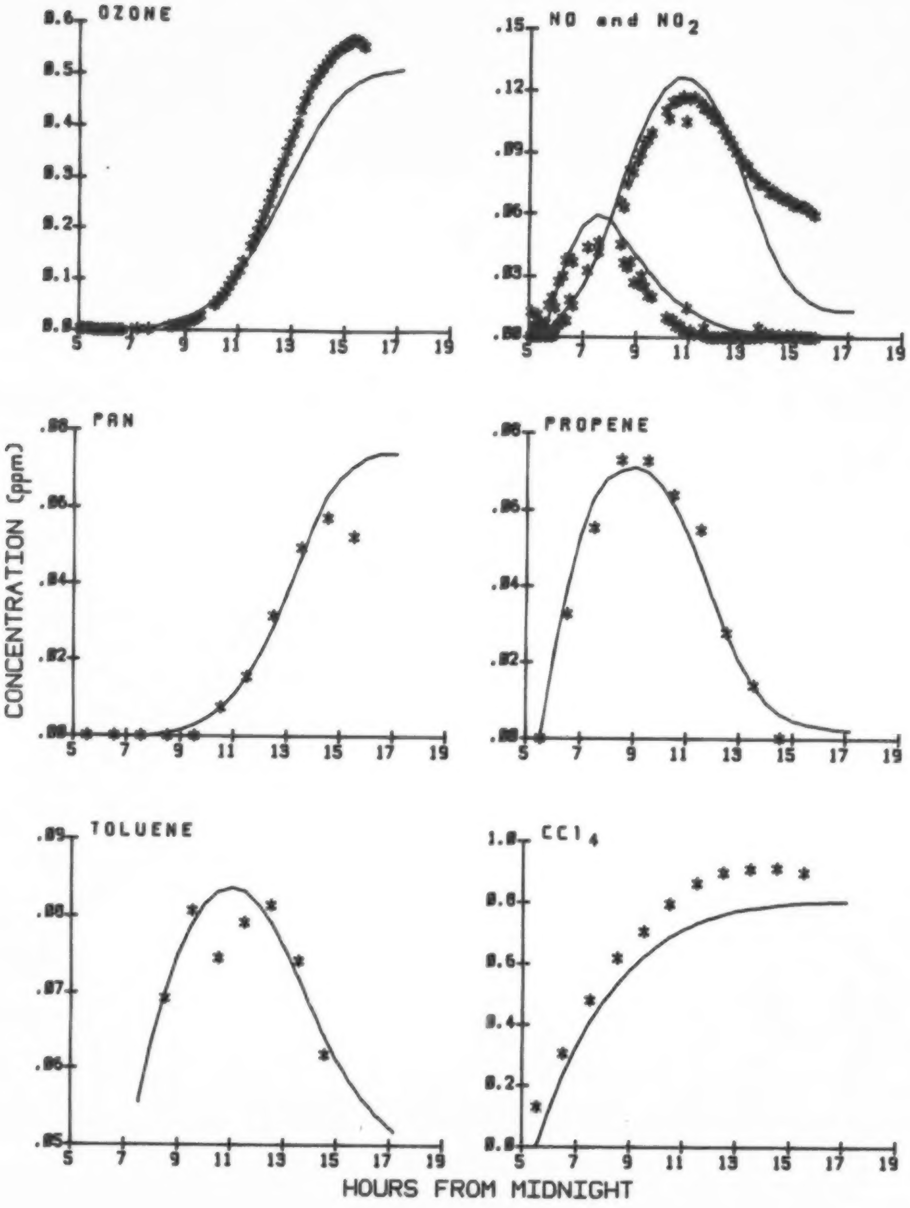

Figure IV-101. Experimental and calculated concentration-time plots for representative species observed in the UNC dynamic injection propene + n-butane + toluene run JN1483B.
* = Experimental data.
----- = Model calculation.

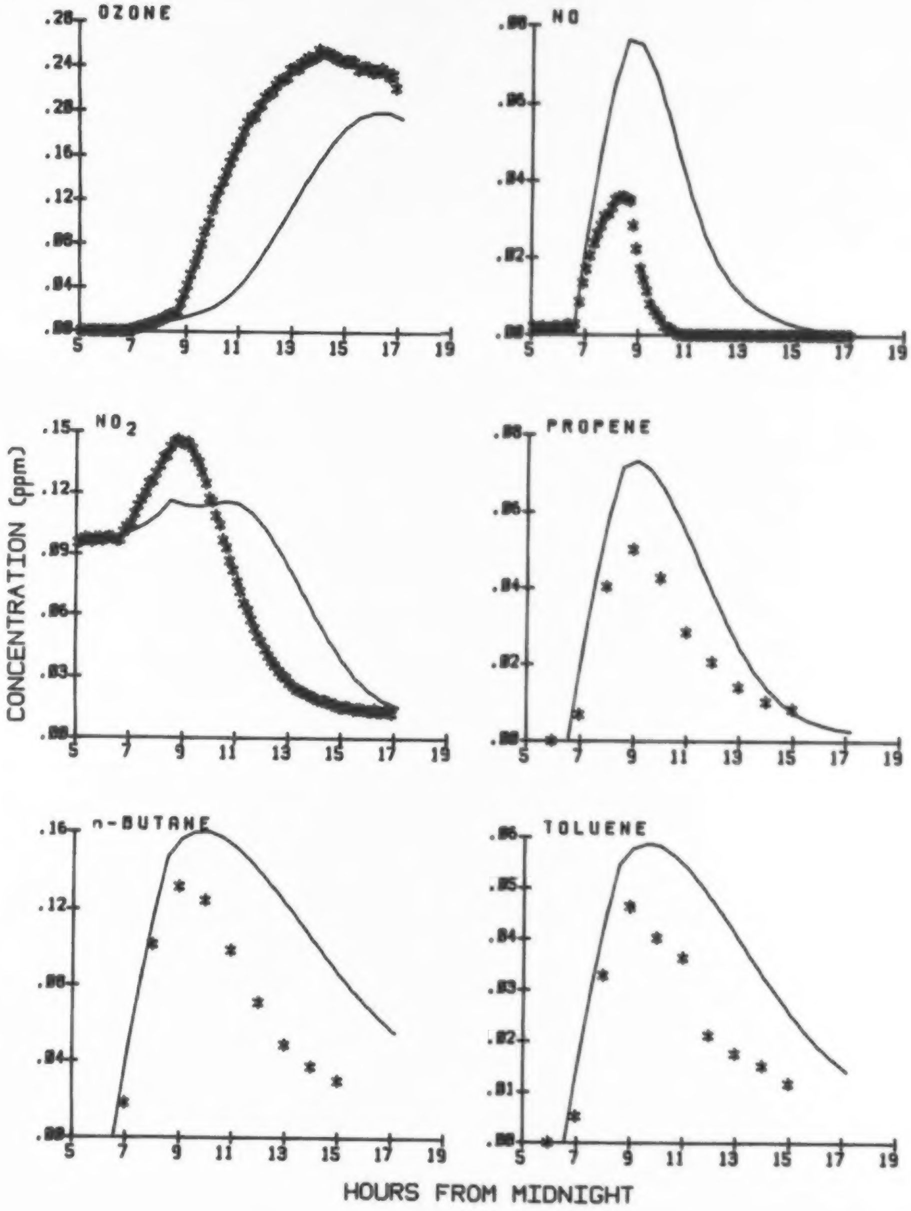

Figure IV-102. Experimental and calculated concentration-time plots for representative species observed in the UNC dynamic dilution and injection propene + n-butane + toluene run AU2683B.

* = Experimental data.

----- = Model calculation.

results are discussed in the appropriate sections above. In all cases except for the two PBT runs which were poorly simulated, where the fits were better in the simulation of the static sides, the quality of fits obtained in modeling the dynamic side was comparable to those obtained in modeling the static experiment. This is indicated in Table IV-53, where the relative discrepancies in the calculated ozone yields and NO oxidation/ozone formation times for the static and dynamic experiments are compared. This indicates that in general if the model performed adequately in simulating the results of static experiments, it was also satisfactory in simulating the results of experiments carried out under dynamic conditions, provided that the special conditions employed in the dynamic experiments were appropriately represented in the model.

Table IV-53. Comparison of Discrepancies in Model Predictions of Ozone Yields and Times Required to Achieve Half the Experimental Change in ([$O_3$]-[NO]) for Static and Dynamic Experiments Carried Out at the Same Time

| Run Date | Expt-Calc/Expt Ozone Maxima | | Expt-Calc/Expt NO Oxidation Times | |
|---|---|---|---|---|
| | Static | Dynamic | Static | Dynamic |
| Sep 04, 1982 | -0.13 | 0.00 | -0.24 | -0.21 |
| Jul 17, 1983 | -0.28 | -0.20 | 0.21 | 0.10 |
| Sep 13, 1982 | -0.19 | -0.26 | -0.07 | 0.15 |
| Jul 21, 1983 | -0.19 | -0.13 | 0.07 | 0.10 |
| Jul 29, 1983 | -0.10 | -0.18 | -0.20 | -0.11 |
| Jun 14, 1983 | -0.12 | -0.12 | -0.05 | 0.05 |
| Aug 18, 1983 | -0.25 | -0.46 | 0.13 | 0.92 |
| Jun 27, 1983 | 0.05 | 0.23 | -0.05 | -0.07 |
| Aug 26, 1983 | -0.25 | -0.22 | 0.06 | 0.64 |

## IV. F. UNC AUTO EXHAUST EXPERIMENTS

Jeffries et al. (1985b) recently completed an experimental program involving irradiations of real and synthetic auto exhaust in the UNC chamber, and 22 exhaust irradiations carried out in that program were modeled in this study. Testing the mechanism against such data is useful since automobile emissions are the single most important contributor to urban photochemical smog and thus the organic mixtures involved may be more representative of the ambient atmosphere than any of the synthetic mixtures used in the chamber runs discussed previously. This also allows the ability of the model to simulate very complex mixtures of organics, including many species which are not explicitly represented in the model, to be assessed.

The experimental study is described in detail by Jeffries et al. (1985b), and is only briefly summarized here. Exhaust from two automobiles, a 1972 Dodge Charger and a 1979 Plymouth Volare, was employed in these experiments, with the vehicles operating at high idle speeds. In some experiments, the exhaust was injected directly into the chamber, and in others the exhaust was first cryogenically trapped and subsequently evaporated and injected into the chamber. In addition, several experiments employing synthetic mixtures designed to represent auto exhaust were carried out in conjunction with these runs, and, for comparative purposes, these are modeled using a similar procedure to represent the organics as used in the auto exhaust runs.

In Section IV-F-1, below, the method used to assign the hydrocarbon composition in the exhaust and the species lumping technique employed is discussed. Although in principle the same general species lumping technique could be employed in modeling these runs as employed when modeling the UNC complex mixture runs discussed in Section IV-E-10, because of time constraints a somewhat simpler version of the "lumped molecule" approach was employed. Following the discussion of the speciation of the exhaust and the lumping approach employed, in Section IV-F-2, the results of the model simulations are summarized.

### 1. Hydrocarbon Speciation and Lumping

Typical hydrocarbon composition profiles for these two vehicles, obtained from Jeffries et al. (1985b) is shown in Table IV-54. The data in the table indicate the complexity and large number of species in the exhaust mixtures. Typically, 30 to 40 species account for 80 percent of the organic carbon. The remaining 20 percent consists of small amounts of many different compounds, some of which (e.g., higher alkenes) may be important to the reactivity of the mixture. The data in Table IV-54 were obtained from separate analyses, carried out in 1984, of the exhaust from these vehicles running in fast idle mode.

For the purpose of modeling the auto exhaust irradiations and the associated synthetic exhaust experiments, a simple "lumped molecule" approach, where selected individual species were employed to represent groups of similar species (without averaging of rate constants or mechanistic parameters as used in modeling the complex mixture runs discussed in Section IV-E-10), was employed. The representative species used in the model, and the individual species they represented in modeling the runs discussed in this section are listed in Table IV-55. The measured species and those assigned to represent the unspeciated hydrocarbons (see below) were assigned to the classes on a ppmC basis, with the molar concentrations in ppm being computed using the carbon numbers of the surrogate species.

The rate constants and reaction mechanisms of the representative alkenes and aromatics used in these model calculations are those given in Section II and were not modified for the purpose of using them as lumped species in these calculations. The rate constants and mechanistic and product yield parameters (i.e., the parameters p1 through pC, etc., defined in Section II-F-3) for the lumped alkane species "$C_4$-$C_5$"" were obtained by averaging the rate constants for n-butane, n-pentane, isobutane, and isopentane, the parameters for the lumped alkane species "$C_6$ plus" were obtained by averaging the parameters for n-hexane, n-heptane, n-octane, 2,3-dimethylbutane, 2-methylpentane, 2,3-dimethylpentane, and isooctane. In both cases each compound was weighed equally in the parameters for these in the averages. The parameters for these individual

Table IV-54. Normalized Hydrocarbon Composition of Exhaust from the Vehicles Employed in the UNC Auto Exhaust Study. (Data from Table 6 in Appendix C of Jeffries et al. 1985b. Vehicles Operated Using the Federal Test Procedure at High Idle)

| Species[a] | 1972 Dodge Charger | 1979 Plymouth Volare |
|---|---|---|
| Alkanes: | | |
| Ethane | 0.0074 | 0.0041 |
| Propane | 0.0026 | 0.0044 |
| n-Butane | 0.0417 | 0.0632 |
| Isobutane | 0.0103 | 0.0073 |
| n-Pentane | 0.0263 | 0.0279 |
| Isopentane | 0.0552 | 0.0720 |
| Cyclopentane | 0.0029 | 0.0037 |
| Cyclohexane | 0.0026 | 0.0016 |
| 2-Methylpentane | 0.0285 | 0.0278 |
| 3-Methylpentane | 0.0189 | 0.0153 |
| 2,2-Dimethylbutane | 0.0069 | 0.0114 |
| Methylcyclopentane | 0.0131 | 0.0133 |
| n-Heptane | 0.0112 | 0.0095 |
| 2-Methylhexane | 0.0023 | 0.0035 |
| Methylcyclohexane | 0.0039 | 0.0064 |
| 2,4-Dimethylpentane | 0.0057 | 0.0086 |
| 3-Methylhexane | 0.0145 | 0.0110 |
| 2,3-Dimethylpentane | 0.0259 | 0.0226 |
| 2,2,3-Trimethylpentane | 0.0030 | 0.0068 |
| 2,3,3-Trimethylpentane | 0.0083 | 0.0091 |
| 2,5-Dimethylhexane | 0.0031 | 0.0113 |
| n-Octane | 0.0052 | 0.0061 |
| 4-Methylheptane | 0.0086 | 0.0100 |
| 2,4-Dimethylhexane | 0.0051 | 0.0231 |
| 2,2,4-Trimethylpentane | 0.0146 | 0.0559 |
| 2,3,4-Trimethylpentane | 0.0034 | 0.0078 |
| 3-Methyloctane | 0.0036 | 0.0044 |
| 2,2,5-Trimethylhexane | 0.0022 | 0.0129 |
| Indane | 0.0027 | 0.0026 |
| Nonane | 0.0021 | 0.0034 |
| 2,4-Dimethylheptane | 0.0019 | 0.0030 |
| 2,3,5-Trimethylhexane | 0.0008 | 0.0015 |
| Alkenes: | | |
| Ethylene | 0.0615 | 0.0444 |
| Propylene | 0.0280 | 0.0117 |
| 1,3-Butadiene | 0.0057 | 0.0030 |
| 1-Butene | 0.0086 | 0.0041 |
| *trans*-2-Butene | 0.0062 | 0.0034 |

(continued)

Table IV-54 (continued) - 2

| Species[a] | 1972 Dodge Charger | 1979 Plymouth Volare |
|---|---|---|
| *cis*-2-Butene | 0.0048 | 0.0028 |
| 2-Methyl-1,3,butadiene | 0.0051 | 0.0064 |
| *cis*-2-Pentene | 0.0051 | 0.0080 |
| *trans*-2-Pentene | 0.0028 | 0.0033 |
| 2-Methyl-2-butene | 0.0028 | 0.0019 |
| Pentyne | 0.0051 | 0.0080 |
| 3-Methyl-1-butene | 0.0030 | 0.0026 |
| 2-Methyl-1-butene | 0.0044 | 0.0032 |
| 1-Pentene | 0.0027 | 0.0025 |
| Cyclopentene | 0.0015 | 0.0016 |
| *cis*-2-Hexene | 0.0023 | 0.0046 |
| 2-Hexene | 0.0029 | 0.0066 |
| 1-Hexene | 0.0013 | 0.0033 |
| n-Hexene | 0.0181 | 0.0104 |
| *Aromatics:* | | |
| Benzene | 0.0394 | 0.0211 |
| Toluene | 0.1239 | 0.0821 |
| m-Xylene | 0.0586 | 0.0437 |
| Ethylbenzene | 0.0180 | 0.0127 |
| Styrene | 0.0052 | 0.0043 |
| 1,3,5-Trimethylbenzene | 0.0084 | 0.0052 |
| 1,2,3-Trimethylbenzene | 0.0063 | 0.0032 |
| o-Xylene | 0.0225 | 0.0158 |
| Isopropylbenzene | 0.0013 | 0.0008 |
| 1,2,4-Trimethylbenzene | 0.0273 | 0.0148 |
| n-Propylbenzene | 0.0051 | 0.0034 |
| 1,3-Diethylbenzene | 0.0028 | 0.0012 |
| Naphthalene | 0.0029 | 0.0012 |
| o-Ethyltoluene | 0.0091 | 0.0067 |
| Tetramethylbenzene | 0.0015 | 0.0007 |
| 1,4-Diethylbenzene | 0.0048 | 0.0028 |
| p-Ethyltoluene | 0.0069 | 0.0040 |
| m-Ethyltoluene | 0.0191 | 0.0110 |
| 1,2-Diethylbenzene | 0.0027 | 0.0012 |
| sec-Butylbenzene | 0.0015 | 0.0017 |
| Butylbenzene | 0.0052 | 0.0033 |
| 1-Methylnaphthalene | 0.0005 | 0.0001 |
| *Other:* | | |
| Acetylene | 0.0510 | 0.1028 |
| Unknowns | 0.0557 | 0.0490 |

[a] Species nomenclature given by Jeffries et al. (1985b) used.

Table IV-55. Assignment of Representative Species Used in the Model Simulations of the UNC Auto Exhaust Irradiations and Related Experiments

| Lumped or Representative Species Used in Model | Compounds Represented |
|---|---|
| C4-C5 | $C_4$ and $C_5$ alkanes |
| $C_6$plus | $\geq C_6$ alkanes and unidentified alkanes |
| Ethene | Ethene |
| Propene | Terminal alkenes (including 1,3-butadiene) |
| trans-2-Butene | Internal alkenes |
| Benzene | Benzene |
| Toluene | Monoalkylbenzenes (including styrene) |
| m-Xylene | Dialkylbenzenes |
| 1,3,5-Trimethylbenzene | Trialkylbenzenes, naphthalenes, and unidentified aromatics |
| Unreactive | Ethane, propane and acetylene |

alkanes used to calculate those for the lumped alkanes are given in the tables in Section II-F-4.

Although hydrocarbon composition data at the level of detail shown in Table IV-48 were not available for the individual experiments, for most runs, Jeffries et al. (1985b) gives speciated data for 10 to 30 of the major compounds, and results of initial total nonmethane hydrocarbon (NMHC) measurements for all the exhaust irradiations. Because of potential interferences in the gas chromatographic (GC) analyses of individual compounds, the initial concentrations summarized by Jeffries et al. (1985b), who took these interferences into account in deriving their recommended values, is used rather than the GC data in the data sets for the individual runs. For the purpose of this program we assume, as do Jeffries et al. (1985b), that the UNC total nonmethane hydrocarbon data are meaningful, though such data are subject to significant uncertainties [see Jeffries et al. (1985b) for a discussion of the NMHC measurements]. Based on the NMHC data, the fraction of unidentified carbon in these runs range from 5 to 50 percent. Hence, complete speciation of the organic mixture was not availiable for many of the experiments, and for these runs, it was necessary to represent the reactions of this "unspeciated carbon" in the model.

The unspeciated carbon in the exhaust runs was assigned to the various representative or surrogate species in the model by first partitioning it into unspeciated alkanes, alkenes, and aromatics using one of the following schemes:

1) 80% alkanes, 5% alkenes, 15% aromatics
2) 90% alkanes, 10% alkenes
3) 100% alkanes.

where the unspeciated alkanes, alkenes, and aromatics were partitioned as follows:

alkanes: 40% $C_4$-$C_5$
60% $C_6$plus

alkenes: 60% propene
40% *trans*-2-butene

aromatics: 30% toluene
50% m-xylene
20% 1,3,5-trimethylbenzene

The choice of schemes depended on the availability of higher alkene and higher aromatic species data. Scheme 1 was used if the data for those two classes were incomplete; scheme 2 was used if data for the alkenes were incomplete, and scheme 3 was used otherwise. Most of the unspeciated species were assumed to be alkanes because there was only limited data for the higher alkanes for the individual runs in the UNC data set. The specific percentages used in these assignments were estimated from the general characteristics of the 1984 idle data given in Table IV-54.

For the runs carried out on July 8, 1983, which involved irradiation of Charger exhaust on one side and Volare exhaust on the other, Jeffries et al. (1985b) gave recommended values only for the total NMHC levels. For modeling those irradiations, we employed the speciation given in Table IV-56, which is based on the data given in Table IV-54. A number of other exhaust irradiations carried out at UNC had only NMHC data, and in principle this assignment could be used in modeling these runs, but these were not modeled in this program because we did not receive the data for them from the UNC researchers.

Table IV-56. Assignment of Species Used for Modeling UNC Auto Exhaust Experiments Which only had Total NMHC Data

| Model Compound | Volare | Charger |
|---|---|---|
| $C_4$-$C_5$ | 0.201 | 0.148 |
| $C_6$plus | 0.318 | 0.234 |
| Ethene | 0.049 | 0.056 |
| Propene | 0.063 | 0.072 |
| trans-2-Butene | 0.028 | 0.032 |
| Benzene | 0.023 | 0.035 |
| Toluene | 0.104 | 0.158 |
| m-Xylene | 0.081 | 0.123 |
| 1,3,5-Trimethylbenzene | 0.023 | 0.035 |
| Formaldehyde | 0.010 | 0.010 |
| Unreactive | 0.111 | 0.108 |

## 2. Results of Model Calculations

The UNC auto exhaust experiments which were modeled are grouped according to the vehicle used and are listed in Table IV-57, along with the initial $NO_x$ and total hydrocarbon levels, and footnotes indicating which runs employed cryogenically trapped exhaust. The synthetic exhaust experiments are also listed on that table. The experimental and calculated ozone yields, NO oxidation/ozone formation times, and PAN yields for those experiments are also given in Table IV-57. The distributions of the discrepancies in the model predictions of these measurements of reactivity are plotted in Figure IV-103, along with the distribution of the discrepancies in predicted formaldehyde yields. Concentration-time plots of

Table IV-57. Summary of Initial Reactant Concentrations and Experimental and Calculated Maximum Ozone and PAN Yields and Times Required to Achieve Half the Experimental Change in ($[O_3]-[NO]$) for the UNC Auto Exhaust Irradiations and Associated Experiments

| Experiment | Initial Concentrations | | | Maximum Ozone Concentration | | | | Time to 1/2 Maximum Expt. ($[O_3]-[NO]$) | | | | Maximum PAN Yields | | | |
|---|---|---|---|---|---|---|---|---|---|---|---|---|---|---|---|
| | $NO_x$ (ppm) | HC (ppmC) | $HC/NO_x$ | Expt (ppm) | Calc (ppm) | Calc -Expt (ppm) | Calc -Expt /Expt | Expt (min) | Calc (min) | Calc -Expt (min) | Calc -Expt /Expt | Expt (ppm) | Calc (ppm) | Calc -Expt (ppm) | Calc -Expt /Expt |
| **1: Volare Exhaust Runns** | | | | | | | | | | | | | | | |
| JN2582R | 0.658 | 0.6 | 0.8 | 0.003 | 0.013 | 0.011 | | 406 | 389 | -17 | -0.04 | | | | |
| JN2982R | 0.244 | 2.5 | 10.1 | 0.704 | 0.658 | -0.046 | -0.07 | 276 | 268 | -7 | -0.03 | 0.065 | 0.080 | 0.015 | 0.23 |
| JN3082R | 0.329 | 2.8 | 8.6 | 0.811 | 0.662 | -0.149 | -0.18 | 196 | 152 | -44 | -0.22 | 0.068 | 0.139 | 0.071 | 1.05 |
| OC0682R | 0.470 | 2.0 | 4.2 | 0.355 | 0.315 | -0.040 | -0.11 | 403 | 383 | -20 | -0.05 | 0.024 | 0.021 | -0.003 | -0.13 |
| AU1183R | 0.226 | 2.2 | 9.5 | 0.850 | 0.732 | -0.118 | -0.14 | 314 | 305 | -10 | -0.03 | 0.032 | 0.058 | 0.027 | 0.85 |
| JN2582B | 0.648 | 0.6 | 0.8 | 0.003 | 0.014 | 0.011 | | 376 | 377 | 2 | 0.00 | | | | |
| JN2982B | 0.260 | 2.5 | 9.5 | 0.766 | 0.663 | -0.102 | -0.13 | 263 | 278 | 15 | 0.06 | 0.070 | 0.085 | 0.015 | 0.22 |
| JN3082B | 0.327 | 3.1 | 9.6 | 0.840 | 0.687 | -0.153 | -0.18 | 185 | 155 | -30 | -0.16 | 0.068 | 0.132 | 0.064 | 0.94 |
| ST2982B | 0.390 | 1.7 | 4.5 | 0.205 | 0.119 | -0.086 | -0.42 | 366 | 397 | 31 | 0.08 | 0.014 | 0.007 | -0.007 | -0.51 |
| JL0283B | 0.184 | 1.7 | 9.2 | 0.697 | 0.698 | 0.001 | 0.00 | 344 | 313 | -31 | -0.09 | 0.043 | 0.046 | 0.003 | 0.08 |
| JL0883B | 0.368 | 1.7 | 4.6 | 0.879 | 0.767 | -0.112 | -0.13 | 424 | 475 | 51 | 0.12 | 0.081 | 0.034 | -0.046 | -0.57 |
| AU1183B | 0.218 | 0.7 | 3.1 | 0.601 | 0.560 | -0.040 | -0.07 | 420 | 404 | -17 | -0.04 | | | | |
| Group Average | 0.360 | 1.8 | 6.2 | 0.560 | 0.491 | -0.069 | -0.14 | 331 | 325 | -6 | -0.03 | 0.052 | 0.067 | 0.015 | 0.24 |
| S. Dev. | 0.159 | 0.9 | 3.6 | 0.330 | 0.291 | 0.059 | 0.11 | 84 | 100 | 27 | 0.10 | 0.024 | 0.047 | 0.036 | 0.60 |
| Avg. Abs. Value | | | | | | 0.073 | 0.14 | | | 22 | 0.08 | | | 0.028 | 0.51 |
| S. Dev. | | | | | | 0.054 | 0.11 | | | 15 | 0.06 | | | 0.026 | 0.37 |
| **2: Charger Exhaust Runs** | | | | | | | | | | | | | | | |
| JL0182R | 0.369 | 3.5 | 9.6 | 0.740 | 0.817 | 0.077 | 0.10 | 316 | 260 | -56 | -0.18 | 0.076 | 0.111 | 0.036 | 0.47 |
| AU0382R | 0.456 | 2.5 | 5.4 | 0.344 | 0.405 | 0.061 | 0.18 | 394 | 373 | -21 | -0.05 | | | | |
| ST1782R[a] | 0.255 | 2.2 | 8.5 | 0.562 | 0.569 | 0.007 | 0.01 | 260 | 281 | 21 | 0.08 | 0.042 | 0.055 | 0.013 | 0.32 |
| ST2982R | 0.392 | 1.7 | 4.4 | 0.073 | 0.101 | 0.028 | 0.38 | 352 | 348 | -4 | -0.01 | | | | |
| JL0283R | 0.178 | 1.6 | 9.2 | 0.595 | 0.600 | 0.004 | 0.01 | 360 | 337 | -23 | -0.06 | 0.041 | 0.042 | 0.000 | 0.01 |

(continued)

Table IV-57 (continued) - 2

| Experiment | Initial Concentrations | | | Maximum Ozone Concentration | | | | Time to 1/2 Maximum Expt. ([$O_3$]-[NO]) | | | | Maximum PAN Yields | | | |
|---|---|---|---|---|---|---|---|---|---|---|---|---|---|---|---|
| | $NO_x$ (ppm) | HC (ppmC) | HC/$NO_x$ | Expt (ppm) | Calc (ppm) | Calc -Expt (ppm) | Calc -Expt /Expt | Expt (min) | Calc (min) | Calc -Expt (min) | Calc -Expt /Expt | Expt (ppm) | Calc (ppm) | Calc -Expt (ppm) | Calc -Expt /Expt |
| JL0883R | 0.372 | 1.7 | 4.7 | 0.756 | 0.650 | -0.106 | -0.14 | 435 | 460 | 25 | 0.06 | 0.092 | 0.043 | -0.049 | -0.53 |
| JL1583R | 0.359 | 2.2 | 6.1 | 0.866 | 0.693 | -0.173 | -0.20 | 377 | 369 | -8 | -0.02 | 0.068 | 0.058 | -0.010 | -0.14 |
| OC0483R | 0.254 | 2.6 | 10.2 | 0.603 | 0.636 | 0.033 | 0.06 | 305 | 238 | -67 | -0.22 | 0.061 | 0.072 | 0.011 | 0.18 |
| JL0182B | 0.352 | 3.6 | 10.2 | 0.759 | 0.760 | 0.002 | 0.00 | 306 | 251 | -55 | -0.18 | 0.079 | 0.124 | 0.045 | 0.56 |
| AU0382B[a] | 0.165 | 1.2 | 7.6 | 0.576 | 0.438 | -0.137 | -0.24 | 419 | 479 | 60 | 0.14 | 0.012 | 0.017 | 0.005 | 0.41 |
| ST1782B | 0.254 | 2.4 | 9.5 | 0.637 | 0.588 | -0.049 | -0.08 | 373 | 382 | 9 | 0.02 | 0.045 | 0.055 | 0.010 | 0.22 |
| OC0682B | 0.466 | 2.0 | 4.2 | 0.450 | 0.357 | -0.093 | -0.21 | 414 | 394 | -20 | -0.05 | 0.026 | 0.023 | -0.004 | -0.14 |
| JL1583B | 0.352 | 2.3 | 6.4 | 0.922 | 0.773 | -0.149 | -0.16 | 376 | 344 | -32 | -0.09 | 0.063 | 0.069 | 0.006 | 0.10 |
| Group Average | 0.325 | 2.3 | 7.4 | 0.606 | 0.568 | -0.038 | -0.02 | 361 | 347 | -13 | -0.04 | 0.055 | 0.061 | 0.006 | 0.13 |
| S. Dev. | 0.096 | 0.7 | 2.3 | 0.226 | 0.199 | 0.085 | 0.18 | 52 | 75 | 36 | 0.11 | 0.024 | 0.033 | 0.024 | 0.32 |
| Avg. Abs. Value | | | | | | 0.071 | 0.14 | | | 31 | 0.09 | | | 0.017 | 0.28 |
| S. Dev. | | | | | | 0.058 | 0.11 | | | 21 | 0.07 | | | 0.017 | 0.19 |
| 3: Synthetic Mixture Runs | | | | | | | | | | | | | | | |
| OC0783R[b] | 0.334 | 2.7 | 7.9 | 0.178 | 0.491 | 0.312 | 1.75 | 394 | 286 | -108 | -0.27 | 0.056 | 0.078 | 0.022 | 0.40 |
| OC0483B[c] | 0.251 | 2.2 | 8.7 | 0.642 | 0.670 | 0.028 | 0.04 | 369 | 268 | -101 | -0.27 | 0.060 | 0.070 | 0.010 | 0.16 |
| OC0783B[c] | 0.345 | 2.7 | 7.8 | 0.451 | 0.618 | 0.168 | 0.37 | 360 | 245 | -116 | -0.32 | 0.101 | 0.110 | 0.009 | 0.09 |
| Group Average | 0.310 | 2.5 | 8.2 | 0.424 | 0.593 | 0.169 | 0.72 | 374 | 266 | -108 | -0.29 | 0.072 | 0.086 | 0.014 | 0.22 |
| S. Dev. | 0.051 | 0.3 | 0.5 | 0.233 | 0.092 | 0.142 | 0.90 | 17 | 21 | 7 | 0.03 | 0.025 | 0.021 | 0.007 | 0.16 |
| Avg. Abs. Value | | | | | | 0.169 | 0.72 | | | 108 | 0.29 | | | 0.014 | 0.22 |
| S. Dev. | | | | | | 0.142 | 0.90 | | | 7 | 0.03 | | | 0.007 | 0.16 |

[a] Cryogenically trapped exhaust employed.
[b] UNCMIX + COMARO run.
[c] Synthetic exhaust run.

```
-------------------------------------------------------------------------
 Calc.-Expt.      Volare             Charger            Synthetic
Maximum Ozone                                            Mixtures
-------------------------------------------------------------------------

      < -0.33     :                  :                  :
-0.33 - -0.27     :                  :                  :
-0.27 - -0.21     :                  :                  :
-0.21 - -0.15     :1                 :1                 :
-0.15 - -0.09     :1111              :1111              :
-0.09 - -0.03     :1111              :1                 :
-0.03 -  0.03     :111               :1111              :1
 0.03 -  0.09     :                  :111               :
 0.09 -  0.15     :                  :                  :
 0.15 -  0.21     :                  :                  :1
 0.21 -  0.27     :                  :                  :
 0.27 -  0.33     :                  :                  :1
      >  0.33     :                  :                  :

-------------------------------------------------------------------------
 Calc.-Expt.
 /Expt. NO Ox-     Volare             Charger            Synthetic
idation Times                                             Mixtures
-------------------------------------------------------------------------

      < -0.55     :                  :                  :
-0.55 - -0.45     :                  :                  :
-0.45 - -0.35     :                  :                  :
-0.35 - -0.25     :                  :                  :111
-0.25 - -0.15     :11                :111               :
-0.15 - -0.05     :1                 :111               :
-0.05 -  0.05     :111111            :1111              :
 0.05 -  0.15     :111               :111               :
 0.15 -  0.25     :                  :                  :
 0.25 -  0.35     :                  :                  :
 0.35 -  0.45     :                  :                  :
 0.45 -  0.55     :                  :                  :
      >  0.55     :                  :                  :

-------------------------------------------------------------------------
```

Figure IV-103. Plots of distributions in discrepancies in model predictions of maximum ozone yields, times required to achieve half the maximum experimental change in ($[O_3]-[NO]$), ethene half-lives, and PAN and formaldehyde yields for the UNC auto exhaust irradiations and associated experiments. Codes for experiments in PAN, formaldehyde, and ethene plots:
1 = Volare exhaust, 2 = Charger exhaust,
3 = Synthetic mixture runs.

```
----------------------------------------------------------------------
    Calc.-Expt./Calc.                   Calc.-Expt./Calc.
       PAN Yields                     Formaldehyde Yields
----------------------------------------------------------------------

    < -0.5     :112                     < -0.5     :1111111111222222233
-0.5 - -0.4    :                   -0.5 - -0.4     :2
-0.4 - -0.3    :                   -0.4 - -0.3     :22
-0.3 - -0.2    :                   -0.3 - -0.2     :23
-0.2 - -0.1    :122                -0.2 - -0.1     :
-0.1 -  0.0    :                   -0.1 -  0.0     :2
 0.0 -  0.1    :123                 0.0 -  0.1     :
 0.1 -  0.2    :223                 0.1 -  0.2     :
 0.2 -  0.3    :112                 0.2 -  0.3     :2
 0.3 -  0.4    :23                  0.3 -  0.4     :
 0.4 -  0.5    :22                  0.4 -  0.5     :
    >  0.5     :1112                    >  0.5     :

----------------------------------------------------------------------
       Calc.-Expt./Calc.
       Ethene Half Lives
----------------------------------------------------------------------
    < -0.5    :
-0.5 - -0.4   :
-0.4 - -0.3   :
-0.3 - -0.2   :13
-0.2 - -0.1   :12223
-0.1 -  0.0   :1111222223
 0.0 -  0.1   :1111222
 0.1 -  0.2   :22
 0.2 -  0.3   :
 0.3 -  0.4   :
 0.4 -  0.5   :
    >  0.5    :

----------------------------------------------------------------------
```

Figure IV-103 (continued)

selected species for representative experiments are given in Figures IV-104 through IV-108, where Figures IV-104 and IV-105 show data for runs using exhaust from the Plymouth Volare at two different hydrocarbon/$NO_x$ ratios, Figures IV-106 and IV-107 show data from runs using exhaust from the Charger, and Figure IV-108 shows data from the synthetic exhaust experiment carried out at the same time as the Charger exhaust experiment shown on Figure IV-107.

In general, the performance of the model in simulating the results of these auto exhaust runs was suprisingly good, especially in view of the greater uncertainties involved in modeling these experiments and the general variability of the performance of the model in simulating other groups of UNC chamber runs, where the initial reactant concentrations are more precisely known. In particular, the performance of the model was comparable to, and indeed slightly better than, the simulations of the UNC complex mixture runs discussed in Section IV-E-10. In addition, it is interesting to note that the model performance in simulating the JL0883 runs, which had only total NMHC data, was comparable to the simulations of the other experiments, though the ozone maximum yield was slightly underpredicted in both runs. (Concentration-time data for run JL0883R are shown in Figure IV-106.) The relatively good performance of the model in simulating these runs suggests either that the speciation of the exhaust in these runs is adequately characterized, or that the model is not very sensitive to the uncertainties involved, or that some cancellation of errors is occurring.

As indicated in Figure IV-103, there are some differences in the distribution of the discrepancies in the model predictions for the model simulations of the exhaust from the two vehicles, though it is not clear whether these differences are significant. In general, the model had a somewhat greater tendency to overpredict ozone yields when simulating experiments using exhaust from the Volare, while the simulations of the runs involving the Charger tended to have a wider distribution of the discrepancies in the predictions of the NO oxidation/ozone formation times. However, in most cases the discrepancies in the model predictions in ozone yields and timing are relatively small, and have no apparent dependence on the initial hydrocarbon or $NO_x$ levels, or their ratio.

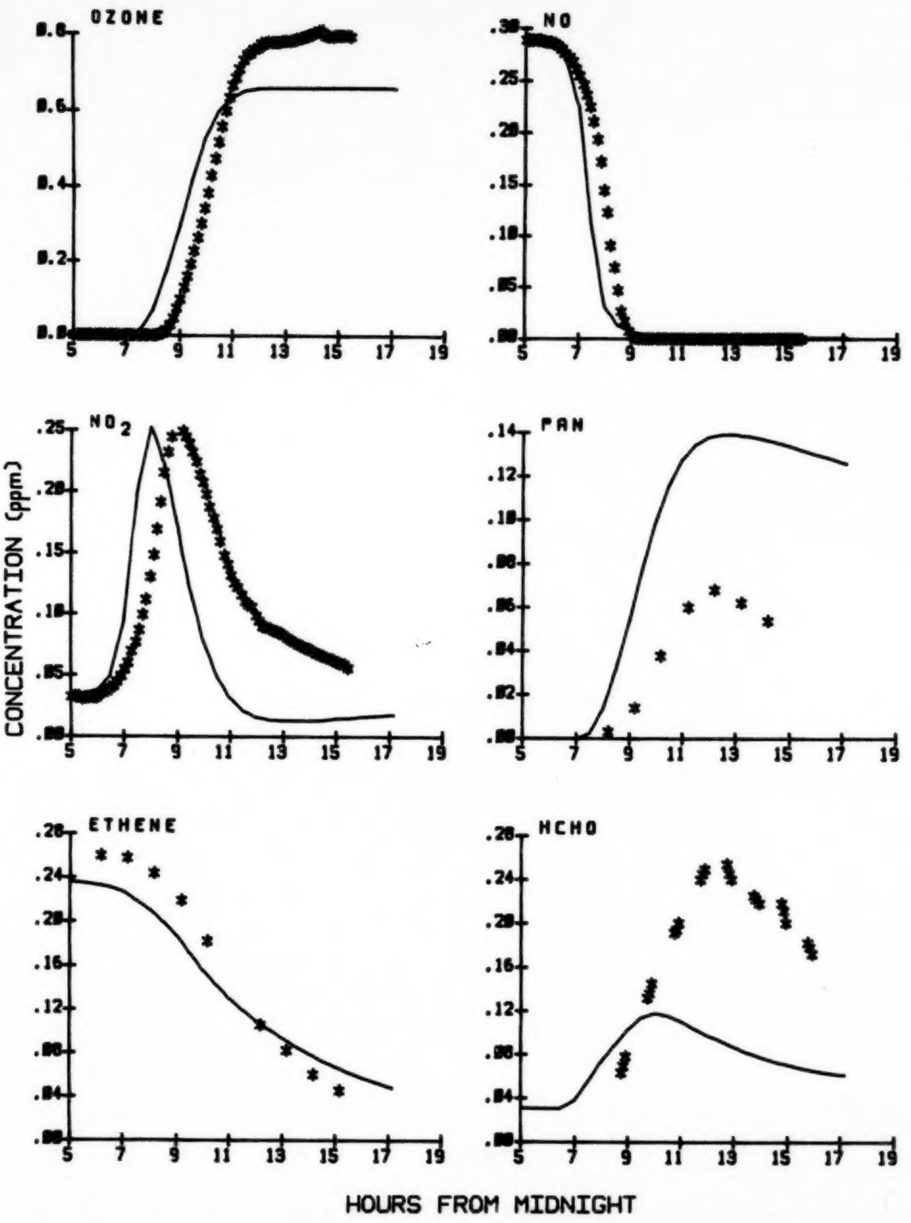

Figure IV-104. Experimental and calculated concentration-time plots for selected species observed in the UNC Volare exhaust irradiation JN3082R.
* = Experimental data.
----- = Model calculation.

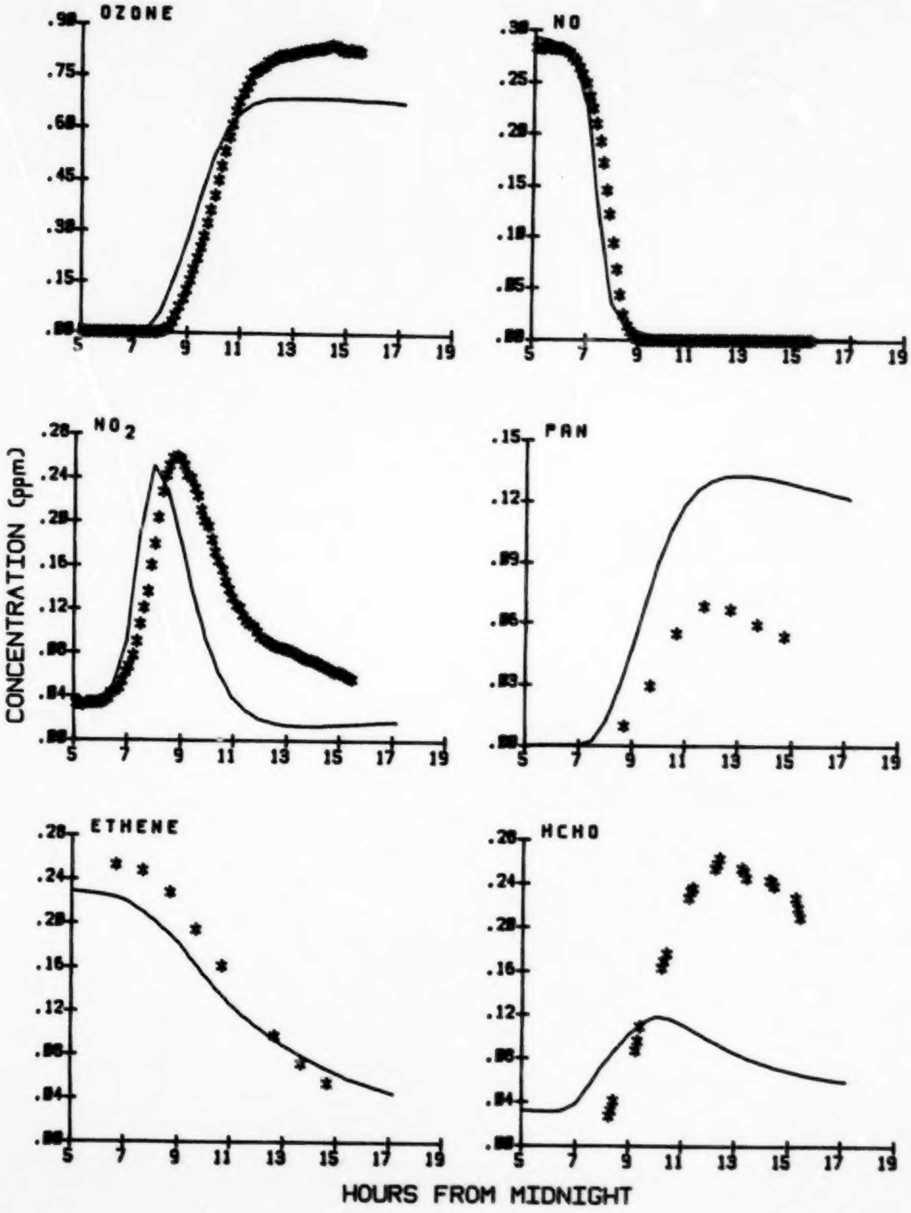

Figure IV-105. Experimental and calculated concentration-time plots for selected species observed in the UNC Volare exhaust irradiation JN3082B.

* = Experimental data.

----- = Model calculation.

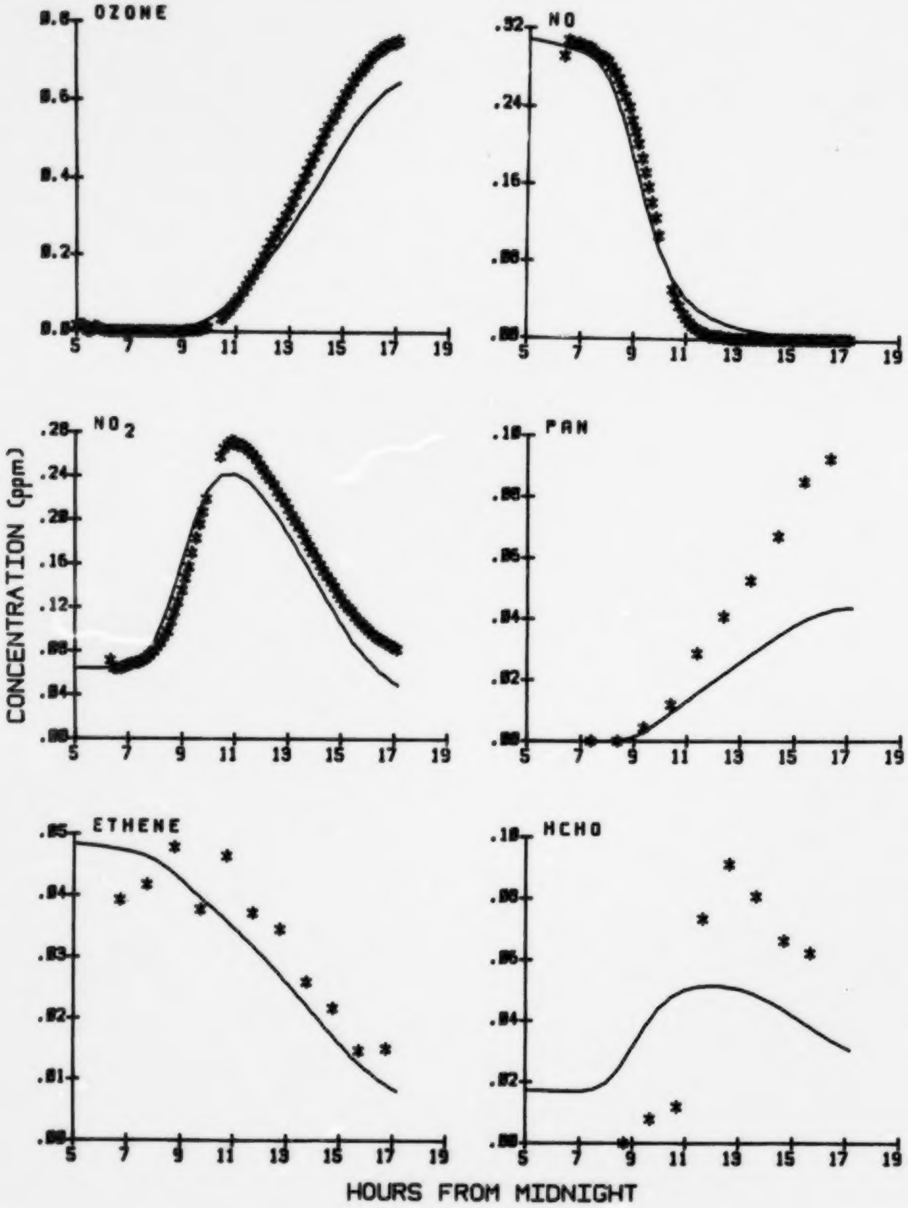

Figure IV-106. Experimental and calculated concentration-time plots for selected species observed in the UNC Charger exhaust irradiation JL0883R.
* = Experimental data.
----- = Model calculation.

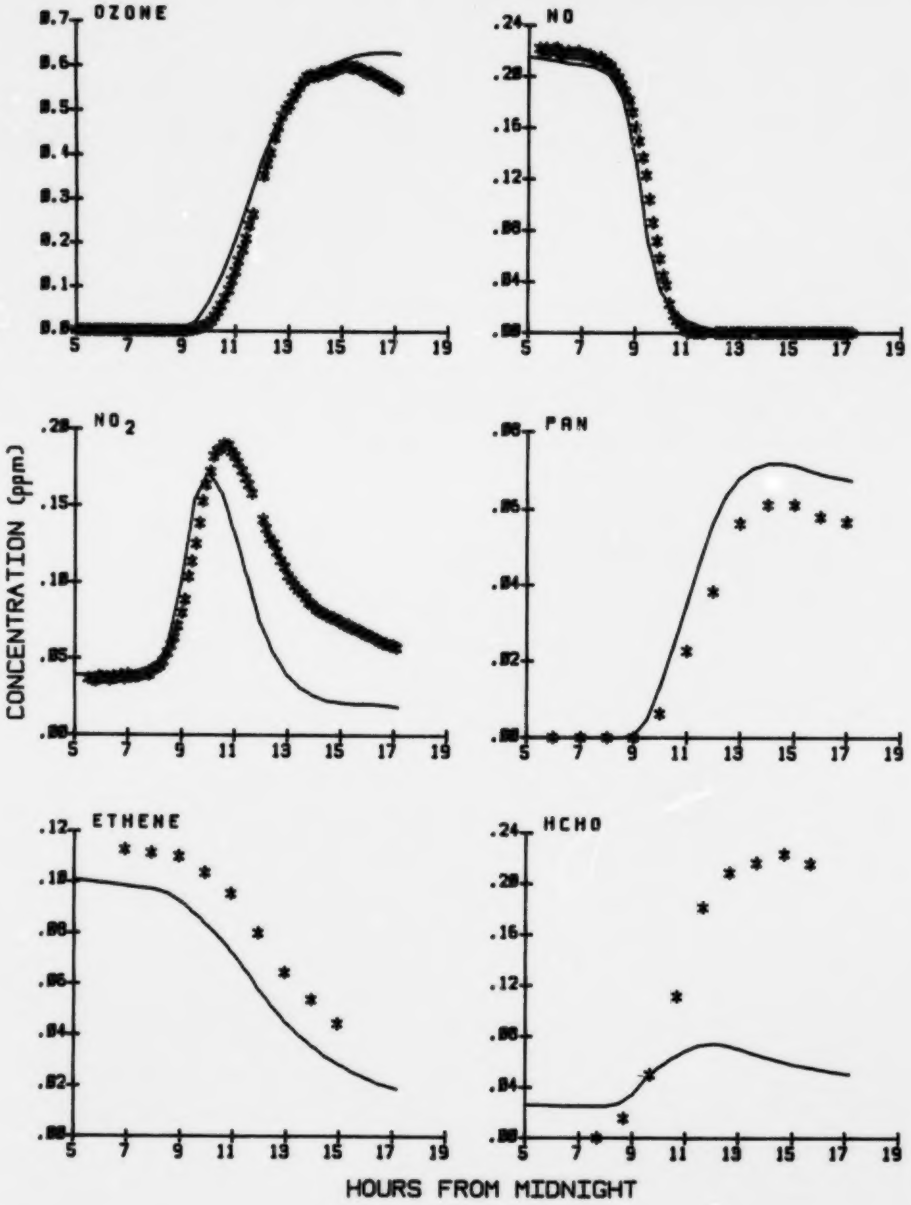

Figure IV-107. Experimental and calculated concentration-time plots for selected species observed in the UNC Charger exhaust irradiation OC0483R.
* = Experimental data.
----- = Model calculation.

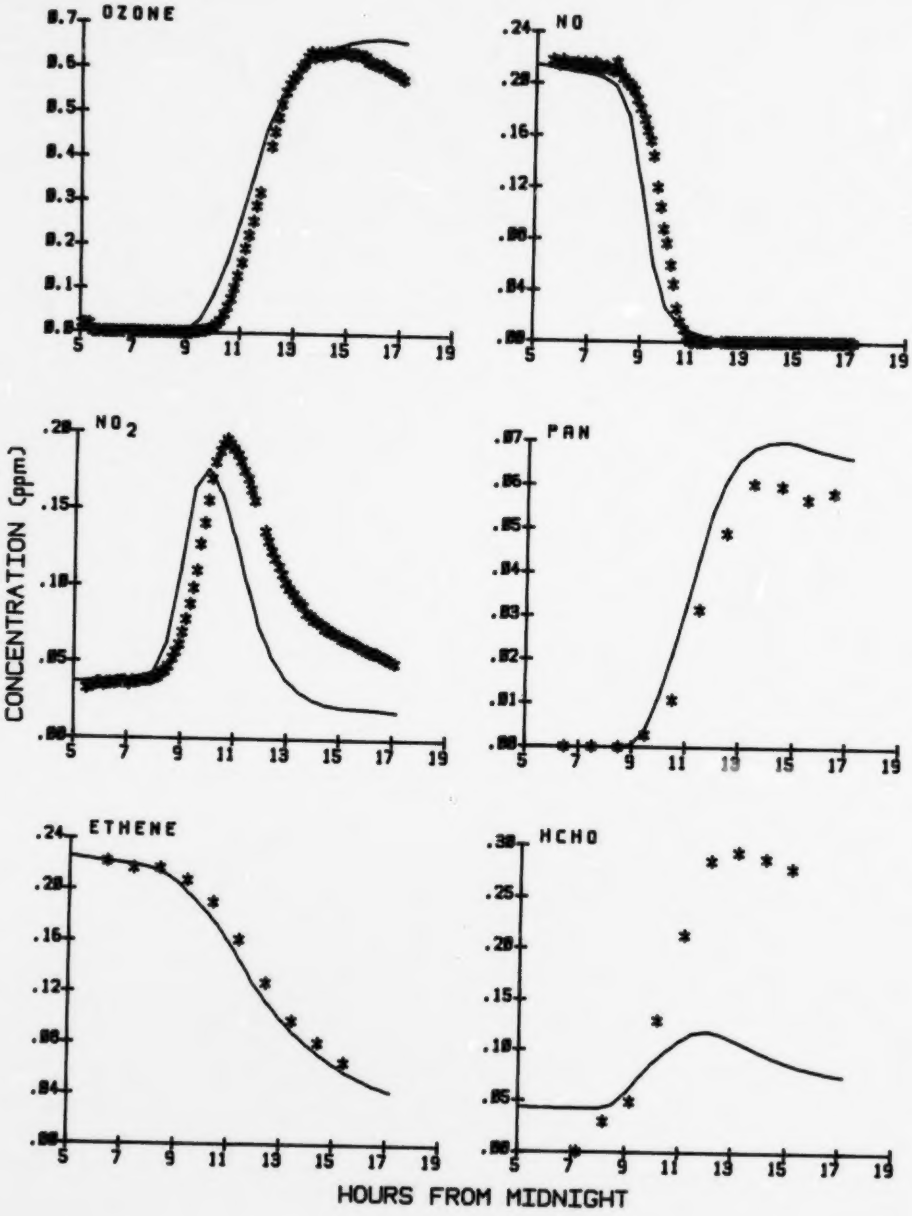

Figure IV-108. Experimental and calculated concentration-time plots for selected species observed in the UNC synthetic exhaust irradiation OC0483B.
* = Experimental data.
----- = Model calculation.

The simulations of the exhaust experiments also gave generally good fits to the observed ethene half-lives, though it should be pointed out that for some runs, the UNC ethene data suffers from interference from other, less reactive compounds, which means that the measured ethene half-life would be slightly longer than the true value. [This is why in some runs the initial ethene concentrations recommended by Jeffries et al. (1985b), and used in our model simulations, is somewhat lower than the experimental values, as shown in Figures IV-104 through IV-107.] Despite this problem, ethene is chosen for testing the model predictions of organic consumption rates, because it is the only relatively rapidly reacting species which is represented in the model explicitly.

The model tended to overpredict PAN yields observed in most exhaust irradiations, though this could be attributed, at least in part, to the lumping technique employed, where in many cases compounds which form PAN in their photooxidations are used in the model to represent compounds which would form PPN or other higher peroxy acyl nitrates. (For example, toluene, which forms PAN in its photooxidation, is used in the model to represent the reactions of ethyl benzene, which by analogous reactions is expected to form PPN and not PAN.) The model significantly underpredicts formaldehyde yields observed in these experiments, but this is in line with the results obtained in modeling essentially all UNC runs employed in this program. In fact, one would expect the approach of representing the reactions of larger molecules (such as ethylbenzene) by smaller ones (such as toluene) to result in consistent overpredictions of formaldehyde.

It is interesting to note that the runs where the model performance was the poorest were not exhaust runs, but were irradiations of known mixtures. In particular, known mixtures were irradiated on both sides of the chamber on October 7, 1983, and the simulations of both these mixtures significantly overpredicted the observed reactivity. The other known mixture irradiation associated with these experiments was carried out on the "blue" side of the chamber three days earlier, with a Charger exhaust irradiation being simultaneously carried out on the "red" side. In this set of irradiations, the model performance in simulating the results from the known mixture side was comparable to that for the exhaust side, as is shown in Figures IV-107 and IV-108, which gives experimental and calculated concentration-time data for these runs.

# SECTION V

# SUMMARY, CONCLUSIONS, AND FUTURE EFFORTS

The first phase of this research program achieved its objective in updating and comprehensively testing a detailed chemical mechanism which can be adapted for incorporation into air quality simulation models for control strategy assessments. In this phase, the detailed, "lumped molecule," mechanisms of Atkinson et al. (1982a) and Lurmann et al. (1986) were updated based on recent relevant laboratory results and results of tests against environmental chamber experiments, and chemical mechanisms for a number of new species were developed. Substantial modifications were made to previous aromatic photooxidation mechanisms and the approach used to represent the reactions of the higher ($\geq C_5$) alkanes, several significant changes concerning the mechanisms of the alkenes and the ketones were made, and a new approach was developed to represent the reactions of peroxy radicals under conditions where radical-radical reactions become important. These updated mechanisms were tested, using a consistent set of assumptions regarding environmental chamber effects, against the results of over 400 environmental chamber experiments carried out in four different environmental chambers operated by two different research groups. This is, we believe, the most comprehensive testing program for atmospheric reaction mechanisms carried out to date as a single study, and this study has allowed the performance of state-of-the-art mechanisms in simulating results of environmental chamber experiments to be assessed in detail.

However, despite the progress made, a number of uncertainties remain in our understanding of potentially important areas of the chemical mechanisms. Furthermore, the testing of the mechanisms has revealed a number of discrepancies between the predictions of the model and the experimental results. Many of these discrepancies were random in nature, and can be attributed to uncertainties in characterizing chamber effects or light intensity, but other discrepancies may be due to errors in the updated mechanisms. These discrepancies and uncertainties indicate additional areas of research required to improve the validity of current atmospheric reaction mechanisms, and concurrently in our confidence in the predictions of models which incorporate such mechanisms. The major areas of uncertainty in the mechanisms, and the areas where the current model does not well simulate the environmental chamber data, are summarized in the following sections.

Among these areas of needed research are improved characterization of chamber effects and light characteristics associated with environmental chamber experiments, to allow for more unambiguous testing of the chemical mechanisms. At the present time, if the model performs poorly in simulating the results of a given experiment, it is not always clear whether this is due to problems with the chemical mechanism or in characterizing the conditions of the experiment. Because of this, it is necessary to test the model predictions against a large number of experiments to determine if the discrepancies are due to systematic problems with the model, or to uncertainties in the characterization of conditions of individual runs, which are expected to be more random in nature. Fortunately, in many cases, the large data base of environmental chamber experiments used in this program allows systematic, as opposed to random, discrepancies to be observed. However, even where such systematic discrepancies are observed, the possibility that it is due to systematic errors in chamber or light intensity characterization, as opposed to errors in the chemistry, cannot always be ruled out.

Despite the problem areas in the mechanism and uncertainties in chamber and light intensity characterization, the model was able to simulate reasonably well the major results of the majority of the experiments used for model testing, particularly those employing complex mixtures more representative of urban atmospheres. Thus the predictive power of the detailed mechanism which was developed and tested in this program is sufficient that it is suitable for condensation for use in air quality simulation models, and models incorporating this mechanism can be employed by regulatory and planning officials with the confidence that they are based on our best current understanding of atmospheric reaction mechanisms and results of smog chamber experiments. Nevertheless, it is clear that the mechanism developed in this program is yet one further step in the progressive development of detailed chemical mechanisms, and that future updates, testing, and adaptation will be appropriate as information regarding the uncertain areas of the mechanism, or the major uncertain chamber effects and light intensity characteristics, become available.

The progress made in the updating and the testing of the chemical mechanism carried out in this program, and the uncertainties, discrepancies, and problem areas encountered are summarized below. Section V-A summarizes the updates of the reaction mechanism and the areas of uncertainty, and indicates those portions of the mechanisms which had to be adjusted to improve the fits to the environmental chamber data. Section V-B summarizes the results of the testing program, indicating the areas where the model performed well or exhibited systematic discrepancies, and the uncertainties introduced by incompletely characterized chamber effects and other problems associated with environmental chamber experiments. Finally, in Section V-C, the work being carried out in the remainder of this program in adapting these mechanisms to atmospheric modeling is briefly summarized and discussed.

## V. A. UPDATED CHEMICAL MECHANISMS AND REMAINING UNCERTAINTIES

### 1. Mechanism Updates and Species Represented

The chemical mechanism developed in this program is an updated and expanded version of the mechanism of Lurmann et al. (1984, 1986), which, in turn, is an update of the earlier mechanism of Atkinson et al. (1982a). The species included in the new mechanisms, and the major differences between the mechanisms developed in this program and the previous mechanisms of Atkinson et al. (1982a) and Lurmann et al. (1984, 1986), are as follows:

Inorganics. The reactions of the inorganic species NO, $NO_2$, $O_3$, CO, $NO_3$, $N_2O_5$, HONO, $HONO_2$, $HO_2NO_2$, OH, $HO_2$, $O(^3P)$, $H_2O_2$ and $SO_2$ are represented explicitly. This mechanism differs from that of Atkinson et al. (1982a) and Lurmann et al. (1984, 1986) in that the reactions of $O(^3P)$ atoms are represented explicitly rather than being lumped in other reactions, and differs from that of Atkinson et al. (1982a) in that a reaction between $HO_2$ and $NO_3$ is included. Some minor rate constant updates, based primarily on the recent reviews of Atkinson and Lloyd (1984) and NASA (1985), are also included.

Alkanes. The reactions of ethane, propane, n-butane, and isobutane are represented explicitly. The reactions of the higher alkanes n-pentane through n-nonane, 2-methyl butane, 2-methyl pentane, 2,3-dimethyl butane, 2,4-dimethyl pentane, and 2,2,4-trimethyl pentane (isooctane) are represented using a "lumped reaction" approach which represents the net effects of their overall reactions. However, for atmospheric modeling purposes, the reactions of many of these species can be lumped together, and indeed for the purposes of testing the model against the results of auto exhaust irradiations carried out at UNC (Jeffries et al. 1985b) all alkanes were lumped into three classes: unreactive, $C_4$-$C_5$ alkanes, and $\geq C_6$ alkanes. Other than the number of species represented and some updates in estimates of branching ratios based on the recent review of Carter and Atkinson (1985), the major difference between this and the earlier mechanisms is that in the present mechanism the formation of alkyl nitrates in the reactions of NO with hydroxy-substituted peroxy radicals is assumed to be zero, in contrast with earlier mechanisms in which the nitrate yields were assumed to be the same as those from the unsubstituted radicals. This modification was made to improve the fits of model predictions to n-heptane, n-octane, and n-nonane-$NO_x$-air environmental chamber experiments.

Alkenes. The reactions of ethene, propene, 1-butene, trans-2-butene, and isobutene are represented explicitly. However, for atmospheric modeling purposes, it is appropriate to lump together the reactions of the alkenes which react at similar rates, and for this purpose a general lumped monoalkene model, which can be used to represent different alkenes which react at different rates as a single species, was developed. The alkene mechanisms developed in this program differ from those in the previous models of Atkinson et al. (1982a) and Lurmann et al. (1984, 1986) in that (a) the present mechanism includes the reactions of the alkenes with $O(^3P)$ atoms and $NO_3$ radicals; (b) several modifications were made to the highly uncertain ozone + alkene mechanisms based on recent laboratory data and adjustments required to fit the results of the environmental chamber experiments, and (c) the formation of organic nitrates from the reactions of NO with the hydroxy-substituted peroxy radicals formed in the reactions of the butenes were assumed to be zero, instead of the non-negligible ~8% nitrate yields assumed in the previous models of Atkinson et al. (1982a) and Lurmann et al. (1984, 1986). The latter modification was also made in order to improve the fits to the environmental chamber experiments.

Aromatic Hydrocarbons. The reactions of benzene, toluene, o- and m-xylene, and 1,3,5-trimethylbenzene are represented explicitly in the model, though for the purposes of atmospheric modeling the reactions of the xylenes can be lumped together. The details of the ring-opening processes in the reactions of these aromatic hydrocarbons, and the subsequent reactions of many of the ring-opening products, are not known. These reactions are represented by parameterized, semi-empirical mechanisms, with the photolysis rates of the uncharacterized products being adjusted to fit the environmental chamber data. The aromatic mechanism developed in this program differs considerably from those in the earlier models in that at the time those were developed it was believed that the ring-opening processes could be represented by a well-defined sequence of fragmentation reactions which form α-dicarbonyls and unsaturated 1,4-dicarbonyls. More recent product data indicate that this ring-opening mechanism is incomplete, and that the major ring-opening pathways and the ring-opening products are, in fact, unknown.

Photooxidation Products. The reactions of the photooxidation products formaldehyde, acetaldehyde, propionaldehyde, acetone, methyl ethyl ketone (MEK), glycolaldehyde, 3-pentanol, glyoxal, methylglyoxal, biacetyl, PAN, PPN, PBzN, 2-butyl nitrate and 4-heptyl nitrate, and the reactions of OH radicals with benzaldehyde and of $NO_3$ radicals with phenol and o-cresol, are represented explicitly. The photolysis of benzaldehyde, the reactions of OH radicals with phenolics, and the reactions of the uncharacterized aromatic ring-opening products are represented by parameterized mechanisms with the parameters being adjusted in some cases to fit the environmental chamber data. In a number of cases, the "lumped molecule" approach is employed in which one or more of these representative photooxidation products is used to represent the reactions of other species, in order to limit the number of product species represented explicitly. For example, propionaldehyde was used to represent the reactions of the higher aldehydes, MEK was used to represent the higher ketones, appropriate combinations of propionaldehyde, MEK, and 3-pentanol were used to represent the bi- and poly-functional products formed in the photooxidations of the higher alkanes, and 2-butyl and/or 4-heptyl nitrates were used to represent the reactions of the $\geq C_4$ nitrates formed from the higher alkanes. The mechanism developed in this program thus employs a greater variety of representative photooxidation products than do the previous mechanisms of Atkinson et al. (1982a) and Lurmann et al. (1984, 1986). In addition, the acetone and MEK mechanisms developed in this program use photodecomposition quantum yields of 0.1 and 0.07, respectively, rather than unity as assumed previously.

Peroxy Radical Reactions. While the reactions of NO with the peroxy and acyl peroxy radicals formed in the photooxidations of the various compounds listed above are represented explicitly, as they were in previous mechanisms, new approaches were developed to allow for a more efficient representation of the reactions of these species with $HO_2$ and with other peroxy or acyl peroxy radicals. These radical-radical reactions were shown to be significant under conditions when $NO_x$ is depleted, but explicitly representing or all the possible combination reactions of the many different peroxy or acyl peroxy radicals in the mechanisms, or all the different hydroperoxides which can be formed when they react with $HO_2$, would increase the number of reactions and species in the mechanisms excessively. The peroxy + peroxy radical reactions were represented in the new mechanism by including the reactions of the individual peroxy or acyl peroxy radicals with the pseudo-species "$RO_2$" and "$RCO_3$", which were used to represent the total concentrations of all peroxy and acyl peroxy radicals, respectively. (These latter pseudo-species were calculated by including them as products in any reaction forming peroxy or acyl peroxy radicals, and including in the model separate pseudo-reactions to represent their sink processes. Including these species in the model as separately integrated species has the additional advantage that it allows the steady-state approximation to be employed for the many individual peroxy or acyl peroxy species in the model, significantly reducing the total number of species which have to be integrated by the model calculation software.) The reactions of the hydroperoxides formed in the reactions of the peroxy or acyl peroxy radicals were represented by the pseudo-specie "-OOH" plus the set of oxygenated products formed when the individual radicals react in the presence of NO, with a photolysis reaction of "-OOH" being included in the model to represent the radical regeneration which results when the individual hydroperoxides photolyze. This approach involves a number of approximations, but test calculations using simplified mechanisms with the peroxy + peroxy or peroxy + $HO_2$ reactions represented explicitly showed that the errors introduced by this representation are relatively minor, especially when compared to the much more severe errors introduced by ignoring them altogether.

## 2. Major Uncertainties in the Mechanisms

Although substantial progress has been made in recent years in improving our understanding of the detailed chemical reactions occurring when organics are irradiated in the presence of $NO_x$, substantial areas of uncertainty still remain. In several areas, primarily concerning the reactions of aromatics, our knowledge of the detailed reactions occurring are so incomplete that we had no choice but to employ arbitrary assumptions or empirical models. In other portions of the mechanism, uncertain parameters in the model were adjusted in order to achieve acceptable fits of the model simulations to the results of relevant environmental chamber experiments, and in other areas highly uncertain estimates had to be made. The major areas of uncertainty which we believe are involved in the present mechanism, including those areas where parameters had to be adjusted to improve fits to the chamber experiments, are briefly summarized below.

The largest general area of uncertainty continues to be the photooxidation mechanism of the aromatic hydrocarbons and their reaction products. Ring opening is an important reaction pathway for the aromatics, yet only a relatively small fraction of the ring-opening products have been quantitatively identified, and the subsequent reactions of the products expected (and observed in qualitative product studies) to be formed, are unknown. Unfortunately, it is clear that these uncharacterized ring-opening products are highly reactive and cannot be ignored, since if they are, the reactivity observed in essentially all aromatic-$NO_x$-air irradiations is significantly underpredicted. Previously published models for aromatics, including those of Atkinson et al. (1982a) and Lurmann et al. (1984, 1986), were all based on assuming higher yields of $\alpha$-dicarbonyls from aromatics than is now known to be the case, with the rapid photolysis of these species supplying the radicals necessary to account for the observed reactivity. In addition, none of those models were tested against experiments using blacklight irradiation, where the $\alpha$-dicarbonyl photolysis is sufficiently slow that reactivity is underpredicted even if the high $\alpha$-dicarbonyl yields are assumed. Thus in this model we had to assume that the uncharacterized ring-opening products photolyze at rates comparable to those of the $\alpha$-dicarbonyls, with their photolysis rates being adjusted to fit the data. Although the photolysis rates adjusted to fit results of experiments employing a solar simulator were different than those required to fit experiments using blacklight irradiation, by assuming that this product photolyze only at wavelengths $\lesssim$350 nm, the observed reactivity in both chambers, and in most outdoor chamber irradiations, could be simulated with a consistent model.

Since the identity and the details of the reactions of the aromatic ring-opening products are unknown, no attempt was made to represent them explicitly in this model. Rather, the products formed from a given aromatic hydrocarbon were lumped together as a single specie, whose reaction mechanism was based on that employed in the previous models of Atkinson and co-workers to represent the reactions of the unsaturated 1,4-dicarbonyls. It was assumed that the OH radical reactions of these species, which are non-negligible despite their rapid assumed photolysis, involve the formation of PAN-analogs, since including this $NO_x$ sink resulted in improved predictions of maximum ozone yields. However, the possibilities that the $NO_x$ sink(s) involved are totally different, and that the presently uncharacterized ring-opening products react via pathways which are not analogous to those assumed in this model, have not been ruled out.

The reactions of the ring-opening products are not the only areas of uncertainty in the aromatic photooxidation mechanisms. Other uncertain areas, or areas where parameters were adjusted for the model to better fit the data, are as follows: (1) The OH + phenol and cresol mechanisms are totally unknown, and no attempt was made to represent them explicitly. The reactions involved were represented in this model by an empirical model with two parameters, adjusted to fit the results of the single o-cresol-$NO_x$ run carried out in the SAPRC EC. (2) Organic nitrate formation from the reactions of NO with OH-aromatic-$O_2$ adducts was assumed to be negligible, and yielded better fits to the data. Assuming this radical sink to be important (and correcting for the loss of radicals by using higher ring-opening product photolysis rates) results in incorrect predictions of the effect of reactivity on the hydrocarbon/$NO_x$ ratios in the benzene system. (3) The reaction of $NO_3$ radicals with nitrophenols was added to the model to provide a $NO_x$ sink and improve the fits to the observed maximum ozone yields. (4) The mechanism and products formed from the photolysis of benzaldehyde is unknown. The photolysis rate was adjusted to fit the results of EC experiments, and only unreactive species were assumed to be formed to fit the data. (5) Although, based on an extrapolation from elevated temperature data, it was initially assumed that there is a 7% abstraction pathway in the reaction of OH radicals with benzene, we found that assuming this in our model resulted in unsatisfactory simulations of the benzene runs, so this process was assumed not to be important under tropospheric conditions. (6) The yields of phenolic products from the xylenes and trimethylbenzenes are unknown, and were estimated based on those in the toluene system. Thus, despite progress in recent years, further studies of the mechanisms of the photooxidations of aromatics, and their reaction products, are urgently needed.

Another major area of uncertainty in the present model concerns the mechanism of the reactions of ozone with propene and the higher alkenes. Assumptions regarding these reactions, particularly regarding the amount of radicals produced, can have significant effects on the chemical mechanism predictions. Although there have been numerous studies of these reactions, for alkenes other than ethene the available data are not sufficient to unambiguously establish the exact mechanism, or products formed, under atmospheric conditions. In this model, based on the recent data of Hatakeyama et al. (1984) which indicate lower stabilization yields in the reactions of the "hot biradicals" formed in the ozone-alkene reactions, we initially estimated that the radical yields in the reaction of ozone with propene were higher than assumed in the previous mechanisms of Atkinson et al. (1982a) and Lurmann et al. (1984, 1986). However, in order to fit the chamber data, the radical yields had to be adjusted back down to approximately the levels assumed in the previous models. Although no separate adjustments were made to improve the fits to experiments employing 1-butene and *trans*-2-butene, the results of these experiments were not particularly well simulated, and such adjustments may be appropriate. The ozone + isobutene mechanism is also totally unknown and had to be adjusted based on the results of a single experiment. Despite this it was not possible to fit both the reactivity observed and the PAN yield with the same model. Although it appears that we now have a reasonably good understanding of the ozone + ethene reaction mechanism under atmospheric conditions, it is clear that this is not so for the higher alkenes, and that further work, specifically addressed at unambiguously establishing radical yields under atmospheric conditions, is necessary.

Another area of the reaction mechanism for the butenes where the model was adjusted concerned the organic nitrate yield from the reactions of NO with the OH-butene-$O_2$ adducts formed from the OH + butene reactions. By analogy with reactions of NO with the unsubstituted $C_4$ peroxy radicals formed from n-butane, Atkinson et al. (1982a) assumed that 8% nitrate formation occurred, but we obtained better fits to the chamber data if the nitrate yield was assumed to be negligible. Recent studies by Shepson et al. (1985) on the analogous reactions in the propene system suggests that some nitrate formation does occur, but that it is less important than estimated by analogy with the alkane systems.

The reaction mechanisms of the higher alkanes are also not without major areas of uncertainty where the model had to be adjusted to yield satisfactory fits to the chamber data. The most important uncertainty concerns the reactions of the species formed following hydrogen shift isomerizations of longer-chain alkoxy radicals, which are major reaction routes in the photooxidations of alkanes with chains of five carbons or more. In particular, organic nitrate yields in the reactions of NO with the hydroxy-substituted peroxy radicals formed in these reactions are not known. It had previously been assumed that the nitrate yields from the reactions of NO with these radicals is similar to that for unsubstituted $RO_2$ radicals with the same number of carbons. However, we found that if this is assumed then the reactivity observed in $NO_x$-air irradiations of n-heptane through n-nonane are significantly underpredicted, and that better fits are obtained if no nitrates are formed from these hydroxy-substituted peroxy radicals. Thus, our updated model assumes that nitrate formation from these reactions is negligible (consistent with our assumptions regarding the reactions of the hydroxy-substituted radicals formed from the butenes). However, this adjusted model tends to overpredict maximum ozone yields observed in higher alkane-$NO_x$-air runs where a "true" ozone maximum is obtained, suggesting that the model needs additional $NO_x$ sinks, which this nitrate formation reaction would provide.

The alkane photooxidation mechanisms have other areas of uncertainty, though in terms of affecting predictions of overall reactivity and maximum ozone yields, those regarding nitrate formation reactions are clearly the most important. The photooxidations of many of the higher alkanes are characterized by many competing alkoxy radical reactions, and although a systematic set of procedures for estimating these branching ratios has been developed and incorporated into this model, these estimates are uncertain in many cases. Studies of the kinetics of the decomposition, isomerizations, and reactions with $O_2$ of a much wider variety of alkoxy radicals than presently available are necessary to reduce the uncertainties in these estimates.

Although recent laboratory studies have substantially reduced the uncertainties concerning the photolysis rates of formaldehyde and acetaldehyde, there remain uncertainties regarding the quantum yields for other oxygenates whose reactions are incorporated in this model. The quantum yields for the photolysis of methyl ethyl ketone are unknown, and those for the photolysis of acetone and propionaldehyde are uncertain. Unfortunately, the available chamber data are inadequate to comprehensively test the quantum yields assumed in the present model. The wavelength dependences of the quantum yields for the photolysis of the $\alpha$-dicarbonyls are unknown, though a comparison of biacetyl photolysis rates under blacklight and solar simulator irradiation tends to support the assumption incorporated in this model that they are wavelength independent.

The $HO_2$ + formaldehyde reaction mechanism is still highly uncertain, and under some conditions assumptions regarding this reaction can significantly affect model predictions. The previous experimental studies of this reaction have involved analyses of complex chemical systems which are subject to significant ambiguities and uncertainties. In this model, we had to choose between the various published rate constants, based on which value gave the best fit of model simulations to results of formaldehyde-$NO_x$-air and ethene-$NO_x$-air chamber experiments which were found to be sensitive to this parameter.

Significant progress has been made in our understanding of the reactions of the inorganic species incorporated into this model and, in terms of affecting model simulations of chamber experiments or photochemical smog formation, most of the remaining areas of uncertainty are believed to be minor compared to the much greater uncertainties in the reactions of the organic species. Probably the greatest uncertainty in this area concerns the extent to which the $N_2O_5$ + $H_2O$ reaction occurs in the gas phase, and whether it should be included in airshed models. The most recent experimental study of Atkinson et al. (1986b) shows that the homogeneous gas-phase reaction of $N_2O_5$ with water vapor is slow, with a 298 K rate constant $<1.5 \times 10^{-21}$ $cm^3$ $molecule^{-1}$ $sec^{-1}$. Indeed, it is likely that the homogeneous gas phase reaction is negligibly slow. However, an analysis of ambient air data suggests that an "effective" rate coefficient for this reaction of $\sim 3 \times 10^{-21}$ $cm^3$ $molecule^{-1}$ $sec^{-1}$ at 298 K is appropriate for ambient lower tropospheric modeling; though this "effective" rate coefficient may represent other processes such as dry deposition (Atkinson et al. 1986a). Environmental chamber data are not useful in testing this, since this reaction is known to occur on chamber walls, and it must be included as part of the chamber effects model.

It should also be pointed out that the uncertainties listed above are applicable to the reaction mechanisms of the specific organics which are represented explicitly in the mechanisms developed in this program, and not the additional uncertainties associated with representing the reactions of other compounds or (especially) other classes of compounds in the atmosphere. It is assumed that the set of compounds represented explicitly in this model are adequate to represent the reactions of most of the alkanes, alkenes, aromatic hydrocarbons, and simple oxygenates which are emitted into urban atmospheres, but the applicability of this assumption to many of the other emitted organics is highly uncertain. In particular, the species represented explicitly in this model may not be good surrogates for the reactions of, for example, the naphthalenes, the biogenically emitted organics, heteroatom-containing organics, bi- and polyfunctional compounds, high molecular weight organics, etc., which are also emitted in many, if not most, urban areas. If the reactions of such organics are important in affecting air quality in any airshed of interest, additional research is required to to determine the most appropriate manner to represent the atmospheric reactions of such species in the air quality models.

## V. B. SUMMARY OF RESULTS OF TESTING PROGRAM

The chemical mechanisms developed in this program were tested against the data obtained from over 400 environmental chamber experiments, carried out in four different environmental chambers by two different research groups. The chambers from which data were used were the 150,000-liter dual outdoor chamber at the University of North Carolina (UNC), the 5800-liter evacuable indoor chamber (EC) at the Statewide Air Pollution Research Center at U. C. Riverside (SAPRC), the SAPRC 6400-liter indoor Teflon chamber (ITC), and the SAPRC 50,000-liter dual outdoor Teflon chamber (OTC). The experiments used for model testing ranged in complexity from pure air, $NO_x$-air, and aldehyde-air runs used for chamber characterization purposes, through single component-$NO_x$-air irradiations employing a variety of representative alkanes, alkenes, aromatic hydrocarbons, aldehydes and ketones, to $NO_x$-air irradiations of simple and complex mixtures of organics and real and synthetic auto exhaust. The most comprehensive set of experiments used in this program were from the UNC chamber, but the set of experiments from the SAPRC EC was almost as comprehensive in terms of the number and variety of characterization and single component-$NO_x$-air runs. The major set of experiments from the other two SAPRC chambers were irradiations of various surrogate hydrocarbon-$NO_x$ mixtures (including many carried out under multi-day conditions), but a more limited set of characterization and single component-$NO_x$-air runs from those chambers was also available for this program. The major results from model simulations of these experiments are summarized below.

In order to carry out this testing program, procedures were developed to represent the light intensities and spectral distributions of the light sources used in the different chambers, and the various chamber effects, (radical sources, $NO_x$ offgassing rates, etc.), in a consistent manner for all four chambers. A number of uncertainties in these chamber-dependent parameters were identified which could significantly impact the results of the model testing, as discussed below. While the standard testing procedure involved no run-to-run adjustment of uncertain chamber-dependent parameters to optimize the fits of the model predictions to experimental results, a number of exploratory calculations were carried out to assess the effects of these parameters on the fits of the model calculations to the experimental data, and for the n-butane-$NO_x$-air runs a limited number of calculations were conducted to determine the quality of fits which resulted when magnitude of the chamber radical source was adjusted. While such run-to-run adjustment would obviously yield better fits, such a procedure defeats the purpose of this testing program since it could mask systematic errors in the chemical mechanism.

### 1. Chamber Effects and Light Source Characterization and Uncertainties

In this section, the chamber- and run-dependent parameters which were taken into account in the testing of the mechanism against environmental chamber data are summarized, and the most important areas of uncertainty are indicated. As discussed above and summarized below, many of the cases of poor fits of model simulations to experimental results are probably due to uncertainties in these parameters. An improvement in our understanding of these uncertainties would result in increased utility of environmental chamber data in providing more rigorous and unambiguous tests of the chemical mechanisms than currently possible.

Light Intensity and Spectral Distribution. The correct quantification of the intensity and spectral distribution of the chamber light sources is probably the most important requirement in modeling environmental chamber experiments, since these determine the rate constants for the photolysis reactions which drive the overall photochemical processes. This is not a significant uncertainty in the model simulations of the indoor chamber experiments, since periodic $NO_2$ actinometry data are available to determine the overall intensity, and periodic measurements of the spectral distribution of the light sources determine the relative spectral distributions. However, this does represent a potentially significant uncertainty in modeling the outdoor chamber experiments, which use natural sunlight whose intensity and spectral distribution vary with time, and which are affected by local meteorological effects, the albedos of nearby surfaces, and effects of transmission of sunlight through the chamber walls.

While systematic procedures were derived for calculating the time-varying light intensities and spectral distributions from the available light monitoring data, these procedures involve a number of presently unverified assumptions. In particular, in modeling both the UNC and SAPRC OTC chamber experiments it was necessary to assume that (1) the relative spectral distributions given as a function of zenith angle by Peterson (1976) for his "best estimate" surface albedos apply to sunlight reaching both the UNC and the SAPRC outdoor chambers at all times, including overcast or partly cloudy conditions; (2) the overall light intensity at all wavelengths which affect the photolysis reactions in the model are proportional to the UV radiometer readings, with the proportionality factor being derived from empirical UV vs $k_1$ relationships and theoretically calculated $k_1$ values; and (3) passage of the sunlight through the Teflon chamber walls and reflection from nearby surfaces does not affect the spectral distribution of the light reaching the interior of the chamber, or the manner in which the overall light intensity varies with zenith angle. This latter assumption is uncertain for both outdoor chambers, and it is particularly uncertain for the UNC chamber since (1) no reliable data are presently available concerning either the $NO_2$ photolysis rates inside the UNC chamber or the light intensity inside the chamber compared to outside; (2) the use of a reflective surface on the floor of the UNC chamber may enhance the light intensity inside that chamber in a manner which depends on the zenith angle; and (3) the Teflon walls of the UNC chamber are rarely changed, and buildup of contaminants on the walls, or "solarization" of the walls, may preferentially the lower wavelength radiation. [Jeffries (private communication) has unpublished data suggesting that this may be the case.] These factors are neglected in our calculation of photolysis rates inside the UNC chamber, but they may well be highly significant.

Chamber Radical Sources. It has been recognized for a number of years that it is necessary to include in the model provisions for uncharacterized chamber-dependent continuous radical sources when simulating environmental chamber experiments. The magnitude of the radical sources used in the model simulations of the SAPRC chamber experiments were determined based on results of radical tracer-$NO_x$-air experiments carried out to measure this effect, and it was assumed that the magnitude of this effect in the UNC chamber was similar to that in the SAPRC ITC and OTC, which have similar types of surfaces. The modeling of the $NO_x$-air, CO-

$NO_x$-air, and n-butane-$NO_x$-air experiments carried out in the UNC chamber, which are extremely sensitive to this parameter, indicated that this assumption is probably appropriate. However, from the point of view of testing chemical mechanisms, the major problem caused by the chamber radical source is not that its exact chemical and physical cause is unknown, but that it tends to vary in magnitude from run to run. This results in a significant scatter in the quality of fits of the model simulations of experiments employing compounds, such as the alkanes, for which the homogeneous radical sink processes are more important than the homogeneous radical sources in their photooxidation mechanisms. This variability significantly limits the utility of environmental chamber experiments for testing chemical mechanisms for such compounds, since poor fits of the unadjusted model simulations to the data can always be attributed to the known variability of the radical source. Fortunately, for $NO_x$-air irradiations employing more reactive compounds such as the alkenes and aromatics, or complex mixtures containing these compounds, the homogeneous radical sources involved in their photooxidations are sufficient that the magnitude of the chamber radical source is not the dominant factor in affecting the quality of the fits of the model simulations to the data. Thus if poor fits of the model predictions to the experimental data are obtained, they are more likely due to other problems with the model.

$NO_x$ Offgassing. Offgassing of $NO_x$ from the chamber walls can be important for experiments employing low (<0.1 ppm) injected $NO_x$ levels, and it is necessary to assume non-negligible $NO_x$ offgassing for the model to simulate the results of aldehyde-air and pure air irradiations. In this program, we used a simple light-dependent model for $NO_x$ offgassing, with its rate being determined by $k_1$ times a constant factor which depended only on the chamber, with the proportionality factor being adjusted to fit the results of the acetaldehyde-air irradiations carried out in each of the four chambers. However, this simple $NO_x$ offgassing model is probably an oversimplification, especially for the outdoor chambers, where it was not possible to accurately simulate both the PAN and the ozone data in the acetaldehyde-air runs. However, insufficient data are available to indicate more appropriate methods to represent this effect, and development of more complex and speculative methods to represent $NO_x$ offgassing, or adjusting its rate from run-to-run, was not considered to be consistent with the objectives and scope of this program. Fortunately, sensitivity calculations carried out indicate that $NO_x$ offgassing plays a relatively minor role in affecting the simulations of experiments employing more than ~0.2 ppm of injected $NO_x$.

Offgassing of Organic Contaminants. The experimental $NO_x$-air and (for the UNC chamber) pure air irradiation data indicate the presence of low levels of reactive organic contaminants in each of the four chambers. These could be present either in the diluent air used in the experiments, or emitted from the chamber walls during the course of the irradiation. However, the amount of excess NO to $NO_2$ conversion in the $NO_x$-air irradiations, or of ozone formation in the pure air irradiations, is sufficiently low that in organic-$NO_x$-air irradiations the reactivity of the injected organics is always much greater than that of any organic contaminants. This effect was hence ignored in our simulations of the organic-$NO_x$-air experiments.

It has been assumed in previous modeling studies of the UNC chamber experiments that formaldehyde offgassing makes a significant contribution to the radical source in that chamber. However, comparison of results of test calculations carried out in this program with NO to $NO_2$ conversion rates observed in the UNC $NO_x$-air irradiations, and with formaldehyde levels measured using a sensitive laser absorption technique in a pure air irradiation in the UNC chamber, indicated that if formaldehyde offgassing occurs in that chamber, it is at a rate which is much too low to account for the chamber radical source.

Initial Nitrous Acid. There is evidence that nitrous acid (HONO), a powerful photoinitiator, is initially present in many environmental chamber experiments, either introduced as a contaminant together with the injected $NO_x$, or formed heterogeneously from $NO_2$ (see below). The photolysis of this initially present HONO can cause significant radical formation in the initial stages of irradiations, and it thus represents a component of the chamber radical source, though it is less important than the continuous chamber radical source in affecting the results of simulations. Direct and indirect measurements of initial HONO in SAPRC EC runs (Carter et al. 1982a, Pitts et al. 1983) indicate that assuming initial HONO to be present at levels of ~7% of the initial $NO_2$ is appropriate, though it can vary from run to run by as much as a factor of two. The initial HONO levels appropriate for use in modeling the other chamber runs are more uncertain, but we assumed that they are less than in the EC runs since HONO formation from $NO_2$ in the dark is slower in Teflon film chambers (Pitts et al. 1984). In this model testing program, the initial HONO used in the simulations of all of the EC runs was assumed to be 7% of the initial $NO_2$, and in modeling the runs carried out in the other Teflon film chambers, it was assumed to be negligible. The initial HONO levels probably vary from run-to-run, and treating them as an adjustable parameter would probably improve the fits to the results of some runs. However, such run-to-run adjustment of unknown parameters was not carried out in this testing program.

Ozone Wall Loss. The dark decay of ozone to the walls of environmental chambers is a well recognized phenomenon, and is relatively easy to measure by carrying out ozone dark decay experiments. Such data are available for all four chambers, and the decay rates used in the model simulations were obtained from the results of these experiments. These rates are variable, but the magnitude of the ozone decay rates in these chambers, while non-negligible, are sufficiently low that the variability does not represent significant uncertainties in the model simulations.

Heterogeneous Hydrolysis Reactions. The model also contains provision for the surface-dependent hydrolyses of $N_2O_5$, forming nitric acid and/or wall-absorbed $NO_x$, and $NO_2$, forming nitrous acid and wall-absorbed $NO_x$. The former reaction represents a $NO_x$ sink process which may affect predictions of maximum ozone yields in experiments where this is affected by the availability of $NO_x$, and the latter reaction makes a relatively minor contribution to the chamber radical source. These reactions are reasonably well characterized in the SAPRC EC, and data are available for Teflon-film chambers which allow their rates to be estimated for the SAPRC ITC and OTC, and for the UNC chamber. The estimates of their rates in the OTC and (especially) the UNC chamber are uncertain, but they are estimated to be slower than in the SAPRC ITC, where these reactions are relatively slow compared to their rates in the EC. The impact of the uncertainties in the rates of these processes on results of the model simulations were not investigated in this program, but because of their relatively low rates in the Teflon film chambers (where the variability and the uncertainties are the greatest), we do not believe this to be a major source of uncertainty in the model simulations, especially when compared to other uncertainties in chamber characterization.

### 2. Results of Model Testing

The predictive capabilities of the mechanism developed in this program were evaluated by comparing the predicted and experimental maximum ozone yields, NO oxidation and ozone formation times, reactant half-lives, and selected product yields. For the purpose of comparing the accuracy of the model in simulating the rates of NO consumption and ozone formation, a new "timing" statistic, defined as the time required to achieve one-half of the maximum experimental change in the quantity ($[O_3]-[NO]$), was employed. This "timing" measurement was found to avoid many of the problems of simpler methods which have been employed to assess model performance, such as times to maximum $O_3$, times to maximum $NO_2$, etc. The averages and ($1\sigma$) standard deviations of the percentage differences between the model predictions and experimental measurements of maximum ozone yields, NO oxidation/ozone formation times, and selected organic reactant half-lives are summarized in Table V-1 for the single organic-$NO_x$-air runs, and in Table V-2 for the runs employing simple and complex mixtures. These fits, and the fits to the observed yields of selected products, are summarized below for the various types of runs.

Aldehyde-$NO_x$-Air Runs. The model exhibited a number of disagreements with the experimental data for the aldehyde-$NO_x$ irradiations, although it is not clear to what extent this is due to problems with the mechanism, since in many cases different results were obtained in simulating experiments carried out in different chambers. The formaldehyde consumption rates were significantly and consistently overpredicted in the simulations of the UNC formaldehyde runs, but much less so in the simulations of those runs carried out in the EC. While this may be due to problems with characterizing the UV light intensity in the UNC chamber, the discrepancies in the aldehyde half-lives are in the opposite direction in the simulations of the UNC acetaldehyde and propionaldehyde-$NO_x$-air runs. The model had a consistent tendency to underpredict the ozone yields in most of the aldehyde runs, except for the UNC formaldehyde-$NO_x$-air runs, where the results

**Table V-1. Summary of Average Percent Discrepancies in Model Predictions of Maximum Ozone Yields, Times Required to Achieve Half the Maximum Experimental Change in ([$O_3$]-[NO]), and Reactant Half-Lives for the Single Organic $NO_x$-Air Irradiations**

| Organic Reactant | Chamber | No. Runs | Average Percent Discrepancy | | |
|---|---|---|---|---|---|
| | | | Maximum Ozone | NO Oxidation Time | Reactant Half-Life |
| Formaldehyde | EC | 5 | 13 ± 1 | -13 ± 25 | -14 ± 32 |
| | ITC | 1 | | -10 | |
| | OTC | 2 | -22 ± 9 | 1 ± 6 | |
| | UNC | 7 | -3 ± 31 | -14 ± 8 | -30 ± 8 |
| Acetaldehyde and propionaldehyde | EC | 2 | -15 ± 13 | 9 ± 11 | 30 |
| | UNC | 5 | -36 ± 2 | 4 ± 8 | 16 ± 7 |
| Acetone | UNC | 1 | 104 | -26 | 22 |
| Methyl ethyl ketone | UNC | 2 | -15 ± 3 | -4 ± 12 | 12 ± 7 |
| Ethene | EC | 6 | -2 ± 25 | 11 ± 37 | 14 ± 37 |
| | UNC | 6 | 8 ± 22 | -4 ± 16 | -7 ± 17 |
| Propene | EC | 15 | 27 ± 33 | -16 ± 30 | 1 ± 29 |
| | ITC | 3 | 2 ± 20 | -17 ± 12 | 0 ± 6 |
| | OTC | 5 | 19 ± 18 | -10 ± 15 | 2 ± 6 |
| | UNC | 22 | -5 ± 21 | -9 ± 15 | -11 ± 13 |
| Propene (dynamic) | UNC | 5 | -15 ± 10 | 1 ± 16 | |
| 1-Butene | EC | 3 | -33 ± 13 | 27 ± 32 | 51 ± 17 |
| | UNC | 4 | 63 ± 39 | -27 ± 4 | -24 ± 3 |
| *trans*-2-Butene | EC | 3 | -33 ± 8 | 48 ± 16 | 68 ± 8 |
| | UNC | 1 | -13 | -8 | -8 |
| Isobutene | ITC | 1 | 8 | -33 | -25 |
| n-Butane | EC | 14 | 11 ± 48 | -10 ± 46 | |
| | ITC | 3 | 216 ±108 | -46 ± 35 | |
| | OTC | 1 | | -67 | |
| | UNC | 7 | 8 ± 73 | 1 ± 27 | |
| $\geq C_5$ Alkanes | EC | 6 | 33 ± 21 | -10 ± 20 | |
| | ITC | 8 | 2 ± 44 | 22 ± 38 | |
| | UNC | 6 | 63 ± 72 | -17 ± 15 | |
| Benzene | ITC | 6 | 19 ± 5 | -15 ± 11 | |
| Toluene | EC | 13 | 16 ± 8 | -11 ± 24 | |
| | ITC | 2 | 5 | -27 ± 21 | |
| | UNC | 5 | 94 ±102 | -13 ± 11 | |
| Xylenes | EC | 4 | -6 ± 17 | -5 ± 13 | 63 ± 52 |
| | ITC | 2 | -28 | -25 ± 26 | 16 ± 33 |
| | UNC | 4 | -18 ± 13 | -10 ± 13 | 10 ± 25 |
| 1,3,5-Trimethylbenzene | EC | 3 | 3 ± 3 | -1 ± 1 | 5 ± 8 |
| | ITC | 5 | -32 ± 11 | -23 ± 16 | 9 ± 38 |

Table V-2. Summary of Average Percent Discrepancies in Model Predictions of Maximum Ozone Yields, Times Required to Achieve Half the Maximum Experimental Change in ($[O_3]$-[NO]), and Reactant Half-Lives for the Organic-$NO_x$-Air Irradiations Employing Mixtures of Organics

| Mixture | Chamber | No. Runs | Average Percent Discrepancy: Maximum Ozone | Average Percent Discrepancy: NO Oxidation Time | Average Percent Discrepancy: Reactant Half-Life[a] |
|---|---|---|---|---|---|
| Mixed alkenes | EC | 9 | -25 ± 21 | 37 ± 33 | 55 ± 25 |
| | UNC | 4 | -35 ± 40 | 22 ± 39 | 99 ± 88 |
| Mixed alkanes | EC | 2 | 6 ± 5 | 3 ± 12 | |
| Mixed aromatics | UNC | 2 | 9 ± 12 | -5 ± 11 | 5 ± 12[b] |
| Alkane + alkene | EC | 5 | 20 ± 9 | 8 ± 14 | 5 ± 15 |
| | UNC | 7 | 17 ± 42 | -11 ± 15 | -5 ± 13 |
| Other known mixtures (with all reactants represented explicitly) | EC | 18 | 16 ± 14 | -9 ± 9 | 11 ± 13 |
| | ITC | 24 | 21 ± 35 | -42 ± 8 | -9 ± 13 |
| | OTC | 25 | 20 ± 19 | -5 ± 16 | 12 ± 19 |
| | UNC | 9 | -10 ± 22 | 0 ± 13 | -1 ± 14 |
| Known mixtures (dynamic) | UNC | 4 | -14 ± 29 | 39 ± 47 | |
| Known mixtures (with species lumping) | UNC | 25 | 21 ± 95 | -10 ± 15 | 6 ± 16[c] |
| Auto exhaust | UNC | 25 | -7 ± 16 | -4 ± 10 | |

[a] Half-life discrepancy given for propene unless otherwise indicated.
[b] Half-life discrepancy given for o-xylene.
[c] Half-life discrepancy given for ethene.

were highly variable in this regard. Predictions of PAN yields from acetaldehyde and propionaldehyde were highly variable, but indicated no systematic discrepancies.

Ketone-$NO_x$-Air Runs. Only three such runs were available for model testing, one for acetone and two for MEK. The model significantly overpredicted the reactivity observed in the acetone run, but underpredicted the reactivity in the MEK runs. Better fits could be obtained by adjusting the ketone photodecomposition quantum yields, but in view of the limited number of runs, the uncertainties in light characterization for the UNC chamber, and the variability of the model simulations of the UNC aldehyde-$NO_x$-air runs, this was not considered to be appropriate. This set of experiments is not considered to be adequate for any comprehensive testing of models for ketones.

Ethene and Propene-$NO_x$-Air Runs. A reasonably comprehensive set of runs are available for testing the chemical mechanisms for these alkenes, and the model generally performed much better in simulating these runs than in simulating the aldehyde runs. This is despite the fact that the chemical reaction mechanisms for formaldehyde and (for propene) acetaldehyde are important components of the overall chemical mechanism for these two alkenes. The model tended to overpredict the ozone yields observed in the EC and OTC propene runs, but on the average the model predictions for ozone were consistent with the ozone yields observed in the other two chambers. The propene model overpredicted the PAN and acetaldehyde yields (by approximately 20%, typically), but this may be within the experimental uncertainties. The predictions of formaldehyde yields from these alkenes was reasonably consistent with the majority of the formaldehyde data from the SAPRC runs and closely fit those measured by a laser absorption technique in several UNC runs. However, the predicted formaldehyde yields were consistently lower than the formaldehyde yields measured by the technique used in most UNC runs, and this was the case for essentially all types of runs where formaldehyde is formed as a product.

Butene-$NO_x$-Air Runs. The performance of the model in simulating the relatively limited number of 1-butene, trans-2-butene and isobutene-$NO_x$-air runs was not particularly satisfactory, but again the discrepancies depended on the chamber employed. The reactivity in the 1-butene runs was significantly underpredicted in the EC experiments and overpredicted in the UNC experiments. The reactivities in the trans-2-butene runs carried out in the EC were consistently underpredicted, but slightly overpredicted in the single run carried out in the UNC chamber. Only one isobutene-$NO_x$-air run was available for model testing, and the PAN yield observed in that run was not consistent with model predictions. We conclude that the available data do not provide comprehensive tests for the mechanisms of the reactions of these compounds and that further laboratory and environmental chamber studies are required before mechanisms for the reactions of these compounds can be considered to be adequately established.

n-Butane-$NO_x$-Air Runs. While the results of model simulations of the n-butane runs were highly variable, this is due to the extreme sensitivity of these runs to the chamber radical source, and significantly better fits could be obtained if the magnitude of the radical source was adjusted from run-to-run. The disagreements between predicted and experimental data using the unadjusted model appeared to be random, and thus were probably not due to errors in the mechanism. However, if the radical source was adjusted to optimize the fits to ozone, then the model tends to underpredict the NO oxidation/ozone formation time and overpredict the product yields observed in the SAPRC runs, by ~20-30%. This suggests a systematic problem with the ozone predictions of the n-butane mechanism, although the data are not conclusive in this regard.

$\geq C_5$ Alkane-$NO_x$-Air Runs. The results of the model simulations of the runs employing the higher alkanes were also variable, and simulations of these runs are also sensitive to the chamber radical source. However, in general the model for the higher alkanes appears to agree, on the average, with the experimental data in its predictions of the "timing" observed in these runs, but it also appears that the model has a tendency to overpredict the ozone yields under conditions where "true" ozone maxima were obtained. This suggests that there may be $NO_x$ (but not radical) sinks in the reactions of these compounds which were not being taken into account in this mechanism. However, at the present time it is not clear what causes these $NO_x$ sinks. The model predictions appear to be reasonably consistent with the oxygenated product yields observed in the 2,3-dimethylbutane runs, but not with those observed in the runs employing isopentane and isooctane, suggesting that the branching ratio estimates for certain alkoxy radical reactions need revision.

Aromatic-$NO_x$-Air Runs. While the model gave reasonably good predictions to the overall reactivity observed in the benzene, toluene, xylene, and 1,3,5-trimethylbenzene-$NO_x$-air runs modeled in this program, this was primarily due to the adjustment of photolysis rates of unknown aromatic ring-opening products. However, a number of discrepancies between the model and the experimental data were still observed. The models for benzene and toluene tended to overpredict ozone yields, while ozone tended to be underpredicted in the models for the xylenes and 1,3,5-trimethylbenzene. The model tends to overpredict PAN yields from toluene and the xylenes, and underpredict it from 1,3,5-trimethylbenzene. However, these predictions of PAN could be improved by adjusting the mechanism for the reactions of the unknown ring-opening products. The model also consistently underpredicts the rate of consumption of the aromatic towards the end of the experiments, (which causes an overprediction of the overall half lives), though their consumption rates during the initial periods of the runs are reasonably well predicted. It is clear that further refinements of the mechanisms for these aromatics are required. However, considering the many gaps in our present knowledge of major areas of this mechanism, the performance of the model is probably as good as can reasonably be expected at the present time.

Dynamic Experiments. Several propene-$NO_x$-air and propene + n-butane + toluene-$NO_x$-air runs carried out at UNC under "dynamic" conditions, where some or all of the reactants were continuously injected during the experiment or where the chamber contents were diluted at relatively high rates, were modeled. The fits of the model predictions to the results of these runs were variable, but generally were similar in quality to the fits to comparable "static" runs, indicating that these "dynamic" experiments do not reveal additional problems with the model which were not indicated by the tests using the much larger set of "static" runs.

$NO_x$-Air Runs with Organic Mixtures. The performance of the model in simulating runs employing mixtures of organics was comparable to its performance in simulating results of the single organic runs, though there were cases where systematic discrepancies were observed. Fewer systematic discrepancies are expected in the simulations of mixtures because of the tendency for errors in the mechanism of any given organic in the mixture to be offset by compensating errors in the mechanisms for the other organics present. However, the model consistently underpredicted the reactivity observed in the mixed alkene runs carried out in both the EC and UNC chambers, and consistently overpredicted the rates of NO oxidation and ozone formation in the ITC runs employing mixtures of organics. The underprediction of reactivity in the alkene runs suggests problems with the alkene and/or aldehyde mechanisms, but the overprediction of NO oxidation/ozone formation rates in the ITC runs is more likely due to chamber characterization problems. Thus, as shown in Table V-1, a similar tendency was observed in the simulations of most of the types of single organic runs carried out in the ITC. There also appears to be a moderate tendency to overpredict ozone in the simulations of the EC and the OTC runs, which appears to be less in the case of the simulations of the runs carried out in the UNC chamber.

A few of the UNC runs employing known mixtures were simulated very poorly, either due to problems with chamber characterization or errors in specifying initial reactant concentrations in the model, and this contributed to the high standard deviations of the average discrepancies noted in several cases in Table V-2. Fewer cases of gross discrepancies were observed in the simulations of the SAPRC runs, and in some cases this made the systematic discrepancies more evident. However, on the average the UNC runs were simulated about as well, and in some cases better, than the SAPRC runs.

Auto Exhaust Irradiations. The performance of the model in simulating the UNC auto exhaust irradiations was suprisingly good, especially considering the greater uncertainties involved in speciating the reactants present in those experiments, and its more variable performance in simulating the UNC runs containing known mixtures. This may be a result of greater care possibly being taken in controlling and characterizing the conditions of these experiments, but it also may be an example of compensating errors in the mechanism and/or in the speciation of the reactants. In any case, the good performance of the model in simulating these runs is fortunate from the point of view of the objectives of this program, since automobile exhaust is a significant contributor to the emissions into urban atmospheres.

In summary, while there were a number of individual chamber experiments which were not well simulated by the model, the model was able to simulate reasonably well the major results observed in a majority of the experiments. The greatest discrepancies observed were generally of a random nature, with no apparent correlation between the initial organic and $NO_x$ levels or organic/$NO_x$ ratios and the discrepancies observed. It is probable that such random discrepancies are due more to variabilities in the experimental conditions, or chamber or lighting effects, than to errors in the chemical mechanism. Although, as noted above, a number of cases of systematic discrepancies were observed, indicating problems with the mechanism or systematic errors in the way the chamber-dependent or lighting parameters were characterized, in most cases the systematic discrepancies were less than the run-to-run variability of the fits.

This testing program has resulted in a detailed assessment of the strengths and weaknesses of this mechanism in simulating the results of environmental chamber experiments; and these results, documented in Section IV of this report, will serve as a basis against which the performance of future kinetic mechanisms can be compared. In general, the performance of this model in simulating the results of these experiments, when taken as a group, is probably as good as can be expected considering the variability of chamber conditions and our current state of knowledge of chamber effects and the $NO_x$-air photooxidation mechanisms of organic compounds. Thus, until alternative or updated mechanisms yield better predictions to the results of these experiments (without run-to-run adjustment of parameters), or until further relevant kinetic, mechanistic, or environmental chamber data become available, we believe that the mechanism developed and tested in this program represents the current state-of-the-art, and as such is suitable for adaptation to atmospheric modeling. This, as discussed below, is the objective of the second phase of this program.

## V. C. ADAPTATION OF THE MECHANISM FOR ATMOSPHERIC MODELING

The goal of this research program is to provide the EPA with updated and evaluated chemical mechanisms for use in urban-scale ozone modeling. The detailed chemical mechanism developed and tested in Phase I of the program, described in this report, will be adapted for use in air quality simulation models in Phase II. This section describes the general approach planned for Phase II of this program.

Atmospheric modeling differs from environmental chamber modeling in numerous aspects. Firstly, the speciation of ambient hydrocarbons is generally complex and not well known, in contrast to most chamber experiments where the reactant concentrations are accurately known. Secondly, given typical mixing layer heights of several hundred to a few thousand meters, the surface area-to-volume ratio in the atmosphere is much smaller than in environmental chambers. Thus, most of the heterogeneous reactions which ar[illegible]ortant in many chamber experiments can be probably be ignored in atmosp[illegible]c ozone modeling. (Some heterogeneous loss processes such as dry deposition to ground and particulate surfaces nevertheless need to be included in the atmospheric modeling.) Thirdly, atmospheric models must simulate other physical processes besides chemistry, such as transport, diffusion, emissions entrainment, etc., and cannot devote 100% of the computational resources available to solving the chemistry alone. Given the uncertainties in organic speciation and computer resource constraints, it is difficult to justify including as much chemical detail in atmospheric modeling as is employed in environmental chamber modeling, where computer constraints are much less of a factor, and where a maximum chemical accuracy is the objective.

In Phase II of this program we plan to adapt the mechanism for use in EPA's photochemical box model, OZIPM version 3.0, for use with the Empirical Kinetic Modeling Approach (EKMA). Even though the OZIPM air quality model can accommodate fairly large chemical mechanisms, some condensation of the mechanism will be performed prior to installing the mechanism in OZIPM. The mechanism condensation will be accomplished primarily by invoking lumping approximations and eliminating reactions which are shown to be unimportant under airshed modeling conditions. We plan to use lumping approximations similar to those used for modeling the

UNC automobile exhaust irradiations, based on the fact that automobile exhaust is a major contributor to ambient hydrocarbons in urban areas and that satisfactory results were obtained for modeling irradiated auto exhaust using a modest level of speciation. The recommended organic classes and corresponding lumped or surrogate species are shown in Table V-3.

Table V-3. Organic Classes and Corresponding Lumped or Surrogate Species Recommended for Use in Atmospheric Modeling

| Organic Class | Lumped or Surrogate Species |
|---|---|
| $C_4$-$C_5$ Alkanes | Lumped $C_4$-$C_5$ Alkane |
| $>C_5$ Alkanes | Lumped $>C_5$ Alkane |
| Ethene | Ethene |
| Terminal Alkenes | Propene |
| Internal Alkenes | trans-2-Butene |
| Mono-alkylbenzenes | Toluene |
| Di-alkylbenzenes | m-Xylene |
| Tri-alkylbenzenes | 1,3,5-Trimethylbenzene |
| Formaldehyde | Formaldehyde |
| Higher Aldehydes | Acetaldehyde |

The organic lumping scheme shown in Table V-3 is similar to that used in the ALW mechanism with the exceptions that two, rather than one, classes of $>C_3$ alkanes and three, rather than two, classes of alkylbenzenes are employed. Since OZIPM is primarily used for one-day simulations, we do not plan to include separate reactions for less reactive species such as benzene and propane. Instead, we recommend lumping a fraction (~40%) of the ambient benzene and propane concentrations (or emissions) with the $C_4$-$C_5$ alkanes. Testing will be carried out to determine which reactions can safely be eliminated and to ensure that the mechanism installed into OZIPM provides predictions very similar to the fully, detailed chemical mechanism for complex mixtures.

A sensitivity analysis will be carried out to assess the effects of various input parameters on OZIPM's predicted control strategy requirements. The input parameters with the largest influence on the control requirements will be identified and varied within their range of uncertainties. The likely parameters to be studied include the hydrocarbon compositions of ambient air and emissions, hydrocarbon to $NO_x$ ratio, initial concentrations of radical initiators such as aldehydes and HONO, and the concentrations of ozone and hydrocarbons aloft. The effects of these parameters will be investigated under several sets of atmospherically likely meteorological conditions.

Another version of the chemical mechanism will be developed for use in multi-cell Lagrangian and Eulerian photochemical air quality models, such as the Urban Airshed Model (UAM). This version of the mechanism will be designed for use in multi-day simulations and will be significantly more condensed and parameterized than the mechanism installed into OZIPM. This version of the mechanism will be designed to be used with steady-state and other numerical approximations that minimize the number of integrated chemical species and reactions. The predictions from this version will be compared with the those from the version installed into OZIPM to ensure that both versions perform similarly over a wide range of conditions.

In addition, guidelines for the correct use of the mechanisms in atmospheric simulation models will be developed. These will include information for classifying the individual organic compounds into the lumped hydrocarbon classes and default organic speciation profiles for ambient urban air and emissions. These will be fully documented in the final report for the second phase of this program.

# VI. REFERENCES

Altshuller, A. P., Kopczynski, S. L., Lonneman, W. A., Becker, T. L. and Slater, R. (1967): Environ. Sci. Technol., 1, 899.

Amimoto, S. T., Force, A. P., Wiesenfeld, J. R. and Young, R. H. (1980): J. Chem. Phys., 73, 1244.

Arnold, I., Comes, F. J. and Moortgat, G. K. (1977): Chem. Phys., 24, 211.

Atkinson, R. and Pitts, J. N., Jr. (1977): J. Chem. Phys., 67, 38.

Atkinson, R. and Pitts, J. N., Jr. (1978): J. Chem. Phys., 68, 2992.

Atkinson, R., Carter, W. P. L., Darnall, K. R., Winer, A. M. and Pitts, J. N., Jr. (1980): Int. J. Chem. Kinet. 12, 779.

Atkinson, R., Lloyd, A. C. and Winges, L. (1982a): Atmos. Environ., 16, 1341.

Atkinson, R., Aschmann, S. M., Carter, W. P. L. and Winer, A. M. (1982b): Int. J. Chem. Kinet., 14, 919.

Atkinson, R., Aschmann, S. M., Carter, W. P. L., Winer, A. M. and Pitts, J. N., Jr. (1982c): J. Phys. Chem., 86, 4563.

Atkinson, R., Carter, W. P. L. and Winer, A. M. (1983a): J. Phys. Chem., 87, 2012.

Atkinson, R., Carter, W. P. L. and Winer, A. M. (1983b): J. Phys. Chem. 87, 1605.

Atkinson, R., Carter, W. P. L. and Winer, A. M. (1983c): "Evaluation of Hydrocarbon Reactivities for Use in Control Strategies," Final Report to the California Air Resources Board Contract No. A0-105-32, May.

Atkinson, R. and Carter, W. P. L. (1984): Chem. Rev., 84, 437.

Atkinson, R. and Lloyd, A. C. (1984): J. Phys. Chem. Ref. Data, 13, 315.

Atkinson, R., Plum, C. N., Carter, W. P. L., Winer, A. M. and Pitts, J. N., Jr. (1984a): J. Phys. Chem., 88, 1210.

Atkinson, R., Aschmann, S. M., Carter, W. P. L., Winer, A. M. and Pitts, J. N., Jr. (1984b): Int. J. Chem. Kinet., 16, 1085.

Atkinson, R., Carter, W. P. L., Plum, C. N., Winer, A. M. and Pitts, J. N., Jr. (1984c): Int. J. Chem. Kinet. 16, 887.

Atkinson, R., Tuazon, E. C. and Carter, W. P. L. (1985): Int. J. Chem. Kinet., 17, 725.

Atkinson, R. (1986): Chem. Rev., 86, 69.

Atkinson, R., Winer, A. M. and Pitts, J. N., Jr. (1986a): Atmos. Environ., 20, 331.

Atkinson, R., Tuazon, E. C., Mac Leod, H., Aschmann, S. M. and Winer, A. M. (1986b): Geophys. Res. Lett., 13, 117.

Baldwin, A. C., Barker, J. R., Golden, D. M. and Hendry, D. G. (1977): J. Phys. Chem., 81, 2483.

Bandow, H. and Washida, N. (1985a): Bull. Chem. Soc. Jpn., 58, 2541.

Bandow, H. and Washida, N. (1985b): Bull. Chem. Soc. Jpn., 58, 2549.

Bandow, H., Washida, N. and Akimoto, H. (1985): Bull. Chem. Soc. Jpn., 58, 2531.

Barnes, I., Bastian, V., Becker, K. H., Fink, E. H. and Zabel, F. (1981): Chem. Phys. Lett., 83, 459.

Barnes, I., Becker, K. H., Fink, E. H., Reimer, A., Zabel, F. and Niki, H. (1985): Chem. Phys. Lett., 115, 1.

Beaucheme, J. H., Bekowies, P. J., McAfee, J. M., Winer, A. M., Zafonte, L. and Pitts, J. N., Jr. (1973): Proc. 7th Conf. on Space Simulation, Los Angeles, CA, NASA Spec. Publ. 336, pp. 811-825, November 12-14.

Biermann, H. W., Zetzsch, C. and Stuhl, F. (1978): Ber. Bunsenges Phys. Chem., 82, 633.

Brock, J. C. and Watson, R. T. (1980a): Chem. Phys., 46, 477.

Brock, J. C. and Watson, R. T. (1980b): Chem. Phys. Lett., 71, 371.

Burrows, J. P., Tyndall, G. S. and Moortgat, G. K. (1985): Chem. Phys. Lett., 119, 193.

Calvert, J. G. and Pitts, J. N., Jr. (1966): Photochemistry, John Wiley & Sons, Inc., New York, NY.

Cantrell, C. A., Stockwell, W. R., Anderson, L. G., Busarow, K. L., Perner, D., Schmeltekopf, A., Calvert, J. G. and Johnston, H. S. (1985): J. Phys. Chem., 89, 139.

Carter, W. P. L., Lloyd, A. C., Sprung, J. L. and Pitts, J. N., Jr. (1979a): Int. J. Chem. Kinet., 11, 45.

Carter, W. P. L., Darnall, K. R., Graham, R. A., Winer, A. M. and Pitts, J. N., Jr. (1979b): J. Phys. Chem., 83, 2305.

Carter, W. P. L., Winer, A. M. and Pitts, J. N., Jr. (1981a): Environ. Sci. Technol., 15, 829.

Carter, W. P. L., Atkinson, R., Winer, A. M. and Pitts, J. N., Jr. (1981b): Int. J. Chem. Kinet., 13, 735.

Carter, W. P. L., Winer, A. M. and Pitts, J. N., Jr. (1982a): Atmos. Environ., 16, 113.

Carter, W. P. L., Atkinson, R., Winer, A. M. and Pitts, J. N., Jr. (1982b): Int. J. Chem. Kinet., 14, 1071.

Carter, W. P. L., Winer, A. M., Atkinson, R., Dodd, M. C., Long, W. D. and Aschmann, S. M. (1984): "Atmospheric Photochemical Modeling of Turbine Engine Fuels. Phase I. Experimental Studies," Final Report to the U. S. Air Force, ESL-TR-84-32, September.

Carter, W. P. L. and Atkinson, R. (1985): J. Atmos. Chem., 3, 377.

Carter, W. P. L., Dodd, M. C., Long, W. D., Atkinson, R. and Dodge, M. C. (1985): "Outdoor Chamber Study to Test Multi-Day Effects," EPA-600/3-84-115, March.

Carter, W. P. L., Atkinson, R., Long, W. D., Parker, L. N. and Dodd., M. C. (1986): "Effects of Methanol Substitution of Multi-Day Air Pollution Episodes," Final Report on California Air Resources Board Contract No. A3-125-32, April.

Cox, R. A. and Penkett, S. A. (1972): J. Chem. Soc. Faraday Trans. I., 68, 1735.

Cox, R. A. and Tyndall, G. S. (1979): Chem. Phys. Lett., 63, 490.

Cox, R. A. and Tyndall, G. S. (1980): J. Chem. Soc. Faraday Trans. II, 76, 153.

Cox, R. A., Patrick, K. F. and Chant, S. A. (1981): Environ. Sci. Technol., 15, 587.

Cvetanovic, R. J. (1963): Adv. Photochem., 1, 115.

Cvetanovic, R. J. (1976): 12th Int. Symp. Free Radicals, Laguna Beach, CA, January 4-9.

Demerjian, K. L., Kerr, J. A. and Calvert, J. G. (1974): Adv. Environ. Sci. Technol., 4, 1.

Demerjian, K. L. and Schere, K. L. (1979): Proceedings of the APCA Specialty Conference on Ozone/Oxidants: Interaction with the Total Environment, Air Pollution Control Association, Houston, TX, October 14-17.

Demerjian, K. L. (1982): Personal communication to J. Seinfeld.

Dimitriades, B. (1970): "On the Function of Hydrocarbon and Nitrogen Oxides in Photochemical Smog Formation," U. S. Bureau of Mines, Report of Investigations, RI-7433, September.

Dodge, M. C. and Bufalini, J. J. (1972): unpublished smog chamber data cited in Demerjian et al. (1974).

Dodge, M. C. (1977): "Combined Use of Modeling Techniques and Smog Chamber Data to Derive Ozone-Precursor Relationships," EPA-600/3-77-001.

Dodge, M. C. and Arnts, R. R. (1979): Int. J. Chem. Kinet., 11, 399.

Doyle, G. J., Bekowies, P. J., Winer, A. M. and Pitts, J. N., Jr. (1977): Environ. Sci. Technol., 11, 45.

Dumdei, B. E. and O'Brien, R. J. (1984): Nature, 311, 248.

Fairchild, C. E., Stone, E. J. and Lawrence, G. M. (1978): J. Chem. Phys., 69, 3632.

Falls, A. H. and Seinfeld, J. H. (1978): Environ. Sci. Technol., 12, 1398.

Gardner, E. P., Wijayaratne, R. D. and Calvert, J. G. (1984): J. Phys. Chem., 88, 5069.

Gitchell, A., Simonaitis, R. and Heicklen, J. (1974): J. Air Pollut. Control Assoc., 24, 357.

Glasson, W. A. and Tuesday, C. S. (1970): Environ. Sci. Technol., 4, 916.

Graedel, T. E., Farrow, L. A. and Weber, T. A. (1976): Atmos. Environ., 10, 1095.

Graham, R. A. and Johnston, H. S. (1978): J. Phys. Chem., 82, 254.

Graham, R. A., Winer, A. M. and Pitts, J. N., Jr. (1978): J. Chem. Phys., 68, 4505.

Greenblatt, G. D. and Wiesenfeld, J. R. (1983): J. Chem. Phys., 78, 4924.

Gutman, D. G., Sanders, N. and Butler, J. E. (1982): J. Phys. Chem., 86, 66.

Harker, A. B., Ho, W. and Ratto, J. J. (1977): Chem. Phys. Lett., 50, 394.

Harris, G. W., Carter, W. P. L., Winer, A. M., Pitts, J. N., Jr., Platt, U. and Perner, D. (1982): Environ. Sci. Technol., 16, 414.

Hatakeyama, S. Kobayashi, H. and Akimoto, H. (1984): J. Phys. Chem., 88, 4736.

Hayes, S. R. et al. (1980): "Evaluation of Requirements for the Control of Ozone and Nitrogen Dioxide in the South Coast Air Basin," SAI No. 218-BS80-178, prepared for National Commission of Air Quality, October.

Hecht, T. A., Seinfeld, J. H. and Dodge, M. C. (1974): Environ. Sci. Technol., 8, 327.

Hendry, D. G. and Kenley, R. A. (1977): J. Am. Chem. Soc., 99, 3198.

Hendry, D. G., Baldwin, A. C., Barker, J. R. and Golden, D. M. (1978): "Computer Modeling of Simulated Photochemical Smog," EPA-600/3-78-059, June.

Herron, J. T. and Huie, R. E. (1977): J. Am. Chem. Soc., 99, 5430.

Horowitz, A. and Calvert, J. G. (1982): J. Phys. Chem., 86, 3105.

Hoshino, M., Akimoto, H. and Okuda, M. (1978): Bull. Chem. Soc. Japan, 51, 718.

Hov, Ø. and Derwent, R. G. (1981): J. Air Pollut. Control Assoc., 31, 1260.

Howard, C. J. (1977): J. Chem. Phys., 67, 5258.

Hurt, P. R. and Lurmann, F. (1982): "Application of EKMA to Kern County," ERT Document No. P-A753-2, Environmental Research & Technology, Inc., Westlake Village, CA, January.

Izumi, K., Mizouchi, M., Yoshioka, M., Murano, K. and Fukuyama, T. (1984): Environ. Sci. Technol., 18, 116.

Japar, S. M. and Niki, H. (1975): J. Phys. Chem., 79, 1629.

Jeffries, H. E., Sexton, K. G. and Salmi, C. N. (1981): "Effects of Chemistry and Meteorology on Ozone-Control Calculations Using Simple Trajectory Models and the EKMA Procedure," EPA-450/4-81-034, November.

Jeffries, H. E., Kamens, R. M., Sexton, K. G. and Gerhardt, A. A. (1982): "Outdoor Smog Chamber Experiments to Test Photochemical Models," EPA-600/3-82-016A, April.

Jeffries, H. E., Sexton, K. G., Kamens, R. M. and Holleman, M. S. (1985a): "Outdoor Chamber Studies to Test Photochemical Models: Phase II," EPA-600/3-85-029.

Jeffries, H. E., Sexton, K. G., Morris, T. P., Jackson, M., Goodman, R. G., Kamens, R. M. and Holleman, M. S. (1985b): "Outdoor Smog Chamber Experiments Using Automobile Exhaust," EPA-600/3-85-032.

Jeffries, H. E., Sexton, K. G. and Holleman, M. S. (1985c): "Outdoor Smog Chamber Experiments: Reactivity of Methanol Exhaust," EPA-460/3-85-009a.

Jeffries, H. E., Sexton, K. G., Kamens, R. M. and Holleman, M. S. (1985d): "Outdoor Smog Chamber Experiments: Reactivity of Methanol Exhaust. Part II. Quality Assurance and Data Processing System Description," EPA-460/3-85-009b.

Johnston, H. S., Chang, S. G. and Whitten, G. (1974): J. Phys. Chem., 78, 1.

Kamens, R. M., Jeffries, H. E., Sexton, K. G. and Gerhardt, A. A. (1981): "Smog Chamber Experiments to Test Oxidant Related Control Strategy Issues," EPA-600/3-82-014, November.

Kan, C. S., Calvert, J. G. and Shaw, J. H. (1980): J. Phys. Chem., 84, 3411.

Kan, C. S., Su, F., Calvert, J. G. and Shaw, J. H. (1981): J. Phys. Chem., 85, 2359.

Kenley, R. A., Davenport, J. E. and Hendry, D. G. (1981): J. Phys. Chem., 85, 2740.

Kerr, J. A. and Moss, S. J. (1981): Handbook of Bimolecular and Termolecular Gas Reactions, Vol. I, CRC Press, Inc., Boca Raton, FL.

Killus, J. P. and Whitten, G. Z. (1982a): "A New Carbon-Bond Mechanism for Air Quality Simulation Modeling," EPA-600/3-82-041, April.

Killus, J. P. and Whitten, G. Z. (1982b): Atmos. Environ., 16, 1973.

Killus, J. P. and Whitten, G. Z. (1983): Atmos. Environ. 17, 1597.

Kircher, C. C. and Sander, S. P. (1984): J. Phys. Chem., 88, 2082.

Kircher, C. C., Margitan, J. J. and Sander, S. P. (1984): J. Phys. Chem., 88, 4370.

Kuntz, R. L., Kopczynski, S. L. and Bufalini, J. J. (1973): Environ. Sci. Technol., 7, 1119.

Laity, J. L., Burstein, G. F. and Appel, B. R. (1973): Photochemical Smog and the Atmospheric Reactions of the Solvents, in Solvents Theory and Practice, R. W. Tess (Ed.), Adv. Chem. Series, 124, 95.

Leone, J. A. and Seinfeld, J. H. (1984a): Int. J. Chem. Kinet., 16, 159.

Leone, J. A. and Seinfeld, J. H. (1984b): "Evaluation of Chemical Reaction Mechanisms for Photochemical Smog. Part II. Quantitative Evaluation of the Mechanisms," EPA-600/3-84-063, November.

Leone, J. A., Flagan, R. C., Grosjean, D. and Seinfeld, J. H. (1985): Int. J. Chem. Kinet., 17, 177.

Lloyd, A. C., Lurmann, F. W., Godden, D. A., Hutchins, J. F., Eschenroeder, A. Q. and Nordsieck, R. A. (1979): "Development of the ELSTAR Photochemical Air Quality Simulation Model and its Evaluation Relative to the LARPP Data Base," ERT Document No. P-5287-500, prepared for the Coordinating Research Council by Environmental Research & Technology, Inc., Westlake Village, CA.

Lorenz, K., Rhasa, D., Zellner, R. and Fritz, B. (1985): Ber. Bunsenges Phys. Chem., 89, 341.

Lurmann, F. W., Lloyd, A. C. and Atkinson, R. (1984): "Gas Phase Chemistry," ADOM/TADAP Model Development Program, Volume 6, ERT Document No. P-B980-530, July.

Lurmann, F. W., Lloyd, A. C. and Atkinson, R. (1986): J. Geophys. Res., in press.

Madronich, S. and Felder, W. (1985): J. Phys. Chem., 89, 3556.

Magnotta, F. and Johnston, H. S. (1980): Geophys. Res. Lett., 7, 769.

Majer, J. R., Naman, S-A. M. A. and Robb, J. C. (1969): Trans. Faraday Soc., 65, 1846-1853.

Malko, M. W. and Troe, J. (1982): Int. J. Chem. Kinet., 14, 399.

Manzanares, E. R., Sato, M. and Lee, L. C. (1984): unpublished data.

Marinelli, W. J., Swanson, D. M. and Johnston, H. S. (1982): J. Chem. Phys., 76, 2864.

Martinez, J. R. and Maxwell, C. (1981): "Evaluation of the Empirical Kinetic Modeling Approach (EKMA), as a Prediction of Maximum Ozone," presented at the EKMA Workshop, Research Triangle Park, NC, December 15-16.

McRae, G. J. and Seinfeld, J. H. (1983): Atmos. Environ., 17, 501.

McRae, G. J., Leone, J. A. and Seinfeld, J. H. (1983): "Evaluation of Chemical Reaction Mechanisms for Photochemical Smog. Part I. Mechanism Description and Documentation," U. S. Environmental Protection Agency, Report No. EPA-600/3-83-086.

Meyrahn, H., Moortgat, G. K. and Warneck, P. (1982): 15th Int. Conf. Photochem., Stanford, CA.

Molina, M. J. and Arguello, G. (1979): Geophys. Res. Lett., 6, 953.

Molina, L. T. and Molina, M. J. (1981): J. Photochem., 15, 97.

Moortgat, G. K. and Warneck, P. (1975): Naturforsch., 30A, 835.

Moortgat, G. K., Kudszus, E. and Warneck, P. (1977): J. Chem. Soc. Faraday Trans. II, 73, 1216.

Moortgat, G. K. and Kudszus, E. (1978): Geophys. Res. Lett., 5, 191.

NASA (1983): "Chemical Kinetics and Photochemical Data for Use in Stratospheric Modeling," Evaluation Number 6, JPL Publication 83-62, September 15.

NASA (1985): "Chemical Kinetics and Photochemical Data for Use in Stratospheric Modeling," Evaluation No. 7, JPL Publication 85-37, July 1.

NBS (1978): "Reaction Rate and Photochemical Data for Atmospheric Chemistry - 1977," Hampson, R. F., Jr. and Garvin, D. (Eds.), National Bureau of Standards Special Publication 513, May.

Niki, H., Daby, E. E. and Weinstock, B. (1972): Adv. Chem. Series., 113, 16.

Niki, H., Maker, P. D., Savage, C. M. and Breitenbach, L. P. (1977): Chem. Phys. Lett. 46, 327.

Niki, H., Maker, P. D., Savage, C. M. and Breitenbach, L. P. (1978): J. Phys. Chem., 82, 135.

Niki, H., Maker, P. D., Savage, C. M. and Breitenbach, L. P. (1979): In Nitrogenous Air Pollutants, Grosjean, D. (Ed.), Ann Arbor Press, Ann Arbor, MI.

Niki, H., Maker, P. D., Savage, C. M. and Breitenbach, L. P. (1981a): Chem. Phys. Lett., 80, 499.

Niki, H., Maker, P. D., Savage, C. M. and Breitenbach, L. P. (1981b): J. Phys. Chem., 85, 1024.

Niki, H., Maker, P. D., Savage, C. M. and Breitenbach, L. P. (1982): J. Phys. Chem., 86, 3825.

Niki, H., Maker, P. D., Savage, C. M. and Breitenbach, L. P. (1984): J. Phys. Chem., 88, 2116.

Niki, H., Maker, P. D., Savage, C. M. and Breitenbach, L. P. (1985): Int. J. Chem. Kinet., 17, 547.

Ohta, T., Bandow, H. and Akimoto, H. (1982): Int. J. Chem. Kinet., 14, 173.

Paraskevopoulos, G. and Cvetanovic, R. J. (1971): Chem. Phys. Lett., 9, 603.

Paraskevopoulos, G., Singleton, D. L. and Irwin, R. S. (1983): Chem. Phys. Lett., 100, 83.

Paraskevopoulos, G. and Irwin, R. S. (1984): J. Chem. Phys., 80, 259.

Patrick, R. and Pilling, M. J. (1982): Chem. Phys. Lett., 91, 343.

Penner, J. E. and Walton, J. J. (1982): "Air Quality Model Update," Lawrence Livermore Laboratory Report UCID-19300, University of California, Livermore, CA, 55 pp.

Perner, D., Schmeltekopf, A., Winkler, R. H., Johnston, H. S., Calvert, J. G., Cantrell, C. A. and Stockwell, W. R. (1985): J. Geophys. Res., 90, 3807.

Perry, R. A., Atkinson, R. and Pitts, J. N., Jr. (1977a): J. Phys. Chem., 81, 296.

Perry, R. A., Atkinson, R. and Pitts, J. N., Jr. (1977b): J. Phys. Chem., 81, 1607.

Peterson, J. T. (1976): "Calculated Actinic Fluxes (290-700 nm) for Air Pollution Photochemistry Applications," EPA-600/4-76-025, June.

Pitts, J. N. Jr., Darnall, K., Carter, W. P. L., Winer, A. M. and Atkinson, R. (1979): "Mechanisms of Photochemical Reactions in Urban Air," EPA-600/3/79-110, November.

Pitts, J. N., Jr., Atkinson, R., Carter, W. P. L., Winer, A. M. and Tuazon, E. C. (1983): "Chemical Consequences of Air Quality Standard and of Control Implementation Programs," Final Report to the California Air Resources Board Contract No. A1-030-32, April.

Pitts, J. N., Jr., Sanhueza, E., Atkinson, R., Carter, W. P. L., Winer, A. M., Harris, G. W. and Plum, C. N. (1984): Int. J. Chem. Kinet., 16, 919.

Plum, C. N., Sanhueza, E., Atkinson, R., Carter, W. P. L. and Pitts, J. N., Jr. (1983): Environ. Sci. Technol., 17, 479.

Ravishankara, A. R. and Mauldin, R. L., III, (1985): J. Phys. Chem., 89, 3144.

Rinke, M. and Zetzsch, C. (1984): Ber. Bunsenges Phys. Chem., 88, 55.

Saeger, M. (1977): "An Experimental Determination of the Specific Photolysis Rate of Nitrogen Dioxide," Masters Thesis, University of North Carolina, Chapel Hill, NC.

Sakamaki, F., Akimoto, H. and Okuda, M. (1981): Environ. Sci. Technol., 15, 665.

Sakamaki, F., Hatakeyama, S. and Akimoto, H. (1983): Int. J. Chem. Kinet., 15, 1013.

Sander, S. P. and Peterson, M. E. (1984): J. Phys. Chem., 88, 1566.

Shepson, P. B. and Heicklen, J. (1982a): J. Photochem, 18, 169.

Shepson, P. B. and Heicklen, J. (1982b): J. Photochem., 19, 215.

Shepson, P. B., Edney, E. O. and Corse, E. W. (1984): J. Phys. Chem., 88, 4122.

Shepson, P. B., Edney, E. O., Kleindienst, T. E., Pittman, J. H., Namie, G. R. and Cupitt, L. T. (1985): Environ. Sci. Technol., 19, 849.

Singleton, D. L., Furuyama, S., Cvetanovic, R. J. and Irwin, R. S. (1975): J. Chem. Phys., 63, 1003.

Sparks, R. K., Carlson, L. R., Shobatake, K. Kowalozyk, M. L. and Lee, Y. T. (1980): J. Chem. Phys., 72, 1401.

Stockwell, W. R. and Calvert, J. G. (1978): J. Photochem., 8, 193.

Stockwell, W. R. and Calvert, J. G. (1983): Atmos. Environ., 17, 2231.

Su, F., Calvert, J. G., Shaw, J. H., Niki, H., Maker, P. D., Savage, C. M. and Breitenbach, L. P. (1979a): Chem. Phys. Lett., 65, 221.

Su, F., Calvert, J. G. and Shaw, J. H. (1979b): J. Phys. Chem., 83, 3185.

Su, F., Calvert, J. G. and Shaw, J. H. (1980): J. Phys. Chem., 84, 239.

Taylor, W. D., Allston, T. D., Moscato, M. J., Fazekas, G. B., Kozlowski, R. and Takacs, G. A. (1980): Int. J. Chem. Kinet., 12, 231.

Thrush, B. A. and Tyndall, G. S. (1982a): J. Chem. Soc. Faraday Trans. II, 78, 1469.

Thrush, B. A. and Tyndall, G. S. (1982b): J. Chem. Phys. Lett., 92, 232.

Trevor, P. L., Black, G. and Barker, J. R. (1982): J. Phys. Chem., 86, 1661.

Tuazon, E. C., Atkinson, R., Plum, C. N., Winer, A. M. and Pitts, J. N., Jr. (1983): Geophys. Res. Lett., 10, 953.

Tuazon, E. C., Sanhueza, E., Atkinson, R., Carter, W. P. L., Winer, A. M. and Pitts, J. N., Jr. (1984a): J. Phys. Chem., 88, 3095.

Tuazon, E. C., Atkinson, R., Mac Leod, H., Biermann, H. W., Winer, A. M., Carter, W. P. L. and Pitts, J. N., Jr. (1984b): Environ. Sci. Technol., 18, 981.

Tuazon, E. C., Mac Leod, H., Atkinson, R. and Carter, W. P. L. (1986): Environ. Sci. Technol., 20, 383.

Vegret, B., Rayez, J. C. and Lesclaux, R. (1982): J. Phys. Chem., 86, 3424.

Whitten, G. Z., Killus, J. P. and Hogo, H. (1980a): "Modeling of Simulated Photochemical Smog with Kinetic Mechanisms," EPA-600/3-80-028a.

Whitten, G. Z., Hogo, H. and Killus, J. P. (1980b): Environ. Sci. Technol., 14, 690.

Whitten, G. Z., Killus, J. P. and Johnson, R. G. (1985): "Modeling of Auto Exhaust Smog Chamber Data for EKMA Development," EPA-600/3-85-025.

Wilson, K. W. and Doyle, G. J. (1970): "Investigation of Photochemical Reactivities of Organic Solvents," Stanford Research Institute Report, EPA Contract HCPA 22-61-125, September.

Wine, P. H. and Ravishankara, A. R. (1982): Chem. Phys., 69, 365.

Wine, P. H., Thompson, R. J., Ravishankara, A. R., Semmes, D. H., Gump, C. A., Torabi, A. and Nicovich, J. M. (1984): J. Phys. Chem., 88, 2095.

Winer, A. M., Peters, J. W., Smith, J. P. and Pitts, J. N., Jr. (1974): Environ. Sci. Technol., 8, 1118.

Winer, A. M., Graham, R. A., Doyle, G. J., Bekowies, P. J., McAfee, J. M. and Pitts, J. N., Jr. (1980): Adv. Environ. Sci. Technol., 10, 461.

Zafonte, L., Rieger, P. L. and Holmes, J. R. (1977): Environ. Sci. Technol., 11, 483.